

Synthesis, structures
and reactivity studies of
P-bis(trimethylsilyl)methyl-substituted
 $\sigma^3\lambda^3$ -oxaphosphirane complexes

Dissertation
zur
Erlangung des Doktorgrades (Dr. rer. nat.)
der
Mathematisch-Naturwissenschaftlichen Fakultät
der
Rheinischen Friedrich-Wilhelms-Universität Bonn

vorgelegt von
Janaina Marinas Pérez
aus
Recife, Brasilien

Bonn, 2010

Angefertigt mit Genehmigung der Mathematisch-Naturwissenschaftlichen Fakultät der
Rheinischen Friedrich-Wilhelms-Universität Bonn

1. Gutachter: Prof. Dr. R. Streubel

2. Gutachter: Prof. Dr. E. Niecke

Eingereicht am: 11.10.2010

Tag der Promotion: 13.01.2011

Diese Dissertation ist auf dem Hochschulschriftenserver der ULB Bonn

http://hss.ulb.uni-bonn.de/diss_online/ elektronisch publiziert

Erscheinungsjahr: 2011

Some of the results of this Thesis were previously published

- J. Marinas Pérez, C. Albrecht, H. Helten, G. Schnakenburg, R. Streubel, „Competing ring cleavage of transient *O*-protonated oxaphosphirane complexes: 1,3-oxaphospholane and η^2 -Wittig ylide complex formation“ *J. Chem. Soc., Chem. Comm.* **2010**, 46, 7244-7246.
- J. Marinas Pérez, H. Helten, B. Donnadieu, C. A. Reed, R. Streubel, „Protonation-Induced Rearrangement of an Oxaphosphirane Complex“ *Angew. Chem. Int. Ed.* **2010**, 49(14), 2615-2618.
- H. Helten, J. Marinas Pérez, J. Daniels, R. Streubel, „First Bronsted Acid-Induced Ring Expansion of an Oxaphosphirane Complex: A Combined Experimental and DFT Study“, *Organometallics* **2009**, 28(4), 1221-1226.
- R. Streubel, M. Bode, J. Marinas Pérez, G. Schnakenburg, J. Daniels, M. Nieger, P. G. Jones, „Facile Synthesis of Pentacarbonyltungsten(0) Complexes with Oxaphosphirane Ligands“, *Z. Anorg. Allg. Chem.* **2009**, 635(8), 1163-1171.
- A. Özbolat, G. von Frantzius, J. Marinas Pérez, M. Nieger, R. Streubel, „Strong evidence for a transient phosphinidenoid complex“, *Angew. Chem. Int. Ed.* **2007**, 46(48), 9327-9330.

Conference contributions

- J. Marinas Pérez, R. Streubel, 2th Deutsch-Österreichischer Mitarbeiterworkshop Hauptgruppenelementchemie, Bad Münster am Stein, 28. October **2007**; „*Ring expansion reactions of oxaphosphirane complexes – first examples*“, (Oral presentation).
- J. Marinas Pérez, M. Bode, H. Helten, R. Streubel, 5th European Workshop on Phosphorus Chemistry, Regensburg/Germany, 10. March **2008**; “*Synthesis and ring expansion reactions of oxaphosphirane complexes*“, (Oral presentation).

- J. Marinas Pérez, H. Helten, R. Streubel, 15th International Conference on Chemistry of Phosphorus Compounds, St Petersburg/Russia, 25.-30. March **2008**; “*First Acid induced Ring-Expansion Reactions of an Oxaphosphirane Complex*“, Poster, P-109.
- J. Marinas Pérez, Group Seminar Prof. C. Reed, Riverside/USA, 16. **2009**; “*Synthesis and reactions of oxaphosphirane complexes*”, (Oral presentation).
- J. Marinas Pérez, H. Helten, R. Streubel, 6th European Workshop on Phosphorus Chemistry, Florence/Italy, March **2009**; “*Acid induced ring-expansion of an oxaphosphirane transition metal complex: the quest for o-protonation*”, Poster, P-36.
- J. Marinas Pérez, R. Streubel, 3rd Deutsch-Österreichischer Mitarbeiter-Workshop, Tecklenburg/Germany, 4.-5. April **2009**; „*Acid induced ring-expansion reactions of an oxaphosphirane transition metal complex: the quest for o-protonation* “, (Oral presentation).
- J. Marinas Pérez, H. Helten, R. Streubel, 12th International Symposium on Inorganic Ring Systems, Goa, India, August **2009**; „*Protonation and Ring expansion of an Oxaphosphirane Complex*”, Poster, P-39.

Danksagung

Bei Herrn Prof. Dr. Rainer Streubel bedanke ich mich herzlich für die Themenstellung, die hervorragenden Arbeitsbedingungen, seine wertvollen Ratschläge und Anregungen, die großzügige Bereitstellung von Mitteln zur Anfertigung dieser Arbeit, sowie das Ermöglichen meiner Auslandsaufenthalte und der Teilnahme an diversen Tagungen.

Bei Herrn Prof. E. Niecke bedanke ich mich herzlich für sein Interesse und die Übernahme des Koreferates.

Herrn Prof. C. A. Reed danke ich für die freundliche Aufnahme in seiner Arbeitsgruppe in der University of California at Riverside. Darüberhinaus danke ich allen Mitarbeitern der Arbeitsgruppe für die gute Zusammenarbeit, insbesondere Dr. Evgenii Stoyanov und Irina Stoyanova für die Einarbeitung in die Carboranchemie.

Dr. Holger Helten und O. Krahe danke ich für die theoretischen Untersuchungen und für die Anregungen und Diskussionen.

Für die Anfertigung von Einkristallrötgenstrukturanalysen gilt mein Dank Herrn Dr. Gregor Schnakenburg, Herrn Dr. Jörg Daniels und Herrn Dr. Bruno Donnadieu.

Dr. Maurice van Gastel danke ich für die Einführung in die EPR-Spektroskopie.

Weiterhin danke ich allen Mitarbeitern der Zentralanalytik der Chemischen Institute. Vor allem geht mein Dank für die Aufnahme zahlreicher Spektren und die Durchführung der NMR-Sondermessungen an Frau Karin Prochnicki. Darüberhinaus danke ich Frau Hannelore Spitz, Frau Ulrike Weynand und Herrn Claus Schmidt für die Aufnahme von NMR-Spektren, Frau Christine Sondag und Frau Dr. Marianne Engeser für die Aufnahme von MS-Spektren, Frau Anna Martens für die Durchführung der Elementaranalysen sowie den Mitarbeitern des Chemikalienlagers, Glasbläserei, der Mechanik- und der Elektrowerkstatt.

Allen Mitarbeiter des AK Streubel: Gerd von Frantzius, Holger Helten, Maren Bode, Stefan Fankel, Christian Schulten, Carolin Albrecht, Vitaly Nesterov, Lili Duan, Aysel Özbolat-Schön und Susanne Saurbrey, vielen Dank für die hervorragende Zusammenarbeit und auch ausserhalb des Labors vorhandene Unterstützung.

Ausserdem danke ich auch allen ACF-, Bachelor- und Austausch-Praktikanten, die mich bei meiner Arbeit unterstützt haben.

Mein besonderer Dank gilt meiner Familie und meinen Eltern.

An expert is a person who has made all the mistakes that can be made in a very narrow field.

Niels Bohr.

Table of contents

I. Introduction to oxygen-containing <i>P</i> -three-membered heterocycles.....	1
I.I Introduction to phosphinidenoid complex chemistry	19
II. Aim of the thesis.....	22
III. Synthesis of $\sigma^3\lambda^3$ -oxaphosphirane complexes VII using transiently formed Li/Cl phosphinidenoid complexes	23
III.1 Synthesis of (bis(trimethylsilyl)methyl)dichlorophosphane complexes	23
III.2 Synthesis of <i>C</i> -aryl- <i>P</i> -bis(trimethylsilyl)methyl-substituted oxaphosphirane complexes	26
III.3 Synthesis of new <i>C</i> -alkyl- <i>P</i> -bis(trimethylsilyl)methyl-substituted oxaphosphirane complexes	32
III.4 Synthesis of <i>C</i> -disubstituted- <i>P</i> -bis(trimethylsilyl)methyl-substituted oxaphosphirane complexes	37
III.5 Synthesis of the first spiro-oxaphosphirane complex	41
III.6 Scopes and limitations of the phosphinidenoid complex method in the synthesis of oxaphosphirane complexes	46
IV. Investigations on the reactivity of <i>P</i> -bis(trimethylsilyl)methyl-substituted - $\sigma^3\lambda^3$ -oxaphosphirane complexes VII	52
IV.1 Acid-induced ring expansion reactions of <i>C</i> -phenyl-oxaphosphirane complexes.....	54
IV.1.1 Synthesis of the 1,3,4-dioxaphospholane complexes from <i>C</i> -phenyl-oxaphosphirane complexes	55
IV.1.1.1 Synthesis of 3,5-diphenyl-1,3,4-dioxaphospholane complexes	58
IV.1.1.2 Synthesis of 2-alkyl-1,3,4-dioxaphospholane complexes	62
IV.1.2 Investigations on the reaction mechanism of the acid-induced ring expansion reaction	65
IV.2 Acid-induced ring-opening reactions of the oxaphosphirane complex 16a	70
IV.2.1 Formation of <i>side-on</i> bonded P=C pentacarbonyltungsten(0) complexes through acid-induced ring-opening reactions	70
IV.2.2.1 Hydrogen chloride induced ring-opening reaction	83
IV.2.2.2 Synthesis of oxaphosphirane complexes VII using a chloro(hydroxymethyl)phosphane complex and LDA	90
IV.3 Ring-opening reactions of the oxaphosphirane complex 16a using fluoroboronic acid	95

V.1 Introduction into the ring-opening reactions of the oxiranes using Ti(III) complexes as SET reagents	103
V.2 Ring-opening reactions of the oxaphosphirane complex 16a using <i>in situ</i> generated Ti(III) complexes as SET reagents.....	108
V.2.1 Proposed mechanism for the formation of phosphaalkene complexes 102a,b	111
V.2.2 Reactivity of the phosphaalkene complexes 102a,b	113
VI. Summary	117
VII. Experimental part.....	126
VII.1. Preparative methods.....	126
VII.2 Measuring methods and devices	126
VII.2.1 Melting point determination	126
VII.2.2 Elemental analysis	126
VII.2.3 Mass spectrometry	126
VII.2.4 NMR spectroscopy.	127
VII.2.5 UV/vis spectroscopy.....	127
VII.2.6 Infrared spectroscopy.....	127
VII.2.7 Crystal structure analysis	127
VII.2.8 Chemicals	128
VII.2.9 Working procedure	130
VII.3 General procedure for the synthesis of [(bis(trimethylsilyl)methyl)dichlorophosphane]pentacarbonylchromium(0), - molybdenum(0) and -tungsten(0) [24-26]	131
VII.3.1 Synthesis of [(bis(trimethylsilyl)methyl)dichlorophosphane] pentacarbonylchromium(0) [26]	132
VII.3.2 Synthesis of [(bis(trimethylsilyl)methyl)dichlorophosphane] pentacarbonylmolybdenum(0) [25].....	133
VII.3.3 Synthesis of [(bis(trimethylsilyl)methyl)dichlorophosphane] pentacarbonyltungsten(0) [24]	134
VII.4 Synthesis of [2-bis(trimethylsilyl)methyl-3-phenyl-oxaphosphirane- kP]pentacarbonylchromium(0) [29]	135
VII.5 Synthesis of [2-bis(trimethylsilyl)methyl-3-phenyl-oxaphosphirane- kP]pentacarbonylmolybdenum(0) [30]	137
VII.6 General procedure for the synthesis of $\sigma^3\lambda^3$ -oxaphosphirane complexes.	139

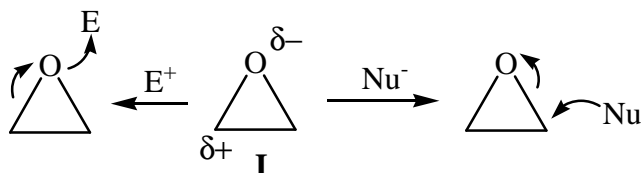
VII.6.1 Synthesis of [2-bis(trimethylsilyl)methyl-3-phenyl-oxaphosphirane- <i>kP</i>]pentacarbonyltungsten(0) [16a]	139
VII.6.2 Synthesis of [2-bis(trimethylsilyl)methyl-3-(2-methylphenyl)-oxaphosphirane- <i>kP</i>]pentacarbonyltungsten(0) [33]	141
VII.6.3 Synthesis of [2-bis(trimethylsilyl)methyl-3-(2-methoxyphenyl)-oxaphosphirane- <i>kP</i>]pentacarbonyltungsten(0) [34]	143
VII.6.4 Synthesis of [2-bis(trimethylsilyl)methyl-3- <i>tert</i> -butyl-oxaphosphirane- <i>kP</i>]pentacarbonyltungsten(0) [36]	144
VII.6.5 Synthesis of [2-bis(trimethylsilyl)methyl-3- <i>iso</i> -propyl-oxaphosphirane- <i>kP</i>]pentacarbonyltungsten(0) [37]	146
VII.6.6 Synthesis of [2-bis(trimethylsilyl)methyl-3- <i>n</i> -propyl-oxaphosphirane- <i>kP</i>]pentacarbonyltungsten(0) [38]	148
VII.6.7 Synthesis of the [2-bis(trimethylsilyl)methyl-3-methyl-oxaphosphirane- <i>kP</i>]pentacarbonyltungsten(0) [39]	149
VII.6.8 Synthesis of the [2-bis(trimethylsilyl)methyl-3-dimethyl-oxaphosphirane- <i>kP</i>]pentacarbonyltungsten(0) [42]	151
VII.6.9 Synthesis of the [2-bis(trimethylsilyl)methyl-3-diphenyl-oxaphosphirane- <i>kP</i>]pentacarbonyltungsten(0) [41]	153
VII.6.10 Synthesis of the [1-oxa-2-(bis(trimethylsilyl)methyl)phosphaspiro [2.5]octane- <i>kP</i>] pentacarbonyltungsten(0) [46a,b].....	154
VII.7 Reactions of [(bis(trimethylsilyl)methyl)dichlorophosphane]pentacarbonyltungsten(0) [24] with 2-adamantanone, 2,2,4,4-tetramethyl-3-pentanone and 3,3-dimethylbutan-2-one	157
VII.8 Reactions of [(bis(trimethylsilyl)methyl)dichlorophosphane]pentacarbonyltungsten(0) [24] with 1,1,3,3-tetramethylurea, N,N-dimethylformamide and tetrahydro-1,3-dimethylpyrimidin-2(<i>H</i>)-one	157
VII.9 Reaction of [dichlorophenylphosphane]pentacarbonyltungsten(0) [48] with benzaldehyde	158
VII.10 Attempts of synthesis of [(cyclopenta-1,3-dienyl)dichlorophosphane]pentacarbonyltungsten(0) [49]	159
VII.11 Attempts to complexation of (1,3,5-tri- <i>tert</i> -butylbenzyl)dichlorophosphane [50]....	159
VII.12 Attempts to complexation of (1,3,5-trimethylbenzyl)dichlorophosphane [51]	160
VII.13 Synthesis of [(bis(trimethylsilyl)methyl)dichlorophosphane]borane [52]	160

VII.14 General procedure for the synthesis of [2-(bis(trimethylsilyl)methyl)-2,5-diphenyl-1,3,4-dioxaphospholane]pentacarbonylchromium(0), molybdenum(0) and tungsten(0) [62-64a,b]	162
VII.14.1 Synthesis of [2-(bis(trimethylsilyl)methyl)-2,5-diphenyl-1,3,4-dioxaphospholane] pentacarbonylchromium(0) [62a,b]	162
VII.14.2 Synthesis of 1[2-(bis(trimethylsilyl)methyl)-2,5-diphenyl-1,3,4-dioxaphospholane] pentacarbonylmolybdenum(0) [63a,b]	165
VII.14.3 Synthesis of [2-(bis(trimethylsilyl)methyl)-2,5-diphenyl-1,3,4-dioxaphospholane] pentacarbonyltungsten(0) [64a,b]	168
VII.14.4 Synthesis of [2-(bis(trimethylsilyl)methyl)-2-methyl-5-phenyl-1,3,4-dioxaphospholane] pentacarbonyltungsten(0) [65a,b]	171
VII.14.5 Synthesis of [2-(bis(trimethylsilyl)methyl)-2- <i>iso</i> -propyl-5-phenyl-1,3,4-dioxaphospholane] pentacarbonyltungsten(0) [66a,b]	174
VII.15 Synthesis of { η^2 -[phenylmethylene{bis(trimethylsilyl)methyl}hydroxyphosphonium] pentacarbonyltungsten(0)}trifluoromethanesulfonate [72a,b]	177
VII.16 Synthesis of { η^2 -[phenylmethylene(bis(trimethylsilyl)methyl)hydroxyphosphonium] pentacarbonyltungsten(0)}2,3,4,5,6,7,8,9,10,11,12-undecachloro-1-carbadodecaborate [73]	179
VII.16.1 Synthesis of (bis(trimethylsilyl)methyl)-1-(phenylmethyl)phosphinic acid [74]	180
VII.17 Reaction of oxaphosphirane complex [46a] with triflic acid	181
VII.18 Synthesis of [bis(trimethylsilyl)methyl-1,1-(hydroxyphenyl)methyl chlorophosphane] pentacarbonyltungsten(0) [85a,b-85c]	183
VII.19 Synthesis of [2-bis(trimethylsilyl)methyl-3-phenyl-oxaphosphirane- <i>kP</i>] pentacarbonyltungsten(0) [16b]	187
VII.20 Synthesis of [(bis(trimethylsilyl)methyl)fluoro-1,1-(hydroxyphenyl)methylphosphane]pentacarbonyltungsten(0) [90, 91]	189
VII.21 Synthesis of η^2 -[(phenyl)methylene(bis(trimethylsilyl)methyl)fluorohydroxyphosphorane] pentacarbonyltungsten(0) [92]	191
VII.22 Synthesis of [(bis(trimethylsilyl)methyl)-1-phenylmethyldene phosphane] pentacarbonyltungsten(0) [102a,b]	192

VII.23 Synthesis of [benzyl(bis(trimethylsilyl)methyl)chlorophosphane] pentacarbonyltungsten(0) [113]	194
IIX. Literature.....	197
IX. Appendix	203

I. Introduction to oxygen-containing three-membered *P*-heterocycles

Epoxides, also called oxiranes **I**, are three membered heterocycles with one oxygen and two carbons atoms in the ring system which approximately defines an equilateral triangle. The chemical behavior of oxiranes is governed by two factors: the ring strain^[1] and the basicity of the oxygen ring atom. The reactions of epoxides with nucleophiles and/or electrophiles generally involve heterocyclic ring-opening via cleavage of the C-O bond (Scheme 1).^[2]



Scheme 1. Ring-opening of oxiranes **I** induced by electrophilic or nucleophilic attack.^[2]

Every year, a huge number of publications on oxiranes appear in the literature. As consequence of the rapid development in synthetic methods, the investigation of chemical reactions, and hence utilization of oxiranes, oxiranes occupy a central position among cyclic organic compounds.^[2,3] Thus, ring-opening reactions of epoxides have been applied industrially to produce a variety of bulk chemicals.

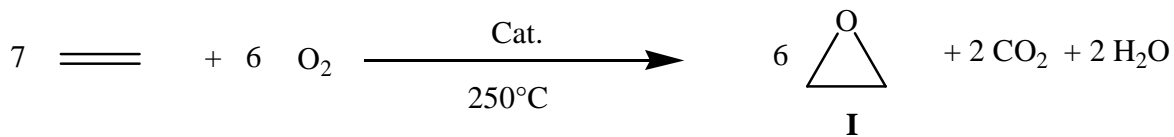
The simplest and most interesting epoxide is called ethylene oxide, which was first reported in 1859 by the french chemist Charles-Adolphe Wurtz.^[4] Ethylene oxide is a major industrial chemical and is consistently ranked among the top 25 highest production volume chemicals produced in the world. In 2003, 16 domestic suppliers of ethylene oxide were identified in USA.^[5] Overall, ethylene oxide demand is expected to grow at around 5% per year – globally. World consumption of ethylene oxide in 2007 was 19.9 million tones, some studies estimates that 13-14 new ethylene oxide plants will come on-stream until 2011 all over the world.

The largest outlet for ethylene oxide is ethylene glycol, which accounts for three-quarters of ethylene oxide global consumption. Mono ethylene glycol is the primary glycol which is used

mainly to make polyester, used in the production of textiles, followed by automotive antifreezes.

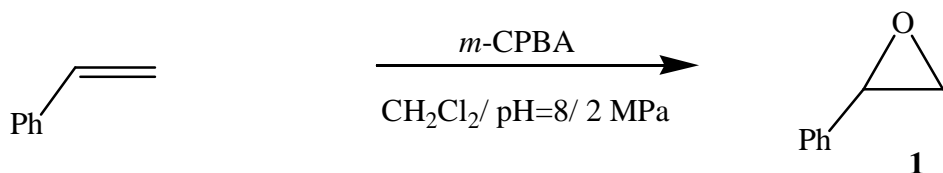
The second largest outlet for ethylene oxide, at 9% of total consumption, is as surface active agents, primarily non-ionic alkyl phenol ethoxylates and detergent alcohol ethoxylates. The alkyl phenol ethoxylates are used as non-ionic surfactants or as intermediates for the production of anionic alcohol ether sulphates/phosphates for home laundry and dishwashing formulations. Another important derivatives of the ethylenoxide are epoxy resins, which are used as coating agent in the automobile industry and for electrical devices.

The usual industrial procedure to synthesize ethylene oxide is the direct oxidation of alkenes with oxygen in the presence of silver catalysts.^[6] The yield under industrial conditions stands at 83-84%. This high yield is due to extensive research by big producers, driven by enormous cost savings potential (Scheme 2).



Scheme 2. Chemical equation of the industrial production of ethylene oxide.^[6]

This process is not effective enough in case of the production of other bulkier oxirane derivatives. In this case the direct formation of epoxides by olefin oxidation with the use of either transition metal catalysts or of simple organic ketone-based catalysts is once again considerably more elegant and environmentally friendly (Scheme 3).^[7,8]



Scheme 3. Example of the synthesis of oxirane derivative **1** using *m*-CPBA as an oxidant reagent.^[7]

Interestingly, oxaziridines **II** (Figure 1), in which one of the CR₂ moieties is formally exchanged by an NR group, have received much less attention. The first example was synthesized in 1956^[9] and originally called oxaziranes or isonitrones.

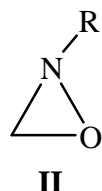
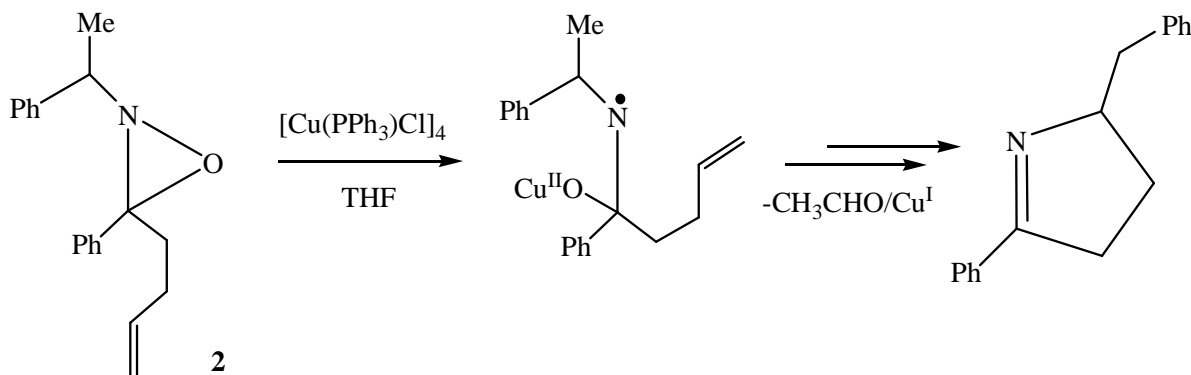


Figure 1. Representation of oxaziridine derivatives; R denotes ubiquitous organic substituents.

The presence of an inherently weak N-O bond in a strained ring promised a group of compounds of unusually high reactivity. The presence of a chiral center at the nitrogen and unshared electrons at the oxygen atom make the stereochemical isomerism at nitrogen possible.

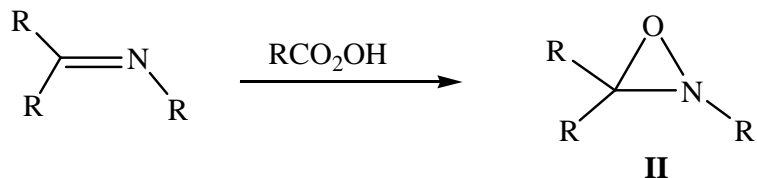
Oxaziridines can be used as oxygenating or aminating agent in so-called heteroatom transfer reactions.^[9] The oxaziridines are very versatile compounds, for example both acid and base catalyzed ring-opening of oxaziridines can lead to unique functionality, like hydroxyl amines or ketones.

Upon reaction with Cu complexes they can also build nitrogen-centered radicals via Single-Electron Transfer (SET) reactions (Scheme 4).^[10]



Scheme 4. Example of a single-electron transfer reaction of oxaziridine derivative **2**.^[10]

In analogy with the synthesis of oxiranes the epoxidation of the C-N double bond of imines leads to oxaziridines, as first described by Krimm (Scheme 5);^[11] peracetic acid and *m*-CPBA are mainly used for this purpose.



Scheme 5. Most important synthetic method for oxaziridine derivatives **II**; R denotes ubiquitous organic substituents.^[11]

Oxasiliranes **III** (Figure 2),^[12] which are the silicon analogous of oxiranes are much more reactive and up to now only few examples of oxasilirane derivatives have been established.^[13] The first stable oxasilirane was isolated in 1982^[14] (Figure 3), after almost thirty years of investigations four new oxasiliranes could be isolated by Stalke^[15] through stabilization of the three-membered heterocycle by a nitrogen-donor ligand (Figure 3).

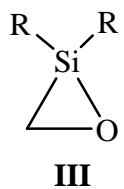


Figure 2. Representation of oxasiliranes **III**; R denotes ubiquitous organic substituents.

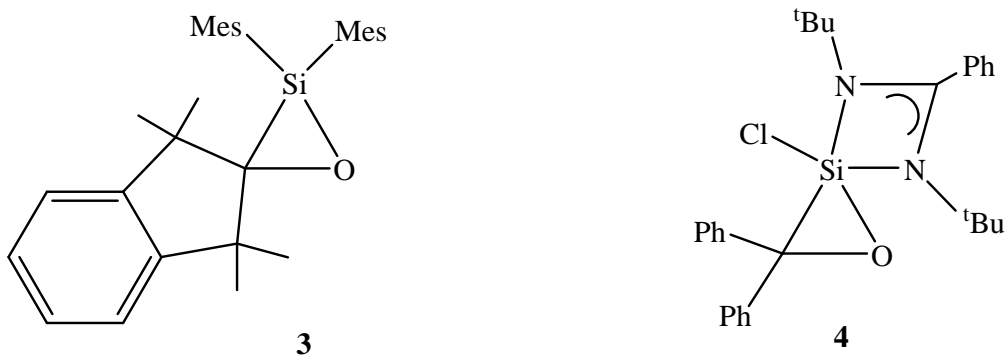


Figure 3. First isolated oxasilirane compound **3**^[14] and recently established oxasilirane **4**.^[15]

The phosphorus analogues **IV** of the oxiranes, so-called $\sigma^3\lambda^3$ -oxaphosphiranes, are experimentally still unknown but they have been claimed as reactive intermediates.^[16]

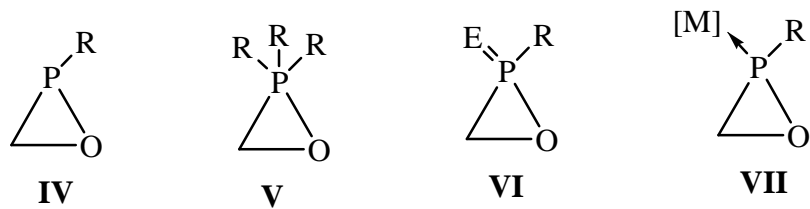
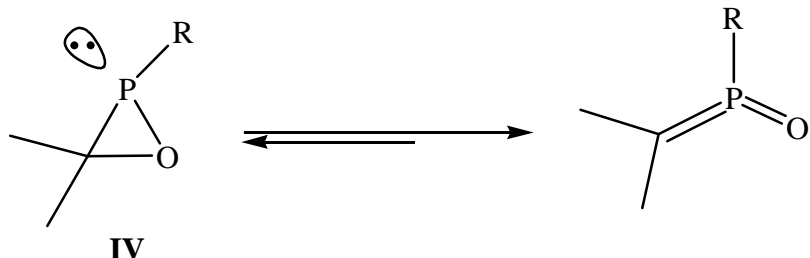


Figure 4. Representation of possible oxaphosphirane derivatives with phosphorus in different oxidation states and bonding environments; R denotes ubiquitous organic substituents; E denotes O or N substituent; [M] denotes a carbonyl transition metal group.

Until now only a few examples of $\sigma^5\lambda^5$ -, $\sigma^4\lambda^5$ -oxaphosphirane derivatives **V**, **VI** or $\sigma^3\lambda^3$ -oxaphosphirane complexes **VII** are known, which might be due to the used synthetic methodologies (too laborious and often low yields) and, therefore, a broad development of their chemistry was hampered. Nevertheless, the history of the synthesis and theoretical studies of these compounds will be discussed in more detail in this chapter.

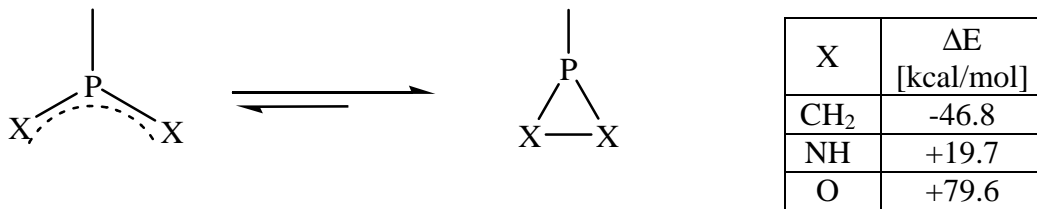
Although non-ligated $\sigma^3\lambda^3$ -oxaphosphirane derivatives **IV** are still unknown, theoretical investigations are available^[16] that predict existence, although rearrangements might occur.^[16, 17] Among those is the valence isomerisation of oxaphosphiranes **IV** (Scheme 6) that proceed via ring-opening and formation of $\sigma^3\lambda^5$ -alkylidene(oxo)phosphoranes, which was recognised by Schoeller, early on.^[17]



Scheme 6. Possible valence isomerisation of $\sigma^3\lambda^3$ -oxaphosphiranes **IV**.^[17]

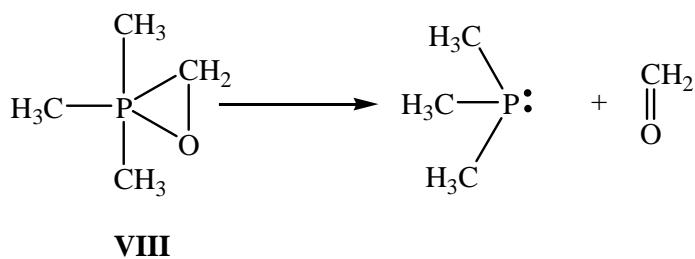
Theoretical investigations of the enthalpic contributions of ring-opening/closing reactions of three-membered heterocycles having one phosphorus atom were studied by Schoeller using *ab-initio* methods (SCF/CEPA-1 level) (Scheme 7). He showed that the nature of the substituents can shift the equilibrium to one or the other side.^[17] In case of the carbon moiety ($X = \text{CH}_2$) the three-membered heterocycle is preferred (exothermic reaction), whereas in case of oxygen ($X = \text{O}$) the open form is preferred (endothermic reaction). Further calculations showed that the difference in energy between the open and the closed form is

also influenced by the substituents at the carbon ($X = \text{CH}_2$) and phosphorus center and thus could determine the relative stabilities of both forms (open and closed ring).



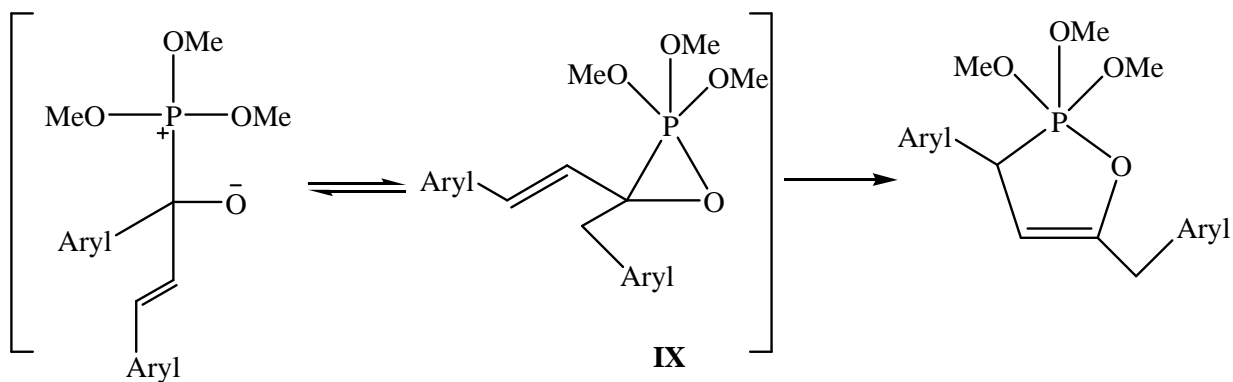
Scheme 7. Calculations on the ring-opening / closing reaction of three-membered heterocycles having one phosphorus center as reported by Schoeller.^[17]

More recently, DFT calculations on $\sigma^5\lambda^5$ -oxaphosphiranes **V** were reported by Quin and co-workers, which also reported NMR chemical shift calculations on different phosphoranes; they found that the three-membered ring in **VIII** was unstable and ring-cleavage might occur yielding the corresponding phosphane and ketone (Scheme 8). Nevertheless, an optimized geometry was obtained for **VIII**, and a calculated NMR shift for the parent compound was reported (${}^3\text{P}$ NMR: $\delta = -221$ ppm).^[18]



Scheme 8. Ring-cleavage reaction of the $\sigma^5\lambda^5$ -oxaphosphirane **VIII** as proposed by Quin.^[18]

In 1996, a new kind of ring-enlargement was proposed: a vinyl cyclopropane cyclopentene-type rearrangement of the transiently formed 3-vinyl-substituted oxaphosphirane **IX**; however, no strong evidence was provided for the existence of the latter.^[19, 20]



Scheme 9. Proposed rearrangement of 3-vinyl-substituted $\sigma^5\lambda^5$ -oxaphosphirane **IX**.^[19]

In 2003, Lammertsma tried to calculate the parent $\sigma^3\lambda^3$ -oxaphosphirane **IV**, but the structure was not stable at the Hartree Fock level and opened to form a phosphacarbonyl-ylide,^[21] and, therefore, no ring-strain could be calculated for this species (but see also below). By contrast, the parent azaphosphirene^[35] was obtained as confirmed minimum and the ring strain was calculated to 26.5 kcal/mol.

The most recent theoretical investigations on oxaphosphiranes were done by Neese and Streubel,^[16] in which the non-ligated $\sigma^3\lambda^3$ -oxaphosphirane and other CH₃OP isomers were calculated; structures and relative energies are displayed in Table 1. In this series, the most stable isomer was predicted to be the phosphinidene oxide **XIV**; methylene(oxo)phosphorane **XI** is about 9 kcal/mol more stable than **X**. Since **XI** is obtained from **X** by valence isomerisation (formally cleavage of the C-O bond), this means that the ring strain must be considerable high (see also below), as Schoeller's calculations also had predicted previously.^[17] Close in energy to **XIV** (and **XVI**) is the combination of PH₃ and CO (**XV**), which result from decomposition. An isomer very high in energy, is **XVII**, a hydroxylcarbene with a C-bonded phosphanyl group revealing a pyramidal phosphorus coordination environment (Table 1).

Table 1. Relative energies (to compound **XIV**) of the investigated isomers of CH₃OP; structures were optimized at the SCS-MP2/TZVPP level. Energy cc-pVQZ basis set); ZPE calculated by using RI-SCS-MP2/TZVPP. Color code: O: red; C: green; P: purple; H: white.^[16]

ΔE Kcal/mol	X	XI	XII	XIII	XIV	XV	XVI	XVII
CCSD(T)	25.0	14.9	18.1	57.0	0.0	8.9	4.3	66.4
B3LYP	25.6	15.1	16.2	55.2	0.0	10.2	4.7	65.1

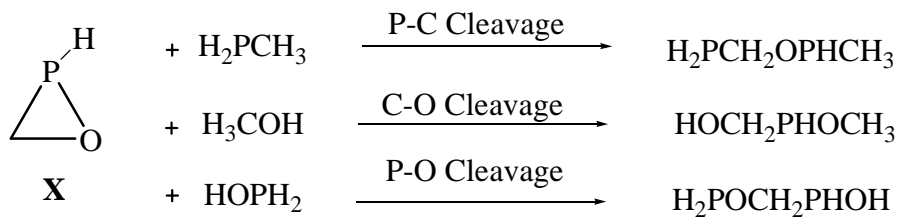
The authors also made the first theoretical investigation on metal-bound oxaphosphirane and isomers (type **VII**) to approach the experimental situation being actively investigated by the group of Streubel. They studied the situation for all structural motifs if bound to a Cr(CO)₅ fragment. Since several binding modes of the complex fragment can be envisaged for each species (P-bound, O-bound, C-bound, and various *side-on* bonded modes), a considerable number of possible structures arise; selected isomers are shown in Table 2.

Consistent with the results obtained on the small model systems, which is isomer **XVIII**, the terminal phosphinidene oxide complex^[22] was calculated to be the most stable isomer. Here the combination of a strong Cr-P bond, a strong P=O bond, and the stability of the methyl group together provide the thermodynamic sink in this series of isomers. Species **XVIII**, is energetically relatively well isolated, since the next stable species are more than 10–15 kcal·mol⁻¹ less stable. The parent oxaphosphirane complex **XXII** is predicted to be about 32 kcal·mol⁻¹ less stable than **XVIII**. Thus, if **XXII** can be made, a number of rearrangements could be energetically favourable.

Table 2. Relative energies (to **XVIII**) of some of the investigated chromium complexes of CH_3PO isomers; structures and ZPE were optimized at the BP86/def2-TZVP level. Colour code: O: red; C: green; P: purple; Cr: turquoise; H: white.^[16]

	XVIII	XIX	XX	XXI	XXII
ΔE Kcal/mol	0.0	7.8	11.8	12.8	31.8

All the calculations performed on the oxaphosphirane system showed the tendency of the oxaphosphirane ring to undergo ring-opening to yield the more stable phosphinidene oxide derivatives. Even the oxaphosphirane complexes **VII** are expected to undergo valence isomerisation to the open form. The large ring strain seems to be the driving force that destabilizes this kind of heterocycle. To get more insight into this problem, Neese *et al.* also performed calculations on the ring strain^[16] of the oxaphosphirane **X** (Table 3) and oxaphosphirane complex **XXIII** (Table 4), in comparison with the oxirane **I** (Table 5). For their calculations they used the concept of homodesmic reactions (Schemes 10-12). In such reactions the number and type of bonds and the valences of all atoms are preserved.^[23] The ring strain is then obtained by changing the sign of the reaction energy. Geometries were optimized with BP86/def2-TZVP for homodesmic reactions of the oxaphosphirane **X** as well as for the trimethyl substituted oxaphosphirane κ -P Cr(CO)₅ complex **XXIII**.

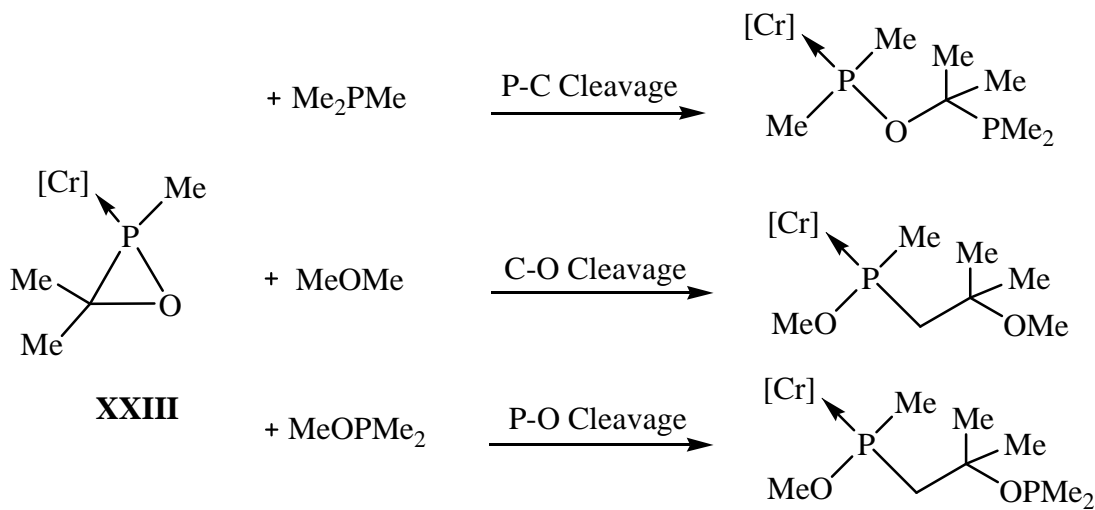


Scheme 10. Homodesmic reactions of oxaphosphirane **X**.^[16]

Table 3. Ring strain of 20 kcal/mol from homodesmic reactions of oxaphosphirane **X** (TZVPP basis set), ZPE calculation and geometry optimization using BP86/def2-TZVP.^[16]

	B3LYP	SCS-MP2	CCSD(T)
P-C cleavage	20.8	23.1	23.6
C-O cleavage	21.2	22.7	23.6
P-O cleavage	19.7	21.8	22.3
mean value	20.5	22.5	23.2

It is evident from the numbers, that the ring strain in oxaphosphiranes is indeed significant ~22-23 kcal/mol (Table 5). Comparison between the oxaphosphiranes and oxirane reveals that the former are slightly less strained by ~3 kcal/mol. While the effect of the binding to the metal fragment is predicted to be small by SCS-MP2, a large effect is observed in the B3LYP calculations.

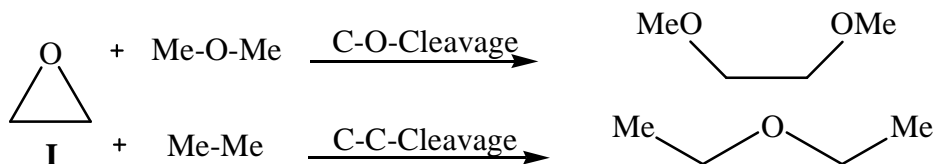


Scheme 11. Homodesmic reactions of the oxaphosphirane $\text{Cr}(\text{CO})_5$ complex **XXIII** ($[\text{Cr}] = \text{Cr}(\text{CO})_5$).^[16]

Table 4. Ring strain of (13 kcal/mol) from homodesmotic reactions of complex **XXIII** (TZVPP basis set), ZPE calculation and geometry optimization using BP86/def2-TZVP.^[16]

	B3LYP	SCS-MP2
P-C cleavage	13.1	21.6
C-O cleavage	12.2	21.1
P-O cleavage	12.9	23.4
mean value	12.8	22.0

C-O bond cleavage is clearly preferred for the oxirane **I** ring-opening (Table 5), but in case of the oxaphosphirane complex **XXIII**, the C-O cleavage is only slightly preferred to the P-O bond cleavage (Table 4) by B3LYP.



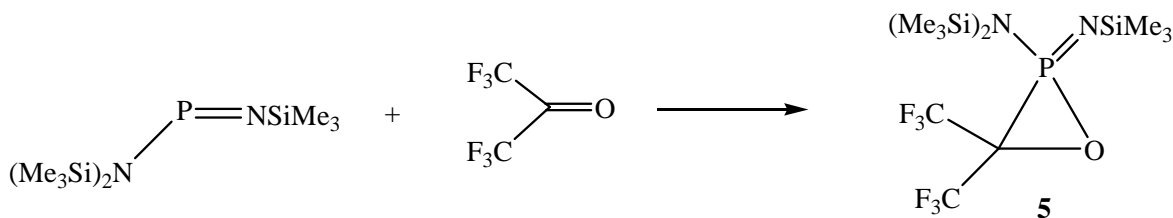
Scheme 12. Homodesmic reactions of oxirane **I**.^[16]

Table 5. Ring strain of 23 kcal/mol from homodesmic reactions of oxirane **I** (TZVPP basis set), ZPE calculation and geometry optimization at BP86/def2-TZVP.^[16]

	B3LYP	SCS-MP2	CCSD(T)
C-C cleavage	24.3	25.8	27.2
C-O cleavage	22.7	24.3	25.7
mean value	23.5	25.0	26.4

Nevertheless, theoretical investigations on real oxaphosphirane, yet isolated, have not been performed so far and the latter calculations could only describe a trend on the stability of this kind of compounds but not the real one. In fact, despite these calculations which predict a high ring strain, some derivatives of oxaphosphiranes **V**, **VI** and especially **VII** were experimentally confirmed.

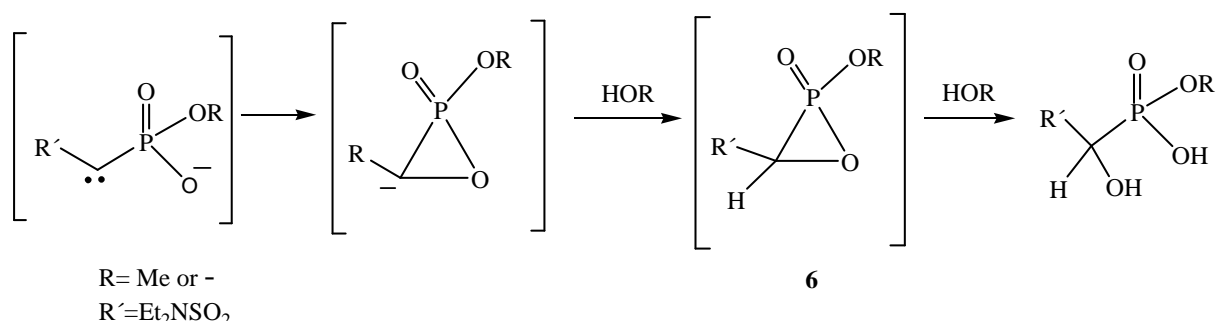
The chemistry of oxaphosphiranes having phosphorus in high coordination dates back to 1978, when the first synthesis of a $\sigma^4\lambda^5$ -oxaphosphirane derivative **VI** was described by Röschenthaler and Schmutzler using Niecke's imino phosphane^[24] and hexafluoro acetone (Scheme 13).^[25]



Scheme 13. Synthesis of the first oxaphosphirane derivative **5**.^[25]

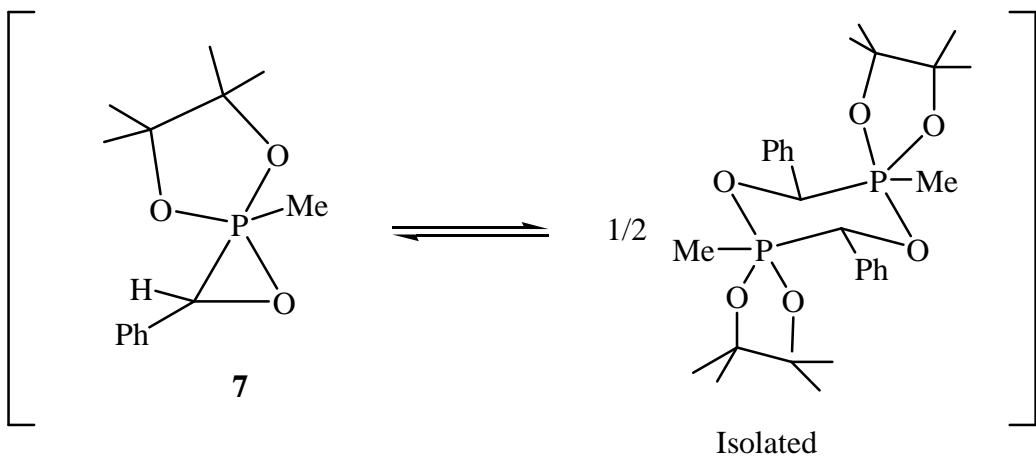
This kind of [2+1] cycloaddition reactions with hexafluoro acetone were previously known with transition metals like Ni or Rh but not for main group elements.^[26,27] Some years later Niecke *et al.* performed some investigations on this reaction and found that the substituents at the nitrogen atom could direct the reaction towards a [2+1] cycloaddition yielding oxaphosphiranes or into a [2+2] reaction yielding oxazaphosphetidines.^[28]

In 1982, intermediacy of a $\sigma^4\lambda^5$ -oxaphosphirane *P*-oxide derivative **VI** was claimed by Bartlett.^[29] Instead of the Wolff-rearrangement to explain the migration of an oxygen substituent from phosphorus, they proposed (without experimental evidence) a mechanism involving cyclization of a carbene intermediate, protonation, and subsequent reaction of the oxaphosphirane **6** by nucleophilic attack on phosphorus (Scheme 14).



Scheme 14. Mechanism proposed by Bartlett on the formation and transformation of the transient oxaphosphirane **6**.^[29]

Some years later, NMR and mass evidence was provided by Boisdan and Barrans who investigated a monomer-dimer-equilibrium of a $\sigma^5\lambda^5$ -oxaphosphirane **V**.^[30] The oxaphosphirane **7** seemed to be unstable and the equilibrium was shifted to the dimer, which was isolated.



Scheme 15. Equilibrium proposed by Boisdan and Barrans between the oxaphosphirane intermediate **7** and its dimer.^[30]

Albeit recent theoretical investigations^[31] predict easy decomposition of the oxaphosphirane into phosphane and carbonyl derivatives, further evidence for the existence of a $\sigma^5\lambda^5$ -oxaphosphirane derivative **V** was gained by Butenschön.^[32] In this case the oxaphosphirane **8** was isolated and its identity established by NMR spectroscopic and mass spectrometric studies (Figure 5).

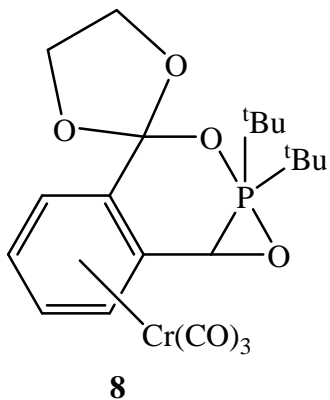
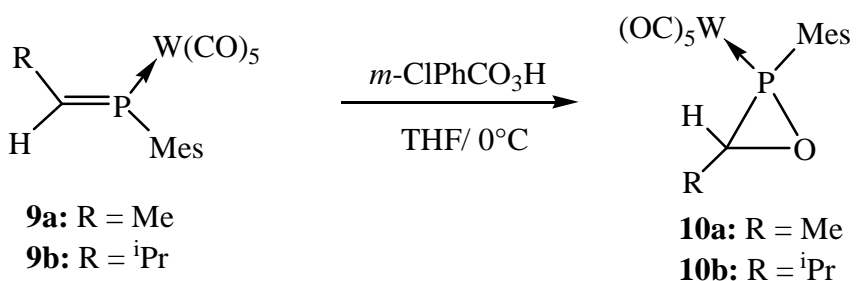


Figure 5. Oxaphosphirane **8**, isolated by Butenschön *et al.*^[32]

In 1990, Mathey showed that $\sigma^3\lambda^3$ -oxaphosphirane complexes **VII** can be obtained through epoxidation of phosphaalkene complexes with *m*-CPBA, which represents a further breakthrough.^[33] As oxidation of unligated phosphaalkenes occurs preferentially at the phosphorus atom, it is necessary to block the lone pair to mimick alkenes. In their report they showed that the phosphaalkene complex derivatives **9a,b** reacted with meta-chloroperbenzoic acid (*m*-CPBA) to yield the oxaphosphirane complexes **10a,b** (Scheme 16). The X-ray single-crystal structure analysis of complex **10b** confirmed for the first time the existence of an oxaphosphirane ring in a transition metal complex.



Scheme 16. Synthesis of oxaphosphirane complexes **10a,b** via epoxidation of phosphaalkene complexes **9a,b** with *m*-CPBA.^[33]

M. Schröder (in the group of Regitz) continued the work of Mathey in the field of the synthesis of oxaphosphirane complex using the same methodology.^[34] He succeeded to

synthesize and characterize new oxaphosphirane complexes not only with tungsten, but also with chromium and manganese (Figure 6), and he pointed out the necessity of having a sterically demanding substituent at phosphorus to stabilize the three-membered heterocycle. The difficulties to synthesize the corresponding phosphaalkene complexes and to work with the *m*-CPBA, most of the targeted oxaphosphirane complexes decomposed in an acid medium and/or were stable at low temperatures only, hampered the number of oxaphosphirane complexes accessible via this method.

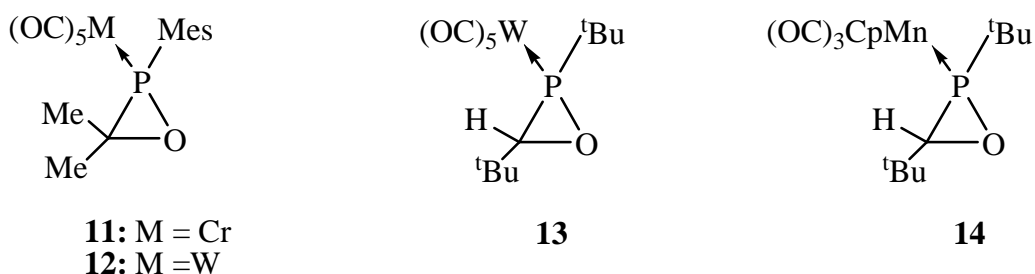
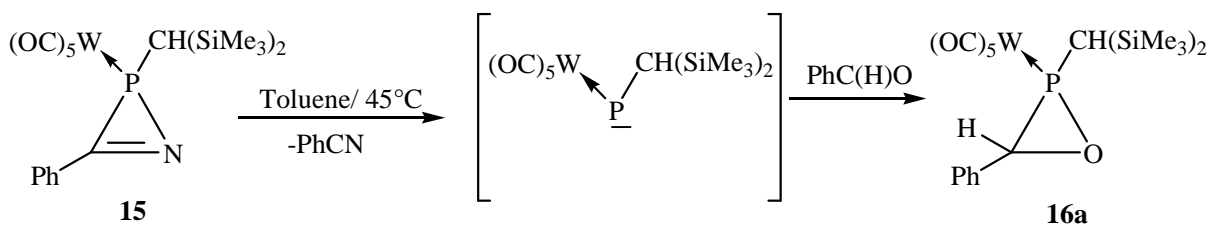


Figure 6. Oxaphosphirane complexes **11-14** synthesized by Schröder.^[34]

In 1994, Streubel *et al.* described a new synthetic route to oxaphosphirane complexes **VII**; they used the thermally induced ring cleavage of a 2*H*-azaphosphirene complex^[35] in the presence of an aldehyde^[36] or a ketone^[37] derivative; in the latter case a side-reaction to a benzo[c]-1,2-oxaphospholane complex occurred. In the case of benzaldehyde a transiently phosphinidene complex was formed, which reacted with the aldehyde and led exclusively to the oxaphosphirane complex **16a** (Scheme 17) which crystallized as a *RS/SR* diastereomers mixture. Surprisingly, no [3+2] cycloaddition reactions were observed under these conditions, and thus no five-membered heterocycles were formed.



Scheme 17. Synthesis of $\sigma^3\lambda^3$ -oxaphosphirane complex **16a** using 2*H*-azaphosphirene tungsten complex **15**.^[36]

Further investigations showed that the reaction of 2*H*-azaphosphirene complex **15** with carbonyl compounds having alkyl groups attached to the carbonyl carbon atom, did not yield the corresponding oxaphosphirane complexes.^[38] Instead, acyclic products having PH-functional groups were obtained. Related results were reported by the group of Mathey at about the same time.^[39]

As this method to synthesize oxaphosphirane complexes requires 2*H*-azaphosphirene tungsten complex **15** as starting material, which is a precious compound, i.e., obtained via a multi-step synthetic process, and it can't be applied to other aldehydes or ketones than the ones described before, doesn't make it suitable as standard method for the synthesis of $\sigma^3\lambda^3$ -oxaphosphirane complexes.

I.1 Introduction to phosphinidenoid complex chemistry

Phosphinidenoids **XXV** are the phosphorus analogous of carbenoids **XXIV** (Fig. 7).^[41] The latter can be structurally described as organometallic compounds containing a main group metal and an electronegative element at the same atom. They show high thermal lability and an ambiphilic reaction behaviour, i.e., they can react with nucleophiles, with electrophiles or like singlet carbenes.

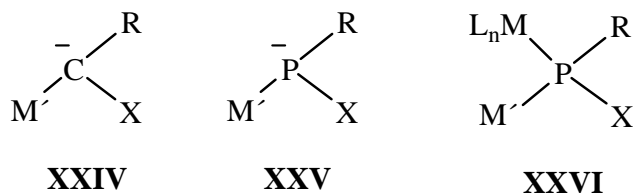
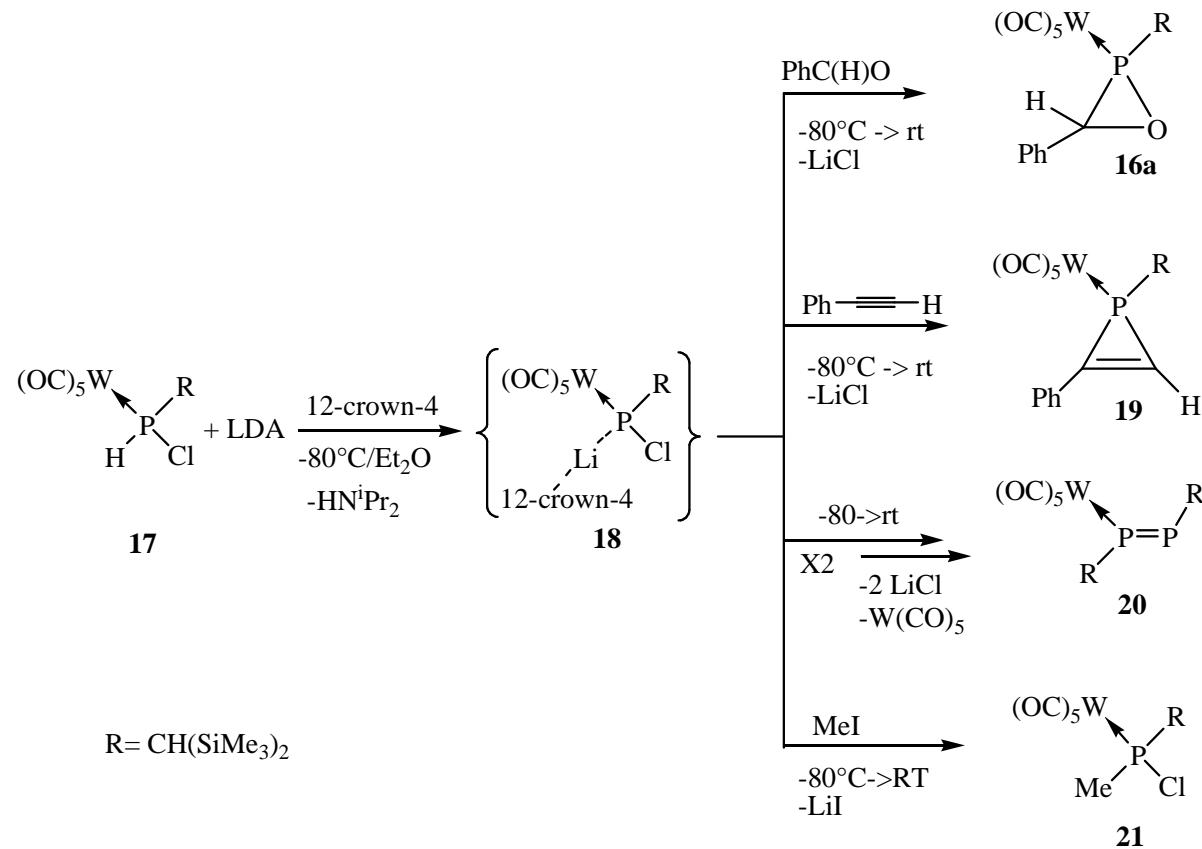


Figure 7. Carbenoid (**XXIV**), phosphinidenoid (**XXV**), phosphinidenoid complex (**XXVI**) (R denotes an organic substituent; M': Main group metal; X: Halogene; ML: Transition metal complex fragment).

While studying the chemistry of Li/X phosphinidenoid complexes **XXVI** a new synthetic route to $\sigma^3\lambda^3$ -oxaphosphirane complexes **VII** was recently developed by Özbolat-Schön, in the group of Streubel.^[40] She found that transiently formed Li/Cl phosphinidenoid complexes **XXVI** show an interesting reactivity and could react with different trapping agents or π -systems to yield different phosphorus containing complexes, as oxaphosphirane complex **16a** (Scheme 18). The related phosphinidenoid complex **18** was selectively obtained via deprotonation of chloro(organo)phosphane complex **17**^[42] with lithium diisopropylamide (LDA) in the presence of 12-crown-4. This transient Li/Cl phosphinidenoid complex was fully characterized by means of NMR spectroscopy at low temperature. Warming up in the absence of any trapping reagent led to *E*-diphosphene complex **20**,^[43] while in the presence of

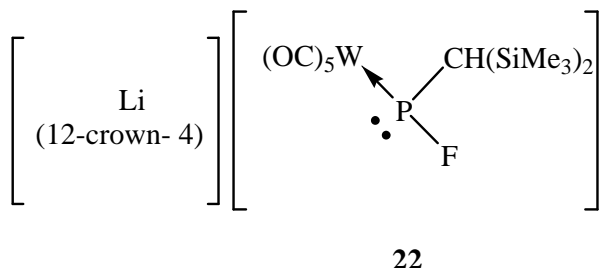
π -system such as phenyl acetylene or benzaldehyde the formation of 1*H*-phosphirene complex **19** and oxaphosphirane complex **16a** as formal [2+1] cycloaddition products were observed (Scheme 18).^[40]



Scheme 18. Synthesis and reactivity of *P*-bis(trimethylsilyl)methyl-substituted Li/Cl-phosphinidenoid complex **18**.^[40]

The phosphinidenoid complex **18** not only reacts like a “phosphinidene complex” but the generation of complex **18** in the presence of methyl iodide yielded the *P*-methyl-substituted chlorophosphane complex **21** (Scheme 18) as the sole phosphorus-containing product, thus confirming the nucleophilic reactivity and the unambiguously existence of complex **18** as intermediate.

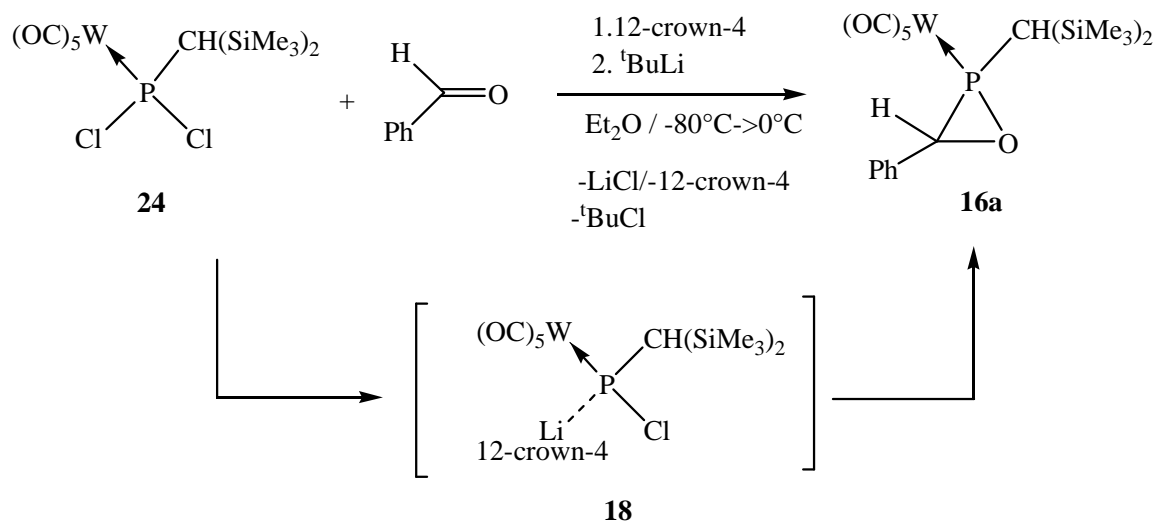
Another phosphinidenoid complex derivative, the *P*-bis(trimethylsilyl)methyl-substituted Li/F-phosphinidenoid complex **22**,^[44] showing higher stability than the Li/Cl derivative **18**, was confirmed by low-temperature NMR, MAS-NMR spectroscopic experiments, and its structure as ion pair further evidenced by X-ray crystallographic measurements.



22

Figure 8. Molecular structure of the isolated Li/F-phosphinidenoid complex **22**.^[44]

Another major synthetic breakthrough was achieved, when oxaphosphirane complex **16a** was synthesized from the easily accessible complex $[\text{W}(\text{CO})_5(\text{RPCl}_2)]$ (**24**) ($\text{R} = \text{CH}(\text{SiMe}_3)_2$) using *tert*-butyllithium and benzaldehyde (Scheme 19);^[40,45] here, the formation of the transient phosphinidenoid complex **18** was also proposed.



Scheme 19. Synthesis of the oxaphosphirane complex **16a** using dichlorophosphane complex **24**.^[40,45]

II. Aim of the thesis

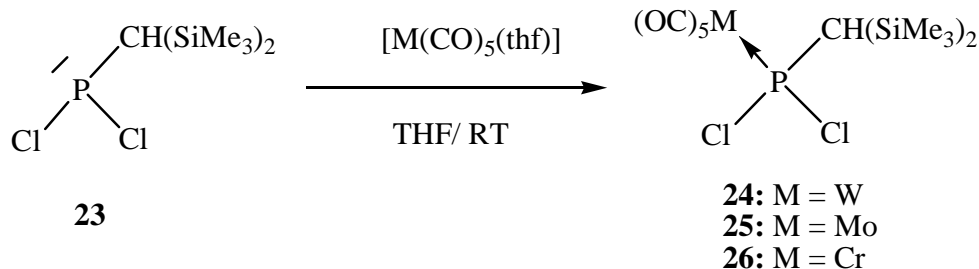
The aim of this work was to study the applicability of the novel route using Li/Cl phosphinidenoid complexes and various carbonyl derivatives to obtain a broad set of oxaphosphirane complexes, thus being able to explore the chemistry of $\sigma^3\lambda^3$ -oxaphosphirane complexes **VII** in more detail.

Further major objective was to investigate the reactivity of oxaphosphirane complexes with particular emphasis on its relationship to oxirane chemistry, *i.e.*, ring-opening reactions.

III. Synthesis of $\sigma^3\lambda^3$ -oxaphosphirane complexes **VII** using transiently formed Li/Cl phosphinidenoid complexes

III.1 Synthesis of (bis(trimethylsilyl)methyl)dichlorophosphane complexes

To synthesize new oxaphosphirane complexes using the Li/Cl phosphinidenoid complex route, the dichloro(organo)phosphane complexes (**24-26**) were used as starting materials due to their easy access compared to the chloro(organo)phosphane complex **17**; the latter is in fact the result of the thermal decomposition of the 2*H*-azaphosphhirene complex **15** in the presence of $[\text{Et}_3\text{NH}]\text{Cl}$.^[42]



Scheme 20. Synthesis of the (bis(trimethylsilyl)methyl)dichlorophosphane complexes (**24-26**).

Here, the complexes **24-26** were synthesized via complexation of the dichlorophosphane **23**^[46] with $[\text{M}(\text{CO})_5(\text{thf})]$ ^[47] ($\text{M} = \text{Cr}, \text{Mo}, \text{W}$) (Scheme 20); the required $[\text{M}(\text{CO})_5(\text{thf})]$ complexes were synthesized via photolysis of the corresponding $\text{M}(\text{CO})_6$ complexes or alternatively from the $[\text{M}(\text{CO})_5\text{CH}_3\text{CN}]$.^[48] The tungsten complex **24**^[49] had been obtained before via an unconventional way: the thermolysis of the 2*H*-azaphosphhirene complex **15** in the presence of CCl_4 yielded complex **24** in low yields, which was then exchanged for the complexation route in order to obtain better yields (85 %).^[49] The light sensitive

molybdenum complex **25** could only be isolated with a relatively low yield of 32 % and the photolysis of Mo(CO)₆ had to be performed in the presence of the dichloro-(organophosphane) **23**; selected data of complexes **24-26** are given in Table 6.

Table 6. Selected NMR data (CDCl₃) of complexes **24-26**.

	$\delta^{31}\text{P}$ [ppm] ($J_{\text{W,P}}$ [Hz])	$\delta(^1\text{H})$ [ppm] ($J_{\text{P,H}}$ [Hz])		$\delta(^{13}\text{C}\{^1\text{H}\})$ [ppm] ($J_{\text{P,C}}$ [Hz])		
		CH(SiMe ₃) ₂	CH ₃	<i>cis</i> -CO	<i>trans</i> -CO	CH
24	157.6 (330.8)	2.24 (8.3)	0.41	196.3 (7.8)	198.9 (44.5)	43.8 (2.3)
25	203.1	1.99 (10.5)	0.34	201.7 (10.3)	207.1 (46.0)	41.5 (29.7)
26	236.2	2.03 (10.4)	0.34	214.2 (14.5)	219.6 (1.3)	44.6 (26.6)

The chromium complex **26** showed a ${}^3\text{P}\{^1\text{H}\}$ NMR resonance downfield shifted with respect to the complexes **25** and **24**. These so-called $\Delta\delta$ -values (the differences between the phosphorus resonances of transition metal complexes having the same ligand) is a common feature of coordinated trivalent phosphorus compounds.^[50] Complex **24** had a phosphorus tungsten coupling constant of 330 Hz, in accordance with the literature.^[49,51] All ¹H and ¹³C {¹H} NMR data of the three complexes were very similar to each other, e.g., in the ¹H NMR spectra they all showed only one signal for the SiMe₃ groups. The complex **24** had a ${}^2J_{\text{P,H}}$ and ${}^1J_{\text{P,C}}$ couplings for the CH(SiMe₃)₂ group, which was slightly smaller than those of complexes **25**, **26**. In complex **26** the *trans*-CO carbon had a smaller phosphorus–carbon coupling constant magnitude than the *cis*-CO groups, which is also a common feature of pentacarbonyl phosphane chromium complexes.^[52,53]

Mass spectrometric investigations (EI, ¹⁸⁴W for complex **24**, ⁵²Cr for complex **26** and ⁹⁸Mo for complex **25**) showed the preference of the molecule radical cations (m/z 585 for complex **24**, m/z 489 for complex **25** and m/z 452 for complex **26**) to extrude CO before loosing a chlorine atom; the formation of the [(SiMe₃)^{•+}] (m/z 73) as base peak was observed in all cases.

Light yellow single-crystals of complexes **25** and **26** were obtained from concentrated *n*-pentane solutions. X-ray diffraction analysis showed that complex **26** crystallized in the monoclinic crystal system, P₂₁/n, like complex **24** (structures are shown in Figure 9), while complex **25** crystallized in the P₂₁/c space group.^[49] The P–Cl bonds are slightly longer than in complex **24** (2.058 Å). The W–P bond in complex **24** is shorter (2.4589(7))^[49] than the Mo–P bond in complex **25**, this feature can be also observed in the oxaphosphirane complexes and azaphosphirene complexes.^[42] The other crystallographic data of complexes **25**, **26** are very similar to complex **24**; further details on structure solution and refinement can be found in the appendix under GSTR 140 and GSTR 150.

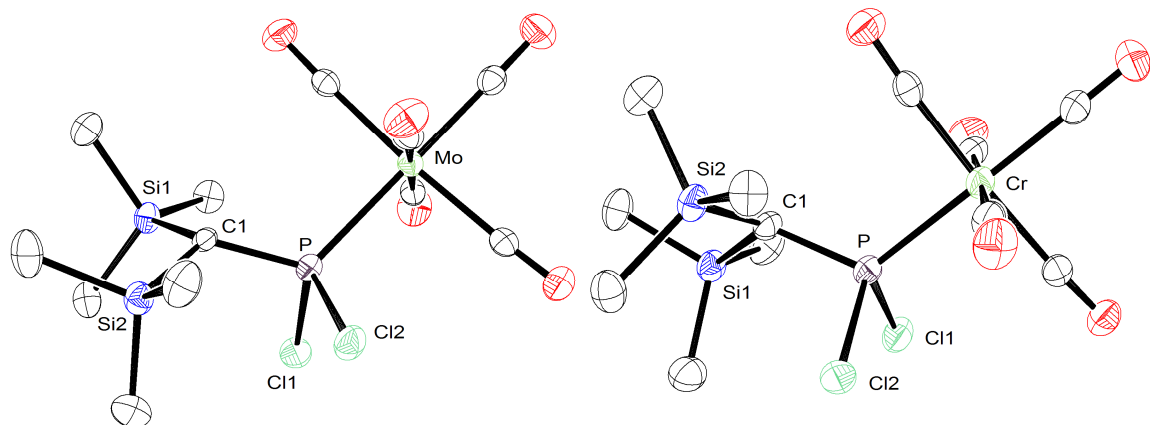
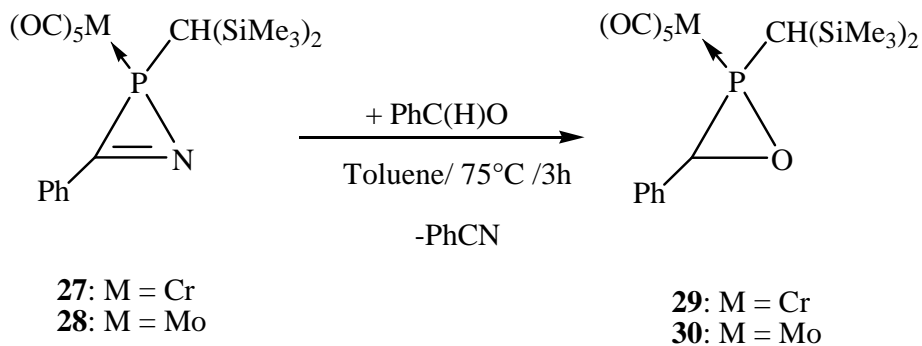


Figure 9. Molecular structure of complexes **25** (left side) and **26** (right side) in the crystal (ellipsoids represent 50% probability level, hydrogen atoms are omitted for clarity). Selected bond lengths (Å) and angles (°) of complex **26**: Cr–P 2.3177(10), P–Cl(1) 2.0639(12), P–Cl(2) 2.0636(12), P–C(1) 1.803(3), M–P–C(1) 120.14(11), C(1)–P–Cl(1) 106.25(10), Cl(1)–P–Cl(2) 96.57(5); Selected bond lengths (Å) and angles (°) of complex **25**: Mo–P 2.4670(11), P–Cl(1) 2.0611(14), P–Cl(2) 2.0629(14), P–C(1) 1.806(4), M–P–C(1) 119.90(12), C(1)–P–Cl(1) 106.50(12), Cl(1)–P–Cl(2) 96.81(6).

III.2. Synthesis of *C*-aryl-*P*-bis(trimethylsilyl)methyl-substituted oxaphosphirane complexes

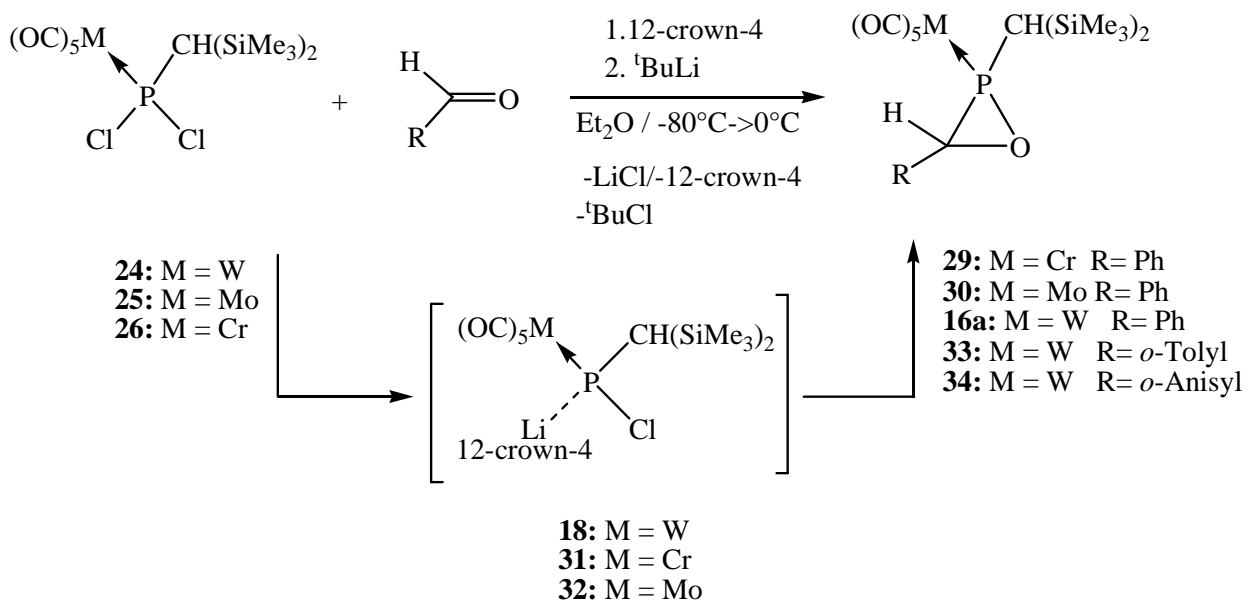
As described beforehand, the oxaphosphirane complex **16a** was first synthesized via thermolysis of a 2*H*-azaphosphirene complex (Scheme 17),^[36] but its chromium and molybdenum analogues were still unknown. They also have been first synthesized from the corresponding 2*H*-azaphosphirene Cr and Mo complexes (**27** and **28**^[54]). The increase of the temperature reaction from 45°C to 75°C made the synthesis much faster and selective, but this route still requires a multi-step synthesis of the starting material, which makes it were expensive and time demanding (Scheme 21).



Scheme 21. Synthesis of the oxaphosphirane complexes **29** and **30** from their 2*H*-azaphosphirene complexes **27** and **28**.

Therefore attention was drawn to the Li/Cl phosphinidenoid complex route, which would make the synthesis much easier and effective (Scheme 22). In this work, only the *C*-phenyl-substituted oxaphosphirane complexes **29** (M = Cr), **30** (M = Mo) were synthesized, although this route could be also transferred to other aldehyde derivatives for all the metals of the group 6 elements. Further reactions to obtain *C*-aryl-substituted oxaphosphirane complexes were then and therefore only performed with the tungsten derivatives.

Lithiation at low temperature of the appropriate dichloro(organo)phosphane complexes **24**-**26** in the presence of 12-crown-4 to form the transient Li/Cl phosphinidenoid complexes **18**, **31** and **32**^[60] and subsequent addition of benzaldehyde (**16a**, **29**, **30**), *o*-tolylaldehyde (**29**) or *o*-anisaldehyde (**30**) yielded selective the desired oxaphosphirane complexes (Scheme 22).



Scheme 22. Synthesis of the C-aryl-oxaphosphirane complexes **16a**,^[36] **29-30** through reaction of transiently formed Li/Cl phosphinidenoid complexes **18**, **31** and **32**.^[60]

It should be pointed out that if the reaction mixture was left at ambient temperature for 24 hours, decomposition of the oxaphosphirane complexes was observed. Because of this low stability the yields after chromatography were only relatively good, 60-64 % for complex **16a**, **29**, **33**, **30** and only 30 % for the molybdenum oxaphosphirane complex **30**, which is also light sensitive; structurally important NMR data are shown in Table 7.

Table 7. Selected NMR data (CDCl_3) of the oxaphosphirane complexes **29-34** and **16a**.^[36]

	$\delta^{31}\text{P}$ [ppm] ($^1J_{\text{W},\text{P}}$ [Hz])	$\delta(^1\text{H})$ [ppm] ($J_{\text{P},\text{H}}$ [Hz])		$\delta(^{13}\text{C}\{^1\text{H}\})$ [ppm] ($J_{\text{P},\text{C}}$ [Hz])	
		$\text{CH}(\text{SiMe}_3)_2$	CHAr	$\text{CH}(\text{SiMe}_3)_2$	CHAr
29	91.0	1.13	4.37	31.0 (24.2)	57.2 (24.2)
30	65.4	1.10 (2.2)	4.36 (1.6)	30.5 (25.2)	56.7 (22.3)
16a	38.2 (307.7)	1.28	4.40 (1.8)	30.5 (18.8)	57.9 (27.5)
33	41.0 (306.6)	1.14	4.26	32.7 (20.3)	57.9 (24.5)
34	39.2 (305.5)	1.16	4.46	30.4 (20.2)	54.7 (28.2)

The $^{31}\text{P}\{^1\text{H}\}$ NMR data of complexes **29**, **30** and **16a**^[36] (Table 7) showed again the $\Delta\delta$ values expected for the transition metals of group 6 elements. All C-aryl-substituted oxaphosphirane tungsten complexes showed a similar chemical shift and similar phosphorus-tungsten coupling constants around 305 Hz.

The ^1H NMR data of the $\underline{\text{CH}}(\text{SiMe}_3)_2$ protons (underlined) of these complexes were up-field in comparison with the respective dichloro(organo)phosphane complexes **24-26**, and they had smaller or no phosphorus-proton coupling constant; this was also observed in the case of other *P*-bis(trimethylsilyl)methyl three-membered heterocycles.^[52,42] The ^1H NMR shifts of the $\text{C}(\text{H})\text{Ar}$ protons were around 4.40 ppm and they also showed a small or no $^{2+3}J_{\text{P},\text{H}}$ coupling. The $^{13}\text{C}\{^1\text{H}\}$ NMR data of the carbon atoms of the $\underline{\text{CH}}(\text{SiMe}_3)_2$ group were up-fielded to the dichlorophosphane complexes **24-26** but they showed a similar $^1J_{\text{P},\text{C}}$ coupling constant in the range of 18.8-25.2 Hz. The $\underline{\text{CH}}(\text{Ar})$ showed resonances in the narrow range of 54.7-57.9 ppm with a $^{1+2}J_{\text{P},\text{C}}$ coupling constant value of 22.3-28.2 Hz; the latter phosphorus-carbon couplings are significantly larger than those of other three-membered, saturated phosphorus heterocyclic ligands such as phosphiranes^[57] and azaphosphoridines bound to a pentacarbonyltungsten(0) unit.^[36]

Mass spectrometric investigations (EI, 70eV) of oxaphosphirane complexes **16a**, **29-34** revealed that the molecule radical cations of **16a** (m/z 620), **29** (m/z 488), **30** (m/z 534), **33** (m/z 634, Figure 10), **34** (m/z 650), preferentially undergo ring-opening to yield $[(M(CO)_5PCH(SiMe_3)_2)^{•+}]$ (m/z 514 for M: ^{184}W , m/z 372 for M: ^{52}Cr and m/z 427 for ^{98}Mo) and subsequently extrude CO to give a series of cations (m/z 486 for M: ^{184}W (Figure 10), m/z 372 for M: ^{52}Cr and m/z 399 for ^{98}Mo).

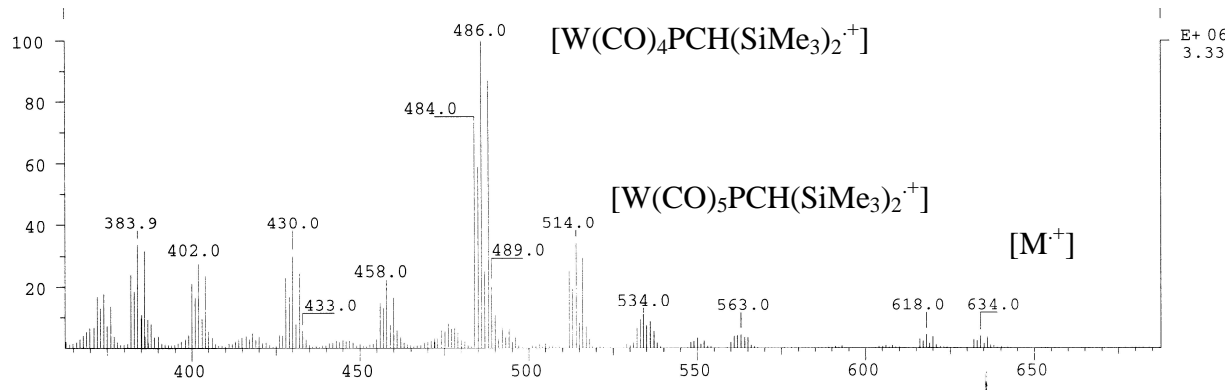


Figure 10. Mass spectra (EI, 70eV) of complex **33**.

The IR spectra of complexes **16a**, **29-34** showed three main signals in the carbonyl absorption range caused by the $M(CO)_5$ group, which display a local C_{4v} symmetry. For this symmetry three bands are expected: one E_1 and two A_1 modes.^[55] The UV/Vis spectra of the oxaphosphirane complexes **16a**, **29-34** showed one λ_{max} value at about 235 nm ($\epsilon = 0.45$), which can be attributed to the $\pi-\pi^*$ electron transitions related to the aryl group. In addition, shoulders appeared at λ_{max} values about 300 nm, which can be attributed to charge-transfer transitions of the carbonyl groups.^[56]

Suitable single crystals for X-ray diffractometric analysis of complexes **29**, **30**, **33** and **34** were obtained from concentrated *n*-pentane solutions; the structures are displayed in Fig. 11 and 12. The X-ray crystal structure of complex **16a** was already described in the literature.^[36]

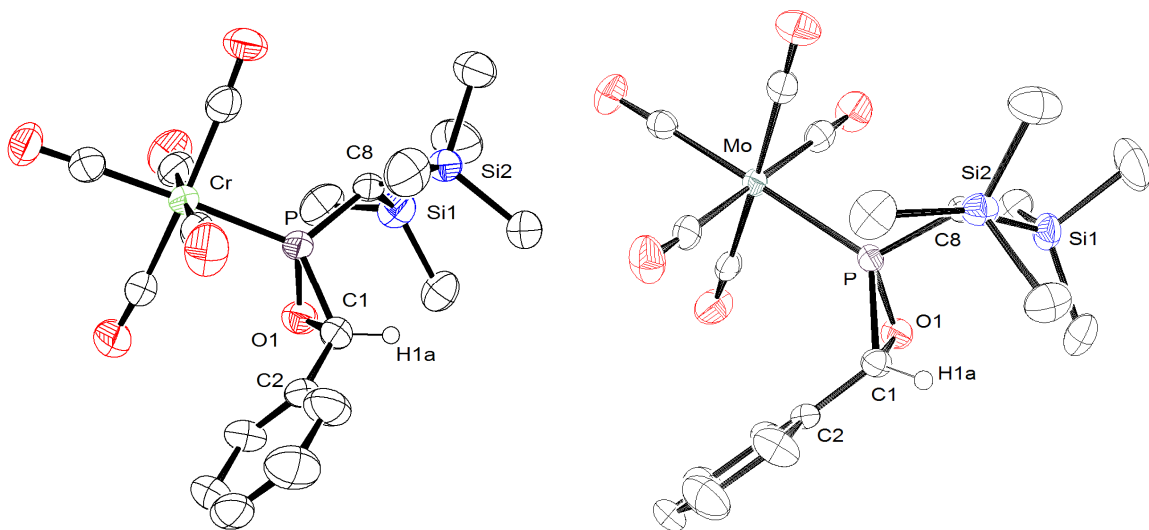


Figure 11. Molecular structure of the oxaphosphirane complexes **29** (left side) and **30** (right side) in the crystal (ellipsoids represent 50% probability level, hydrogen atoms except H1a are omitted for clarity). Selected bond lengths (\AA) and angles ($^\circ$) of oxaphosphirane complex **29**: Cr-P 2.3181(13), P-O(1) 1.682(3), C(1)-O(1) 1.491(6), P-C(1) 1.793(4), P-O(1)-C(1) 68.5(2), C(1)-P-O(1) 50.7(2), O(1)-C(1)-P 60.8(2); Selected bond lengths (\AA) and angles ($^\circ$) of oxaphosphirane complex **30**: Mo-P 2.4675(7), P-O(1) 1.6786(16), C(1)-O(1) 1.482(2), P-C(1) 1.795(2), P-O(1)-C(1) 68.90(10), C(1)-P-O(1) 50.37(8), O(1)-C(1)-P 60.72(10). Further details on structure solution and refinement can be found in the appendix under GSTR084 (complex **29**) and GREG 116 (complex **30**).

All complexes **16a**, **29-34** crystallized in the same space group, triclinic P(-1), as racemic mixture of *RS/SR* diastereomers. The bond angles were very similar among the oxaphosphirane complexes **16a**, **29-34**, *e.g.*, they had acute endocyclic angles at phosphorus of about 50° . This holds true also for all bond lengths except the phosphorus metal distances. The Cr-P distance (2.318(13) \AA) was the shortest one, as expected, but the W-P distance is

slightly shorter than the Mo-P distance. This trend was also observed in *P*-Cp*-oxaphosphirane derivatives.^[51]

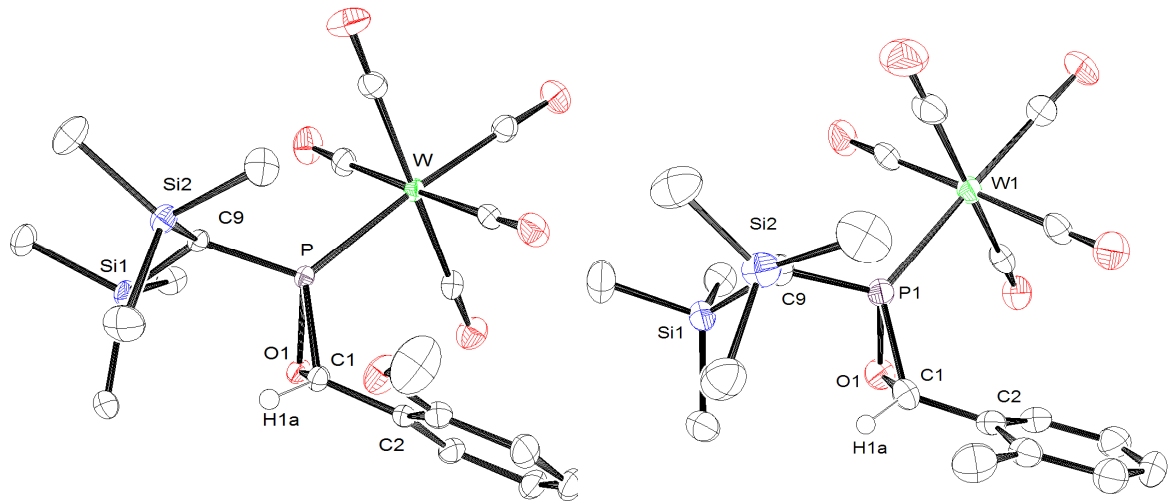
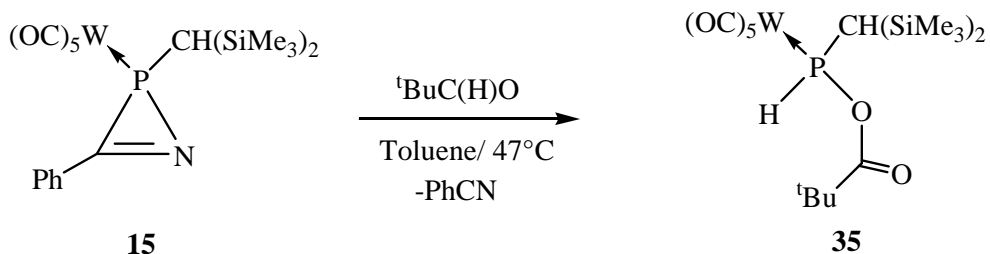


Figure 12. Molecular structures of complex **34** (left side) and one independent molecule of complex **33** (right side) in the crystal (50 % probability level; hydrogen atoms except H1a are omitted for clarity). Selected bond lengths (\AA) and angles ($^{\circ}$) of complex **33**: W-P 2.4597(14), P-O(1) 1.667(4), C(1)-O(1) 1.486(6), P-C(1) 1.805(5), P-O(1)-C(1) 69.6(3), C(1)-P-O(1) 50.5(2), O(1)-C(1)-P 59.9(2); Selected bond lengths (\AA) and angles ($^{\circ}$) of complex **34** (Two independent molecules, one molecule of *n*-pentane in the unit cell. The data for only one molecule are presented as the other is not significantly different): W-P 2.4631(5), P-O(1) 1.6701(13), C(1)-O(1) 1.467(2), P-C(1) 1.790(2), P-O(1)-C(1) 69.23(9), C(1)-P-O(1) 50.01(8), O(1)-C(1)-P 60.76(9). Further details on structure solution and refinement can be found in the appendix under GSTR072 (complex **33**) and GSTR 105 (complex **34**).

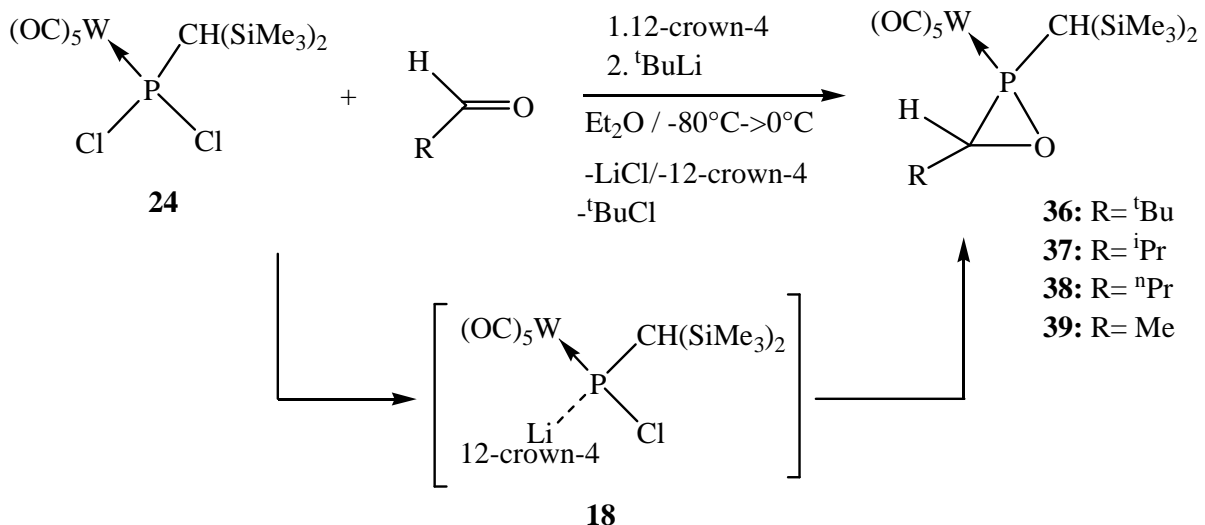
III.3. Synthesis of *C*-alkyl-*P*-bis(trimethylsilyl)methyl-substituted oxaphosphirane complexes

Attempts to synthesize new *C*-alkyl substituted oxaphosphirane complexes were already performed by Ostrowski through the thermolysis of the 2*H*-azaphosphirene complex **15**. In particular, studies to synthesize the *tert*-butyl *C*-substituted oxaphosphirane complex did not yield the desired oxaphosphirane complex but the *tert*-butylcarbonyloxy(alkyl)phosphane complex **35** (Scheme 23).^[38]



Scheme 23. Synthesis of the complex **35** via thermolysis of complex **15**.^[38]

In this chapter the synthesis of novel *C*-alkyl substituted oxaphosphirane complexes using the phosphinidenoid complex route was performed. The reaction of dichlorophosphane **24** with alkyl substituted aldehydes yielded selectively the oxaphosphirane complexes **36-38** in moderate yields after column chromatography (50-55%) (Scheme 24).



Scheme 24. Synthesis of oxaphosphirane complexes **36-39** through reaction of transiently formed Li/Cl phosphinidenoid complex **18** and aldehydes.^[45]

The oxaphosphirane complex **39** ($R = \text{Me}$) was also formed, but decomposed after few hours in solution. Therefore, only the NMR data of complex **39** were obtained. In general, the *C*-alkyl substituted oxaphosphirane complexes were isolated in lower yields than the aryl derivatives, partly due to rapid decomposition. Although it seemed apparent that the aryl group stabilize the oxaphosphirane complexes most probably because of electronic effects, it was not the case for the *P*-Cp* oxaphosphirane complexes,^[51] in which the *C*-methyl substituted oxaphosphirane complex was stable.

Nevertheless, the utility of the new phosphinidenoid complex route to synthesize oxaphosphirane complexes was proven, where other routes had failed before.

The $^{31}\text{P}\{\text{H}\}$ NMR spectroscopic data (Table 8) of the oxaphosphirane complexes **36-39** were very similar (22.5-30.9 ppm) and the shifts slightly up-fielded to the *C*-aryl substituted oxaphosphirane complexes **33**, **34**. The phosphorus-tungsten coupling constants were also slightly smaller (298.7-302.6 Hz) than for the aryl derivatives. There is no obvious trend

between the steric demand of the substituent at the carbon center of the ring and the $^{31}\text{P}\{\text{H}\}$ NMR chemical shift.

Table 8. Selected NMR data (CDCl_3) of the oxaphosphirane complexes **36- 39**.

	$\delta^{31}\text{P}$ [ppm] ($^1J_{\text{W},\text{P}}$ [Hz])	$\delta(^1\text{H})$ [ppm] ($J_{\text{P},\text{H}}$ [Hz])		$\delta(^{13}\text{C}\{\text{H}\})$ [ppm] ($J_{\text{P},\text{C}}$ [Hz])	
		<u>CH(SiMe₃)₂</u>	<u>CHR</u>	<u>CH(SiMe₃)₂</u>	<u>CHR</u>
36	22.5 (298.8)	1.25	2.70	33.6 (15.4)	67.1 (28.5)
37	31.9 (298.8)	1.05	2.75 (9.8)	28.7 (17.1)	62.9 (28.7)
38	27.7 (302.6)	1.15	3.10 (9.8)	28.5 (16.4)	57.4 (30.7)
39	30.9 (298.7)	1.05	3.15	28.5 (16.3)	53.8 (32.9)

The ^1H NMR data of the CH(SiMe₃)₂ protons of complexes **36-39** were very similar to the *C*-aryl substituted oxaphosphirane complexes, too, and did not show any phosphorus hydrogen couplings. On the other hand the CHR protons showed resonances at around 3 ppm, and in the case of complexes **37**, **38** ($\text{R} = ^i\text{Pr}, ^n\text{Pr}$) they showed a relative big $^{2+3}J_{\text{P},\text{H}}$ value (9.8 Hz) compared to the oxaphosphirane complexes **36** and **39**.

In case of complex **39**, there was a phosphorus hydrogen coupling of 15.9 Hz between the CH_3 group attached to the ring and the phosphorus atom, although no $^{2+3}J_{\text{P},\text{H}}$ constant could be found for the CH(Me) proton. This interesting phenomenon was also observed in the *C*-methyl substituted oxaphosphirane complex having a Cp^* moiety attached to the phosphorus.^[51]

The $^{13}\text{C}\{\text{H}\}$ NMR spectroscopic data of complexes **36-39** revealed similar trends for the resonances of the CH(SiMe₃)₂ carbon atoms (Table 8), they were found in the narrow range of 28.5 to 33.6 ppm with a $^1J_{\text{P},\text{C}}$ value of 15.1 to 17.1 Hz. The CHR carbon atoms of the complexes **36** and **37** were more deshielded than the one of the *C*-aryl substituted oxaphosphirane complexes; oxaphosphirane complex **38** doesn't follow this trend.

The mass spectrometric experiments (EI, 70eV, ^{184}W) revealed again that the molecule radical cations of **36** (m/z 620), **37** (m/z 488), **38** (m/z 534) undergo ring fragmentation in all cases followed by loss of one molecule CO, forming the base peak (m/z 486), which was assigned to $[(\text{CO})_4\text{WPCH}(\text{SiMe}_3)_2]^{•+}$.

The infrared spectroscopy of complexes **36-38** showed again the same symmetry ($\text{C}_{4\text{v}}$) in the $\text{W}(\text{CO})_5$ fragment. Three bands were found in the carbonyl absorption range, two weak bands at higher frequencies due to $\text{A}_1^{(1)}$ ($\sim 2070 \text{ cm}^{-1}$) and B_1 ($\sim 1990 \text{ cm}^{-1}$) modes, and another very strong band at lower frequencies ($\sim 1930 \text{ cm}^{-1}$) most probably due to overlapping of the E and $\text{A}_1^{(2)}$ modes.

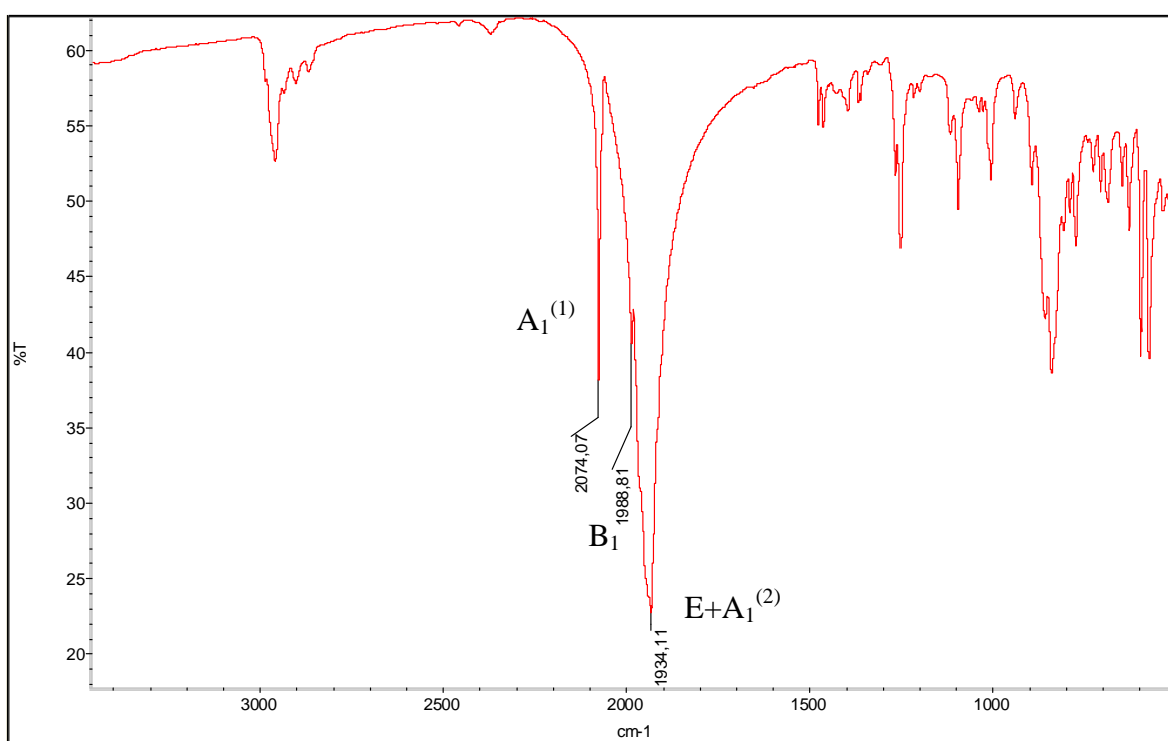


Figure 13. Infrared spectrum of complex **36**.

The UV/vis studies for these oxaphosphirane complexes showed a λ_{max} around 240 nm and a shoulder at around 300 nm, which can be assigned to a metal–ligand charge transfer (MLCT) process.^[56]

Only complex **36** could be determinate by X-ray diffraction studies, in this case the oxaphosphirane complex crystallized in the monoclinic space group $P\ 2_1/1$, which breaks the tendency of the other oxaphosphirane complexes to the triclinic space group. It was also found as mixture of *RS/SR* diastereomers (Figure 14).

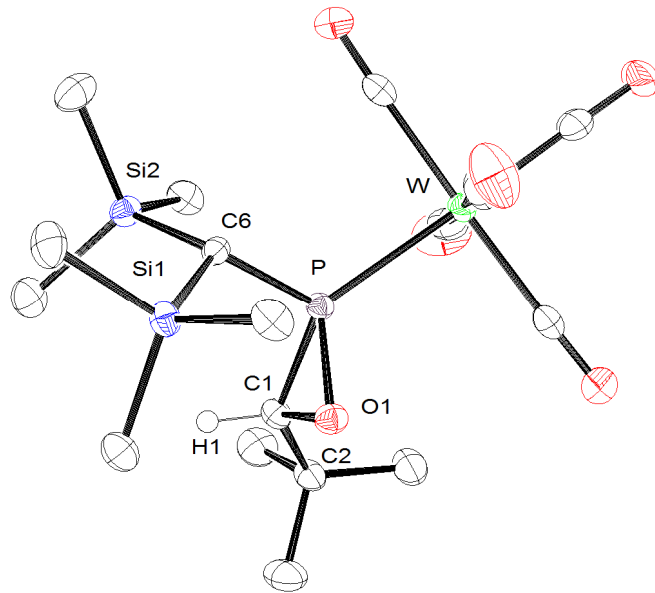
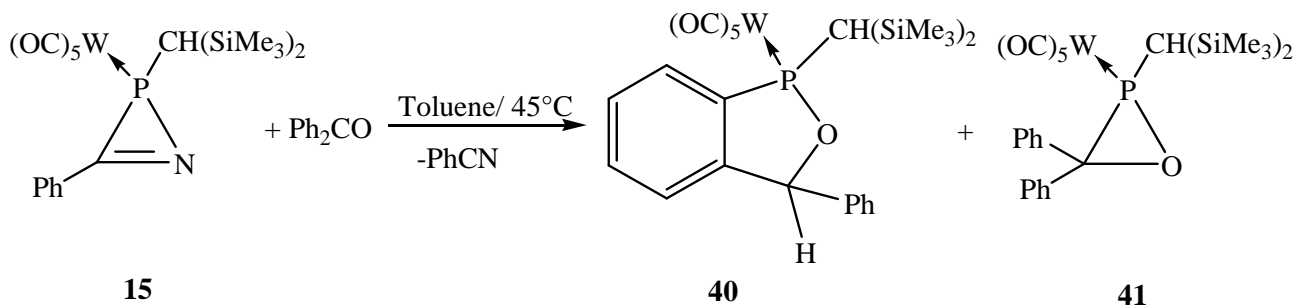


Figure 14. Molecular structure of oxaphosphirane complex **36** in the crystal (50 % probability level; hydrogen atoms except H1 are omitted for clarity). Selected bond lengths (\AA) and angles ($^{\circ}$): W-P 2.4804(8), P-O(1) 1.669(2), C(1)-O(1) 1.487(4), P-C(1) 1.784(3), P-O(1)-C(1) 68.58(16), C(1)-P-O(1) 50.88(13), O(1)-C(1)-P 60.54(14). Further details on structure solution and refinement can be found in the appendix under GSTR071.

The crystal structure of complex **36** showed the typical acute endocyclic angle at the phosphorus atom (50.8°) and similar bond lengths. This proves that, at least for the *C*-aryl/alkyl oxaphosphirane complexes, the P-W distance is unaffected by the *C*-substitution pattern of the ligand.

III.4 Synthesis of *C*-disubstituted-*P*-bis(trimethylsilyl)methyl-substituted oxaphosphirane complexes

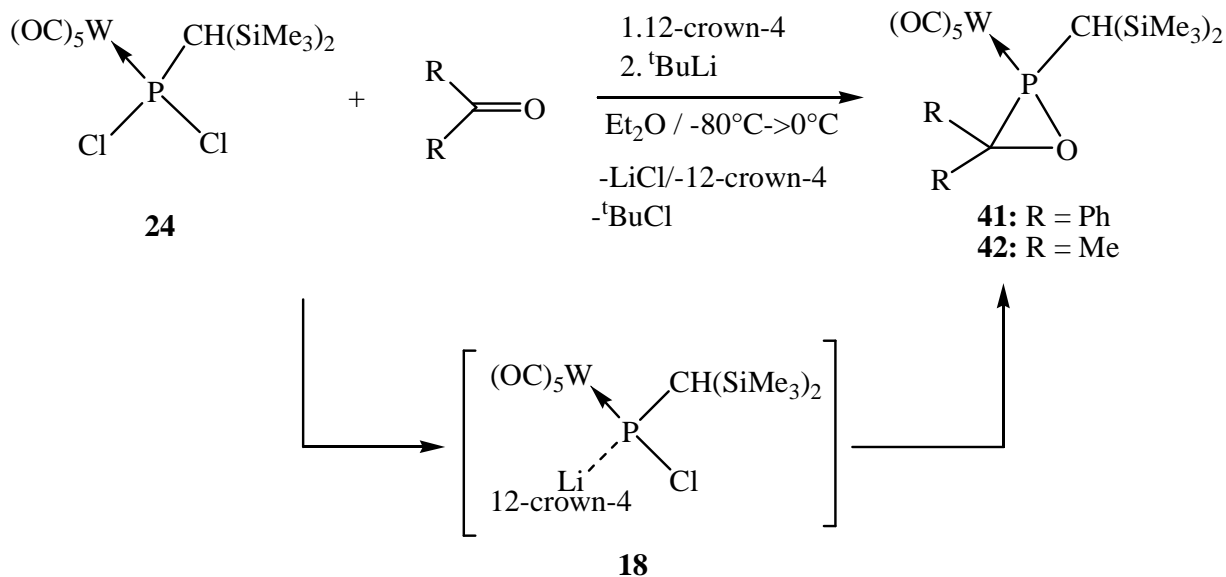
As mentioned in the introduction, Schröder was able to synthesize two different *C*-disubstituted oxaphosphirane metal complexes (complexes **11**, **12**), but before it was Ostrowski who synthesized the first *C*-disubstituted oxaphosphirane complex **41** via [2+1] cycloaddition of a transient terminal phosphinidene complex, generated from the 2*H*-azaphosphirene complex **15**, with benzophenone (Scheme 25). Unfortunately, complex **41** was obtained as by-product only (10 % after chromatography), while the major product was the benzoxaphospholane complex **40**.^[36]



Scheme 25. Synthesis of oxaphospholane complex **40** and oxaphosphirane complex **41**.^[36]

If the phosphinidenoid complex route was applied, much better yields were obtained in the synthesis of the *C*-disubstituted oxaphosphirane complex **41**. When the complex **24** and benzophenone were employed, the oxaphosphirane complex **41** was the major product (80%) in the reaction mixture, although a by-product (${}^{31}\text{P}\{{}^1\text{H}\}$ NMR: 140 ppm, ${}^1\text{J}_{\text{W},\text{P}} = 278$ Hz) was observed in small quantities. After column chromatography the oxaphosphirane complex **41** was obtained in pure form; single-crystals were grown from *n*-pentane solution and used for X-ray diffractometric studies.

Further studies showed that the phosphinidenoid complex route is especially useful in oxaphosphirane complex synthesis if ketones (or aldehydes) having a low boiling point shall be used. Thus when acetone was used, the oxaphosphirane complex **42** was obtained selectively (yield : 49%) (Scheme 26).



Scheme 26. Synthesis of oxaphosphirane complexes **41**, **42** through reaction of transiently formed Li/Cl phosphinidenoid complex **18**.

As the analytical data of complex **41**, published in the literature,^[36] were not complete, the missing data could be obtained (Table 9). The phosphorus chemical shift of complex **41** was very close to the *C*-dimethyl complex **42**, but its phosphorus-tungsten coupling constant almost 10 Hz larger. The $^2J_{P,H}$ value of the $\text{CH}(\text{SiMe}_3)_2$ proton of the complex **41** was also unusually large (16 Hz) in comparison with complex **42**. The CH_3 moieties of complex **42** showed relative $^3J_{P,H}$ values of 9.11-15.01 Hz. The $^{13}\text{C}\{^1\text{H}\}$ NMR data of both *C*-disubstituted complexes were very close to those of the *C*-monosubstituted oxaphosphirane complexes **36-39**, no influence of the substitution at the carbon atom on the ring into the $^{13}\text{C}\{^1\text{H}\}$ NMR data was found.

Table 9. Selected NMR data (CDCl_3) of the oxaphosphirane complexes **41** and **42**.

	$\delta^{31}\text{P}$ [ppm] ($^1\text{J}_{\text{W},\text{P}}$ [Hz])	$\delta(^1\text{H})$ [ppm] ($J_{\text{P},\text{H}}$ [Hz])			$\delta(^{13}\text{C}\{^1\text{H}\})$ [ppm] ($J_{\text{P},\text{C}}$ [Hz])	
		$\text{CH}(\text{SiMe}_3)_2$	R^{a}	R^{a}	$\text{CH}(\text{SiMe}_3)_2$	CR_2
41	52.2 (305.5)	1.31 (15.9)	7.6	7.6	23.9 (38.2)	69.9 (20.5)
42	55.6 (296.2)	1.25 (3.0)	1.46 (15.0)	1.63 (9.1)	30.5 (17.4)	61.1 (31.0)

^a**41** R = Ph; **42** R = Me

Suitable crystals for X-ray diffractometric studies of complexes **41** and **42** were obtained from concentrated *n*-pentane solutions (Figure 15 and 16). Surprisingly, all bond lengths and angles in the oxaphosphirane ring of complexes **42** and **41** were in the normal range of the other oxaphosphirane complexes presented in this work. One interesting feature of the molecular structure of complex **41** is that the position of the $\text{CH}(\text{SiMe}_3)_2$ proton (H14) is on the opposite side of the $\text{W}(\text{CO})_5$ group, most probably due the steric effect of the two phenyl groups attached to C1. Complex **41** crystallized as a mixture of *R/S* diastereomers in the orthorhombic (Fdd2) crystal system while the oxaphosphirane complex **42** crystallized on the monoclinic space group P 2₁/n again as a mixture of *R/S* diastereomers.

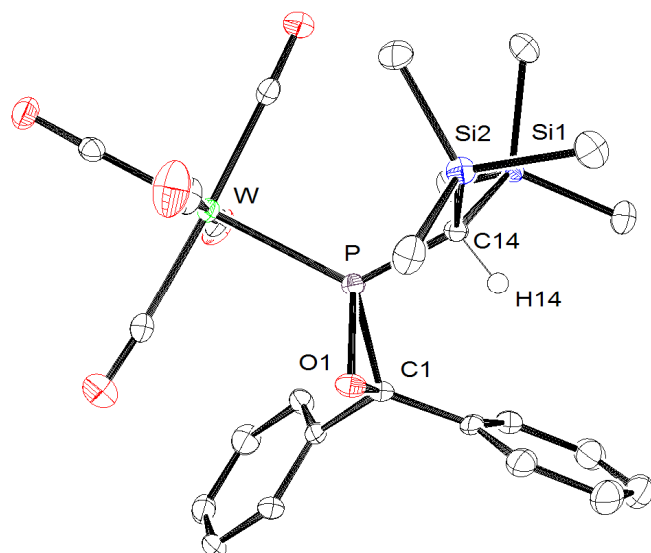


Figure 15. Molecular structure of oxaphosphirane complex **41** in the crystal (50 % probability level; hydrogen atoms except H14 are omitted for clarity). Selected bond lengths (\AA) and angles ($^{\circ}$) : W-P 2.4802(8), P-O(1) 1.671(2), C(1)-O(1) 1.485(3), P-C(1) 1.811(3), P-O(1)-

C(1) 69.74(14), C(1)-P-O(1) 50.29(12), O(1)-C(1)-P 59.96(13). Further details on structure solution and refinement can be found in the appendix under GSTR145.

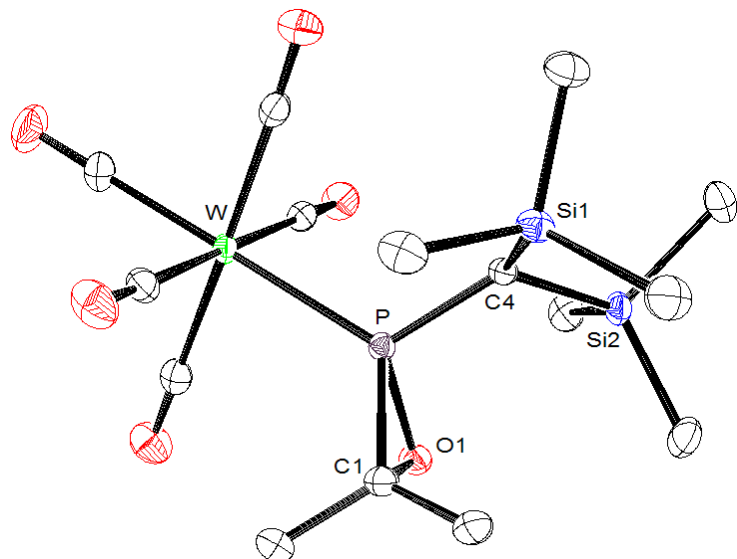
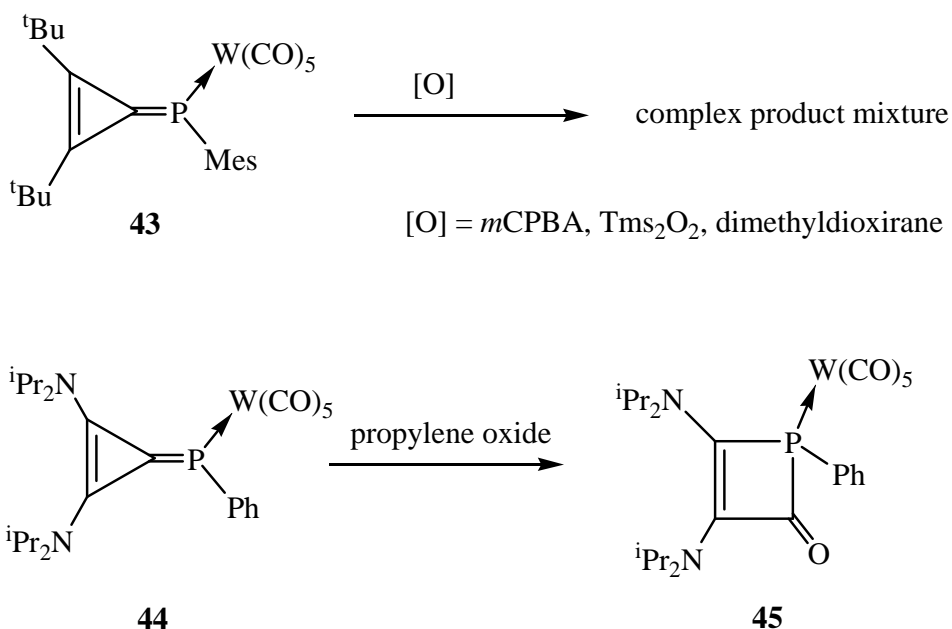


Figure 16. Molecular structure of oxaphosphirane complex **42** in the crystal (50 % probability level; hydrogen atoms are omitted for clarity). Selected bond lengths (\AA) and angles ($^{\circ}$) : W-P 2.4805(5), P-O(1) 1.6672(13), C(1)-O(1) 1.495(2), P-C(1) 1.7949(18), P-O(1)-C(1) 68.92(9), C(1)-P-O(1) 51.00(7), O(1)-C(1)-P 60.08(8). Further details on structure solution and refinement can be found in the appendix under GSTR100.

III.5 Synthesis of the first spiro-oxaphosphirane complex

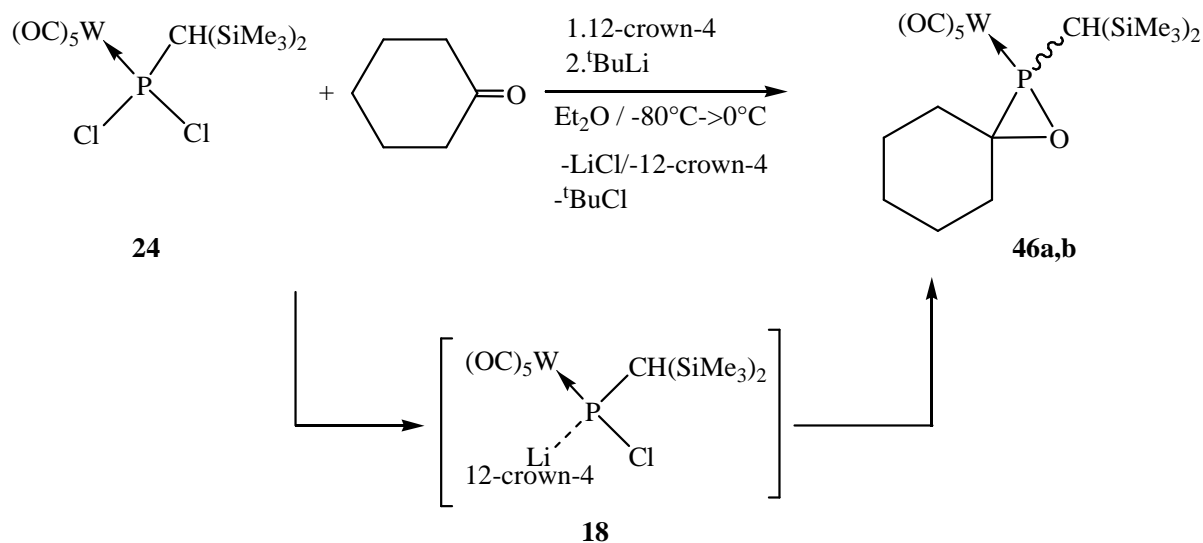
Until now, all attempts to synthesize oxaphospha-spiropentanes through oxidation of phosphaalkenes with inverse electron density, made by Schröder,^[34] and more recently performed by Bertrand and Mathey,^[58] failed. In both cases, cyclopropenyliden-type phosphine complexes (**43**, **44**) were used having a positive charge delocalized over the cyclopropenylidium unit and a negative charge localised at the phosphorus center. In case of complex **43**, Schröder could not detect an oxaphosphirane complex nor identify other products.^[34] Complex **44** yielded the phosphacyclobutenone complex **45** only,^[58] thus paralleling the oxaspiropentene-cyclobutenone conversion;^[59] the authors also performed DFT calculations on the spiro-oxaphosphirane and found it to be 46.0 kcal/mol less stable than the isomeric four-membered heterocycle.



Scheme 27. Unsuccessful attempts to synthesize spirooxaphosphirane complexes.^[34,58]

Despite these discouraging results the synthesis of a spiro-oxaphosphirane complex derivative was attempted using the phosphinidenoid complex route, which was successful

and the first examples, the complexes **46a,b**, were obtained using complex **24** and cyclohexanone (Scheme 28). The two isomeric oxaphosphirane complexes (ratio: 77:23) were isolated after column chromatography, whereby **46a** was obtained in pure form (yield 10%), while **46b** was obtained as mixture with **46a** (yellow oil, yield: 58%).



Scheme 28. Synthesis of the oxaphosphirane complexes **46a,b** through reaction of transiently formed Li/Cl phosphinidenoid complex **18** with cyclohexanone.

Both isomeric oxaphosphirane complexes **46a** and **46b** had identical tungsten-phosphorus coupling constants (295.6 Hz) but 10 ppm difference between their $^{31}\text{P}\{\text{H}\}$ NMR chemical shift values (Table 10). There was also a large difference between their $^2J_{\text{P},\text{H}}$ values of the $\text{CH}(\text{SiMe}_3)_2$ proton, the major isomer **46a** displayed a value of 15.9 Hz, while the minor isomer **46b** showed a “normal” value of 2.9 Hz compared to the other oxaphosphirane complexes reported in this work. On the other hand, there were no such significant differences in their $^{13}\text{C}\{\text{H}\}$ NMR data and in comparison with the other oxaphosphirane complexes **36-39**.

Table 10. Selected NMR data of oxaphosphirane complexes **46a,b** (CDCl_3).

	$\delta^{31}\text{P}$ [ppm] ($^1J_{\text{W},\text{P}}$ [Hz])	$\delta(^1\text{H})$ [ppm] ($J_{\text{P},\text{H}}$ [Hz])	$\delta(^{13}\text{C}\{^1\text{H}\})$ [ppm] ($J_{\text{P},\text{C}}$ [Hz])
		$\text{CH}(\text{SiMe}_3)_2$	$\text{CH}(\text{SiMe}_3)_2$
46a	47.1 (295.6)	1.20 (15.9)	23.4 (38.8) 65.7 (27.3)
46b	57.6 (295.7)	1.24 (2.9)	23.0 (38.0) 65.0 (29.6)

Noteworthy are also the differences in their ^{29}Si NMR data: complex **46a** showed a doublet at -1.50 ppm with a $^2J_{\text{P},\text{Si}}$ value of 5.8 Hz and one singlet at 4.0, while the oxaphosphirane complex **46b** showed two doublets, one at -1.30 ppm with a $^2J_{\text{P},\text{Si}}$ value of 6.5 Hz and a second one at 0.90 ppm with a $^2J_{\text{P},\text{Si}}$ of 8.2 Hz. Until now all other characterized oxaphosphirane complexes had displayed two doublets with similar values to complex **46b**.

Mass spectrometric investigations (EI, 70eV, ^{184}W) using a mixture of oxaphosphirane complexes **46a,b** showed the molecule radical cation of **46a,b** (m/z 612) followed by ring cleavage and loss of one molecule CO to form $[(\text{OC})_4\text{WPCH}(\text{SiMe}_3)_2]^{\bullet+}$ (m/z 486) and the $[(\text{SiMe}_3)^{\bullet+}]$ fragment (m/z 73) was found to be the base peak.

It is not clear if the diasteromery of complex **46a,b** is due to the possible *R* or *S* configuration at the phosphorus center or to the different conformation, boat or chair, of the cyclohexane unit. As only suitable crystals for X-ray diffractometric studies of complex **46a** (Figure 17) but not of complex **46b** were obtained from a concentrated *n*-pentane solution, this question remained open. Like most of the oxaphosphirane complexes, complex **46a** crystallized in the triclinic system P (-1). The phosphorus center displayed a *S* configuration, although the tetrahedral symmetry is much distorted. The endocyclic angle at the phosphorus was even smaller than in the other oxaphosphirane complexes reported herein. The C(1)-O(1) bond length was also clearly shorter than in the other oxaphosphirane complexes under study in this work.

The cyclohexane group adopts a chair conformation almost perpendicular, 89.66° , to the oxaphosphirane ring plane (Figure 18).

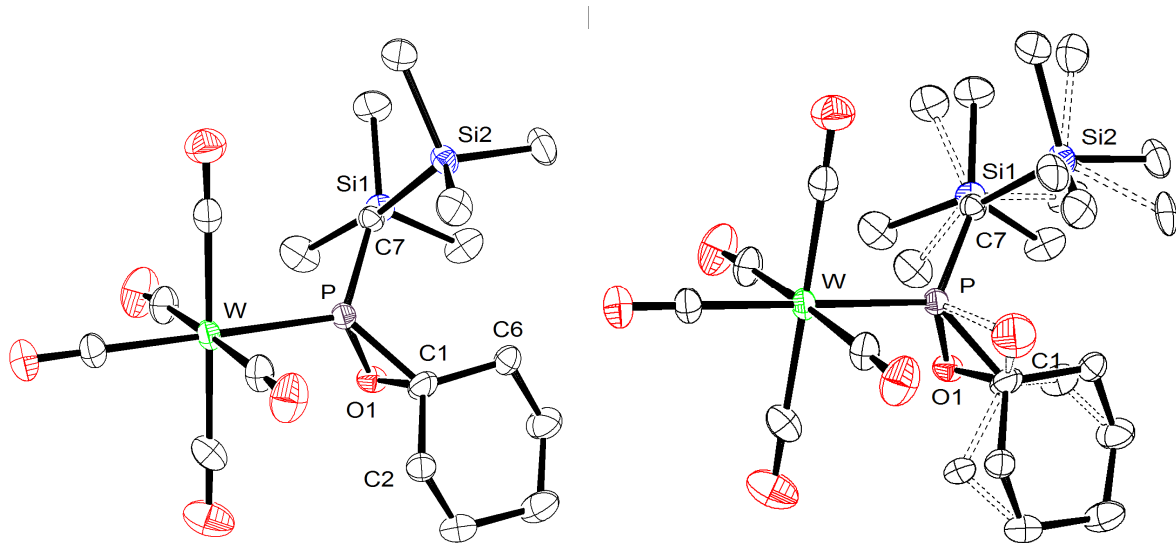


Figure 17. Molecular structure of oxaphosphirane complex **46a** in the crystal (50 % probability level; 60 % main orientation on phenyl group and oxaphosphirane ring; only the crystallographic data of the main structure are given while the second disordered structure is mainly the same; hydrogen atoms are omitted for clarity; reduced form on the left side). Selected bond lengths (\AA) and angles ($^\circ$): W-P 2.4740(7), P-O(1) 1.676(3), C(1)-O(1) 1.416(4), P-C(1) 1.778(3), P-O(1)-C(1) 69.59(17), C(1)-P-O(1) 48.31(13), O(1)-C(1)-P 62.10(15). Further details on structure solution and refinement can be found in the appendix under GSTR138.

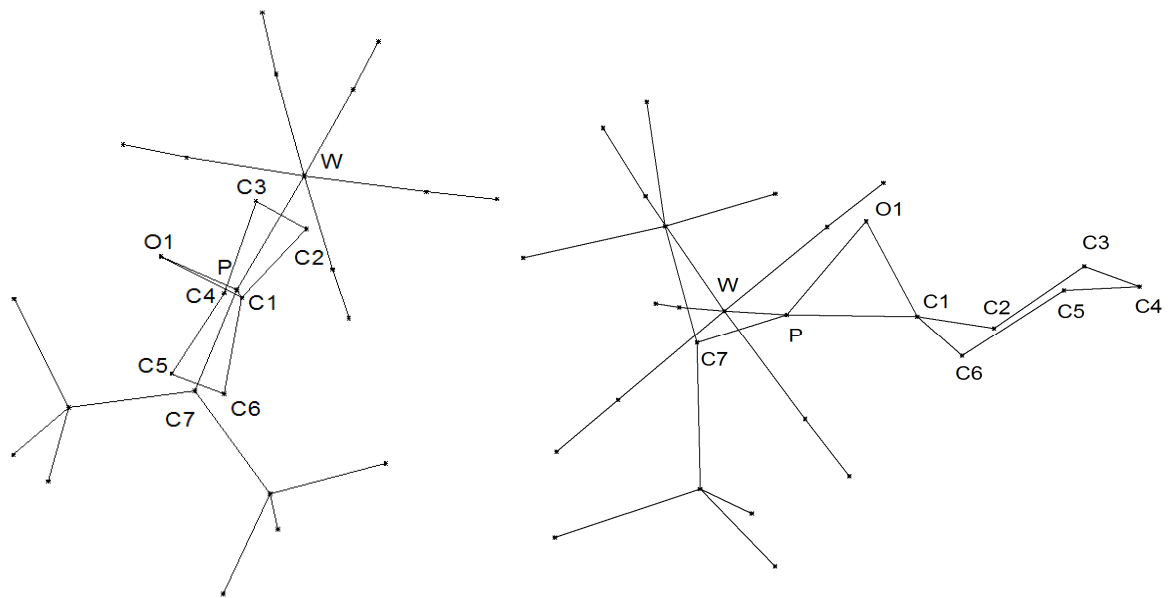
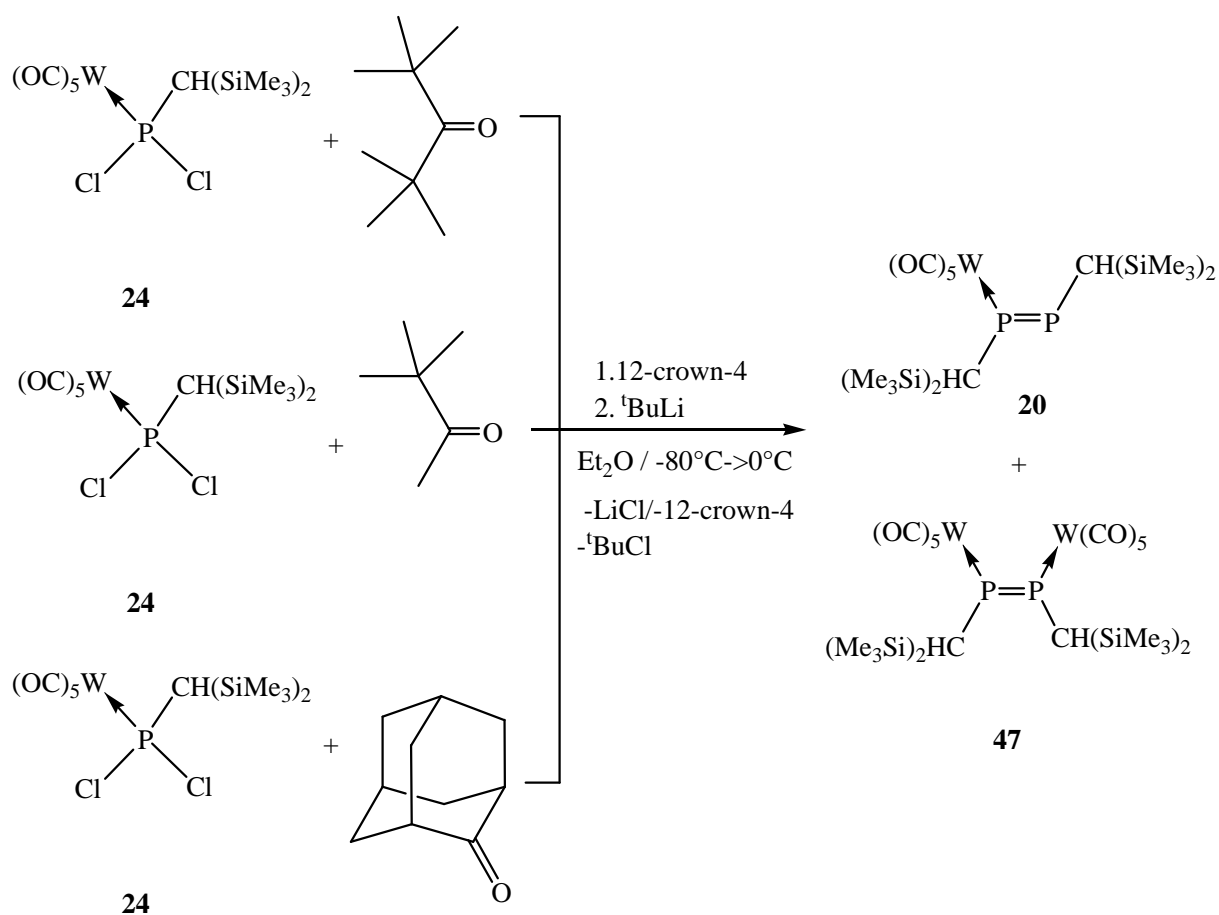


Figure 18. View of the reduced and simplified molecular structure of complex **46a** along the P-C1 axis (left side) and from the oxaphosphirane plane (right side).

III.6 Scope and limitations of the phosphinidenoid complex method in the synthesis of oxaphosphirane complexes

One of the principal advantages of the transient formed Li/Cl phosphinidenoid complex route is the versatility in the election of the trapping agent (aldehydes or ketones), although some steric limitations were found, *e.g.*, if very bulky ketones, like 2-adamantanone (Figure 19), 2,2,4,4-tetramethylpentan-3-one or even 3,3-dimethylbutan-2-one were used, no oxaphosphirane complexes were observed by ^{31}P NMR spectroscopy but the formation of the diphosphene complex **20**^[43] and **47**^[60] (Scheme 29); the latter were always formed if the phosphinidenoid complex **18** was warmed up in the absence of an effective trapping reagent.^[60]



Scheme 29. Reaction of complex **24** with very bulky ketones.

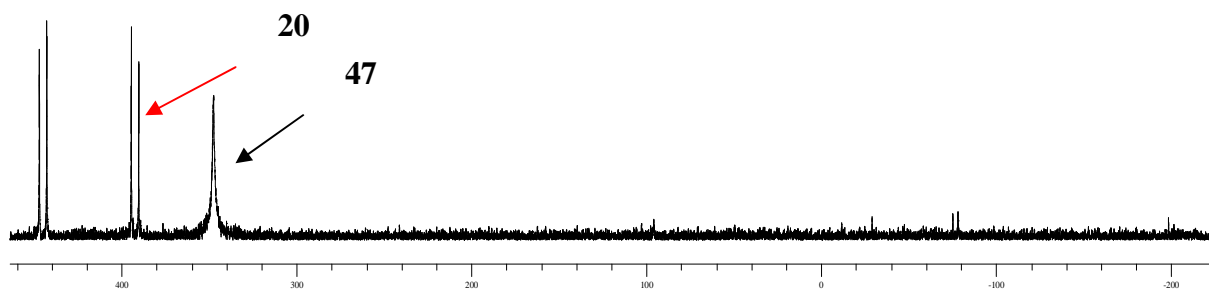
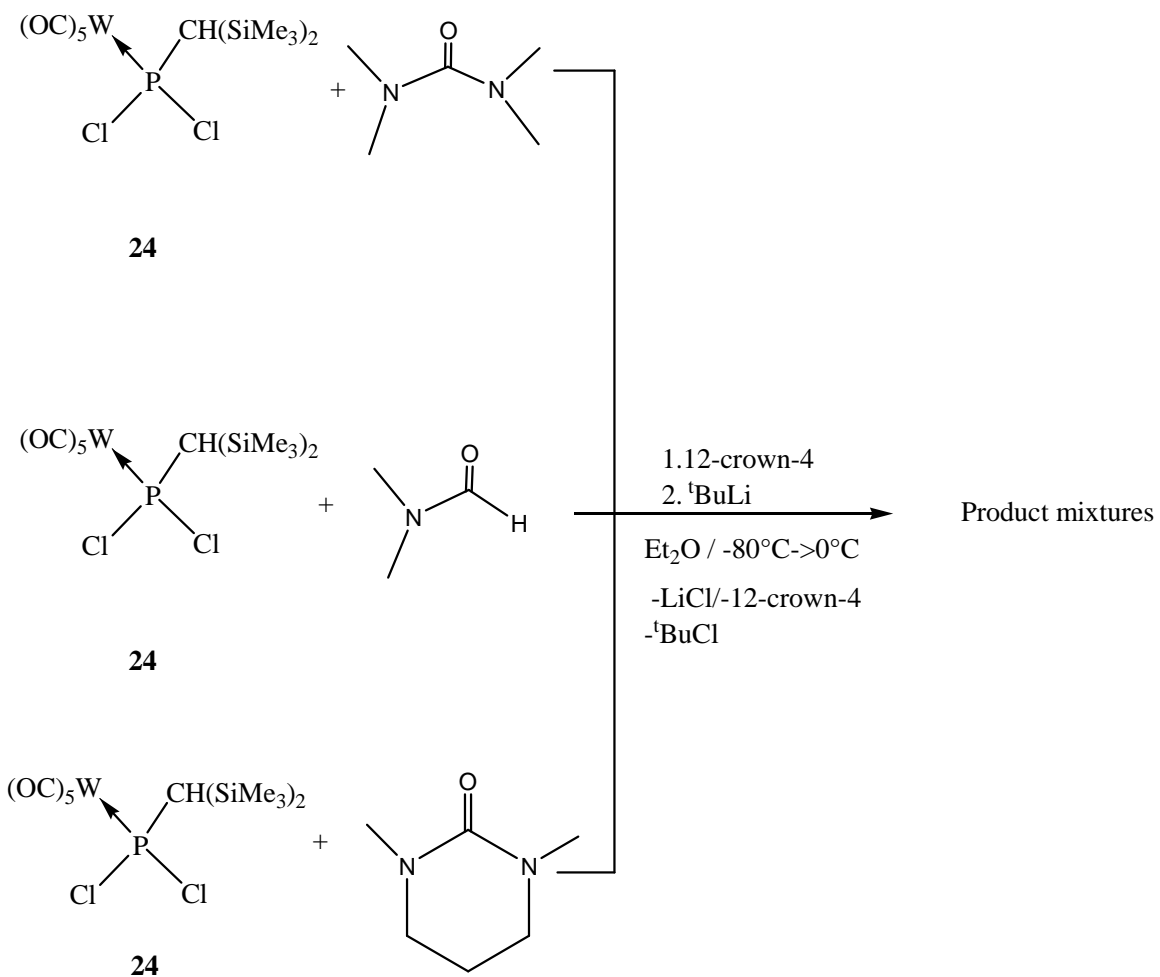


Figure 19. $^{31}\text{P}\{\text{H}\}$ NMR spectra of the reaction of complex **24** with 2-adamantanone.

Also if *N*-functionalized aldehydes or ketones (dimethylformamide, tetramethylurea or tetrahydro-1,3-dimethylpyrimidin-2(*IH*)-one (Scheme 30)) were used as trapping agents, the formation of the desired oxaphosphirane complexes could not be observed. If dimethylformamide was used as trapping agent, the results were not reproducible: the $^{31}\text{P}\{\text{H}\}$ NMR data of the reaction mixtures displayed a signal at -23.0 ppm with a $^1J_{\text{W},\text{P}} = 312$ Hz, which appeared in all spectra but in a different ratio. The same resonance was also found in a very unselective reaction with dimethylurea.



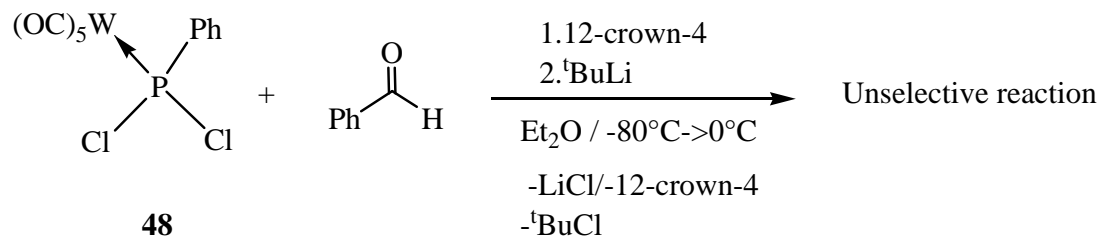
Scheme 30. Attempts to synthesize *N*-functionalized oxaphosphirane complexes.

If tetrahydro-1,3-dimethylpyrimidin-2-one was employed the $^{31}\text{P}\{\text{H}\}$ NMR spectra (r.t.) showed a mixture of unidentified products in the range of 20 to 50 ppm, showing a broad signals and one sharp signal at 10 ppm with $^1J_{\text{W},\text{P}} = 233$ Hz. $^{31}\text{P}\{\text{H}\}$ NMR monitoring at low temperature revealed only the formation of the phosphinidenoid complex **18** before it then reacted to yield non-identified products.

So far this work was focused on the synthesis of *P*-bis(trimethylsilyl)methyl substituted oxaphosphirane complexes, which together with the *P*-Cp* and *P*-^tBu and *P*-Mes-substituted complex derivatives were the only substituents that had enabled the isolation of the targeted compounds. Therefore, a part of this study was devoted to establish Li/Cl phosphinidenoid

complexes with less bulky substituents at phosphorus; preliminary results will be reported hereafter.

First, $[\text{W}(\text{CO})_5(\text{PhPCl}_2)]^{[61]}$ (**48**) was chosen as example of an easy-to-access starting material, which was synthesized via coordination of the commercially available dichloro(phenyl)phosphane. The chlorine/lithium exchange reaction in complex **48** followed the same protocol as before and yielded, in the case of benzaldehyde, a mixture of products as revealed through the $^{31}\text{P}\{^1\text{H}\}$ NMR spectra (Figure 20) and which showed resonances between 150 and -150 ppm; none of them could be assigned to a corresponding *P*-Ph substituted oxaphosphirane complex



Scheme 31. Attempt to synthesize a *P*-phenyl substituted oxaphosphirane complex.

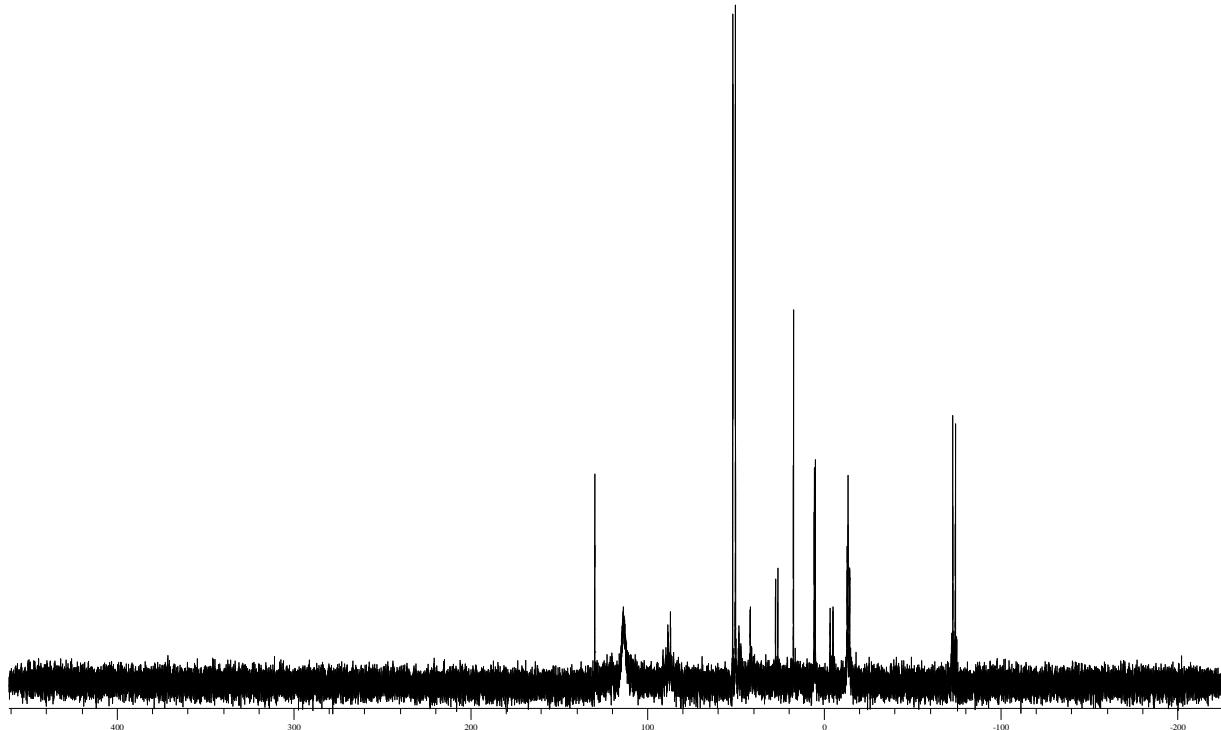
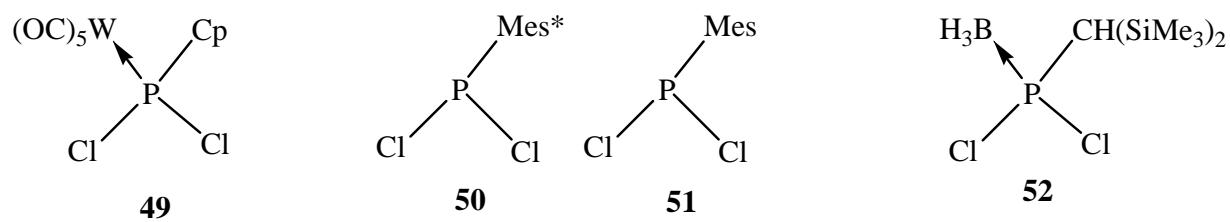


Figure 20. $^{31}\text{P}\{\text{H}\}$ NMR spectra of the reaction solution of complex **48** with aldehyde.

In order to examine if the less bulky *P*-Cp complex **49** could be used, instead of the *P*-Cp* complex, its synthesis was attempted via the reaction of CpPCl₂^[62] with [W(CO)₅(thf)] but its isolation was not achieved because of partial decomposition during the column chromatography.



Scheme 32. Attempted new dichlorophosphane complexes.

As Schröder had already demonstrated that *P*-Mes substituted oxaphosphirane complexes could be synthesized using the “oxidation method”, it seemed likely to attempt the synthesis

via the "phosphinidenoid complex route" employing either a Mes (1,3,5-trimethylbenzyl) or Mes* (1,3,5-tri-*tert*-butylbenzyl) as substituent at phosphorus. Unfortunately, the corresponding dichloro(aryl)phosphanes **51**^[63] and **50**^[64] did not react with [W(CO)₅(thf)], and thus no reactions could be performed.

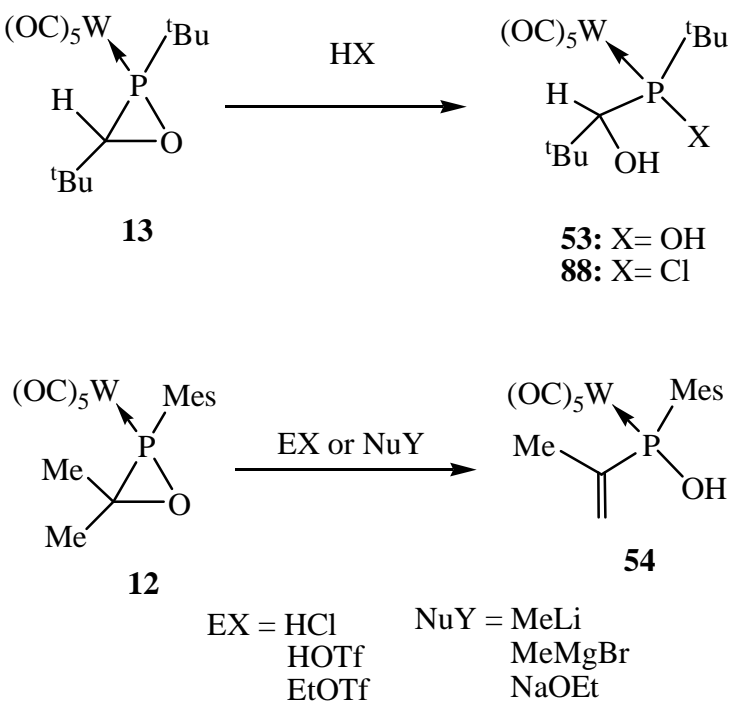
As many phosphane derivatives form adducts with various boranes,^[65] the complexation of the phosphane **23** with BH₃·THF was studied. Furthermore, recent studies had revealed that some phosphine-borane adducts were stable towards lithiation conditions.^[66] Therefore, it was assumed that such adducts might be applicable to the synthesis of oxaphosphirane borane complexes using the "phosphinidenoid complex route". Together with the perspective of a facilitated decomplexation of such oxaphosphirane borane complexes to yield non-ligated oxaphosphiranes was very attractive. Attempts to synthesized the phosphane-borane complex **52** (Scheme 32) were only partly successful as decomplexation occurred during evaporation of the solvent and the complex could not be isolated in pure form.

Lithiation under standart conditions of the phosphane-borane complex **52** in the presence of aldehyde in order to synthesized oxaphosphirane borane complexes led only to very unselective and not reproducible reactions. The spectra showed different resonances at low field (between -77 and -150 ppm with $J_{P,H}$ values around 180 Hz) and at high field (between 160 and 200 ppm).

Complexation of phosphane **50** and **51** using BH₃·THF were, as in case of [W(CO)₅(thf)], not successful. In case of dichloro(phenyl)phosphane, partially complexation occurred in toluene (³¹P NMR: 149.88 ppm, $^1J_{P,B} = 22.89$ Hz) but the borane complex could not be characterized because of the decomplexation while removing the solvent to give the free phosphane.

IV. Investigations on the reactivity of *P*-bis(trimethylsilyl)methyl-substituted- $\sigma^3\lambda^3$ -oxaphosphirane complexes

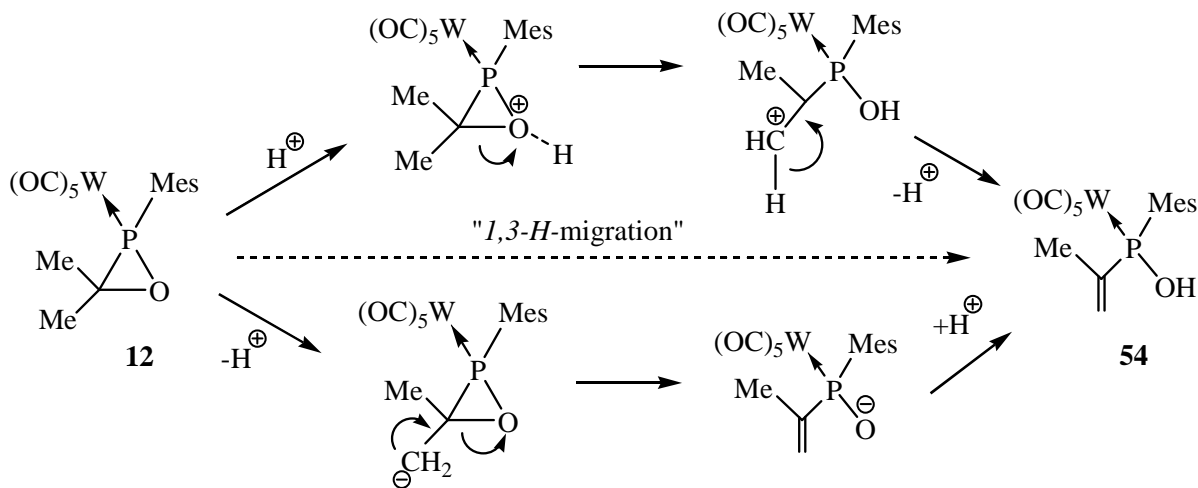
Schröder was the first to report on the chemistry of isolated $\sigma^3\lambda^3$ -oxaphosphirane complexes **VII**, whereby he had exclusively investigated the reactivity of the oxaphosphirane complexes **12** and **13** towards few electrophiles and nucleophiles (Scheme 33).^[34] Apparently, the “oxidation methodology” did not allow a broader study of oxaphosphirane complexes as stated by himself.^[33]



Scheme 33. Reactivity studies on the oxaphosphiranes complexes **12** and **13**, performed by Schröder.^[34]

He studied the ring-opening behavior of the oxaphosphirane complex **13** towards water and HCl and observed that the phosphane complexes **53** and **88** were formed through P-O bond cleavage. He proposed that the formation of these products should occur through protonation of the oxaphosphirane ring at the oxygen atom and subsequent nucleophilic attack. On the

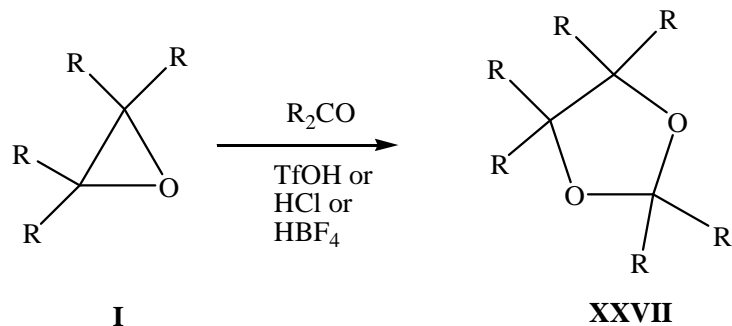
other hand and surprisingly, complex **12** didn't show any reactivity towards water and strong electrophiles such as TfOH, HCl, and EtOTf, but did react with strong nucleophiles such as MeLi, MeMgBr, and NaOEt, whereby C-O bond cleavage and 1,3-proton shift occurred to give complex **54** as the only isolated product in all cases (Scheme 34). In the proposed mechanism,^[34] the last protonation step was due to the work-up process, *i.e.*, column chromatography.



Scheme 34. Mechanism proposed by Schröder for the formation of complex **54** from oxaphosphirane complex **12**.^[34]

IV.1 Acid-induced ring expansion reactions of C-phenyl-oxaphosphirane complexes

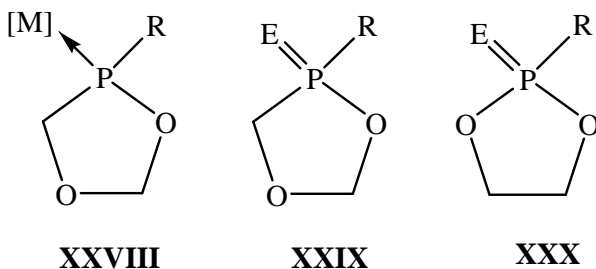
As described in the first chapter, a major aim of this work was to investigate the chemical behavior of oxaphosphirane complexes in comparison to oxiranes. It is well known that oxiranes can undergo ring expansion reactions in the presence of π -systems induced by different Brønsted acids (Scheme 35).^[67-69] If ketones or aldehydes were used as π -systems, dioxolanes **XXVII** were formed as result of a ring expansion reaction (Scheme 35). In case of an acid-induced ring expansion reaction of the $\sigma^3\lambda^3$ -oxaphosphirane complexes **VII** this would result in the formation of 1,3,4-dioxaphospholane complexes.



Scheme 35. Examples of acid-induced ring expansion reactions using $TfOH$,^[67] HCl ^[68] or HBF_4 ^[69] as Brønsted acids.

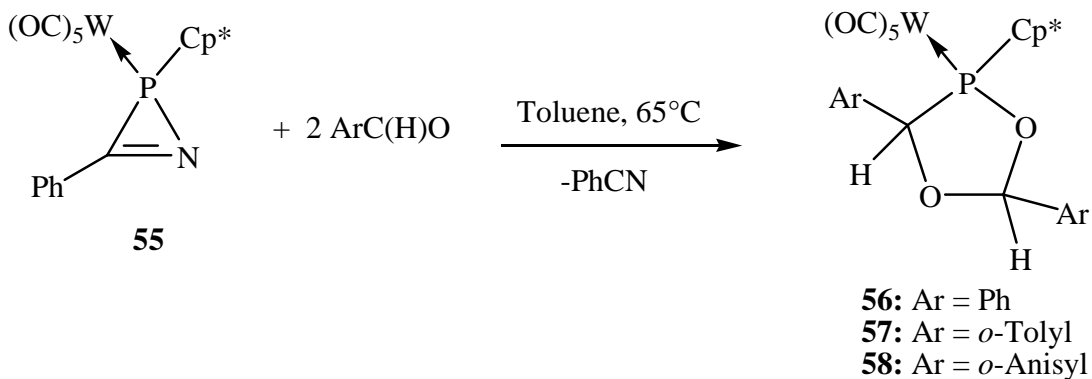
IV.1.1 Synthesis of 1,3,4-dioxaphospholane complexes from C-phenyl oxaphosphirane complexes

Until now only three examples of $1,3,4-\sigma^3\lambda^3$ -dioxaphospholane complexes **XXVIII** are known,^[51,70] and there is also not much literature about their P^V analogues **XXIX**,^[29,71] albeit the interest in **XXIX** as possible precursor for polymers. The 1,3,2-dioxaphospholanes **XXX** (Scheme 36) have attracted a great deal of interest over the years because of their applicability as precursors for polymeric and/or copolymeric materials,^[72] some of which are fire-resistant and some biodegradable.^[73] Consequently, several valuable synthetic methods have been developed for their synthesis.



Scheme 36. Dioxaphospholanes **XXIX**, **XXX** and complexes thereof **XXVIII**; R denotes ubiquitous organic substituents; E denotes O or lone pair; [M] denotes a $W(CO)_5$ group.

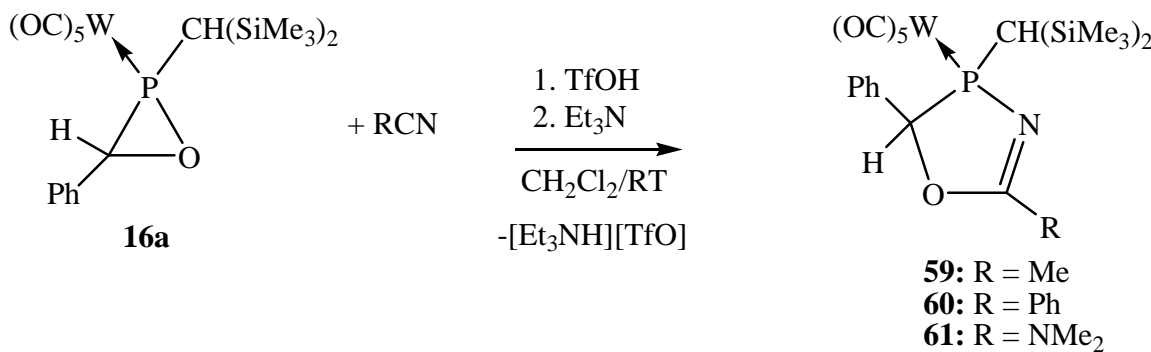
The synthesis of $1,3,4-\sigma^3\lambda^3$ -dioxaphospholane complexes appears to be more challenging as one might think. The only three $1,3,4-\sigma^3\lambda^3$ -dioxaphospholane complexes known until now, complexes **56-58**^[51, 70] were synthesized through thermolysis of the P -Cp*-2H-azaphosphirene complex **55** in the presence of aldehydes (Scheme 37).^[74] When the same reaction conditions were applied to a mixture of the 2H-azaphosphirene complex **15** and benzaldehyde, the oxaphosphirane complex **16a** was obtained.^[36]



Scheme 37. Synthesis of the 1,3,4 - $\sigma^3\lambda^3$ dioxaphospholane complexes **56-58** via thermolysis of 2*H*-azaphosphirene complex **51**.^[51,70]

First attempts of Bode to synthesize 1,3,4 - $\sigma^3\lambda^3$ -dioxaphospholane complexes via thermolysis reactions starting from *P*-Cp*-oxaphosphirane complexes in the presence of aldehydes failed and P-C cage complexes were formed, instead, via C-O bond cleavage.^[75] Surprisingly, own studies on thermal ring-opening reactions of oxaphosphirane complex **16a** failed, too, as **16a** didn't react under the same conditions.

Shortly afterwards, I had developed a new method for the ring expansion reaction of oxaphosphirane complex **16a**, which were the first examples of Brønsted acid-induced P-O bond selective ring expansion reactions of a transition metal coordinated $\sigma^3\lambda^3$ -oxaphosphirane complex.^[76] This method provided high yield access to 4,5-dihydro-1,3,4-oxazaphosphole complexes **59-61** from complex **16a** using trifluoromethane sulfonic acid in the presence of different carbonitriles, followed by treatment with triethylamine (Scheme 38).



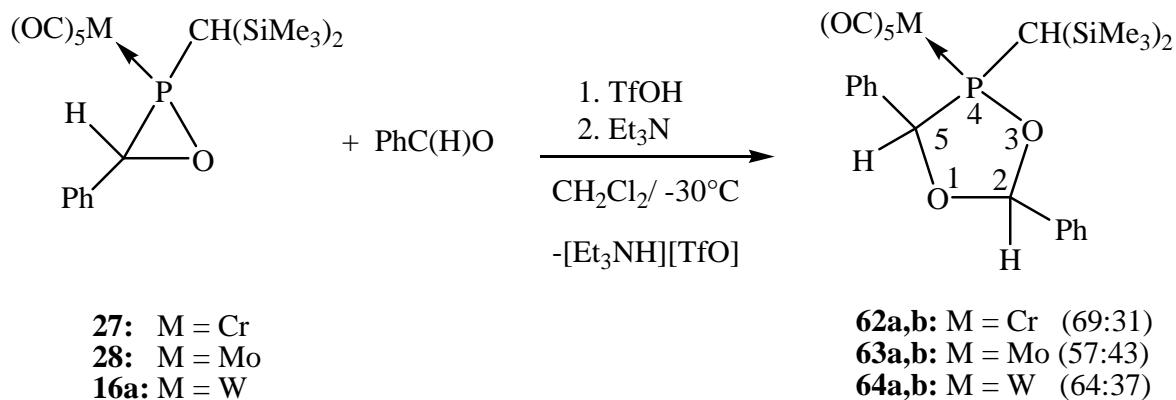
Scheme 38. Brønsted acid-induced ring expansion reactions of oxaphosphirane complex **16a**.^[76]

Because of its selectivity, under mild conditions, this method was very promising for P-heterocyclic synthesis, in general, and for the synthesis of 1,3,4- $\sigma^3\lambda^3$ -dioxaphospholane complexes **XXVIII**, especially.

First attempts to synthesize 1,3,4- $\sigma^3\lambda^3$ -dioxaphospholane complexes using oxaphosphirane complex **16a**, benzaldehyde and one eq. of TfOH and, subsequently, NEt₃ at ambient temperature were not successful: the desired product was found only as a minor product, while the major product showed a ³¹P{¹H} NMR resonance at 49 ppm without tungsten satellites, and which couldn't be isolated because decomposition during column chromatography. Upon lowering the reaction temperature to -30°C, the reaction became more selective and the 1,3,4- $\sigma^3\lambda^3$ -dioxaphospholane complexes were found as the major products, although the formation of the by-product (about 30%) having no tungsten satellites was also observed. The reactions could not be performed below -30°C, to increase the selectivity of the reaction, because of the low solubility of the acid in dichloromethane at very low temperatures. The formation of this compound and investigation on the reaction mechanism will be discussed later in chapter IV.2.1.

IV.1.1.1 Synthesis of 3,5-diphenyl-1,3,4-dioxaphospholane complexes

The first aspect to be investigated was if there is any metal dependency on the product formation. Therefore, the oxaphosphirane complexes **16a**, **29**, **30** were reacted with benzaldehyde and TfOH in CH₂Cl₂ at -30°C and, subsequently, with NEt₃, which yielded the 1,3,4-dioxaphospholane complexes **62-64a,b** as a mixture of two diastereomers (see Scheme 39 for ratios); the complexes were isolated after column chromatography in moderate yields (25-26 %).



Scheme 39. Synthesis of 1,3,4-dioxaphospholane complexes **62-64a,b**.

As expected the ³¹P NMR data of the complexes **62-64a,b** showed the influence of the metal fragment as the complexes **62a,b** (M = Cr) are more deshielded than complexes **63a,b** and **64a,b** (Table 11). In each case, there is only a small difference of 0.2-0.3 ppm between both diastereomers **a,b** and in the case of the complexes **62a,b** both showed the same tungsten-phosphorus coupling constant of 281 Hz. No correlation could be found between the ²J_{P,H} values of the CH(SiMe₃)₂ moiety and the ³¹P{¹H} NMR resonance of both diastereomers in solution.

The C⁵-H protons (Scheme 39, numbering according to the Hantzsch-Widman system^[12]) showed a ¹H NMR resonance in the narrow range of 5.32-5.80 ppm with a ²⁺⁵J_{P,H} value between 14.3 and 20 Hz. The C²-H protons were also found very close to each other 6.09-6.72 ppm. Whereas complexes **62-63a,b** did not show couplings of the C²-H with the phosphorus, a small coupling of 4.1 and 1.8 Hz was determined for complexes **64a,b**. The ¹³C{¹H} NMR resonances were all found in the expected range and were also very similar for all metal complexes.^[70] The values of the ²⁺⁴J_{P,C} constant of the C⁵-centres are around 5 Hz smaller than those of C², except for complexes **64a,b**, where the J_{P,C} values were very similar for both complexes.

Table 11. Selected NMR data (CDCl₃) of 1,3,4-dioxaphospholane complexes **62-64a,b**.

	$\delta^{31}\text{P}$ [ppm] (¹ J _{W,P} [Hz])	$\delta(^1\text{H})$ [ppm] ($J_{\text{P},\text{H}}$ [Hz])			$\delta(^{13}\text{C}\{^1\text{H}\})$ [ppm] ($J_{\text{P},\text{C}}$ [Hz])		
		CH(SiMe ₃) ₂	C ⁵ -H	C ² -H	CH(SiMe ₃) ₂	C ⁵	C ²
62a	180.4	1.65 (20.0)	5.64 (23.8)	6.09	22.0 (36.2)	88.4 (5.2)	102.6 (10.3)
62b	181.2	2.00 (19.5)	5.39 (20.2)	6.68	25.1 (36.2)	91.6 (2.6)	102.5 (15.5)
63a	154.4	1.92 (17.9)	5.32 (15.5)	6.72	20.3 (36.8)	88.7 (5.8)	102.8 (10.4)
63b	154.7	1.58 (18.7)	5.70 (20.9)	6.08	21.9 (36.2)	91.9 (2.6)	101.7 (8.4)
64a	130.6 (281.0)	1.80 (19.9)	5.40 (14.3)	6.50 (4.1)	22.5 (29.4)	93.0 (7.8)	101.8 (8.1)
64b	130.8 (281.0)	2.10 (19.0)	5.80 (19.4)	6.10 (1.8)	20.6 (29.8)	89.5 (11.3)	103.2 (10.3)

The mass spectrometric experiments (EI, ¹⁸⁴W for complex **64a,b**, ⁹⁸Mo for complex **63a,b** and ⁵²Cr for complex **62a,b**) on the 1,3,4-dioxaphospholane complexes **62-64a,b** showed the preference of the molecule radical cations (m/z 594 for complexes **62a,b**, m/z 640 for complexes **63a,b** and m/z 726 for complexes **64a,b**) to extrude PhC(H)O to give m/z 488 for complexes **62a,b**, m/z 534 for complexes **63a,b** and m/z 620 for complexes **64a,b**, before loosing CO.

The IR spectra of complexes **62-64a,b** showed one strong absorption band in the carbonyl range ($\sim 1930\text{-}1940 \text{ cm}^{-1}$) which was very broad, most probably as result of the overlapping of bands, and another weak band at approximately 2070 cm^{-1} .

The UV/visible spectra of the complexes **62-64a,b** showed one λ_{\max} at around 235 nm and shoulders that appear at λ_{\max} values around 300 nm due to metal- ligand charge-transfer transitions.^[55]

Suitable crystals for X-ray diffractometry were obtained from concentrated *n*-pentane solutions (Figure 21). Both complexes crystallized in the same crystal system, monoclinic, but in different space groups P 2₁/n for complex **62a** and P 2₁/c for complex **64a**.

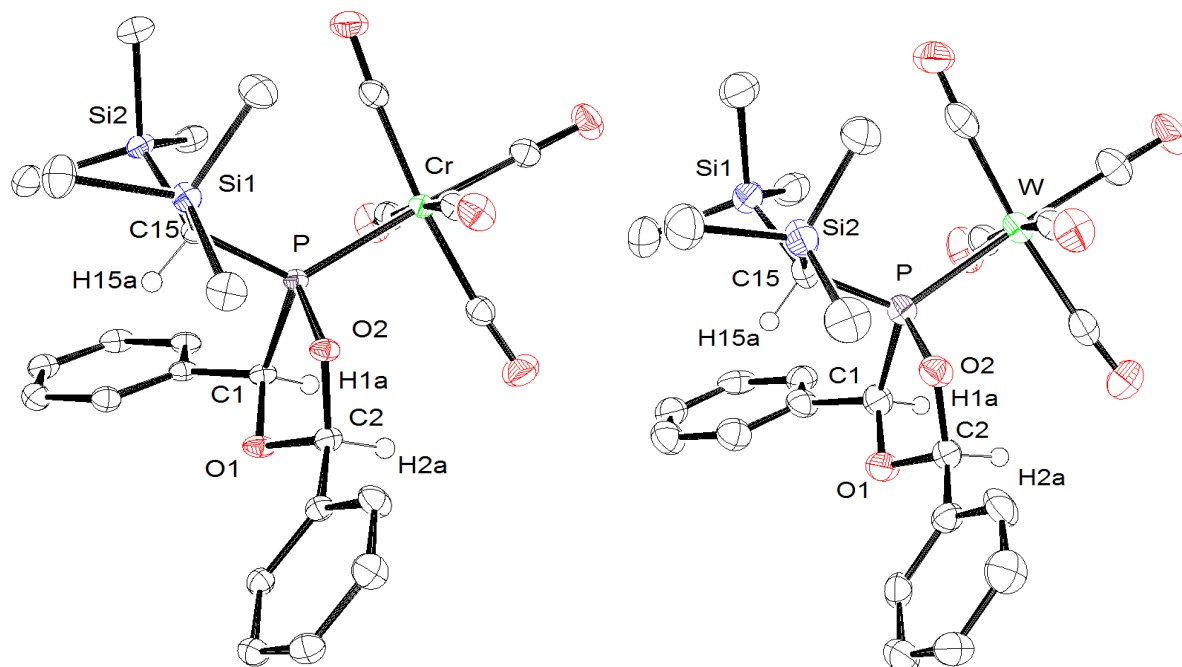


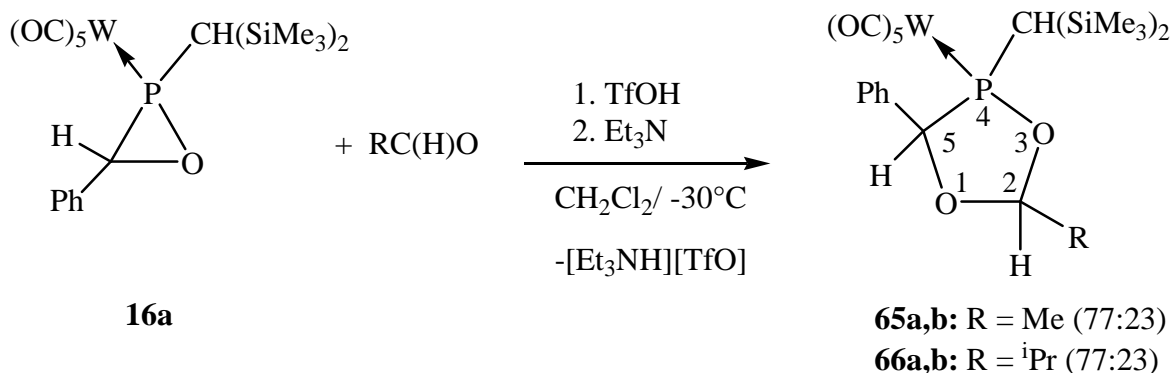
Figure 21. Molecular structures of 1,3,4-dioxaphospholane complexes **62a** (left side) and **64a** (right side) in the crystal (50 % probability level; hydrogen atoms except H1, H2 and H15a are omitted for clarity). Selected bond lengths (\AA) and angles ($^\circ$) of 1,3,4-dioxaphospholane complexes **62a**: Cr-P 2.3673(4), P-O(2) 1.6536(8), C(1)-O(1) 1.4295(13), P-C(1) 1.9239(12), P-C(15) 1.8208(12), O(1)-C(2) 1.3988(14), O(2)-C(2) 1.4377(14), C(1)-P-O(2) 90.05(4), P-

C(1)-O(1) 102.39(7), C(1)-O(1)-C(2) 108.29(9), O(2)-C(2)-O(1) 106.84(9), P-O(2)-C(2) 111.74(7), C(1)-P-O(2)-C(2) 12.52; Selected bond lengths (\AA) and angles ($^\circ$) of 1,3,4-dioxaphospholane complexes **64a**: W-P 2.5107(19), P-O(2) 1.656(4), C(1)-O(1) 1.433(7), P-C(1) 1.920(7), P-C(15) 1.835(7), O(1)-C(2) 1.396(7), O(2)-C(2) 1.445(7), C(1)-P-O(2) 90.3(3), P-C(1)-O(1) 102.1(4), C(1)-O(1)-C(2) 108.9(5), O(2)-C(2)-O(1) 106.2(5), P-O(2)-C(2) 111.5(4), C(1)-P-O(2)-C(2) 13.41. Further details on structure solution and refinement can be found in the appendix under GSTR099 (complex **62a**) and GSTR137 (complex **64a**).

The structures of both 1,3,4-dioxaphospholane complexes **62**, **64a** showed a non-planar dioxaphospholane ring having an envelope conformation as central unit with two phenyl groups and the $\text{CH}(\text{SiMe}_3)_2$ group adopting positions at the same side of the five-membered ring; in both complexes O(1) points 0.53 \AA out of the best plane (C(1)-P-O(2)-C(2)). Probably due to steric effects, the $\text{CH}(\text{SiMe}_3)_2$ groups adopt a relative orientation towards the $\text{M}(\text{CO})_5$ moiety such as that the CH group is facing the two phenyl groups, which is in marked contrast to the situation found in the starting materials, complexes **29**, **16a**. The P-C(1) distances are unusually long for a P-Csp³ single bond,^[77] but similar values had been observed before in related heterocyclic complexes.^[78] The $\text{M}(\text{CO})_5$ moieties have a distorted octahedral geometry, and the *cis*-CO are slightly bend to the *trans*-CO (C(25)-W-C(26) 86 $^\circ$) due to the bulkiness of the dioxaphospholane ligand.

IV.1.1.2 Synthesis of 2-alkyl-1,3,4-dioxaphospholane complexes

As the investigation of Bode had revealed that only 2-aryl-substituted 1,3,4-dioxaphospholane complexes **56-58** are accessible via the thermolysis method, and because of the necessity of a high reaction temperature other more volatile aldehydes such as alkyl derivatives were not examined, it seemed to be attractive to test the new Brønsted acid-induced ring expansion methodology. The reaction of oxaphosphirane complex **16a** with acetaldehyde and isobutyraldehyde yielded 2-alkyl-substituted 1,3,4-dioxaphospholane complexes **65a,b** (yield 23 %) and complexes **66a,b** (yield 21 %) under standard conditions (Scheme 40). Again the formation of by-products was observed, which did not reveal the existence of *P*-bound pentacarbonyltungsten moieties, and, interestingly, the same diasteroisomer ratio (77:23) was found for both complexes **65-66a,b**.



Scheme 40. Synthesis of 2-alkyl substituted 1,3,4- $\sigma^3\lambda^3$ -dioxaphospholane complexes **65-66a,b**.

The new complexes showed $^{31}\text{P}\{\text{H}\}$ NMR resonances around 130 ppm with almost the same $^1J_{\text{W},\text{P}}$ coupling constant of about 280 Hz (Table 12). The $\text{CH}(\text{SiMe}_3)_2$ and the $\text{C}^2\text{-H}$ proton showed similar $J_{\text{P},\text{H}}$ values. An interesting structural feature was that the major isomers (**65**, **66a**) had the largest $^2J_{\text{P},\text{H}}$ values between the $\text{CH}(\text{SiMe}_3)_2$ and the phosphorus. The $\text{C}^2\text{-H}$

protons showed again a smaller $^{3+4}J_{P,H}$ values (1-2 Hz) than the C⁵-H protons. In case of their $^{13}\text{C}\{\text{H}\}$ NMR data a difference of almost 10 Hz in the $^1J_{P,C}$ values of the CH(SiMe₃)₂ carbon between both diastereomers was observed, which was not the case for the 2-phenyl-1,3,4-dioxaphospholane complexes **64a,b**.

Table 12. Selected NMR data (CDCl₃) of 1,3,4- dioxaphospholane complexes **65-66a,b**.

	$\delta^{31}\text{P}$ [ppm] ($^1J_{W,P}$ [Hz])	$\delta^{(\text{H})}$ [ppm] ($J_{P,\text{H}}$ [Hz])			$\delta^{(13}\text{C}\{\text{H}\})$ [ppm] ($J_{P,C}$ [Hz])		
		CH(SiMe ₃) ₂	C ⁵ -H	C ² -H	CH(SiMe ₃) ₂	C ⁵	C ²
65a	132.0 (279.7)	1.80 (19.1)	5.45 (19.7)	5.13 (1.7)	20.5 (20.6)	92.0 (8.4)	99.0 (9.0)
65b	130.0 (279.7)	1.81 (13.0)	5.45 (14.3)	5.80 (2.1)	21.0 (29.7)	101.0 (10.3)	87.5 (11.7)
66a	131.0 (281.0)	1.60 (19.8)	5.45 (20.4)	5.00 (1.5)	20.5 (20.0)	108.0 (8.4)	110.1 (11.6)
66b	129.5 (279.7)	1.80 (11.9)	5.20 (14.4)	5.25 (1.0)	19.5 (30.3)	93.0 (8.4)	110.4 (11.6)

Mass spectrometric studies (EI, 70 eV, ^{184}W) of complexes **65-66a,b** showed the preference of the molecule radical cations (m/z 664 for complexes **65a,b** and m/z 692 for complexes **66a,b**) to extrude MeC(H)O for complexes **65a,b**, and $^i\text{PrC(H)O}$ for complexes **66a,b** to give m/z 620, following by loss of benzaldehyde and CO thus forming the basis peak m/z 486, which was assigned to $[(\text{W}(\text{CO})_4\text{PCH}(\text{SiMe}_3)_2)^{•+}]$ in both cases.

IR spectroscopic studies of complexes **65-66a,b** showed the typical bands due to the W(CO)₅ fragment, one strong bond at approximately 1945 cm⁻¹ and a medium band at approximately 2070 cm⁻¹. The UV/Vis spectra also showed the typical bands due to metal-ligand charge-transfer transitions groups at 235 and 300 nm.

Suitable crystals for X-ray diffractometry of complex **66a** were, again, obtained from a concentrated *n*-pentane solution (Figure 22); it also crystallized in the monoclinic crystal

system, P 2₁/c like complex **64a**. The dioxaphospholane ring also showed a non-planar situation of an envelope conformation, where the O(1) atom points out 0.724 Å of the best plane given by C(1)-P-O(2)-C(2); the respective torsion angle is 1.79 °. The P-C(1) is slightly longer than in the complex **64a**. The H(1) and H(2) protons adopting positions at the same side of the five-membered ring as the W(CO)₅ group, while the CH(SiMe₃)₂ proton (H12a) adopts a relative orientation towards the metal fragment, like in case of the complex **62, 64a**.

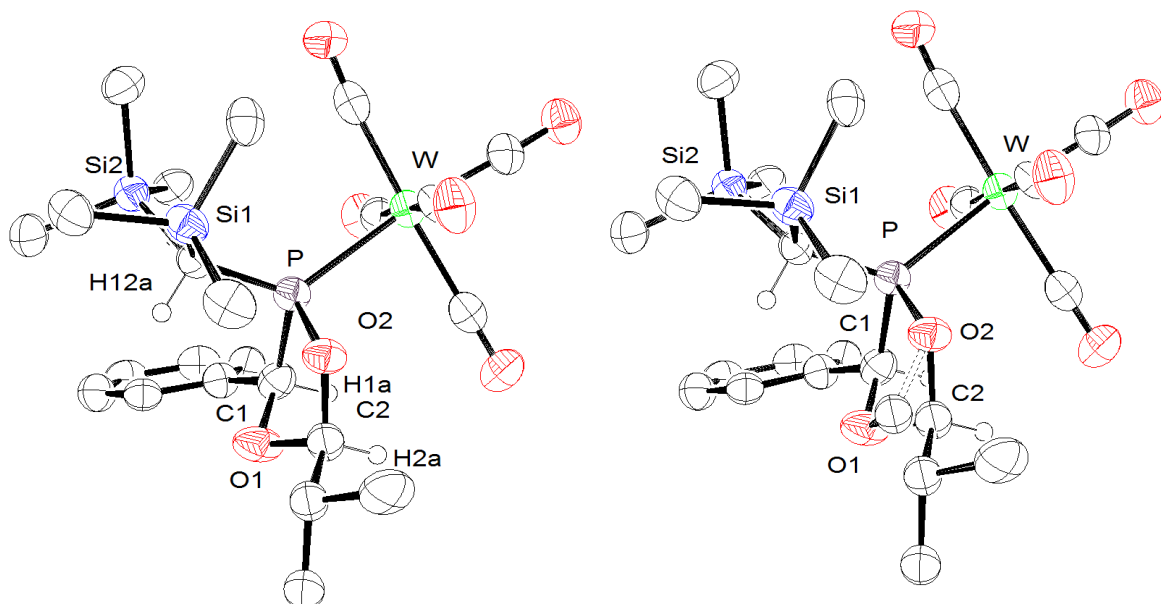
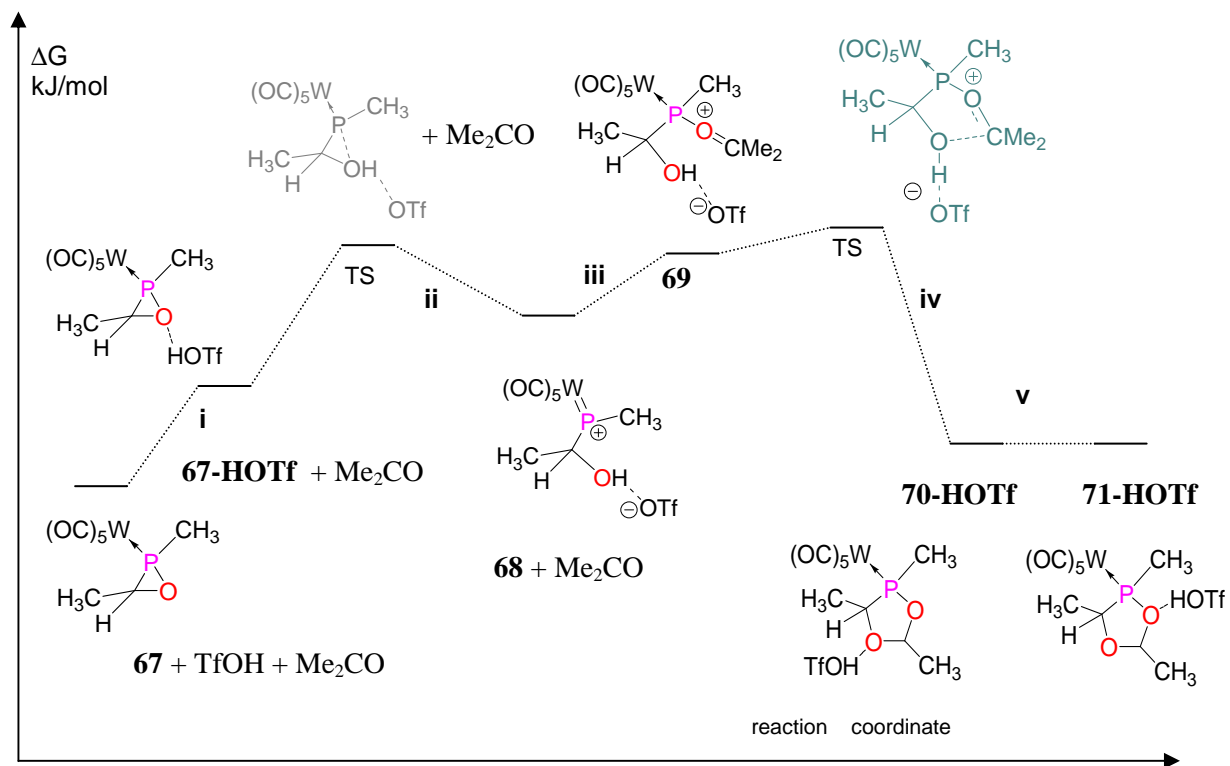


Figure 22. Molecular structure of 1,3,4-dioxaphospholane complex **66a** in the crystal (50 % probability level; reduce structure on the left side; 90 % main orientation on ⁱPr group; hydrogen atoms except H1a, H2a and H12a are omitted for clarity). Selected bond lengths (Å) and angles (°) : W-P 2.502(2), P-O(2) 1.642(6), C(1)-O(1) 1.427(10), P-C(1) 1.862(10), P-C(12) 1.808(9), O(1)-C(2) 1.446(15), O(2)-C(2) 1.472(16), C(1)-P-O(2) 88.6(4), P-C(1)-O(1) 102.8(6), C(1)-O(1)-C(2) 101.6(8), O(2)-C(2)-O(1) 103.5(10), P-O(2)-C(2) 112.8(7), C(1)-P-O(2)-C(2) 1.79. Further details on structure solution and refinement can be found in the appendix under GSTR139.

IV.1.2 Investigations on the reaction mechanism of the acid-induced ring expansion reaction

The crystal structure of the 1,3,4-dioxaphosphole complex **66a**, confirmed the insertion of one aldehyde unit into the oxaphosphirane ring through P-O bond cleavage. To gain more insight into the reaction mechanism theoretical studies were performed by Helten using a *P*-, *C*-methyl model system for oxaphosphirane complex **67** instead of the real structure complex **16a** and Me₂CO as model ketone. Oxaphosphirane complex **67** and triflic acid can form a loose associate, **67**-HOTf (Scheme 41), in which the proton of triflic acid is not transferred to the oxaphosphirane ring but forms an O-H-O hydrogen bond with the oxaphosphirane oxygen center. This undergoes spontaneous ring-opening and generation of phosphonium complex **68**; during the reaction the triflic acid proton is transferred to the former oxaphosphirane oxygen. The latter is then attacked by the carbonyl compound through the oxygen center, thus leading to the acyclic intermediate **69**, which undergoes subsequent cyclization. Compared to the acid-induced ring expansion of **67** with nitriles,^[76] three important differences deserve special attention: 1) the formation of the intermediate **69** is less favoured than the analogous formation of the *Ritter-type* adduct from the reaction of **68** with acetonitrile, 2) the barrier of the subsequent cyclization is, with respect to **69** significantly lower, and 3) in the cyclization step the proton that stemmed from TfOH is back-transferred to the triflate anion, and the system has no possibility for stabilization through protonation of a heteroatom of the five-membered ring. In the case of the reaction with nitriles, the resulting 4,5-dihydro-1,3,4-oxazaphosphole complexes are finally protonated at the nitrogen center, which renders the reaction irreversible. Here, in the products **70**-HOTf and **71**-HOTf, the triflic acid proton is bound *via* hydrogen bonding to the O¹ or the O³ center of the dioxaphospholane complex, respectively, and none of them is clearly favoured over the other. Consequently, the last step, vi, corresponds then largely to the deprotonation of triflic acid by

the amine, and is, as anticipated, highly exergonic. Comparison of the reactions with the model aldehyde and the model keton reveals that the major difference is found for the cyclization step (iv), as this is considerably less exergonic if Me_2CO rather than CH_2O is employed. In combination with the aforementioned issues 1–3, this supports the assumption that the reaction with ketones might be reversible (theoretical studies of the formation of *O*-protonated 1,3-dioxolanes predicted the possibility of a very fast (0.05 ps) ring-opening reaction^[79]) before the deprotonation is carried out. As the total number of particles during the ring expansion reaction decreases, the overall reaction entropy is negative: $-219 \text{ J}\cdot\text{mol}^{-1}\cdot\text{K}^{-1}$ for the sum of the steps ii, iii, and iv. This explains the necessity for performing the reaction—including the deprotonation—at low temperature.



Scheme 41. Computed pathway for the reaction of oxaphosphirane complex **67** with acetone in the presence of TfOH. The sum of free energies of the reactants **67**+TfOH+Me₂CO was arbitrarily taken as the zero point of the ΔG scale.

Table 13. Calculated thermochemical data for reactions of **67** with TfOH and R₂CO (R = H, Me; B3LYP/aug-TZVP/ECP-60-MWB(W), COSMO CH₂Cl₂ // RI-BLYP/aug-SV(P)/ECP-60-MWB(W), COSMO CH₂Cl₂); all values in kJ · mol⁻¹.

Reaction ^[a]	ΔG^\ddagger_{298}	$\Delta_R G_{298}$		
i	[b]	+13.6		
ii	+31.5	+25.1		
R = H		R = CH ₃		
	ΔG^\ddagger_{298}	$\Delta_R G_{298}$	ΔG^\ddagger_{298}	$\Delta_R G_{298}$
iii	[c]	+24.9	[c]	+34.3
iv	[c]	-81.9	+9.3	-44.1
v	[b]	-7.8	[b]	-0.7
vi ^[d]	[b]	-81.5	[b]	-96.9

^[a] Cf. Scheme 41. ^[b] Not calculated. ^[c] Not located. ^[d] Deprotonation of **67**-HOTf by NMe₃; not shown in Scheme 41.

The formation of two diastereomers was not taken into account in these calculations. The preference for this stereochemistry, as determined by the crystal structures of the major isomers of complexes **64a** and **66a**, can be convincingly explained only through calculations of the transition state in pathway **iv** (Scheme 41). Supposedly the small energy barrier corresponds to the transition state in which the C⁵-H and C²-H protons point towards the W(CO)₅ fragment, where both protons could be weak coordinated to the triflate anion placed at the same ring side.

Attempts to characterize the proposed *O*-protonated 1,3,4-dioxaphospholane complexes **70**-HOTf analogous by NMR spectroscopy at room temperature failed. Therefore, ³¹P{¹H}

NMR monitoring of the reaction course was performed for complexes **64a,b** at low temperature (Figure 23).

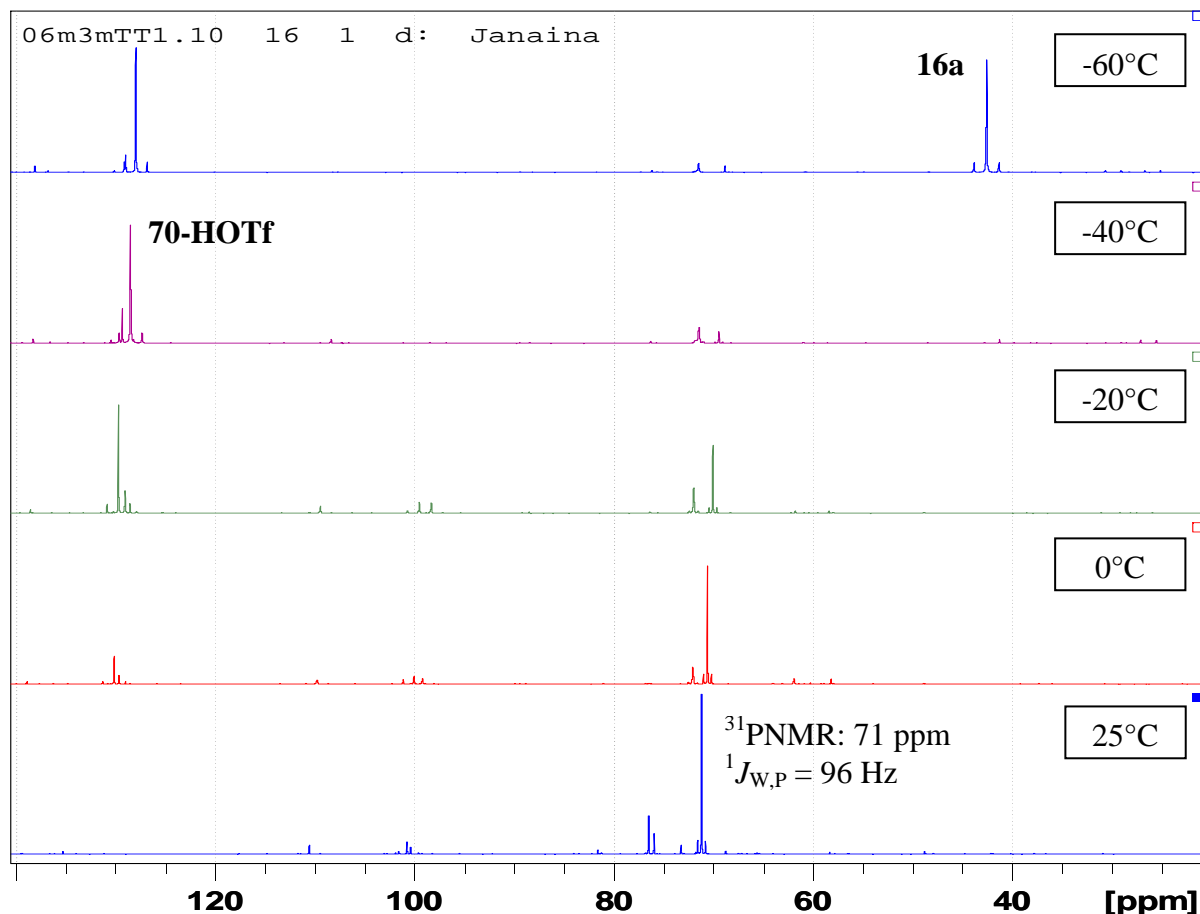


Figure 23. $^{31}\text{P}\{\text{H}\}$ NMR monitoring of the reaction course of the 1,3,4-dioxaphospholane complexes **64a,b** formation.

The reaction was performed at -60°C , without the subsequent addition of NEt_3 , and allowed to warm up to ambient temperature (Figure 23). The formation of the *O*-protonated-1,3,4-dioxaphospholane complexes **70-HOTf** analogous was already observed at -60°C (128.0 ppm, $^1\text{J}_{\text{P},\text{W}} = 276.5$ Hz (30%) and 130 ppm, $^1\text{J}_{\text{P},\text{W}} = 276.5$ Hz (70%)), although the reaction was not complete and some starting material (complex **16a**, 42 ppm, $^1\text{J}_{\text{P},\text{W}} = 309.0$ Hz) had remained.

The products at 128 and 130 ppm did not show any additional phosphorus proton coupling. Somehow, this is in contrast with the case of the *N*-protonated 1,3,4-oxazaphosphole complexes, in which a coupling was observed between the N-H and the phosphorus atom. This probably points to a O¹-bonded proton and, surprisingly, the resonance and the tungsten-phosphorus coupling constant of the *O*-protonated-1,3,4-dioxaphospholane complex are very close to the values of the neutral complex. The reaction of complex **16a** with the aldehyde in the presence of TfOH is complete at -30°C, and the formation of two new products around 70 ppm was observed. During the warm-up process the signal at 128 ppm vanished while the one at 71 ppm grew in. At ambient temperature only these two signals, one at 71 ppm having a very small tungsten-phosphorus coupling constant of 96.1 Hz and another less intense signal at 72 ppm with a $^1J_{W,P} = 106$ Hz were observed. The *O*-protonated 1,3,4-oxazaphospholane complex **70-HOTf** analogous was only stable at low temperature (-60 to -20°C) which explains the necessity to perform the ring expansion and the deprotonation reaction at low temperature. The nature and reactivity of the by-products formed at room temperature will be discussed in the next chapter.

IV.2 Acid induced ring-opening reactions of the oxaphosphirane complex **16a**

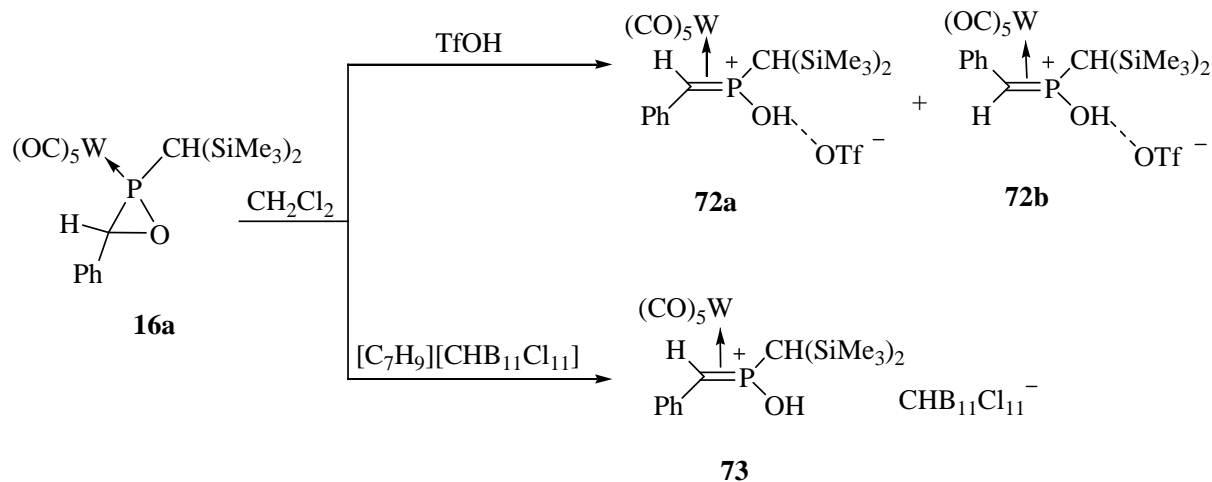
This chapter will be focussed on investigations of the acid-induced ring-opening reactions of the *P*-bis(trimethylsilyl)methyl- $\sigma^3\lambda^3$ -oxaphosphirane complexes **VII** using the oxaphosphirane tungsten complex **16a**; it was chosen because of its easy accessibility and the helpful information obtainable through the phosphorus-tungsten coupling constant in $^{31}\text{P}\{^1\text{H}\}$ NMR experiments.

IV.2.1 Formation of *side-on* bonded P=C pentacarbonyltungsten(0) complexes through acid-induced ring-opening reactions

To study the first step of the mechanism of the oxaphosphirane ring-opening reactions, proposed and described in detail in chapter IV.1, *i.e.*, bonding and stability of the *O*-protonated oxaphosphirane complex proposed in the theoretical calculations (complex **67**-HOTf, Scheme 41), oxaphosphirane complex **16a** was reacted with triflic acid in the absence of any trapping agent (Scheme 42).

When a CH_2Cl_2 solution of the oxaphosphirane complex **16a** was treated at room temperature with one equivalent of triflic acid the solution color immediately changed from light yellow to deep green (UV/Vis (CH_2Cl_2)): λ ($\log \epsilon$): 248 (0.45), 287 (0.08) nm, these bands are 10 nm red-shifted compared to the oxaphosphirane complex **16a**). The formation of one major product was observed by $^{31}\text{P}\{^1\text{H}\}$ NMR spectroscopy. Surprisingly, the data of which were

very similar to those of the final product, observed in the monitoring of the reaction of oxaphosphirane complex **16a** with aldehyde and triflic acid (Figure 23) at low temperature. Close inspection of all NMR data showed the selective formation of two isomers in a ratio of 86:14. Complex **72a** displayed a $^{31}\text{P}\{\text{H}\}$ MNR resonance at 73.8 ppm with a small tungsten-phosphorus coupling constant of 113.2 Hz, whereas complex **72b** showed a $^{31}\text{P}\{\text{H}\}$ NMR resonance at 72.3 ppm with an even smaller $^1\text{J}_{\text{W},\text{P}}$ coupling of 97.9 Hz. Neither ^1H nor $^{13}\text{C}\{\text{H}\}$ NMR spectroscopy nor IR spectroscopy on **72a,b** was particularly informative and attempts to separate **72a** from **72b** via column chromatography or crystallization failed. Therefore the nature of these products couldn't be fully explained until the same reaction was performed with the acid $[\text{C}_7\text{H}_9][\text{CHB}_{11}\text{Cl}_{11}]$ (Scheme 42) and the crystal structure unambiguously confirmed the *side-on* complex **73**.^[80]



Scheme 42. Formation of the *side-on* complexes **72a,b** and **73** through protonation of complex **16a**.^[80]

The characterization of complexes **72** and **73** appeared to be difficult as fast decomplexation of the cationic ligand occurred, *i.e.*, decomposition of the *side-on* complexes. Because of the polar nature of **72a,b** and **73** they did not dissolve in non-polar solvents such as *n*-pentane,

and if other, more polar organic solvent were used such as THF or diethyl ether decomplexation occurred readily. But luckily they were stable in dichloromethane solutions for 2-3 days at room temperature.

A further observation merits a note: if small amounts of air came inside the reaction vessel, a faster decomposition occurred to give a blue solution, but further attempts to isolate the decomposition product using column chromatography or crystallization failed. NMR spectroscopic experiments revealed the absence of the pentacarbonyltungsten moiety and thus clearly suggested that elimination of $\text{W}(\text{CO})_5$ must have taken place. The formation of (bis(trimethylsilyl)methyl)-1-phenylmethylphosphinic acid **74** was supported by a set of resonances for a CH_2Ph unit and mass spectrometric studies (EI), which revealed the molecular radical cation (m/z 314). To proof this proposal, the mixture of complexes **72a,b** was reacted with little amounts of water, which led to decomplexation and rearrangement to give **74**.

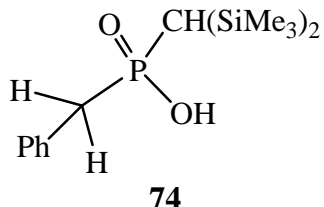


Figure 24. Decomposition product of the complexes **72a,b**, the phosphinic acid **74**.

The superior crystallizing properties of carborane anions as counter ions for reactive cations^[81] suggested that X-ray structural information might be obtained using a carborane acid instead of triflic acid. Thus, reaction of complex **16a** with the toluenium ion salt $[\text{C}_7\text{H}_9][\text{CHB}_{11}\text{Cl}_{11}]$, a somewhat weaker acid than triflic acid but having a less basic anion,^[82] was performed under similar conditions and led exclusively to the single product **73** displaying similar, although not identical, NMR data (Table 14).

All compounds showed small tungsten-phosphorus coupling constant due to the *side-on* bonding to the metal complex moiety.^[83] The ¹H NMR values showed differences of the CHPh proton between the two *E, Z*-isomers **72a,b**; complex **72a** showed a resonance at 3.20 ppm with a ²J_{P,H} value of 17.4 Hz, which was in accordance with the data of the complex **73** and therefore the same *E*-configuration was assigned to both complexes, while the minor isomer **72b** showed a smaller ²J_{P,H} coupling of only 3.8 Hz.

Table 14. Selected NMR data of the *side-on* complexes **72a,b** and **73** (CDCl₃ for **72a,b**, CD₂Cl₂ for complex **73**); ^acould not be measured.

	$\delta^{31}\text{P}$ [ppm] ($^1\text{J}_{\text{W,P}}$ [Hz])	$\delta(^1\text{H})$ [ppm] ($J_{\text{P,H}}$ [Hz])		$\delta(^{13}\text{C}\{^1\text{H}\})$ [ppm] ($J_{\text{P,C}}$ [Hz])	
		CH(SiMe ₃) ₂	CHPh	CH(SiMe ₃) ₂	CHPh
72a	73.8 (113.2)	0.40 (10.5)	3.20 (16.3)	18.1 (24.6)	15.0 (16.5)
72b	72.3 (97.9)	1.00 (8.7)	4.10 (3.8)	- ^a	- ^a
73	75.5 (118.0)	1.00 (6.9)	3.40 (17.4)	21.0 (21.6)	17.9 (15.9)

Special attention required the ¹³C{¹H} NMR data of the CHPh atom of complexes **72a, 73** which is almost 40 ppm up-field shifted with respect to the oxaphosphirane complex **16a**, thus revealing some degree of sp³ character of this carbon centre in the *side-on* complexes. As a consequence of the *side-on* coordination all CO groups showed only one resonance in solution with a small ²J_{P,C} coupling of 9.7 Hz. The ²⁹Si{¹H} NMR data also differed from oxaphosphirane complexes as they showed two doublets at 3.4 and 14.1 ppm, respectively, with larger phosphorus-silicon coupling constants of 4.7 and 14.8 Hz. The IR spectrometric data confirmed the existence of a hydroxyl group attached to the phosphorus, which showed a sharp signal at 3387 cm⁻¹ for complex **73**. In case of the complexes **72a,b** a very broad signal at 3500 cm⁻¹ was observed. Here, this band was even broader than that of pure triflate acid, probably due to H-bonding of the triflate to the OH group.

In the solid state the molecular structure of **73** revealed a coordinated methylene phosphonium ion that is *side-on* bonded to the W(CO)₅ group (Figure 25).

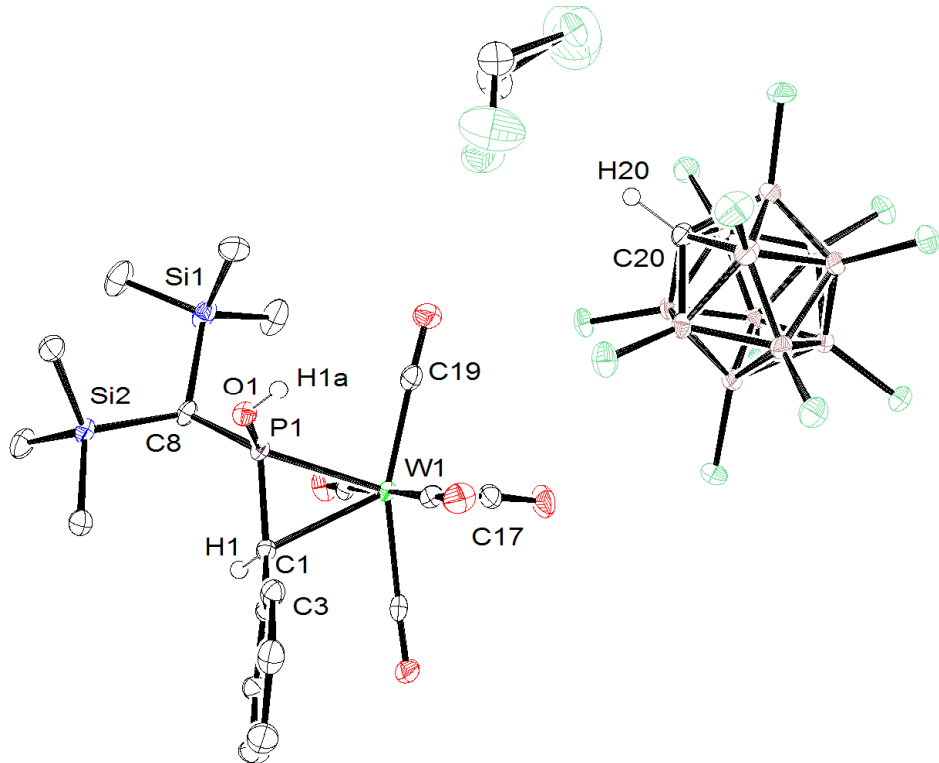


Figure 25. Structure of **73**·CH₂Cl₂ in the crystal (50% probability level; hydrogen atoms except H1, H1a, H20 are omitted for clarity). Selected bond lengths [Å] and angles [°] : W-P 2.4513(5), W-C(1) 2.4489(17), P-O(1) 1.5935(14), P-C(1) 1.7394(18), C(1)-W-P 41.58(4), P(1)-C(1)-W 69.28(9), C(1)-P(1)-W 69.14(6). Further details on structure solution and refinement can be found in the appendix.

The *P*-OH group formed a weak H-bond to Cl(6) of the carborane anion: O-H = 1.75 Å, H···Cl = 2.51 Å, O···Cl = 3.26 Å and ∠O-H-Cl = 177°. Comparison of the cationic ligand in **73** with structurally characterized free methylene phosphonium ions in [(*i*Pr₂N)₂P=C(SiMe₃)₂][OTf]^[84] and [(*t*Bu)₂P=C(Ph)₂][AlCl₄]^[85] showed that the P-C(1) bond in **73** is lengthened approximately 0.1 Å by coordination to tungsten – but is still shorter than

a typical P-C single bond. The environments at the P and C(1) centers deviate from the planarity expected of a *side-on* coordinated, Z-configurated P-C double bond in **XXXI**, which points to a contribution of the structure **XXXII** to the ground state (Scheme 43).

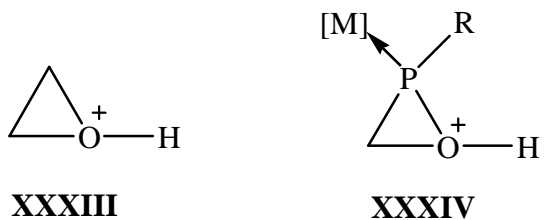


Scheme 43. Canonical formulae **XXXI** and **XXXII** of the ligand-metal bonding in **72a,b** and **73**.

The very close similarity of the NMR spectroscopic data for the triflic acid products **72a,b** and the carborane acid product **73** suggested that they all have the same fundamental cationic structure. Given the greater basicity and smaller size of the triflate anion relative to $\text{CHB}_{11}\text{Cl}_{11}^-$, the difference between the complexes **72** and **73** probably lies in the ability of triflate to engage in stronger H-bonding with the *P*-OH group of the cation. Finally, the appearance of two isomers **72a** and **72b** is presumably explained in terms of a haptotropic shift via diasteromeric transition states. Since the free energy preference of complex **72a** over complex **72b** is only a few kJ/mol, calculations performed by Helten,^[80] the absence of isomers of complex **73** suggested that an explanation must include H-bonding of the triflate anion.

Low temperature $^{31}\text{P}\{^1\text{H}\}$ NMR investigations were performed onto the reaction course, in the hope to find an oxaphosphiranium intermediate, the phosphorus analogue of oxiranium derivatives **XXXIII**^[86-92] which are often proposed intermediates of acid-catalyzed oxirane ring-opening reactions. The oxaphosphiranium derivatives are still unknown but in principle, κP metal coordination of a $\sigma^3\lambda^3$ -oxaphosphirane complex **VII** should divert protonation to

yield *O*-protonated complexes **XXXIV** (Scheme 44), and kinetic stabilization with a bulky *P*-substituent might allow observation of a closed-ring cation.



Scheme 44. Derivatives of oxiranium **XXXIII** and O-H oxaphosphiranium complexes **XXXIV** ([M] denotes a $M(CO)_5$ group).

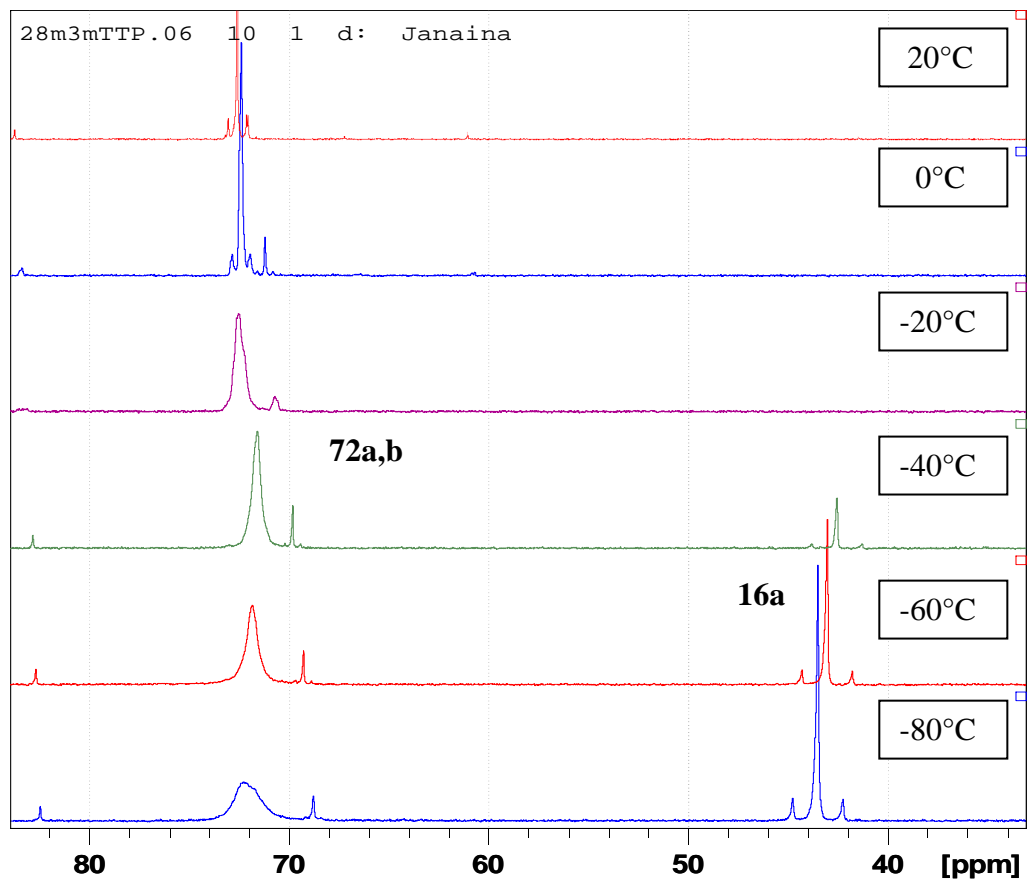
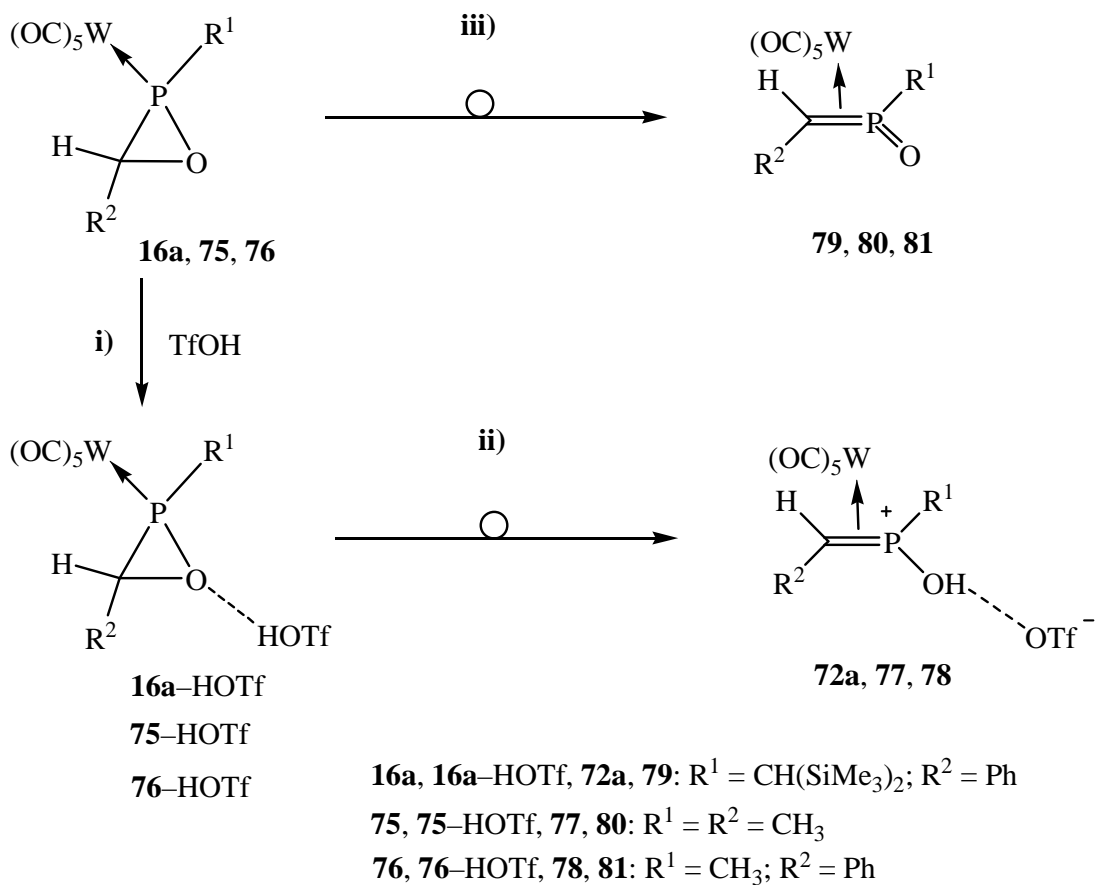


Figure 26. $^{31}\text{P}\{\text{H}\}$ NMR spectroscopic monitoring of the formation of complexes **72a,b**.

Unfortunately no other signal besides complexes **72a,b** was observed even at -80°C although a very small peak (3%) could be observed around 82 ppm (Figure 26). At this temperature some starting material, complex **16a**, was still observed in the $^{31}\text{P} \{^1\text{H}\}$ NMR spectra, while the complexes **72a,b** displayed a broad signal. During warm-up all starting material reacted to give the *side-on* complexes, and the signals of which were getting sharper.

To get further insight into the reaction of the oxaphosphirane complex **16a** with triflic acid, DFT calculations were performed by Helten on two model complexes, **75** ($\text{R}^1 = \text{R}^2 = \text{CH}_3$) and **76** ($\text{R}^1 = \text{CH}_3, \text{R}^2 = \text{Ph}$) and on the full system of complex **16a** (Scheme 45, reactions **i**, **ii**).^[80] Furthermore, the valence isomerisation of **16a**, **75**, **76** to methylene oxophosphorane complexes **79-80** (**iii**) was computed for comparison. The relative free energies are given in Table 15.



Scheme 45. Computed TfOH-induced ring-opening and valence isomerisation of complexes **16a**, **75** and **76**.^[80]

Table 15. Calculated thermo chemical data for reactions shown in Scheme 45 (all values in kJ/mol; B3LYP/aug-TZVP/ECP-60-MWB(W) COSMO (CH_2Cl_2) // RI-BLYP/aug-SV(P)/ECP-60-MWB(W) COSMO (CH_2Cl_2)).^[a] Not calculated.^[80]

Rct.	$R^1 = R^2 = CH_3$		$R^1 = CH_3$ $R^2 = Ph$		$R^1 = CH(SiMe_3)_2$ $R^2 = Ph$	
	ΔG^\ddagger_{298}	$\Delta_R G_{298}$	ΔG^\ddagger_{298}	$\Delta_R G_{298}$	ΔG^\ddagger_{298}	$\Delta_R G_{298}$
i)	[a]	+13.6	[a]	+17.2	[a]	+29.5
ii)	+75.5	-32.6	+44.8	-43.1	+53.3	-30.2
iii)	+134.3	+4.4	+96.6	-2.8	+123.6	+14.9

In the first, slightly endergonic step (i) the oxaphosphirane complex and triflic acid formed an associate (**16a–HOTf**, **75–HOTf**, **76–HOTf**) where the acid proton is bound to the oxaphosphirane oxygen center via O–H–O hydrogen bonding. Upon proton transfer, C–O

ring bond cleavage and haptotropic shift of the W(CO)₅ fragment proceeded in a concerted manner (**ii**), leading to the exergonic formation of the final products **72a**, **77** and **78**. This explains why the *O*-protonated oxaphosphirane complex **16a** was not observed, even at -80 °C. The barrier for this process was strongly influenced in the calculations by the oxaphosphirane *C*-substituent, decreasing considerably if a phenyl substituent is present (R² at C³). This was also apparent from the transition state structures (Figure 27). When R² = Ph, lengthening of the C–O bond was significantly less pronounced, indicating an earlier transition state; in each case the TfOH proton was already transferred to the ring oxygen. During cleavage of the C–O bond, the positive charge that was emerging at the C³ center is effectively stabilized by the phenyl group through π -electron conjugation. The nature of the *P*-substituent had a rather small effect on the thermo chemical data. Thus, the model system **75** was sufficient to provide an accurate description of this reaction. Valence isomerisation (**iii**), without preceding activation by an acid, was almost thermo neutral for the three systems computed, but the barriers were considerably higher than those of reaction (**ii**).

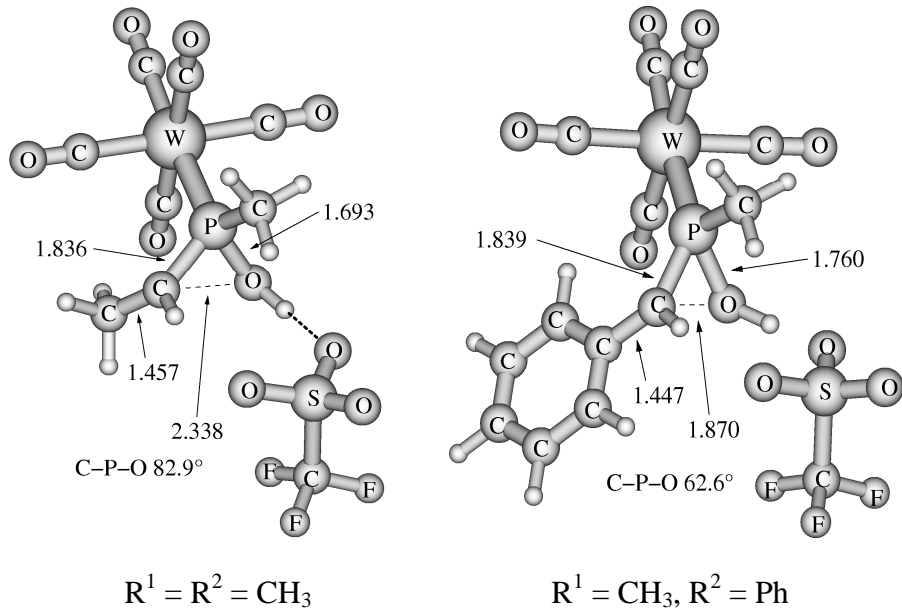


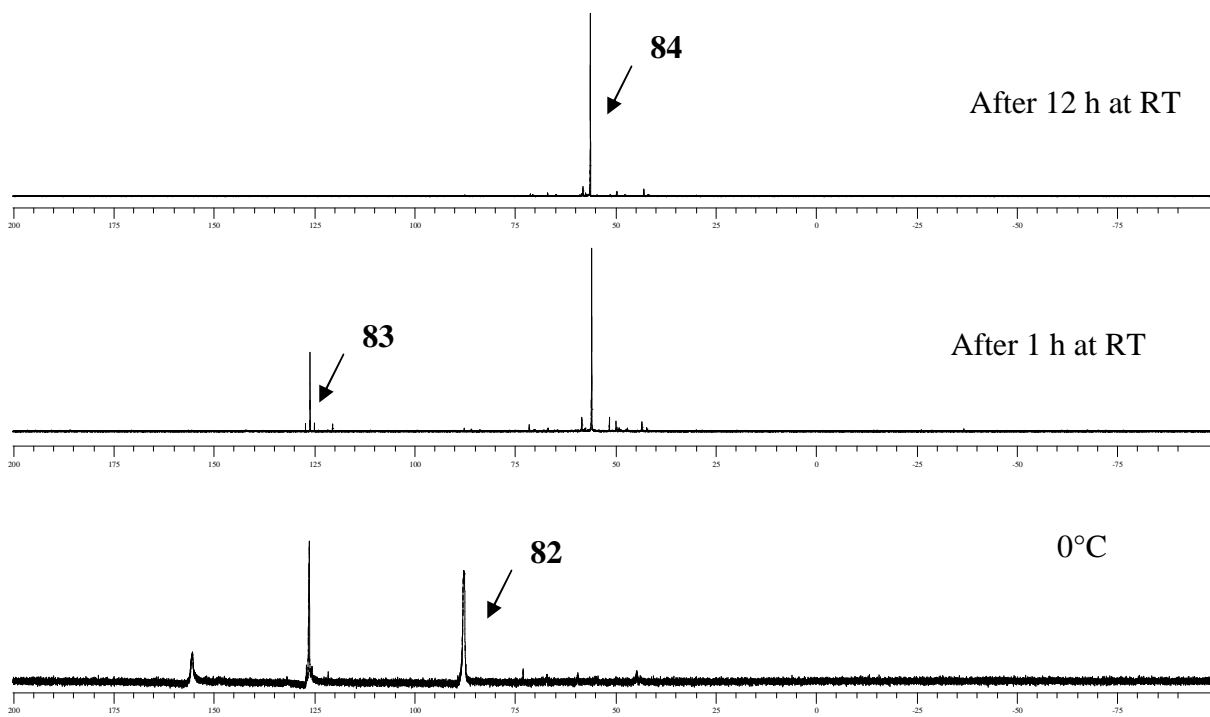
Figure 27. Calculated structures of the transition states of the TfOH-induced ring-opening (**ii**) of two model systems, **75**-HOTf (left side) and **76**-HOTf (right side). Bond distances are giving in Å.^[80]

Also in the presented DFT calculations, the *C*-phenyl substituent stabilizes the transition state, while the presence of the bulky $CH(SiMe_3)_2$ group at phosphorus causes a significant increase of the barrier.

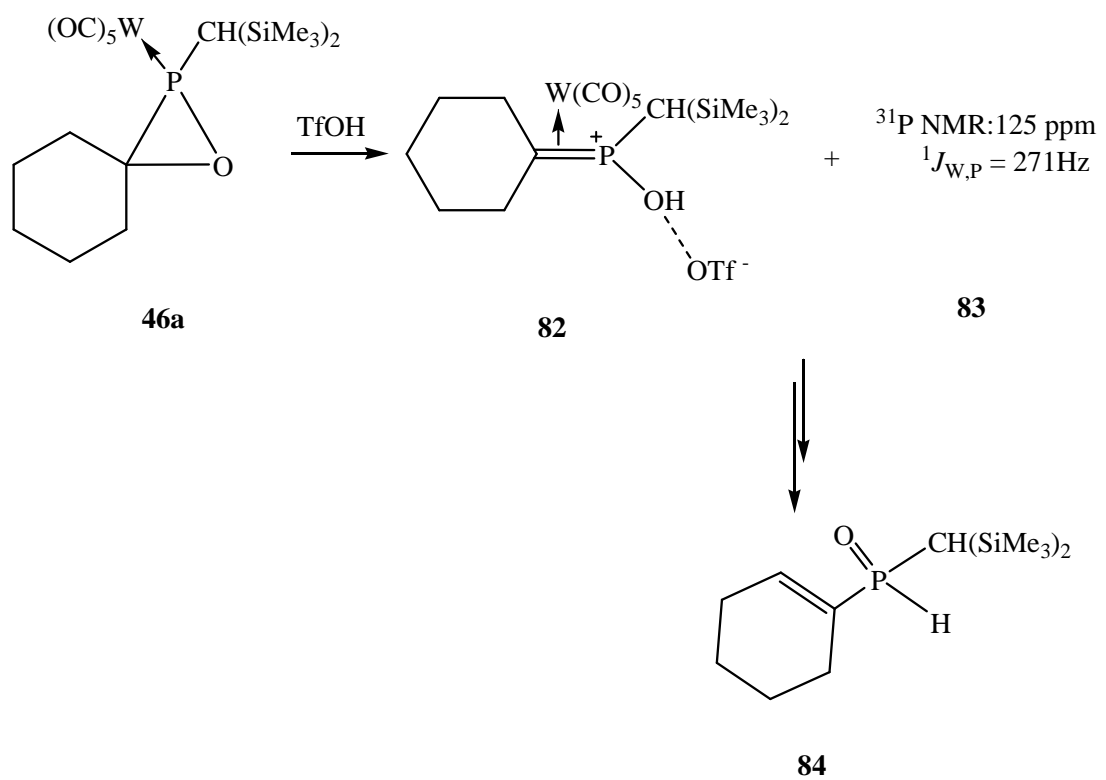
It is noteworthy that, from the experimental studies, no *side-on* complexes were found when either oxaphosphirane complex **12**^[34] or the *P*-Cp^{*}-oxaphosphirane complex^[51] were protonated with TfOH and thus the combination of the phenyl group at the carbon atom and the $CH(SiMe_3)_2$ at the phosphorus atom seems to be ideal for the formation of this class of coordination compounds.

To confirm this hypothesis, protonation with triflic acid of the spiro oxaphosphirane **46a** was also monitored by low temperature $^{31}P\{^1H\}$ NMR spectroscopy (Scheme 46). In this case the formation of *side-on* complex **82** ($^{31}P\{^1H\}$ MNR: 87 ppm, $^1J_{W,P} = 94$ Hz) was observed at low temperature together with some by-products: one resonance appeared at 125 ppm with a

$^1J_{W,P} = 270$ Hz (15%) and another resonance at 150 ppm, which was only stable below -10°C and which didn't enable the determination of the phosphorus-tungsten coupling constant. The $^{31}\text{P}\{\text{H}\}$ NMR data of the former product can be compared with the complex **54**, proposed by Schröder, and which might have been formed via proton-shift ($^{31}\text{P}\{\text{H}\}$ NMR: 123.4 ppm, $^1J_{W,P} = 271$ Hz). Unfortunately, the *side-on* complex **82** decomposed rapidly at room temperature to yield compound **84** with a resonance at 56 ppm and which revealed a large $^1J_{P,H}$ coupling constant of 507 Hz. The by-product at 125 ppm (**83**) also reacted after some hours, to give the same product, apparently. NMR studies on compound **84** suggested decomplexation of the *side-on* complex followed by rearrangement of a P-OH to yield a (H)P=O moiety^[93] and some kind of proton migration (Scheme 47).



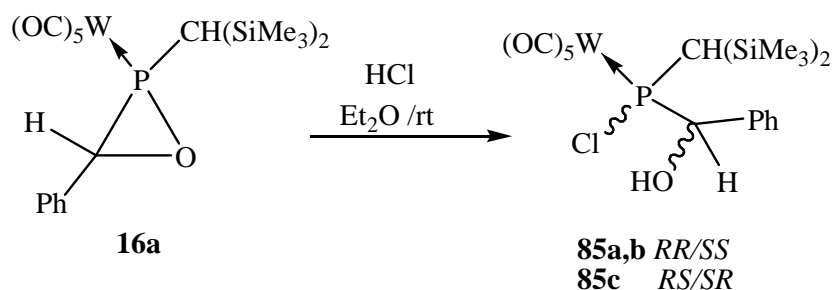
Scheme 46. $^{31}\text{P}\{\text{H}\}$ NMR monitoring of the reaction of complex **46a** with TfOH.



Scheme 47. Proposed course of the reaction of **46a** with TfOH.

IV.2.2.1 Hydrogen chloride induced ring-opening reaction

After these surprising findings in the case of super acids investigating the reactivity of the oxaphosphirane complex **16a** towards other Brønsted acids that posses stronger coordinating anions was of great interest. First, hydrogen chloride was chosen as acid in order to enable comparison with the investigations of Schröder.^[34] The protonation of the oxaphosphirane complex **16a** was performed with HCl gas (Scheme 48) in diethyl ether at ambient temperature and yielded a diastereomeric mixture of complexes **85a,b** and **85c**.



Scheme 48. Reaction of oxaphosphirane complex **16a** with $\text{HCl}_{(\text{g})}$.

Surprisingly, the $^{31}\text{P}\{^1\text{H}\}$ NMR data of the reaction mixture showed two resonances, one at 126.1 ppm with a tungsten-phosphorus coupling of 275 Hz and a very broad signal at 142.0 ppm ($W_{\text{H}1/2} = 100$ Hz), whereby the broadening of the NMR signal was not due to polymerization, as checked by GPC, but to a coalescence process (see below) of the two resonances of complexes **85a,b**.

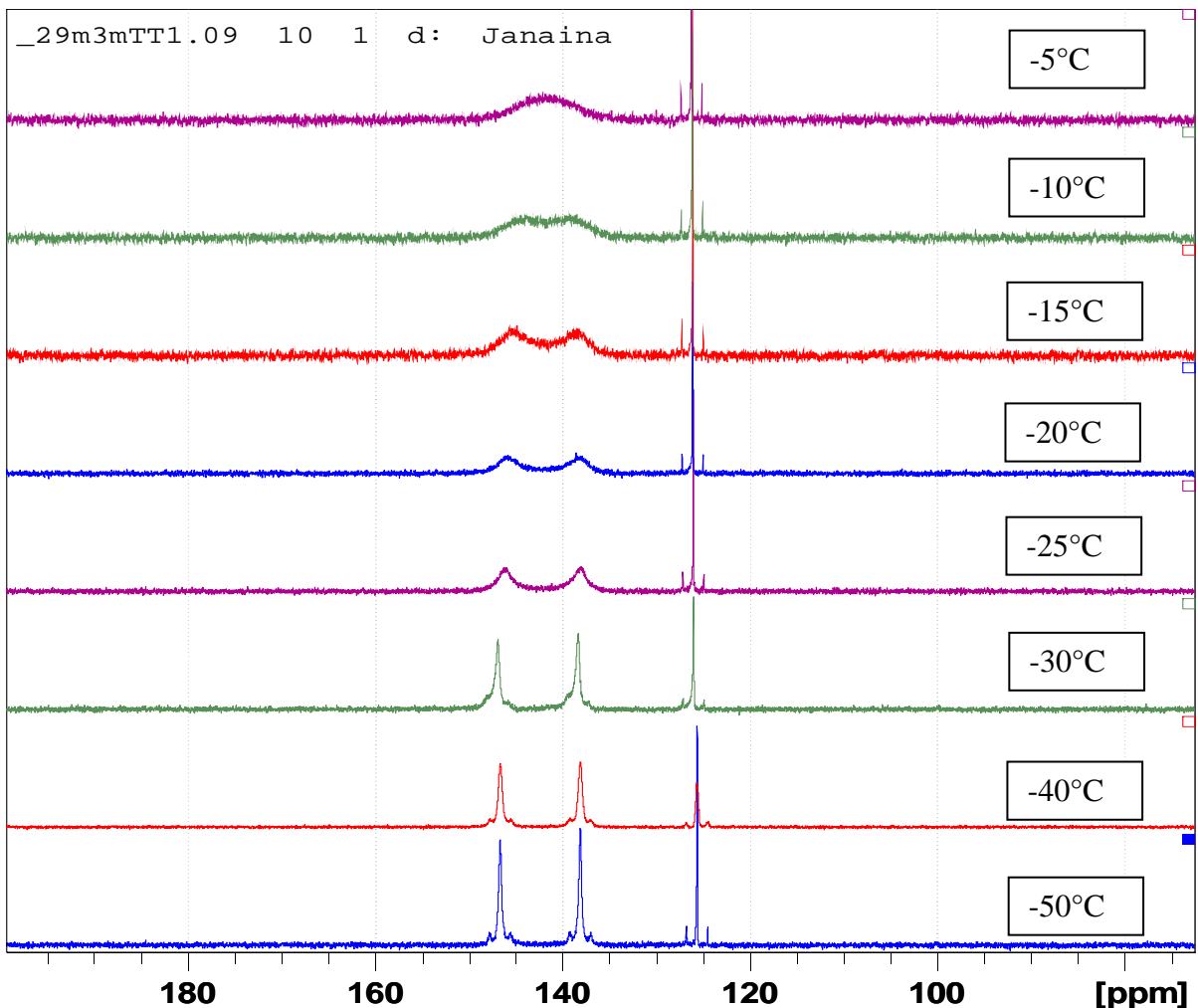


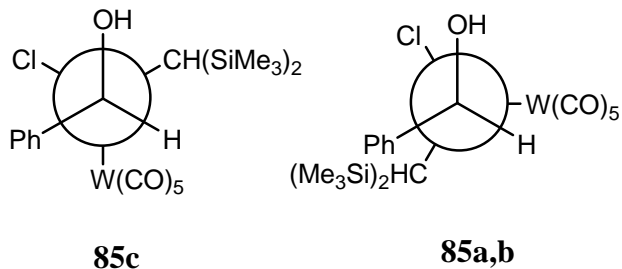
Figure 28. Low temperature $^{31}\text{P}\{\text{H}\}$ NMR measurements of a mixture of complexes **85a,b**-**85c**.

$^{31}\text{P}\{\text{H}\}$ NMR measurements of the reaction mixture (Figure 28) at low temperature revealed that the coalescence temperature was achieved at -5°C . The tungsten-phosphorus coupling constants and the ^{31}P NMR resonances of complexes **85a,b** were determined at -50°C although they still showed a significant broadening ($W_{\text{H}1/2} = 30\text{ Hz}$). No changes were observed in the sharp signal of complex **85c** at 126 ppm.

To explain the presence of three resonances at low temperature in the $^{31}\text{P}\{\text{H}\}$ NMR studies and the coalescence process, two different factors should bear in mind, the both chiral centers

in complexes **85a-c**, expressed as meso and rac isomers, together with a possible H bonding between the chlorine center and the hydroxyl group, which creates a chiral plane and thus gives rise to another isomer. In particular, the coalescence processes as observed by $^{31}\text{P}\{\text{H}\}$ NMR spectroscopy can be assigned to an intramolecular H-bonding, which was reported for molybdenum and tungsten phosphate aquo complexes.^[94]

The intramolecular H-bonding in complexes **85a,b** is favoured if the chlorine atom is closer to the hydroxy function (see Newman projections in Scheme 49) which means in an eclipsed conformation and which shall be sterically unusual. The $\text{CH}(\text{SiMe}_3)_2$ proton could then present two different conformations in this situation, it could be pointing towards the $\text{W}(\text{CO})_5$ or to the phenyl group. This interconversion can not take place at low temperature, and thus giving rise to two different ^{31}P NMR resonances as proven by further investigations (next chapter). The crystal structure of complex **85c** not only confirmed the presence of *RS/SR* meso form in the solid state in an *anti* conformation (Figure 30) but also the absence of H-bonding.



Scheme 49. Newman projections of complexes **85a-c**.

The kinetic parameters of the coalescence process were calculated from the $^{31}\text{P}\{\text{H}\}$ NMR data below the coalescence temperature, supposedly being a first order kinetic process.^[96,97] The first order rate constant (*k*) is inversely proportional to the conformer lifetime. Representation of the $\ln(k/T)$ vs $(1/T)$ (Figure 29) gave an enthalpy value of $\Delta H^\# = -5.6 \text{ J/mol}$ and an entropy value of $\Delta S^\# = -205.15 \text{ J/Kmol}$. The relative small value of $\Delta H^\#$ suggested a weak H-bonding interaction.^[95]

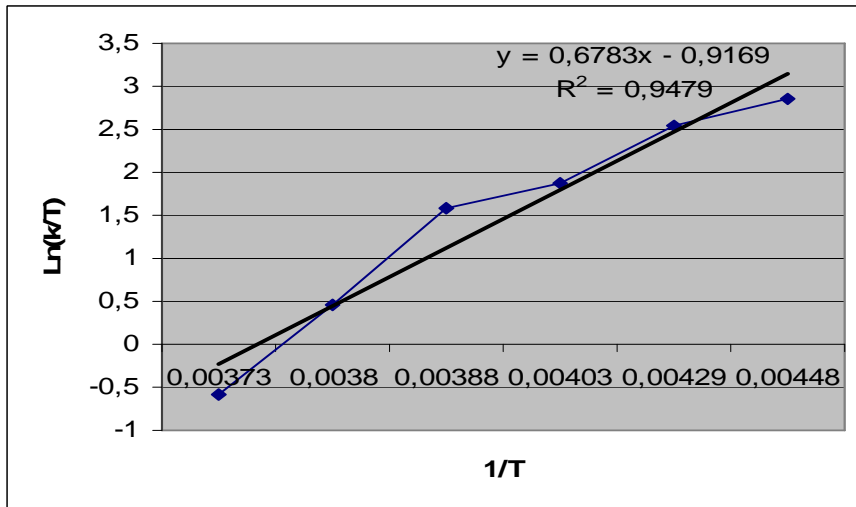


Figure 29. Representation of $\ln(K/T)$ vs. $1/T$ for the coalescence process of complexes **85a,b**.

Attempts to isolate complex **85c** from **85a,b** by column chromatography or recrystallization failed; they only could be partially separated by sequential and repeated washing with *n*-pentane at low temperature. Curiously all complexes **85a,b** and **85c** were white powders, but when they were dissolved again the diethyl ether solution became blue after some minutes; most probably, small amounts of unknown impurities were formed, a related problem was already observed for the unstable hydroxyl-substituted complexes **87** and **88a,b** (Scheme 50 and 51).

Selected NMR data of complexes **85a,b-85c** are displayed in Table 16. It is noteworthy that all diastereomers have almost the same tungsten-phosphorus coupling constant of 275 Hz but they differ very much in their $^{31}\text{P}\{\text{H}\}$ NMR resonances (**85c**: 126 ppm (even at -50°C); **85a,b**: 142 ppm at ambient temperature, 146.6 ppm and 138.7 ppm at -50°C).

The ^1H NMR data of both complexes **85a,b**, showed only one resonance at RT for each proton, which split into two broad signals at -50°C for both the $\text{CH}(\text{SiMe}_3)_2$ and the $\text{PH}(\text{Ph})$ protons (Table 16). The $^{13}\text{C}\{\text{H}\}$ NMR data also showed only one resonance at RT except for

the carbon atom CH(SiMe₃)₂ which appeared as a broad signal even at low temperature. The same overall picture resulted for the ²⁹Si{¹H} NMR data of complexes **85a,b** showing two broad signals at 1.1 and 1.5 ppm at ambient and low temperature. Very characteristic for complexes **85a,b** was the ¹J_{P,C} of the CHPh atom, which is 11 Hz larger than in complex **85c**.

Table 16. Selected NMR data (CDCl₃) of complexes **85a,b** and **85c**.

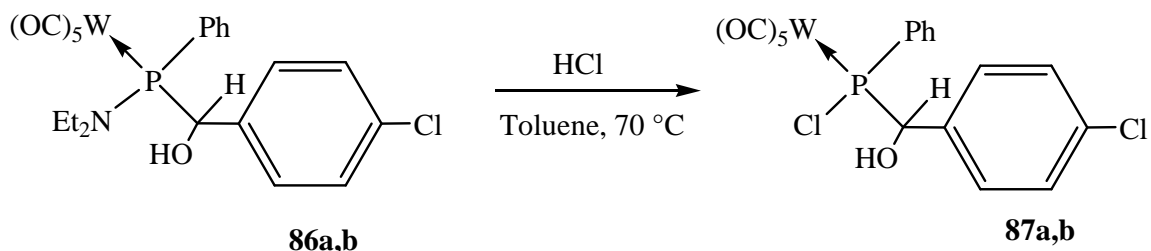
	$\delta^{31}\text{P}$ [ppm] ($^1J_{\text{W,P}}$ [Hz])	$\delta(^1\text{H})$ [ppm] ($J_{\text{P,H}}$ [Hz])		$\delta(^{13}\text{C}\{^1\text{H}\})$ [ppm] ($J_{\text{P,C}}$ [Hz])	
		CH(SiMe ₃) ₂	CHPh	CH(SiMe ₃) ₂	CHPh
85a,b	142.0 (broad)	2.31 (12.3)	5.34 (20.8)	30.0 (broad)	80.2 (21.3)
	146.6/138.7 ^a (274.0)	1.89/2.70 ^a (broad)	5.00/5.45 ^a (broad)	- ^{a,b}	- ^{a,b}
85c	126.1 (275.0)	1.51 (16.7)	5.36 (14.3)	25.8 (28.9)	79.1 (9.9)

^a Temperature of measurement -50°C. ^b Only broadening of the signals can be detected.

The IR spectroscopic data of complexes **85a,b-85c** showed a similar pattern for the carbonyl ligands. In the case of the OH group a sharp signal at 3525 cm⁻¹ was found for complex **85c** while complex **85a,b** showed both a broad signal at 3400 cm⁻¹ due to the H-bonding interactions. Mass spectrometric (EI, 70eV, ¹⁸⁴W) studies of complexes **85a,b** and **85c** showed the same molecular peak (m/z 656), similar fragmentation and the same base peak due to the [(SiMe₃)^{•+}] (m/z 73).

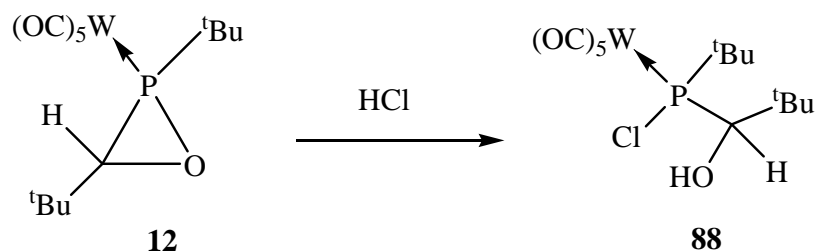
The crystal structure of complex **85c** unambiguously revealed that ring-opening of a transient *O*-protonated oxaphosphirane complex had taken place and chlorine was bound to the phosphorus center. Complex **85c** represents the first structurally confirmed example of a chloro(hydroxymethyl)phosphane complex, which is an unusual compound as only two other derivatives were found in the literature. It also represents a complex of a phosphorus-analogue of 1-chloro-1-hydroxyethane derivatives, better known in biology as vicinal halo

alcohol derivatives.^[98] The first example of such a complex was synthesized by Mathey *et al.*^[99] via reaction of the amino substituted precursors **86a,b** with HCl (Scheme 50), but complexes **87a,b** could not be fully characterized and only their mass and ³¹P NMR data were obtained because of its low stability.



Scheme 50. Synthesis of the *P*-chloro-(hydroxymethyl)phenylphosphane complex **87a,b**.^[99]

The second derivative, described in the literature, complex **88**,^[34] was also synthesized from an oxaphosphirane complex **12** using HCl, but again it was not fully characterized, only their mass and NMR data were obtained because its decomposition during the chromatography. Only in case of complex **87a,b** the formation of two diastereomers was observed, but not in case of complex **88**.



Scheme 51. Synthesis of complex **88** from oxaphosphirane complex **12** via addition of HCl.^[34]

The crystal structure of the complex **85c** (triclinic, space group P (-1)) was slightly disordered, having a OH group main orientation of 77 %. It showed a mixture of SR/RS

configured molecules in the unit cell. Therefore, complexes **85a,b** supposedly have a *RR/SS* configuration; selected structural data of complex **85c** are displayed below. As described before the $\text{CH}(\text{SiMe}_3)_2$ proton (H8a) is pointing towards the $\text{W}(\text{CO})_5$ group, while the OH group is pointing away. The W-P and Cl-P bond lengths are slighter longer than in the related dichloro(organo)phosphane complex **24**.^[49]

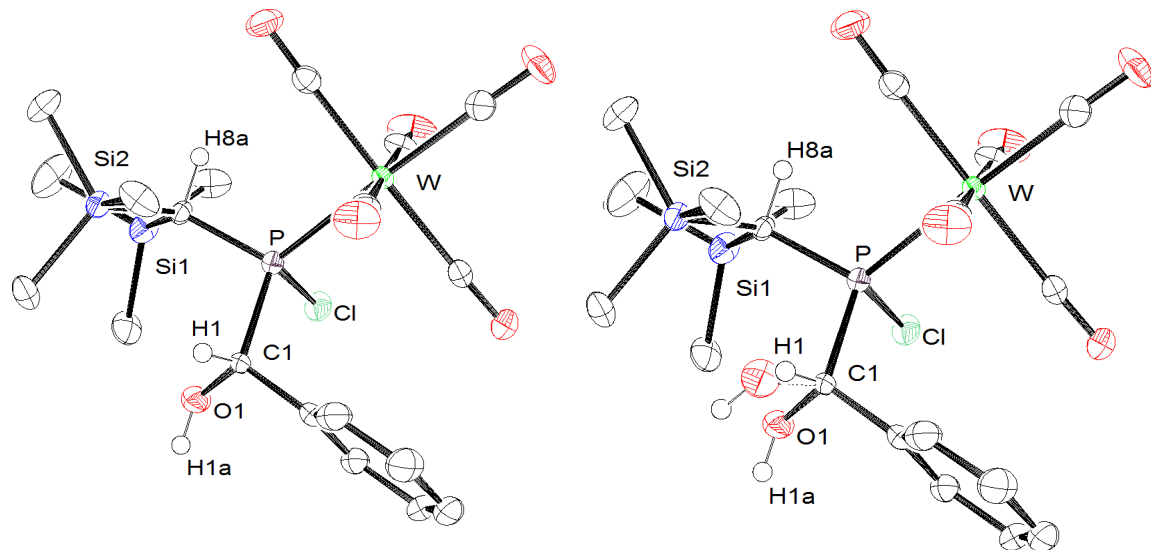
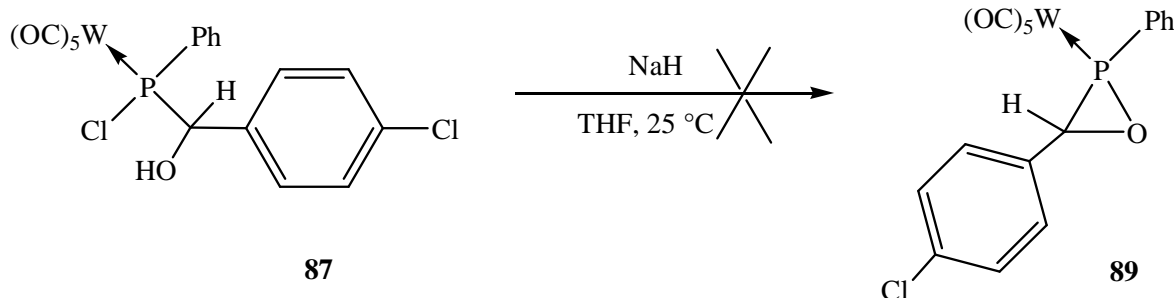


Figure 30. Structure of complex **85c** in the crystal (50% probability level; OH group main orientation 77 %; hydrogen atoms except H1, H1a and H8a are omitted for clarity; reduced structure on the left side). Selected bond lengths [Å] and angles [°] : W-P 2.5000(9), P-Cl 2.0830(13), P-C(1) 1.886(3), P-C(8) 1.823(3), C(1)-O(1) 1.378(5), C(1)-O(1s) 1.231, W-P-C(l) 122.03(12), C(8)-P-W 116.92(11), Cl-P-W 106.45(5). Further details on structure solution and refinement can be found in the appendix under GSTR074.

IV.2.2.2 Synthesis of oxaphosphirane complexes **VII** using a chloro(hydroxymethyl)organophosphane complex and LDA

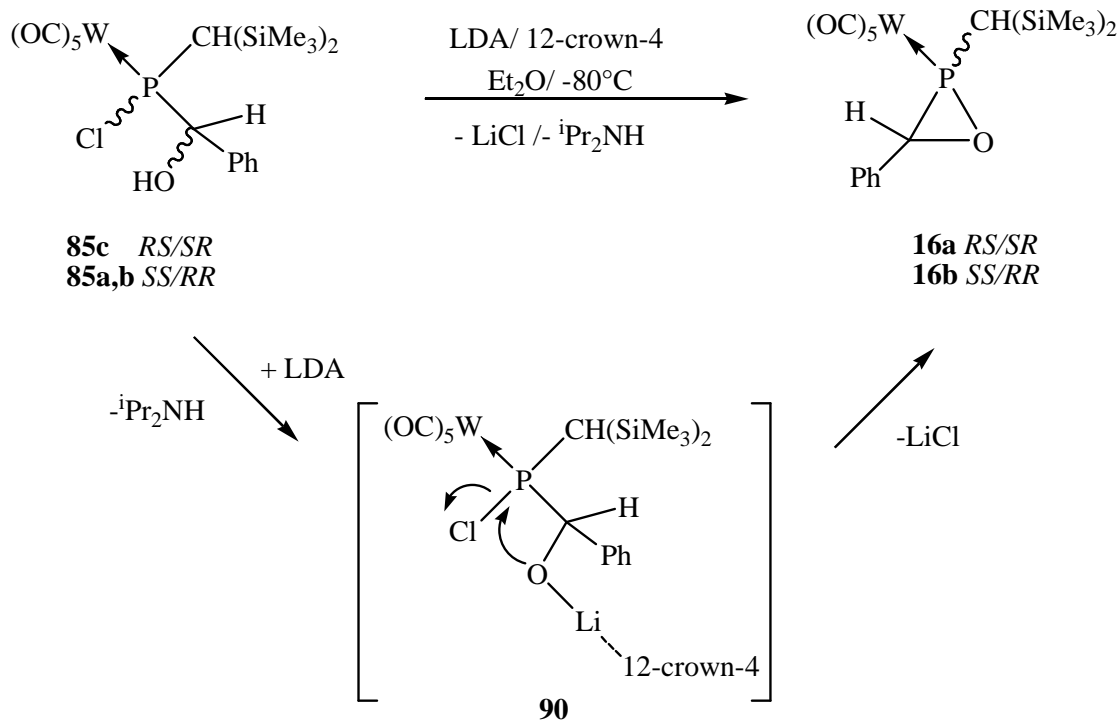
Although the synthesis of oxaphosphirane complexes **VII** via the phosphinidenoid complex route, presented in this work, showed many advantages compared to the previously established “oxidation or phosphinidene complex-transfer methods”, the search for new methods to synthesize oxaphosphirane complexes still represents a challenge. Therefore, the opportunity to find an alternative route starting from the chloro(hydroxymethyl)phosphane complexes **85a,b** and/or **85c** was examined. Interestingly, this idea was not entirely new but it was hampered by the difficulty in synthesising the required starting material, and the idea of Mathey *et al.*^[99] to use NaH as deprotonating agent turned out to be ineffective (Scheme 52).



Scheme 52. Attempted synthesis of oxaphosphirane complex **89** using complex **87**.^[99]

As the mixture of complexes **85a,b** and **85c** was stable in solution it was suitable for this propose and, instead of NaH, LDA was used as base at low temperature in order to avoid nucleophilic substitution at phosphorus. Interestingly, the presence of 12-crown-4 was required to make the reaction more selective (Scheme 53). Without crown ether, the desired oxaphosphirane complexes were observed only as by-products (~10%) in a very unselective reaction. ³¹P{¹H} NMR spectroscopic reaction monitoring revealed the formation of both diasteromers of the oxaphosphirane complex **16a,b**. If complex **85c** (as the complete

separation of both complexes was not possible, still 8% **85a,b** was present) was used, the formation of the diastereomer **16a** was preferred (70:30). In case of complexes **85a,b** (with 8% of **85c** as impurity) was used, the diastereomer **16b** was preferably formed (ratio: 30:70). This indicates the retention of configuration as the main pathway in a nucleophilic reaction. It seems plausible that the formation of the oxaphosphirane complexes **16a,b** occurred via an intermolecular *neighboring-group mechanism*^[100] in which the transiently formed alkoxide in **90** nucleophilically attacks the phosphorus center and expels the chloride (Scheme 53). In this type of reactions, typical for the formation of epoxides and lactones, the configuration is retained.



Scheme 53. Synthesis of the oxaphosphirane complexes **16a,b** from the chloro(hydroxy-methyl)phosphane complexes **85a,b** and **85c**.

Selected NMR data of the new complex **16b**, displayed in Table 17, revealed that the $^{31}\text{P}\{^1\text{H}\}$ NMR resonance was up-field shifted by 8 ppm in comparison to **16a** and had a significantly

smaller tungsten-phosphorus coupling constant of 292.3 Hz (vs. 307.7 Hz in **16a**). The ^1H NMR resonances of the $\text{CH}(\text{SiMe}_3)_2$ and CHPh protons of complex **16b** had chemical shifts similar to those of **16a**, but the 17 Hz difference in the $^2J_{\text{P},\text{H}}$ couplings of the $\text{CH}(\text{SiMe}_3)_2$ protons was significant and as such close to those obtained for the isomers of the spiro oxaphosphirane complexes **46a,b**. The most surprising result was that the $^{13}\text{C}\{^1\text{H}\}$ NMR shift of the $\text{CH}(\text{SiMe}_3)_2$ atom was found at 19.1 ppm, which was very much up-field in comparison with all the oxaphosphirane complexes known so far. Furthermore, a $^1J_{\text{P},\text{C}}$ value of 39.3 Hz for the same carbon atom was observed, almost 10 Hz larger than the coupling constant determined for complex **16a**.^[36]

Table 17. Selected NMR data (CDCl_3) of complexes **16a,b**.

	δ ^{31}P [ppm] ($^1J_{\text{W},\text{P}}$ [Hz])	$\delta(^1\text{H})$ [ppm] ($J_{\text{P},\text{H}}$ [Hz])		$\delta(^{13}\text{C}\{^1\text{H}\})$ [ppm] ($J_{\text{P},\text{C}}$ [Hz])	
		$\text{CH}(\text{SiMe}_3)_2$	CHPh	$\text{CH}(\text{SiMe}_3)_2$	CHPh
16a ^[36]	38.2 (307.7)	1.28	4.40 (1.8)	30.5 (18.8)	57.9 (27.5)
16b	31.0 (292.3)	1.28 (17.2)	4.50 (5.8)	19.1 (39.3)	62.5 (22.3)

There were also considerable changes in the ^{29}Si NMR data of complex **16b**, which displayed two doublets: one at -0.1 ppm with a $^2J_{\text{P},\text{Si}}$ coupling of 3.5 Hz and one at 4.5 ppm with a $^2J_{\text{P},\text{Si}}$ coupling of 1.3 Hz, and thus being significantly larger than those of the oxaphosphirane complex **16a**.^[36]

The mass spectrometric data (EI, 70eV, ^{184}W) of complex **16b** showed identical main fragmentation to the oxaphosphirane complex **16a** (molecular peak m/z 620, 15%), the $[(\text{CH}(\text{SiMe}_3)_2\text{PW}(\text{CO})_4)^{\bullet+}]$ fragment (m/z 486) was found as base peak again.

After purification by low temperature chromatography and washing with *n*-pentane, suitable single-crystals for X-ray diffraction studies of complex **16b** were obtained from a concentrated *n*-pentane solution (Figure 31).

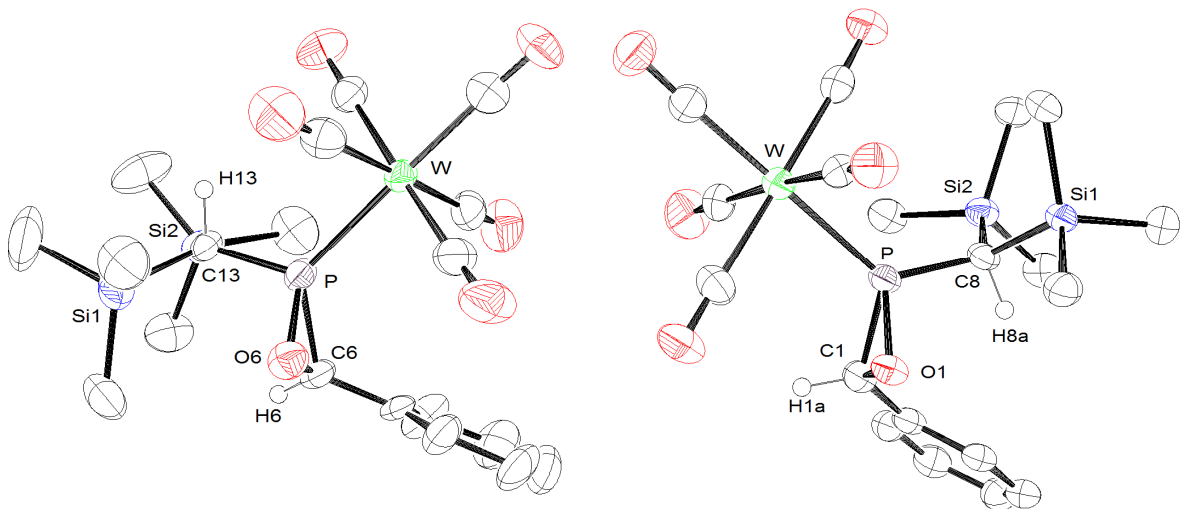


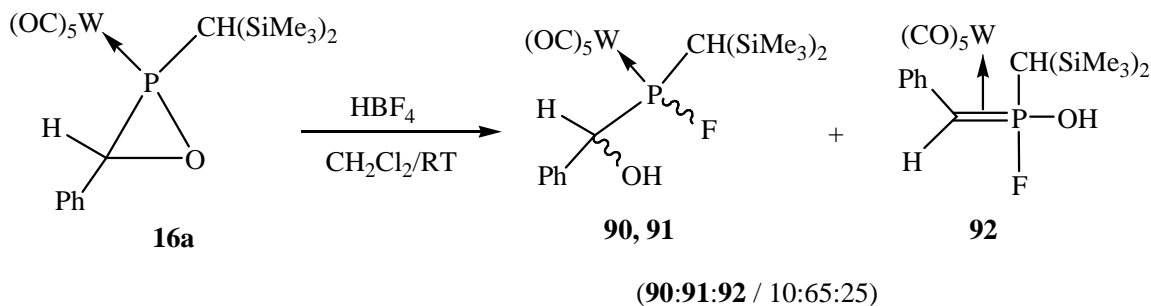
Figure 31. Molecular structure of the (previously known) oxaphosphirane complex **16a** (left side)^[36] and its diastereomer **16b** (right side) in the crystal (50 % probability level; hydrogen atoms except H1a, H8a for complex **16b** and H6, H13 for complex **16a** are omitted for clarity). Selected bond lengths [Å] and angles [°] of complex **16a**^[36]: W-P 2.462(2), P-O(1) 1.668(6), C(1)-O(1) 1.480(9), P-C(1) 1.802(7), P-O(1)-C(1) 69.6, C(1)-P-O(1) 50.3, O(1)-C(1)-P 60.1; Selected bond lengths [Å] and angles [°] of complex **16b**: W-P 2.4692(14), P-O(1) 1.668(3), C(1)-O(1) 1.480(6), P-C(1) 1.804(5), P-O(1)-C(1) 69.7(2), C(1)-P-O(1) 50.26(19), O(1)-C(1)-P 60.1(2). Further details on structure solution and refinement can be found in the appendix under GSTR146.

The oxaphosphirane complex **16a** crystallized in the triclinic system, space group P (-1), as a mixture of *RS/SR* diastereomers,^[36] whereas the complex **16b** crystallized in the monoclinic system, space group P2₁/c, as a racemic mixture of *RR/SS* diastereomers. Another particular feature of complex **16b** was the orientation of the CH(SiMe₃)₂ proton (H8a), in a *trans*-

eclipsed position to the W(CO)₅ moiety, contrary to the complex **16a** which displayed a *syn*-eclipsed conformation. The fact that chloro(hydroxymethyl)phosphane complexes **85a,b** yielded preferably oxaphosphirane complex **16b** suggested that they should possess *RR/SS* conformation. The bond lengths and angles of both oxaphosphirane complexes **16a,b** were essentially identical and no influence of the stereochemistry onto the structural parameters of the oxaphosphirane complexes **16a,b** could be found.

IV.3 Ring-opening reactions of the oxaphosphirane complex **16a** using fluoroboronic acid

Protonation of the oxaphosphirane complex **16a** with $\text{HBF}_4 \cdot \text{Et}_2\text{O}$ in dichloromethane yielded a mixture of three complexes (ratio: 10:65:25) according to the three $^{31}\text{P}\{^1\text{H}\}$ NMR signals (Scheme 54).^[115] The minor product (~10 %) had a very broad signal at 201 ppm ($W_{\text{H}1/2} = 420$ Hz) with a $^1J_{\text{P},\text{F}}$ coupling of ~826 Hz, and which was assigned to complex **90** and could be a diastereomer of complex **91**. It seems to be related to the situation of **85a,b** but having now the fluorine and the proton atom of the OH group which can build H-F interactions. Unfortunately, complex **90** decomposed during column chromatography (Figure 32). The signal of the major product was assigned to fluorophosphane complex **91** (~65 %) and the third signal to the *side on* complex **92** (~25 %). Complex **91** showed a $^{31}\text{P}\{^1\text{H}\}$ NMR resonance at 198.1 ppm (Table 18) with a tungsten-phosphorus coupling constant of 296 Hz, which was 20 ppm larger than the chlorine complexes **85a,b**. The phosphorus-fluorine coupling constant of 826.0 Hz is typical for a directly to phosphorus bonded fluorine.^[99]



Scheme 54. Reaction of the oxaphosphirane complex **16a** with $\text{HBF}_4 \cdot \text{Et}_2\text{O}$.^[115]

[ref]

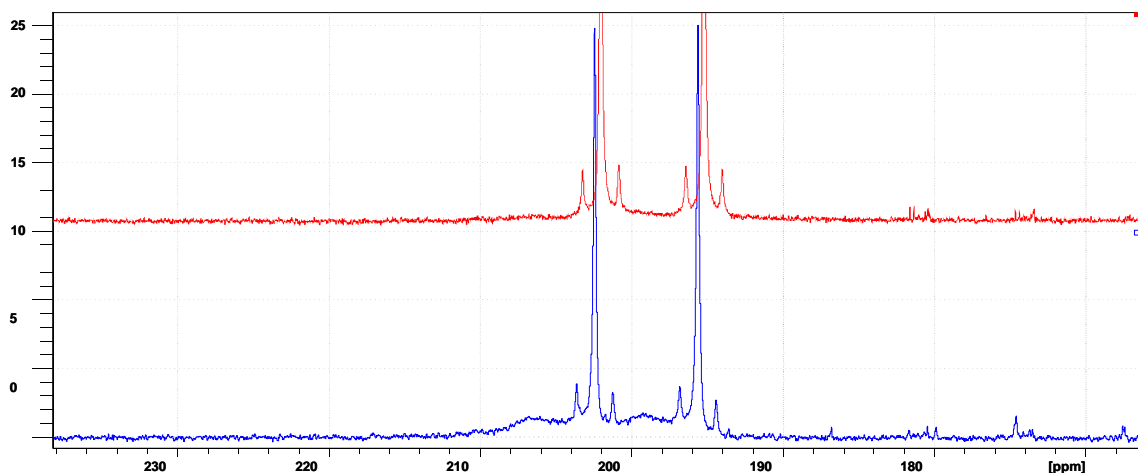


Figure 32. Detail of the $^{31}\text{P}\{^1\text{H}\}$ NMR spectra of the reaction mixture in which complexes **90** and **91** are present (bottom) or absent (**90**) after column chromatography (top).

The ^1H and $^{13}\text{C}\{^1\text{H}\}$ NMR data of the P-F containing complex **91** were similar of those of complexes **85a,b**. The CHPh proton had a small $^3J_{\text{H,F}}$ coupling of 6.6 Hz and didn't show any coupling to phosphorus, surprisingly. In the $^{13}\text{C}\{^1\text{H}\}$ NMR spectra the CH(SiMe₃)₂ carbon showed a broad signal like the complexes **85a,b**. Curiously, the CHPh carbon atom displayed a pseudo-quartet, whereby the $^1J_{\text{P,C}}$ and $^2J_{\text{F,C}}$ coupling had almost identical values.

Table 18. Selected NMR data (CDCl₃) of complexes **92** and **91**.

	$\delta^{31}\text{P}$ [ppm] ($^1J_{\text{W,P}}/^1J_{\text{P,F}}$ [Hz])	$\delta(^1\text{H})$ [ppm] ($J_{\text{P,H}}/J_{\text{H,F}}$ [Hz])		$\delta(^{13}\text{C}\{^1\text{H}\})$ [ppm] ($J_{\text{P,C}}/J_{\text{F,C}}$ [Hz])		$\delta(^{19}\text{F}\{^1\text{H}\})$ [ppm] ($J_{\text{P,F}}$ [Hz])
		CH(SiMe ₃) ₂	CHPh	CH(SiMe ₃) ₂	CHPh	
91	198.1 (296.3/826.0)	1.89 (15.7/-)	5.35 (-/6.6)	30.0 (broad)	78.1 (17.0/17.0)	-123.1 (851.9)
92	143.5 (144.0/1043.0)	0.85 (20.0/-)	3.40 (17.4/-)	13.0 (17.0)	66.0 (broad)	-71.5 (1059.7)

The mass spectra (EI) of complex **91** showed loss of CO units and revealed a high stability of the P-F bond. The infrared spectra of complex **91** confirmed unambiguously the presence of the hydroxyl group showing a sharp absorption signal at 3585 cm⁻¹.

Single crystals of complex **91** (Figure 33), obtained from a *n*-pentane solution showed a mixture of *RR/SS* diastereomers, contrary to the complex **85c** which showed a *RS/SR* configuration. Complex **91** crystallize in the monoclinic ($P2_1/n$) crystal system and showed similar structural data as complex **85c**.

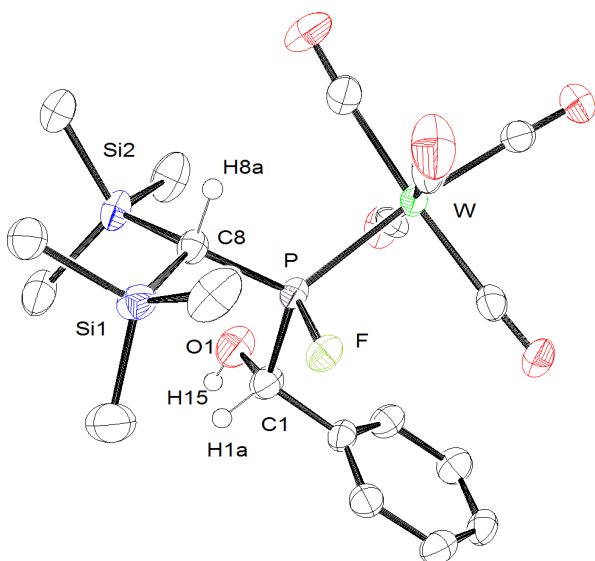


Figure 33. Structure of complex **91** in the crystal (50% probability level; hydrogen atoms except H1a, H8a and H15 are omitted for clarity). Selected bond lengths [Å] and angles [°] : W-P 2.4684(12), P-F 1.603(3), P-C(1) 1.874(5), P-C(8) 1.810(4), C(1)-O(1) 1.396(6), W-P-C(1) 120.95(17), C(8)-P-W 119.46(16), F-P-W 107.27(11). Further details on structure solution and refinement can be found in the appendix under GSTR167.

The *side-on* complex **92** could be only observed in the reaction mixture and had only a relative low stability. Like the other *side-on* complexes reported in this work, it easily undergoes decomplexation and decomposition if donor solvents or small amounts of air are

present. It also showed a relatively small $^1J_{W,P}$ coupling constant of 144.0 Hz due to the *side-on* coordination of the pentacarbonyltungsten fragment to the P-C bond, whereby the increase of 20 Hz (compared to complex **73**) is indicative for the influence of the *P*-bounded fluorine atom. A comparison of **92** with the phosphorus ylide κC -pentacarbonyltungsten complex **93**, isolated by Fischer *et al.* (Figure 34),^[101] which didn't show any phosphorus-carbon coupling constant for the carbonyl carbons and which revealed *cis* and *trans*-CO resonances in the $^{13}C\{^1H\}$ NMR, led further support to the assignment of **92** as an η^2 -W(CO)₅ Wittig-ylide complex.

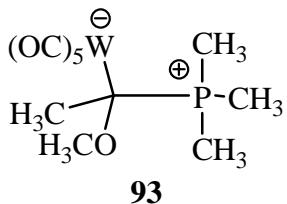


Figure 34. Phosphorus ylide κC -complex **93** as proposed by Fischer.^[101]

The *side-on* coordination was also supported by the single $^{13}C\{^1H\}$ NMR resonance of the pentacarbonyl group – as expected for the η^2 coordination^[80] – at 197.5 with a $^2J_{P,C}$ coupling of 10.9 Hz. The $^{29}Si\{^1H\}$ NMR spectra were also helpful to identify the *side-on* coordination mode as the presence of two doublets, one at 4.1 ppm with a $^2J_{P,Si}$ value of 4.7 Hz and another one at 15.0 ppm with a $^2J_{P,Si}$ value of 14.9 Hz, revealed the similarity to the other *side-on* complexes **72a,b** and **73**.

The presence of the hydroxyl group seems to be compatible with the fluorine at the same phosphorus atom. There are not many examples of phosphorus(III) compounds – and none of P(V) compounds – having a fluorine atom and a hydroxyl function attached to the same phosphorus atom; one example of a P(III) derivative is the complex **94** synthesized by Mathey *et al.* (Figure 35).^[102]

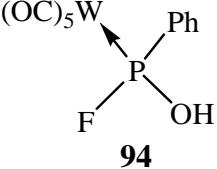
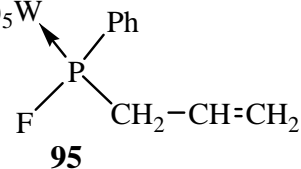
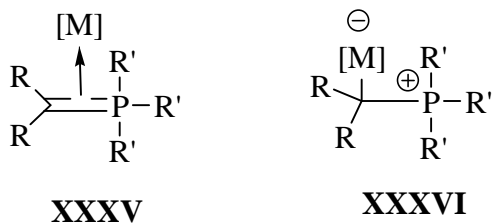
 94	 95
^{31}P NMR (CDCl_3): $\delta = 167.7$ ppm $(^1J_{\text{W},\text{P}} = 343$ Hz, $^1J_{\text{P},\text{F}} = 1031$ Hz)	^{31}P NMR (hexane): $\delta = 170.7$ ppm $(^1J_{\text{W},\text{P}} = 298$ Hz, $^1J_{\text{P},\text{F}} = 867$ Hz)
^{19}F -NMR (CDCl_3): $\delta = -55.8$ ppm $(^1J_{\text{P},\text{F}} = 1031$ Hz)	

Figure 35. Selected NMR data of complex **94**^[102] and complex **95**.^[99]

The difference of almost 50 ppm in the $^{19}\text{F}\{^1\text{H}\}$ NMR of complexes **92** and **91** seems to be due to the hydroxyl group position in complex **92**.^[102] The $^{19}\text{F}\{^1\text{H}\}$ NMR values of the *side-on* complex **92** are comparable to those of complex **94**. The presence of a hydroxyl and a fluoro function attached to the same phosphorus atom increased the $^1J_{\text{P},\text{F}}$ value notably: there is approximately 164 Hz difference between complexes **94** and **95**.^[99, 102] The same trend was observed in complex **92**, which showed a huge $^1J_{\text{P},\text{F}}$ value because of the hydroxyl function. The IR spectrum of complex **92** showed a broad absorption signal at 3373 cm^{-1} due to the OH moiety. After literature survey (20.06.2010), it turned out that the *side-on* complex **92** was the first example of a η^2 Wittig ylide complex of type **XXXV** (Scheme 55).



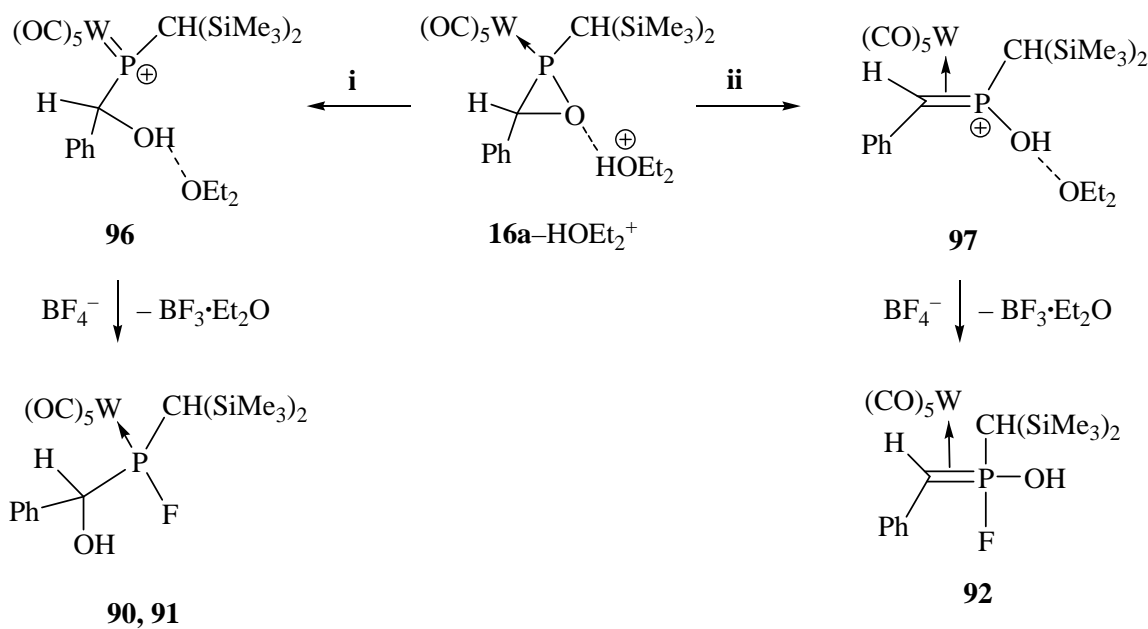
Scheme 55. Wittig η^2 **XXXV** and η^1 ylide complexes **XXXVI**.^[112-118]

Phosphorus ylides^[103] are the “key player” of the so-called Wittig reaction, which is of great importance in olefin chemistry and has various industrial applications;^[104,105] the discovery

yielded G. Wittig the Nobel prize in 1979. The double bond between the phosphorus and the carbon atom in the Wittig ylides can be described by canonical formulae such as ylen and/or the 1,2-dipolar ylide. *P*-Metallo derivatives of phosphorus ylides^[106-108] as well as carbon-bound derivatives^[109-111] had been studied before, but also ylidene η^1 -complexes **XXXVI** had been already established.^[112-118]

Two possible pathways for the formation of the two different products, the fluorophosphane complexes **90**, **91** might result from the protonation of the oxygen atom of the oxaphosphirane complex **16a** and fluoride-induced ring-opening via P-O bond cleavage. On the other hand, the *side-on* complex **92** might be formed in a competing reaction from the rearranged product **97** formed via *O*-protonation followed by fluoride attack on the phosphorus of **97**; it should be noted that tetrafluoroborate might have reacted instead.

Once again, Helten performed DFT calculations (Table 19) to examine the preference for P-O bond cleavage (of **16a**) over *side-on* complex formation upon approach of a super-acid towards the oxaphosphirane complex oxygen center (Scheme 56).



Scheme 56. Computed acid-induced ring-opening reaction of complex **16a**.^[115]

Table 19. Calculated thermo chemical data for reactions shown in Scheme 56 (all values in kJ/mol; B3LYP/aug-TZVP/ECP-60-MWB(W), COSMO (CH₂Cl₂) // RI-BLYP/aug-SV(P)/ECP-60-MWB(W), COSMO (CH₂Cl₂)).

i)	ΔG^\ddagger_{298}	+19.3
	$\Delta_R G_{298}$	+2.5
ii)	ΔG^\ddagger_{298}	+51.3
	$\Delta_R G_{298}$	-40.2

In order to find an explanation for the divergent behavior with respect to P–O vs. C–O bond cleavage, both reactions were computed by means of DFT calculations starting from **16a**–HOEt₂⁺, where the acid proton, mediated through diethyl ether, is bound to the oxaphosphirane oxygen center via O–H–O hydrogen bonding (Scheme 56); relative free energies are given in Table 19. The formation of complexes **90**, **91**, can be explained by

assuming *O*-protonation of **16a** to be the first step, which then is followed by a kinetically preferred P–O bond cleavage and formation of the phosphonium complex **96** which can be attack for the fluorine atom at the two different diastereofacial sites. However, in the case of **16a** the reaction is endergonic and, hence, complex **96** may partly reacts back to **16a** and via reaction **ii** to give complex **97**. Subsequently, a transfer of fluoride from tetrafluoroborate onto **97** to give **92** might take place.

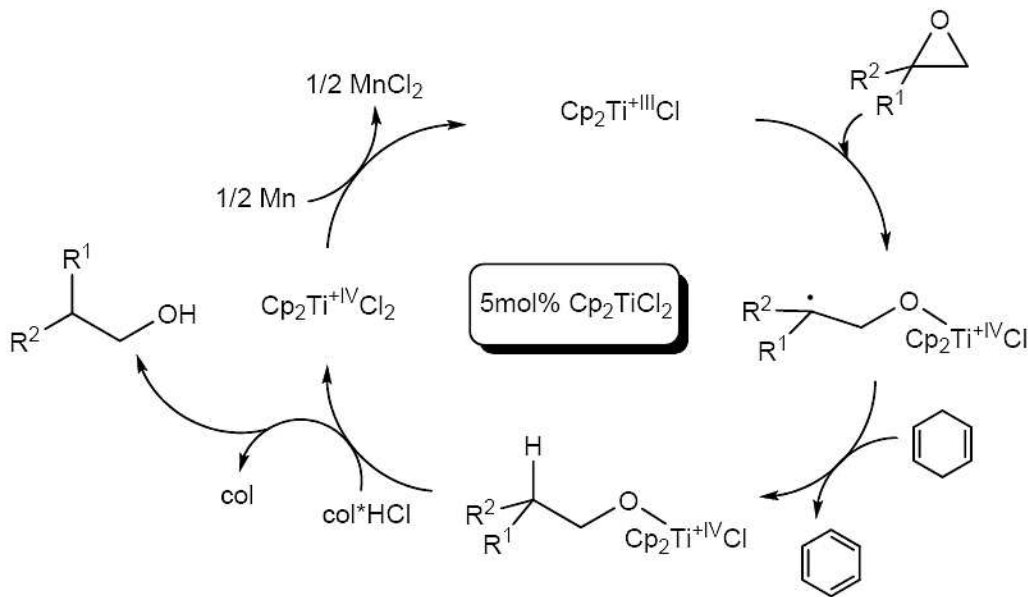
V.1 Introduction into ring-opening reactions of oxiranes using Ti(III) complexes as SET reagents

One of the major aims of this work was to compare the ring-opening chemistry of oxiranes (epoxides) with oxaphosphirane complexes. Oxiranes are among the most and best investigated three-membered heterocycles in organic chemistry, and it is well known that they can undergo ring-opening reactions with low valent Ti species, as reported by Nugent and Rajan Babu reported for the reductive epoxide ring-opening using titanocene(III) derivatives.^[116] They used isolated $[\text{Cp}_2\text{TiCl}]_2$ (or generated *in situ* from Cp_2TiCl_2 and granulated zinc) as SET (Single Electron Transfer) reagents (Scheme 57).



Scheme 57. *In situ* formation of reactive Ti(III) complexes.^[116]

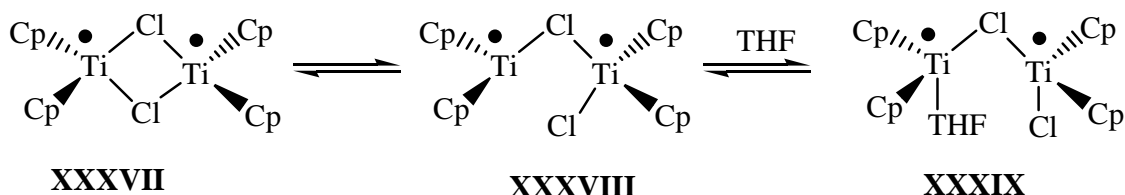
A general advantage of radical reactions compared to ionic reactions is the higher functional group tolerance. This is specially important in the synthesis of highly functionalized compounds, e.g. complex natural products, where the Cp_2TiCl induced radical epoxide opening is well established.^[117] Subsequently, Gansäuer *et al.* developed a catalytic version of the reaction which was reported in 1998.^[118] After reduction and epoxide ring-opening, the carbon centered radical is saturated by hydrogen transfer from 1,4-cyclohexadiene. Regeneration of Cp_2TiCl was achieved by protonation of the oxygen, which is bound to titanium using 2,4,6-collidine hydrochloride (col·HCl); this provides also the chlorine for renewing Cp_2TiCl_2 (Scheme 58)



Scheme 58. Titanocene(III) complex-catalyzed reductive epoxide opening.^[118]

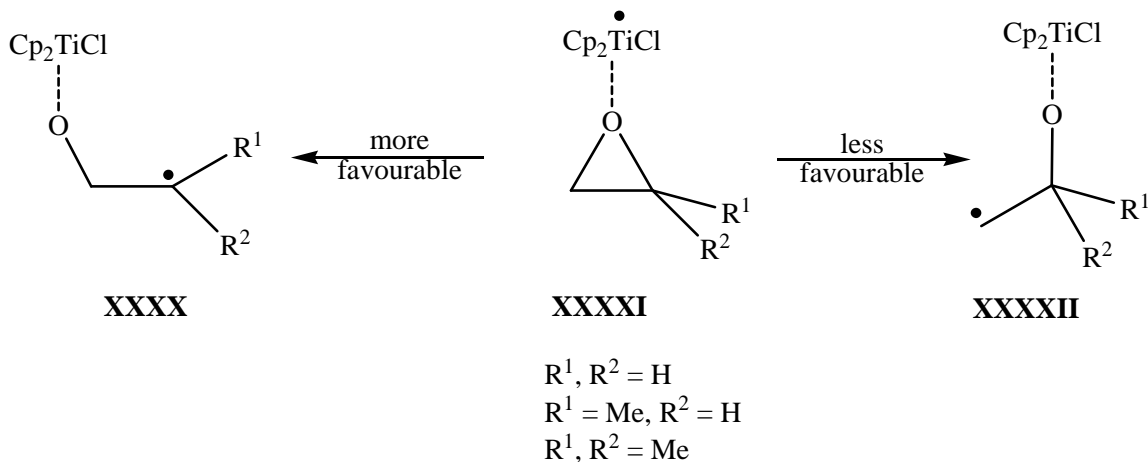
The catalytic epoxide ring-opening by titanocene(III) was extended by Gansäuer *et al.* to enantioselective ring-opening of *meso*-epoxides by employing substoichiometric quantities of titanocene complexes with chiral ligands.^[119]

The nature of the compounds derived from titanocene dichloride by reduction was studied in detail by electrochemical studies and UV spectroscopy.^[120] Specially the structure and behavior of “Cp₂TiCl” in THF solution is of interest as it is known that in the solid state dicyclopentadienyltitanium(III) chloride appears as dimer, bridged by two chlorine atoms and features a strong interaction between the two d¹ electrons at each Ti (**XXXVII** in Scheme 59).^[121]



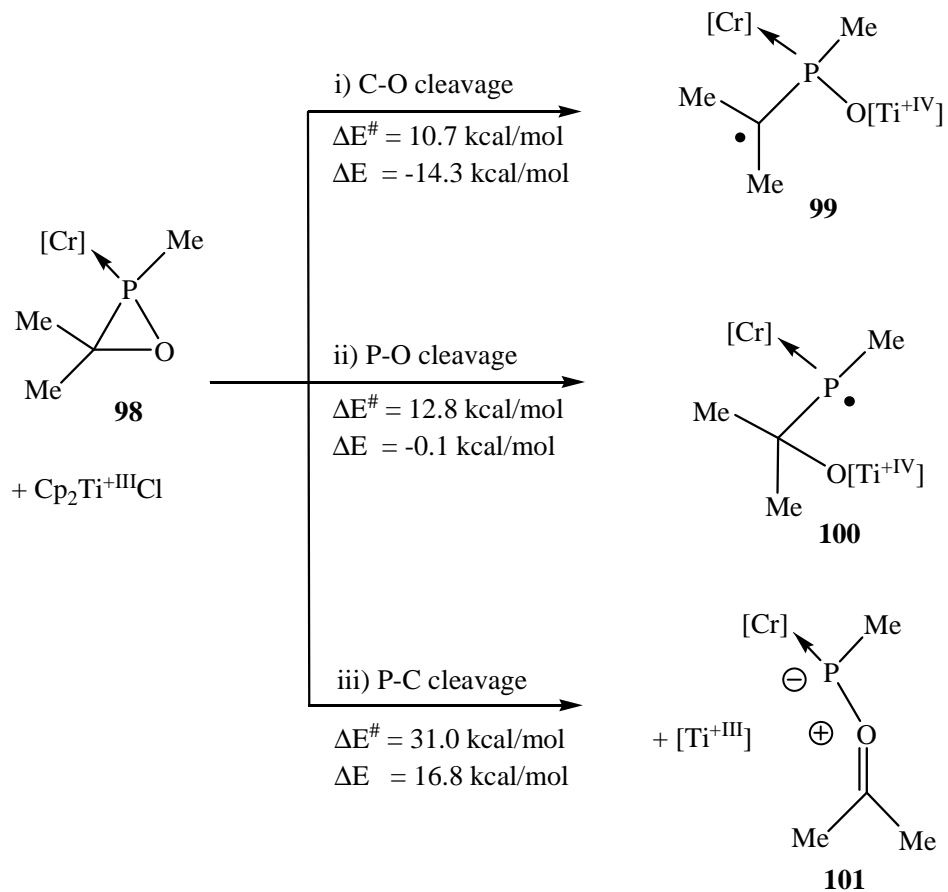
Scheme 59. Half-open dimers **XXXVIII** and **XXXIX**, proposed to be involved in epoxide ring-opening.^[121]

In solution a rapid equilibrium between half-open dimers and the dimer **XXXVII** were proposed, thus having an accessible coordination site (**XXXVIII** and **XXXIX** in Scheme 59). The free coordination site can be occupied by solvent molecules, *i.e.*, THF. Dimerisation increases according to the principle of activation of electrophiles by electrophiles through dimeric association.^[122] This will result in a faster formation of epoxide-titanocene complexes, and possibly also influences the activation energy of the epoxide ring-opening step. In the case of epoxides (oxiranes) one of the two carbon-oxygen bonds can be reductively cleaved, so that the carbon-carbon bond remains and one of the carbons (probably the most substituted one) become the new radical centre (Scheme 60).^[116]



Scheme 60. Possible ring-opening reactions of oxirane complexes.^[124]

As oxaphosphirane chemistry represented a new area of research, the reaction course of ring-opening process was not easy to predict evident, especially which of the three ring-bonds will preferably be cleaved and which center will become the radical center and/or have the highest spin density. To examine this theoretically Neese and Streubel performed calculations on the three possible pathways reactions of the oxaphosphirane complex **98** with Ti(III) species (Scheme 61).^[16]



Scheme 61. Calculated possible pathways of the oxaphosphirane complex ring-opening reaction with Ti(III) complexes, BP86/def2-tzvp.^[16]

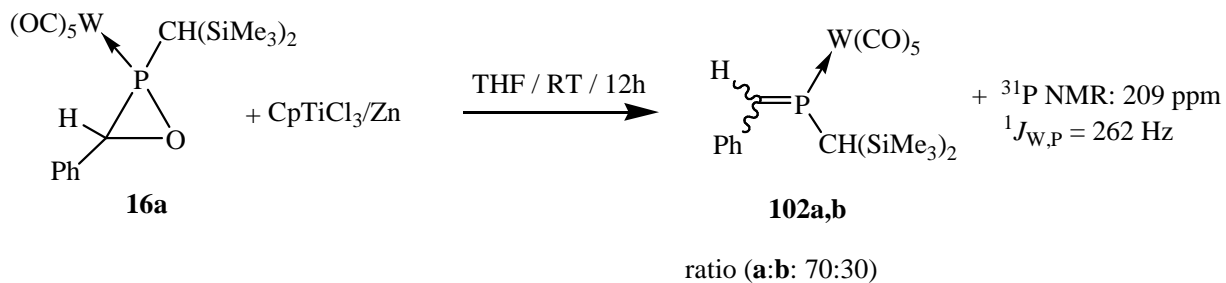
For the CpTiCl_2 -induced oxaphosphirane ring-opening low barriers were calculated for paths including C-O and P-O bond cleavage processes; more difficult was to estimate the selectivity of the reactions. The C-O bond cleavage (Scheme 61) leads to complex **99** having a ligand with a carbon-centered radical and a stable Ti(IV)-O bond, in close analogy to the

epoxide-based $\{\text{Cp}_2\text{TiCl}\}$ chemistry.^[123] Cleavage of the P-O bond leads to complex **100** with a ligand possessing a P-centered radical with a spin-population of roughly 0.66 unpaired electrons that is bound to a $\text{Cr}(\text{CO})_5$ fragment having a spin-population of roughly 0.2 unpaired electrons in the t_{2g} -orbitals. Therefore the resulting ligand in **99** might be described as a phosphanyl complex-substituted alkoxytitanium(IV) complex. Finally, opening of the P-C bond leads to dissociation of the Ti(III) fragment and formation of a high-energy product **101**, a phosphacarbonyl-ylide complex,^[37] which displays an acetone moiety coordinated to the *P*-center of the terminal phosphinidene chromium complex. Of the three products the most stable one by far is the C-O bond cleavage product **99** that is about 15 kcal·mol⁻¹ more stable than **100**, and almost 30 kcal·mol⁻¹ more stable than **101**. In the epoxide chemistry the ring-opening reaction is close to thermoneutral according to all theoretical calculations performed so far.^[123] In keeping with the thermodynamic results, the calculations showed that the lowest transition state occurs for the C-O bond cleavage and is calculated to be 10.7 kcal·mol⁻¹ compared to 8.7 kcal·mol⁻¹ obtained for the analogous $\{\text{Cp}_2\text{TiCl}\}$ /epoxide chemistry at the same level of theory.^[123]

From comparative calculations with $\text{Mo}(\text{CO})_5$ and $\text{W}(\text{CO})_5$ instead of $\text{Cr}(\text{CO})_5$ coordinated at phosphorus it was deduced that the influence of the metal fragment on the reactivity with CpTiCl_2 is negligible.^[124] Comparison of the three calculated ring-openings with Cp_2TiCl , CpTiCl_2 and TiCl_3 showed that increasing Lewis-acidity is expected to increase the reactivity significantly. Therefore, it appeared to be attractive to carry out the first comparative study of the reductive ring-opening of oxaphosphirane complexes.

V.2 Ring-opening reactions of the oxaphosphirane complex **16a** using *in situ* generated Ti(III) complexes as SET reagents

Reaction of oxaphosphirane complex **16a** with *in situ* prepared CpTiCl₂ (from CpTiCl₃ and zinc in THF) led to the formation of the phosphaalkene complexes **102a,b** (Scheme 62); in addition, small amounts of a compound at 209 ppm (¹J_{W,P} = 262 Hz) was observed in the reaction solution. Unfortunately, all complexes **102a,b** were very unstable in solution, therefore, only some NMR data could be obtained (Table 20).



Scheme 62. Formation of the phosphaalkene complexes **102a,b** from oxaphosphirane complex **16a**.

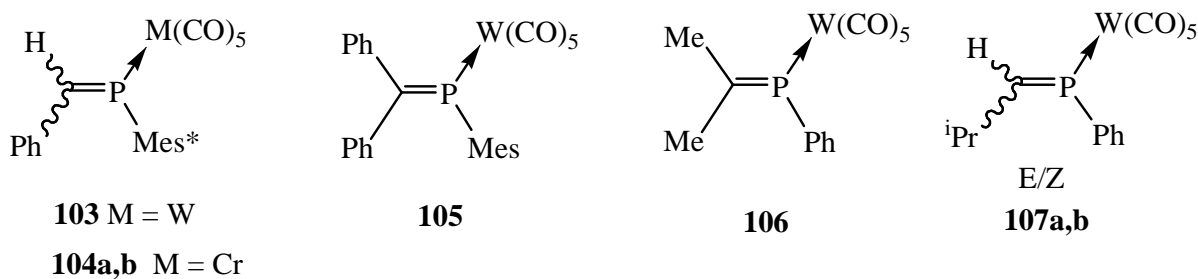
Besides their low-field ³¹P{¹H} NMR resonances, structurally supportive for the assignment to the complexes **102a,b** were the ¹³C{¹H} NMR data, especially the signals at 165.1 and 167.0 ppm with a ¹J_{P,C} coupling of about 40 Hz, which confirmed the presence of a P,C double bond. The resonances of the CH=P protons were found at 8.25 ppm (**102a**) and at 8.80 ppm (**102b**), which are in the same range as the values found for the complexes **104a,b**^[128] (Scheme 63, Table 20). It is also noteworthy to note the substantial differences between the resonances of the CH(SiMe₃)₂ protons of both isomers **102a,b** (almost 1.5 ppm)

and also their $^2J_{\text{P},\text{H}}$ coupling constant values were significantly different (**102a**: 20 Hz and **102b**: 5.3 Hz).

Table 20. Selected NMR data (THF-d⁸) of complexes **102a,b**.

	$\delta^{31}\text{P}$ [ppm] ($^1J_{\text{W,P}}$ [Hz])	$\delta(^1\text{H})$ [ppm] ($J_{\text{P,H}}$ [Hz])		$\delta(^{13}\text{C}\{^1\text{H}\})$ [ppm] ($J_{\text{P,C}}$ [Hz])	
		CH(SiMe ₃) ₂	CHPh	CH(SiMe ₃) ₂	CHPh
102a	212.0 (260.0)	3.05 (20.0)	8.25 (17.5)	23.5 (19.6)	165.1 (39.0)
102b	219.0 (260.0)	1.50 (5.3)	8.80 (20.3)	34.0 (16.8)	167.0 (40.0)

Some examples of η^1 -bound phosphaalkene pentacarbonyltungsten complexes were reported so far, most of them synthesized through “Phospha-Witting reactions” (cf. Scheme 56).^[125-129] Among them only complexes **104a,b**,^[128] **105**,^[125] were fully characterized, and for all other phosphaalkene complexes only their $^{31}\text{P}\{^1\text{H}\}$ NMR data (Table 21) were given because of the instability of these compounds. In case of complexes **104** and **107** the formation of two diasteromers was also observed.



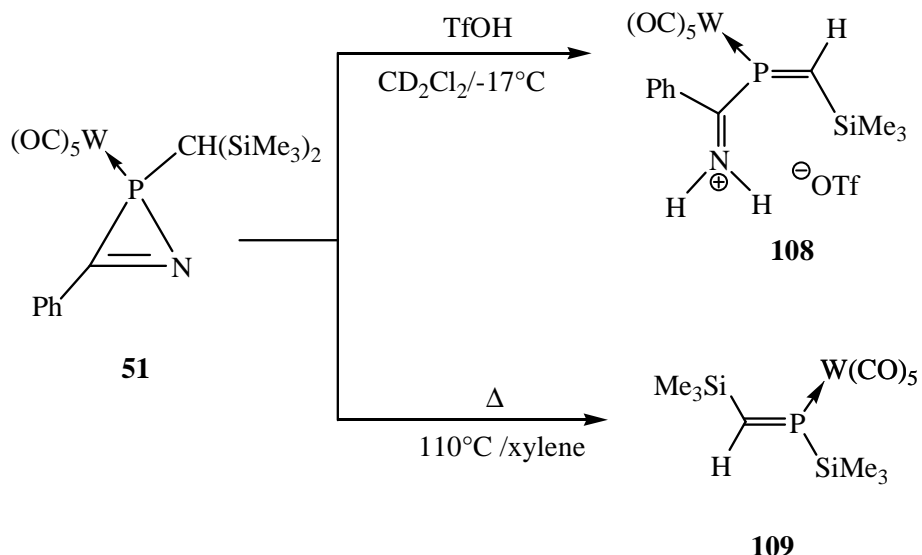
Scheme 63. Literature-described phosphaalkene pentacarbonyltungsten complexes.^[125-129]

Table 21. $^{31}\text{P}\{^1\text{H}\}$ NMR data of complexes **103-107a,b**.

	103 ^[126]	105 ^[127]	106 ^[125, 129]	107a ^[125,129]	107b ^[125, 129]
$\delta^{31}\text{P}$ [ppm] ($^1J_{\text{W,P}}$ [Hz])	212 (271)	195 (264)	176 (261)	186 (259)	191 (-)

As it can be concluded from table 29 and 21 the $^{31}\text{P}\{^1\text{H}\}$ NMR data of complexes **102a,b** agreed very well with those found in the literature.

Two more closely related phosphaalkene complexes were obtained from the 2*H*-azaphosphirene complex **51** via two different methods. The complex **108**^[130] was obtained as part of the result of the protonation of the complex **51** at low temperature and complex **109**^[131] from the rearrangement of a SiMe₃ group of a transiently formed phosphinidene complex at 110°C.



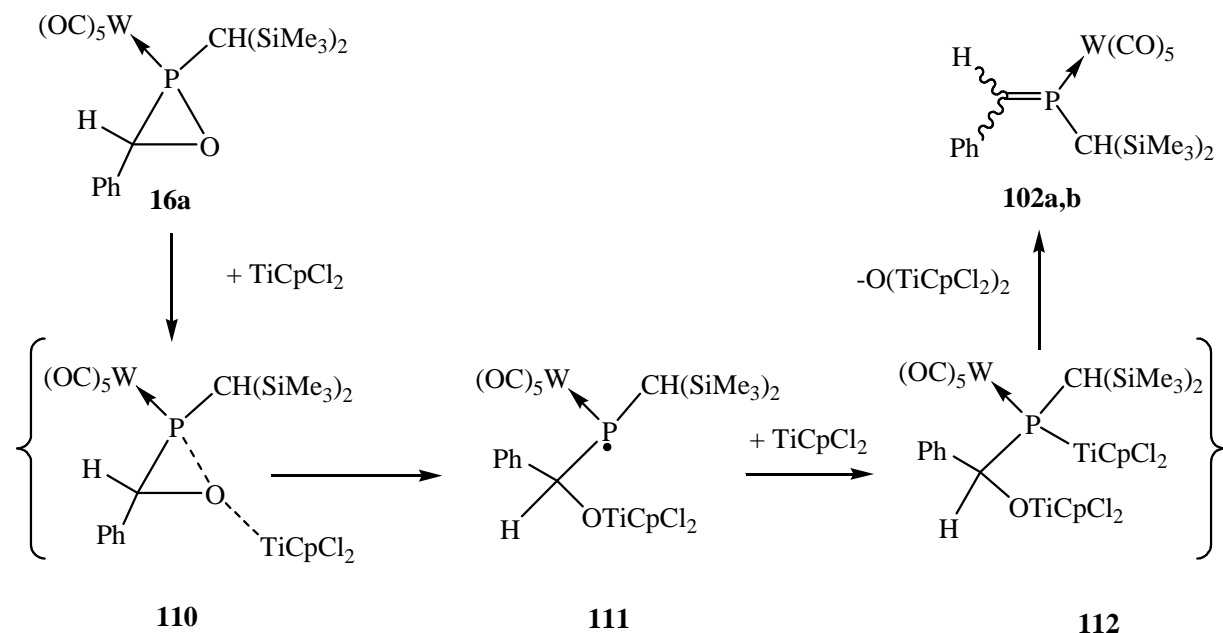
Scheme 64. Synthesis of phosphaalkene complexes **108**, **109**.

In both cases the formation of one diastereomer was observed: *Z* in the case of complex **108** and *E* for **109**. Unfortunately, the NMR data of these complexes differed too much to those of complexes **102a,b** and no comparison of the stereochemistry could be done (³¹P{¹H} NMR complex **108**: 223.3 ppm ¹J_{W,P} = 293.0 Hz, complex **109**: 295.5 ppm ¹J_{W,P} = 217.5 Hz; ¹H NMR for the P=CH proton complex **108**: 8.52 ppm ²J_{P,H} = 1.5 Hz, complex **109**: 9.83 ppm, ²J_{P,H} = 32 Hz). Other attempts to clarify the *Z/E* configuration of complexes **102a,b** by ¹H-NOE experiments failed (all isomers showed a correlation of the CHPh with the SiMe₃ groups, which can be only explained by the wrong assignment of the T1(spin-lattice relaxation time)).^[132] As the phosphaalkene complexes **102a,b** could not be crystallized or further purified by chromatography, its stereochemistry remained unclear.

V.2.1 Proposed mechanism for the formation of phosphaalkene complexes

102a,b

Based on the theoretical investigations of Neese and Streubel^[16] and assuming an analogy to oxiranes, the following mechanism for the formation of the phosphaalkene complexes **102a,b** was proposed (Scheme 65).



Scheme 65. Proposed mechanism for the formation of phosphaalkene complexes **102a,b**.

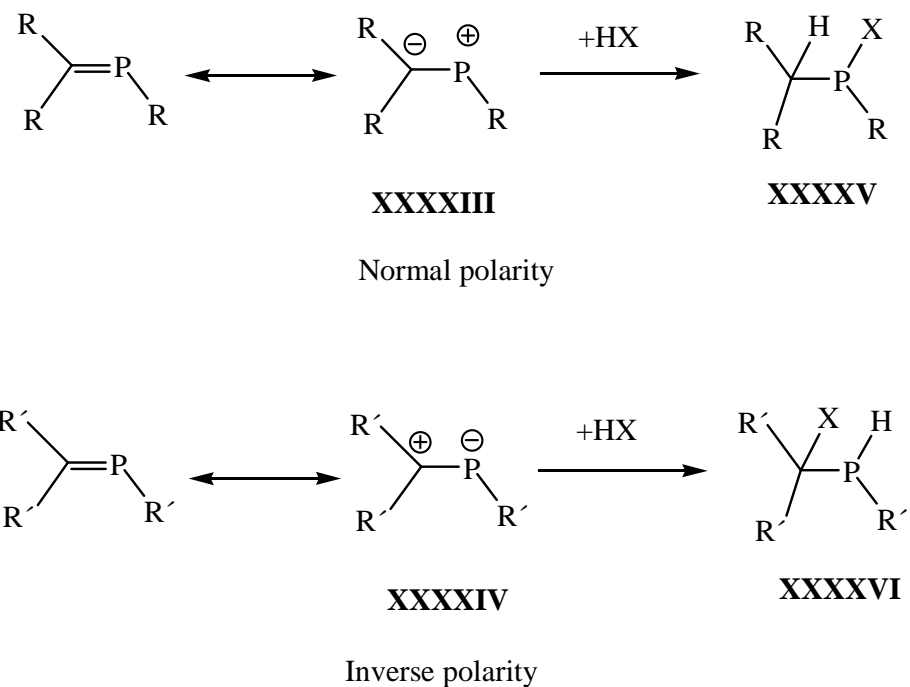
The first step could be a weak coordination of the titanium(III) complex to the oxygen atom of **16a** that leads to a reductive cleavage of the P-O bond to yield **111**. The P-centered radical complex **111** reacted with a second TiCpCl_2 moiety, present in solution, to form the intermediate complex **112** possessing a Ti-P and O-Ti bond, which is unstable and eliminates $\text{O}(\text{TiCpCl}_2)_2$ to furnish complexes **102a,b** as final deoxygenation products.

A similar mechanism was recently proposed for the deoxygenation of epoxides,^[137] which also required an excess of TiCpCl_3 to complete the reaction due to the coordination of two

TiCpCl₂ moieties in the product that then eliminates O(TiCpCl₂)₂ in the last step. In line with the proposed mechanism was the observation that the reaction of the oxaphosphirane complex **16a** was not so effective if “Cp₂TiCl” was used; it didn’t form complexes **102a,b** as effective as TiCpCl₂. This points to severe steric restraints as the bonding of two Cp₂TiCl groups within a **112**-related complex would impose steric repulsion between these groups and the W(CO)₅ and CH(SiMe₃)₂ groups.

V.2.2 Reactivity of the phosphaalkene complexes **102a,b**

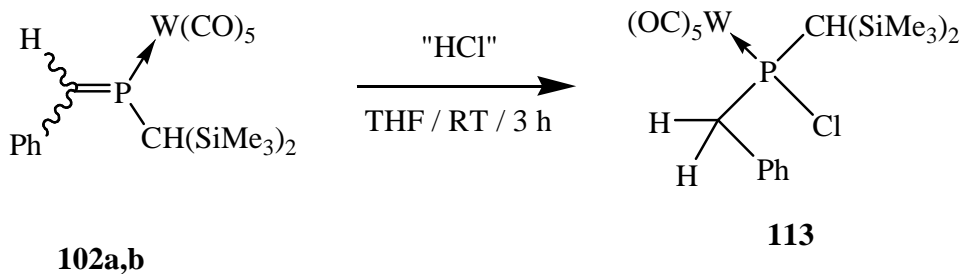
Phosphaalkene complexes and phosphaalkene derivatives could possess similar reactivity if the HOMO is defined by the π -system of the P-C double bond, and thus by its electronic properties. In general, phosphaalkenes can show a “normal polarity”,^[138] in which the phosphorus has a formal positive charge and the carbon the negative (**XXXXIII**) or an “inverse polarity”,^[139] in which the phosphorus has a negative charge and the carbon a positive (**XXXXIV**) (Scheme 66).



Scheme 66. Reactivity of phosphaalkenes compound towards protic compounds.

Complexes having normally polarised phosphaalkene ligands usually react with protic compounds via 1,2 addition so that the proton is added to the carbon center,^[140] while the inverted phosphaalkenes react to yield P-H compounds (Scheme 66).^[141]

Solutions of freshly prepared complexes **102a,b** showed a high sensitivity towards traces of air and/or water, the latter might have caused the formation of HCl and thus 1,2-addition of HCl to form selectively chlorophosphane complex **113** (Scheme 67) which was isolated and unambiguously characterized by single-crystal X-ray diffractometry .



Scheme 67. Proposed formation of chlorophosphane complex **113** from phosphaalkene complexes **102a,b**.

Although plausible, the origin of HCl was not apparent or proven. Earlier on, some studies pointed out that titanium(III) chloride, having water coordinated, could act as hydrogen donor and react with free chlorine radicals in the reaction solution.^[142] On the other hand Ti(IV) species can be easily hydrolyzed by water to form HCl.^[143]

The selected NMR data of **113** are shown in Table 22. The chlorophosphane complex **113**, displayed a $^{31}\text{P}\{\text{H}\}$ NMR resonance at 124.9 ppm with a tungsten-phosphorus coupling constant of 278 Hz thus being very close to the data of complexes **85a,b**.

Table 22. Selected NMR data (CDCl_3) of complex **113**.

	$\delta^{31}\text{P}$ [ppm] ($^1J_{\text{W,P}}$ [Hz])	$\delta(^1\text{H})$ [ppm] ($J_{\text{P,H}}$ / $^2J_{\text{H,H}}$ [Hz])			$\delta(^{13}\text{C}\{^1\text{H}\})$ [ppm] ($J_{\text{P,C}}$ [Hz])	
		$\text{CH}(\text{SiMe}_3)_2$	H^1	H^2	$\text{CH}(\text{SiMe}_3)_2$	CH_2
113	124.9 (278.0)	1.88 (10.2)	3.50 (10.1/13.6)	3.90 (13.9/13.6)	30.5 (16.2)	45.5 (10.4)

And again, the ^1H and $^{13}\text{C}\{^1\text{H}\}$ NMR data were very similar to those of the complexes **85a,b-85c**: The CH_2 moiety showed a $^{13}\text{C}\{^1\text{H}\}$ NMR signal at 45.5 ppm with $^1J_{\text{P,C}}$ coupling of 10.4 Hz and the diastereotopic protons showed a $^2J_{\text{H,H}}$ coupling of 13.6 Hz; the $^3J_{\text{P,H}}$ couplings of H^1 and H^2 differed by almost 4 Hz.

Colourless crystals of complex **113**, suitable for X-ray diffractometric studies, were obtained from a concentrated *n*-pentane solution. The crystal structure (triclinic, space group P (-1)) of complex **113** was slightly disordered (Figure 36); selected structural data are shown below and as their parameters are very close to the chlorophosphane complexes reported before in this work it will not discussed further.

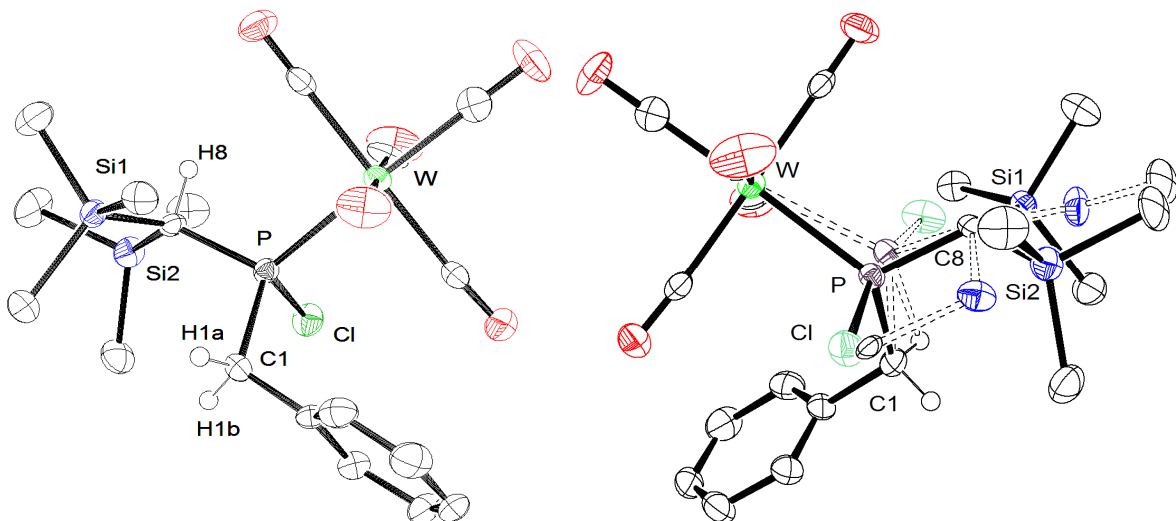
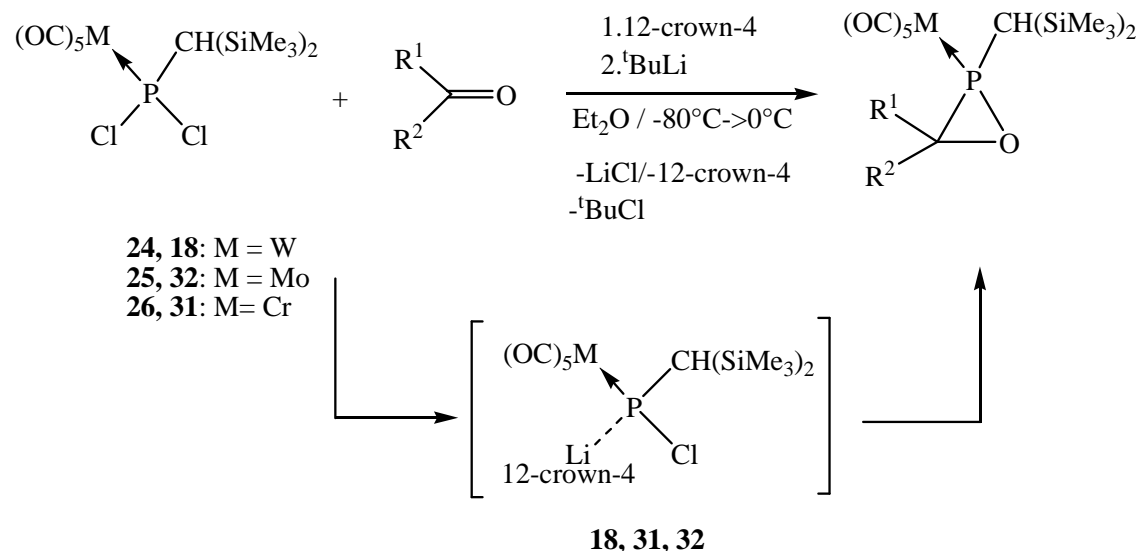


Figure 36. Molecular structure of chlorophosphane complex **113** in the crystal (50 % probability level; main orientation 90 %; hydrogen atoms except H1 and H2 are omitted for clarity; reduced structure on the left). Selected bond lengths [\AA] and angles [$^\circ$]: W-P 2.5032(16), P-Cl 2.098(2), P-C(1) 1.856(5), P-C(8) 1.821(5), W-P-C(l) 122.89(19), C(8)-P-W 117.11(18), Cl-P-W 105.74(8). Further details on structure solution and refinement can be found in the appendix under GSTR070.

VI. Summary

The aim of this thesis was to investigate scope and limitations of the new method based on recently discovered transiently formed species, the Li/Cl phosphinidenoid complexes, in the synthesis of oxaphosphirane complexes of the group 6 metal triade. Another important part of this work was focused on ring-opening and ring-expansion reactions using Brønstedt acids and Ti(III) complexes, which were accompanied by theoretical studies, kindly performed by Helten and Krahe as mentioned.

In the first chapter the synthesis of the new oxaphosphirane complexes **29-30**, **33-39** and **41**, **42** synthesized from dichloro(organo)phosphane complexes **24-26** ($R = CH(SiMe_3)_2$; for chromium, molybdenum and tungsten) via chlorine/lithium exchange in the presence of 12-crown-4 and carbonyl derivatives (Scheme 68) is presented and selected spectroscopic data discussed.



16a: $M = W; R^1 = H; R^2 = Ph$
29: $M = Cr; R^1 = H; R^2 = Ph$
30: $M = Mo; R^1 = H; R^2 = Ph$

33: $M = W; R^1 = H; R^2 = o\text{-Tolyl}$
34: $M = W; R^1 = H; R^2 = o\text{-Anisy}$
36: $M = W; R^1 = H; R^2 = tBu$
37: $M = W; R^1 = H; R^2 = iPr$
38: $M = W; R^1 = H; R^2 = nPr$
39: $M = W; R^1 = H; R^2 = Me$

41: $M = W; R^1 = R^2 = Ph$
42: $M = W; R^1 = R^2 = Me$

Scheme 68. Synthesis of new oxaphosphirane complexes via the reaction of transiently formed Li/Cl phosphinidenoid complexes **18**, **31** and **32**.

In general, pure oxaphosphirane complexes are stable at ambient temperature under inert gas atmosphere and only complex **39** showed a reduced stability in solution and could be characterized only from the reaction solution. Most of these complexes could be crystallized and thus structurally confirmed by single-crystal X-ray diffractometry; complex **41** is shown as one representative example in Figure 37.

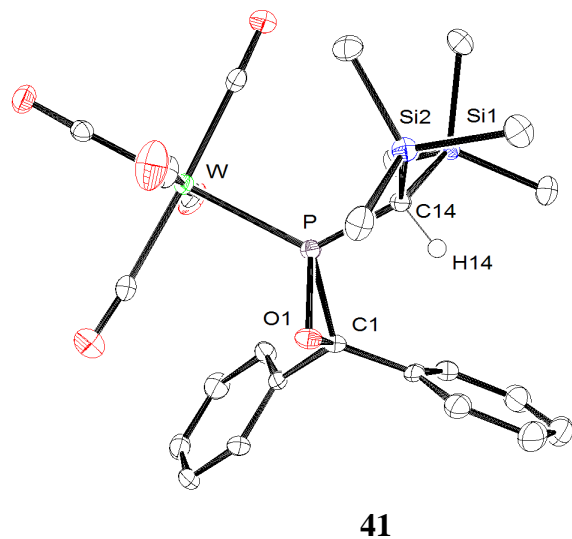
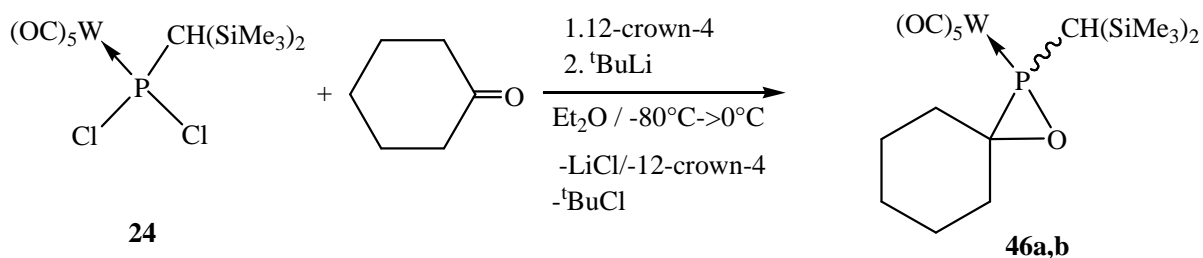


Figure 37. Molecular structure of complex **41** in the crystal (hydrogen atoms except H14 omitted for clarity).

It was also possible to synthesize the first spiro-oxaphosphirane complexes **46a,b** (Scheme 69), which showed an unusual form of isomerism. The molecular structure of complex **46a** was unambiguously elucidated by X-ray diffractometry (Figure 38).



Scheme 69. Synthesis of the spiro-oxaphosphirane complexes **46a,b**.

The crystallographic parameters of all oxaphosphirane complexes presented in this work are very similar and only little influence on the C-substitution pattern onto the oxaphosphirane ring parameters was observed.

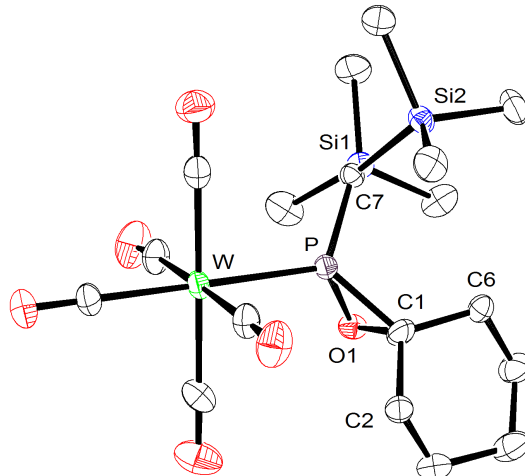
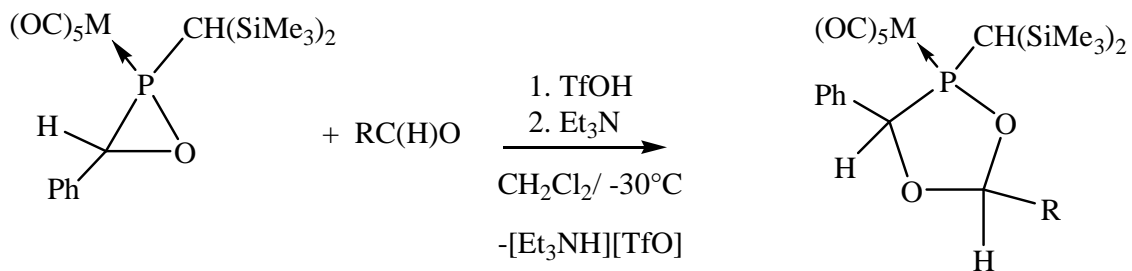


Figure 38. Molecular structure of complex **46a** in the crystal (hydrogen atoms omitted for clarity).

Although the transient Li/Cl phosphinidenoid complexes showed a high selectivity in all cases mentioned beforehand, the limits of this method came to the fore if very bulky ketones or *N*-functionalized aldehydes or ketones were employed. In these cases the formation of oxaphosphirane complexes was not observed and unknown side-reactions took place.

In the second chapter the chemical behavior of oxaphosphirane complexes was studied first with special focus on ring enlargement reactions. Acid-induced ring expansion reactions of the chromium, molybdenum and tungsten oxaphosphirane complexes **16a**, **29**, **30** was achieved using triflic acid, in the presence of carbonyl derivatives, and subsequent treatment with triethylamine to form the 1,3,4-dioxaphospholane complexes **62-66a,b** (Scheme 70).



- 62a,b:** M = Cr; R = Ph
- 63a,b:** M = Mo; R = Ph
- 64a,b:** M = W; R = Ph
- 65a,b:** M = W; R = ⁱPr
- 66a,b:** M = W; R = Me

Scheme 70. Synthesis of 1,3,4-dioxaphospholane complexes **62-66a,b**.

Although the yields were relatively low in some cases, because of side-reactions of the protonated 1,3,4-dioxophospholane derivatives observed by low temperature $^{31}\text{P}\{^1\text{H}\}$ NMR reaction monitoring, the derivatives **62-66a** were isolated in pure form through column chromatography; a mechanistic proposal for the product formation is described. In all molecular structures the preferred (typical) stereochemistry was such as the organic substituents at the five-membered ring adopted a *cis* position, whereas the W(CO)₅ group was bound in a *trans* fashion; one example is shown in Figure 39.

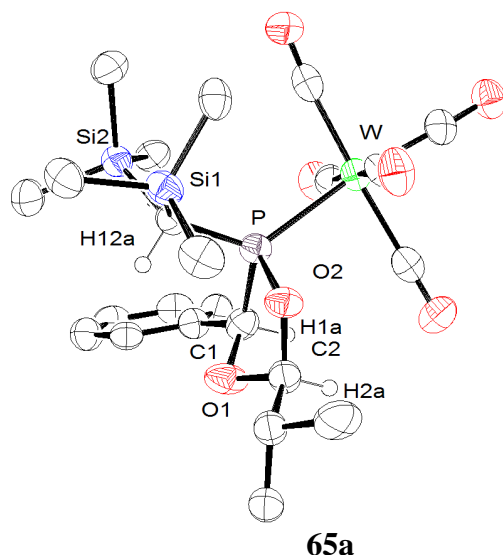
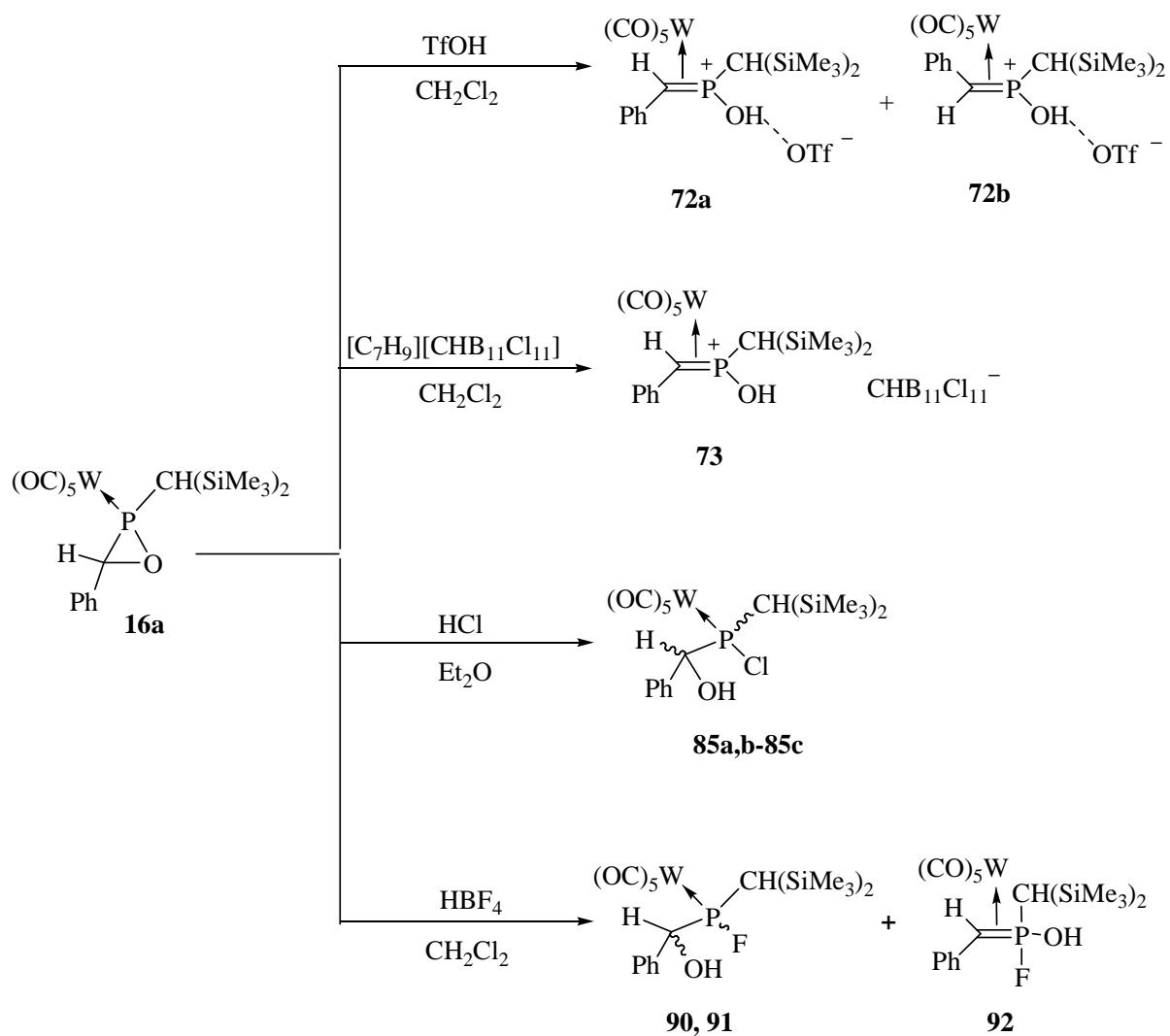


Figure 39. Molecular structure of complex **65a** in the crystal (hydrogen atoms except H1a, H2a and H12a omitted for clarity).

In chapter IV.2, experimental and theoretical studies were undertaken to get insight into the acid induced ring-opening reactions of the oxaphosphirane complex **16a** in the absence of trapping reagents. Here, the reactions of **16a** with triflic acid, a toluenium carbaboranid, hydrochloric acid and fluoroboronic acid were investigated and the products either isolated (**73**, **85c**, **90**) or characterized from the reaction mixture (**72** and **92**) (Scheme 71).



Scheme 71. Acid-induced ring-opening reactions of complex **16a**.

Of particular interest is the surprising formation of the *side-on* complexes after *O*-protonation of the oxaphosphirane complex **16a** using TfOH or [C₇H₉][CHB₁₁C₁₁], which was proven by

NMR studies and the crystal structure in the case of complex **73** (Figure 40); DFT calculations were performed onto the formation of the η^2 coordinated $\text{W}(\text{CO})_5$ complex.

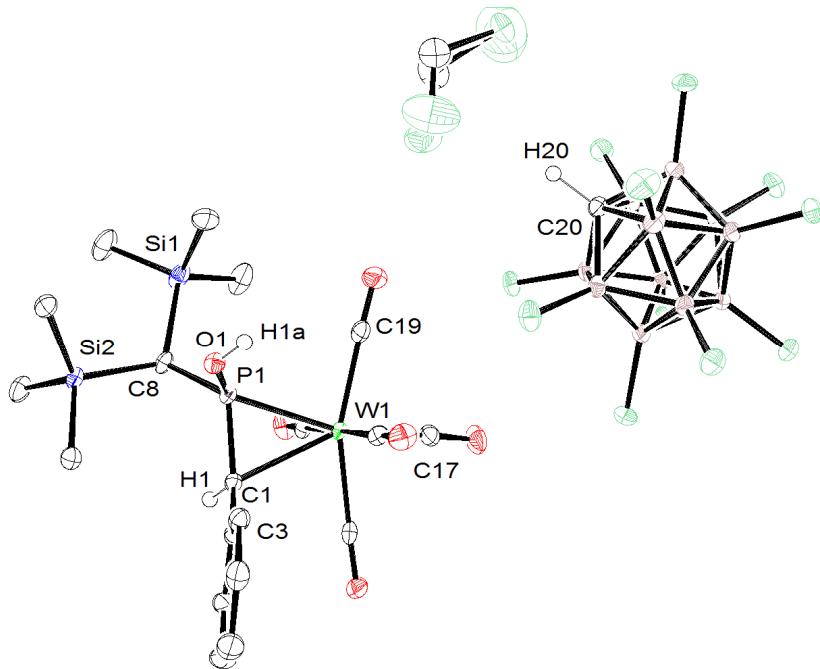


Figure 40. Molecular structure of complex **73** in the crystal (hydrogen atoms except H1, H1a and H20 omitted for clarity).

Protonation of the oxaphosphirane complex **16a** with HCl yielded a mixture of chlorophosphane complexes **85a-c** via P-O bond cleavage (Scheme 71); the structure of complex **85c** was unambiguously confirmed (Figure 41). Interestingly, resonance signals of complexes **85a,b** showed coalescence in the $^{31}\text{P}\{\text{H}\}$ NMR spectra, which was investigated and the process analysed with respect to its underlying kinetics by low temperature NMR spectroscopic measurements.

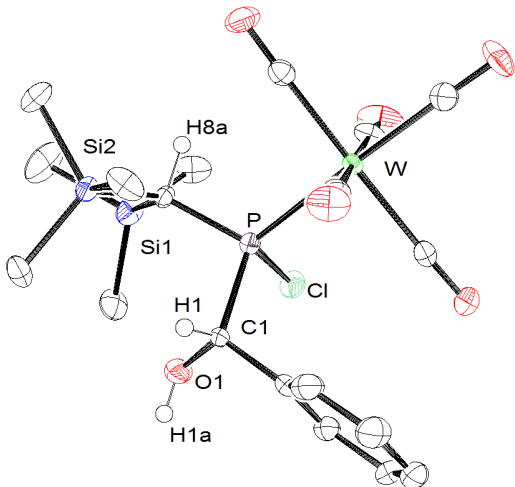
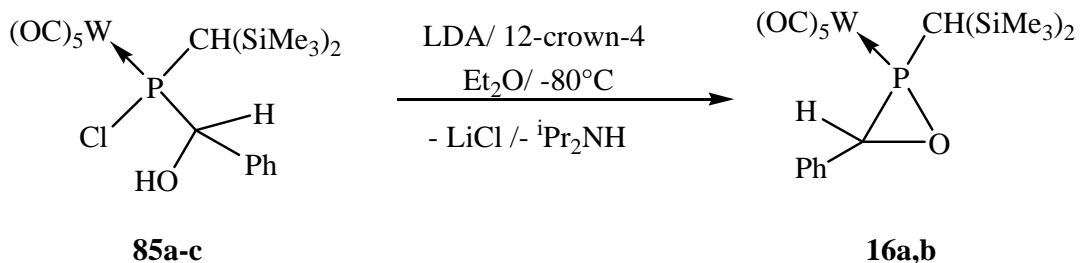


Figure 41. Molecular structure of complex **85c** in the crystal (hydrogen atoms except H1, H1a and H8a omitted for clarity).

In the reaction of **16a** with HBF_4 the outcome was (perhaps) even more surprising as two different products were obtained, the fluorophosphane complexes **90**, **91** (structurally confirmed by X-ray diffractometry) and the *side-on* complex **92** (Scheme 71); the latter represented the first example of a η^2 -Wittig ylide complex. The formation of these complexes could be explained on the basis of DFT calculations and provided information about two possible reactions pathways that involve P-O and C-O bond cleavages.

A novel synthetic route to oxaphosphirane complexes was discovered, presented in chapter IV.2.2.2, which is the deprotonation of the chlorophosphane complexes **85a-c** (Scheme 72). The reaction yielded a mixture of diastereomeric oxaphosphirane complexes **16a,b**. The structure of complex **16b** was unambiguously established by X-ray crystallography (Fig. 42, right) and confirmed the *RR/SS* constitution of this isomer.



Scheme 72. Synthesis of oxaphosphirane complexes **16a,b** from chloro(diorgano)phosphane complexes.

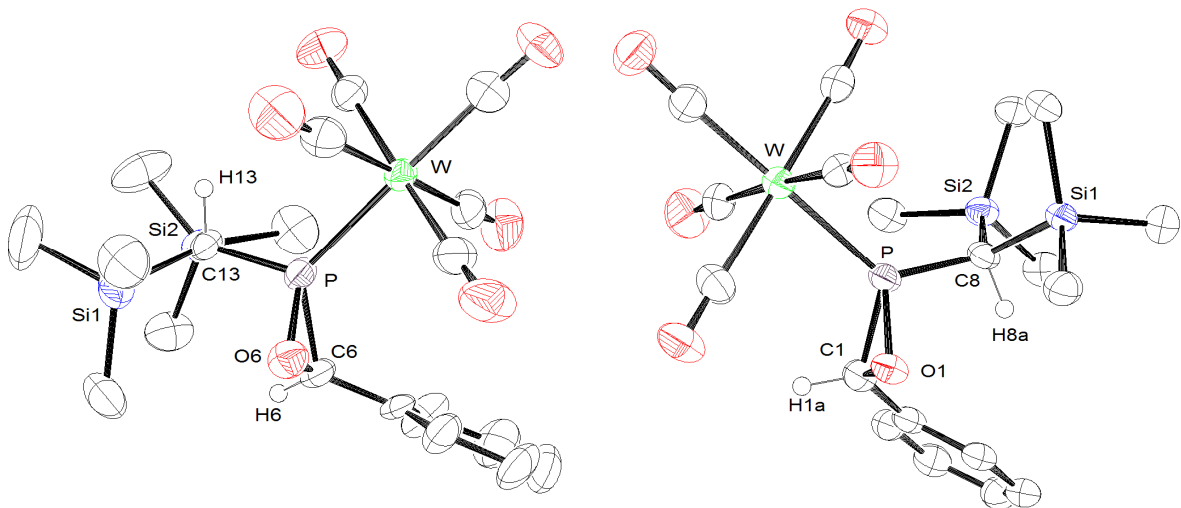
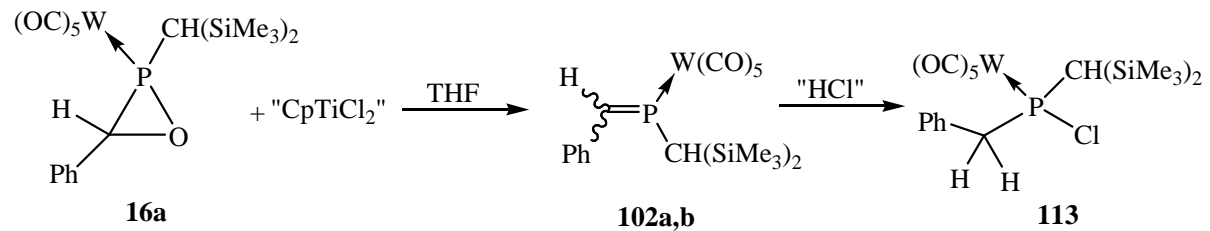


Figure 42. Comparison of the molecular structure of oxaphosphirane complex **16a** (left side)^[36] and its diastereomer **16b** (right side) in the crystal (hydrogen atoms except H1a, H8a for complex **16b** and H6, H13 for complex **16a**^[36] are omitted for clarity).

First investigations of SET reactions of oxaphosphirane complex **16a** using *in situ* prepared “CpTiCl₂” are presented in chapter V. These reactions led to a deoxygenation of the oxaphosphirane complex and formation of the phosphaalkene complexes **102a,b** (Scheme 73), which were not stable towards traces of air and reacted further to give the

chloro(diorgano)phosphane complex **113** as final product, which was also structurally confirmed.



Scheme 73. SET reaction of complex **16a** using Ti(III) species.

VII. EXPERIMENTAL PART

VII.1. Preparative methods

All reactions and manipulation were carried out under an atmosphere of dried argon ((BTS catalyst (Merck) heated at 100–130°C, phosphorus pentoxide, and silica gel), using standard Schlenk techniques with conventional glassware. Solvents were dried according to standard procedures^[144] and stored in brown-glass bottles over sodium wire and under inert-gas atmosphere. Most products were purified by low-temperature column chromatography using chromatographic columns equipped with integrated cooling mantles cooled with a connected cryostat. All devices were evacuated and refilled with Ar to avoid any moisture before perform the reactions.

VII.2 Measuring methods and devices

VII.2.1 Melting point determination

The melting points were recorded using from a Büchi (530 or S) capillary apparatus.

VII.2.2 Elemental analysis

Elemental analyses were performed using an elementary vario EL analytical gas chromatograph.

VII.2.3 Mass spectrometry

Electron ionization (EI) mass spectra were recorded on a Kratos MS 50 spectrometer (70eV).

VII.2.4 NMR spectroscopy

NMR spectra were recorded on a Bruker AX 300 spectrometer (^{11}B : 96.3 MHz, ^{29}Si : 60 MHz, ^{31}P : 121.5 MHz, ^{19}F : 282.4 MHz, ^{13}C : 75.0 MHz and ^1H : 300.1 MHz) or on or a Bruker Avance 400 spectrometer (^1H : 400.13 MHz; ^{13}C : 100.6 MHz; ^{29}Si : 79.5 MHz; ^{31}P : 161.9 MHz) at 30°C using CDCl_3 , CD_2Cl_2 or THF d⁸ as solvents and internal standards; shifts are given relative to external tetramethylsilane (^1H , ^{13}C , ^{29}Si), boron trifluoride diethyl etherate in CDCl_3 (^{11}B), trichlorofluoromethane (^{19}F) and 85% H_3PO_4 (^{31}P).

VII.2.5 UV/vis spectroscopy

UV/vis spectra were recorded on a UV-1650PC Shimadzu spectrometer spectrometer (λ = 190–1100 nm) using dichloromethane as solvent and quartz glass cells from the company Hellma with an optical path length of 1 cm at ambient temperature.

VII.2.6 Infrared spectroscopy

IR spectra were recorded on a Thermo Nicolet 380 spectrometer using KBr or nujol for the samples preparation. In case of complex **73** the crystals were measured on a Shimadzu-8300 FITR spectrometer placed inside the glove box.

VII.2.7 Crystal structure analysis

Crystal structures were recorded on a Nonius Kappa CCD diffractometer^[145], Nonius MACH3 diffractometer or a Bruker APEX-II CCD diffractometer with MoK α - 10829 (complex **73**). The structures were solved by Patterson methods or Direct Methods (SHELXS-97)^[147, 148] and refined by full-matrix least squares on F₂ (SHELXL-97).^[146, 148] All non-hydrogens atoms were refined anisotropically. Hydrogen atoms were included isotropically using the riding model on the bound

atoms; in some (denoted) cases hydrogen atoms were located in the Fourier difference electron density. Absorption corrections were carried out analytically or semi-empirically from equivalents.

VII.2.8 Chemicals

The following chemicals were commercially available and in some cases purified before used (producer name in brackets):

- Tungsten hexacarbonyl (Aldrich)
- *n*-butyllithium (1.6 M in hexane, Aldrich, Acros)
- *t*-butyllithium (1.6 M in hexane, Aldrich, Acros)
- Triethylamine (Aldrich)
- Acetone (Acros)
- 2-adamantanone (Aldrich)
- 2,2,4,4-tetramethyl-3-pentanone (Aldrich)
- 3,3-dimethylbutan-2-one (Aldrich)
- 1,1,3,3-tetramethylurea (Acros)
- *N,N*-dimethylformamide (Acros)
- Tetrahydro-1,3-dimethylpyrimidin-2(*IH*)-one (Aldrich)
- Silica gel Merck 60 (0.063-0.2 mm, pH = 6.5-7.5, Merck)
- Aluminium oxide Merck 90 actief neutral (70-230 mesh ASTM, Merck)
- Trifluoromethanesulfonic acid (Aldrich)
- 12-crown-4 (Merck)
- Acetaldehyde (Acros)
- Benzaldehyde (KMF)
- Fluoroboronic acid (1M in diethyl ether, Merck)
- Butyraldehyde (Merck)

- Chromium hexacarbonyl (Aldrich)
- Diisopropylamine (Aldrich)
- Isobutyraldehyde (Merck)
- Molybdenum hexacarbonyl (Aldrich)
- *o*-Anisaldehyde (Aldrich)
- *o*-Tolylaldehyde (Aldrich)
- Pivalinaldehyde (Acros)
- Benzonitrile (Acros)
- Borane THF complex 1M in THF (Merck)
- Cyclohexanone (Acros)
- Benzophenone (Acros)
- Cyclopentadienyltitaniumdichloride (Acros)
- Bis(cyclopentadienyl)titanium dichloride (Acros)
- Zinc (Aldrich)

The following compounds were synthesized according to published procedures

- (Bis(trimethylsilyl)methyl)dichlorophosphane^[46]
- [2-Bis(trimethylsilyl)methyl-3-phenyl-2*H*-azaphosphhirene-P]pentacarbonylchromium(0)^[54]
- [2-Bis(trimethylsilyl)methyl-3-phenyl-2*H*-azaphosphhirene-P]pentacarbonylmolybdenum(0)^[54]
- (Cyclopenta-1,3-dienyl)dichlorophosphane^[62]
- [dichlorophenylphosphane]pentacarbonyltungsten(0)^[61]
- (1,3,5-tri-*tert*-butylbenzyl)dichlorophosphane^[64]
- (1,3,5-trimethylbenzyl)dichlorophosphane^[63]

- Toluinium-2,3,4,5,6,7,8,9,10,11,12-undecachloro-1-carbadodecaborate^[82]

VII.2.9 Working procedure

The working procedure with the chemicals was accomplished using fume hoods and/or glove boxes according to the valid legislation (in agreement with the dangerous material regulation). All work resulting in this sense took place in appropriate protective clothing available in the laboratory. The already used solvents were collected in the canisters and properly removed according with the waste policy. The used silica gel was likewise supplied to the solid wastes.

VII.3 General procedure for the synthesis of
[(bis(trimethylsilyl)methyl)dichlorophosphane]pentacarbonylchromium(0),-
molybdenum(0) and -tungsten(0) [24-26]

Procedure A:

8.5 mmol of metalhexacarbonyl (1.87g Cr(CO)₆; 2.25 g Mo(CO)₆; 3.00 g W(CO)₆) were placed in a photochemical reactor and suspended in 300 mL THF. The suspension was photolysed with a 150 W medium-pressure mercury arc -UV-Lamp (TQ150, Heraeus Noblelight, Hanau, Germany) for 45 minutes. The yellow solution was transferred to a Schlenk flask via a double-ended needle and 1.77 g (6.8 mmol) of (bis(trimethylsilyl)methyl)dichlorophosphane **23** was added. The solution was then stirred (12 h) at ambient temperature. The solvent was removed under reduced pressure ($\sim 10^{-2}$ mbar) and the product was purified by column chromatography (Al₂O₃, -20 °C, h = 7 cm, ϕ = 5cm, eluent: petroleum ether (200 mL)).

Procedure B:

10.0 mmol of the acetonitrile metal(0) complex (2.55 g Cr(CO)₅CH₃CN; 4.00 g W(CO)₅CH₃CN) were dissolved in 50 mL of THF. 2.00 g (8.0 mmol) of (bis(trimethylsilyl)methyl)dichlorophosphane **23** was added and the solution was stirred at ambient temperature for 48 h. After the reaction was completed, the solvent was removed under reduced pressure ($\sim 10^{-2}$ mbar) and the product was purified by column chromatography (Al₂O₃, -20 °C, h = 5 cm, ϕ = 5cm, eluent: petroleum ether (200 mL)).

VII.3.1 Synthesis of [bis(trimethylsilyl)methyldichlorophosphane] pentacarbonylchromium(0) **[26]**

Procedure A: Yield: 1.85 g (60 %)

Procedure B: Yield: 2.50 g (70 %)

Empirical formula: $C_{12}H_{19}Cl_2CrO_5PSi_2$

Molecular weight: 453.32 g/mol

Melting point: 65°C

1H NMR (300 MHz, CDCl₃, 30°C): $\delta = 0.34$ (s, 18H, Si(CH₃)₃), 2.03 (d, 1H, $^2J_{P,H} = 10.4$ Hz CH(Si(CH₃)₃)₂).

$^{13}C\{^1H\}$ NMR (75 MHz, CDCl₃, 30°C): $\delta = 3.0$ (d, $^3J_{P,C} = 3.9$ Hz, Si(CH₃)₃), 44.6 (d, $^1J_{P,C} = 26.6$ Hz, CH(Si(CH₃)₃)₂), 214.2 (d, $^2J_{P,C} = 14.5$ Hz, *cis*-CO), 219.6 (d, $^2J_{P,C} = 1.3$ Hz, *trans*-CO).

$^{29}Si\{^1H\}$ NMR (60 MHz, CDCl₃, 30°C): $\delta = 2.3$ (d, $^2J_{P,Si} = 4.5$ Hz, Si(CH₃)₃).

^{31}P NMR (121.5 MHz, CDCl₃, 30°C): $\delta = 236.2$ (d, $^2J_{P,H} = 10.1$ Hz).

Mass spectrometry (EI, ^{52}Cr): m/z (%) = 452 (30) [$M^{•+}$], 396 (10) [$(M-2CO)^{•+}$], 368 (10) [$(M-3CO)^{•+}$], 340 (30) [$(M-4CO)^{•+}$], 312 (90) [$(M-5CO)^{•+}$], 73 (100) [(SiMe₃) $^{•+}$].

IR (KBr, only v(CO)): $\tilde{\nu}$ [cm⁻¹] = 1947 (s), 1969 (s), 2017 (w), 2075(w).

UV/vis (CH₂Cl₂): λ (log ε): 218.1 (0.25), 236.3 (2.61), 290.0 (0.06) nm

Elemental analysis: C [%] H [%]

Calculated 31.79 4.22

Found 31.76 4.38

VII.3.2 Synthesis of [(bis(trimethylsilyl)methyl)dichlorophosphane]

pentacarbonylmolybdenum(0) [25]

Procedure A: The molybdenumhexacarbonyl and the (bis(trimethylsilyl)methyl)phosphane **23** were photolysed together in the UV reactor for 2 h, and stirring for further 4 h at RT.

Yield: 1.08 g (32%)

Empirical formula: C₁₂H₁₉Cl₂MoO₅PSi₂

Molecular weight: 497.27 g/mol

Melting point: 70°C

¹H NMR (300 MHz, CDCl₃, 30°C): δ = 0.34 (s, 18H, Si(CH₃)₃), 1.99 (d, 1H, ²J_{P,H} = 10.5 Hz CH(Si(CH₃)₃)₂).

¹³C{¹H} NMR (75 MHz, CDCl₃, 30°C): δ = 0.7 (d, ³J_{P,C} = 3.7 Hz, Si(CH₃)₃), 41.5 (d, ¹J_{P,C} = 29.7 Hz, CH(Si(CH₃)₃)₂), 201.7 (d, ²J_{P,C} = 10.3 Hz, *cis*-CO), 207.1 (d, ²J_{P,C} = 46.0 Hz, *trans*-CO).

$^{29}\text{Si}\{\text{H}\}$ NMR (60 MHz, CDCl_3 , 30°C): $\delta = 2.2$ (d, $^2J_{\text{P},\text{Si}} = 2.9$ Hz, $\text{Si}(\text{CH}_3)_3$).

^{31}P NMR (121.5 MHz, CDCl_3 , 30°C): $\delta = 203.1$ (d, $^2J_{\text{P},\text{H}} = 10.1$ Hz).

Mass spectrometry (EI, ^{98}Mo): m/z (%) = 498 (20) [$\text{M}^{\bullet+}$], 442 (30) [$(\text{M}-2\text{CO})^{\bullet+}$], 414 (15) [$(\text{M}-3\text{CO})^{\bullet+}$], 386 (30) [$(\text{M}-4\text{CO})^{\bullet+}$], 356 (30) [$(\text{M}-5\text{CO})^{\bullet+}$], 73 (100) [$(\text{SiMe}_3)^{\bullet+}$].

IR (KBr, $\nu(\text{CO})$): $\tilde{\nu}$ [cm $^{-1}$] = 1974(w), 1969 (w), 2020 (s), 2083(s).

UV/vis (CH_2Cl_2): λ (log ε): 235 (0.96), 290 (0.17) nm.

Elemental analysis: C [%] H [%]

Calculated 28.98 3.85

Found 28.98 4.14

VII.3.3 Synthesis of [(bis(trimethylsilyl)methyl)dichlorophosphane] pentacarbonyltungsten(0) **[24]**

The analytical data of complex **24** was already published in the literature.^[49]

Procedure A: Yield 3.20 g (80 %)

Procedure B: Yield 4.00 g (85 %)

VII.4 Synthesis of [2-bis(trimethylsilyl)methyl-3-phenyl-oxaphosphirane-*k*P]pentacarbonylchromium(0) [29]

Procedure A:

4.12 g (8.5 mmol) complex **27** and 0.86 mL benzaldehyde (8.5 mmol) were dissolved in 25 mL Toluene and heated to 75 °C under stirring for 3 hours. The solvents were then removed in vacuo ($\sim 10^{-2}$ mbar) and the product purified by column chromatography (SiO_2 , -20°C, $h = 6 \text{ cm}$, $\phi = 3 \text{ cm}$, eluent: petroleum ether: diethyl ether 80:20, (350 mL)). Pale yellow solid.

Yield: 2.48 g 60 %

Procedure B:

0.99 g (2.18 mmol) of complex **26** and 0.28 mL (1.74 mmol) of 12-crown-4 were dissolved in 25 mL diethyl ether at -80°C. Then 1.63 mL (2.39 mmol) of a solution of $^t\text{BuLi}$ 1.6 M in *n*-pentane were dropwise added while stirring. The solution was stirred for five minutes at this temperature and then 0.22 mL (2.18 mmol) benzaldehyde were added.

The brown suspension was stirred for additional 90 min, while gently warming to 0°C and then allowed to warm up to ambient temperature. The solvents were then removed in vacuo ($\sim 10^{-2}$ mbar) and the residue extracted with 30 mL of *n*-pentane. The product was purified by column chromatography (Al_2O_3 , -30°C, $h=1 \text{ cm}$, $\phi = 2 \text{ cm}$, petroleum ether 50 mL)

Yield: 0.44 g (41%)

Empirical formula: $\text{C}_{19}\text{H}_{25}\text{O}_6\text{PSi}_2\text{Cr}$

Molecular weight: 488.54 g/mol

Melting point: 108°C

¹H NMR (300 MHz, CDCl₃, 30°C): δ = 0.32 (s, 9H, Si(CH₃)₃), 0.39 (s, 9H, Si(CH₃)₃), 1.13 (s, 1H, CH(Si(CH₃)₃)₂), 4.37 (s, 1H, PhC(H)O), 7.40 (m, 5H, Ph-H).

¹³C{¹H} NMR (75 MHz, CDCl₃, 30°C): δ = -0.3 (d, ³J_{P,C} = 3.8 Hz, Si(CH₃)₃), 0.0 (d, ³J_{P,C} = 21.9 Hz, Si(CH₃)₃), 31.0 (d, ¹J_{P,C} = 24.2 Hz, CH(Si(CH₃)₃)₂), 57.2 (d, ¹⁺²J_{P,C} = 24.2 Hz, PCOH), 123.9 (d, ³J_{P,C} = 3.2 Hz, o-Ph), 126.1 (d, ³J_{P,C} = 2.2 Hz, Ph), 126.5 (d, ³J_{P,C} = 2.2 Hz, Ph), 133.1 (s, ipso-Ph), 212.9 (d, ²J_{P,C} = 15.8 Hz, cis-CO), 217.7 (d, ²J_{P,C} = 3.2 Hz, trans-CO).

²⁹Si{¹H} NMR (60 MHz, CDCl₃, 30°C): δ = -0.1 (d, ²J_{P,Si} = 5.5 Hz, Si(CH₃)₃), 0.1 (d, ²J_{P,Si} = 7.6 Hz, Si(CH₃)₃).

³¹P{¹H} NMR (121.5 MHz, CDCl₃, 30°C): δ = 91.0.

Mass spectrometry (EI, ⁵²Cr): m/z (%) = 488 (15) [M•⁺], 354 (100) [(M-PhCOH-CO)^{•+}], 348 (50) [(M-5CO)^{•+}], 270 (70) [(M-PhCOH-4CO)^{•+}], 242 (60) [(M-PhCOH-5CO)^{•+}].

IR (KBr, ν(CO)): ν [cm⁻¹] = 1946 (w), 1995 (w), 2070 (s).

UV/Vis (CH₂Cl₂): λ (log ε): 233.5 (1.14), 203.1 (1.20) nm.

Elemental analysis: C [%] H [%]

Calculated 46.71 5.16

Found 47.80 5.61

VII.5 Synthesis of [2-bis(trimethylsilyl)methyl-3-phenyl-oxaphosphirane-*k*P]pentacarbonylmolybdenum(0) [30]

Method A:

0.90 g (1.8 mmol) complex **28** and 0.18 mL benzaldehyde (1.8 mmol) were dissolved in 4 mL Toluene and heated to 75 °C under stirring for 3 hours. The solvents were then removed in vacuo ($\sim 10^{-2}$ mbar) and the product purified by column chromatography (SiO_2 , -20°C, $h = 6 \text{ cm}$, $\phi = 3 \text{ cm}$, eluent petroleum ether: diethyl ether 80:20, (150 mL)). Pale yellow solid.

Yield: 0.45g (50 %)

Method B:

0.60 g (1.20 mmol) of complex **25** and 0.20 mL (1.20 mmol) of 12-crown-4 were dissolved in 15 mL diethyl ether at -80°C. Then 0.75 mL (1.32 mmol) of a solution of $^t\text{BuLi}$ 1.6 M in *n*-pentane were dropwise added while stirring. The solution was stirred for five minutes at this temperature and then 0.12 mL (1.20 mmol) benzaldehyde were added.

The brown suspension was stirred for additional 90 min, while gently warming to 0°C and then allowed to warm up to ambient temperature. The solvents were then removed in vacuo ($\sim 10^{-2}$ mbar) and the residue extracted with 20 mL of *n*-pentane. The product was purified by column chromatography (Al_2O_3 , -30°C, $h = 1 \text{ cm}$, $\phi = 1 \text{ cm}$, petroleum ether (50 mL)).

Yield: 0.20 g (30%)

Empirical formula: $\text{C}_{19}\text{H}_{25}\text{MoO}_6\text{PSi}_2$ Molecular weight: 532.48 g/mol

Melting point: 110°C

¹H NMR (300 MHz, CDCl₃, 30°C): δ = 0.32 (s, 9H, Si(CH₃)₃), 0.38 (s, 9H, Si(CH₃)₃), 1.10 (d, 1H, ²J_{P,H} = 2.2 Hz CH(Si(CH₃)₃)₂), 4.36 (d, 1H, ²⁺³J_{P,H} = 1.6 Hz, PhC(H)O), 7.28 (s, 1H, Ph), 7.36 (m, 2H, Ph), 7.38 (m, 2H, Ph).

¹³C{¹H} NMR (75 MHz, CDCl₃, 30°C): δ = -0.3 (d, ³J_{P,C} = 3.8 Hz, Si(CH₃)₃), 0.0 (d, ³J_{P,C} = 2.5 Hz, Si(CH₃)₃), 30.5 (d, ¹J_{P,C} = 25.2 Hz, CH(Si(CH₃)₃)₂), 56.7 (d, ¹⁺²J_{P,C} = 22.3 Hz, PCOH), 123.5(d, ³J_{P,C} = 3.5 Hz, Ph), 126 (d, ³J_{P,C} = 2.5 Hz, Ph), 126.5 (d, ³J_{P,C} = 2.2 Hz, Ph), 133.1 (s, *i*-Ph), 201.8 (d, ²J_{P,C} = 10.6 Hz, *cis*-CO), 209.9 (d, ²J_{P,C} = 35.6 Hz, *trans*-CO).

²⁹Si{¹H} NMR (60 MHz, CDCl₃, 30°C): δ = -0.58 (d, ²J_{P,Si} = 5.5 Hz, Si(CH₃)₃), 0.65 (d, ²J_{P,Si} = 7.6 Hz, Si(CH₃)₃).

³¹P NMR (121.5 MHz, CDCl₃, 30°C): δ = 65.4.

Mass spectrometry (EI, ⁹⁸Mo): m/z (%) = 534 (18) [M•⁺], 399 (100) [(M-PhCOH-CO)^{•+}], 394 (60) [(M-5CO)^{•+}].

IR (KBr, v(CO)): ν [cm⁻¹] = 1953 (w), 2002 (w), 2079 (s).

UV-vis (CH₂Cl₂): λ (log ε): 301 (0.43), 236 (2.61), 210 (1.92) nm

Elemental analysis: C [%] H [%]

Calculated 42.86 4.73

Found 43.47 5.19

VII.6 General procedure for the synthesis of the $\sigma^3\lambda^3$ -oxaphosphirane complexes

To a solution of 200 mg (0.31 mmol) of complex **24** and 12-crown-4 (0.31 mmol) in 10 mL of diethyl ether a solution of 0.2 mL (1.6 M, 0.31 mmol) *tert*-butyllithium was added dropwise at -80°C while stirring. The solution was stirred for five minutes at this temperature and then 0.31 mmol of the corresponding aldehyde were added. The solution was stirred for additional 90 min, while gently warming to 0°C and then allowed to warm up to ambient temperature. The solvents were then removed in vacuo ($\sim 10^{-2}$ mbar) and the residue extracted with 20 mL of *n*-pentane. The products were purified by column chromatography (Al₂O₃, -30°C, h = 1 cm, ϕ = 1 cm, petroleum ether (50 mL)).

VII.6.1 Synthesis of [2-bis(trimethylsilyl)methyl-3-phenyl-oxaphosphirane-*k*P]pentacarbonyltungsten (0) [**16a**]

Synthesized according to the general procedure for the synthesis of the $\sigma^3\lambda^3$ -oxaphosphirane complexes using 31 μ L of benzaldehyde.

Most of the analytical data can be found in the literature, they were measured again due to the important role of the oxaphosphirane complex **16a** in this work.

Yield: 127.4 mg (60%)

Empirical formula: C₁₉H₂₅O₆PSi₂W Molecular weight: 620.04 g/mol

Melting point: 96°C

¹H NMR (300 MHz, CDCl₃, 30°C): δ = 0.30 (s, 9H, Si(CH₃)₃), 0.39 (s, 9H, Si(CH₃)₃), 1.28 (s, broad, 1H, CH(Si(CH₃)₃)₂), 4.40 (d, 1H, ²⁺³J_{P,H} = 1.8 Hz, PhC(H)O), 7.10 (m_c, 3H, Ph), 7.36 (m_c, 2H, Ph).

¹³C{¹H} NMR (75 MHz, CDCl₃, 30°C): δ = -0.3 (d, ³J_{P,C} = 4.2 Hz, Si(CH₃)₃), 0.0 (d, ³J_{P,C} = 2.2 Hz, Si(CH₃)₃), 30.5 (d, ¹J_{P,C} = 18.8 Hz, CH(Si(CH₃)₃)₂), 57.9 (d, ¹⁺²J_{P,C} = 27.5 Hz, PCOH), 123.5 (d, ³J_{P,C} = 3.2 Hz, Ph), 126.1 (d, J = 2.9 Hz, Ph), 126.7 (d, J = 2.3 Hz, Ph), 133.3 (s, p-Ph), 192.7 (d, ²J_{P,C} = 8.4 Hz, cis-CO), 194.9 (d, ²J_{P,C} = 35.6 Hz, trans-CO).

²⁹Si{¹H} NMR (60 MHz, CDCl₃, 30°C): δ = 0.2 (d, ²J_{P,Si} = 5.6 Hz, Si(CH₃)₃), 1.5 (d, ³J_{P,Si} = 8.0 Hz, Si(CH₃)₃).

³¹P NMR (121.5 MHz, CDCl₃, 30°C): δ = 38.2 (s_{sat}, ¹J_{W,P} = 307.7 Hz).

Mass spectrometry (EI, 70 eV, ¹⁸⁴W): m/z (%) = 620 (20) [M^{•+}], 514 (15) [(M-Ph(H)CO)^{•+}], 486 (15) [(M-Ph(H)CO-CO)^{•+}], 428 (50) [(M-PhC(H)O-3CO)^{•+}], 400 (60) [(M-Ph(H)CO-4CO)^{•+}]; 86 (100) [(CH(Si(CH₃)₃)₂)^{•+}].

IR (KBr, v(CO)): ̄ [cm⁻¹] = 1880 (s), 1924 (m), 2077 (w), 2067(w).

UV/vis (CH₂Cl₂): λ (log ε): 235 (0.45), 299 (0.08) nm.

Elemental analysis: C [%] H [%]

Calculated 36.78 4.06

Found 36.99 4.36

VII.6.2 Synthesis of [2-bis(trimethylsilyl)methyl-3-(2-methylphenyl)-oxaphosphirane-*k*P]pentacarbonyltungsten(0) [33]

Synthesized according to the general procedure for the synthesis of the $\sigma^3\lambda^3$ -oxaphosphirane complexes using 36 μL of tolualdehyde.

Yield: 130.2 mg (60%)

Empirical formula: $\text{C}_{20}\text{H}_{27}\text{O}_6\text{PSi}_2\text{W}$ Molecular weight: 634.04 g/mol

Melting point: 98°C

^1H NMR (300 MHz, CDCl_3 , 30°C): $\delta = 0.16$ (s, 9H, $\text{Si}(\text{CH}_3)_3$), 0.22 (s, 9H, $\text{Si}(\text{CH}_3)_3$), 1.14 (s, broad signal, 1H, $\text{CH}(\text{Si}(\text{CH}_3)_3)_2$), 2.33 (s, 3H, *p*- CH_3), 4.26 (s, 1H, PhC(H)O), 7(m, 4H, Ph).

$^{13}\text{C}\{\text{H}\}$ NMR (75 MHz, CDCl_3 , 30°C): $\delta = 1.6$ (d, $^3J_{\text{P,C}} = 3.14$ Hz, $\text{Si}(\text{CH}_3)_3$), 1.8 (d, $^3J_{\text{P,C}} = 2.3$ Hz, $\text{Si}(\text{CH}_3)_3$), 32.7 (d, $^1J_{\text{P,C}} = 20.3$ Hz, $\underline{\text{CH}}(\text{Si}(\text{CH}_3)_3)_2$), 57.9 (d, $^{1+2}J_{\text{P,C}} = 24.5$ Hz, PC(H)O), 125.6 (d, $^3J_{\text{P,C}} = 2.1$ Hz, Ar), 125.7 (d, $J_{\text{P,C}} = 4.3$ Hz, Ar), 127.6 (d, $J_{\text{P,C}} = 2.6$ Hz,

Ar), 129.6 (d, $J_{P,C} = 2.3$ Hz, Ar), 128.0 (s, *ipso*-Ar), 131.3 (s, *i*-Ar), 193.9 (d, $^2J_{P,C} = 8.4$ Hz, *cis*-CO), 195.1 (d, $^2J_{P,C} = 34.9$ Hz, *trans*-CO).

$^{29}\text{Si}\{\text{H}\}$ NMR (60 MHz, CDCl_3 , 30°C): $\delta = -0.8$ (d, $^2J_{\text{P},\text{Si}} = 4.7$ Hz, $\text{Si}(\text{CH}_3)_3$), 1.3 (d, $^2J_{\text{P},\text{Si}} = 7.2$ Hz, $\text{Si}(\text{CH}_3)_3$).

^{31}P NMR (121.5 MHz, CDCl_3 , 30°C): $\delta = 41.0$ (s_{sat}, $^1J_{\text{P},\text{W}} = 306.6$ Hz).

Mass spectrometry (EI, 70 eV, ^{184}W): m/z (%) = 634(10) [$\text{M}^{\bullet+}$], 514 (40) [($\text{M}-\text{Ar}-\text{C}(\text{H})\text{O}$) $^{\bullet+}$], 486 (100) [($\text{M}-\text{Ar}-\text{C}(\text{H})\text{O}-\text{CO}$) $^{\bullet+}$].

IR (KBr, v(CO)): $\tilde{\nu}$ [cm⁻¹] = 1923 (w), 1993, (s), 2075 (w), 2957(w).

UV/vis (CH_2Cl_2): λ (log ε) : 231 (0.29), 290 (0.04) nm.

Elemental analysis: C [%] H [%]

Calculated 37.86 4.29

Found 38.12 4.57

VII.6.3 Synthesis of [2-bis(trimethylsilyl)methyl-3-(2-methoxyphenyl)-oxaphosphirane-*k*P]pentacarbonyltungsten (0) **[34]**

Synthesized according to the general procedure for the synthesis of the $\sigma^3\lambda^3$ -oxaphosphirane complexes using 42 mg of *o*-anisaldehyde.

Yield: 142.5 mg (64%)

Empirical formula: C₂₀H₂₇O₇PSi₂W Molecular weight: 650.41 g/mol

Melting point: 99°C

¹H NMR (300 MHz, CDCl₃, 30°C): δ = 0.22 (s, 9H, Si(CH₃)₃), 0.30 (s, 9H, Si(CH₃)₃), 1.16 (s, br, 1H, CH(Si(CH₃)₃)₂), 3.79 (s, 3H, OCH₃), 4.46 (s, 1H, ArC(H)O), 6.79 (m, 3H, Ar), 6.79 (m, 1H, Ar).

¹³C{¹H}NMR (75 MHz, CDCl₃, 30°C): δ = -0.8 (d, ³J_{P,C} = 4.2 Hz, Si(CH₃)₃), 0.0 (d, ³J_{P,C} = 2.2 Hz, Si(CH₃)₃), 30.4 (d, ¹J_{P,C} = 20.2 Hz, CH(Si(CH₃)₃)₂), 52.6 (s, OCH₃), 54.7 (d, ¹⁺²J_{P,C} = 28.2 Hz, PC(H)O), 107.3 (d, ³J_{P,C} = 2.24 Hz, Ar), 118.3 (d, J_{P,C} = 2.4 Hz, Ar), 121.7 (s, *i*-Ar), 124.3 (d, J_{P,C} = 4.3 Hz, Ar), 126.8 (d, J_{P,C} = 2.6 Hz, Ar), 155.23 (d, J_{P,C} = 2.6 Hz, *i*-Ar), 192.9 (d, ²J_{P,C} = 8.4 Hz, *cis*-CO), 195.2 (d, ²J_{P,C} = 34.7 Hz, *trans*-CO).

²⁹Si{¹H} NMR (60 MHz, CDCl₃, 30°C): δ = 0.0 (d, ²J_{P,Si} = 5.5 Hz, Si(CH₃)₃), 1.2 (d, ²J_{P,Si} = 8.0 Hz, Si(CH₃)₃).

³¹P NMR (121.5 MHz, CDCl₃, 30°C): δ = 39.2 (s_{sat}, ¹J_{P,W} = 305.5 Hz).

Mass spectrometry (EI, 70 eV, ^{184}W): m/z (%) = 650 (60) [M^+], 566 (40) [$(\text{M}-3\text{CO})^+$], 514 (15) [$(\text{M}-\text{Ar}-\text{C}(\text{H})\text{O})^+$], 73 (100) [$(\text{Si}(\text{CH}_3)_3)^+$].

IR (KBr, $\nu(\text{CO})$): $\tilde{\nu}$ [cm $^{-1}$] = 1915 (s), 1992(w), 2075 (w).

UV/vis (CH_2Cl_2): λ (log ε): 232 (0.35), 292 (0.06) nm.

Elemental analysis: C [%] H [%]

Calculated 36.93 4.18

Found 37.30 4.42

VII.6.4 Synthesis of [2-bis(trimethylsilyl)methyl-3-*tert*-butyl-oxaphosphirane-*kP*]pentacarbonyltungsten(0) [36]

Synthesized according to the general procedure for the synthesis of the $\sigma^3\lambda^3$ -oxaphosphirane complexes using 35 μL of pivalinaldehyde.

Yield: 100.4 mg (50%)

Empirical formula: $\text{C}_{17}\text{H}_{29}\text{O}_6\text{PSi}_2\text{W}$ Molecular weight: 600.39 g/mol

Melting point: 94°C

¹H NMR (300 MHz, CDCl₃, 30°C): δ = 0.24 (s, 9H, Si(CH₃)₃), 0.31 (s, 9H, Si(CH₃)₃), 1.10 (s, 9H, (CH₃)₃), 1.25 (s, 1H, CH(Si(CH₃)₃)₂), 2.70 (s, 1H, PC(H)O).

¹³C{¹H}NMR (75 MHz, CDCl₃, 30°C): δ = 0.7 (d, ³J_{P,C} = 4.5 Hz, Si(CH₃)₃), 1.5 (d, ³J_{P,C} = 2.3 Hz, Si(CH₃)₃), 24.5 (d, ²J_{P,C} = 4.0 Hz, CH₃), 27.3 (d, ²J_{P,C} = 4.0 Hz, 2CH₃), 31.0 (s, C(CH₃)₃), 33.6 (d, ²J_{P,C} = 15.4 Hz, CH(Si(CH₃)₃)₂), 67.1 (d, ¹⁺²J_{P,C} = 28.5 Hz, PC(H)O), 195.5 (d, ²J_{P,C} = 8.4 Hz, *cis*-CO), 196.5 (d, ²J_{P,C} = 33.6 Hz, *trans*-CO).

²⁹Si{¹H} NMR (60 MHz, CDCl₃, 30°C): δ = -0.0 (d, ²J_{P,Si} = 7.8 Hz, Si(CH₃)₃), 2.0 (d, ²J_{P,Si} = 4.5 Hz, Si(CH₃)₃).

³¹P NMR (121.5 MHz, CDCl₃, 30°C): δ = 22.5 (s_{sat}, ¹J_{P,W} = 298.8 Hz).

Mass spectrometry (EI, 70 eV, ¹⁸⁴W): m/z (%) = 600 (13) [M^{•+}], 557 (30) [(M-CO-O)^{•+}], 527 (20)[(M-2CO-O)^{•+}], 514 (40) [(M-^tBu-C(H)O)^{•+}], 486 (100) [(M-^tBu-C(H)O-CO)^{•+}].

IR (KBr, ν(CO)): ν [cm⁻¹] = 1934 (s), 1986(w), 2076 (w).

UV/vis (CH₂Cl₂): λ (log ε): 237 (0.48), 301 (0.05) nm.

Elemental analysis: C [%] H [%]

Calculated 34.01 4.87

Found 33.88 4.86

VII.6.5 Synthesis of [2-bis(trimethylsilyl)methyl-3-*iso*-propyl-oxaphosphirane-*kP*]pentacarbonyltungsten(0) [37]

Synthesized according to the general procedure for the synthesis of the $\sigma^3\lambda^3$ -oxaphosphirane complexes using 28 μL of isobutyraldehyde.

Yield: 106.3 mg (53%)

Empirical formula: $\text{C}_{16}\text{H}_{27}\text{O}_6\text{PSi}_2\text{W}$

Molecular weight: 586.37 g/mol

Melting point: 86°C

^1H NMR (300 MHz, CDCl_3 , 30°C): $\delta = 0.25$ (s, 9H, $\text{Si}(\text{CH}_3)_3$), 0.30 (s, 9H, $\text{Si}(\text{CH}_3)_3$) 1.05 (m, 1H, $\underline{\text{CH}}(\text{Si}(\text{CH}_3)_3)_2$), 1.17 (d, 3H, $^2J_{\text{H,H}} = 6.5$ Hz, CH_3), 1.21 (d, 3H, $^2J_{\text{H,H}} = 6.7$ Hz, CH_3), 1.60 (m, 1H, $\underline{\text{CH}}(\text{CH}_3)_2$), 2.75 (d, 1H, $^{2+3}J_{\text{P,H}} = 9.8$ Hz, PC(H)O).

$^{13}\text{C}\{^1\text{H}\}$ NMR (75 MHz, CDCl_3 , 30°C): $\delta = -0.4$ (d, $^3J_{\text{P,C}} = 4.5$ Hz, $\text{Si}(\text{CH}_3)_3$), 0.0 (d, $^3J_{\text{P,C}} = 2.6$ Hz, $\text{Si}(\text{CH}_3)_3$), 17.2 (s, $\text{CH}\underline{\text{CH}}_3$), 17.4 (d, $^1J_{\text{P,C}} = 11.6$ Hz, $\text{CH}\underline{\text{CH}}_3$), 29.0 (d, $\underline{\text{CH}}\text{CH}_3$, $^3J_{\text{P,C}} = 3.3$ Hz), 28.7 (d, $\underline{\text{CH}}(\text{Si}(\text{CH}_3)_3)_2$, $^3J_{\text{P,C}} = 17.1$ Hz), 62.9 (d, $^{1+2}J_{\text{P,C}} = 28.7$ Hz, PC(H)O), 193.4 (d, $^2J_{\text{P,C}} = 8.4$ Hz, *cis*-CO), 195 (d, $^2J_{\text{P,C}} = 33.6$ Hz, *trans*-CO).

$^{29}\text{Si}\{^1\text{H}\}$ NMR (60 MHz, CDCl_3 , 30°C): $\delta = -1.8$ (d, $^2J_{\text{P,Si}} = 4.8$ Hz, $\text{Si}(\text{CH}_3)_3$), 0.1 (d, $^2J_{\text{P,Si}} = 8.0$ Hz, $\text{Si}(\text{CH}_3)_3$).

$^{31}\text{P}\{^1\text{H}\}$ NMR (121.5 MHz, CDCl_3 , 30°C): $\delta = 31.9$ (s_{sat} , $^1J_{\text{P,W}} = 298.8$ Hz).

^{31}P NMR (121.5 MHz, CDCl_3 , 30°C): $\delta = 31.9$ (d_{sat} , $^1J_{\text{P},\text{W}} = 298.8$ Hz, $^2J_{\text{P},\text{H}} = 11.4$ Hz).

Mass spectrometry (EI, 70 eV, ^{184}W): m/z (%) = 586 (15) [$\text{M}^{•+}$], 543 (30) [$(\text{M}-^i\text{Pr})^{•+}$], 514 (40) [$(\text{M}-^i\text{Pr}-\text{C}(\text{H})\text{O})^{•+}$], 486 (100) [$(\text{M}-^i\text{Pr}-\text{C}(\text{H})\text{O}-\text{CO})^{•+}$].

IR (KBr, $\nu(\text{CO})$): $\tilde{\nu}$ [cm $^{-1}$] = 1930 (s), 1986 (w), 2067(w).

UV/vis (CH_2Cl_2): λ ($\log \varepsilon$): 237 (0.47), 293 (0.06) nm.

Elemental analysis: C [%] H [%]

Calculated 32.77 4.64

Found 32.68 4.65

VII.6.6 Synthesis of [2-bis(trimethylsilyl)methyl-3-*n*-propyl-oxaphosphirane-*k*P]pentacarbonyltungsten(0) [38]

Synthesized according to the general procedure for the synthesis of the $\sigma^3\lambda^3$ -oxaphosphirane complexes using 27 μL of butyraldehyde.

Yield: 110.1 mg (55%)

Empirical formula: $\text{C}_{16}\text{H}_{27}\text{O}_6\text{PSi}_2\text{W}$ Molecular weight: 586.37 g/mol

Melting point: 68°C

^1H NMR (300 MHz, CDCl_3 , 30°C): $\delta = 0.25$ (s, 9H, $\text{Si}(\text{CH}_3)_3$), 0.29 (s, 9H, $\text{Si}(\text{CH}_3)_3$), 1.05 (t, 3H, $^2J_{\text{H,H}} = 6.5$, CH_3), 1.15 (s, 1H, $\underline{\text{CH}}(\text{Si}(\text{CH}_3)_3)_2$), 1.60 (mc, 2H, CH_2), 1.80 (m, 2H, CH_2), 3.1 (d, 1H, $^2J_{\text{P,H}} = 9.8$ Hz, $\text{PC}(\text{H})\text{O}$).

$^{13}\text{C}\{^1\text{H}\}$ NMR (75 MHz, CDCl_3 , 30°C): $\delta = -0.6$ (d, $^3J_{\text{P,C}} = 4.5$ Hz, $\text{Si}(\text{CH}_3)_3$), 0.0 (d, $^3J_{\text{P,C}} = 2.2$ Hz, $\text{Si}(\text{CH}_3)_3$), 11.9 (s, $\text{CH}_2\underline{\text{CH}}_3$), 17.8 (d, $^2J_{\text{P,C}} = 6.1$ Hz, CH_2), 28.5 (d, $^3J_{\text{P,C}} = 16.4$ Hz, $\underline{\text{CH}}(\text{Si}(\text{CH}_3)_3)_2$), 31.4 (d, $^3J_{\text{P,C}} = 30.7$ Hz, CH_2), 57.4 (d, $^{1+2}J_{\text{P,C}} = 30.7$ Hz, $\text{PC}(\text{H})\text{O}$), 193.5 (d, $^2J_{\text{P,C}} = 8.4$ Hz, *cis*-CO), 195.0 (d, $^2J_{\text{P,C}} = 33.6$ Hz, *trans*-CO).

$^{29}\text{Si}\{^1\text{H}\}$ NMR (60 MHz, CDCl_3 , 30°C): $\delta = -1.8$ (d, $^2J_{\text{P,Si}} = 4.8$ Hz, $\text{Si}(\text{CH}_3)_3$), 0.1 (d, $^2J_{\text{P,Si}} = 8.0$ Hz, $\text{Si}(\text{CH}_3)_3$).

$^{31}\text{P}\{^1\text{H}\}$ NMR (121.5 MHz, CDCl_3 , 30°C): $\delta = 27.7$ (s_{sat} , $^1J_{\text{W,P}} = 302.6$ Hz).

³¹P NMR (121.5 MHz, CDCl₃, 30°C): δ = 27.7 (d_{sat}, ¹J_{W,P} = 302.6 Hz, ²J_{P,H} = 10.0 Hz).

Mass spectrometry (EI, 70 eV, ¹⁸⁴W): m/z (%): 586 (20) [M^{•+}], 543 (27) [(M-ⁿPr)^{•+}], 514 (35) [(M-ⁿPr-C(H)O)^{•+}], 486 (100) [(M-ⁿPr-C(H)O-CO)^{•+}].

IR (KBr, v(CO)): ν [cm⁻¹] = 1930 (s), 1986(w), 2076 (w).

UV/vis (CH₂Cl₂): λ (log ε): 239 (0.51), 297 (0.07) nm.

Elemental analysis: C [%] H [%]

Calculated 32.77 4.64

Found 32.20 4.56

VII.6.7 Synthesis of [2-bis(trimethylsilyl)methyl-3-methyl-oxaphosphirane-*k*P]pentacarbonyltungsten(0) [39]

To a solution of 160 mg (0.27 mmol) of complex **24** and 12-crown-4 (0.27 mmol) in 3 mL diethyl ether was added dropwise 0.2 mL of a solution (1.6 M in *n*-pentane, 0.31 mmol) *tert*-butyllithium at -80°C while stirring. The solution was stirred for five minutes at this temperature and then 30 μL (0.54 mmol) of acetaldehyde was added. The solution was stirred for additional 90 min, while gently warming to 0 °C and then allowed to warm up to ambient temperature. The solvents were then removed in vacuo (~10⁻² mbar) and the residue extracted with 5 mL of *n*-pentane. The residue was dissolved in CDCl₃ and the NMR data

were measured overnight. After the measure the oxaphosphirane complex **39** had decomposed.

Empirical formula: C₁₄H₂₃O₆PSi₂W

Molecular weight: 558.31 g/mol

¹H NMR (300 MHz, CDCl₃, 30°C): δ = 0.15 (s, 9H, Si(CH₃)₃), 0.19 (s, 9H, Si(CH₃)₃), 1.05 (s, br, 1H, CH(Si(CH₃)₃)₂), 1.46 (dd, ²J_{P,H} = 15.9 Hz, ²J_{H,H} = 5.9 Hz, 3H, CH₃), 3.15 (q, 1H, ²J_{H,H} = 5.98 Hz, PC(H)O).

¹³C{¹H}NMR (75 MHz, CDCl₃, 30°C): δ = -0.6 (d, ³J_{P,C} = 4.5 Hz, Si(CH₃)₃), 0.0 (d, ³J_{P,C} = 2.3 Hz, Si(CH₃)₃), 14.8 (d, ³J_{P,C} = 2.9 Hz, CH₃), 28.5 (d, ³J_{P,C} = 16.3 Hz, CH(Si(CH₃)₃)₂), 53.8 (d, ¹⁺²J_{P,C} = 32.9 Hz, PCOH), 193.4 (d, ²J_{P,C} = 8.6 Hz, *cis*-CO), 195.7 (d, ²J_{P,C} = 33.7 Hz, *trans*-CO).

²⁹Si{¹H} NMR (60 MHz, CDCl₃, 30°C): δ = -0.7 (d, ²J_{P,Si} = 5.1 Hz, Si(CH₃)₃), 0.9 (d, ²J_{P,Si} = 8.0 Hz, Si(CH₃)₃).

³¹P{¹H} NMR (121.5 MHz, CDCl₃, 30°C): δ = 30.9 (s_{sat}, ¹J_{P,W} = 298.7 Hz).

³¹P NMR (121.5 MHz, CDCl₃, 30°C): δ = 30.9 (q_{sat}, ¹J_{P,W} = 298.7 Hz, ²J_{P,H} = 15.9 Hz).

VII.6.8 Synthesis of [2-bis(trimethylsilyl)methyl-3,3-dimethyl-oxaphosphirane-*k*P]pentacarbonyltungsten(0) [42]

1 g (1.7 mmol) of complex **24** were dissolved in 25 mL of Et₂O, then 0.19 mL (1.2 mmol) of 12-crown-4 were added and the solution was cooled down to -80°C. 1.25 mL (1.9 mmol) of a 1.6 M solution of ^tBuLi was added dropwise while stirring and after 10 min 0.37 mL (5.1 mmol) of acetone was added and the reaction was allowed to warm up until 0°C. The solvents were removed under vacuum ($\sim 10^{-2}$ mbar). The product was extracted with a mixture of 2 mL Et₂O/ 20 mL *n*-pentane. The product was purified by column chromatography (Al₂O₃, -30°C, h = 1cm, ϕ = 2 cm, petroleum ether (100 mL); petroleum ether/ diethyl ether 1:1 (100 mL)).

The first and the second fraction yielded white oil which was washed with *n*-pentane giving a white powder.

Yield: 0.480 g (49%)

Empirical formula: C₁₅H₂₅O₆PSi₂W

Molecular weight: 572.34 g/mol

Melting point: 71°C

¹H NMR (300 MHz, CDCl₃, 30°C): δ = 0.19 (s, 9H, Si(CH₃)₃), 0.22 (d, 9H, ⁴J_{P,H} = 0.55 Hz, Si(CH₃)₃), 1.25 (d, 1H, ²J_{P,H} = 3.04 Hz, CH(Si(CH₃)₃)₂), 1.46 (d, 1H, ³J_{P,H} = 15.01 Hz, CH₃), 1.63 (d, 1H, ³J_{P,H} = 9.11 Hz, CH₃).

$^{13}\text{C}\{\text{H}\}$ NMR (75 MHz, CDCl_3 , 30°C): $\delta = -0.4$ (d, $^3J_{\text{P,C}} = 3.8$ Hz, $\text{Si}(\text{CH}_3)_3$), 0.0 (d, $^3J_{\text{P,C}} = 2.6$ Hz, $\text{Si}(\text{CH}_3)_3$), 20.0 (d, $^3J_{\text{P,C}} = 1.3$ Hz, CH_3), 23.0 (d, $^3J_{\text{P,C}} = 9.1$ Hz, CH_3), 30.5 (d, $^1J_{\text{P,C}} = 17.4$ Hz, $\underline{\text{C}}\text{H}(\text{Si}(\text{CH}_3)_3)_2$), 61.1 (d, $^{1+2}J_{\text{P,C}} = 31.0$ Hz, $\underline{\text{P}}\text{CO}(\text{CH}_3)_2$), 192.7 (d, $^2J_{\text{P,C}} = 8.4$ Hz, *cis*-CO), 195.0 (d, $^2J_{\text{P,C}} = 32.9$ Hz, *trans*-CO).

$^{29}\text{Si}\{\text{H}\}$ NMR (60 MHz, CDCl_3 , 30°C): $\delta = -1.0$ (d, $^2J_{\text{P,Si}} = 6.5$ Hz, $\text{Si}(\text{CH}_3)_3$), 1.2 (d, $^2J_{\text{P,Si}} = 8.4$ Hz, $\text{Si}(\text{CH}_3)_3$).

$^{31}\text{P}\{\text{H}\}$ NMR (121.5 MHz, CDCl_3 , 30°C): $\delta = 55.6$ (s_{sat} , $^1J_{\text{P,W}} = 296.2$ Hz).

^{31}P NMR (121.5 MHz, CDCl_3 , 30°C): $\delta = 55.6$ (m_{sat} , $^1J_{\text{P,W}} = 296.2$ Hz).

Mass spectrometry (EI, 70 eV, ^{184}W): m/z (%) = 571(15) [$\text{M}^{\bullet+}$], 557(15) [$(\text{M}-\text{Me})^{\bullet+}$], 516(30) [$(\text{M}-2\text{CO})^{\bullet+}$], 486 (100) [$(\text{M}-3\text{CO})^{\bullet+}$], 73 (50) [$(\text{SiMe}_3)^{\bullet+}$].

IR (KBr, $\nu(\text{CO})$): $\tilde{\nu}$ [cm $^{-1}$] = 1880 (s), 1924 (w), 2077 (s), 2067(s).

UV/vis (CH_2Cl_2): λ ($\log \varepsilon$) 234 (0.51), 305 (0.05) nm.

Elemental analysis: C [%] H [%]

Calculated 31.48 4.40

Found 31.26 4.42

VII.6.9 Synthesis of [2-bis(trimethylsilyl)methyl-3-diphenyl-oxaphosphirane-*k*P]pentacarbonyltungsten(0) [41]

0.4 g (0.7 mmol) of complex **24** were dissolved in 15 mL of Et₂O, then 0.11 mL (0.7 mmol) of 12-crown-4 were added and the solution was cooled down to -80°C. 0.45 mL (0.7 mmol) of a 1.6 M solution of ^tBuLi was added dropwise while stirring and after 10 min 1.28 g (7 mmol) of benzophenone was added and the reaction was allowed to warm up to room temperature. The solvents were removed under vacuum ($\sim 10^{-2}$ mbar). The product was extracted with a mixture of 1 mL Et₂O/ 10 mL *n*-pentane. The product was purified by column chromatography (Al₂O₃, -30°C, *h*= 1cm, ϕ = 2 cm, petroleum ether (100 mL); petroleum ether/ diethyl ether 4:1 (100 mL)).

The first and the second fraction yielded a yellow oil, which was washed with *n*-pentane and thus giving a light yellow powder after drying in *vacuo*. Suitable crystals for X-ray diffractometry were obtained from a concentrated *n*-pentane solution.

Yield: 166 mg (35%)

Empirical formula: C₂₅H₂₉O₆PSi₂W

Molecular weight: 696.2 g/mol

The ³¹P and ¹³C NMR data of oxaphosphirane complex **41** was already described in the literature,^[38] but as the analytical data were incomplete all the NMR data were measured again.

¹H NMR (300 MHz, CDCl₃, 30°C): δ = 0.00 (s, 9H, Si(CH₃)₃), 0.31 (s, 9H, Si(CH₃)₃), 1.31 (d, 1H, ²J_{P,H} = 15.9 Hz, CH(Si(CH₃)₃)₂), 7.6 (m, Ph).

$^{13}\text{C}\{\text{H}\}$ NMR (75 MHz, CDCl_3 , 30°C): δ = 0.4 (d, $^3J_{\text{P,C}} = 4.9$ Hz, $\text{Si}(\text{CH}_3)_3$), 0.9 (d, $^3J_{\text{P,C}} = 2.9$ Hz, $\text{Si}(\text{CH}_3)_3$), 23.9 (d, $^3J_{\text{P,C}} = 38.2$ Hz, $\underline{\text{C}}\text{H}(\text{Si}(\text{CH}_3)_3)_2$), 69.9 (d, $^{1+2}J_{\text{P,C}} = 20.5$ Hz, PCO), 127.0 (s, Ph), 128.2 (s, Ph), 128.3 (s, Ph), 128.4 (s, Ph), 128.6 (s, ph), 129.2 (s, Ph), 130.1 (s, *i*-Ph), 132.4 (s, *i*-Ph), 194.3 (d, $^2J_{\text{P,C}} = 8.0$ Hz, *cis*-CO), 196.5 (d, $^2J_{\text{P,C}} = 34.6$ Hz, *trans*-CO).

$^{29}\text{Si}\{\text{H}\}$ NMR (60 MHz, CDCl_3 , 30°C): δ = -1.50 (d, $^2J_{\text{P,Si}} = 5.8$ Hz, $\text{Si}(\text{CH}_3)_3$), 4.0 (s, $\text{Si}(\text{CH}_3)_3$).

$^{31}\text{P}\{\text{H}\}$ NMR (121.5 MHz, CDCl_3 , 30°C): δ = 52.2 (s_{sat} , $^1J_{\text{P,W}} = 305.5$ Hz).

^{31}P NMR (121.5 MHz, CDCl_3 , 30°C): δ = 52.2 (d_{sat} , $^1J_{\text{P,W}} = 305.5$ Hz, $^2J_{\text{P,H}} = 15.8$ Hz).

Mass spectrometry (EI, 70 eV, ^{184}W): m/z (%) = 696 (20) [$\text{M}^{\bullet+}$], 668 (12) [(M-CO) $^{\bullet+}$], 612 (48) [(M-3CO) $^{\bullet+}$], 556 (36) [(M-5CO) $^{\bullet+}$], 514 (16) [(M- $\text{C}_{13}\text{H}_{11}\text{O}$) $^{\bullet+}$], 486 (54) [(M- $\text{C}_{13}\text{H}_{11}\text{O}$ -CO) $^{\bullet+}$], 73 (100) [(SiMe₃) $^{\bullet+}$].

VII.6.10 Synthesis of [1-oxa-2-(bis(trimethylsilyl)methyl)phosphaspiro[2.5]octane-*k*P]pentacarbonyltungsten(0) [46a,b]

0.275 g (0.47 mmol) of complex **24** were dissolved in 6 mL of Et₂O, then 60 μL (0.38 mmol) of 12-crown-4 were added and the solution was cooled down to -80°C. 0.40 mL (0.61 mmol) of a 1.6 M ^tBuLi solution were added dropwise while stirring and after 10 min 0.15 mL (1.41 mmol) of cyclohexanone were added and the reaction was allowed to warm up until 0°C. The

solvents were removed under vacuum ($\sim 10^{-2}$ mbar). The products were extracted with a mixture of 0.5 mL Et₂O/ 5 mL *n*-pentane and purified by column chromatography (Al₂O₃, -30°C, h = 1cm, ϕ = 1cm, petroleum ether). The first fraction yielded the pure **46a** (Yield **46a** 30 mg 10%) while the second fraction yielded a mixture of both isomers **46a,b** as yellow oil.

Yield 46a,b: 0.168 g 58%

Empirical formula: C₁₈H₂₉O₆PSi₂W Molecular weight: 612.1 g/mol

Analytical data of complex **46a** (ratio 77%):

¹H NMR (300 MHz, CDCl₃, 30°C): δ = 0.22 (s, 9H, Si(CH₃)₃, 0.27 (s, 9H, Si(CH₃)₃, 1.20 (d, 1H, ²J_{P,H} = 15.9 Hz, CH(Si(CH₃)₃)₂), 1.7 (m, 6H, CH₂), 1.8 (m, 4H, CH₂).

¹³C{¹H}NMR (75 MHz, CDCl₃, 30°C): δ = -0.1 (d, ³J_{P,C} = 4.9 Hz, Si(CH₃)₃), -0.0 (d, ³J_{P,C} = 2.9 Hz, Si(CH₃)₃), 22.2 (d, ¹J_{P,C} = 5.45 Hz, CH₂), 23.1 (d, ³J_{P,C} = 2.18 Hz, CH₂), 23.4 (d, ³J_{P,C} = 38.8 Hz, CH(Si(CH₃)₃)₂), 33.0 (d, J_{P,C} = 6.7 Hz, CH₂), 65.7 (d, ¹⁺²J_{P,C} = 27.3 Hz, PCO), 194.1 (d, ²J_{P,C} = 8.2 Hz, *cis*-CO), 196.1 (d, ²J_{P,C} = 32.6 Hz, *trans*-CO).

²⁹Si{¹H} NMR (60 MHz, CDCl₃, 30°C): δ = -1.50 (d, ²J_{P,Si} = 5.8 Hz, Si(CH₃)₃), 4.0 (s, Si(CH₃)₃).

³¹P{¹H} NMR (121.5 MHz, CDCl₃, 30°C): δ = 47.1 (s_{sat}, ¹J_{P,W} = 295.6 Hz).

³¹P NMR (121.5 MHz, CDCl₃, 30°C): δ = 47.1 (dq_{sat}, ¹J_{P,W} = 295.6 Hz, ²J_{P,H} = 14.8 Hz, ²J_{P,H} = 12.6 Hz).

Mass spectrometry (EI, 70 eV, ^{184}W): m/z (%) = 612 (30) [$\text{M}^{\bullet+}$], 584 (20) [$(\text{M}-\text{CO})^{\bullet+}$], 556 (15) [$(\text{M}-2\text{CO})^{\bullet+}$], 514 (40) [$(\text{M}-\text{C}_6\text{H}_{10}\text{O})^{\bullet+}$], 486 (15) [$(\text{M}-\text{C}_6\text{H}_{10}\text{O}-\text{CO})^{\bullet+}$], 73 (100) [$(\text{SiMe}_3)^{\bullet+}$].

IR (Nujol, $\nu(\text{CO})$): $\tilde{\nu}$ [cm $^{-1}$] = 1942 (m), 1986(s), 2074 (s).

UV/vis (CH_2Cl_2): λ (log ε): 238 (0.47), 295 (0.06) nm.

Elemental analysis: C [%] H [%]

Calculated	35.30	4.77
Found	35.14	4.70

Analytical data of complex **46b** (ratio 23%):

^1H NMR (300 MHz, CDCl_3 , 30°C): δ = 0.18 (s, 9H, $\text{Si}(\text{CH}_3)_3$), 0.21 (s, 9H, $\text{Si}(\text{CH}_3)_3$), 1.24 (d, 1H, $^2J_{\text{P},\text{H}} = 2.9$ Hz, $\text{CH}(\text{Si}(\text{CH}_3)_3)_2$), 1.55 (m, 6H, CH_2), 1.7 (m, 4H, CH_2).

$^{13}\text{C}\{^1\text{H}\}$ NMR (75 MHz, CDCl_3 , 30°C): δ = -0.2 (d, $^3J_{\text{P},\text{C}} = 4.2$ Hz, $\text{Si}(\text{CH}_3)_3$), 0.2 (d, $^3J_{\text{P},\text{C}} = 2.4$ Hz, $\text{Si}(\text{CH}_3)_3$), 21.6 (d, $^1J_{\text{P},\text{C}} = 8.2$ Hz, CH_2), 22.5 (d, CH_2 , $^3J_{\text{P},\text{C}} = 2.8$ Hz), 23.0 (d, $^3J_{\text{P},\text{C}} = 38.0$ Hz, $\text{CH}(\text{Si}(\text{CH}_3)_3)_2$), 32.2 (d, $J_{\text{P},\text{C}} = 7.1$ Hz, CH_2), 65.0 (d, $^{1+2}J_{\text{P},\text{C}} = 29.6$ Hz, PCO), 193.8 (d, $^2J_{\text{P},\text{C}} = 8.2$ Hz, *cis*-CO), 196.6 (d, $^2J_{\text{P},\text{C}} = 32.6$ Hz, *trans*-CO).

$^{29}\text{Si}\{^1\text{H}\}$ NMR (60 MHz, CDCl_3 , 30°C): δ = -1.3 (d, $^2J_{\text{P},\text{Si}} = 6.5$ Hz, $\text{Si}(\text{CH}_3)_3$), 0.9 (d, $^2J_{\text{P},\text{Si}} = 8.2$ Hz, $\text{Si}(\text{CH}_3)_3$).

$^{31}\text{P}\{\text{H}\}$ NMR (121.5 MHz, CDCl_3 , 30°C): $\delta = 57.6$ (s_{sat} , $^1J_{\text{P},\text{W}} = 295.7$ Hz).

^{31}P NMR (121.5 MHz, CDCl_3 , 30°C): $\delta = 57.6$ (br_{sat} , $^1J_{\text{P},\text{W}} = 295.7$ Hz).

VII.7 Reactions of [(bis(trimethylsilyl)methyl)dichlorophosphane] pentacarbonyltungsten(0) [24] with 2-adamantanone, 2,2,4,4-tetramethyl-3-pentanone and 3,3-dimethylbutan-2-one

The same general procedure as the synthesis of the oxaphosphirane complex **16a** was used, changing the ketone stoichiometric from 1 eq, to 3 eq and 10 eq in relation to complex **24**. In all cases only the formation of complexes **20**^[43] and **47**^[60] was observed.

VII.8 Reactions of [(bis(trimethylsilyl)methyl)dichlorophosphane] pentacarbonyltungsten(0) [24] with 1,1,3,3-tetramethylurea, *N,N*-dimethylformamide and tetrahydro-1,3-dimethylpyrimidin-2(*IH*)-one

The same general procedure as the synthesis of the oxaphosphirane complex **16a** was used, changing the dimethylformamide stoichiometric from 1 eq, to 2 eq and 5 eq in relation to complex **24**.

1 eq (^{31}P NMR): 130.1 ppm $^1J_{\text{W,P}} = 276.8$ Hz (80%), -25 ppm $^1J_{\text{W,P}} = 287$ Hz (20%).

2 eq (^{31}P NMR): 96 ppm $^1J_{\text{W,P}} = 259.1$ Hz (10%), 89.0 ppm $^1J_{\text{W,P}} = 252.0$ Hz (10%), -25 ppm $^1J_{\text{W,P}} = 287$ Hz (80%).

5 eq (^{31}P NMR): 77.8 ppm $^1J_{\text{W,P}} = 272$ Hz, $^1J_{\text{P,H}} = 323$ Hz (60%), 54.8 ppm $^1J_{\text{W,P}} = 268$ Hz, $^1J_{\text{P,H}} = 352$ Hz (10%), -23.0 ppm $^1J_{\text{W,P}} = 312$ Hz (30%).

The same general procedure as the synthesis of the oxaphosphirane complex **16a** was used, changing the *N,N*-dimethylformamide stoichiometric from 1 eq, to 2 eq and 5 eq in relation to complex **24**.

In all cases the main product show a $^{31}\text{P}\{\text{H}\}$ NMR resonance at -23 ppm with $^1J_{\text{W,P}} = 312$ Hz and a mixture unidentified products from 50 to 20 ppm.

The same general procedure as the synthesis of the oxaphosphirane complex **16a** was used, changing the tetrahydro-1,3-dimethylpyrimidin-2(*IH*)-one stoichiometric from 1 eq, to 2 eq and 5 eq in relation to the complex **24**.

In all cases the main product show the $^{31}\text{P}\{\text{H}\}$ NMR spectra at room temperature show a mixture of unidentified products from 50 to 20 ppm, broad signal and one small signal at 10 ppm with $^1J_{\text{W,P}} = 233$ Hz. $^{31}\text{P}\{\text{H}\}$ NMR monitoring at low temperature show only the formation of the phosphinidenoid complex **18**^[60] before reacted to the other products.

VII.9 Reaction of [dichlorophenylphosphane]pentacarbonyltungsten(0) **[48]** with benzaldehyde

100 mg (20 mmol) complex **48** were dissolved in 5 mL Et₂O. 32 μL (0.20 mmol) 12-crown-4 were added and the solution cooled down to -80°C. 21 μL (0.40 mmol) *tert*-buthyllithium

were added under stirring and after 2 min 113 μ L (0.20 mmol) benzaldehyde. The solution was allowed to warm up to room temperature and a $^{31}\text{P}\{\text{H}\}$ NMR spectra of the reaction solution was taken. The spectra showed many signals between 50 and 10 ppm, which could not be identified.

VII.10 Attempts to synthesized [(cyclopenta-1,3-dienyl)dichlorophosphane]-pentacarbonyltungsten(0) [49]

0.334 g (2 mmol) $\text{W}(\text{CO})_5\text{CH}_3\text{CN}$ were dissolved in 30 mL THF and 0.730 g (2 mmol) of (cyclopenta-1,3-dienyl)dichlorophosphane added. $^{31}\text{P}\{\text{H}\}$ NMR spectroscopy of the reaction solution show a signal at 129.5 ppm ($^1J_{\text{W},\text{P}} = 343,3$ Hz (80%)) after 30 h, which was assigned to the phosphane complex and another at 162.8 assigned to the free phosphane. After column flash chromatography (Al_2O_3 , $\phi = 2$ cm, $h = 2$ cm, $T = -20$ °C, time: 10 min, petroleum ether (200 mL)) and NMR measurement a new signal at 114 ppm ($^1J_{\text{W},\text{P}} = 339$ Hz) appeared, and thus no pure complex **49** could be isolated.

VII.11 Attempted complexation of (1,3,5-tri-*tert*-butylbenzyl)dichlorophosphane [50]

1.60 g (4.5 mmol) $\text{W}(\text{CO})_6$ were dissolved in 160 mL THF and 45 min at -10°C photolysized. Then 1.64 g (4.7 mmol) of (1,3,5-tri-*tert*-butylbenzyl)dichlorophosphane^[64] were added. The mixture was stirred for four days in the dark; no complexation was observed after this time.

VII.12 Attempted complexation of (1,3,5-trimethylbenzyl)dichlorophosphane [51]

2.13 g (6.1 mmol) W(CO)₆ were dissolved in 160 mL THF and 45 min at -10°C photolysized. Then 1.17 g (5.3 mmol) of (1,3,5-trimethylbenzyl)dichlorophosphane^[63] were added. The mixture was stirred for four days in the dark; no complexation was observed after this time.

VII.13 Attempted synthesis of
[(bis(trimethylsilyl)methyl)dichlorophosphane]borane [52]

1.5 g (5.74 mmol) of (bis(trimethylsilyl)methyl)dichlorophosphane **24** was dissolved in 5 mL toluene and 6.3 mL (6.31 mmol) of a solution BH₃.THF 1M were added. After 12 h stirring the solvent was removed at reduce pressure ($\sim 10^{-2}$ mbar) and the residue washed with petroleum ether. The complex **52** was obtained as white semi solid compound because of the partial decomplexation of complex **52** into the liquid dichlorophosphane **23**.

Yield: 0.95 g (60%)

Empirical formula: C₇H₂₂BCl₂PSi₂ Molecular weight: 275.11 g/mol

¹H NMR (300 MHz, CDCl₃, 30°C): δ = 0.39 (s, 18H, Si(CH₃)₃), 1.50 (q, 3H, ¹J_{B,H} = 100.0 Hz BH₃), 1.72 (d, 1H, ²J_{P,H} = 13.88 Hz, CH(Si(CH₃)₃)₂).

¹³C{¹H}NMR (75 MHz, CDCl₃, 30°C): δ = 2.9 (d, ³J_{P,C} = 3.6 Hz, Si(CH₃)₃), 32.7 (d, ¹J_{P,C} = 27.8 Hz, CH(Si(CH₃)₃)₂).

$^{29}\text{Si}\{\text{H}\}$ NMR (60 MHz, CDCl_3 , 30°C): $\delta = 2.5$ (broad signal).

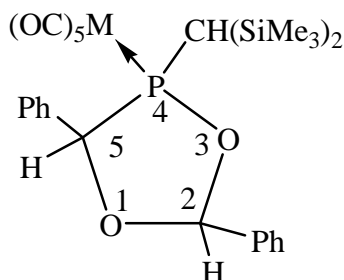
^{31}P NMR (121.5 MHz, CDCl_3 , 30°C): $\delta = 177.7$ (d, $^1J_{\text{P,B}} = 33.1$ Hz).

$^{11}\text{B}\{\text{H}\}$ NMR (96 MHz, CDCl_3 , 30°C): $\delta = -26.3$ (d, $^1J_{\text{P,B}} = 23.5$ Hz).

^{11}B NMR (96 MHz, CDCl_3 , 30°C): $\delta = -26.3$ (dq, $^1J_{\text{P,B}} = 21.2$ Hz, $^1J_{\text{B,H}} = 103.3$ Hz).

VII.14 General procedure for the synthesis of [2-(bis(trimethylsilyl)methyl)-2,5-diphenyl-1,3,4-dioxaphospholane]pentacarbonylchromium(0), molybdenum(0) and tungsten(0) **[62-64a,b]**

(0.6 mmol) of the appropriate oxaphosphirane complex (0.293 g oxaphosphirane complex **29**, 0.320 g oxaphosphirane complex **30**, 0.428 g oxaphosphirane complex **16a**) were dissolved in 10 mL dichloromethane. 100 μ L (1.4 mmol) of benzaldehyde were added and the solution was cooled down to -30°C. 62 μ L (0.6 mmol) of TfOH were added while stirring, the orange solution was then stirring for 10 minutes at low temperature. After addition of the Net_3 100 μ L (0.6 mmol), the solution turned yellow. The solvent was removed under reduced pressure ($\sim 10^{-2}$ mbar) and the oily residue was subjected to column chromatography. (Al₂O₃, -30°C, h = 1cm, ϕ = 2cm, petroleum ether (200 mL); petroleum ether/ diethyl ether 4:1 (200 mL)). The first fraction yielded **62-64a**, while the second fraction yielded a mixture of isomers **62a,b-64a,b** in each case.



VII.14.1 Synthesis of [2-(bis(trimethylsilyl)methyl)-2,5-diphenyl-1,3,4-dioxaphospholane]pentacarbonylchromium(0) **[62a,b]**

Synthesized according to the general procedure for the [2-(bis(trimethylsilyl)methyl)-2,5-diphenyl-1,3,4-dioxaphospholane]pentacarbonylmetal(0).

Empirical formula: C₂₆H₃₁O₇PSi₂Cr Molecular weight: 594.6 g/mol

Analytical data of complex **62a** (ratio 69%):

Yield: 44 mg 13%

Melting point: 128°C

¹H NMR (300 MHz, CDCl₃, 30°C): δ = -0.20 (s, 9H, Si(CH₃)₃), 0.50 (s, 9H, Si(CH₃)₃, 1.65 (d, 1H, ²J_{P,H} = 20.0 Hz, CH(Si(CH₃)₃)₂), 5.64 (d, 1H, ²⁺⁵J_{P,H} = 23.8 Hz, C⁵-H), 6.09 (s, 1H, C²-H), 7.5 (m, 5H, Ph).

¹³C{¹H}NMR (75 MHz, CDCl₃, 30°C): δ = 1.7 (d, ³J_{P,C} = 3.2 Hz, Si(CH₃)₃), 2.3 (d, ³J_{P,C} = 2.3 Hz, Si(CH₃)₃), 22.0 (d, ¹J_{P,C} = 36.2 Hz, CH(SiCH₃)₃), 88.4 (d, ¹⁺⁴J_{P,C} = 5.2 Hz, C⁵), 102.6 (d, ²⁺³J_{P,C} = 10.3 Hz, C²), 125.5 (s, Ph), 127.2 (d, J_{P,C} = 3.4 Hz, Ph), 127.2 (d, J_{P,C} = 3.2 Hz, Ph), 127.3 (s, Ph), 128.0 (d, J_{P,C} = 1.2 Hz, Ph), 128.7 (s, Ph), 132.1 (d, J_{P,C} = 1.8 Hz, *i*-Ph), 136.5 (d, J_{P,C} = 1.23 Hz, *i*-Ph), 214.7 (d, ²J_{P,C} = 13.7 Hz, *cis*-CO), 218.7 (d, ²J_{P,C} = 5.27 Hz, *trans*-CO).

²⁹Si{¹H} NMR (60 MHz, CDCl₃, 30°C): δ = -3.8 (d, ²J_{P,Si} = 10.5 Hz, Si(CH₃)₃), 3.0 (d, ²J_{P,Si} = 3.6 Hz, Si(CH₃)₃).

³¹P{¹H} NMR (121.5 MHz, CDCl₃, 30°C): δ = 180.4.

³¹P NMR (121.5 MHz, CDCl₃, 30°C): δ = 180.4 (t, ²J_{P,H} = 19.1 Hz).

Mass spectrometry (EI, ^{52}Cr): m/z (%) = 594 (50) [$\text{M}^{\bullet+}$], 566 (20)[(M-CO) $^{\bullet+}$], 510 (15)[(M-3CO) $^{\bullet+}$], 454 (100)[(M-5CO) $^{\bullet+}$], 348 (50) [(M-5CO-PhCHO) $^{\bullet+}$].

IR (Nujol, v(CO)): $\tilde{\nu}$ [cm $^{-1}$] = 1934 (s), 2060 (m).

UV/vis (CH_2Cl_2): λ (log ε): 265 (3.31), 348 (0.39) nm.

Elemental analysis: C [%] H [%]

Calculated 52.3 5.30

Found 52.7 5.30

Analytical data of the complex **62b** (from a 59:41 mixture with **62a**):

Yield: 88 mg 26%

^1H NMR (300 MHz, CDCl_3 , 30°C): δ = -0.20 (s, 9H, $\text{Si}(\text{CH}_3)_3$), 0.10 (s, 9H, $\text{Si}(\text{CH}_3)_3$, 2.00 (d, 1H, $^2J_{\text{P},\text{H}} = 19.5$ Hz, $\underline{\text{CH}}(\text{Si}(\text{CH}_3)_3)_2$), 5.39 (d, 1H, $^{2+5}J_{\text{P},\text{H}} = 20.2$ Hz, $\text{C}^5\text{-H}$), 6.68 (s, 1H, $\text{C}^2\text{-H}$), 7.5 (m, 5H, Ph).

$^{13}\text{C}\{^1\text{H}\}$ NMR (75 MHz, CDCl_3 , 30°C): δ = 1.7 (d, $^3J_{\text{P},\text{C}} = 3.2$ Hz, $\text{Si}(\text{CH}_3)_3$), 2.3 (d, $^3J_{\text{P},\text{C}} = 2.3$ Hz, $\text{Si}(\text{CH}_3)_3$), 25.1 (d, $^1J_{\text{P},\text{C}} = 36.2$ Hz, $\underline{\text{CH}}(\text{Si}(\text{CH}_3)_3)_2$), 91.6 (d, $^{1+4}J_{\text{P},\text{C}} = 2.6$ Hz, C^5), 102.5 (d, $^{2+3}J_{\text{P},\text{C}} = 15.5$ Hz, C^2), 124.5 (s, Ph), 126.5 (d, $J_{\text{P},\text{C}} = 3.4$ Hz, Ph), 127.3 (d, $J_{\text{P},\text{C}} = 3.2$ Hz, Ph), 127.4 (s, Ph), 128.1 (d, $J_{\text{P},\text{C}} = 2.0$ Hz, Ph), 128.5 (s, Ph), 132.7 (d, $J_{\text{P},\text{C}} = 3.1$ Hz, *i*-

Ph), 134.5 (d, $J_{P,C} = 2.45$ Hz, *i*-Ph), 215.2 (d, $^2J_{P,C} = 13.7$ Hz, *cis*-CO), 219.0 (d, $^2J_{P,C} = 5.45$ Hz, *trans*-CO).

$^{29}\text{Si}\{\text{H}\}$ NMR (60 MHz, CDCl_3 , 30°C): $\delta = -4.0$ (d, $^2J_{\text{P},\text{Si}} = 11.6$ Hz, $\text{Si}(\text{CH}_3)_3$), 2.4 (d, $^2J_{\text{P},\text{Si}} = 3.8$ Hz, $\text{Si}(\text{CH}_3)_3$).

$^{31}\text{P}\{\text{H}\}$ NMR (121.5 MHz, CDCl_3 , 30°C): $\delta = 181.2$.

^{31}P NMR (121.5 MHz, CDCl_3 , 30°C): $\delta = 181.2$ (t, $^2J_{\text{P},\text{H}} = 16.5$ Hz).

VII.14.2 Synthesis of [2-(bis(trimethylsilyl)methyl)-2,5-diphenyl-1,3,4-dioxaphospholane]pentacarbonylmolybdenum(0) [**63a,b**]

Synthesized according to the general procedure for the [2-(bis(trimethylsilyl)methyl)-2,5-diphenyl-1,3,4-dioxaphospholane]pentacarbonylmetal (0)

Empirical formula: $\text{C}_{26}\text{H}_{31}\text{O}_7\text{PSi}_2\text{Mo}$ Molecular weight: 638.6 g/mol

Analytical data of complex **63a**:

Yield: 48 mg 13%

Melting point: 125°C

¹H NMR (300 MHz, CDCl₃, 30°C): δ = -0.20 (s, 9H, Si(CH₃)₃), 0.10 (s, 9H, Si(CH₃)₃), 1.92 (d, 1H, ²J_{P,H} = 17.9 Hz, CH(Si(CH₃)₃)₂), 5.32 (d, 1H, ²⁺⁵J_{P,H} = 15.5 Hz, C⁵-H), 6.72 (s, 1H, C²-H), 7.5 (m, 5H, Ph).

¹³C{¹H}NMR (75 MHz, CDCl₃, 30°C): δ = 1.3 (d, ³J_{P,C} = 3.7 Hz, Si(CH₃)₃), 2.2 (d, ³J_{P,C} = 2.3 Hz, Si(CH₃)₃), 20.3 (d, ¹J_{P,C} = 36.8 Hz, CH(SiCH₃)₃)₂), 88.7 (d, ¹⁺⁴J_{P,C} = 5.8 Hz, C⁵), 102.8 (d, ²⁺³J_{P,C} = 10.4 Hz, C²), 124.5 (s, Ph), 126.2 (d, J_{P,C} = 3.3 Hz, Ph), 127.4 (s, Ph), 128.0 (d, J_{P,C} = 1.2 Hz, Ph), 128.1 (s, Ph), 132.8 (d, J_{P,C} = 3.2 Hz, i-Ph), 136.7 (d, J_{P,C} = 2.5 Hz, i-Ph), 204.5 (d, ²J_{P,C} = 9.7 Hz, cis-CO), 208.2 (d, ²J_{P,C} = 26.51 Hz, trans-CO).

²⁹Si{¹H} NMR (60 MHz, CDCl₃, 30°C): δ = -3.9 (s, Si(CH₃)₃), 2.7 (d, ²J_{P,Si} = 3.6 Hz, Si(CH₃)₃).

³¹P{¹H} NMR (121.5 MHz, CDCl₃, 30°C): δ = 154.4.

³¹P NMR (121.5 MHz, CDCl₃, 30°C): δ = 154.4 (t, ²J_{P,H} = 16.4 Hz).

Mass spectrometry (EI, ⁹⁸Mo): m/z (%) = 640 (15) [M•⁺], 556 (30) [(M-3CO)^{•+}], 534 (35) [(M-PhCHO)^{•+}], 500 (35) [(M-5CO)^{•+}], 296 (100) [(M-PhCHO-Mo(CO)₅)^{•+}], 281 (60)[(M-PhCHO-Mo(CO)₅-CH₃)^{•+}], 73 (90) [(SiMe₃)^{•+}].

IR (Nujol, ν(CO)): ν [cm⁻¹] = 1941 (s), 1980 (m), 2076 (m).

UV-vis (CH₂Cl₂): λ (log ε): 238 (0.19), 295 (0.03), 343 (0.01) nm.

Elemental analysis: C [%] H [%]

Calculated 48.95 4.89

Found 48.97 4.91

Analytical data of complex **63b** (from a 47:53 mixture with **63a**):

Yield: 96 mg 25%

¹H NMR (300 MHz, CDCl₃, 30°C): δ = -0.20 (s, 9H, Si(CH₃)₃), 0.44 (s, 9H, Si(CH₃)₃), 1.58 (d, 1H, ²J_{P,H} = 18.7 Hz, CH(Si(CH₃)₃)₂), 5.7 (d, 1H, ²⁺⁵J_{P,H} = 20.9 Hz, C⁵-H), 6.08 (s, 1H, C²-H), 7.5 (m, 5H, Ph).

¹³C{¹H}NMR (75 MHz, CDCl₃, 30°C): δ = 1.5 (d, ³J_{P,C} = 4.2 Hz, Si(CH₃)₃), 2.3 (d, ³J_{P,C} = 2.3 Hz, Si(CH₃)₃), 21.9 (d, ¹J_{P,C} = 36.2 Hz, CH(SiCH₃)₃)₂), 91.9 (d, ¹⁺⁴J_{P,C} = 2.6 Hz, C⁵), 101.7 (d, ²⁺³J_{P,C} = 8.4 Hz, C²), 125.3 (s, Ph), 127.0 (d, J_{P,C} = 3.3 Hz, Ph), 127.2 (s, Ph), 127.3 (s, Ph), 128.0 (d, J_{P,C} = 1.2 Hz, Ph), 128.0 (s, Ph), 131.9 (d, J_{P,C} = 1.9 Hz, i-Ph), 134.5 (d, J_{P,C} = 2.6 Hz, i-Ph), 204.0 (d, ²J_{P,C} = 9.0 Hz, cis-CO), 207.9 (d, ²J_{P,C} = 26.5 Hz, trans-CO).

²⁹Si{¹H} NMR (60 MHz, CDCl₃, 30°C): δ = -4.0 (s, Si(CH₃)₃), 1.9 (d, ²J_{P,Si} = 3.9 Hz, Si(CH₃)₃).

³¹P{¹H} NMR (121.5 MHz, CDCl₃, 30°C): δ = 154.7.

³¹P NMR (121.5 MHz, CDCl₃, 30°C): δ = 154.7 (t, ²J_{P,H} = 19.1 Hz).

VII.14.3 Synthesis of [2-(bis(trimethylsilyl)methyl)-2,5-diphenyl-1,3,4-dioxaphospholane]pentacarbonyltungsten(0) [**64a,b**]

Synthesized according to the general procedure for [2-(bis(trimethylsilyl)methyl)-2,5-diphenyl-1,3,4-dioxaphospholane]pentacarbonylmetal(0).

Empirical formula: C₂₆H₃₁O₇PSi₂W Molecular weight: 726.5 g/mol

Analytical data of complex **64a**:

Yield: 57 mg 13%

Melting point: 130°C

¹H NMR (300 MHz, CDCl₃, 30°C): δ = -0.20 (s, 9H, Si(CH₃)₃), 0.10 (s, 9H, Si(CH₃)₃), 1.8 (d, 1H, ²J_{P,H} = 19.9 Hz, CH(Si(CH₃)₃)₂), 5.40 (d, 1H, ²⁺⁵J_{P,H} = 14.3 Hz, C⁵-H), 6.50 (d, 1H, ²J_{P,H} = 4.1 Hz, C²-H), 7.40 (m, 5H, Ph).

¹³C{¹H}NMR (75 MHz, CDCl₃, 30°C): δ = 1.6 (d, ³J_{P,C} = 3.9 Hz, Si(CH₃)₃), 2.4 (d, ³J_{P,C} = 2.3 Hz, Si(CH₃)₃), 22.5 (d, ¹⁺⁴J_{P,C} = 29.4 Hz, CH(SiCH₃)₃), 93.0 (d, ¹J_{P,C} = 7.8 Hz, C⁵), 101.8 (d, ²⁺³J_{P,C} = 8.1 Hz, C²), 125.3 (s, Ph), 127.1 (d, J_{P,C} = 3.2 Hz, Ph), 127.2 (s, Ph), 127.1 (s, Ph), 128.0 (d, J_{P,C} = 1.2 Hz, Ph), 128.1 (s, Ph), 132.0 (d, J_{P,C} = 1.9 Hz, i-Ph), 133.0 (d, J_{P,C} = 3.2 Hz, i-Ph), 195.4 (d, ²J_{P,C} = 7.4 Hz, cis-CO), 196.7 (d, ²J_{P,C} = 27.9 Hz, trans-CO).

²⁹Si{¹H} NMR (60 MHz, CDCl₃, 30°C): δ = -3.6 (d, ²J_{P,Si} = 12.8 Hz, Si(CH₃)₃), 2.0 (d, ²J_{P,Si} = 4.4 Hz, Si(CH₃)₃).

$^{31}\text{P}\{\text{H}\}$ NMR (121.5 MHz, CDCl_3 , 30°C): $\delta = 130.6$ (s_{sat} , $^1J_{\text{W,P}} = 281.0$ Hz).

^{31}P NMR (121.5 MHz, CDCl_3 , 30°C): $\delta = 130.6$ (t_{sat} , $^1J_{\text{W,P}} = 281.0$ Hz, $^2J_{\text{P,H}} = 15.2$ Hz, $^2J_{\text{P,H}} = 17.8$ Hz).

Mass spectrometry (EI, 70 eV, ^{184}W): m/z (%) = 726 (20) [$\text{M}^{\bullet+}$], 620 (20) [(M-PhCHO) $^{\bullet+}$], 514 (20) [(M-2Ph-2CO) $^{\bullet+}$], 196 (100) [(Ph-CO-Ph) $^{\bullet+}$], 73 (10) [(SiMe₃) $^{\bullet+}$].

IR (Nujol, v(CO)): $\tilde{\nu}$ [cm⁻¹] = 1932 (s), 2069 (m).

UV/vis (CH₂Cl₂): λ (log ε): 235 (2.63), 295 (0.18) nm.

Elemental analysis: C [%] H [%]

Calculated 42.98 4.30

Found 43.09 4.15

Analytical data of complex **64b** (from a 54:46 mixture with **64a**):

Yield: 114 mg 26%

^1H NMR (300 MHz, CDCl_3 , 30°C): $\delta = -0.20$ (s, 9H, Si(CH₃)₃), 0.45 (s, 9H, Si(CH₃)₃), 2.1 (d, 1H, $^2J_{\text{P,H}} = 19.0$ Hz, CH(SiCH₃)₂), 5.80 (d, 1H, $^{2+5}J_{\text{P,H}} = 19.4$ Hz, C⁵-H), 6.10 (d, 1H, $^2J_{\text{P,H}} = 1.8$ Hz, C²-H), 7.6 (m, 5H, Ph).

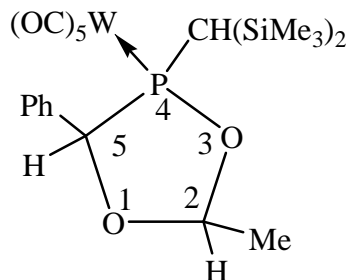
$^{13}\text{C}\{\text{H}\}$ NMR (75 MHz, CDCl_3 , 30°C): $\delta = 1.4$ (d, $^3J_{\text{P,C}} = 3.7$ Hz, $\text{Si}(\text{CH}_3)_3$), 2.2 (d, $^3J_{\text{P,C}} = 2.3$ Hz, $\text{Si}(\text{CH}_3)_3$), 20.6 (d, $^1J_{\text{P,C}} = 29.8$ Hz, $\underline{\text{C}}\text{H}(\text{SiCH}_3)_3)_2$), 89.5 (d, $^{1+4}J_{\text{P,C}} = 11.3$ Hz, C^5), 103.2 (d, $^{2+3}J_{\text{P,C}} = 10.3$ Hz, C^2), 124.5 (s, Ph), 126.4 (d, $J_{\text{P,C}} = 3.4$ Hz, Ph), 127.3 (s, Ph), 128.0 (d, $J_{\text{P,C}} = 1.2$ Hz, Ph), 128.4 (s, Ph), 134.4 (d, $J_{\text{P,C}} = 3.2$ Hz, *i*-Ph), 136.5 (d, $J_{\text{P,C}} = 0.9$ Hz, *i*-Ph), 196.0 (d, $^2J_{\text{P,C}} = 7.4$ Hz, *cis*-CO), 196.4 (d, $^2J_{\text{P,C}} = 27.8$ Hz, *trans*-CO).

$^{29}\text{Si}\{\text{H}\}$ NMR (60 MHz, CDCl_3 , 30°C): $\delta = -3.6$ (d, $^2J_{\text{P,Si}} = 11.9$ Hz, $\text{Si}(\text{CH}_3)_3$), 2.8 (d, $^2J_{\text{P,Si}} = 4.1$ Hz, $\text{Si}(\text{CH}_3)_3$).

$^{31}\text{P}\{\text{H}\}$ NMR (121.5 MHz, CDCl_3 , 30°C): $\delta = 130.8$ (s_{sat}, $^1J_{\text{W,P}} = 281.0$ Hz).

^{31}P NMR (121.5 MHz, CDCl_3 , 30°C): $\delta = 130.8$ (t_{sat}, $^1J_{\text{W,P}} = 281.0$ Hz, $^2J_{\text{P,H}} = 20.3$ Hz, $^2J_{\text{P,H}} = 17.8$ Hz).

VII.14.4 Synthesis of [2-(bis(trimethylsilyl)methyl)-2-methyl-5-phenyl-1,3,4-dioxaphospholane]pentacarbonyltungsten(0) [**65a,b**]



0.300 g (0.48 mmol) of the oxaphosphirane complex **16a** were dissolved in 10 mL dichloromethane. 27 μ L (0.48 mmol) of acetaldehyde were then added and the solution was cooling down to -30°C. 77 μ L (0.48 mmol) of TfOH were added while stirring, the orange solution was stirring for 10 minutes at low temperature before addition of the N e₃ 67 μ L (0.48 mmol). The solution turned into yellow. The solvent was removed under reduced pressure ($\sim 10^{-2}$ mbar) and the oily residue was subjected to column chromatography. (Al_2O_3 , -30°C, $h = 1\text{cm}$, $\phi = 2\text{ cm}$, petroleum ether (200 mL); petroleum ether/ diethyl ether 4:1 (200 mL)). The first fraction yielded **65a**, while the second fraction yielded a mixture of isomers **65a,b**.

Empirical formula: C₂₁H₂₉O₇PSi₂W

Molecular weight: 664.4 g/mol

Analytical data of complex **65a**:

Yield: 38 mg 11%

Melting point: 129°C

¹H NMR (300 MHz, CDCl₃, 30°C): δ = -0.29 (s, 9H, Si(CH₃)₃), 0.28 (s, 9H, Si(CH₃)₃), 1.60 (d, 3H, ³J_{H,H} = 4.9 Hz, CH₃), 1.80 (d, 1H, ²J_{P,H} = 19.1 Hz, CH(Si(CH₃)₃)₂), 5.13 (dq, 1H, ³⁺⁴J_{P,H} = 1.7 Hz, ³J_{H,H} = 4.9 Hz, C²-H), 5.45 (d, 1H, ²⁺⁵J_{P,H} = 19.6 Hz, C⁵-H), 7.35 (m, 5H, Ph).

¹³C{¹H}NMR (75 MHz, CDCl₃, 30°C): δ = 0.3 (d, ³J_{P,C} = 3.9 Hz, Si(CH₃)₃), 1.4 (d, ³J_{P,C} = 1.9 Hz, Si(CH₃)₃), 17.5 (d, ²J_{P,C} = 2.6 Hz, CH₃), 20.5 (d, ¹J_{P,C} = 20.6 Hz, CH(Si(CH₃)₃)₂), 92.0 (d, ¹⁺⁴J_{P,C} = 8.4 Hz, C⁵), 99.0 (d, ²⁺³J_{P,C} = 9.0 Hz, C²), 125.2 (d, J_{P,C} = 3.2 Hz, 2C, Ph), 125.6 (d, ⁵J_{P,C} = 5.2 Hz, *p*-ph), 125.7 (d, J_{P,C} = 3.9 Hz, 2C, Ph), 131.4 (d, ²J_{P,C} = 3.2 Hz, *i*-Ph), 194.5 (d, ²J_{P,C} = 7.1 Hz, *cis*-CO), 197.0 (d, ²J_{P,C} = 27.8 Hz, *trans*-CO).

²⁹Si{¹H} NMR (60 MHz, CDCl₃, 30°C): δ = -3.5 (d, ²J_{P,Si} = 12.3 Hz, Si(CH₃)₃), 2.5 (d, ²J_{P,Si} = 4.3 Hz, Si(CH₃)₃).

³¹P{¹H} NMR (121.5 MHz, CDCl₃, 30°C): δ = 132.0 (s_{sat}, ¹J_{W,P} = 279.7 Hz).

³¹P NMR (121.5 MHz, CDCl₃, 30°C): δ = 132.0 (t_{sat}, ¹J_{W,P} = 279.7 Hz, ²J_{P,H} = 19.07 Hz).

Mass spectrometry (EI, 70 eV, ¹⁸⁴W): m/z (%) = 664 (15) [M^{•+}], 620 (20) [(M-MeCHO)^{•+}], 564 (15) [(M-MeCHO-CO)^{•+}], 536 (20) [(M-MeCHO-3CO)^{•+}], 514 (70) [(M-PhCHO-MeCHO)^{•+}], 486 (100) [(M-PhCHO-MeCHO-CO)^{•+}], 73 (60) [(SiMe₃)^{•+}].

IR (Nujol, ν(CO)): ν [cm⁻¹] = 1936 (s), 1980(m), 2072 (m).

UV-vis (CH₂Cl₂): λ (log ε): 236 (2.97), 287 (0.298) nm

Elemental analysis: C [%] H [%]

Calculated 37.96 4.40

Found 37.54 5.57

Analytical data of complex **65b** (from a 67:33 mixture with **65a**):

Yield: 68 mg 21%

¹H NMR (300 MHz, CDCl₃, 30°C): δ = -0.32 (s, 9H, Si(CH₃)₃), 0.26 (s, 9H, Si(CH₃)₃), 1.40 (d, 3H, ³J_{H,H} = 5.3 Hz, CH₃), 1.81 (d, 1H, ²J_{P,H} = 13.0, CH(SiCH₃)₂), 5.45 (d, 1H, ²⁺⁵J_{P,H} = 14.3 Hz, C⁵-H), 5.80 (dq, 1H, ³⁺⁴J_{P,H} = 2.1 Hz, ³J_{H,H} = 5.3 Hz, C²-H), 7.35 (m, 5H, Ph).

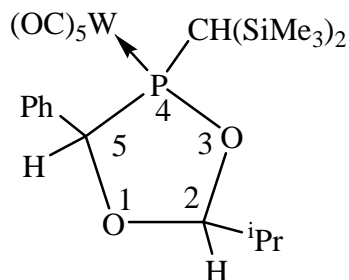
¹³C{¹H}NMR (75 MHz, CDCl₃, 30°C): δ = 0.0 (d, ³J_{P,C} = 3.9 Hz, Si(CH₃)₃), 2.6 (d, ³J_{P,C} = 2.6 Hz, Si(CH₃)₃), 18.0 (d, ³J_{P,C} = 1.9 Hz, CH₃), 21.0 (d, ¹J_{P,C} = 29.7 Hz, CH(Si(CH₃)₃)₂), 87.5 (d, ²⁺³J_{P,C} = 11.7 Hz, C²), 101.0 (d, ¹⁺⁴J_{P,C} = 10.3 Hz, C⁵), 126.2 (d, ⁵J_{P,C} = 4.6 Hz, p-Ph), 126.2 (d, J_{P,C} = 1.9 Hz, 2C, Ph), 126.4 (d, J_{P,C} = 1.9 Hz, 2C, Ph), 131.2 (d, ²J_{P,C} = 3.2 Hz, i-Ph), 194.5 (d, ²J_{P,C} = 7.1 Hz, *cis*-CO), 197.0 (d, ²J_{P,C} = 27.8 Hz, *trans*-CO).

²⁹Si{¹H} NMR (60 MHz, CDCl₃, 30°C): δ = -3.4 (d, ²J_{P,Si} = 12.3 Hz, Si(CH₃)₃), 2.8 (d, ²J_{P,Si} = 3.9 Hz, Si(CH₃)₃).

³¹P{¹H} NMR (121.5 MHz, CDCl₃, 30°C): δ = 130.0 (s_{sat}, ¹J_{W,P} = 279.7 Hz).

³¹P NMR (121.5 MHz, CDCl₃, 30°C): δ = 130.0 (t_{sat}, ¹J_{W,P} = 279.7 Hz, ²J_{P,H} = 16.5 Hz).

VII.14.5 Synthesis of [2-(bis(trimethylsilyl)methyl)-2-*iso*-propyl-5-phenyl-1,3,4-dioxaphospholane]pentacarbonyltungsten(0) [**66a,b**]



0.300 g (0.48 mmol) of the oxaphosphirane complex **16a** were dissolved in 10 mL dichloromethane. 88 μ L (0.90 mmol) of isobutyraldehyde were added and the solution was cooled down to -30°C. 77 μ L (0.48 mmol) of TfOH were added while stirring, the orange solution was stirred for 10 minutes at low temperature before addition of 67 μ L (0.48 mmol) of NEt₃. The solution turned yellow. The solvent was removed under reduced pressure ($\sim 10^{-2}$ mbar) and the oily residue was subjected to column chromatography.(Al₂O₃, -30°C, h = 1cm, ϕ = 2 cm, petroleum ether (200 mL); petroleum ether/ diethyl ether 4:1 (200 mL)). The first fraction yielded **66a**, while the second fraction yielded a mixture of isomers **66a,b**.

Empirical formula: C₂₃H₃₃O₇PSi₂W

Molecular weight: 692.49 g/mol

Analytical data of complex **66a**:

Yield: 40 mg 12%

Melting point: 130°C

¹H NMR (300 MHz, CDCl₃, 30°C): δ = 0.26 (s, 9H, Si(CH₃)₃), 0.30 (s, 9H, Si(CH₃)₃), 1.01 (m, 6H, CH₃), 1.60 (d, 1H, ²J_{P,H} = 19.8 Hz, CH(Si(CH₃)₃)₂), 2.10 (m, 1H, CH(CH₃)₂), 5.00 (d, 1H, ³⁺⁴J_{P,H} = 1.5 Hz, ²J_{H,H} = 7.5, C²-H), 5.45 (d, 1H, ²⁺⁵J_{P,H} = 20.4 Hz, C⁵-H), 7.40 (m, 5H, Ph).

$^{13}\text{C}\{\text{H}\}$ NMR (75 MHz, CDCl_3 , 30°C): $\delta = 1.7$ (d, $^3J_{\text{P,C}} = 3.9$ Hz, $\text{Si}(\text{CH}_3)_3$), 2.6 (d, $^3J_{\text{P,C}} = 1.9$ Hz, $\text{Si}(\text{CH}_3)_3$), 16.0 (s, CH_3), 20.5 (d, $^1J_{\text{P,C}} = 20.0$ Hz, $\underline{\text{CH}}(\text{Si}(\text{CH}_3)_3)_2$), 31.1 (d, $^3J_{\text{P,C}} = 2.5$ Hz, CH), 108.0 (d, $^{1+4}J_{\text{P,C}} = 8.4$ Hz, C⁵), 110.1(d, $^{2+3}J_{\text{P,C}} = 11.6$ Hz, C²), 126.5 (d, $J_{\text{P,C}} = 4.52$ Hz, Ph), 127.2 (d, $J_{\text{P,C}} = 3.87$ Hz, 2C, Ph), 127.9 (d, $J_{\text{P,C}} = 1.9$ Hz, Ph), 133.3 (d, $J_{\text{P,C}} = 3.23$ Hz, *i*-Ph), 196.1 (d, $^2J_{\text{P,C}} = 7.1$ Hz, *cis*-CO), 198.5 (d, $^2J_{\text{P,C}} = 27.8$ Hz, *trans*-CO).

$^{29}\text{Si}\{\text{H}\}$ NMR (60 MHz, CDCl_3 , 30°C): $\delta = -3.5$ (d, $^2J_{\text{P,Si}} = 12.7$ Hz, $\text{Si}(\text{CH}_3)_3$), 2.0 (d, $^2J_{\text{P,Si}} = 4.3$ Hz, $\text{Si}(\text{CH}_3)_3$).

$^{31}\text{P}\{\text{H}\}$ NMR (121.5 MHz, CDCl_3 , 30°C): $\delta = 131.0$ (s_{sat} , $^1J_{\text{W,P}} = 281.0$ Hz).

^{31}P NMR (121.5 MHz, CDCl_3 , 30°C): $\delta = 131.0$ (t_{sat} , $^1J_{\text{W,P}} = 281.0$ Hz, $^2J_{\text{P,H}} = 19.80$ Hz).

Mass spectrometry (EI, 70 eV, ^{184}W): m/z (%) = 692 (50) [$\text{M}^{\bullet+}$], 620 (20)[($\text{M}-^i\text{PrCHO}$) $^{\bullet+}$], 536 (20)[($\text{M}-^i\text{PrCHO}-3\text{CO}$) $^{\bullet+}$], 514 (60) [($\text{M}-\text{PhCHO}-^i\text{PrCHO}$) $^{\bullet+}$], 486 (100)[($\text{M}-\text{PhCHO}-^i\text{PrCHO}-\text{CO}$) $^{\bullet+}$], 73 (90) [$(\text{SiMe}_3)^{\bullet+}$].

IR (Nujol, $\nu(\text{CO})$): $\ddot{\nu}$ [cm⁻¹] = 1953 (s) 2077 (m).

UV/vis (CH_2Cl_2): λ (log ε): 238 (1.48), 300 (0.25) nm.

Elemental analysis: C [%] H [%]

Calculated 39.89 4.80

Found 40.00 4.72

Analytical data of complex **66b** (from a 67:33 mixture with **66a**):

Yield: 77 mg 23%

¹H NMR (300 MHz, CDCl₃, 30°C): δ = -0.20 (s, 9H, Si(CH₃)₃), -0.18 (s, 9H, Si(CH₃)₃), 1.4 (m, 6H, CH₃), 1.80 (d, 1H, ²J_{P,H} = 11.9 Hz, CH(Si(CH₃)₃)₂), 2.00 (m, 1H, CH(CH₃)₂), 5.20 (d, 1H, ³⁺⁴J_{P,H} = 1.00 Hz, ²J_{H,H} = 6.8, C²-H), 5.25 (d, 1H, ²⁺⁵J_{P,H} = 14.4 Hz, C⁵-H), 7.60 (m, 5H, Ph).

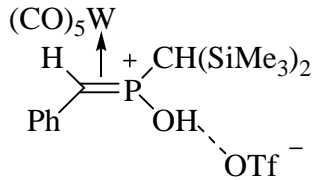
¹³C{¹H}NMR (75 MHz, CDCl₃, 30°C): δ = 1.4 (d, ³J_{P,C} = 3.9 Hz, Si(CH₃)₃), 2.6 (d, ³J_{P,C} = 1.9 Hz, Si(CH₃)₃), 17.0 (s, CH₃), 19.5 (d, ¹J_{P,C} = 30.3 Hz, CH(Si(CH₃)₃)₂), 31.1 (d, ³J_{P,C} = 2.5 Hz, CH), 93.0 (d, ¹⁺⁴J_{P,C} = 8.4 Hz, C⁵), 110.4 (d, ²⁺³J_{P,C} = 11.6 Hz, C²), 126.5 (d, J_{P,C} = 4.5 Hz, Ph), 127.2 (d, J_{P,C} = 3.9 Hz, 2C, Ph), 127.9 (d, J_{P,C} = 1.9 Hz, Ph), 133.3 (d, J_{P,C} = 3.2 Hz, i-Ph), 196.1 (d, ²J_{P,C} = 7.1 Hz, *cis*-CO), 198.5 (d, ²J_{P,C} = 27.8 Hz, *trans*-CO).

²⁹Si{¹H} NMR (60 MHz, CDCl₃, 30°C): δ = -3.4 (d, ²J_{P,Si} = 11.6 Hz, Si(CH₃)₃), 3.0 (d, ²J_{P,Si} = 3.9 Hz, Si(CH₃)₃).

³¹P{¹H} NMR (121.5 MHz, CDCl₃, 30°C): δ = 129.5 (s_{sat}, ¹J_{W,P} = 279.7 Hz).

³¹P NMR (121.5 MHz, CDCl₃, 30°C): δ = 129.5 (t_{sat}, ¹J_{W,P} = 279.7 Hz, ²J_{P,H} = 17.8 Hz).

VII.15 Synthesis { η^2 -[phenylmethylen (bis(trimethylsilyl)methyl)hydroxyphosphonium]pentacarbonyltungsten(0)} trifluoromethanesulfonate [72a,b]



40 mg (0.06 mmol) of complex **16a** were dissolved in 0.6 mL of CH_2Cl_2 and 7 μL (0.07 mmol) of TfOH were added at ambient temperature. After 5 minutes the reaction was completed. The solvent was removed under vacuum ($\sim 10^{-2}$ mbar) and the green oil obtained was dissolved in CDCl_3 .

Yield: 47 mg (92%)

Empirical formula: $\text{C}_{20}\text{H}_{23}\text{F}_3\text{O}_9\text{PSSi}_2\text{W}$

Molecular weight: 770.46 g/mol

Only the complete data for the major isomer, complex **72a** ratio (86%), are given:

^1H NMR (300 MHz, CDCl_3 , 30°C): $\delta = 0.20$ (s, 9H, $\text{Si}(\text{CH}_3)_3$), 0.40 (d, 1H, $^2J_{\text{P},\text{H}} = 10.5$ Hz, $\text{CH}(\text{Si}(\text{CH}_3)_3)_2$, 0.48 (s, 9H, $\text{Si}(\text{CH}_3)_3$), 3.20 (d, 1H, $^2J_{\text{P},\text{H}} = 16.3$ Hz, CHPh), 7.40 (m_c, 5H, Ph).

$^{13}\text{C}\{^1\text{H}\}$ NMR (75 MHz, CDCl_3 , 30°C): $\delta = -0.1$ (d, $^3J_{\text{P},\text{C}} = 4.2$ Hz; $\text{Si}(\text{CH}_3)_3$), 0.1 (d, $^3J_{\text{P},\text{C}} = 2.9$ Hz; $\text{Si}(\text{CH}_3)_3$), 15.0 (d, $^1J_{\text{P},\text{C}} = 16.5$ Hz, CHPh), 18.1 (d, $^1J_{\text{P},\text{C}} = 24.6$ Hz; $\text{CH}(\text{Si}(\text{CH}_3)_3)_2$), 117.0 (q, $^1J_{\text{F},\text{C}} = 317.0$ Hz; SO_3CF_3), 126.5 (d, $^3J_{\text{P},\text{C}} = 2.3$ Hz; Ph), 126.8 (s; Ph), 127.6 (s; *p*-Ph), 134.3 (d, $^2J_{\text{P},\text{C}} = 6.1$ Hz; *i*-Ph), 190.4 (d, $^2J_{\text{P},\text{C}} = 9.7$ Hz; CO).

$^{29}\text{Si}\{\text{H}\}$ NMR (60 MHz, CDCl_3 , 30°C): $\delta = 3.4$ (d, $^2J_{\text{P},\text{Si}} = 4.7$ Hz, $\text{Si}(\text{CH}_3)_3$), 14.1 (d, $^2J_{\text{P},\text{Si}} = 14.8$ Hz, $\text{Si}(\text{CH}_3)_3$).

^{31}P NMR (121.5 MHz, CDCl_3 , 30°C): $\delta = 73.8$ (dd_{sat}, $^1J_{\text{W,P}} = 113.2$ Hz, $^2J_{\text{P,H}} = 16.5$ Hz, $^2J_{\text{P,H}} = 10.5$ Hz).

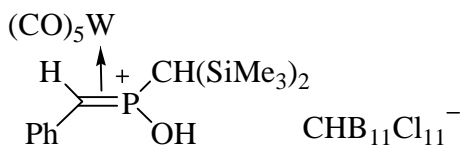
IR (Nujol, cm^{-1}): $\tilde{\nu} = \sim 3500$ (very broad; v(OH); this band is even broader than that of pure triflate acid), 2072 (w; v (CO)), 2002 (m; v (CO)), 1980 (s; v (CO)), 1937 (s; v (CO)), 1870 (m; v (CO)), 844 (m; Ph).

Analytical data of complex **72b** (ratio 14%):

^1H NMR (300 MHz, CDCl_3 , 30°C): $\delta = 0.17$ (s, 9H, $\text{Si}(\text{CH}_3)_3$), 0.58 (s, 9H, $\text{Si}(\text{CH}_3)_3$), 1.00 (d, 1H, $^2J_{\text{P,H}} = 8.7$ Hz, $\text{CH}(\text{Si}(\text{CH}_3)_3)_2$), 4.10 (d, 1H, $^2J_{\text{P,H}} = 3.81$ Hz, CHPh), 7.40 (m_c, 5H, Ph).

^{31}P NMR (121.5 MHz, CDCl_3 , 30°C): $\delta = 72.3$ (dd_{sat}, $^1J_{\text{W,P}} = 97.9$ Hz, $^2J_{\text{P,H}} = 3.7$ Hz, $^2J_{\text{P,H}} = 8.7$ Hz).

[phenylmethylene(bis(trimethylsilyl)methyl)hydroxyphosphonium]pentacarbon yltungsten(0)}_{2,3,4,5,6,7,8,9,10,11,12}-undecachloro-1-carbadodecaborate [73]



33 mg (0.05 mmol) of oxaphosphirane complex **16a** were dissolved in 0.6 mL of CD₂Cl₂ and 30 mg (0.05 mmol) of [C₇H₉][CHB₁₁Cl₁₁] were added at ambient temperature. After 10 min the reaction was completed. Colorless crystals of complex **73** were obtained from diffusion-controlled crystallisation into the reaction solution using *n*-hexane.

Yield: 48 mg (79%)

Empirical formula: C₂₀H₂₇B₁₁Cl₁₁O₆PSi₂W Molecular weight: 1143.31 g/mol

¹H NMR (300 MHz, CD₂Cl₂, 30°C): δ = 0.32 (s, 9H, Si(CH₃)₃), 0.50 (s, 9H, Si(CH₃)₃), 1.00 (d, ²J_{P,H} = 6.9 Hz, CH(Si(CH₃)₃), 3.40 (d, ²J_{P,H} = 17.4 Hz, CHPh), 3.20 (br, 1H, CHB₁₁Cl₁₁), 7.4 (m_c, 3H, Ph), 7.5 (m_c, 2H, Ph).

¹³C{¹H} NMR (75 MHz, CD₂Cl₂, 30°C): δ = 2.4 (d, ³J_{P,C} = 2.7 Hz, Si(CH₃)₃), 2.5 (d, ³J_{P,C} = 4.7 Hz, Si(CH₃)₃), 17.9 (d, ¹J_{P,C} = 15.9 Hz, CHPh), 21.0 (d, ¹J_{P,C} = 21.6 Hz, CH((Si(CH₃)₃)₂), 47.1 (s, CHB₁₁Cl₁₁), 129.0 (d, J_{P,C} = 8.9 Hz, Ph), 129.2 (d, J_{P,C} = 3.5 Hz, Ph), 130.5 (s, *p*-Ph), 136.1 (,; *i*-Ph), 193.0 (d, ²J_{P,C} = 9.6 Hz, CO).

$^{29}\text{Si}\{\text{H}\}$ NMR (60 MHz, CDCl_3 , 30°C): δ = 3.4 (d, $^2J_{\text{P},\text{Si}} = 4.7$ Hz), 14.1 (d, $^2J_{\text{P},\text{Si}} = 14.1$ Hz).

^{31}P NMR (121.5 MHz, CD_2Cl_2 , 30°C): δ = 75.5 (dd_{sat}, $^1J_{\text{W,P}} = 118.0$ Hz, $^2J_{\text{P,H}} = 17.1$ Hz, $^2J_{\text{P,H}} = 11.5$ Hz).

IR (Nujol, cm^{-1}): $\tilde{\nu} = 3387$ (br; v (OH)), 2117 (m; v (CO)), 2067 (m; v (CO)), 2037 (s; v (CO)), 2023 (s; v (CO)), 1992 (m; v (CO)), 831 (m; Ph).

VII.16.1 Synthesis of (bis(trimethylsilyl)methyl)-1-(phenyl)methylphosphinic acid [74]

0.100 g of complex **72a,b** were dissolved in 1 mL Et_2O , the precipitation of the white powder was observed ($\text{W}(\text{CO})_6$). The solvent was removed under reduce pressure ($\sim 10^{-2}$ mbar), and the compound **74** obtained as blue oil.

^1H NMR (300 MHz, CDCl_3 , 30°C): δ = 0.25 (s, 18H, $\text{Si}(\text{CH}_3)_3$), 0.80 (d, 1H, $^2J_{\text{P,H}} = 17.94$ Hz, $\text{CH}(\text{Si}(\text{CH}_3)_3)_2$), 3.50 (d, 2H, $^2J_{\text{P,H}} = 16.6$ Hz, CH_2), 7.25 (m, 2H, Ph), 7.40 (m, 3H, Ph), 10.00 (OH, broad signal).

$^{13}\text{C}\{\text{H}\}$ NMR (75 MHz, CDCl_3 , 30°C): δ = 0.0 (d, $^3J_{\text{P,C}} = 3.2$ Hz, $\text{Si}(\text{CH}_3)_3$), 11.0 (d, $^1J_{\text{P,C}} = 72.4$ Hz, $\text{CH}(\text{Si}(\text{CH}_3)_3)_2$), 37.0 (d, $^1J_{\text{P,C}} = 79.5$ Hz, CH_2), 126.6 (d, $^3J_{\text{P,C}} = 2.3$ Hz, *i*-Ph), 126.8 (d, $J_{\text{P,C}} = 3.8$ Hz, Ph), 127.8 (d, $J_{\text{P,C}} = 3.2$ Hz, 2C, Ph), 128.8 (d, $J_{\text{P,C}} = 5.8$ Hz, 2C, Ph).

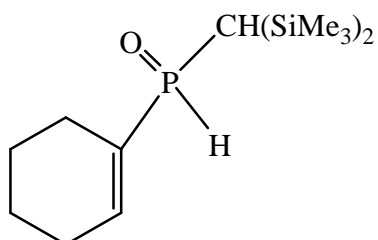
$^{29}\text{Si}\{\text{H}\}$ NMR (60 MHz, CDCl_3 , 30°C): δ = 1.9 (d, $^2J_{\text{P,Si}} = 6.1$ Hz).

^{31}P NMR (121.5 MHz, CDCl_3 , 30°C): δ = 81.61 (pseudoq, $^2J_{\text{P,H}} = 16.53$ Hz).

Mass spectrometry (EI, 70 eV, ^{184}W): m/z (%) = 314 (5) [$\text{M}^{\bullet+}$], 298 (10) [$(\text{M-O})^{\bullet+}$], 223 (7)[$(\text{M-PhCH}_2)^{\bullet+}$], 91 (15) [$(\text{CH}_2\text{Ph})^{\bullet+}$].

VII.17 Reaction of oxaphosphirane complex [46a] with triflic acid

40 mg (0.06 mmol) of oxaphosphirane complex **46a** were dissolved in CDCl_3 and 7 μL (0.07 mmol) of TfOH were added at -50°C. The sample was allowed to warm up to room temperature during the ^{31}P NMR measurement, and then measured again after 12 h at the same temperature.



82

Empirical formula: $\text{C}_{13}\text{H}_{29}\text{OPSi}_2$ Molecular weight: 288.51 g/mol

¹H NMR (300 MHz, CDCl₃, 30°C): δ = -0.18 (s, 9H, Si(CH₃)₃), 0.21 (s, 9H, Si(CH₃)₃), 0.90 (d, 1H, ²J_{P,H} = 16.3 Hz, CH(Si(CH₃)₃)₂), 1.65 (m, 4H, CH₂), 2.10 (m, 2H, CH₂), 2.21(m, 2H, CH₂), 6.79 (d, 1H, ²J_{P,H} = 23.45 Hz, CH), 7.21 (d, 1H, ¹J_{P,H} = 509.0 Hz, PH).

¹³C{¹H}NMR (75 MHz, CDCl₃, 30°C): δ = 0.0 (d, ³J_{P,C} = 4.3 Hz, Si(CH₃)₃), 1.1 (d, ³J_{P,C} = 3.2 Hz, Si(CH₃)₃), 9.4 (d, ¹J_{P,C} = 44.9 Hz, CH(Si(CH₃)₃)₂), 20.0 (s, CH₂), 21.5 (d, ³J_{P,C} = 10 Hz,CH₂), 22.4 (d, *J*_{P,C} = 13.2 Hz, CH₂), 26.1 (d, *J*_{P,C} = 15.5 Hz, CH₂), 124 (d, *J*_{P,C} = 89.3 Hz, *ipso*-CH₂), 148.7 (d, *J*_{P,C} = 8.9 Hz, CH).

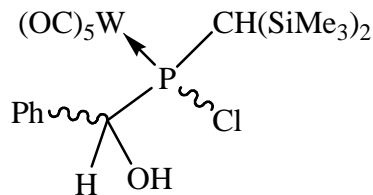
²⁹Si{¹H} NMR (60 MHz, CDCl₃, 30°C): δ = 3.6 (s, Si(CH₃)₃), 3.8 (d, ²J_{P,Si} = 3.1 Hz, Si(CH₃)₃).

³¹P NMR (121.5 MHz, CDCl₃, 30°C): δ = 56.2 (d, ¹J_{P,H} = 508.0).

VII.18 Synthesis of [(bis(trimethylsilyl)methyl)-1,1-(hydroxyphenyl)methylchlorophosphane]pentacarbonyltungsten(0) [85a,b-85c]

A stream of (HCl gas, produced by dropping HCl_{conc} onto CaCl₂, was bubbled into a solution of 0.215 mg (0.347 mmol) of complex **16a** in 20 mL Et₂O at ambient temperature for two hours.

The solvent was removed under reduced pressure ($\sim 10^{-2}$ mbar), and the products fell down after the addition of *n*-pentane. The complexes 85a, b and 85c could be partially separated after successive washing with *n*-pentane.



Analytical data of complex **85c**:

Yield: 50 mg (23%)

Empirical formula: C₁₉H₂₆ClO₆PSi₂W

Molecular weight: 656.84 g/mol

Melting point: 135 °C

¹H NMR (300 MHz, CDCl₃, 30°C): δ = 0.2 (s, 9H, Si(CH₃)₃), 0.48 (s, 9H, Si(CH₃)₃), 1.51 (d, 1H, ²J_{P,H} = 16.7 Hz, CH(SiCH₃)₂), 2.80 (s, w, OH), 5.36 (d, ²J_{P,H} = 14.3 Hz, CHPOH), 7.40 (m, 3H, Ph), 7.68 (m, 2H, Ph).

$^{13}\text{C}\{\text{H}\}$ NMR (75 MHz, CDCl_3 , 30°C): δ = 2.7 (d, $^3J_{\text{P,C}} = 3.1$ Hz, $\text{Si}(\text{CH}_3)_3$), 2.8 (d, $^3J_{\text{P,C}} = 2.7$ Hz, $\text{Si}(\text{CH}_3)_3$), 25.8 (d, $^1J_{\text{P,C}} = 28.9$ Hz, $\underline{\text{C}}\text{H}(\text{Si}(\text{CH}_3)_3)_2$), 79.1 (d, $^1J_{\text{P,C}} = 9.9$ Hz, PCOH), 127.3 (d, 2C, $J_{\text{P,C}} = 1.8$ Hz, Ph), 127.4 (d, 2C, $J_{\text{P,C}} = 2.9$ Hz, Ph), 128.3 (d, $J_{\text{P,C}} = 2.31$ Hz, Ph), 135.9 (d, $J_{\text{P,C}} = 2.0$ Hz, *i*-Ph), 196.0 (d, $^2J_{\text{P,C}} = 6.9$ Hz; *cis*-CO), 197.6 (d, $^2J_{\text{P,C}} = 32.5$ Hz, *trans*-CO).

$^{29}\text{Si}\{\text{H}\}$ NMR (60 MHz, CDCl_3 , 30°C): δ = 0.0 (d, $^2J_{\text{P,Si}} = 6.3$ Hz, $\text{Si}(\text{CH}_3)_3$), 2.6 (d, $^2J_{\text{P,Si}} = 2.2$ Hz, $\text{Si}(\text{CH}_3)_3$).

^{31}P NMR (121.5 MHz, CDCl_3 , 30°C): δ = 126.1 (t_{sat} , $^1J_{\text{W,P}} = 275.0$ Hz, $^2J_{\text{P,H}} = 15.1$ Hz).

Mass spectrometry (EI, 70 eV, ^{184}W): m/z (%) = 656 (15) [$\text{M}^{\bullet+}$], 549 (30) [(M-
PhCH(OH)) $^{\bullet+}$], 514 (10) [(M- PhCH(OH)-Cl) $^{\bullet+}$], 297 (10) [(M- W(CO)5-Cl) $^{\bullet+}$], 73 (100)
[(SiMe_3) $^{\bullet+}$].

IR (KBr, v(CO)): $\tilde{\nu}$ [cm $^{-1}$] = 3525 (m; v (OH)), 2074 (m; v (CO)), 1988 (m; v (CO)), 1934 (s;
v(CO)), 1913 (s; v (CO)), 843 (m; ph).

UV/vis (CH_2Cl_2): λ (log ϵ): 235.6 (1.69), 299.4 (0.23) nm

Elemental analysis: C [%] H [%]

Calculated 34.74 3.99

Found 34.43 4.03

Analytical data of complex **85a,b**:

Yield: 100 mg (47%)

Empirical formula: C₁₉H₂₆ClO₆PSi₂W

Molecular weight: 656.84 g/mol

Melting point: 134 °C

¹H NMR (300 MHz, CDCl₃, 30°C): δ = 0.30 (s, 9H, Si(CH₃)₃), 0.44 (s, 9H, Si(CH₃)₃), 2.31 (d, 1H, ²J_{P,H} = 12.3 Hz, CH(Si(CH₃)₃)₂), 3.80 (s, w; OH), 5.34 (d, ²J_{P,H} = 20.8 Hz, CHPOH), 7.40 (m, 3H, Ph), 7.6 (m, 2H, Ph).

¹³C{¹H}NMR (75 MHz, CDCl₃, 30°C): δ = 2.4 (d, ³J_{P,C} = 3.2 Hz; Si(CH₃)₃), 3.1 (d, ³J_{P,C} = 2.6 Hz; Si(CH₃)₃), 30.0 (broad, CH(Si(CH₃)₃)₂), 80.2 (d, ¹J_{P,C} = 21.3 Hz, PCOH), 127.5 (d, 2C, J_{P,C} = 3.0 Hz, Ph), 127.7 (d, 2C, J_{P,C} = 4.9 Hz, Ph), 128.4 (d, 1C, J_{P,C} = 3.4 Hz, Ph), 136.2 (d, 1C, J_{P,C} = 3.3 Hz, i-Ph), 195.4 (d, ²J_{P,C} = 6.8 Hz; cis-CO), 197.5 (d, ²J_{P,C} = 31.2 Hz; trans-CO).

²⁹Si{¹H} NMR (60 MHz, CDCl₃, 30°C): δ = 1.1 (broad signal, Si(CH₃)₃), 1.5 (broad signal, Si(CH₃)₃).

³¹P NMR (121.5 MHz, CDCl₃, 30°C): δ = 140.0 (br.; Wh/2 = 440 Hz).

³¹P NMR (121.5 MHz, CDCl₃, -40°C): δ = 146.6 (s_{sat}, ¹J_{W,P} = 274.0 Hz); 138.7 (s_{sat}, ¹J_{W,P} = 274.0 Hz).

Mass spectrometry (EI, 70 eV, ^{184}W): m/z (%) = 656 (15) [$\text{M}^{\bullet+}$], 572.0 (20) [$(\text{M}-3\text{CO})^{\bullet+}$], 549 (30) [$(\text{M}-\text{PhCH(OH)})^{\bullet+}$], 516 (10) [$(\text{M}-\text{Ph}-5\text{CO})^{\bullet+}$], 107 (20) [$(\text{PhHCOH})^{\bullet+}$], 73 (100) [$(\text{SiMe}_3)^{\bullet+}$].

IR (Nujol): $\tilde{\nu}$ [cm $^{-1}$] = 3400 (broad; ν (OH)), 2074 (m; ν (CO)), 1987 (s; ν (CO)), 1938 (m; ν (CO)), 1913 (s; ν (CO)), 839 (m; Ph).

UV/vis (CH_2Cl_2): λ (log ϵ): 235.6 (1.69), 299.4 (0.23) nm

Elemental analysis: C [%] H [%]

Calculated 34.74 3.99

Found 34.43 4.03

VII.19 Synthesis of [2-bis(trimethylsilyl)methyl-3-phenyl-oxaphosphirane-*k*P]pentacarbonyltungsten(0) [**16b**]

60 μ L (0.82 mmol) of diisopropylamine were dissolved in 2 mL Et₂O and cooled down to -40 °C. 0.3 mL (0.48 mmol) of a ⁿBuLi (1.6 M in Hexane) solution were added and the solution was stirred for 10 minutes at low temperature. Then the solvent were removed under vacuum ($\sim 10^{-2}$ mbar) to yield the LDA as white powder.

200 mg (0.30 mmol) of complex **85a,b** and 24 μ L (0.15 mmol) of 12-crow-4 were dissolved in 3 mL Et₂O and cooled down to -80°C. The freshly prepared LDA was dissolved in 7 mL of Et₂O and cooling down to -80 °C too. The LDA solution was added via transfer double needle to the first solution. The blue-green solution was stirred for 1 hour in the cooling bath and then stirred further 10 minutes at RT. The solvents were removed under vacuum ($\sim 10^{-2}$ mbar). The product was extracted from the brownish residue with a mixture of 2 mL Et₂O/ 5mL *n*-pentane and purified by column chromatography. (Al₂O₃, -30 °C, h = 1cm, ϕ = 1cm, petroleum ether (50 mL; petroleum ether/ diethyl ether 1:1 (50 mL)).

Yield: 117 mg (58%)

Empirical formula: C₁₉H₂₅O₆PSi₂W

Molecular weight: 620.38 g/mol

Melting point: 102 °C

¹H NMR (300 MHz, CDCl₃, 30°C): δ = 0.00 (s, 9H, Si(CH₃)₃), 0.49 (s, 9H, Si(CH₃)₃), 1.28 (d, ²J_{PH} = 17.2 Hz, 1H, CH(Si(CH₃)₃)₂), 4.50 (d, 1H, ²J_{PH} = 5.8 Hz, PhCHO), 7.40 (m, 5h, Ph).

¹³C{¹H}NMR (75 MHz, CDCl₃, 30°C): δ = -0.79 (d, ³J_{P,C} = 4.5 Hz, Si(CH₃)₃), -0.2 (d, ³J_{P,C} = 3.2 Hz, Si(CH₃)₃), 19.1 (d, ¹J_{P,C} = 39.3 Hz, CH(Si(CH₃)₃)₂), 62.5 (d, ¹J_{P,C} = 22.3 Hz, PCOH), 124.6 (d, 2C, *J*_{P,C} = 1.9 Hz, Ph), 126.0 (d, ⁵J_{P,C} = 1.9 Hz, *p*-Ph), 126.4 (d, 2C, *J*_{P,C} = 1.9 Hz, Ph), 132.2 (d, ²J_{P,C} = 3.6 Hz, *i*-Ph), 193.7 (d, ²J_{P,C} = 8.4 Hz, *cis*-CO), 193.7 (d, ²J_{P,C} = 36.5 Hz, *trans*-CO).

²⁹Si{¹H} NMR (60 MHz, CDCl₃, 30°C): δ = -0.1 (d, ²J_{P,Si} = 3.5 Hz), 4.5 (d, ²J_{P,Si} = 1.3 Hz).

³¹P{¹H} NMR (121.5 MHz, CDCl₃, 30°C): δ = 31.0 (dd_{sat}, ¹J_{P,W} = 292.3 Hz, ²J_{P,H} = 17.9 Hz, ²J_{P,H} = 5.2 Hz).

Mass spectrometry (EI, 70 eV, ¹⁸⁴W): m/z (%) = 620 (15) [M•⁺], 514 (40) [(M-PhCOH)^{•+}], 486 (100) [(M-PhCOH-CO)^{•+}], 458 (40) [(M-PhCOH-2CO)^{•+}], 430 (60) [(M-PhCOH-3CO)^{•+}], 402 (40) [(M-PhCOH-4CO)^{•+}].

IR (KBr, ν(CO)): ν [cm⁻¹] = 1949 (w), 1993 (s), 2082 (s).

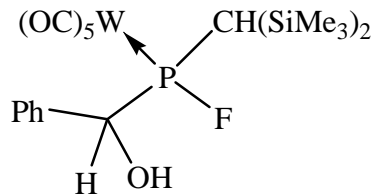
UV/vis (CH₂Cl₂): λ (log ε): 233.6 (0.76), 301.0 (0.09) nm

Elemental analysis: C [%] H [%]

Calculated 36.78 4.06

Found 36.10 4.40

VII.20 Synthesis of [(bis(trimethylsilyl)methyl)fluoro-1,1-(hydroxyphenyl)-methylphosphane]pentacarbonyltungsten(0) [90, 91]



150 mg (0.240 mmol) of complex **16a** were dissolved in 1.5 mL of CH_2Cl_2 and (33 μL , 0.240 mmol) of a solution 1M of $\text{HBF}_4 \cdot \text{Et}_2\text{O}$ were added at room temperature. The mixture was stirred at RT for 10 min and the solvent was removed under vacuum ($\sim 10^{-2}$ mbar).

The residue was subjected to low temperature chromatography ($T = -20^\circ\text{C}$, Al_2O_3 , petroleum ether: CH_2Cl_2). The last fraction yielded complex **91** as white oil. Complex **90** could only be detected in the reaction mixture.

Analytical data of complex **90**:

^{31}P NMR (121.5 MHz, CH_2Cl_2 , 30°C): $\delta = 201.0$ (br; $Wh_{1/2} = 420$ Hz, $^1J_{\text{P},\text{F}} = 826.0$ Hz).

Analytical data of complex **91**:

Yield: 91.4 mg (59%)

Empirical formula: $\text{C}_{19}\text{H}_{26}\text{FO}_6\text{PSi}_2\text{W}$ Molecular weight: 640.4 g/mol

^1H NMR (300 MHz, CDCl_3 , 30°C): $\delta = 0.34$ (s, 9H, $\text{Si}(\text{CH}_3)_3$), 0.37 (d, 9H, $^4J_{\text{F},\text{H}} = 1.1$ Hz, $\text{Si}(\text{CH}_3)_3$), 1.89 (d, 1H, $^2J_{\text{P},\text{H}} = 15.7$ Hz, $\text{CH}(\text{Si}(\text{CH}_3)_3)_2$), 2.39 (d, br, 1H, $^3J_{\text{P},\text{H}} = 24.0$ Hz, OH), 5.35 (d, 1H, $^2J_{\text{H},\text{F}} = 6.6$ Hz, CHOH), 7.45 (m_c, 5H, Ph).

$^{13}\text{C}\{\text{H}\}$ NMR (75 MHz, CDCl_3 , 30°C): $\delta = 1.6$ (dd, $^3J_{\text{P},\text{C}} = 1.9$ Hz, $^4J_{\text{P},\text{F}} = 1.2$ Hz, Si(CH₃)₃), 2.0 (dd, $^3J_{\text{P},\text{C}} = 1.9$ Hz, $^4J_{\text{P},\text{F}} = 1.2$ Hz, Si(CH₃)₃), 30.0 (m_c br, CH(Si(CH₃)₃)₂), 78.1 (qq, $^1J_{\text{P},\text{C}}$ $\approx ^2J_{\text{F},\text{C}} = 17$ Hz, PCOH), 126.6 (dd, $J_{\text{P},\text{C}} = 3.8$ Hz, $J_{\text{F},\text{C}} = 2.3$ Hz, Ph), 127.8 (d, $J_{\text{P},\text{C}} = 1.9$ Hz, Ph), 128.0 (d, $J_{\text{P},\text{C}} = 2.3$ Hz, Ph), 136.7 (s; *i*-Ph), 195.0 (dd, $^2J_{\text{P},\text{C}} = 7.7$ Hz, $^3J_{\text{F},\text{C}} = 3.5$ Hz, *cis*-CO), 197.5 (dd, $^2J_{\text{P},\text{C}} = 30.1$ Hz, $^3J_{\text{F},\text{C}} = 0.9$ Hz, *trans*-CO).

$^{29}\text{Si}\{\text{H}\}$ NMR (60 MHz, CDCl_3 , 30°C): $\delta = 0.0$ (d, $^2J_{\text{P},\text{Si}} = 5.9$ Hz).

^{31}P NMR (121.5 MHz, CDCl_3 , 30°C): $\delta = 198.1$ (dd_{sat}, $^1J_{\text{W},\text{P}} = 296.3$ Hz, $^1J_{\text{P},\text{F}} = 826.0$ Hz).

$^{19}\text{F}\{\text{H}\}$ NMR (282.4 MHz, CDCl_3 , 30°C): $\delta = -123.1$ (d, $^1J_{\text{P},\text{F}} = 851.9$ Hz).

IR (Nujol, cm⁻¹): $\tilde{\nu} = 3585$ (m; v (OH)), 2075 (m; v (CO)), 1987 (s; v (CO)), 1930 (s; v (CO)), 2023 (s; v (CO)), 1992 (m; v (CO)), 844 (m; Ph).

Mass spectrometry (EI, 70 eV, ^{184}W): m/z (%) = 640 (60) [M^{•+}], 612 (20) [(M-CO)^{•+}], 556 (10) [(M-3CO)^{•+}], 316.1 (10) [(M-W(CO)₅)^{•+}], 179 (100) [(M-W(CO)₅-2(CH₃))^{•+}], 73 (80) [(Si(CH₃)₃)^{•+}].

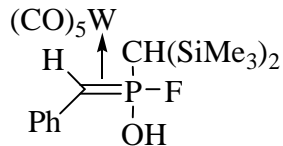
Elemental analysis: C [%] H [%]

Calculated 35.65 4.09

Found 35.82 4.20

VII.21 Synthesis of η^2 -[(phenyl)methylene(bis(trimethylsilyl)methyl)fluoro-hydroxyphosphorane]pentacarbonyltungsten(0) [92]

The same procedure as complex **91** was used to synthesize complex **92** using CDCl_3 as a solvent to measuring the NMR data in the reaction mixture.



¹H NMR (300 MHz, CDCl₃, 30°C): δ = 0.20 (s, 9H, Si(CH₃)₃), 0.30 (d, 9H, ⁴J_{F,H} = 1.1 Hz, Si(CH₃)₃), 0.85 (d, 1H, ²J_{P,H} = 20.0 Hz, CH(SiMe₃)₂), 3.40 (d, 1H, ²J_{P,H} = 17.4 Hz, CHPh), 7.45 (m_c, 5H, Ph).

$^{13}\text{C}\{\text{H}\}$ NMR (75 MHz, CDCl_3): δ = 0.2 (d, $^3J_{\text{P,C}} = 4.3$ Hz, $\text{Si}(\text{CH}_3)_3$), 0.0 (d, $^3J_{\text{P,C}} = 3.0$ Hz, $\text{Si}(\text{CH}_3)_3$), 13.0 (d, $^1J_{\text{P,C}} = 17.0$ Hz, $\underline{\text{CH}}(\text{Si}(\text{CH}_3)_3)_2$), 66.0 (broad, $\underline{\text{CHPh}}$), 126.8 (s, Ph), 127.8 (d, $^2J_{\text{P,C}} = 1.9$ Hz, Ph), 127.3 (d, $J_{\text{P,C}} = 2.2$ Hz, Ph), 136.0 (s, *i*-Ph), 197.5 (d, $^2J_{\text{P,C}} = 10.90$ Hz, CO).

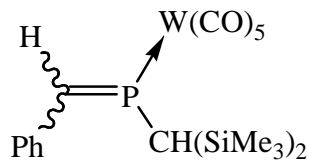
$^{29}\text{Si}\{\text{H}\}$ NMR (60 MHz, CDCl_3 , 30°C): $\delta = 4.1$ (d, $^2J_{\text{P},\text{Si}} = 4.7$ Hz, $\text{Si}(\text{CH}_3)_3$), 15.0 (d, $^2J_{\text{P},\text{Si}} = 14.9$ Hz, $\text{Si}(\text{CH}_3)_3$).

³¹P NMR (121.5 MHz, CDCl₃, 30°C): δ = 143.5 (ddd_{sat}, ¹J_{W,P} = 144.0 Hz, ¹J_{P,F} = 1043.0 Hz, ²J_{P,H} = 20.6 Hz, ²J_{P,H} = 16.8 Hz).

$^{19}\text{F}\{\text{H}\}$ NMR (282.4 MHz, CDCl_3 , 30°C): $\delta = -71.5$ (d, $^1J_{\text{P},\text{F}} = 1059.7$ Hz).

IR (Nujol, cm⁻¹): $\tilde{\nu} = 3373$ (broad signal; v (OH)), 2076 (m; v (CO)), 1980 (s; v (CO)), 1942 (s; v (CO)), 1057 (m), 844 (m; Ph).

VII.22 Synthesis of [(bis(trimethylsilyl)methyl)-1-phenylmethylenephosphane]pentacarbonyltungsten(0) [102a,b]



0.150 g (0.24 mmol) of oxaphosphirane complex **16a**, 0.12 g (0.54 mmol) CpTiCl₃ and 0.04 g Zn (0.60 mmol) were placed in a schlenk tube inside the glove box, and dissolved in 2 mL THF-d8. After 12 h stirring the reaction mixture was subjected to NMR spectroscopic studies.

Empirical formula: C₁₉H₂₅O₅PSi₂W

Molecular weight: 604.38 g/mol

Analytical data of complex **102a** (ratio 65 %):

¹H NMR (300 MHz, THF-d8, 30°C): $\delta = 0.21$ (s, 18H, Si(CH₃)₃), 3.05 (d, 1H, $^2J_{\text{P},\text{H}} = 20.0$ Hz, CH(Si(CH₃)₃)₂), 8.25 (d, 1H, $^2J_{\text{P},\text{H}} = 17.5$ Hz, CHPh), 7.20 (m, 5H, Ph).

$^{13}\text{C}\{\text{H}\}$ NMR (75 MHz, THF-d8, 30°C): δ = -0.0 (s, Si(CH₃)₃), 23.5 (d, $^3J_{\text{P,C}} = 19.6$ Hz, CH(Si(CH₃)₃)₂), 127.6 (d, 2C, $J_{\text{P,C}} = 3.7$ Hz, Ph), 130.5 (d, 2C, $^3J_{\text{P,C}} = 5.2$ Hz, Ph), 132.6 (d, $^2J_{\text{P,C}} = 3.7$ Hz, *i*-Ph), 165.1 (d, $^1J_{\text{P,C}} = 39.0$ Hz, CHPh), 195.4 (d, $^2J_{\text{P,C}} = 9.7$ Hz, *cis*-CO), 197.5 (d, $^2J_{\text{P,C}} = 29.7$ Hz, *trans*-CO).

$^{29}\text{Si}\{\text{H}\}$ NMR (60 MHz, THF-d8, 30°C): δ = 3.1 (d, $^2J_{\text{P,Si}} = 14.8$ Hz, Si(CH₃)₃).

$^{31}\text{P}\{\text{H}\}$ NMR (121.5 MHz, THF-d8, 30°C): δ = 212.0 (s_{sat}, $^1J_{\text{P,W}} = 260.0$ Hz, $^2J_{\text{P,H}} = 18.04$ Hz).

Analytical data of complex **102b** (ratio 25 %):

^1H NMR (300 MHz, THF-d8, 30°C): δ = 0.29 (s, 18H, Si(CH₃)₃), 1.50 (d, 1H, $^2J_{\text{P,H}} = 5.30$ Hz, CH(Si(CH₃)₃)₂), 8.80 (d, 1H, $^2J_{\text{P,H}} = 20.3$ Hz, CHPh), 7.00 (m, 5H, Ph).

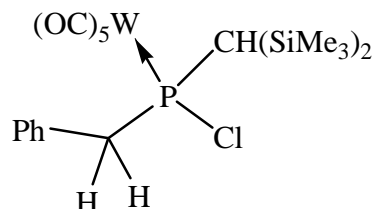
$^{13}\text{C}\{\text{H}\}$ NMR (75 MHz, THF-d8, 30°C): δ = 0.0 (s, Si(CH₃)₃), 34.0 (d, $^3J_{\text{P,C}} = 16.8$ Hz, CH(Si(CH₃)₃)₂), 127.6 (d, 2C, $^3J_{\text{P,C}} = 3.7$ Hz, Ph), 130.5 (d, 2C, $^3J_{\text{P,C}} = 5.2$ Hz, Ph), 132.6 (d, $^2J_{\text{P,C}} = 3.7$ Hz, *i*-Ph), 167.0 (d, $^1J_{\text{P,C}} = 40.0$ Hz, CHPh), 196.4 (d, $^2J_{\text{P,C}} = 9.7$ Hz, *cis*-CO), 198.5 (d, $^2J_{\text{P,C}} = 29.7$ Hz, *trans*-CO).

$^{29}\text{Si}\{\text{H}\}$ NMR (60 MHz, THF-d8, 30°C): δ = 3.3 (d, $^2J_{\text{P,Si}} = 6.3$ Hz, Si(CH₃)₃).

$^{31}\text{P}\{\text{H}\}$ NMR (121.5 MHz, THF-d8, 30°C): δ = 219.0 (s_{sat}, $^1J_{\text{P,W}} = 260.0$ Hz).

³¹P NMR (121.5 MHz, THF-d8, 30°C): δ = 219.0 (dd_{sat}, ¹J_{P,W} = 260.0 Hz, ²J_{P,H} = 20.2 Hz, ²J_{P,H} = 3.1 Hz).

VII.23 Synthesis of [benzyl(bis(trimethylsilyl)methyl)chlorophosphane]-pentacarbonyltungsten(0) [113]



0.150 g (0.24 mmol) of oxaphosphirane complex **16a**, 0.12 g (0.54 mmol) CpTiCl₃ and 0.04 g Zn (0.60 mmol) were placed in a schlenk tube, and dissolved in 2 mL THF. The mixture was stirred at room temperature for 12h in order to form the complexes **102a,b**. The stopper was removed for some minutes and the mixture stirred for 4 h. The colour of the solution changed from blue to yellow.

The solvent was removed under reduced pressure ($\sim 10^{-2}$ mbar). The product was purified by column chromatography (Al₂O₃, -20°C, h = 8 cm, ϕ = 1cm, petroleum ether (100 mL), THF (100 mL)). The last fraction yielded yellow oil which could be crystallized in *n*-pentane.

Yield: 0.123 g (80%)

Empirical formula: C₁₉H₂₆ClO₅PSi₂W

Molecular weight: 640.84 g/mol

Melting point: 151 °C

¹H NMR (300 MHz, CDCl₃, 30°C): δ = 0.30 (s, 9H, Si(CH₃)₃), 0.37 (d, 9H, ³J_{P,H} = 0.5 Hz, Si(CH₃)₃), 1.88 (d, 1H, ²J_{P,H} = 10.2 Hz, CH(Si(CH₃)₃)₂), 3.50 (dd, 1H, ²J_{H,H} = 13.6 Hz, ²J_{P,H} = 10.1 Hz, CH₂Ph), 3.90 (t, 1H, ²J_{H,H} = 13.6 Hz, ²J_{P,H} = 13.9 Hz, CH₂Ph), 7.28 (m, 3H, Ph), 7.32 (m, 2H, Ph).

¹³C{¹H}NMR (75 MHz, CDCl₃, 30°C): δ = 2.1 (d, ³J_{P,C} = 3.8 Hz, Si(CH₃)₃), 2.9 (d, ³J_{P,C} = 2.2 Hz, Si(CH₃)₃), 30.5 (d, ¹J_{P,C} = 16.2 Hz, CH(Si(CH₃)₃)₂), 45.5 (d, ¹J_{P,C} = 10.4 Hz, PCH₂), 126.9 (d, 1C, ⁵J_{P,C} = 3.9 Hz, p-Ph), 127.5 (d, 2C, ¹J_{P,C} = 3.5 Hz, Ph), 129.9 (d, 2C, ¹J_{P,C} = 5.4 Hz, Ph), 132.0 (d, ²J_{P,C} = 4.3 Hz, i-Ph), 196.1 (d, ²J_{P,C} = 7.1 Hz, cis-CO), 198.0 (d, ²J_{P,C} = 32.8 Hz, trans-CO).

²⁹Si{¹H} NMR (60 MHz, CDCl₃, 30°C): δ = -0.7 (d, ²J_{P,Si} = 1.9 Hz, Si(CH₃)₃), 2.5 (d, ²J_{P,Si} = 6.3 Hz, Si(CH₃)₃).

³¹P{¹H} NMR (121.5 MHz, CDCl₃, 30°C): δ = 124.9 (s_{sat}, ¹J_{P,W} = 278).

³¹P NMR (121.5 MHz, CDCl₃, 30°C): δ = 124.9 (d_{sat}, ¹J_{P,W} = 278 Hz, ²J_{P,H} = 9.0 Hz).

Mass spectrometry (EI, 70 eV, ¹⁸⁴W): m/z (%) = 640 (40) [M•⁺], 606 (10) [(M-Cl)^{•+}], 556 (70) [(M-3CO)^{•+}], 500 (20) [(M-5CO)^{•+}], 281 (100) [(M-W-5CO-Cl)^{•+}].

IR (Nujol, ν(CO)): ν [cm⁻¹] = 2082 (m), 1986 (s), 1934 (s), 1910 (m).

UV/vis (CH₂Cl₂): λ (log ε): 233.6 (0.76), 301 (0.09) nm.

Elemental analysis: C [%] H [%]

Calculated 35.61 4.09

Found 35.53 4.20

IIX. Literature

- [1] A. Vila, R. A. Mosquera, *Chem. Phys.* **2003**, 287, 125–135.
- [2] A. Hassner in *The chemistry of Heterocyclic compounds*, Part 3; eds. A. Weisberg, E.C. Taylor, Wiley, New York, 1985, p. 59.
- [3] A. K. Yudin, *Aziridines and Epoxides in Organic Synthesis*, Wiley-VCH, Weinheim, 2006.
- [4] A. Wurtz, *Compt. rend.* **1859**, 48, 101–104.
- [5] Data taking from the 2007 report of UK consultant PCI Xylenes & Polyesters.
- [6] P. P. McClellan, *Ind. Eng. Chem.* **1950**, 42, 2402-2407.
- [7] M. Imuta, H. Ziffer, *J. Org. Chem.* **1979**, 44, 1351-1352.
- [8] Y. Shi in *Modern Oxidation Methods*, Ed. J. E. Bäckyall, Wiley-VCH, Weinheim, 2004, 51-78.
- [9] a) J. P. Freeman, *Oxaziridines. Chemistry of Heterocyclic Compounds*, Chichester, UK, 1985; b) W. D. Emmons, *J. Am. Chem. Soc.* **1956**, 78, 6208-6209.
- [10] J. Aube, X. Peng, Y. Wang, F. Taksuagawa, *J. Am. Chem. Soc.* **1992**, 114, 5466-5468.
- [11] H. Krimm, K. Hamann, German Patent 952, 895 (July 11, 1952).
- [12] H. W. Powell, *Pure Appl. Chem.* **1983**, 55, 2, 409-416.
- [13] a) W. Ando, M. Ikeno, A. Sekiguchi, *J. Am. Chem. Soc.* **1977**, 99, 6447-6449; b) P. Jutzi, D. Eikenberg, E. A. Bunte, A. Moehrke, B. Neumann, H. G. Stammier, *Organometallics* **1996**, 15, 1930-1934; c) Y. Wang, M. Dolg, *Tetrahedron* **1999**, 55, 12751-12756; d) V. N. Khabashesku, K. N. Kud, J. L. Margrave, L. Fredin, *Organomet. Chem.* **2000**, 595, 248-260.
- [14] W. Ando, Y. Hamada, A. Sekiguchi, *Tetrahedron Lett.* **1982**, 23, 5323-5326.
- [15] R. S. Ghadwal, S. S. Sen, H. W. Roesky, M. Granitzka, D. Kratzert, S. Merkel, D. Stalke, *Angew. Chem. Int. Ed. Engl.* **2010**, 49, 3952-3955.
- [16] O. Krahe, F. Neese, R. Streubel, *Chem. Eur. J.* **2009**, 15, 2594-2601.
- [17] W. W. Schoeller in *Multiple Bonds and Low Coordination in Phosphorus Chemistry*, Eds. M. Regitz, O. J. Scherer, Georg Thieme Verlag, Stuttgart, 1990, p. 23.
- [18] D. B. Chesnut, L. D. Quin, *Tetrahedron* **2005**, 61, 12343–12349.
- [19] I. Petnehazy, G. Clementis, Z. M. Jaszay, L. Toeke, C. D. Hall, *J. Chem. Soc. Perkin Trans. 2* **1996**, 11, 2279-2284.
- [20] I. J. Borowitz, M. Anschel, S. Firstenberg, *J. Org. Chem.* **1967**, 32, 1723-1729.
- [21] T. P. M. Goumans, A. W. Ehlers, K. Lammertsma, E. U. Würthwein, *Eur. J. Org. Chem.* **2003**, 2941-2946.
- [22] A stable terminal phosphinidene oxide complex was reported: E. Niecke, M. Engelmann, H. Zorn, B. Krebs, G. Henkel, *Angew. Chem.* **1980**, 92, 738–739; *Angew. Chem. Int. Ed. Engl.* **1980**, 19, 710 –712.
- [23] P. George, M. Trachtman, C. W. Bock, A. M. Brett, *Tetrahedron* **1976**, 32, 317-319.
- [24] E. Niecke, W. Flick, *Angew. Chem.* **1973**, 85, 586-587; *Angew. Chem. Int. Ed. Engl.* **1973**, 12, 585-586.
- [25] G. V. Röschenthaler, K. Sauerbrey, R. Schmutzler, *Chem. Ber.* **1978**, 111, 3105-3111.
- [26] J. Browning, M. Green, F. G. A. Stone, *J. Chem. Soc. A.* **1971**, 454-457.
- [27] A. J. Mukhedhar, V. A. Mukhedhar, F. G. A. Stone, M. Green, *J. Chem. Soc. A.* **1970**, 3166-3171.
- [28] E. Niecke, D. Gudat, W. W. Schoeller, P. Rademacher, *J. Chem. Soc.; Chem. Commun.* **1985**, 1050-1051.
- [29] P. A. Bartlett, N. I. Carruthers, B. M. Winter, K. P. Long, *J. Org. Chem.* **1982**, 47, 1284-1291.
- [30] M. T. Boisdon, J. Barrans, *J. Chem. Soc.; Chem. Commun.* **1988**, 615-617.

- [³¹] a) H. Ikeda, S. Inagaki, *J. Phys. Chem. A* **2001**, *105*, 10711-10718; b) D. B. Chesnut, L. D. Quin, *Tetrahedron* **2005**, *61*, 12343-12349; c) L. I. Savostina, R. M. Aminova, V. F. Mironov, *Rus. J. General. Chem.* **2006**, *76*, 1031.
- [³²] M. Schnebel, I. Weidner, R. Wartchow, H. Butenschön, *Eur. J. Org. Chem.* **2003**, 4363-4372.
- [³³] S. Bauer, A. Marinetti, L. Ricard, F. Mathey, *Angew. Chem.* **1990**, *102*, 1188-1189; *Angew. Chem. Int. Ed. Engl.* **1990**, *29*, 1166-1167.
- [³⁴] M. Schröder, Dissertation, Universität Kaiserslautern, 1999.
- [³⁵] R. Streubel, J. Jeske, P. G. Jones, R. Herbst-Irmer, *Angew. Chem.* **1994**, *106*, 115-117; *Angew. Chem. Int. Ed. Engl.* **1994**, *33*, 80-82.
- [³⁶] R. Streubel, A. Kusenberg, J. Jeske, P.G. Jones, *Angew. Chem.* **1994**, *106*, 2564-2565; *Angew. Chem. Int. Ed. Engl.* **1994**, *33*, 2427-2428.
- [³⁷] R. Streubel, A. Ostrowski, H. Wilkens, F. Ruthe, J. Jeske, P. G. Jones, *Angew. Chem.* **1997**, *109*, 409-413; *Angew. Chem. Int. Ed. Engl.* **1997**, *36*, 378-381.
- [³⁸] A. Ostrowski, Dissertation, Technische Universität Braunschweig, 1997.
- [³⁹] Y. Inubushi, N. H. Tran Huy, F. Mathey, *J. Chem. Soc., Chem. Commun.* **1996**, 1903-1904.
- [⁴⁰] A. Özbolat, G. von Frantzius, J. M. Pérez, M. Nieger, R. Streubel, *Angew. Chem.* **2007**, *119*, 48, 9488-9491; *Angew. Chem. Int. Ed.* **2007**, *46*, 48, 9327-9330.
- [⁴¹] M. Braun, *The Chemistry of Organolithium Compounds*, Chapter 13; eds. Z. Rappaport, I. Marek, Wiley, 2004, p. 829-891.
- [⁴²] R. Streubel, S. Priemer, F. Ruthe, P. G. Jones, *Eur. J. Inorg. Chem.* **2000**, 1253-1259.
- [⁴³] H. Lang, O. Orama, G. Huttner, *J. Organomet. Chem.* **1985**, *291*, 293-309.
- [⁴⁴] A.Özbolat, G. v. Frantzius, W. Hoffbauer, R. Streubel, *Dalton Trans.* **2008**, *20*, 2674-2676.
- [⁴⁵] M. Bode, J. M. Pérez, G. Schnakenburg, J. Daniels, R. Streubel, *Z. Anorg. Allg. Chem.* **2009**, *635*, 8, 1163-1171.
- [⁴⁶] M. J. S. Gynane, A. Hudson, M. F. Lappert, P. P. Power, H. Goldwhite *Dalton Trans.* **1980**, 2428 – 2433.
- [⁴⁷] W. Strohmeier, *Angew. Chem.* **1964**, *76*, 873-881; *Angew. Chem. Int. Ed. Engl.* **1964**, *3*, 730-737.
- [⁴⁸] U. Koelle, *J. Organomet. Chem.* **1977**, *133*, 53-58.
- [⁴⁹] A. A. Khan, C. Wismach, P. G. Jones, R. Streubel, *Dalton Trans.* **2003**, *12*, 2483-2487.
- [⁵⁰] J. Mason, *Multinuclear NMR*, Plenum Press, New York, 1987.
- [⁵¹] Maren Bode, Dissertation, Universität Bonn, 2009.
- [⁵²] H. Wilkens, A. Ostrowski, J. Jeske, F. Ruthe, P. G. Jones, R. Streubel, *Organometallics* **1999**, *18*, 5627–5642.
- [⁵³] R. Streubel, H. Wilkens, P. G. Jones, *Chem. Eur. J.* **2000**, *6*, 3997–4000.
- [⁵⁴] R. Streubel, F. Ruthe, P. G. Jones, *Eur. J. Inorg. Chem.* **1998**, *5*, 571-574.
- [⁵⁵] F. A. Cotton, C. S. Kraihanzel, *J. Am. Chem. Soc.* **1962**, *84*, 4432-4438.
- [⁵⁶] S. W. Kirtley in *Comprehensive Organometallic Chemistry*, Vol.3, ed. G. Wilkinson, Pergamon Press, Oxford, 1982.
- [⁵⁷] F. Mathey, *Chem. Rev.* **1990**, *90*, 997-1025.
- [⁵⁸] N. H. Tran Huy, B. Donnadieu, G. Bertrand, F. Mathey, *Organometallics* **2010**, *29*, 1302–1304.
- [⁵⁹] a) B. Halton, M. J. Cooney, H. Wong, *J. Am. Chem. Soc.* **1994**, *116*, 11574-11575; b) P. Bickers, B. Halton, A. J. Kay, P. T. Northcote, *Aust. J. Chem.* **1999**, *52*, 647-652.
- [⁶⁰] Aysel Özbulat-Schön planned Dissertation, Universität Bonn.
- [⁶¹] A. Marinetti, S. Bauer, L. Ricard, F. Mathey, *Organometallics* **1990**, *93*, 793-798.
- [⁶²] B. Deschamps, F. Mathey, *Phosphorus, Sulfur, Silicon Rel. Elem.* **1983**, *17*, 317-23.
- [⁶³] a) H. Goldwhite, J. Kaminski, G. Millhauser, J. Ortiz, M. Vargas, L. Vertal, *J. Organomet. Chem.* **1986**, *310*, 21-25; b) S. T. Liddle, K. Izod *Organometallics* **2004**, *23*, 5550-5559; d) R. T. Hawkins, W. J. Lennarz, H. R. Snyder *J. Am. Chem. Soc.* **1960**, *82*, 3053-3059.

- [⁶⁴] a) S. Freeman, M. J. P. Harger, *J. Chem. Soc. Perkin Trans.* **1987**, 6, 1399-1406; b) K. Issleib, H. Schmidt, C. Wirkner *Z. Anorg. Allg. Chem.* **1982**, 488, 75-79.
- [⁶⁵] a) P. Knochel, H. Ilia, T. J. Korn, O. Baron, *Handbook of Functionalized Organometallics*, Ed. P. Knochel, Wiley CH Verlag, Weinheim, 2005, p 45-108; b) A. H. Cowley, M. C. Damasco *J. Am. Chem. Soc.* **1971**, 6815-6821; c) R. M. Kren, M. A. Mathur, H. H. Sisler, *Inorg. Chem.* **1974**, 13, 174-177; d) R. K. Kanjolia, D. K. Srivastava, C. L. Watkins, L. K. Krannich *Inorg. Chem.* **1989**, 28, 3341-3345.
- [⁶⁶] S. Juge *Phosphorus, Sulfur, Silicon Rel. Elem.* **2008**, 183, 233-248.
- [⁶⁷] W. R. Hardie, J. E. Aaron, US patent, No 33,055,665.
- [⁶⁸] G. S. Alieva, L. G. Truzhenikova, I. N. Belova, *Zh. Obshch. Khim.* **1962**, 32, 3634-3635.
- [⁶⁹] A. A. Gevorkyan, P. I. Kazaryan, O. V. Avakyan, R. A. Vardanyan, *Khim. Geterotsikl. Soedin.* **1991**, 1, 33-36.
- [⁷⁰] M. Bode, M. Nieger, R. Streubel, *Organometallics* **2007**, 26, 245-246.
- [⁷¹] Z. S. Novikova, I. L. Odinets, I. F. Lutsenko, *Zh. Obshch. Khim.* **1987**, 57, 706-7.
- [⁷²] As most results are described in patents, just some selected references: a) X. J. Huang, Z. K. Xu, L. S. Wan, Z. G. Wang, J. L. Wang, *Macromol. Biosci.* **2005**, 5, 322-330; b) L. Fontaine, D. Derouet, J. C. Brosse, *Eur. Polym. J.* **1990**, 26, 865-870; c) T. Biela, P. Klosinski, S. Penczek, *J. Polym. Sci. Part A: Polym. Chem.* **1989**, 27, 763-774; d) H. Yasuda, M. Sumitani, A. Akamura, *Macromolecules* **1981**, 14, 458-460.
- [⁷³] a) S.W. Huang, J. Wang, P. C. Zhang, H. Q. Mao, R. X. Zhuo, K. Zhuo, W. Leong, *Biomacromolecules* **2004**, 5, 306-311; b) Y. Iwasaki, K. Akiyoshi, *Macromolecules* **2004**, 37, 7637-7642.
- [⁷⁴] R. Streubel, U. Rohde, J. Jeske, F. Ruthe, P. G. Jones, *Eur. J. Inorg. Chem.* **1998**, 2005-2012.
- [⁷⁵] M. Bode, G. Schnakenburg, P. G. Jones, R. Streubel, *Organometallics* **2008**, 27, 11, 2664-2667.
- [⁷⁶] H. Helten, J. M. Perez, J. Daniels, G. Schnakenburg, *Organometallics* **2009**, 28, 1221-1226.
- [⁷⁷] F. H. Allen, O. Kennard, D. G. Watson, L. Brammer, A. G. Orpen, R. Taylor, *J. Chem. Soc., Perkin Trans. II* **1987**, S1-S19.
- [⁷⁸] Hendrik Wilkens, Dissertation, Universität von Braunschweig, 2000.
- [⁷⁹] A. Curioni, W. Andreoni, J. Hutter, H. Schiffer, M. Parrinello, *J. Am. Chem. Soc.* **1994**, 116, 11251-11255.
- [⁸⁰] J. M. Pérez, H. Helten, B. Donnadieu, C. A. Reed, R. Streubel, *Angew. Chem* **2010**, 122, 14, 2670-2674; *Angew. Chem. Int. Ed.* **2010**, 49, 14, 2615-2618.
- [⁸¹] C. A. Reed, *Acc. Chem. Res.* **2009**, 43, 121-128.
- [⁸²] C. A. Reed, *J. Chem. Soc., Chem. Commun.* **2005**, 1669-1677.
- [⁸³] Examples of neutral η^2 -bound phosphaalkene-type ligands: a) A. H. Cowley, R. A. Jones, C. A. Stewart, A. L. Stuart, J. L. Atwood, W. E. Hunter, H.-M. Zhang, *J. Am. Chem. Soc.* **1983**, 105, 3737-3738; b) S. I. Al-Resayes, S. I. Klein, H. W. Kroto, M. F. Meidine, J. F. Nixon, *J. Chem. Soc., Chem. Commun.* **1983**, 930-932; c) T. A. van der Knaap, L. W. Jenneskens, H. J. Meeuwissen, F. Bickelhaupt, D. Walther, E. Dinjus, E. Uhlig, A. L. Spek, *J. Organomet. Chem.* **1983**, 254, C33-C36; d) A. H. Cowley, R. A. Jones, J. G. Lasch, N. C. Norman, C. A. Stewart, A. L. Stuart, J. L. Atwood, W. E. Hunter, H.-M. Zhang, *J. Am. Chem. Soc.* **1984**, 106, 7015-7020; e) B. Deschamps, F. Mathey, *J. Chem. Soc., Chem. Commun.* **1985**, 1010-1012; f) M. H. A. Benvenutti, P. B. Hitchcock, J. L. Kiplinger, J. F. Nixon, T. G. Richmond, *J. Chem. Soc., Chem. Commun.* **1997**, 1539-1540; g) M. Yoshifuji, Y. Ichikawa, N. Yamada, K. Toyota, *J. Chem. Soc., Chem. Commun.* **1998**, 27-28; h) P. Kramkowski, M. Scheer, *Eur. J. Inorg. Chem.* **2000**, 1869-1876; i) C. Peters, H. Disteldorf, E. Fuchs, S. Werner, S. Stutzmann, J. Bruckmann, C. Krüger, P. Binger, H. Heydt, M. Regitz, *Eur. J. Org. Chem.* **2001**, 3425-3435; j) C. Jones, C. Schulten, A. Stasch, *J. Chem. Soc., Dalton Trans.* **2007**, 1929-1933.

- [⁸⁴] A. Igau, A. Baceiredo, H. Grützmacher, H. Pritzkow, G. Bertrand, *J. Am. Chem. Soc.* **1989**, *11*, 6853-6854.
- [⁸⁵] H. Pritzkow, H. Grützmacher, *Angew. Chem.* **1992**, *104*, 92–94; *Angew. Chem. Int. Ed. Engl.* **1992**, *31*, 99-101.
- [⁸⁶] I. Agranat, Y. Shih, Y. Bentor, *J. Am. Chem. Soc.* **1974**, *96*, 1259-1260.
- [⁸⁷] B. Van de Graff, P. P. Dymerski, F. W. McLafferty, *J. Chem. Soc., Chem. Comm.* **1975**, 978-979.
- [⁸⁸] B. H. Solka, M. E. Russell, *J. Phys. Chem.* **1974**, *78*, 1268-1273.
- [⁸⁹] P. O. Momoh, E. Xie, S. A. Abrash, M. Meot-Ner, M. S. El Shall, *J. Phys. Chem. A* **2008**, *112*, 6066-6073.
- [⁹⁰] S. Antoniotti, S. Antonczak, J. Golebiowski, *Theor. Chem. Acc.* **2004**, *112*, 290-297.
- [⁹¹] W. J. Bouma, J. K. MacLeod, L. Radom, *J. Am. Chem. Soc.* **1979**, *101*, 5540-5545.
- [⁹²] Y. Zhao, D. G. Truhlar, *J. Org. Chem.* **2007**, *72*, 295-298.
- [⁹³] L. A. Hamilton, P. S. Landis in *Organic Phosphorus Compounds*, Eds. G. M. Kosolapoff, L. Maier, V 4, p 463, Wiley Interscience, New York, London, Sydney, Toronto, 1972.
- [⁹⁴] a) S. Uchida, K. Inumaru, M. Misono, *J. Phys. Chem. B* **2000**, *104*, 8108-8115; b) J. N. Barrows, M. T. Pope, *Inorg. Chim. Acta* **1993**, *213*, 91-98.
- [⁹⁵] M. D. Pluth, R. G. Bergman, K. N. Raymond, *J. Am. Chem. Soc.* **2008**, *130*, 6362–6366.
- [⁹⁶] H. S. Gutowsky, H. N. Chengt, *J. Chem. Phys.* **1975**, *63*, 6, 2439-2441.
- [⁹⁷] F. P. Gasparro, N. H. Kolodny, *J. Chem. Ed.* **1977**, *54*, 258-261.
- [⁹⁸] R. M. Jong, J. J. W. Tiesinga, A Villa, L. Tang, D. B. Janssen, B. W. Dijkstra, *J. Am. Chem. Soc.* **2005**, *127*, 38, 13338-13343.
- [⁹⁹] A. Marinnetti, F. Mathey, *Phosphorus, Sulfur, Silicon Rel. Elem.* **1984**, *19*, 311-317.
- [¹⁰⁰] J. March, *Advanced Organic Chemistry: Reactions, Mechanisms and Structure*; 4th ed.; Wiley-Interscience: New York, 1992; p 308-326.
- [¹⁰¹] F. R. Kreissl, E. O. Fischer, C. G. Kreiter, H. Fischer, *Chem. Ber.* **1973**, *106*, 1262-1276.
- [¹⁰²] F. Bienewald, N. H. Tran Huy, F. Mathey, *Organic and organometallic synthesis* **1999**, 701-704.
- [¹⁰³] a) G. Wittig, U. Schöllkopf, *Chem. Ber.* **1954**, *97*, 1318-1330; b) G. Wittig, W. Haag, *Chem. Ber.* **1955**, *88*, 1654-1666.
- [¹⁰⁴] H. Pommer, P. C. Thieme, Top. Curr. Chem.: *Industrial applications of the Wittig Reaction*; Springer: Berlin/Heidelberg, 1983.
- [¹⁰⁵] a) H. Schmidbaur, *Pure Appl. Chem.* **1980**, *52*, 1057-1062; b) H. Schmidbaur, *Pure Appl. Chem.* **1978**, *50*, 19-25; c) H. Schmidbaur, *Acc. Chem. Res.* **1975**, *8*, 62-70.
- [¹⁰⁶] W. V. Konze, V. G. Young, R. J. Angelici, *Organometallics* **1998**, *17*, 1569-1581.
- [¹⁰⁷] I. P. Lorenz, W. Pohl, H. Niith M. Schmidt, *J. Organomet. Chem.* **1994**, *475*, 211-221.
- [¹⁰⁸] H. Schmidbaur, *Angew. Chem.* **1983**, *95*, *12*, 980-1000; *Angew. Chem., Int. Engl.* **1983**, *22*, 907-927.
- [¹⁰⁹] G. L. Crocco, K. E. Lee, J. A. Gladysz, *Organometallics* **1990**, *9*, 2819-2831.
- [¹¹⁰] G. Erker, P. Czisch, C. Kriiger, J. M. Wallis, *Organometallics* **1985**, *4*, 2059-2060.
- [¹¹¹] Xi. Li, A. Wang, H. Sun, L. Wang, S. Schmidt, K. Harms, J. Sundermeyer, *Organometallics* **2007**, *26*, 3456-3460.
- [¹¹²] H. El Amouri, M. Gruselle, Y. Besace, J. Vaissermann, G. Jaouent, *Organometallics* **1994**, *13*, 2244-2251.
- [¹¹³] J. F. Hoover, J. M. Stryker, *Organometallics* **1988**, *7*, 2082-2084.
- [¹¹⁴] A. Wang, H. Sun, X. Li, *Organometallics* **2009**, *28*, 5285-5288.
- [¹¹⁵] J. M. Pérez, C. Albrecht, H. Helten, G. Schnakenburg, R. Streubel, *J. Chem. Soc., Chem. Comm.* **2010**, accepted.
- [¹¹⁶] a) T. V. RajanBabu, W. A. Nugent, *J. Am. Chem. Soc.* **1994**, *116*, 986-997; b) W. A. Nugent, T. V. RajanBabu, *J. Am. Chem. Soc.* **1989**, *111*, 4525-4527; c) W. A. Nugent, T. V. RajanBabu, *J. Am. Chem. Soc.* **1988**, *110*, 8561-8562.

- [¹¹⁷] J. M. Cuerva, J. Justicia, J. L. Oller-López, J. E. Oltra, *Top. Curr. Chem.* **2006**, *264*, 63-91; A. F. Barrero, J. F. Q. d. Moral, E. M. Sánchez, J. F. Arteaga, *Eur. J. Org. Chem.* **2006**, 1627-1641.
- [¹¹⁸] a) A. Gansäuer, M. Pierobon, H. Bluhm, *Angew. Chem. Inter. Ed.* **1998**, *37*, 101-103; b) A. Gansäuer, H. Bluhm, M. Pierobon, *J. Am. Chem. Soc.* **1998**, *120*, 12849-12859; c) A. Gansäuer, H. Bluhm, *J. Chem. Soc.; Chem. Comm.* **1998**, 2143-2144.
- [¹¹⁹] A. Gansäuer, H. Bluhm, *Chem. Rev.* **2000**, *100*, 2771-2788.
- [¹²⁰] R. J. Enemærke, J. Larsen, T. Skrydstrup, K. Daasbjerg, *Organometallics* **2004**, *23*, 1866-1867.
- [¹²¹] a) R. S. P. Coutts, P. C. Wailes, *J. Organomet. Chem.* **1973**, *47*, 375-382; b) R. L. Martin, G. Winter, *J. Chem. Soc.* **1965**, 4709-4714.
- [¹²²] E. Negishi, *Chem. Eur. J.* **1999**, *5*, 41-420.
- [¹²³] a) K. Daasbjerg, H. Swith, S. Grimme, M. Gerenkamp, C. Mücke-Lichtenfeld, A. Gansäuer, A. Barchuk, F. Keller, *Angew. Chem.* **2006**, *118*, 2095-2097; b) A. Gansäuer, A. Barchuk, F. Keller, M. Schmitt, S. Grimme, M. Gerenkamp, C. Mücke-Lichtenfeld, K. Daasbjerg, H. Swith, *J. Am. Chem. Soc.* **2007**, *129*, 1359-1371.
- [¹²⁴] O. Krahe, Diplomarbeit, Universität Bonn, 2009.
- [¹²⁵] A. Marinetti, F. Mathey, *Angew. Chem.* **1988**, *100*, *10*, 1435-1437.
- [¹²⁶] M. Yoshifuji, K. Shibayama, T. Hashida, K. Toyota, T. Niitsu, I. Matsuda, T. Sato, N. Inamoto, *J. Organomet. Chem.* **1986**, *311*, 63-67.
- [¹²⁷] H. Estiagh- Hosseini, H. W. Kroto, J. F. Nixon, M. Jamil Maah, M. J. Taylor, *J. Chem. Soc., Chem. Comm.* **1981**, 199-200.
- [¹²⁸] M. Yoshifuji, K. Toyota, N. Inamoto, *Tetrahedron Lett.* **1985**, *26*, *l4*, 1727-1730.
- [¹²⁹] A. Marinetti, S. Bauer, L. Ricard, F. Mathey *Organometallics* **1990**, *9*, 793-798.
- [¹³⁰] H. Helten, M. Engeser, D. Gudat, R. Schilling, G. Schnakenburg, M. Nieger, R. Streubel, *Chem. Eur. J.* **2009**, *15*, 2602-2616.
- [¹³¹] E. Ionescu, Dissertation, Universität Bonn, 2005.
- [¹³²] Charles P. Slichter, *Principles of Magnetic Resonance*, Ed. Springer: Berlin and New York, Third Edition, 1996, p 651.
- [¹³³] J. G. Kenworthy, J. Myatt, P. F. Todd, *Phys. Org. J. Chem. Soc. (B)*, **1970**, 791-794.
- [¹³⁴] E. Samuel, J. Vedel, *Organometallics* **1989**, *8*, 237-241.
- [¹³⁵] M. Kilner, G. Parkin, *J. Organomet. Chem.* **1986**, *302*, 181-191.
- [¹³⁶] Cetinkaya, A. Hudson, M. F. Lappert, H. Goldwhite, *J. Chem. Soc., Chem. Commun.* **1982**, 609-610.
- [¹³⁷] a) A. F. Mateos, S. E. Madrazo, P. H. Teijon, R. R. Gonzalez, *Eur. J. Org. Chem.* **2010**, *5*, 856-861; b) J. Justicia, T. Jimenez, S. P. Morcillo, J. M. Cuerva, J. E. Oltra, *Tetrahedron* **2009**, *65*, *52*, 10837-1084; c) A. Gansauer, A. Fleckhaus, M. A. Lafont, A. Okkel, K. A. Anoop, F. Neese, *J. Am. Chem. Soc.* **2009**, *131*, *46*, 16989-16999.
- [¹³⁸] W. W. Schoeller, E. Niecke, *J. Chem. Soc., Chem. Commun.* **1982**, 569-570; b) C. Thomson, *J. Chem. Soc., Chem. Commun.* **1977**, 322-323; c) T. A. van der Knaap, T. C. Klebach, F. Visser, F. Bickelhaupt, F. Ros, E. J. Baerends, C. H. Stam, M. Konjin, *Tetrahedron* **1984**, *40*, 765-776.
- [¹³⁹] L. Weber, *Eur. J. Inorg. Chem.* **2000**, *12*, 2425-2441.
- [¹⁴⁰] A. Merien, J. P. Majoral, M. Revel, J. Navech, *Tetrahedron Lett.* **1983**, *24*, 1975-1978.
- [¹⁴¹] a) R. Appel, C. Casser, *Chem. Ber.* **1985**, *118*, 3419-3423; b) E. Niecke, E. Symalla, *Chimia* **1985**, *39*, 320-322.
- [¹⁴²] J. Jin, M. Newcomb, *J. Org. Chem.* **2008**, *73*, 7901-7905.
- [¹⁴³] H. Köpf, S. Grabowski, R. Voigtländer, *J. Organomet. Chem.* **1981**, *216*, 185-190.
- [¹⁴⁴] D. D. Perrin, W. L. F. Armarego, D. R. Perrin, *Purification of Laboratory Chemicals*, Pergamon Press Oxford, 1988.

- [¹⁴⁵] a) Collect data collection software, Nonius B.V., 1999; b) Z. Otwinoski, W. Minor in Processing of X-ray Diffraction Data Collected in Oscillation Mode, Methods in Enzymology, Vol. 276: Macromolecular Crystallography, Part A (Eds.: C.W. Carter, Jr., R. M. Sweet), Academic Press, 1997, p. 307–326.
- [¹⁴⁶] G. M. Sheldrick, *Acta Crystallogr., Sect. A* **2008**, *64*, 112–122.
- [¹⁴⁷] SHELXL-97, G. M. Sheldrick, University of Göttingen, 1997.
- [¹⁴⁸] SHELXS-97, G. M. Sheldrick, *Acta Crystallogr., Sect. A* **1990**, *46*, 467–473.

IX. Appendix

IX.1. Abbreviations used

t-BuLi: *tert*-butyllithium

n-BuLi: *n*-butyllithium

Ph: Phenyl

Ar: Aryl

M: Metal

Et₃N: triethyl amine

TfOH: triflic acid

DCM: Dichloro methane

THF: tetrahydrofuran

h: hours

min: minutes

mL: milliliter solution at ambient temperature

M: mol x L⁻¹

MS: Mass Spectrometry

EI: Electron collision Ionization

s: singlet

d: doublet

t: triplet

m: multiplet

s_{sat}: Singlet with Satellites

RT: room temperature

IR: Infrared

w: weak

m: medium

s: strong

vs: very strong

eq: equivalent

Å: Angstrom (= 10⁻¹⁰ m)

Cp: Cyclopentadienyl-

Cp* : 1,2,3,4,5-Pentamethylcyclopenta-2,4-dien-1-yl-

CSD: Cambridge Structural Database

EA: Elemental Analysis

g: gramme

Hz: Hertz

KBr: Kalium bromide

m/z: Mass to Charge ratio

m_c : complicated multiplet

$^nJ_{X,Y}$: Coupling constant (From X with Y through n bonds) [Hz]

Me: Methyl

nm: Nanometer

NMR: Nuclear Magnetic Resonance

EPR: Electron Paramagnetic Resonance

ppm: parts per million

LDA: Lithium diisopropyl amine

Dppe: 1,2-bis(diphenylphosphino)ethane

Mes: 1,3,5-trimethylbenzyl-

Mes*:1,3,5-tri-*tert*-butylbenzyl-

o-DCB : *ortho*-dichloro benzene

PhCN: Benzonitrile

IX.2. Crystal data

i.[Bis(trimethylsilyl)methyldichlorophosphane]pentacarbonylchromium(0) [26]

(A1)

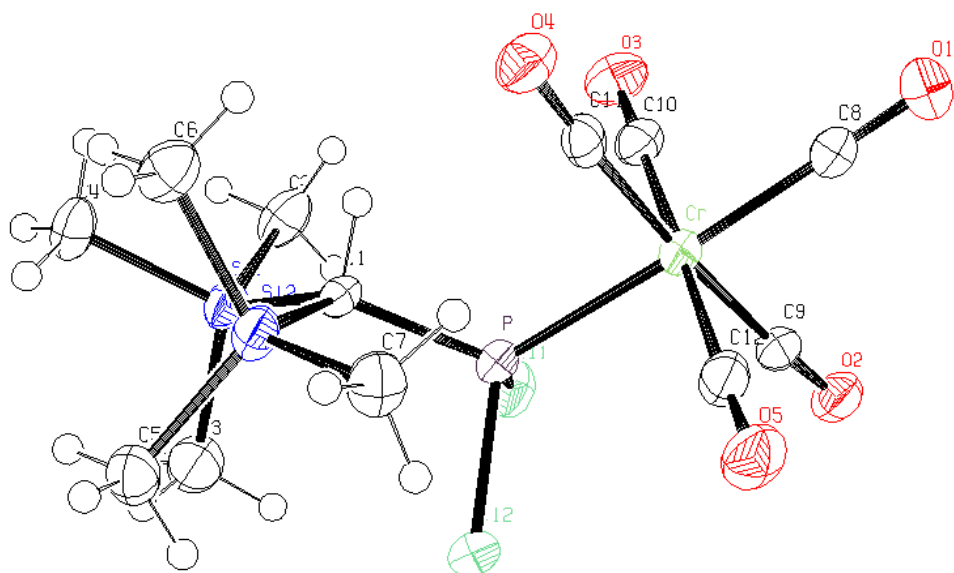


Table i.1. Crystal data and structure refinement for [26].

Identification code	GSTR140, Greg1237
Device Type	Nonius KappaCCD
Empirical formula	C12 H19 Cl2 Cr O5 P Si2
Formula weight	453.32
Temperature	123(2) K
Wavelength	0.71073 Å
Crystal system, space group	Monoclinic, P 21/n
Unit cell dimensions deg.	a = 14.7650(11) Å alpha = 90 deg. b = 9.4473(8) Å beta = 99.880(5) c = 14.7941(12) Å gamma = 90 deg.
Volume	2033.0(3) Å ³
Z, Calculated density	4, 1.481 Mg/m ³
Absorption coefficient	1.039 mm ⁻¹
F(000)	928
Crystal size	0.36 x 0.28 x 0.08 mm

Theta range for data collection	3.53 to 27.51 deg.
Limiting indices	-15<=h<=19, -12<=k<=11, -15<=l<=19
Reflections collected / unique	11844 / 4520 [R(int) = 0.0687]
Completeness to theta = 27.51	96.6 %
Absorption correction	Semi-empirical from equivalents
Max. and min. transmission	0.9215 and 0.7062
Refinement method	Full-matrix least-squares on F^2
Data / restraints / parameters	4520 / 3 / 214
Goodness-of-fit on F^2	0.966
Final R indices [I>2sigma(I)]	R1 = 0.0427, wR2 = 0.0875
R indices (all data)	R1 = 0.0912, wR2 = 0.0986
Largest diff. peak and hole	0.523 and -0.453 e.A^-3

Table i.2. Atomic coordinates ($\times 10^4$) and equivalent isotropic displacement parameters ($\text{\AA}^2 \times 10^3$) for [26].
U(eq) is defined as one third of the trace of the orthogonalized Uij tensor.

	x	y	z	U(eq)
C(1)	2520(2)	2574(3)	-738(2)	24(1)
C(2)	4284(2)	3084(4)	-1601(2)	40(1)
C(3)	3923(3)	139(4)	-854(3)	42(1)
C(4)	2794(2)	1294(4)	-2597(2)	38(1)
C(5)	1514(2)	-356(4)	-951(2)	36(1)
C(6)	697(2)	2265(4)	-2029(2)	38(1)
C(7)	612(2)	1912(4)	-37(2)	35(1)
C(8)	1995(2)	7059(4)	1298(2)	30(1)
C(9)	3382(2)	5335(3)	1936(2)	26(1)
C(10)	3118(2)	6154(4)	179(2)	29(1)
C(11)	1384(2)	5340(3)	-62(2)	26(1)
C(12)	1625(2)	4336(4)	1698(2)	31(1)
C1(1)	4320(1)	3206(1)	615(1)	34(1)
C1(2)	2797(1)	1339(1)	1175(1)	35(1)
Cr	2369(1)	5271(1)	930(1)	25(1)
O(1)	1776(2)	8145(3)	1506(2)	43(1)
O(2)	3986(2)	5450(2)	2523(2)	34(1)
O(3)	3564(2)	6698(3)	-278(2)	40(1)
O(4)	789(2)	5455(3)	-669(2)	37(1)
O(5)	1188(2)	3806(3)	2154(2)	43(1)
P	2902(1)	3156(1)	426(1)	24(1)
Si(1)	3393(1)	1763(1)	-1416(1)	28(1)
Si(2)	1348(1)	1591(1)	-927(1)	28(1)

Table i.3. Bond lengths [Å] and angles [deg] for [26].

C(1)-P	1.803(3)
C(1)-Si(1)	1.922(3)

C(1)-Si(2)	1.942(3)
C(1)-H(1)	1.0000
C(2)-Si(1)	1.868(4)
C(2)-H(2A)	0.9800
C(2)-H(2B)	0.9800
C(2)-H(2C)	0.9800
C(3)-Si(1)	1.853(4)
C(3)-H(3A)	0.9800
C(3)-H(3B)	0.9800
C(3)-H(3C)	0.9800
C(4)-Si(1)	1.872(3)
C(4)-H(4A)	0.9800
C(4)-H(4B)	0.9800
C(4)-H(4C)	0.9800
C(5)-Si(2)	1.856(4)
C(5)-H(5A)	0.9800
C(5)-H(5B)	0.9800
C(5)-H(5C)	0.9800
C(6)-Si(2)	1.858(4)
C(6)-H(6A)	0.9800
C(6)-H(6B)	0.9800
C(6)-H(6C)	0.9800
C(7)-Si(2)	1.870(3)
C(7)-H(7A)	0.9800
C(7)-H(7B)	0.9800
C(7)-H(7C)	0.9800
C(8)-O(1)	1.133(4)
C(8)-Cr	1.887(4)
C(9)-O(2)	1.138(4)
C(9)-Cr	1.922(3)
C(10)-O(3)	1.143(4)
C(10)-Cr	1.891(3)
C(11)-O(4)	1.148(4)
C(11)-Cr	1.882(3)
C(12)-O(5)	1.129(4)
C(12)-Cr	1.925(3)
Cl(1)-P	2.0639(12)
Cl(2)-P	2.0636(12)
Cr-P	2.3177(10)
P-C(1)-Si(1)	119.46(16)
P-C(1)-Si(2)	114.08(15)
Si(1)-C(1)-Si(2)	113.24(16)
P-C(1)-H(1)	102.3
Si(1)-C(1)-H(1)	102.3
Si(2)-C(1)-H(1)	102.3
Si(1)-C(2)-H(2A)	109.5
Si(1)-C(2)-H(2B)	109.5
H(2A)-C(2)-H(2B)	109.5
Si(1)-C(2)-H(2C)	109.5
H(2A)-C(2)-H(2C)	109.5
H(2B)-C(2)-H(2C)	109.5
Si(1)-C(3)-H(3A)	109.5
Si(1)-C(3)-H(3B)	109.5
H(3A)-C(3)-H(3B)	109.5
Si(1)-C(3)-H(3C)	109.5
H(3A)-C(3)-H(3C)	109.5
H(3B)-C(3)-H(3C)	109.5
Si(1)-C(4)-H(4A)	109.5
Si(1)-C(4)-H(4B)	109.5
H(4A)-C(4)-H(4B)	109.5
Si(1)-C(4)-H(4C)	109.5
H(4A)-C(4)-H(4C)	109.5

H(4B)-C(4)-H(4C)	109.5
Si(2)-C(5)-H(5A)	109.5
Si(2)-C(5)-H(5B)	109.5
H(5A)-C(5)-H(5B)	109.5
Si(2)-C(5)-H(5C)	109.5
H(5A)-C(5)-H(5C)	109.5
H(5B)-C(5)-H(5C)	109.5
Si(2)-C(6)-H(6A)	109.5
Si(2)-C(6)-H(6B)	109.5
H(6A)-C(6)-H(6B)	109.5
Si(2)-C(6)-H(6C)	109.5
H(6A)-C(6)-H(6C)	109.5
H(6B)-C(6)-H(6C)	109.5
Si(2)-C(7)-H(7A)	109.5
Si(2)-C(7)-H(7B)	109.5
H(7A)-C(7)-H(7B)	109.5
Si(2)-C(7)-H(7C)	109.5
H(7A)-C(7)-H(7C)	109.5
H(7B)-C(7)-H(7C)	109.5
O(1)-C(8)-Cr	178.7(3)
O(2)-C(9)-Cr	176.3(3)
O(3)-C(10)-Cr	179.3(3)
O(4)-C(11)-Cr	176.5(3)
O(5)-C(12)-Cr	179.0(3)
C(11)-Cr-C(8)	88.22(14)
C(11)-Cr-C(10)	88.72(13)
C(8)-Cr-C(10)	90.25(14)
C(11)-Cr-C(9)	176.17(14)
C(8)-Cr-C(9)	88.59(14)
C(10)-Cr-C(9)	89.17(13)
C(11)-Cr-C(12)	91.94(14)
C(8)-Cr-C(12)	90.89(14)
C(10)-Cr-C(12)	178.70(15)
C(9)-Cr-C(12)	90.23(14)
C(11)-Cr-P	92.21(10)
C(8)-Cr-P	175.98(11)
C(10)-Cr-P	85.76(10)
C(9)-Cr-P	90.82(10)
C(12)-Cr-P	93.09(10)
C(1)-P-Cl(2)	102.70(11)
C(1)-P-Cl(1)	106.25(10)
Cl(2)-P-Cl(1)	96.57(5)
C(1)-P-Cr	120.14(11)
Cl(2)-P-Cr	118.90(4)
Cl(1)-P-Cr	109.21(4)
C(3)-Si(1)-C(2)	111.41(18)
C(3)-Si(1)-C(4)	108.60(17)
C(2)-Si(1)-C(4)	104.64(16)
C(3)-Si(1)-C(1)	111.44(15)
C(2)-Si(1)-C(1)	111.23(15)
C(4)-Si(1)-C(1)	109.25(15)
C(5)-Si(2)-C(6)	111.90(17)
C(5)-Si(2)-C(7)	105.61(16)
C(6)-Si(2)-C(7)	106.65(17)
C(5)-Si(2)-C(1)	111.05(15)
C(6)-Si(2)-C(1)	106.05(15)
C(7)-Si(2)-C(1)	115.61(15)

Table i.4. Anisotropic displacement parameters ($\text{\AA}^2 \times 10^3$) for [26]
The anisotropic displacement factor exponent takes the form:
 $-2 \pi^2 [h^2 a^*{}^2 U_{11} + \dots + 2 h k a^* b^* U_{12}]$

	U11	U22	U33	U23	U13	U12
C(1)	28(2)	27(2)	17(2)	2(1)	2(1)	0(2)
C(2)	38(2)	58(3)	26(2)	0(2)	8(2)	-5(2)
C(3)	44(2)	45(2)	38(2)	-1(2)	5(2)	12(2)
C(4)	43(2)	48(2)	24(2)	-10(2)	9(2)	-6(2)
C(5)	44(2)	33(2)	33(2)	-4(2)	12(2)	-5(2)
C(6)	34(2)	46(2)	32(2)	2(2)	1(2)	-4(2)
C(7)	34(2)	38(2)	35(2)	-3(2)	13(2)	-7(2)
C(8)	37(2)	31(2)	21(2)	-2(1)	2(1)	1(2)
C(9)	33(2)	26(2)	21(2)	2(1)	9(1)	-1(2)
C(10)	31(2)	32(2)	24(2)	1(2)	1(2)	0(2)
C(11)	29(2)	25(2)	26(2)	-4(1)	11(2)	1(2)
C(12)	34(2)	33(2)	25(2)	-2(2)	4(2)	-1(2)
Cl(1)	29(1)	43(1)	28(1)	-7(1)	0(1)	3(1)
Cl(2)	51(1)	30(1)	22(1)	5(1)	6(1)	2(1)
Cr	31(1)	25(1)	19(1)	-1(1)	5(1)	0(1)
O(1)	57(2)	33(2)	39(2)	-7(1)	7(1)	7(1)
O(2)	38(1)	38(1)	24(1)	1(1)	2(1)	-4(1)
O(3)	39(1)	48(2)	34(2)	10(1)	8(1)	-3(1)
O(4)	35(1)	45(2)	28(1)	1(1)	1(1)	3(1)
O(5)	50(2)	47(2)	34(2)	2(1)	17(1)	-9(1)
P	29(1)	26(1)	18(1)	0(1)	3(1)	0(1)
Si(1)	32(1)	33(1)	21(1)	-3(1)	6(1)	1(1)
Si(2)	30(1)	32(1)	21(1)	-2(1)	5(1)	-5(1)

Table i.5. Hydrogen coordinates ($\times 10^4$) and isotropic displacement parameters ($\text{Å}^2 \times 10^3$) for [26].

	x	y	z	U(eq)
H(1)	2360	3488	-1068	29
H(2A)	4803	3038	-1090	60
H(2B)	4017	4037	-1634	60
H(2C)	4500	2872	-2177	60
H(3A)	3463	-618	-909	64
H(3B)	4150	332	-203	64
H(3C)	4436	-156	-1151	64
H(4A)	3246	966	-2964	57
H(4B)	2475	2131	-2888	57
H(4C)	2345	541	-2559	57
H(5A)	914	-827	-1054	54
H(5B)	1870	-668	-364	54
H(5C)	1847	-601	-1449	54
H(6A)	1035	2045	-2527	57
H(6B)	621	3292	-1989	57
H(6C)	91	1813	-2153	57
H(7A)	-1	1514	-245	52
H(7B)	561	2933	61	52
H(7C)	891	1458	539	52

Table i.6. Torsion angles [deg] for [26].

O(4)-C(11)-Cr-C(8)	33(4)
O(4)-C(11)-Cr-C(10)	-57(4)

O(4)-C(11)-Cr-C(9)	-1(6)
O(4)-C(11)-Cr-C(12)	124(4)
O(4)-C(11)-Cr-P	-143(4)
O(1)-C(8)-Cr-C(11)	-73(15)
O(1)-C(8)-Cr-C(10)	16(15)
O(1)-C(8)-Cr-C(9)	105(15)
O(1)-C(8)-Cr-C(12)	-165(15)
O(1)-C(8)-Cr-P	23(16)
O(3)-C(10)-Cr-C(11)	47(28)
O(3)-C(10)-Cr-C(8)	-41(28)
O(3)-C(10)-Cr-C(9)	-130(28)
O(3)-C(10)-Cr-C(12)	168(100)
O(3)-C(10)-Cr-P	139(28)
O(2)-C(9)-Cr-C(11)	-5(6)
O(2)-C(9)-Cr-C(8)	-38(4)
O(2)-C(9)-Cr-C(10)	52(4)
O(2)-C(9)-Cr-C(12)	-129(4)
O(2)-C(9)-Cr-P	138(4)
O(5)-C(12)-Cr-C(11)	-99(20)
O(5)-C(12)-Cr-C(8)	-11(20)
O(5)-C(12)-Cr-C(10)	140(17)
O(5)-C(12)-Cr-C(9)	77(20)
O(5)-C(12)-Cr-P	168(20)
Si(1)-C(1)-P-Cl(2)	-87.24(17)
Si(2)-C(1)-P-Cl(2)	51.24(17)
Si(1)-C(1)-P-Cl(1)	13.6(2)
Si(2)-C(1)-P-Cl(1)	152.07(13)
Si(1)-C(1)-P-Cr	138.03(14)
Si(2)-C(1)-P-Cr	-83.49(18)
C(11)-Cr-P-C(1)	16.89(15)
C(8)-Cr-P-C(1)	-79.1(15)
C(10)-Cr-P-C(1)	-71.67(15)
C(9)-Cr-P-C(1)	-160.77(15)
C(12)-Cr-P-C(1)	108.95(15)
C(11)-Cr-P-Cl(2)	-110.77(10)
C(8)-Cr-P-Cl(2)	153.2(15)
C(10)-Cr-P-Cl(2)	160.68(11)
C(9)-Cr-P-Cl(2)	71.57(10)
C(12)-Cr-P-Cl(2)	-18.71(11)
C(11)-Cr-P-Cl(1)	139.91(10)
C(8)-Cr-P-Cl(1)	43.9(15)
C(10)-Cr-P-Cl(1)	51.36(11)
C(9)-Cr-P-Cl(1)	-37.74(10)
C(12)-Cr-P-Cl(1)	-128.02(11)
P-C(1)-Si(1)-C(3)	60.8(2)
Si(2)-C(1)-Si(1)-C(3)	-78.0(2)
P-C(1)-Si(1)-C(2)	-64.1(2)
Si(2)-C(1)-Si(1)-C(2)	157.05(17)
P-C(1)-Si(1)-C(4)	-179.15(19)
Si(2)-C(1)-Si(1)-C(4)	42.0(2)
P-C(1)-Si(2)-C(5)	-100.3(2)
Si(1)-C(1)-Si(2)-C(5)	40.8(2)
P-C(1)-Si(2)-C(6)	137.89(18)
Si(1)-C(1)-Si(2)-C(6)	-81.0(2)
P-C(1)-Si(2)-C(7)	19.9(2)
Si(1)-C(1)-Si(2)-C(7)	161.04(16)

ii.[(Bis(trimethylsilyl)methyl)dichlorophosphane]pentacarbonylmolybdenum(0)

[25]

(A1)

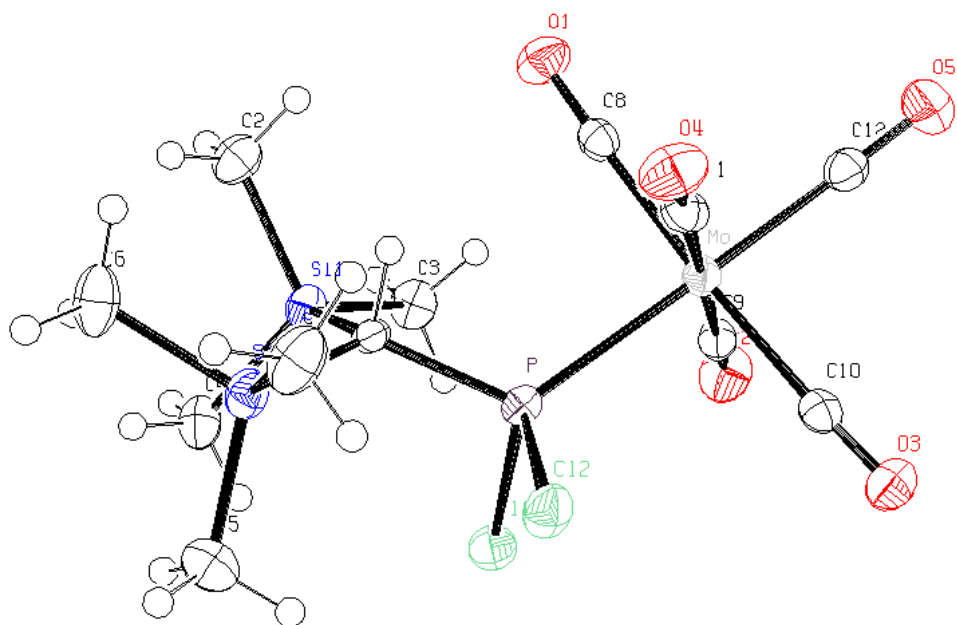


Table ii.1. Crystal data and structure refinement for [25].

Identification code	Greg1200, GSTR150
Device Type	Nonius KappaCCD
Empirical formula	C12 H19 Cl2 Mo O5 P Si2
Formula weight	497.26
Temperature	123(2) K
Wavelength	0.71073 Å
Crystal system, space group	Monoclinic, P 21/c
Unit cell dimensions	a = 14.8589(9) Å alpha = 90 deg. b = 9.6397(9) Å beta = 129.985(4) deg.
	c = 19.0963(17) Å gamma = 90 deg.
Volume	2095.8(3) Å^3
Z, Calculated density	4, 1.576 Mg/m^3
Absorption coefficient	1.088 mm^-1
F(000)	1000
Crystal size	0.28 x 0.20 x 0.20 mm

Theta range for data collection	2.78 to 28.00 deg.
Limiting indices	-19<=h<=14, -12<=k<=12, -24<=l<=25
Reflections collected / unique	15919 / 4922 [R(int) = 0.0986]
Completeness to theta = 28.00	97.1 %
Absorption correction	Semi-empirical from equivalents
Max. and min. transmission	0.8118 and 0.7505
Refinement method	Full-matrix least-squares on F^2
Data / restraints / parameters	4922 / 5 / 214
Goodness-of-fit on F^2	0.801
Final R indices [I>2sigma(I)]	R1 = 0.0404, wR2 = 0.0612
R indices (all data)	R1 = 0.1061, wR2 = 0.0739
Largest diff. peak and hole	0.817 and -1.016 e.A^-3

Table ii.2. Atomic coordinates ($x \times 10^4$) and equivalent isotropic displacement parameters ($\text{Å}^2 \times 10^3$) for [25].
U(eq) is defined as one third of the trace of the orthogonalized Uij tensor.

	x	y	z	U(eq)
C(1)	3277(3)	2494(4)	-2475(2)	18(1)
C(2)	2747(3)	2774(4)	-4290(2)	32(1)
C(3)	686(3)	3104(4)	-4366(2)	30(1)
C(4)	2469(3)	5361(4)	-3490(3)	31(1)
C(5)	4779(4)	4883(4)	-1076(3)	41(1)
C(6)	5388(3)	3763(4)	-2207(3)	38(1)
C(7)	5878(3)	1994(4)	-723(3)	38(1)
C(8)	1421(3)	-359(4)	-3708(3)	23(1)
C(9)	-212(4)	667(4)	-3444(3)	24(1)
C(10)	1443(3)	-394(4)	-1561(3)	22(1)
C(11)	3015(4)	-1205(4)	-1857(3)	25(1)
C(12)	651(3)	-2165(4)	-3041(3)	26(1)
Cl(1)	1648(1)	3703(1)	-2195(1)	32(1)
Cl(2)	3706(1)	1850(1)	-688(1)	32(1)
Mo	1413(1)	-295(1)	-2655(1)	21(1)
O(1)	1437(2)	-448(3)	-4304(2)	35(1)
O(2)	-1096(2)	1201(3)	-3862(2)	39(1)
O(3)	1481(2)	-514(3)	-948(2)	31(1)
O(4)	3926(2)	-1711(3)	-1404(2)	38(1)
O(5)	230(3)	-3254(3)	-3263(2)	42(1)
P	2493(1)	1924(1)	-2097(1)	21(1)
Si(1)	2296(1)	3444(1)	-3642(1)	24(1)
Si(2)	4812(1)	3291(1)	-1608(1)	26(1)

Table ii.3. Bond lengths [Å] and angles [deg] for [25].

C(1)-P	1.806(4)
--------	----------

C(1)-Si(2)	1.918(4)
C(1)-Si(1)	1.939(3)
C(1)-H(1A)	1.0000
C(2)-Si(1)	1.861(4)
C(2)-H(2A)	0.9800
C(2)-H(2B)	0.9800
C(2)-H(2C)	0.9800
C(3)-Si(1)	1.869(4)
C(3)-H(3A)	0.9800
C(3)-H(3B)	0.9800
C(3)-H(3C)	0.9800
C(4)-Si(1)	1.862(4)
C(4)-H(4A)	0.9800
C(4)-H(4B)	0.9800
C(4)-H(4C)	0.9800
C(5)-Si(2)	1.859(4)
C(5)-H(5A)	0.9800
C(5)-H(5B)	0.9800
C(5)-H(5C)	0.9800
C(6)-Si(2)	1.873(4)
C(6)-H(6A)	0.9800
C(6)-H(6B)	0.9800
C(6)-H(6C)	0.9800
C(7)-Si(2)	1.867(4)
C(7)-H(7A)	0.9800
C(7)-H(7B)	0.9800
C(7)-H(7C)	0.9800
C(8)-O(1)	1.156(4)
C(8)-Mo	2.019(4)
C(9)-O(2)	1.132(4)
C(9)-Mo	2.069(4)
C(10)-O(3)	1.141(4)
C(10)-Mo	2.062(4)
C(11)-O(4)	1.147(4)
C(11)-Mo	2.024(4)
C(12)-O(5)	1.154(4)
C(12)-Mo	2.001(4)
C1(1)-P	2.0611(14)
C1(2)-P	2.0629(14)
Mo-P	2.4670(11)
P-C(1)-Si(2)	119.45(18)
P-C(1)-Si(1)	113.74(18)
Si(2)-C(1)-Si(1)	113.65(18)
P-C(1)-H(1A)	102.3
Si(2)-C(1)-H(1A)	102.3
Si(1)-C(1)-H(1A)	102.3
Si(1)-C(2)-H(2A)	109.5
Si(1)-C(2)-H(2B)	109.5
H(2A)-C(2)-H(2B)	109.5
Si(1)-C(2)-H(2C)	109.5
H(2A)-C(2)-H(2C)	109.5
H(2B)-C(2)-H(2C)	109.5
Si(1)-C(3)-H(3A)	109.5
Si(1)-C(3)-H(3B)	109.5
H(3A)-C(3)-H(3B)	109.5
Si(1)-C(3)-H(3C)	109.5
H(3A)-C(3)-H(3C)	109.5
H(3B)-C(3)-H(3C)	109.5
Si(1)-C(4)-H(4A)	109.5
Si(1)-C(4)-H(4B)	109.5
H(4A)-C(4)-H(4B)	109.5
Si(1)-C(4)-H(4C)	109.5

H(4A)-C(4)-H(4C)	109.5
H(4B)-C(4)-H(4C)	109.5
Si(2)-C(5)-H(5A)	109.5
Si(2)-C(5)-H(5B)	109.5
H(5A)-C(5)-H(5B)	109.5
Si(2)-C(5)-H(5C)	109.5
H(5A)-C(5)-H(5C)	109.5
H(5B)-C(5)-H(5C)	109.5
Si(2)-C(6)-H(6A)	109.5
Si(2)-C(6)-H(6B)	109.5
H(6A)-C(6)-H(6B)	109.5
Si(2)-C(6)-H(6C)	109.5
H(6A)-C(6)-H(6C)	109.5
H(6B)-C(6)-H(6C)	109.5
Si(2)-C(7)-H(7A)	109.5
Si(2)-C(7)-H(7B)	109.5
H(7A)-C(7)-H(7B)	109.5
Si(2)-C(7)-H(7C)	109.5
H(7A)-C(7)-H(7C)	109.5
H(7B)-C(7)-H(7C)	109.5
O(1)-C(8)-Mo	177.4(3)
O(2)-C(9)-Mo	178.8(4)
O(3)-C(10)-Mo	176.6(3)
O(4)-C(11)-Mo	179.5(4)
O(5)-C(12)-Mo	178.6(4)
C(12)-Mo-C(8)	88.23(15)
C(12)-Mo-C(11)	89.99(15)
C(8)-Mo-C(11)	88.83(15)
C(12)-Mo-C(10)	88.31(15)
C(8)-Mo-C(10)	175.41(15)
C(11)-Mo-C(10)	88.16(15)
C(12)-Mo-C(9)	90.93(15)
C(8)-Mo-C(9)	92.26(15)
C(11)-Mo-C(9)	178.60(15)
C(10)-Mo-C(9)	90.81(15)
C(12)-Mo-P	175.77(11)
C(8)-Mo-P	92.20(11)
C(11)-Mo-P	85.81(11)
C(10)-Mo-P	91.03(11)
C(9)-Mo-P	93.26(10)
C(1)-P-Cl(1)	102.82(13)
C(1)-P-Cl(2)	106.50(12)
Cl(1)-P-Cl(2)	96.81(6)
C(1)-P-Mo	119.90(12)
Cl(1)-P-Mo	119.52(6)
Cl(2)-P-Mo	108.32(5)
C(2)-Si(1)-C(4)	112.06(18)
C(2)-Si(1)-C(3)	106.50(18)
C(4)-Si(1)-C(3)	105.78(18)
C(2)-Si(1)-C(1)	105.96(17)
C(4)-Si(1)-C(1)	111.30(16)
C(3)-Si(1)-C(1)	115.27(17)
C(5)-Si(2)-C(7)	111.29(19)
C(5)-Si(2)-C(6)	108.4(2)
C(7)-Si(2)-C(6)	105.09(19)
C(5)-Si(2)-C(1)	111.59(18)
C(7)-Si(2)-C(1)	111.08(17)
C(6)-Si(2)-C(1)	109.10(17)

Table ii.4. Anisotropic displacement parameters ($\text{\AA}^2 \times 10^3$) for [25]
The anisotropic displacement factor exponent takes the form:
 $-2 \pi^2 [h^2 a^{*2} U_{11} + \dots + 2 h k a^* b^* U_{12}]$

	U11	U22	U33	U23	U13	U12
C(1)	21(2)	19(2)	19(2)	-1(2)	15(2)	1(2)
C(2)	33(3)	39(3)	28(2)	5(2)	21(2)	4(2)
C(3)	22(2)	35(2)	26(2)	5(2)	13(2)	4(2)
C(4)	29(2)	30(2)	37(2)	7(2)	22(2)	1(2)
C(5)	44(3)	39(3)	40(3)	-14(2)	26(2)	-13(2)
C(6)	20(2)	49(3)	38(3)	9(2)	15(2)	-4(2)
C(7)	23(2)	55(3)	36(3)	7(2)	19(2)	5(2)
C(8)	20(2)	21(2)	25(2)	-2(2)	13(2)	-3(2)
C(9)	25(2)	23(2)	25(2)	0(2)	17(2)	-2(2)
C(10)	19(2)	19(2)	26(2)	2(2)	14(2)	3(2)
C(11)	32(2)	19(2)	24(2)	3(2)	18(2)	3(2)
C(12)	28(2)	27(2)	27(2)	3(2)	19(2)	4(2)
Cl(1)	36(1)	27(1)	46(1)	-2(1)	32(1)	3(1)
Cl(2)	32(1)	41(1)	21(1)	-2(1)	17(1)	-8(1)
Mo	21(1)	20(1)	23(1)	1(1)	15(1)	0(1)
O(1)	33(2)	45(2)	28(2)	-5(1)	21(2)	-2(2)
O(2)	29(2)	45(2)	43(2)	11(2)	22(2)	12(2)
O(3)	33(2)	34(2)	31(2)	6(1)	23(2)	7(1)
O(4)	33(2)	47(2)	35(2)	5(1)	22(2)	13(1)
O(5)	48(2)	32(2)	53(2)	-5(2)	35(2)	-7(2)
P	22(1)	23(1)	22(1)	0(1)	16(1)	0(1)
Si(1)	22(1)	26(1)	24(1)	5(1)	15(1)	2(1)
Si(2)	21(1)	31(1)	25(1)	0(1)	15(1)	-3(1)

Table ii.5. Hydrogen coordinates ($\times 10^4$) and isotropic displacement parameters ($\text{\AA}^2 \times 10^3$) for [25].

	X	Y	Z	U(eq)
H(1A)	3450	1598	-2631	22
H(2A)	2270	3214	-4893	48
H(2B)	2632	1767	-4363	48
H(2C)	3578	2987	-3955	48
H(3A)	277	3500	-4976	45
H(3B)	390	3533	-4084	45
H(3C)	548	2102	-4419	45
H(4A)	3295	5608	-3152	47
H(4B)	2222	5671	-3148	47
H(4C)	1982	5811	-4091	47
H(5A)	4318	4707	-882	62
H(5B)	4419	5642	-1521	62
H(5C)	5583	5140	-543	62
H(6A)	6168	4184	-1769	57
H(6B)	4853	4426	-2697	57
H(6C)	5446	2927	-2468	57
H(7A)	6671	2223	-490	57
H(7B)	5663	1066	-996	57
H(7C)	5860	2013	-219	57

Table ii.6. Torsion angles [deg] for [25].

O(5)-C(12)-Mo-C(8)	56(16)
O(5)-C(12)-Mo-C(11)	-33(16)
O(5)-C(12)-Mo-C(10)	-121(16)
O(5)-C(12)-Mo-C(9)	148(16)
O(5)-C(12)-Mo-P	-40(17)
O(1)-C(8)-Mo-C(12)	-39(7)
O(1)-C(8)-Mo-C(11)	51(7)
O(1)-C(8)-Mo-C(10)	2(9)
O(1)-C(8)-Mo-C(9)	-130(7)
O(1)-C(8)-Mo-P	137(7)
O(4)-C(11)-Mo-C(12)	168(100)
O(4)-C(11)-Mo-C(8)	80(37)
O(4)-C(11)-Mo-C(10)	-104(37)
O(4)-C(11)-Mo-C(9)	-61(39)
O(4)-C(11)-Mo-P	-13(37)
O(3)-C(10)-Mo-C(12)	47(6)
O(3)-C(10)-Mo-C(8)	6(7)
O(3)-C(10)-Mo-C(11)	-43(6)
O(3)-C(10)-Mo-C(9)	138(6)
O(3)-C(10)-Mo-P	-129(6)
O(2)-C(9)-Mo-C(12)	112(17)
O(2)-C(9)-Mo-C(8)	-159(17)
O(2)-C(9)-Mo-C(11)	-18(21)
O(2)-C(9)-Mo-C(10)	24(17)
O(2)-C(9)-Mo-P	-67(17)
Si(2)-C(1)-P-Cl(1)	86.9(2)
Si(1)-C(1)-P-Cl(1)	-51.87(19)
Si(2)-C(1)-P-Cl(2)	-14.3(2)
Si(1)-C(1)-P-Cl(2)	-153.06(15)
Si(2)-C(1)-P-Mo	-137.60(15)
Si(1)-C(1)-P-Mo	83.7(2)
C(12)-Mo-P-C(1)	78.3(15)
C(8)-Mo-P-C(1)	-17.51(17)
C(11)-Mo-P-C(1)	71.15(17)
C(10)-Mo-P-C(1)	159.23(17)
C(9)-Mo-P-C(1)	-109.90(17)
C(12)-Mo-P-Cl(1)	-153.4(15)
C(8)-Mo-P-Cl(1)	110.79(12)
C(11)-Mo-P-Cl(1)	-160.55(12)
C(10)-Mo-P-Cl(1)	-72.47(11)
C(9)-Mo-P-Cl(1)	18.40(12)
C(12)-Mo-P-Cl(2)	-44.1(15)
C(8)-Mo-P-Cl(2)	-139.88(12)
C(11)-Mo-P-Cl(2)	-51.22(12)
C(10)-Mo-P-Cl(2)	36.86(11)
C(9)-Mo-P-Cl(2)	127.72(12)
P-C(1)-Si(1)-C(2)	-137.6(2)
Si(2)-C(1)-Si(1)-C(2)	81.2(2)
P-C(1)-Si(1)-C(4)	100.3(2)
Si(2)-C(1)-Si(1)-C(4)	-40.8(2)
P-C(1)-Si(1)-C(3)	-20.1(3)
Si(2)-C(1)-Si(1)-C(3)	-161.27(19)
P-C(1)-Si(2)-C(5)	-60.5(3)
Si(1)-C(1)-Si(2)-C(5)	78.2(2)
P-C(1)-Si(2)-C(7)	64.3(3)
Si(1)-C(1)-Si(2)-C(7)	-156.93(19)
P-C(1)-Si(2)-C(6)	179.7(2)
Si(1)-C(1)-Si(2)-C(6)	-41.5(2)

iii.[2-Bis(trimethylsilyl)methyl-3-phenyl-oxaphosphirane-

KP]pentacarbonylchromium(0) [29]

(B1)

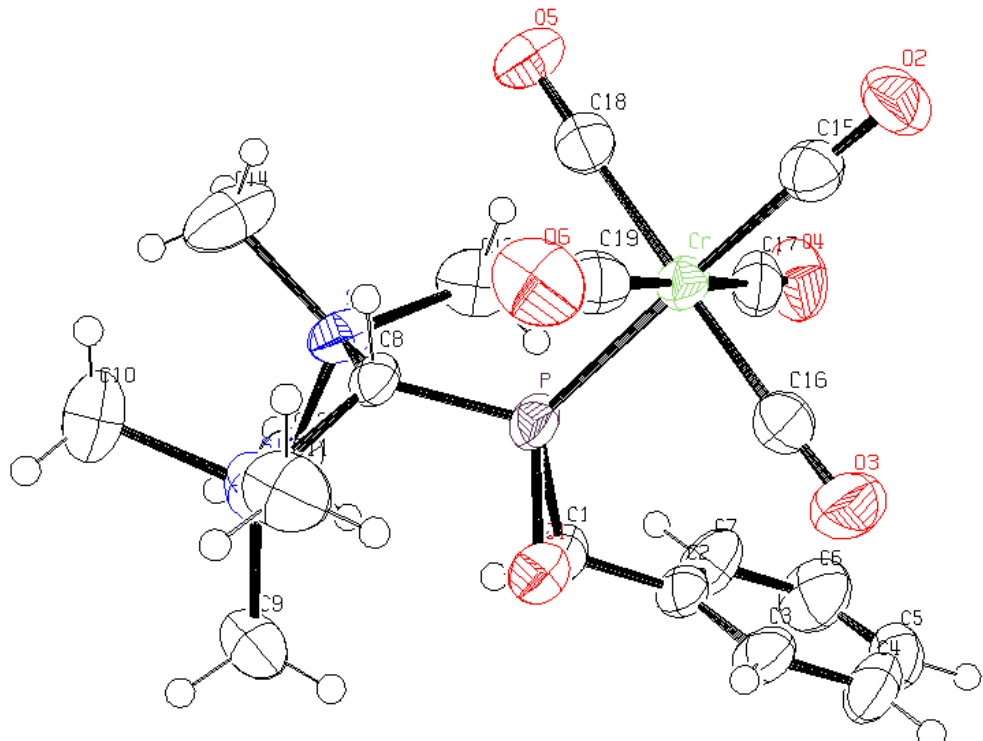


Table iii.1. Crystal data and structure refinement for [29].

Identification code	GSTR084, Greg820
Device Type	STOE IPDS 2T
Empirical formula	C19 H25 Cr O6 P Si2
Formula weight	488.54
Temperature	123(2) K
Wavelength	0.71073 Å
Crystal system, space group	Triclinic, P -1
Unit cell dimensions deg.	a = 8.8967(6) Å alpha = 86.974(5) b = 10.5532(6) Å beta = 88.606(5) deg. c = 13.9398(9) Å gamma = 67.430(5) deg.
Volume	1206.85(13) Å^3
Z, Calculated density	2, 1.344 Mg/m^3

Absorption coefficient	0.669 mm^-1
F(000)	508
Crystal size	0.25 x 0.10 x 0.04 mm
Theta range for data collection	2.09 to 27.00 deg.
Limiting indices	-11<=h<=10, -13<=k<=13, -17<=l<=17
Reflections collected / unique	11847 / 5180 [R(int) = 0.0629]
Completeness to theta = 27.00	98.3 %
Absorption correction	Semi-empirical from equivalents
Max. and min. transmission	0.96483 and 0.91912
Refinement method	Full-matrix least-squares on F^2
Data / restraints / parameters	5180 / 12 / 268
Goodness-of-fit on F^2	0.854
Final R indices [I>2sigma(I)]	R1 = 0.0586, wR2 = 0.1319
R indices (all data)	R1 = 0.1181, wR2 = 0.1500
Largest diff. peak and hole	1.154 and -0.471 e.A^-3

Table iii.2. Atomic coordinates (x 10^4) and equivalent isotropic displacement parameters (A^2 x 10^3) for [29]. U(eq) is defined as one third of the trace of the orthogonalized Uij tensor.

	x	y	z	U(eq)
C(1)	7778(6)	5196(5)	8587(3)	45(1)
C(2)	8264(6)	6289(4)	8950(3)	40(1)
C(3)	7214(7)	7294(5)	9510(3)	50(1)
C(4)	7680(8)	8299(5)	9833(4)	60(2)
C(5)	9150(8)	8321(5)	9614(4)	60(2)
C(6)	10211(8)	7311(7)	9062(5)	73(2)
C(7)	9763(7)	6281(6)	8736(4)	62(2)
C(8)	6858(5)	3744(4)	7135(3)	35(1)
C(9)	6883(7)	2183(6)	9119(4)	57(1)
C(10)	6180(11)	1107(7)	7303(5)	92(2)
C(11)	3715(7)	3729(7)	8038(4)	70(2)
C(12)	9889(7)	4076(6)	6243(4)	66(2)
C(13)	10403(7)	1634(5)	7585(4)	57(1)
C(14)	8872(8)	1810(7)	5640(4)	83(2)
C(15)	4077(6)	9059(5)	5932(3)	45(1)
C(16)	4441(7)	8388(5)	7771(4)	51(1)
C(17)	7141(7)	7748(5)	6566(4)	49(1)
C(18)	5764(6)	6476(5)	5478(3)	43(1)
C(19)	3295(7)	6990(5)	6701(3)	49(1)
Cr	5184(1)	7414(1)	6638(1)	37(1)
O(1)	6039(4)	5391(3)	8736(2)	46(1)
O(2)	3380(5)	10090(3)	5515(2)	56(1)

O(3)	3887(6)	9016(4)	8429(3)	72(1)
O(4)	8308(5)	7940(4)	6488(3)	66(1)
O(5)	6069(5)	5946(4)	4764(2)	56(1)
O(6)	2130(5)	6764(4)	6745(3)	72(1)
P	6510(2)	5415(1)	7561(1)	40(1)
Si(1)	5921(2)	2712(2)	7931(1)	54(1)
Si(2)	9006(2)	2789(1)	6666(1)	47(1)

Table iii.3. Bond lengths [Å] and angles [deg] for [29].

C(1)-O(1)	1.491(6)
C(1)-C(2)	1.493(6)
C(1)-P	1.793(4)
C(1)-H(1A)	1.0000
C(2)-C(7)	1.356(8)
C(2)-C(3)	1.378(7)
C(3)-C(4)	1.377(7)
C(3)-H(3A)	0.9500
C(4)-C(5)	1.345(9)
C(4)-H(4A)	0.9500
C(5)-C(6)	1.378(9)
C(5)-H(5A)	0.9500
C(6)-C(7)	1.393(8)
C(6)-H(6A)	0.9500
C(7)-H(7A)	0.9500
C(8)-P	1.800(4)
C(8)-Si(2)	1.904(5)
C(8)-Si(1)	1.907(5)
C(8)-H(8A)	1.0000
C(9)-Si(1)	1.841(5)
C(9)-H(9A)	0.9800
C(9)-H(9B)	0.9800
C(9)-H(9C)	0.9800
C(10)-Si(1)	1.881(6)
C(10)-H(10A)	0.9800
C(10)-H(10B)	0.9800
C(10)-H(10C)	0.9800
C(11)-Si(1)	1.848(6)
C(11)-H(11A)	0.9800
C(11)-H(11B)	0.9800
C(11)-H(11C)	0.9800
C(12)-Si(2)	1.876(7)
C(12)-H(12A)	0.9800
C(12)-H(12B)	0.9800
C(12)-H(12C)	0.9800
C(13)-Si(2)	1.849(5)
C(13)-H(13A)	0.9800
C(13)-H(13B)	0.9800
C(13)-H(13C)	0.9800
C(14)-Si(2)	1.841(5)
C(14)-H(14C)	0.9800
C(14)-H(14B)	0.9800
C(14)-H(14A)	0.9800
C(15)-O(2)	1.157(5)
C(15)-Cr	1.873(5)
C(16)-O(3)	1.146(6)
C(16)-Cr	1.894(5)
C(17)-O(4)	1.133(6)
C(17)-Cr	1.904(6)
C(18)-O(5)	1.142(5)
C(18)-Cr	1.897(5)

C(19)-O(6)	1.149(6)
C(19)-Cr	1.896(6)
Cr-P	2.3181(13)
O(1)-P	1.682(3)
O(1)-C(1)-C(2)	116.0(4)
O(1)-C(1)-P	60.8(2)
C(2)-C(1)-P	124.5(3)
O(1)-C(1)-H(1A)	114.8
C(2)-C(1)-H(1A)	114.8
P-C(1)-H(1A)	114.8
C(7)-C(2)-C(3)	119.8(4)
C(7)-C(2)-C(1)	119.6(4)
C(3)-C(2)-C(1)	120.6(5)
C(4)-C(3)-C(2)	119.8(5)
C(4)-C(3)-H(3A)	120.1
C(2)-C(3)-H(3A)	120.1
C(5)-C(4)-C(3)	121.2(5)
C(5)-C(4)-H(4A)	119.4
C(3)-C(4)-H(4A)	119.4
C(4)-C(5)-C(6)	119.1(5)
C(4)-C(5)-H(5A)	120.4
C(6)-C(5)-H(5A)	120.4
C(5)-C(6)-C(7)	120.3(6)
C(5)-C(6)-H(6A)	119.9
C(7)-C(6)-H(6A)	119.9
C(2)-C(7)-C(6)	119.7(6)
C(2)-C(7)-H(7A)	120.1
C(6)-C(7)-H(7A)	120.1
P-C(8)-Si(2)	114.2(2)
P-C(8)-Si(1)	113.9(2)
Si(2)-C(8)-Si(1)	117.1(2)
P-C(8)-H(8A)	103.1
Si(2)-C(8)-H(8A)	103.1
Si(1)-C(8)-H(8A)	103.1
Si(1)-C(9)-H(9A)	109.5
Si(1)-C(9)-H(9B)	109.5
H(9A)-C(9)-H(9B)	109.5
Si(1)-C(9)-H(9C)	109.5
H(9A)-C(9)-H(9C)	109.5
H(9B)-C(9)-H(9C)	109.5
Si(1)-C(10)-H(10A)	109.5
Si(1)-C(10)-H(10B)	109.5
H(10A)-C(10)-H(10B)	109.5
Si(1)-C(10)-H(10C)	109.5
H(10A)-C(10)-H(10C)	109.5
H(10B)-C(10)-H(10C)	109.5
Si(1)-C(11)-H(11A)	109.5
Si(1)-C(11)-H(11B)	109.5
H(11A)-C(11)-H(11B)	109.5
Si(1)-C(11)-H(11C)	109.5
H(11A)-C(11)-H(11C)	109.5
H(11B)-C(11)-H(11C)	109.5
Si(2)-C(12)-H(12A)	109.5
Si(2)-C(12)-H(12B)	109.5
H(12A)-C(12)-H(12B)	109.5
Si(2)-C(12)-H(12C)	109.5
H(12A)-C(12)-H(12C)	109.5
H(12B)-C(12)-H(12C)	109.5
Si(2)-C(13)-H(13A)	109.5
Si(2)-C(13)-H(13B)	109.5
H(13A)-C(13)-H(13B)	109.5
Si(2)-C(13)-H(13C)	109.5

H(13A)-C(13)-H(13C)	109.5
H(13B)-C(13)-H(13C)	109.5
Si(2)-C(14)-H(14C)	109.5
Si(2)-C(14)-H(14B)	109.5
H(14C)-C(14)-H(14B)	109.5
Si(2)-C(14)-H(14A)	109.5
H(14C)-C(14)-H(14A)	109.5
H(14B)-C(14)-H(14A)	109.5
O(2)-C(15)-Cr	178.4(4)
O(3)-C(16)-Cr	175.2(5)
O(4)-C(17)-Cr	177.5(5)
O(5)-C(18)-Cr	177.6(4)
O(6)-C(19)-Cr	178.4(5)
C(15)-Cr-C(16)	88.1(2)
C(15)-Cr-C(19)	91.5(2)
C(16)-Cr-C(19)	87.8(2)
C(15)-Cr-C(18)	89.8(2)
C(16)-Cr-C(18)	175.8(2)
C(19)-Cr-C(18)	88.7(2)
C(15)-Cr-C(17)	90.7(2)
C(16)-Cr-C(17)	94.1(2)
C(19)-Cr-C(17)	177.2(2)
C(18)-Cr-C(17)	89.6(2)
C(15)-Cr-P	177.98(16)
C(16)-Cr-P	89.95(14)
C(19)-Cr-P	88.15(15)
C(18)-Cr-P	92.17(14)
C(17)-Cr-P	89.74(14)
C(1)-O(1)-P	68.5(2)
O(1)-P-C(1)	50.7(2)
O(1)-P-C(8)	107.47(19)
C(1)-P-C(8)	108.3(2)
O(1)-P-Cr	118.24(12)
C(1)-P-Cr	127.73(15)
C(8)-P-Cr	121.98(14)
C(9)-Si(1)-C(11)	111.5(3)
C(9)-Si(1)-C(10)	107.6(3)
C(11)-Si(1)-C(10)	107.6(3)
C(9)-Si(1)-C(8)	113.7(2)
C(11)-Si(1)-C(8)	108.3(2)
C(10)-Si(1)-C(8)	107.9(3)
C(14)-Si(2)-C(13)	110.3(3)
C(14)-Si(2)-C(12)	109.0(3)
C(13)-Si(2)-C(12)	107.1(3)
C(14)-Si(2)-C(8)	108.0(3)
C(13)-Si(2)-C(8)	113.5(2)
C(12)-Si(2)-C(8)	108.8(2)

Table iii.4. Anisotropic displacement parameters ($\text{\AA}^2 \times 10^3$) for [29].

The anisotropic displacement factor exponent takes the form:
 $-2 \pi^2 [h^2 a^{*2} U_{11} + \dots + 2 h k a^* b^* U_{12}]$

	U11	U22	U33	U23	U13	U12
C(1)	52(3)	34(2)	47(3)	-5(2)	-13(2)	-13(2)
C(2)	46(3)	39(2)	36(2)	-3(2)	-13(2)	-16(2)
C(3)	57(3)	57(3)	41(3)	-13(2)	-2(2)	-27(3)

C(4)	69(4)	49(3)	61(3)	-20(2)	-10(3)	-20(3)
C(5)	81(4)	48(3)	61(3)	3(2)	-30(3)	-36(3)
C(6)	71(3)	89(3)	77(3)	-16(3)	-7(3)	-47(3)
C(7)	55(3)	70(3)	67(3)	-25(2)	-6(2)	-27(2)
C(8)	37(2)	35(2)	36(2)	-5(2)	-9(2)	-15(2)
C(9)	57(3)	56(3)	62(3)	15(2)	-7(3)	-27(3)
C(10)	128(7)	73(4)	99(5)	-15(4)	-8(5)	-64(5)
C(11)	55(4)	90(4)	71(4)	12(3)	-10(3)	-38(3)
C(12)	44(3)	83(4)	66(4)	-1(3)	5(3)	-18(3)
C(13)	51(3)	54(3)	53(3)	-9(2)	-6(2)	-4(3)
C(14)	67(4)	92(5)	64(4)	-36(3)	-15(3)	3(3)
C(15)	44(3)	47(3)	44(3)	-3(2)	-5(2)	-17(2)
C(16)	63(4)	38(3)	46(3)	3(2)	-12(3)	-11(2)
C(17)	54(3)	33(2)	59(3)	-1(2)	-18(3)	-17(2)
C(18)	39(3)	45(3)	49(3)	1(2)	-10(2)	-18(2)
C(19)	47(3)	54(3)	44(3)	3(2)	-8(2)	-15(3)
Cr	42(1)	32(1)	36(1)	-3(1)	-10(1)	-10(1)
O(1)	48(2)	47(2)	44(2)	-7(1)	-2(2)	-20(2)
O(2)	58(2)	45(2)	55(2)	13(2)	-10(2)	-11(2)
O(3)	94(3)	54(2)	47(2)	-10(2)	-5(2)	-4(2)
O(4)	54(3)	54(2)	97(3)	3(2)	-16(2)	-27(2)
O(5)	62(2)	64(2)	42(2)	-17(2)	-3(2)	-23(2)
O(6)	53(3)	85(3)	81(3)	10(2)	-9(2)	-30(2)
P	46(1)	32(1)	40(1)	-4(1)	-14(1)	-13(1)
Si(1)	55(1)	53(1)	60(1)	5(1)	-10(1)	-30(1)
Si(2)	42(1)	50(1)	39(1)	-10(1)	-6(1)	-6(1)

Table iii.5. Hydrogen coordinates ($\times 10^4$) and isotropic displacement parameters ($\text{\AA}^2 \times 10^3$) for [29].

	x	y	z	U(eq)
H(1A)	8578	4236	8720	54
H(3A)	6170	7294	9672	60
H(4A)	6948	8989	10218	72
H(5A)	9454	9024	9838	72
H(6A)	11253	7317	8902	88
H(7A)	10504	5576	8365	75
H(8A)	6183	3963	6540	43
H(9A)	6614	2992	9504	86
H(9B)	8067	1748	9039	86
H(9C)	6481	1529	9444	86
H(10A)	7342	563	7211	138
H(10B)	5642	1356	6676	138
H(10C)	5690	565	7693	138
H(11A)	3238	3986	7396	104
H(11B)	3540	4562	8381	104
H(11C)	3195	3180	8394	104
H(12A)	9850	4671	6767	99
H(12B)	9256	4635	5698	99
H(12C)	11021	3594	6042	99
H(13A)	9979	945	7825	86
H(13B)	10487	2172	8118	86
H(13C)	11481	1173	7299	86
H(14C)	9931	1441	5316	125
H(14B)	8052	2416	5188	125
H(14A)	8560	1051	5870	125

Table iii.6. Torsion angles [deg] for [29].

O(1)-C(1)-C(2)-C(7)	-171.7(4)
P-C(1)-C(2)-C(7)	-100.5(5)
O(1)-C(1)-C(2)-C(3)	9.2(6)
P-C(1)-C(2)-C(3)	80.3(6)
C(7)-C(2)-C(3)-C(4)	1.2(7)
C(1)-C(2)-C(3)-C(4)	-179.6(4)
C(2)-C(3)-C(4)-C(5)	-0.1(8)
C(3)-C(4)-C(5)-C(6)	-0.5(8)
C(4)-C(5)-C(6)-C(7)	0.0(9)
C(3)-C(2)-C(7)-C(6)	-1.8(8)
C(1)-C(2)-C(7)-C(6)	179.1(5)
C(5)-C(6)-C(7)-C(2)	1.2(9)
O(2)-C(15)-Cr-C(16)	-4(16)
O(2)-C(15)-Cr-C(19)	84(16)
O(2)-C(15)-Cr-C(18)	172(16)
O(2)-C(15)-Cr-C(17)	-98(16)
O(2)-C(15)-Cr-P	4(20)
O(3)-C(16)-Cr-C(15)	47(6)
O(3)-C(16)-Cr-C(19)	-44(6)
O(3)-C(16)-Cr-C(18)	-12(8)
O(3)-C(16)-Cr-C(17)	138(6)
O(3)-C(16)-Cr-P	-133(6)
O(6)-C(19)-Cr-C(15)	-46(16)
O(6)-C(19)-Cr-C(16)	42(16)
O(6)-C(19)-Cr-C(18)	-135(16)
O(6)-C(19)-Cr-C(17)	173(100)
O(6)-C(19)-Cr-P	132(16)
O(5)-C(18)-Cr-C(15)	-24(11)
O(5)-C(18)-Cr-C(16)	35(13)
O(5)-C(18)-Cr-C(19)	68(11)
O(5)-C(18)-Cr-C(17)	-115(11)
O(5)-C(18)-Cr-P	156(11)
O(4)-C(17)-Cr-C(15)	-67(10)
O(4)-C(17)-Cr-C(16)	-155(10)
O(4)-C(17)-Cr-C(19)	74(11)
O(4)-C(17)-Cr-C(18)	23(10)
O(4)-C(17)-Cr-P	115(10)
C(2)-C(1)-O(1)-P	116.7(4)
C(1)-O(1)-P-C(8)	99.7(3)
C(1)-O(1)-P-Cr	-117.3(2)
C(2)-C(1)-P-O(1)	-103.1(5)
O(1)-C(1)-P-C(8)	-97.9(3)
C(2)-C(1)-P-C(8)	159.0(4)
O(1)-C(1)-P-Cr	98.0(2)
C(2)-C(1)-P-Cr	-5.0(6)
Si(2)-C(8)-P-O(1)	-118.1(2)
Si(1)-C(8)-P-O(1)	20.1(3)
Si(2)-C(8)-P-C(1)	-64.6(3)
Si(1)-C(8)-P-C(1)	73.5(3)
Si(2)-C(8)-P-Cr	100.5(2)
Si(1)-C(8)-P-Cr	-121.34(18)
C(15)-Cr-P-O(1)	6(5)
C(16)-Cr-P-O(1)	14.2(2)
C(19)-Cr-P-O(1)	-73.6(2)
C(18)-Cr-P-O(1)	-162.2(2)
C(17)-Cr-P-O(1)	108.3(2)
C(15)-Cr-P-C(1)	-55(5)
C(16)-Cr-P-C(1)	-46.3(3)
C(19)-Cr-P-C(1)	-134.0(3)
C(18)-Cr-P-C(1)	137.4(3)

C(17)-Cr-P-C(1)	47.8(3)
C(15)-Cr-P-C(8)	143(5)
C(16)-Cr-P-C(8)	151.7(3)
C(19)-Cr-P-C(8)	63.9(2)
C(18)-Cr-P-C(8)	-24.7(2)
C(17)-Cr-P-C(8)	-114.2(2)
P-C(8)-Si(1)-C(9)	-67.6(3)
Si(2)-C(8)-Si(1)-C(9)	69.2(3)
P-C(8)-Si(1)-C(11)	56.9(3)
Si(2)-C(8)-Si(1)-C(11)	-166.2(3)
P-C(8)-Si(1)-C(10)	173.1(3)
Si(2)-C(8)-Si(1)-C(10)	-50.0(3)
P-C(8)-Si(2)-C(14)	-144.1(3)
Si(1)-C(8)-Si(2)-C(14)	79.1(3)
P-C(8)-Si(2)-C(13)	93.2(3)
Si(1)-C(8)-Si(2)-C(13)	-43.5(3)
P-C(8)-Si(2)-C(12)	-26.0(3)
Si(1)-C(8)-Si(2)-C(12)	-162.7(2)

iv.[2-Bis(trimethylsilyl)methyl-3-phenyl-oxaphosphirane-
kP]pentacarbonylmolybdenum (0) [30]

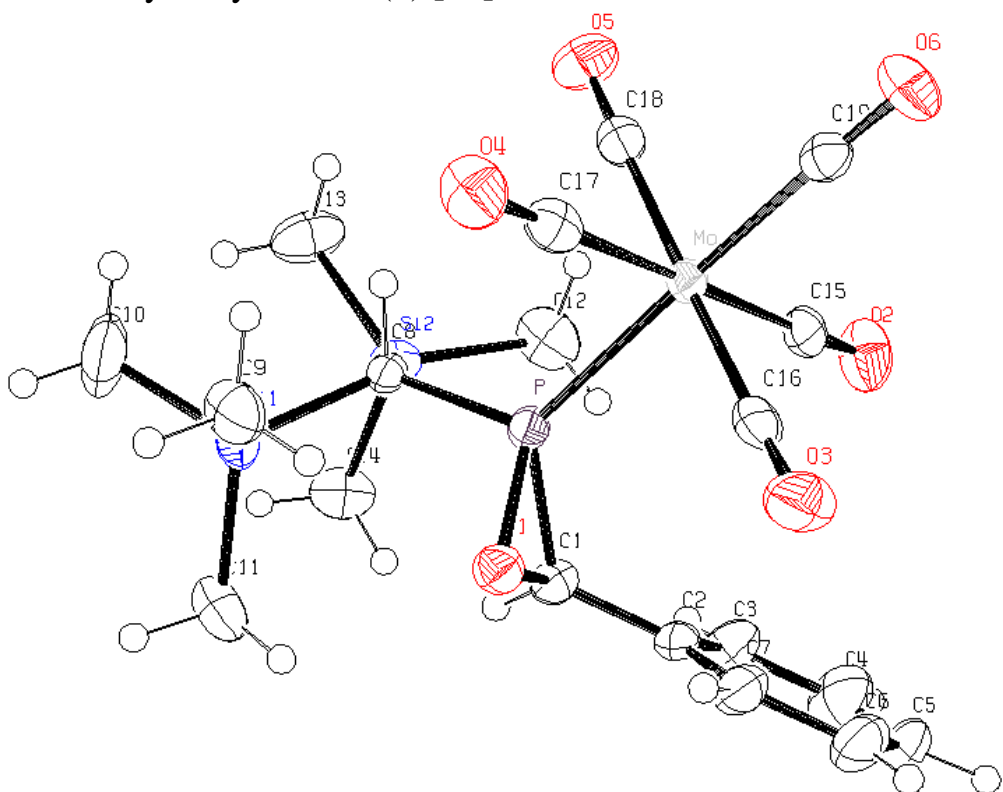


Table iv.1. Crystal data and structure refinement for [30].

Identification code
e:\transfer\d\roentgen\greg116\hauptlsg\mulabs\weiter\greg116

Empirical formula C19 H25 Mo O6 P Si2

Formula weight 532.48

Temperature 123(2) K

Wavelength	0.71073 Å
Crystal system, space group	Triclinic, P -1
Unit cell dimensions 87.1032(12) deg.	a = 8.8987(2) Å alpha =
88.3077(13) deg.	b = 10.6956(3) Å beta =
68.9673(17) deg.	c = 13.9288(5) Å gamma =
Volume	1235.70(6) Å^3
Z, Calculated density	2, 1.431 Mg/m^3
Absorption coefficient	0.722 mm^-1
F(000)	544
Crystal size	0.40 x 0.24 x 0.20 mm
Theta range for data collection	2.57 to 29.11 deg.
Limiting indices	-12<=h<=12, -14<=k<=14, -19<=l<=18
Reflections collected / unique	18795 / 6450 [R(int) = 0.0664]
Completeness to theta = 29.11	97.1 %
Absorption correction	Semi-empirical from equivalents
Max. and min. transmission	0.8691 and 0.7611
Refinement method	Full-matrix least-squares on F^2
Data / restraints / parameters	6450 / 0 / 268
Goodness-of-fit on F^2	0.886
Final R indices [I>2sigma(I)]	R1 = 0.0377, wR2 = 0.0549
R indices (all data)	R1 = 0.0715, wR2 = 0.0606
Largest diff. peak and hole	0.505 and -0.651 e.Å^-3

Table iv.2. Atomic coordinates (x 10^4) and equivalent isotropic displacement parameters (Å^2 x 10^3) for JMP [30].

U(eq) is defined as one third of the trace of the orthogonalized Uij tensor.

	x	y	z	U(eq)
C(1)	7809(3)	5146(2)	8626(2)	26(1)
C(2)	8286(3)	6240(2)	8963(2)	26(1)
C(3)	9839(3)	6201(3)	8793(2)	45(1)
C(4)	10289(4)	7229(3)	9079(2)	58(1)
C(5)	9222(4)	8291(3)	9546(2)	51(1)
C(6)	7691(4)	8321(3)	9735(2)	49(1)
C(7)	7224(3)	7295(3)	9447(2)	35(1)
C(8)	6876(2)	3700(2)	7175(2)	22(1)

C(9)	3738(3)	3694(3)	8101(2)	43(1)
C(10)	6084(4)	1143(3)	7312(2)	66(1)
C(11)	6862(3)	2160(3)	9150(2)	43(1)
C(12)	9870(3)	4100(3)	6257(2)	47(1)
C(13)	8903(3)	1810(3)	5673(2)	52(1)
C(14)	10394(3)	1694(3)	7619(2)	43(1)
C(15)	7197(3)	7834(2)	6589(2)	31(1)
C(16)	4267(3)	8439(2)	7855(2)	31(1)
C(17)	3101(3)	6902(2)	6687(2)	31(1)
C(18)	5786(3)	6423(2)	5402(2)	29(1)
C(19)	3953(3)	9119(3)	5873(2)	28(1)
Mo	5113(1)	7402(1)	6644(1)	22(1)
O(1)	6104(2)	5290(2)	8798(1)	30(1)
O(2)	8355(2)	8057(2)	6531(1)	48(1)
O(3)	3699(2)	9060(2)	8510(1)	49(1)
O(4)	1977(2)	6621(2)	6708(1)	47(1)
O(5)	6116(2)	5890(2)	4686(1)	44(1)
O(6)	3293(2)	10108(2)	5461(1)	44(1)
P	6522(1)	5339(1)	7617(1)	23(1)
Si(1)	5909(1)	2676(1)	7957(1)	34(1)
Si(2)	9012(1)	2815(1)	6696(1)	29(1)

Table iv.3. Bond lengths [Å] and angles [deg] for [30].

C(1)-C(2)	1.481(3)
C(1)-O(1)	1.482(2)
C(1)-P	1.795(2)
C(1)-H(1A)	1.0000
C(2)-C(7)	1.377(3)
C(2)-C(3)	1.382(3)
C(3)-C(4)	1.377(4)
C(3)-H(3A)	0.9500
C(4)-C(5)	1.371(4)
C(4)-H(4A)	0.9500
C(5)-C(6)	1.369(3)
C(5)-H(5A)	0.9500
C(6)-C(7)	1.385(3)
C(6)-H(6A)	0.9500
C(7)-H(7A)	0.9500
C(8)-P	1.804(2)
C(8)-Si(1)	1.904(2)
C(8)-Si(2)	1.911(2)
C(8)-H(8A)	1.0000
C(9)-Si(1)	1.856(2)
C(9)-H(9A)	0.9800
C(9)-H(9B)	0.9800
C(9)-H(9C)	0.9800
C(10)-Si(1)	1.865(3)
C(10)-H(10A)	0.9800
C(10)-H(10B)	0.9800
C(10)-H(10C)	0.9800
C(11)-Si(1)	1.855(3)
C(11)-H(11A)	0.9800
C(11)-H(11B)	0.9800
C(11)-H(11C)	0.9800
C(12)-Si(2)	1.867(2)
C(12)-H(12A)	0.9800
C(12)-H(12B)	0.9800
C(12)-H(12C)	0.9800
C(13)-Si(2)	1.853(3)
C(13)-H(13A)	0.9800

C(13)-H(13B)	0.9800
C(13)-H(13C)	0.9800
C(14)-Si(2)	1.865(2)
C(14)-H(14A)	0.9800
C(14)-H(14B)	0.9800
C(14)-H(14C)	0.9800
C(15)-O(2)	1.139(2)
C(15)-Mo	2.064(2)
C(16)-O(3)	1.150(3)
C(16)-Mo	2.039(3)
C(17)-O(4)	1.142(3)
C(17)-Mo	2.043(2)
C(18)-O(5)	1.151(3)
C(18)-Mo	2.030(3)
C(19)-O(6)	1.143(3)
C(19)-Mo	2.024(3)
Mo-P	2.4675(7)
O(1)-P	1.6786(16)
C(2)-C(1)-O(1)	116.06(19)
C(2)-C(1)-P	123.42(18)
O(1)-C(1)-P	60.72(10)
C(2)-C(1)-H(1A)	115.1
O(1)-C(1)-H(1A)	115.1
P-C(1)-H(1A)	115.1
C(7)-C(2)-C(3)	118.9(2)
C(7)-C(2)-C(1)	121.8(2)
C(3)-C(2)-C(1)	119.3(2)
C(4)-C(3)-C(2)	120.0(3)
C(4)-C(3)-H(3A)	120.0
C(2)-C(3)-H(3A)	120.0
C(5)-C(4)-C(3)	121.0(3)
C(5)-C(4)-H(4A)	119.5
C(3)-C(4)-H(4A)	119.5
C(6)-C(5)-C(4)	119.3(3)
C(6)-C(5)-H(5A)	120.4
C(4)-C(5)-H(5A)	120.4
C(5)-C(6)-C(7)	120.2(3)
C(5)-C(6)-H(6A)	119.9
C(7)-C(6)-H(6A)	119.9
C(2)-C(7)-C(6)	120.6(2)
C(2)-C(7)-H(7A)	119.7
C(6)-C(7)-H(7A)	119.7
P-C(8)-Si(1)	113.33(11)
P-C(8)-Si(2)	114.18(11)
Si(1)-C(8)-Si(2)	118.16(11)
P-C(8)-H(8A)	102.8
Si(1)-C(8)-H(8A)	102.8
Si(2)-C(8)-H(8A)	102.8
Si(1)-C(9)-H(9A)	109.5
Si(1)-C(9)-H(9B)	109.5
H(9A)-C(9)-H(9B)	109.5
Si(1)-C(9)-H(9C)	109.5
H(9A)-C(9)-H(9C)	109.5
H(9B)-C(9)-H(9C)	109.5
Si(1)-C(10)-H(10A)	109.5
Si(1)-C(10)-H(10B)	109.5
H(10A)-C(10)-H(10B)	109.5
Si(1)-C(10)-H(10C)	109.5
H(10A)-C(10)-H(10C)	109.5
H(10B)-C(10)-H(10C)	109.5
Si(1)-C(11)-H(11A)	109.5
Si(1)-C(11)-H(11B)	109.5

H(11A)-C(11)-H(11B)	109.5
Si(1)-C(11)-H(11C)	109.5
H(11A)-C(11)-H(11C)	109.5
H(11B)-C(11)-H(11C)	109.5
Si(2)-C(12)-H(12A)	109.5
Si(2)-C(12)-H(12B)	109.5
H(12A)-C(12)-H(12B)	109.5
Si(2)-C(12)-H(12C)	109.5
H(12A)-C(12)-H(12C)	109.5
H(12B)-C(12)-H(12C)	109.5
Si(2)-C(13)-H(13A)	109.5
Si(2)-C(13)-H(13B)	109.5
H(13A)-C(13)-H(13B)	109.5
Si(2)-C(13)-H(13C)	109.5
H(13A)-C(13)-H(13C)	109.5
H(13B)-C(13)-H(13C)	109.5
Si(2)-C(14)-H(14A)	109.5
Si(2)-C(14)-H(14B)	109.5
H(14A)-C(14)-H(14B)	109.5
Si(2)-C(14)-H(14C)	109.5
H(14A)-C(14)-H(14C)	109.5
H(14B)-C(14)-H(14C)	109.5
O(2)-C(15)-Mo	177.9(2)
O(3)-C(16)-Mo	175.8(2)
O(4)-C(17)-Mo	179.7(2)
O(5)-C(18)-Mo	177.7(2)
O(6)-C(19)-Mo	178.1(2)
C(19)-Mo-C(18)	89.58(9)
C(19)-Mo-C(16)	87.70(9)
C(18)-Mo-C(16)	175.74(10)
C(19)-Mo-C(17)	91.27(9)
C(18)-Mo-C(17)	88.95(9)
C(16)-Mo-C(17)	87.84(10)
C(19)-Mo-C(15)	90.27(9)
C(18)-Mo-C(15)	89.59(9)
C(16)-Mo-C(15)	93.70(10)
C(17)-Mo-C(15)	177.87(9)
C(19)-Mo-P	178.67(7)
C(18)-Mo-P	91.71(7)
C(16)-Mo-P	91.03(7)
C(17)-Mo-P	89.09(7)
C(15)-Mo-P	89.41(7)
C(1)-O(1)-P	68.90(10)
O(1)-P-C(1)	50.37(8)
O(1)-P-C(8)	107.93(9)
C(1)-P-C(8)	108.23(11)
O(1)-P-Mo	119.01(6)
C(1)-P-Mo	127.92(8)
C(8)-P-Mo	121.54(8)
C(11)-Si(1)-C(9)	110.31(12)
C(11)-Si(1)-C(10)	108.78(14)
C(9)-Si(1)-C(10)	108.25(13)
C(11)-Si(1)-C(8)	113.07(11)
C(9)-Si(1)-C(8)	107.98(10)
C(10)-Si(1)-C(8)	108.32(11)
C(13)-Si(2)-C(14)	109.14(13)
C(13)-Si(2)-C(12)	108.82(12)
C(14)-Si(2)-C(12)	108.15(12)
C(13)-Si(2)-C(8)	108.24(11)
C(14)-Si(2)-C(8)	113.26(10)
C(12)-Si(2)-C(8)	109.15(10)

Table iv.4. Anisotropic displacement parameters ($\text{Å}^2 \times 10^3$) for [30].
 The anisotropic displacement factor exponent takes the form:
 $-2 \pi^2 [h^2 a^{*2} U_{11} + \dots + 2 h k a^* b^* U_{12}]$

	U11	U22	U33	U23	U13	U12
C(1)	23(1)	24(1)	28(2)	-3(1)	-4(1)	-4(1)
C(2)	31(1)	25(1)	22(1)	1(1)	-8(1)	-10(1)
C(3)	37(2)	55(2)	48(2)	-18(2)	1(1)	-20(2)
C(4)	55(2)	75(3)	61(2)	-15(2)	2(2)	-44(2)
C(5)	79(2)	41(2)	47(2)	3(2)	-27(2)	-39(2)
C(6)	65(2)	33(2)	44(2)	-11(2)	-12(2)	-10(2)
C(7)	39(2)	33(2)	32(2)	-7(1)	-5(1)	-12(1)
C(8)	23(1)	18(1)	24(1)	-1(1)	-6(1)	-6(1)
C(9)	34(1)	55(2)	47(2)	12(2)	-4(1)	-25(1)
C(10)	86(2)	48(2)	84(3)	-11(2)	6(2)	-47(2)
C(11)	36(2)	39(2)	50(2)	16(1)	-2(1)	-13(1)
C(12)	30(1)	57(2)	51(2)	4(2)	9(1)	-13(1)
C(13)	43(2)	60(2)	41(2)	-19(2)	-4(1)	-4(2)
C(14)	31(1)	48(2)	38(2)	-4(1)	0(1)	-1(1)
C(15)	33(1)	20(1)	36(2)	2(1)	-5(1)	-6(1)
C(16)	36(1)	22(2)	31(2)	5(1)	-5(1)	-6(1)
C(17)	28(1)	29(2)	30(2)	0(1)	1(1)	-3(1)
C(18)	23(1)	30(2)	34(2)	3(1)	-4(1)	-10(1)
C(19)	26(1)	35(2)	26(2)	-3(1)	1(1)	-15(1)
Mo	23(1)	19(1)	24(1)	0(1)	-3(1)	-6(1)
O(1)	31(1)	34(1)	27(1)	-2(1)	2(1)	-15(1)
O(2)	30(1)	41(1)	77(2)	7(1)	-7(1)	-18(1)
O(3)	64(1)	36(1)	34(1)	-6(1)	0(1)	-1(1)
O(4)	30(1)	55(1)	58(1)	9(1)	-3(1)	-20(1)
O(5)	43(1)	55(1)	35(1)	-15(1)	4(1)	-18(1)
O(6)	42(1)	35(1)	48(1)	14(1)	-5(1)	-7(1)
P	24(1)	21(1)	25(1)	-2(1)	-1(1)	-9(1)
Si(1)	34(1)	29(1)	43(1)	5(1)	-2(1)	-17(1)
Si(2)	25(1)	31(1)	28(1)	-3(1)	-2(1)	-4(1)

Table iv.5. Hydrogen coordinates ($\times 10^4$) and isotropic displacement parameters ($\text{Å}^2 \times 10^3$) for [30].

	x	y	z	U(eq)
H(1A)	8611	4221	8747	31
H(3A)	10598	5465	8479	54
H(4A)	11355	7202	8951	69
H(5A)	9541	8999	9736	61
H(6A)	6946	9047	10066	59
H(7A)	6162	7320	9585	42
H(8A)	6217	3908	6578	26
H(9A)	3251	3962	7466	65
H(9B)	3621	4497	8451	65
H(9C)	3198	3162	8461	65
H(10A)	7222	577	7247	100
H(10B)	5612	1403	6672	100

H(10C)	5509	643	7677	100
H(11A)	6609	2948	9540	64
H(11B)	8031	1746	9066	64
H(11C)	6449	1512	9474	64
H(12A)	9862	4677	6782	71
H(12B)	9219	4645	5727	71
H(12C)	10979	3651	6030	71
H(13A)	8064	2363	5231	77
H(13B)	8646	1033	5914	77
H(13C)	9943	1502	5333	77
H(14A)	10025	957	7812	64
H(14B)	10397	2207	8181	64
H(14C)	11486	1328	7348	64

Table iv.6. Torsion angles [deg] for [30].

O(1)-C(1)-C(2)-C(7)	2.9(3)
P-C(1)-C(2)-C(7)	73.7(3)
O(1)-C(1)-C(2)-C(3)	-177.5(2)
P-C(1)-C(2)-C(3)	-106.7(2)
C(7)-C(2)-C(3)-C(4)	-2.1(4)
C(1)-C(2)-C(3)-C(4)	178.3(3)
C(2)-C(3)-C(4)-C(5)	1.0(5)
C(3)-C(4)-C(5)-C(6)	0.5(5)
C(4)-C(5)-C(6)-C(7)	-0.8(4)
C(3)-C(2)-C(7)-C(6)	1.8(4)
C(1)-C(2)-C(7)-C(6)	-178.6(2)
C(5)-C(6)-C(7)-C(2)	-0.4(4)
O(6)-C(19)-Mo-C(18)	-170(6)
O(6)-C(19)-Mo-C(16)	13(6)
O(6)-C(19)-Mo-C(17)	101(6)
O(6)-C(19)-Mo-C(15)	-80(6)
O(6)-C(19)-Mo-P	-4(8)
O(5)-C(18)-Mo-C(19)	-44(5)
O(5)-C(18)-Mo-C(16)	6(6)
O(5)-C(18)-Mo-C(17)	47(5)
O(5)-C(18)-Mo-C(15)	-135(5)
O(5)-C(18)-Mo-P	136(5)
O(3)-C(16)-Mo-C(19)	42(3)
O(3)-C(16)-Mo-C(18)	-8(4)
O(3)-C(16)-Mo-C(17)	-49(3)
O(3)-C(16)-Mo-C(15)	133(3)
O(3)-C(16)-Mo-P	-138(3)
O(4)-C(17)-Mo-C(19)	77(60)
O(4)-C(17)-Mo-C(18)	-12(60)
O(4)-C(17)-Mo-C(16)	165(100)
O(4)-C(17)-Mo-C(15)	-59(61)
O(4)-C(17)-Mo-P	-104(60)
O(2)-C(15)-Mo-C(19)	-81(6)
O(2)-C(15)-Mo-C(18)	9(6)
O(2)-C(15)-Mo-C(16)	-168(6)
O(2)-C(15)-Mo-C(17)	56(7)
O(2)-C(15)-Mo-P	101(6)
C(2)-C(1)-O(1)-P	115.4(2)
C(1)-O(1)-P-C(8)	99.14(13)
C(1)-O(1)-P-Mo	-116.95(11)
C(2)-C(1)-P-O(1)	-103.5(2)
C(2)-C(1)-P-C(8)	157.97(17)
O(1)-C(1)-P-C(8)	-98.52(12)
C(2)-C(1)-P-Mo	-4.7(2)
O(1)-C(1)-P-Mo	98.81(10)

Si(1)-C(8)-P-O(1)	22.83(14)
Si(2)-C(8)-P-O(1)	-116.36(11)
Si(1)-C(8)-P-C(1)	76.02(13)
Si(2)-C(8)-P-C(1)	-63.17(14)
Si(1)-C(8)-P-Mo	-119.98(10)
Si(2)-C(8)-P-Mo	100.82(11)
C(19)-Mo-P-O(1)	30(3)
C(18)-Mo-P-O(1)	-164.63(9)
C(16)-Mo-P-O(1)	12.11(9)
C(17)-Mo-P-O(1)	-75.71(10)
C(15)-Mo-P-O(1)	105.80(10)
C(19)-Mo-P-C(1)	-31(3)
C(18)-Mo-P-C(1)	134.87(11)
C(16)-Mo-P-C(1)	-48.39(11)
C(17)-Mo-P-C(1)	-136.21(11)
C(15)-Mo-P-C(1)	45.30(11)
C(19)-Mo-P-C(8)	169(3)
C(18)-Mo-P-C(8)	-25.75(10)
C(16)-Mo-P-C(8)	151.00(10)
C(17)-Mo-P-C(8)	63.18(10)
C(15)-Mo-P-C(8)	-115.31(10)
P-C(8)-Si(1)-C(11)	-68.52(15)
Si(2)-C(8)-Si(1)-C(11)	68.93(16)
P-C(8)-Si(1)-C(9)	53.81(16)
Si(2)-C(8)-Si(1)-C(9)	-168.74(14)
P-C(8)-Si(1)-C(10)	170.83(14)
Si(2)-C(8)-Si(1)-C(10)	-51.72(18)
P-C(8)-Si(2)-C(13)	-145.65(13)
Si(1)-C(8)-Si(2)-C(13)	77.25(16)
P-C(8)-Si(2)-C(14)	93.20(15)
Si(1)-C(8)-Si(2)-C(14)	-43.91(18)
P-C(8)-Si(2)-C(12)	-27.34(17)
Si(1)-C(8)-Si(2)-C(12)	-164.45(14)

Table iv.7. Hydrogen bonds for [30] [Å and deg.].

D-H...A	d(D-H)	d(H...A)	d(D...A)	\angle (DHA)
C(11)-H(11A)...O(1)	0.98	2.55	3.184(3)	122.4
C(9)-H(9B)...O(1)	0.98	2.70	3.340(3)	123.3

v.[2-Bis(trimethylsilyl)methyl-3-(2-methylphenyl)-oxaphosphirane-
kP]pentacarbonyltungsten (0) [33]

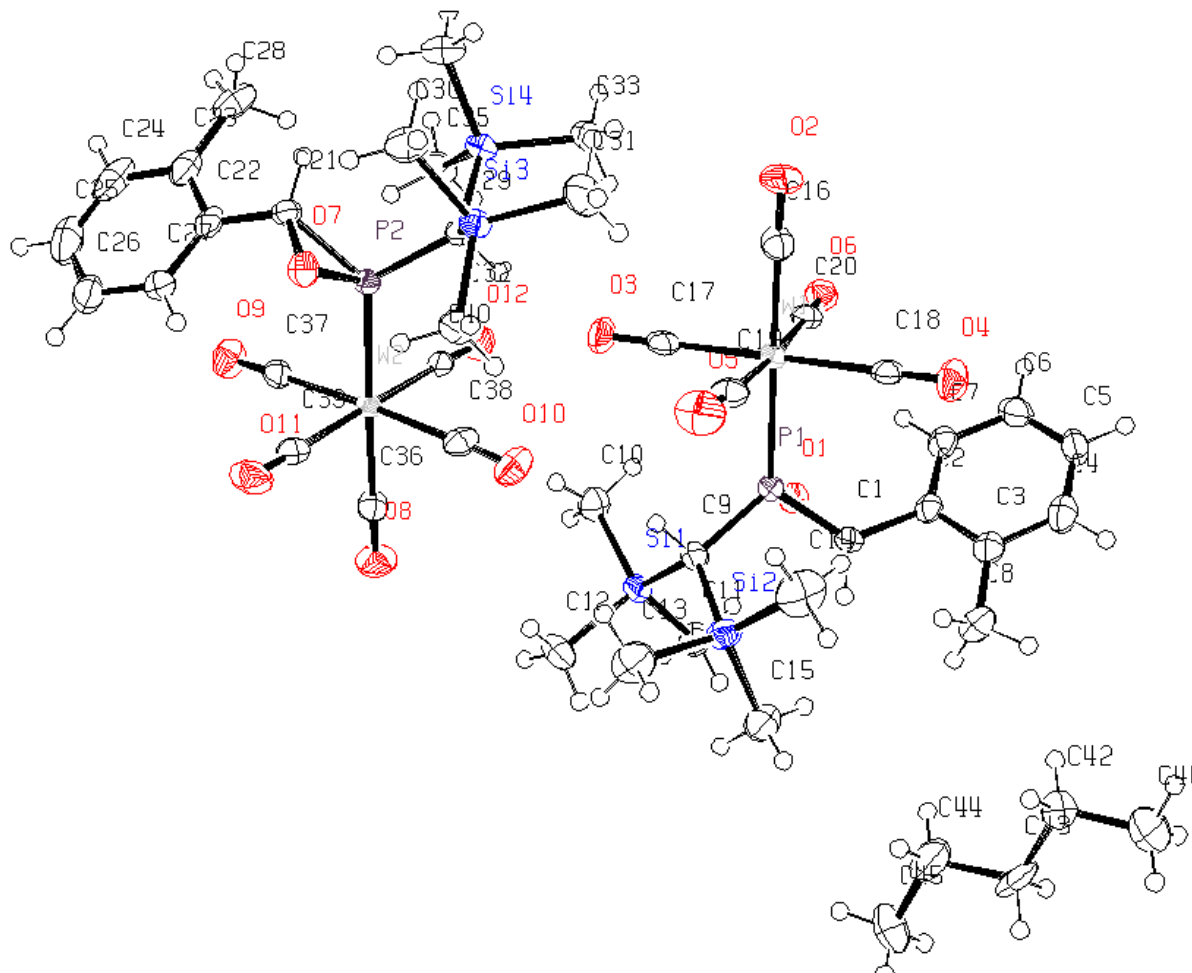


Table v.1. Crystal data and structure refinement for [33].

Identification code	GSTR072, Greg659
Device Type	Nonius KappaCCD
Empirical formula	C ₈₅ H ₁₂₀ O ₂₄ P ₄ Si ₈ W ₄
Formula weight	2609.77
Temperature	123(2) K
Wavelength	0.71073 Å
Crystal system, space group	Triclinic, P -1
Unit cell dimensions 70.7067(18) deg. 80.751(2) deg. 78.910(2) deg.	a = 10.7196(4) Å alpha = b = 15.8421(7) Å beta = c = 16.9897(7) Å gamma =

Volume	2657.58(19) A^3
Z, Calculated density	1, 1.631 Mg/m^3
Absorption coefficient	4.529 mm^-1
F(000)	1290
Crystal size	0.32 x 0.20 x 0.16 mm
Theta range for data collection	2.65 to 28.00 deg.
Limiting indices	-14<=h<=14, -20<=k<=20, -22<=l<=22
Reflections collected / unique	30787 / 12469 [R(int) = 0.0599]
Completeness to theta = 28.00	97.2 %
Absorption correction	Semi-empirical from equivalents
Max. and min. transmission	0.50588 and 0.41709
Refinement method	Full-matrix least-squares on F^2
Data / restraints / parameters	12469 / 4 / 602
Goodness-of-fit on F^2	0.978
Final R indices [I>2sigma(I)]	R1 = 0.0387, wR2 = 0.0743
R indices (all data)	R1 = 0.0694, wR2 = 0.0833
Largest diff. peak and hole	1.400 and -1.692 e.A^-3

Table v.2. Atomic coordinates (x 10^4) and equivalent isotropic displacement parameters (A^2 x 10^3) for [33].

U(eq) is defined as one third of the trace of the orthogonalized Uij tensor.

	x	y	z	U(eq)
C(1)	3488(5)	2181(3)	8078(3)	24(1)
C(2)	4634(5)	2233(4)	8460(3)	26(1)
C(3)	4541(5)	2874(4)	8875(3)	30(1)
C(4)	5653(6)	2927(4)	9187(4)	38(2)
C(5)	6781(6)	2380(5)	9101(4)	41(2)
C(6)	6846(6)	1745(4)	8709(4)	38(2)
C(7)	5768(6)	1666(4)	8390(3)	33(1)
C(8)	3315(6)	3471(4)	9007(4)	41(2)
C(9)	1855(5)	2715(4)	6703(3)	26(1)
C(10)	1799(6)	940(4)	6382(4)	35(1)
C(11)	736(6)	1106(5)	8130(3)	42(2)
C(12)	-672(5)	2144(5)	6602(4)	44(2)
C(13)	-177(7)	4366(5)	6148(4)	51(2)
C(14)	2141(7)	4574(4)	6824(5)	56(2)
C(15)	100(6)	3518(5)	8004(4)	47(2)
C(16)	6815(6)	3027(4)	4995(4)	34(1)
C(17)	4595(5)	2119(4)	5224(3)	33(1)
C(18)	5975(5)	3406(4)	6546(3)	28(1)
C(19)	4266(6)	3939(4)	5229(4)	34(1)

C(20)	6323(5)	1547(4)	6435(3)	26(1)
C(21)	3085(5)	2328(4)	1355(3)	26(1)
C(22)	2319(5)	1896(4)	990(3)	29(1)
C(23)	2916(6)	1183(4)	686(3)	38(2)
C(24)	2156(8)	800(5)	335(4)	53(2)
C(25)	869(8)	1111(6)	295(4)	60(2)
C(26)	290(7)	1821(5)	587(4)	51(2)
C(27)	1019(5)	2213(5)	929(3)	38(2)
C(28)	4309(6)	837(4)	721(4)	47(2)
C(29)	4263(5)	2593(3)	2685(3)	21(1)
C(30)	4789(6)	4233(4)	1089(4)	41(2)
C(31)	5619(6)	4109(4)	2748(4)	46(2)
C(32)	2819(5)	4508(4)	2530(4)	35(1)
C(33)	6838(5)	1679(4)	3384(4)	37(1)
C(34)	6678(6)	2022(4)	1547(4)	43(2)
C(35)	5243(5)	598(4)	2862(4)	35(1)
C(36)	-222(5)	1290(4)	4467(3)	30(1)
C(37)	836(5)	868(4)	2947(3)	29(1)
C(38)	1421(5)	2604(4)	4132(3)	31(1)
C(39)	-144(5)	2728(4)	2870(4)	31(1)
C(40)	2450(5)	746(4)	4213(3)	24(1)
C(41)	1814(16)	5968(13)	10282(11)	59(5)
C(42)	1357(16)	5514(15)	9745(11)	49(4)
C(43)	88(16)	5150(13)	10138(9)	52(6)
C(44)	-380(20)	4687(18)	9617(13)	57(5)
C(45)	-1650(18)	4359(17)	10006(14)	70(7)
O(1)	3657(3)	1425(2)	7717(2)	28(1)
O(2)	7679(4)	3170(3)	4515(3)	43(1)
O(3)	4199(4)	1755(3)	4852(2)	46(1)
O(4)	6367(4)	3766(3)	6916(3)	42(1)
O(5)	3685(5)	4589(3)	4837(3)	56(1)
O(6)	6881(4)	852(3)	6729(2)	34(1)
O(7)	2403(4)	3150(2)	1556(2)	31(1)
O(8)	-979(4)	1037(3)	5000(3)	46(1)
O(9)	636(4)	382(3)	2640(3)	43(1)
O(10)	1515(4)	3081(3)	4498(2)	42(1)
O(11)	-855(4)	3298(3)	2503(3)	47(1)
O(12)	3139(4)	182(3)	4606(2)	36(1)
P(2)	2831(1)	2336(1)	2430(1)	22(1)
P(1)	3493(1)	2417(1)	6963(1)	23(1)
Si(1)	938(1)	1718(1)	6977(1)	28(1)
Si(2)	981(2)	3781(1)	6936(1)	33(1)
Si(3)	4370(1)	3860(1)	2245(1)	26(1)
Si(4)	5748(1)	1738(1)	2606(1)	27(1)
W(1)	5291(1)	2765(1)	5869(1)	24(1)
W(2)	1157(1)	1743(1)	3535(1)	22(1)

Table v.3. Bond lengths [Å] and angles [deg] for [33].

C(1)-O(1)	1.486(6)
C(1)-C(2)	1.505(7)
C(1)-P(1)	1.805(5)
C(1)-H(1A)	1.0000
C(2)-C(7)	1.380(8)
C(2)-C(3)	1.397(7)
C(3)-C(4)	1.407(7)
C(3)-C(8)	1.497(8)
C(4)-C(5)	1.364(9)
C(4)-H(4A)	0.9500
C(5)-C(6)	1.363(8)
C(5)-H(5A)	0.9500

C(6)-C(7)	1.396(7)
C(6)-H(6A)	0.9500
C(7)-H(7A)	0.9500
C(8)-H(8A)	0.9800
C(8)-H(8B)	0.9800
C(8)-H(8C)	0.9800
C(9)-P(1)	1.815(5)
C(9)-Si(2)	1.897(6)
C(9)-Si(1)	1.909(5)
C(9)-H(9A)	1.0000
C(10)-Si(1)	1.864(6)
C(10)-H(10A)	0.9800
C(10)-H(10B)	0.9800
C(10)-H(10C)	0.9800
C(11)-Si(1)	1.874(6)
C(11)-H(11A)	0.9800
C(11)-H(11B)	0.9800
C(11)-H(11C)	0.9800
C(12)-Si(1)	1.861(6)
C(12)-H(12A)	0.9800
C(12)-H(12B)	0.9800
C(12)-H(12C)	0.9800
C(13)-Si(2)	1.861(6)
C(13)-H(13A)	0.9800
C(13)-H(13B)	0.9800
C(13)-H(13C)	0.9800
C(14)-Si(2)	1.879(6)
C(14)-H(14A)	0.9800
C(14)-H(14B)	0.9800
C(14)-H(14C)	0.9800
C(15)-Si(2)	1.860(6)
C(15)-H(15C)	0.9800
C(15)-H(15B)	0.9800
C(15)-H(15A)	0.9800
C(16)-O(2)	1.135(7)
C(16)-W(1)	2.030(6)
C(17)-O(3)	1.156(6)
C(17)-W(1)	2.025(6)
C(18)-O(4)	1.146(6)
C(18)-W(1)	2.054(5)
C(19)-O(5)	1.151(7)
C(19)-W(1)	2.028(7)
C(20)-O(6)	1.140(6)
C(20)-W(1)	2.040(6)
C(21)-C(22)	1.480(7)
C(21)-O(7)	1.482(6)
C(21)-P(2)	1.807(5)
C(21)-H(21A)	1.0000
C(22)-C(27)	1.395(8)
C(22)-C(23)	1.396(8)
C(23)-C(24)	1.404(8)
C(23)-C(28)	1.492(9)
C(24)-C(25)	1.378(11)
C(24)-H(24A)	0.9500
C(25)-C(26)	1.377(11)
C(25)-H(25A)	0.9500
C(26)-C(27)	1.382(8)
C(26)-H(26A)	0.9500
C(27)-H(27A)	0.9500
C(28)-H(28A)	0.9800
C(28)-H(28B)	0.9800
C(28)-H(28C)	0.9800
C(29)-P(2)	1.810(5)

C(29)-Si(4)	1.899(5)
C(29)-Si(3)	1.916(5)
C(29)-H(29A)	1.0000
C(30)-Si(3)	1.860(6)
C(30)-H(30A)	0.9800
C(30)-H(30B)	0.9800
C(30)-H(30C)	0.9800
C(31)-Si(3)	1.863(5)
C(31)-H(31A)	0.9800
C(31)-H(31B)	0.9800
C(31)-H(31C)	0.9800
C(32)-Si(3)	1.863(6)
C(32)-H(32A)	0.9800
C(32)-H(32B)	0.9800
C(32)-H(32C)	0.9800
C(33)-Si(4)	1.869(5)
C(33)-H(33A)	0.9800
C(33)-H(33B)	0.9800
C(33)-H(33C)	0.9800
C(34)-Si(4)	1.870(6)
C(34)-H(34A)	0.9800
C(34)-H(34B)	0.9800
C(34)-H(34C)	0.9800
C(35)-Si(4)	1.878(6)
C(35)-H(35A)	0.9800
C(35)-H(35B)	0.9800
C(35)-H(35C)	0.9800
C(36)-O(8)	1.134(6)
C(36)-W(2)	2.028(6)
C(37)-O(9)	1.129(6)
C(37)-W(2)	2.061(5)
C(38)-O(10)	1.152(6)
C(38)-W(2)	2.032(6)
C(39)-O(11)	1.140(7)
C(39)-W(2)	2.041(7)
C(40)-O(12)	1.141(6)
C(40)-W(2)	2.052(6)
C(41)-C(42)	1.518(14)
C(41)-H(41A)	0.9800
C(41)-H(41B)	0.9800
C(41)-H(41C)	0.9800
C(42)-C(43)	1.543(16)
C(42)-H(42A)	0.9900
C(42)-H(42B)	0.9900
C(43)-C(44)	1.511(14)
C(43)-H(43A)	0.9900
C(43)-H(43B)	0.9900
C(44)-C(45)	1.524(17)
C(44)-H(44A)	0.9900
C(44)-H(44B)	0.9900
C(45)-H(45A)	0.9800
C(45)-H(45B)	0.9800
C(45)-H(45C)	0.9800
O(1)-P(1)	1.667(4)
O(7)-P(2)	1.675(4)
P(2)-W(2)	2.4551(13)
P(1)-W(1)	2.4597(14)
O(1)-C(1)-C(2)	114.6(4)
O(1)-C(1)-P(1)	59.9(2)
C(2)-C(1)-P(1)	122.2(4)
O(1)-C(1)-H(1A)	116.0
C(2)-C(1)-H(1A)	116.0

P(1)-C(1)-H(1A)	116.0
C(7)-C(2)-C(3)	120.3(5)
C(7)-C(2)-C(1)	120.6(5)
C(3)-C(2)-C(1)	119.1(5)
C(2)-C(3)-C(4)	117.1(6)
C(2)-C(3)-C(8)	122.3(5)
C(4)-C(3)-C(8)	120.5(5)
C(5)-C(4)-C(3)	122.5(5)
C(5)-C(4)-H(4A)	118.8
C(3)-C(4)-H(4A)	118.8
C(6)-C(5)-C(4)	119.5(5)
C(6)-C(5)-H(5A)	120.2
C(4)-C(5)-H(5A)	120.2
C(5)-C(6)-C(7)	120.1(6)
C(5)-C(6)-H(6A)	119.9
C(7)-C(6)-H(6A)	119.9
C(2)-C(7)-C(6)	120.4(5)
C(2)-C(7)-H(7A)	119.8
C(6)-C(7)-H(7A)	119.8
C(3)-C(8)-H(8A)	109.5
C(3)-C(8)-H(8B)	109.5
H(8A)-C(8)-H(8B)	109.5
C(3)-C(8)-H(8C)	109.5
H(8A)-C(8)-H(8C)	109.5
H(8B)-C(8)-H(8C)	109.5
P(1)-C(9)-Si(2)	113.7(2)
P(1)-C(9)-Si(1)	114.9(3)
Si(2)-C(9)-Si(1)	117.6(3)
P(1)-C(9)-H(9A)	102.6
Si(2)-C(9)-H(9A)	102.6
Si(1)-C(9)-H(9A)	102.6
Si(1)-C(10)-H(10A)	109.5
Si(1)-C(10)-H(10B)	109.5
H(10A)-C(10)-H(10B)	109.5
Si(1)-C(10)-H(10C)	109.5
H(10A)-C(10)-H(10C)	109.5
H(10B)-C(10)-H(10C)	109.5
Si(1)-C(11)-H(11A)	109.5
Si(1)-C(11)-H(11B)	109.5
H(11A)-C(11)-H(11B)	109.5
Si(1)-C(11)-H(11C)	109.5
H(11A)-C(11)-H(11C)	109.5
H(11B)-C(11)-H(11C)	109.5
Si(1)-C(12)-H(12A)	109.5
Si(1)-C(12)-H(12B)	109.5
H(12A)-C(12)-H(12B)	109.5
Si(1)-C(12)-H(12C)	109.5
H(12A)-C(12)-H(12C)	109.5
H(12B)-C(12)-H(12C)	109.5
Si(2)-C(13)-H(13A)	109.5
Si(2)-C(13)-H(13B)	109.5
H(13A)-C(13)-H(13B)	109.5
Si(2)-C(13)-H(13C)	109.5
H(13A)-C(13)-H(13C)	109.5
H(13B)-C(13)-H(13C)	109.5
Si(2)-C(14)-H(14A)	109.5
Si(2)-C(14)-H(14B)	109.5
H(14A)-C(14)-H(14B)	109.5
Si(2)-C(14)-H(14C)	109.5
H(14A)-C(14)-H(14C)	109.5
H(14B)-C(14)-H(14C)	109.5
Si(2)-C(15)-H(15C)	109.5
Si(2)-C(15)-H(15B)	109.5

H(15C)-C(15)-H(15B)	109.5
Si(2)-C(15)-H(15A)	109.5
H(15C)-C(15)-H(15A)	109.5
H(15B)-C(15)-H(15A)	109.5
O(2)-C(16)-W(1)	179.0(5)
O(3)-C(17)-W(1)	179.6(5)
O(4)-C(18)-W(1)	179.2(5)
O(5)-C(19)-W(1)	176.8(5)
O(6)-C(20)-W(1)	177.1(4)
C(22)-C(21)-O(7)	115.1(4)
C(22)-C(21)-P(2)	124.5(4)
O(7)-C(21)-P(2)	60.3(2)
C(22)-C(21)-H(21A)	115.1
O(7)-C(21)-H(21A)	115.1
P(2)-C(21)-H(21A)	115.1
C(27)-C(22)-C(23)	120.4(5)
C(27)-C(22)-C(21)	120.2(5)
C(23)-C(22)-C(21)	119.4(5)
C(22)-C(23)-C(24)	117.5(6)
C(22)-C(23)-C(28)	122.0(5)
C(24)-C(23)-C(28)	120.5(6)
C(25)-C(24)-C(23)	121.4(7)
C(25)-C(24)-H(24A)	119.3
C(23)-C(24)-H(24A)	119.3
C(24)-C(25)-C(26)	120.7(6)
C(24)-C(25)-H(25A)	119.6
C(26)-C(25)-H(25A)	119.6
C(25)-C(26)-C(27)	118.9(7)
C(25)-C(26)-H(26A)	120.5
C(27)-C(26)-H(26A)	120.5
C(26)-C(27)-C(22)	121.0(6)
C(26)-C(27)-H(27A)	119.5
C(22)-C(27)-H(27A)	119.5
C(23)-C(28)-H(28A)	109.5
C(23)-C(28)-H(28B)	109.5
H(28A)-C(28)-H(28B)	109.5
C(23)-C(28)-H(28C)	109.5
H(28A)-C(28)-H(28C)	109.5
H(28B)-C(28)-H(28C)	109.5
P(2)-C(29)-Si(4)	114.5(3)
P(2)-C(29)-Si(3)	111.7(3)
Si(4)-C(29)-Si(3)	119.6(2)
P(2)-C(29)-H(29A)	102.7
Si(4)-C(29)-H(29A)	102.7
Si(3)-C(29)-H(29A)	102.7
Si(3)-C(30)-H(30A)	109.5
Si(3)-C(30)-H(30B)	109.5
H(30A)-C(30)-H(30B)	109.5
Si(3)-C(30)-H(30C)	109.5
H(30A)-C(30)-H(30C)	109.5
H(30B)-C(30)-H(30C)	109.5
Si(3)-C(31)-H(31A)	109.5
Si(3)-C(31)-H(31B)	109.5
H(31A)-C(31)-H(31B)	109.5
Si(3)-C(31)-H(31C)	109.5
H(31A)-C(31)-H(31C)	109.5
H(31B)-C(31)-H(31C)	109.5
Si(3)-C(32)-H(32A)	109.5
Si(3)-C(32)-H(32B)	109.5
H(32A)-C(32)-H(32B)	109.5
Si(3)-C(32)-H(32C)	109.5
H(32A)-C(32)-H(32C)	109.5
H(32B)-C(32)-H(32C)	109.5

Si(4)-C(33)-H(33A)	109.5
Si(4)-C(33)-H(33B)	109.5
H(33A)-C(33)-H(33B)	109.5
Si(4)-C(33)-H(33C)	109.5
H(33A)-C(33)-H(33C)	109.5
Si(4)-C(34)-H(34A)	109.5
Si(4)-C(34)-H(34B)	109.5
H(34A)-C(34)-H(34B)	109.5
Si(4)-C(34)-H(34C)	109.5
H(34A)-C(34)-H(34C)	109.5
H(34B)-C(34)-H(34C)	109.5
Si(4)-C(35)-H(35A)	109.5
Si(4)-C(35)-H(35B)	109.5
H(35A)-C(35)-H(35B)	109.5
Si(4)-C(35)-H(35C)	109.5
H(35A)-C(35)-H(35C)	109.5
H(35B)-C(35)-H(35C)	109.5
O(8)-C(36)-W(2)	178.7(5)
O(9)-C(37)-W(2)	178.2(5)
O(10)-C(38)-W(2)	176.4(5)
O(11)-C(39)-W(2)	177.9(5)
O(12)-C(40)-W(2)	177.9(5)
C(41)-C(42)-C(43)	112.0(13)
C(41)-C(42)-H(42A)	109.2
C(43)-C(42)-H(42A)	109.2
C(41)-C(42)-H(42B)	109.2
C(43)-C(42)-H(42B)	109.2
H(42A)-C(42)-H(42B)	107.9
C(44)-C(43)-C(42)	112.8(12)
C(44)-C(43)-H(43A)	109.0
C(42)-C(43)-H(43A)	109.0
C(44)-C(43)-H(43B)	109.0
C(42)-C(43)-H(43B)	109.0
H(43A)-C(43)-H(43B)	107.8
C(43)-C(44)-C(45)	111.7(14)
C(43)-C(44)-H(44A)	109.3
C(45)-C(44)-H(44A)	109.3
C(43)-C(44)-H(44B)	109.3
C(45)-C(44)-H(44B)	109.3
H(44A)-C(44)-H(44B)	107.9
C(1)-O(1)-P(1)	69.6(3)
C(21)-O(7)-P(2)	69.5(3)
O(7)-P(2)-C(21)	50.2(2)
O(7)-P(2)-C(29)	107.1(2)
C(21)-P(2)-C(29)	108.5(2)
O(7)-P(2)-W(2)	118.93(15)
C(21)-P(2)-W(2)	128.83(16)
C(29)-P(2)-W(2)	120.97(17)
O(1)-P(1)-C(1)	50.5(2)
O(1)-P(1)-C(9)	109.6(2)
C(1)-P(1)-C(9)	108.9(2)
O(1)-P(1)-W(1)	118.10(15)
C(1)-P(1)-W(1)	127.68(17)
C(9)-P(1)-W(1)	120.96(19)
C(12)-Si(1)-C(10)	107.3(3)
C(12)-Si(1)-C(11)	108.6(3)
C(10)-Si(1)-C(11)	111.0(3)
C(12)-Si(1)-C(9)	108.7(3)
C(10)-Si(1)-C(9)	107.8(3)
C(11)-Si(1)-C(9)	113.2(2)
C(15)-Si(2)-C(13)	109.1(3)
C(15)-Si(2)-C(14)	110.1(3)

C(13)-Si(2)-C(14)	107.4(3)
C(15)-Si(2)-C(9)	111.5(3)
C(13)-Si(2)-C(9)	108.6(3)
C(14)-Si(2)-C(9)	110.1(3)
C(30)-Si(3)-C(32)	110.4(3)
C(30)-Si(3)-C(31)	108.7(3)
C(32)-Si(3)-C(31)	107.4(3)
C(30)-Si(3)-C(29)	112.3(3)
C(32)-Si(3)-C(29)	109.1(2)
C(31)-Si(3)-C(29)	108.9(3)
C(33)-Si(4)-C(34)	107.4(3)
C(33)-Si(4)-C(35)	108.6(3)
C(34)-Si(4)-C(35)	109.3(3)
C(33)-Si(4)-C(29)	109.8(2)
C(34)-Si(4)-C(29)	113.2(3)
C(35)-Si(4)-C(29)	108.3(2)
C(17)-W(1)-C(19)	89.0(2)
C(17)-W(1)-C(16)	92.2(2)
C(19)-W(1)-C(16)	89.9(2)
C(17)-W(1)-C(20)	87.0(2)
C(19)-W(1)-C(20)	175.5(2)
C(16)-W(1)-C(20)	88.2(2)
C(17)-W(1)-C(18)	178.8(2)
C(19)-W(1)-C(18)	91.5(2)
C(16)-W(1)-C(18)	89.0(2)
C(20)-W(1)-C(18)	92.6(2)
C(17)-W(1)-P(1)	88.71(15)
C(19)-W(1)-P(1)	91.77(16)
C(16)-W(1)-P(1)	178.09(17)
C(20)-W(1)-P(1)	90.14(15)
C(18)-W(1)-P(1)	90.15(15)
C(36)-W(2)-C(38)	88.8(2)
C(36)-W(2)-C(39)	91.4(2)
C(38)-W(2)-C(39)	89.4(2)
C(36)-W(2)-C(40)	88.0(2)
C(38)-W(2)-C(40)	90.7(2)
C(39)-W(2)-C(40)	179.4(2)
C(36)-W(2)-C(37)	89.7(2)
C(38)-W(2)-C(37)	178.4(2)
C(39)-W(2)-C(37)	90.0(2)
C(40)-W(2)-C(37)	90.0(2)
C(36)-W(2)-P(2)	177.76(15)
C(38)-W(2)-P(2)	89.02(15)
C(39)-W(2)-P(2)	88.30(15)
C(40)-W(2)-P(2)	92.29(14)
C(37)-W(2)-P(2)	92.48(15)

Table v.4. Anisotropic displacement parameters ($\text{Å}^2 \times 10^3$) for [33]
The anisotropic displacement factor exponent takes the form:
 $-2 \pi^2 [h^2 a^*{}^2 U_{11} + \dots + 2 h k a^* b^* U_{12}]$

	U11	U22	U33	U23	U13	U12
C(1)	20(3)	23(3)	29(3)	-9(2)	1(2)	-4(2)
C(2)	31(3)	29(3)	17(3)	-4(2)	-1(2)	-9(3)
C(3)	34(3)	31(3)	24(3)	-5(3)	0(3)	-10(3)
C(4)	48(4)	41(4)	32(3)	-11(3)	-4(3)	-18(3)

C(5)	35(4)	60(5)	34(3)	-16(3)	-7(3)	-19(3)
C(6)	28(3)	52(4)	29(3)	-7(3)	-2(3)	-4(3)
C(7)	37(3)	44(4)	19(3)	-6(3)	-2(3)	-13(3)
C(8)	50(4)	40(4)	36(4)	-19(3)	-2(3)	-3(3)
C(9)	24(3)	28(3)	29(3)	-11(3)	-3(2)	-5(2)
C(10)	38(3)	31(3)	38(3)	-13(3)	-6(3)	-6(3)
C(11)	41(4)	59(4)	28(3)	-12(3)	2(3)	-23(3)
C(12)	26(3)	55(4)	54(4)	-20(4)	-8(3)	-7(3)
C(13)	58(5)	44(4)	44(4)	-11(3)	-12(4)	15(4)
C(14)	75(5)	23(4)	70(5)	-19(4)	0(4)	-7(4)
C(15)	48(4)	56(5)	40(4)	-21(3)	-6(3)	-1(4)
C(16)	34(3)	34(4)	32(3)	-6(3)	-5(3)	-9(3)
C(17)	22(3)	49(4)	25(3)	-7(3)	7(2)	-12(3)
C(18)	23(3)	33(3)	29(3)	-11(3)	7(2)	-9(3)
C(19)	31(3)	35(4)	31(3)	-5(3)	5(3)	-6(3)
C(20)	21(3)	26(3)	32(3)	-12(3)	5(2)	-7(3)
C(21)	23(3)	30(3)	27(3)	-14(3)	3(2)	-6(3)
C(22)	37(3)	34(3)	16(3)	-3(2)	1(2)	-14(3)
C(23)	50(4)	43(4)	23(3)	-11(3)	1(3)	-16(3)
C(24)	90(6)	51(5)	26(3)	-15(3)	8(4)	-34(4)
C(25)	77(6)	83(6)	35(4)	-15(4)	-7(4)	-50(5)
C(26)	45(4)	85(6)	31(3)	-18(4)	0(3)	-31(4)
C(27)	30(3)	59(4)	30(3)	-20(3)	3(3)	-14(3)
C(28)	67(5)	41(4)	37(4)	-22(3)	9(3)	-9(4)
C(29)	19(3)	26(3)	19(3)	-5(2)	0(2)	-6(2)
C(30)	44(4)	37(4)	35(3)	-4(3)	7(3)	-11(3)
C(31)	44(4)	39(4)	62(5)	-22(4)	-3(3)	-15(3)
C(32)	32(3)	28(3)	46(4)	-17(3)	-1(3)	-3(3)
C(33)	24(3)	42(4)	42(4)	-11(3)	-4(3)	0(3)
C(34)	35(4)	44(4)	45(4)	-15(3)	12(3)	-2(3)
C(35)	29(3)	29(3)	47(4)	-14(3)	-6(3)	1(3)
C(36)	31(3)	28(3)	29(3)	-6(3)	-2(3)	-10(3)
C(37)	25(3)	36(3)	26(3)	-6(3)	0(2)	-12(3)
C(38)	35(3)	31(3)	25(3)	-5(3)	8(3)	-12(3)
C(39)	25(3)	38(4)	27(3)	-10(3)	4(3)	-6(3)
C(40)	22(3)	31(3)	22(3)	-11(3)	2(2)	-9(3)
C(41)	47(10)	68(12)	67(12)	-24(9)	-3(8)	-22(9)
C(42)	39(11)	67(13)	46(10)	-26(8)	-8(8)	-4(9)
C(43)	69(14)	61(18)	31(16)	-32(9)	5(12)	2(11)
C(44)	72(13)	66(13)	41(13)	-29(10)	-5(10)	-4(10)
C(45)	47(11)	94(16)	90(20)	-44(14)	-11(12)	-33(10)
O(1)	31(2)	23(2)	30(2)	-8(2)	-3(2)	-5(2)
O(2)	35(2)	52(3)	38(2)	-9(2)	13(2)	-18(2)
O(3)	45(3)	75(3)	34(2)	-27(2)	4(2)	-33(2)
O(4)	54(3)	40(3)	40(2)	-17(2)	-6(2)	-20(2)
O(5)	56(3)	46(3)	49(3)	4(2)	-7(3)	1(3)
O(6)	30(2)	33(3)	40(2)	-15(2)	-3(2)	-2(2)
O(7)	34(2)	27(2)	30(2)	-6(2)	-8(2)	-4(2)
O(8)	44(3)	50(3)	39(3)	-9(2)	12(2)	-21(2)
O(9)	53(3)	41(3)	42(3)	-15(2)	-5(2)	-22(2)
O(10)	59(3)	38(3)	34(2)	-18(2)	3(2)	-13(2)
O(11)	32(3)	53(3)	43(3)	-4(2)	-5(2)	11(2)
O(12)	40(3)	34(3)	34(2)	-11(2)	-9(2)	2(2)
P(2)	20(1)	26(1)	21(1)	-8(1)	1(1)	-6(1)
P(1)	21(1)	27(1)	22(1)	-9(1)	-1(1)	-5(1)
Si(1)	22(1)	35(1)	27(1)	-10(1)	-1(1)	-8(1)
Si(2)	34(1)	32(1)	31(1)	-12(1)	-1(1)	3(1)
Si(3)	25(1)	24(1)	30(1)	-8(1)	0(1)	-7(1)
Si(4)	21(1)	28(1)	30(1)	-8(1)	1(1)	-5(1)
W(1)	20(1)	29(1)	23(1)	-9(1)	1(1)	-7(1)
W(2)	19(1)	25(1)	23(1)	-8(1)	2(1)	-6(1)

Table v.5. Hydrogen coordinates ($\times 10^4$) and isotropic displacement parameters ($\text{\AA}^2 \times 10^3$) for [33].

	x	y	z	U(eq)
H(1A)	2637	2301	8394	29
H(4A)	5616	3360	9469	46
H(5A)	7517	2440	9312	49
H(6A)	7627	1357	8654	46
H(7A)	5816	1218	8123	40
H(8A)	2647	3097	9292	61
H(8B)	3060	3875	8463	61
H(8C)	3434	3832	9352	61
H(9A)	1966	2911	6076	31
H(10A)	2695	777	6499	52
H(10B)	1756	1243	5780	52
H(10C)	1397	392	6555	52
H(11A)	314	1533	8430	62
H(11B)	1576	835	8327	62
H(11C)	211	629	8235	62
H(12A)	-585	2534	6019	66
H(12B)	-1193	2490	6954	66
H(12C)	-1087	1631	6637	66
H(13A)	-928	4056	6291	77
H(13B)	229	4358	5590	77
H(13C)	-441	4994	6147	77
H(14A)	2391	4862	6228	84
H(14B)	2901	4234	7100	84
H(14C)	1737	5039	7086	84
H(15C)	-256	4082	8131	71
H(15B)	687	3146	8417	71
H(15A)	-596	3186	8028	71
H(21A)	3981	2369	1083	31
H(24A)	2537	317	122	64
H(25A)	375	832	63	73
H(26A)	-597	2037	553	61
H(27A)	630	2707	1127	45
H(28A)	4531	733	1287	71
H(28B)	4803	1283	315	71
H(28C)	4507	268	585	71
H(29A)	4085	2493	3302	26
H(30A)	4129	4117	816	61
H(30B)	5615	3896	949	61
H(30C)	4842	4881	893	61
H(31A)	6463	3836	2555	69
H(31B)	5461	3856	3358	69
H(31C)	5589	4765	2594	69
H(32A)	2611	4307	3140	52
H(32B)	2143	4405	2262	52
H(32C)	2885	5155	2339	52
H(33A)	6405	1475	3952	55
H(33B)	7067	2280	3279	55
H(33C)	7615	1252	3328	55
H(34A)	7082	2556	1457	65
H(34B)	6101	2149	1115	65
H(34C)	7339	1510	1512	65
H(35A)	4426	668	2641	53
H(35B)	5144	317	3472	53
H(35C)	5894	212	2608	53
H(41A)	1147	6454	10373	88

H(41B)	2591	6221	9996	88
H(41C)	2000	5521	10823	88
H(42A)	2018	5007	9674	58
H(42B)	1237	5954	9183	58
H(43A)	208	4715	10703	62
H(43B)	-573	5659	10205	62
H(44A)	267	4165	9563	69
H(44B)	-479	5115	9047	69
H(45A)	-1585	4000	10595	105
H(45B)	-1859	3984	9702	105
H(45C)	-2324	4880	9972	105

Table v.6. Torsion angles [deg] for [33].

O(1)-C(1)-C(2)-C(7)	6.1(7)
P(1)-C(1)-C(2)-C(7)	-62.6(7)
O(1)-C(1)-C(2)-C(3)	-175.0(4)
P(1)-C(1)-C(2)-C(3)	116.3(5)
C(7)-C(2)-C(3)-C(4)	1.9(8)
C(1)-C(2)-C(3)-C(4)	-177.1(5)
C(7)-C(2)-C(3)-C(8)	-176.7(5)
C(1)-C(2)-C(3)-C(8)	4.4(8)
C(2)-C(3)-C(4)-C(5)	-0.4(9)
C(8)-C(3)-C(4)-C(5)	178.2(6)
C(3)-C(4)-C(5)-C(6)	-0.9(9)
C(4)-C(5)-C(6)-C(7)	0.8(9)
C(3)-C(2)-C(7)-C(6)	-2.1(8)
C(1)-C(2)-C(7)-C(6)	176.9(5)
C(5)-C(6)-C(7)-C(2)	0.7(9)
O(7)-C(21)-C(22)-C(27)	-6.0(7)
P(2)-C(21)-C(22)-C(27)	64.0(7)
O(7)-C(21)-C(22)-C(23)	172.3(5)
P(2)-C(21)-C(22)-C(23)	-117.7(5)
C(27)-C(22)-C(23)-C(24)	-1.0(8)
C(21)-C(22)-C(23)-C(24)	-179.3(5)
C(27)-C(22)-C(23)-C(28)	178.6(6)
C(21)-C(22)-C(23)-C(28)	0.4(8)
C(22)-C(23)-C(24)-C(25)	-0.3(9)
C(28)-C(23)-C(24)-C(25)	-179.9(6)
C(23)-C(24)-C(25)-C(26)	1.0(10)
C(24)-C(25)-C(26)-C(27)	-0.6(10)
C(25)-C(26)-C(27)-C(22)	-0.6(10)
C(23)-C(22)-C(27)-C(26)	1.4(9)
C(21)-C(22)-C(27)-C(26)	179.7(5)
C(41)-C(42)-C(43)-C(44)	-179.5(18)
C(42)-C(43)-C(44)-C(45)	-178(2)
C(2)-C(1)-O(1)-P(1)	-114.3(4)
C(22)-C(21)-O(7)-P(2)	116.9(4)
C(21)-O(7)-P(2)-C(29)	100.1(3)
C(21)-O(7)-P(2)-W(2)	-118.2(2)
C(22)-C(21)-P(2)-O(7)	-101.5(5)
C(22)-C(21)-P(2)-C(29)	161.3(5)
O(7)-C(21)-P(2)-C(29)	-97.1(3)
C(22)-C(21)-P(2)-W(2)	-3.6(6)
O(7)-C(21)-P(2)-W(2)	97.9(2)
Si(4)-C(29)-P(2)-O(7)	-114.3(3)
Si(3)-C(29)-P(2)-O(7)	25.6(3)
Si(4)-C(29)-P(2)-C(21)	-61.4(3)
Si(3)-C(29)-P(2)-C(21)	78.5(3)
Si(4)-C(29)-P(2)-W(2)	104.9(2)
Si(3)-C(29)-P(2)-W(2)	-115.1(2)

C(1)-O(1)-P(1)-C(9)	-98.7(3)
C(1)-O(1)-P(1)-W(1)	117.2(2)
C(2)-C(1)-P(1)-O(1)	101.7(5)
O(1)-C(1)-P(1)-C(9)	100.2(3)
C(2)-C(1)-P(1)-C(9)	-158.1(4)
O(1)-C(1)-P(1)-W(1)	-97.7(2)
C(2)-C(1)-P(1)-W(1)	4.0(5)
Si(2)-C(9)-P(1)-O(1)	116.5(3)
Si(1)-C(9)-P(1)-O(1)	-23.1(4)
Si(2)-C(9)-P(1)-C(1)	62.8(3)
Si(1)-C(9)-P(1)-C(1)	-76.8(3)
Si(2)-C(9)-P(1)-W(1)	-100.7(3)
Si(1)-C(9)-P(1)-W(1)	119.7(2)
P(1)-C(9)-Si(1)-C(12)	-176.2(3)
Si(2)-C(9)-Si(1)-C(12)	45.8(4)
P(1)-C(9)-Si(1)-C(10)	-60.2(4)
Si(2)-C(9)-Si(1)-C(10)	161.8(3)
P(1)-C(9)-Si(1)-C(11)	63.0(4)
Si(2)-C(9)-Si(1)-C(11)	-75.0(4)
P(1)-C(9)-Si(2)-C(15)	-92.3(3)
Si(1)-C(9)-Si(2)-C(15)	46.1(4)
P(1)-C(9)-Si(2)-C(13)	147.5(3)
Si(1)-C(9)-Si(2)-C(13)	-74.1(4)
P(1)-C(9)-Si(2)-C(14)	30.1(4)
Si(1)-C(9)-Si(2)-C(14)	168.6(3)
P(2)-C(29)-Si(3)-C(30)	-73.6(3)
Si(4)-C(29)-Si(3)-C(30)	64.1(4)
P(2)-C(29)-Si(3)-C(32)	49.0(3)
Si(4)-C(29)-Si(3)-C(32)	-173.3(3)
P(2)-C(29)-Si(3)-C(31)	165.9(3)
Si(4)-C(29)-Si(3)-C(31)	-56.4(4)
P(2)-C(29)-Si(4)-C(33)	-149.1(3)
Si(3)-C(29)-Si(4)-C(33)	74.3(3)
P(2)-C(29)-Si(4)-C(34)	90.8(3)
Si(3)-C(29)-Si(4)-C(34)	-45.8(4)
P(2)-C(29)-Si(4)-C(35)	-30.6(4)
Si(3)-C(29)-Si(4)-C(35)	-167.2(3)
O(3)-C(17)-W(1)-C(19)	44(76)
O(3)-C(17)-W(1)-C(16)	-46(76)
O(3)-C(17)-W(1)-C(20)	-134(76)
O(3)-C(17)-W(1)-C(18)	156(69)
O(3)-C(17)-W(1)-P(1)	136(76)
O(5)-C(19)-W(1)-C(17)	-24(9)
O(5)-C(19)-W(1)-C(16)	68(9)
O(5)-C(19)-W(1)-C(20)	2(11)
O(5)-C(19)-W(1)-C(18)	157(9)
O(5)-C(19)-W(1)-P(1)	-113(9)
O(2)-C(16)-W(1)-C(17)	-137(31)
O(2)-C(16)-W(1)-C(19)	134(31)
O(2)-C(16)-W(1)-C(20)	-51(31)
O(2)-C(16)-W(1)-C(18)	42(31)
O(2)-C(16)-W(1)-P(1)	-20(35)
O(6)-C(20)-W(1)-C(17)	5(10)
O(6)-C(20)-W(1)-C(19)	-21(11)
O(6)-C(20)-W(1)-C(16)	-87(10)
O(6)-C(20)-W(1)-C(18)	-176(10)
O(6)-C(20)-W(1)-P(1)	94(10)
O(4)-C(18)-W(1)-C(17)	162(37)
O(4)-C(18)-W(1)-C(19)	-87(42)
O(4)-C(18)-W(1)-C(16)	3(42)
O(4)-C(18)-W(1)-C(20)	91(42)
O(4)-C(18)-W(1)-P(1)	-179(100)
O(1)-P(1)-W(1)-C(17)	86.5(2)

C(1)-P(1)-W(1)-C(17)	146.6(3)
C(9)-P(1)-W(1)-C(17)	-53.3(3)
O(1)-P(1)-W(1)-C(19)	175.5(2)
C(1)-P(1)-W(1)-C(19)	-124.5(3)
C(9)-P(1)-W(1)-C(19)	35.7(3)
O(1)-P(1)-W(1)-C(16)	-31(5)
C(1)-P(1)-W(1)-C(16)	29(5)
C(9)-P(1)-W(1)-C(16)	-171(5)
O(1)-P(1)-W(1)-C(20)	-0.4(2)
C(1)-P(1)-W(1)-C(20)	59.6(3)
C(9)-P(1)-W(1)-C(20)	-140.2(2)
O(1)-P(1)-W(1)-C(18)	-93.1(2)
C(1)-P(1)-W(1)-C(18)	-33.0(3)
C(9)-P(1)-W(1)-C(18)	127.2(3)
O(8)-C(36)-W(2)-C(38)	-45(24)
O(8)-C(36)-W(2)-C(39)	-134(24)
O(8)-C(36)-W(2)-C(40)	46(24)
O(8)-C(36)-W(2)-C(37)	136(24)
O(8)-C(36)-W(2)-P(2)	-52(27)
O(10)-C(38)-W(2)-C(36)	-10(9)
O(10)-C(38)-W(2)-C(39)	82(9)
O(10)-C(38)-W(2)-C(40)	-98(9)
O(10)-C(38)-W(2)-C(37)	14(15)
O(10)-C(38)-W(2)-P(2)	170(9)
O(11)-C(39)-W(2)-C(36)	111(14)
O(11)-C(39)-W(2)-C(38)	22(14)
O(11)-C(39)-W(2)-C(40)	117(21)
O(11)-C(39)-W(2)-C(37)	-159(15)
O(11)-C(39)-W(2)-P(2)	-67(14)
O(12)-C(40)-W(2)-C(36)	8(12)
O(12)-C(40)-W(2)-C(38)	97(12)
O(12)-C(40)-W(2)-C(39)	2(28)
O(12)-C(40)-W(2)-C(37)	-82(12)
O(12)-C(40)-W(2)-P(2)	-174(100)
O(9)-C(37)-W(2)-C(36)	2(18)
O(9)-C(37)-W(2)-C(38)	-21(23)
O(9)-C(37)-W(2)-C(39)	-89(18)
O(9)-C(37)-W(2)-C(40)	90(18)
O(9)-C(37)-W(2)-P(2)	-177(100)
O(7)-P(2)-W(2)-C(36)	-89(4)
C(21)-P(2)-W(2)-C(36)	-149(4)
C(29)-P(2)-W(2)-C(36)	47(4)
O(7)-P(2)-W(2)-C(38)	-96.4(2)
C(21)-P(2)-W(2)-C(38)	-156.8(3)
C(29)-P(2)-W(2)-C(38)	39.8(3)
O(7)-P(2)-W(2)-C(39)	-7.0(2)
C(21)-P(2)-W(2)-C(39)	-67.4(3)
C(29)-P(2)-W(2)-C(39)	129.3(3)
O(7)-P(2)-W(2)-C(40)	172.9(2)
C(21)-P(2)-W(2)-C(40)	112.5(3)
C(29)-P(2)-W(2)-C(40)	-50.8(2)
O(7)-P(2)-W(2)-C(37)	82.9(2)
C(21)-P(2)-W(2)-C(37)	22.5(3)
C(29)-P(2)-W(2)-C(37)	-140.8(3)

vi. [2-Bis(trimethylsilyl)methyl-3-(2-methoxyphenyl)-oxaphosphirane-
kP]pentacarbonyltungsten (0) [34]

(A1)

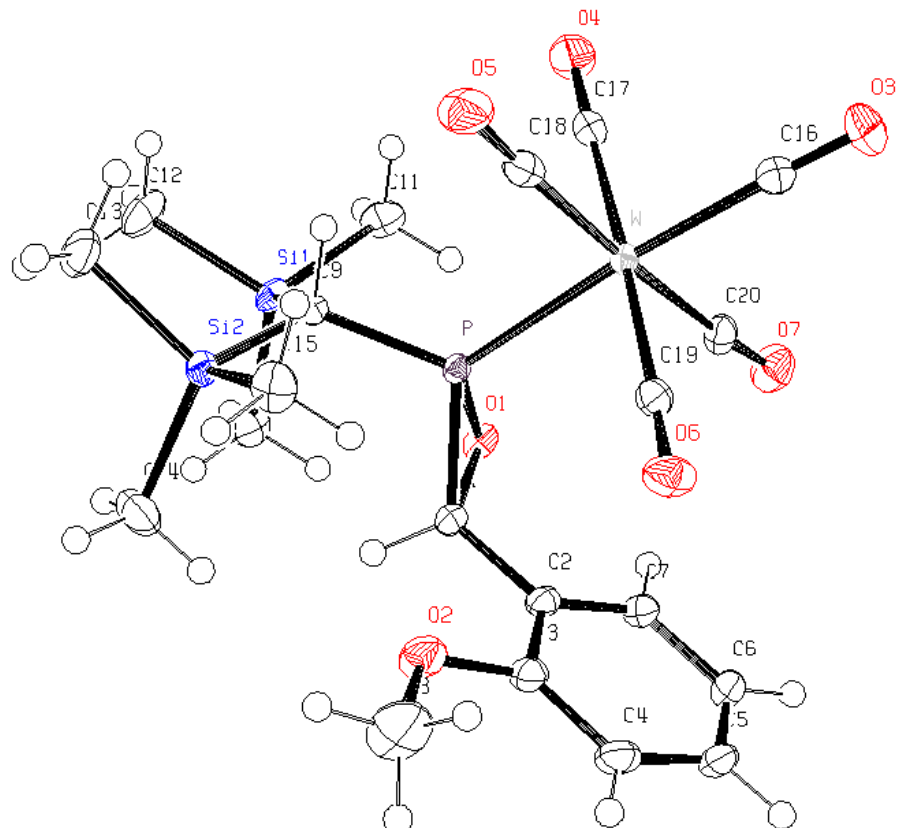


Table vi.1. Crystal data and structure refinement for [34].

Identification code	GSTR105, Greg982f
Device Type	X8-KappaApexII
Empirical formula	C ₂₀ H ₂₇ O ₇ P Si ₂ W
Formula weight	650.42
Temperature	100(2) K
Wavelength	0.71073 Å
Crystal system, space group	Triclinic, P -1
Unit cell dimensions 91.152(2) deg.	a = 10.6733(4) Å alpha =
90.391(2) deg.	b = 10.8524(5) Å beta =
115.605(2) deg.	c = 12.3792(4) Å gamma =
Volume	1292.62(9) Å ³

Z, Calculated density	2, 1.671 Mg/m^3
Absorption coefficient	4.658 mm^-1
F(000)	640
Crystal size	0.60 x 0.60 x 0.32 mm
Theta range for data collection	2.77 to 28.00 deg.
Limiting indices	-14<=h<=14, -9<=k<=14, -16<=l<=15
Reflections collected / unique	15331 / 5996 [R(int) = 0.0279]
Completeness to theta = 28.00	96.2 %
Absorption correction	Semi-empirical from equivalents
Max. and min. transmission	0.3172 and 0.1665
Refinement method	Full-matrix least-squares on F^2
Data / restraints / parameters	5996 / 0 / 288
Goodness-of-fit on F^2	1.028
Final R indices [I>2sigma(I)]	R1 = 0.0176, wR2 = 0.0442
R indices (all data)	R1 = 0.0183, wR2 = 0.0447
Largest diff. peak and hole	1.320 and -0.919 e.A^-3

Table Vi.2. Atomic coordinates ($\times 10^4$) and equivalent isotropic displacement parameters ($\text{\AA}^2 \times 10^3$) for [34].
U(eq) is defined as one third of the trace of the orthogonalized Uij tensor.

	x	y	z	U(eq)
C(1)	7974(2)	8281(2)	8600(2)	16(1)
C(2)	9482(2)	8763(2)	8819(2)	17(1)
C(3)	10414(2)	9926(2)	8302(2)	20(1)
C(4)	11842(2)	10409(2)	8475(2)	26(1)
C(5)	12322(2)	9703(3)	9161(2)	29(1)
C(6)	11423(2)	8570(2)	9686(2)	26(1)
C(7)	9987(2)	8088(2)	9516(2)	21(1)
C(8)	10691(3)	11650(3)	7034(3)	47(1)
C(9)	5427(2)	7020(2)	7271(1)	13(1)
C(10)	4465(2)	7514(2)	9581(2)	24(1)
C(11)	3823(2)	4635(2)	8686(2)	24(1)
C(12)	2343(2)	6215(3)	7770(2)	31(1)
C(13)	4155(2)	8242(3)	5669(2)	30(1)
C(14)	6101(3)	10144(2)	7429(2)	32(1)
C(15)	7251(2)	9057(2)	5601(2)	26(1)
C(16)	8695(2)	4233(2)	6047(2)	21(1)
C(17)	6011(2)	3755(2)	6897(2)	22(1)
C(18)	7183(2)	5699(2)	5268(2)	21(1)
C(19)	9711(2)	7126(2)	6506(2)	19(1)
C(20)	8495(2)	5003(2)	8205(2)	20(1)

O(1)	7073(1)	6942(2)	9031(1)	17(1)
O(2)	9801(2)	10496(2)	7625(1)	27(1)
O(3)	9190(2)	3579(2)	5681(1)	32(1)
O(4)	4975(2)	2811(2)	6957(2)	33(1)
O(5)	6777(2)	5814(2)	4436(1)	34(1)
O(6)	10701(2)	8077(2)	6346(1)	28(1)
O(7)	8803(2)	4708(2)	9005(1)	30(1)
Si(1)	4032(1)	6376(1)	8347(1)	17(1)
Si(2)	5747(1)	8639(1)	6516(1)	17(1)
P	6997(1)	6895(1)	7682(1)	12(1)
W	7873(1)	5415(1)	6734(1)	14(1)

Table vi.3. Bond lengths [Å] and angles [deg] for **[34]**.

C(1)-O(1)	1.467(2)
C(1)-C(2)	1.482(2)
C(1)-P	1.790(2)
C(1)-H(1A)	1.0000
C(2)-C(7)	1.390(3)
C(2)-C(3)	1.396(3)
C(3)-O(2)	1.371(2)
C(3)-C(4)	1.394(3)
C(4)-C(5)	1.389(3)
C(4)-H(4A)	0.9500
C(5)-C(6)	1.370(4)
C(5)-H(5A)	0.9500
C(6)-C(7)	1.402(3)
C(6)-H(6A)	0.9500
C(7)-H(7A)	0.9500
C(8)-O(2)	1.423(3)
C(8)-H(8C)	0.9800
C(8)-H(8B)	0.9800
C(8)-H(8A)	0.9800
C(9)-P	1.8084(17)
C(9)-Si(2)	1.9047(19)
C(9)-Si(1)	1.9096(19)
C(9)-H(9A)	1.0000
C(10)-Si(1)	1.868(2)
C(10)-H(10A)	0.9800
C(10)-H(10B)	0.9800
C(10)-H(10C)	0.9800
C(11)-Si(1)	1.862(2)
C(11)-H(11A)	0.9800
C(11)-H(11B)	0.9800
C(11)-H(11C)	0.9800
C(12)-Si(1)	1.870(2)
C(12)-H(12A)	0.9800
C(12)-H(12B)	0.9800
C(12)-H(12C)	0.9800
C(13)-Si(2)	1.871(2)
C(13)-H(13A)	0.9800
C(13)-H(13B)	0.9800
C(13)-H(13C)	0.9800
C(14)-Si(2)	1.864(2)
C(14)-H(14A)	0.9800
C(14)-H(14B)	0.9800
C(14)-H(14C)	0.9800
C(15)-Si(2)	1.866(2)
C(15)-H(15C)	0.9800
C(15)-H(15B)	0.9800
C(15)-H(15A)	0.9800

C(16)-O(3)	1.141(3)
C(16)-W	2.020(2)
C(17)-O(4)	1.142(3)
C(17)-W	2.040(2)
C(18)-O(5)	1.144(3)
C(18)-W	2.033(2)
C(19)-O(6)	1.136(3)
C(19)-W	2.063(2)
C(20)-O(7)	1.136(3)
C(20)-W	2.057(2)
O(1)-P	1.6701(13)
P-W	2.4631(5)
O(1)-C(1)-C(2)	115.50(15)
O(1)-C(1)-P	60.76(9)
C(2)-C(1)-P	123.31(14)
O(1)-C(1)-H(1A)	115.3
C(2)-C(1)-H(1A)	115.3
P-C(1)-H(1A)	115.3
C(7)-C(2)-C(3)	119.42(18)
C(7)-C(2)-C(1)	121.97(19)
C(3)-C(2)-C(1)	118.61(17)
O(2)-C(3)-C(4)	125.0(2)
O(2)-C(3)-C(2)	114.35(17)
C(4)-C(3)-C(2)	120.67(19)
C(5)-C(4)-C(3)	118.8(2)
C(5)-C(4)-H(4A)	120.6
C(3)-C(4)-H(4A)	120.6
C(6)-C(5)-C(4)	121.38(19)
C(6)-C(5)-H(5A)	119.3
C(4)-C(5)-H(5A)	119.3
C(5)-C(6)-C(7)	119.7(2)
C(5)-C(6)-H(6A)	120.1
C(7)-C(6)-H(6A)	120.1
C(2)-C(7)-C(6)	120.0(2)
C(2)-C(7)-H(7A)	120.0
C(6)-C(7)-H(7A)	120.0
O(2)-C(8)-H(8C)	109.5
O(2)-C(8)-H(8B)	109.5
H(8C)-C(8)-H(8B)	109.5
O(2)-C(8)-H(8A)	109.5
H(8C)-C(8)-H(8A)	109.5
H(8B)-C(8)-H(8A)	109.5
P-C(9)-Si(2)	114.04(10)
P-C(9)-Si(1)	112.18(9)
Si(2)-C(9)-Si(1)	120.03(9)
P-C(9)-H(9A)	102.5
Si(2)-C(9)-H(9A)	102.5
Si(1)-C(9)-H(9A)	102.5
Si(1)-C(10)-H(10A)	109.5
Si(1)-C(10)-H(10B)	109.5
H(10A)-C(10)-H(10B)	109.5
Si(1)-C(10)-H(10C)	109.5
H(10A)-C(10)-H(10C)	109.5
H(10B)-C(10)-H(10C)	109.5
Si(1)-C(11)-H(11A)	109.5
Si(1)-C(11)-H(11B)	109.5
H(11A)-C(11)-H(11B)	109.5
Si(1)-C(11)-H(11C)	109.5
H(11A)-C(11)-H(11C)	109.5
H(11B)-C(11)-H(11C)	109.5
Si(1)-C(12)-H(12A)	109.5
Si(1)-C(12)-H(12B)	109.5

H(12A)-C(12)-H(12B)	109.5
Si(1)-C(12)-H(12C)	109.5
H(12A)-C(12)-H(12C)	109.5
H(12B)-C(12)-H(12C)	109.5
Si(2)-C(13)-H(13A)	109.5
Si(2)-C(13)-H(13B)	109.5
H(13A)-C(13)-H(13B)	109.5
Si(2)-C(13)-H(13C)	109.5
H(13A)-C(13)-H(13C)	109.5
H(13B)-C(13)-H(13C)	109.5
Si(2)-C(14)-H(14A)	109.5
Si(2)-C(14)-H(14B)	109.5
H(14A)-C(14)-H(14B)	109.5
Si(2)-C(14)-H(14C)	109.5
H(14A)-C(14)-H(14C)	109.5
H(14B)-C(14)-H(14C)	109.5
Si(2)-C(15)-H(15C)	109.5
Si(2)-C(15)-H(15B)	109.5
H(15C)-C(15)-H(15B)	109.5
Si(2)-C(15)-H(15A)	109.5
H(15C)-C(15)-H(15A)	109.5
H(15B)-C(15)-H(15A)	109.5
O(3)-C(16)-W	178.01(18)
O(4)-C(17)-W	177.9(2)
O(5)-C(18)-W	177.8(2)
O(6)-C(19)-W	177.37(18)
O(7)-C(20)-W	176.6(2)
C(1)-O(1)-P	69.23(9)
C(3)-O(2)-C(8)	117.45(18)
C(11)-Si(1)-C(10)	111.10(10)
C(11)-Si(1)-C(12)	108.05(11)
C(10)-Si(1)-C(12)	108.33(10)
C(11)-Si(1)-C(9)	106.16(9)
C(10)-Si(1)-C(9)	113.40(9)
C(12)-Si(1)-C(9)	109.68(9)
C(14)-Si(2)-C(15)	108.82(12)
C(14)-Si(2)-C(13)	110.11(11)
C(15)-Si(2)-C(13)	108.47(11)
C(14)-Si(2)-C(9)	113.35(10)
C(15)-Si(2)-C(9)	109.39(9)
C(13)-Si(2)-C(9)	106.59(10)
O(1)-P-C(1)	50.01(8)
O(1)-P-C(9)	107.97(8)
C(1)-P-C(9)	109.21(8)
O(1)-P-W	117.24(5)
C(1)-P-W	125.89(6)
C(9)-P-W	123.04(6)
C(16)-W-C(18)	90.79(8)
C(16)-W-C(17)	90.81(9)
C(18)-W-C(17)	88.04(9)
C(16)-W-C(20)	87.53(8)
C(18)-W-C(20)	176.51(8)
C(17)-W-C(20)	88.93(9)
C(16)-W-C(19)	90.00(9)
C(18)-W-C(19)	89.16(9)
C(17)-W-C(19)	177.09(7)
C(20)-W-C(19)	93.90(8)
C(16)-W-P	175.77(6)
C(18)-W-P	93.05(6)
C(17)-W-P	91.10(6)
C(20)-W-P	88.73(6)
C(19)-W-P	88.28(6)

Table vi.4. Anisotropic displacement parameters ($\text{Å}^2 \times 10^3$) for [34]
The anisotropic displacement factor exponent takes the form:
 $-2 \pi^2 [h^2 a^{*2} U_{11} + \dots + 2 h k a^* b^* U_{12}]$

	U11	U22	U33	U23	U13	U12
C(1)	13(1)	16(1)	17(1)	0(1)	0(1)	5(1)
C(2)	14(1)	20(1)	17(1)	-7(1)	-1(1)	7(1)
C(3)	19(1)	20(1)	21(1)	-5(1)	-2(1)	7(1)
C(4)	15(1)	21(1)	36(1)	-8(1)	2(1)	2(1)
C(5)	14(1)	28(1)	43(1)	-16(1)	-7(1)	8(1)
C(6)	22(1)	28(1)	32(1)	-10(1)	-10(1)	15(1)
C(7)	19(1)	21(1)	23(1)	-6(1)	-5(1)	9(1)
C(8)	34(1)	34(2)	59(2)	22(1)	1(1)	0(1)
C(9)	12(1)	13(1)	15(1)	0(1)	-1(1)	5(1)
C(10)	19(1)	31(1)	23(1)	-4(1)	2(1)	12(1)
C(11)	20(1)	22(1)	23(1)	5(1)	2(1)	1(1)
C(12)	15(1)	49(2)	29(1)	0(1)	0(1)	14(1)
C(13)	28(1)	28(1)	35(1)	7(1)	-10(1)	12(1)
C(14)	47(1)	22(1)	31(1)	-1(1)	-3(1)	19(1)
C(15)	25(1)	24(1)	28(1)	10(1)	6(1)	9(1)
C(16)	19(1)	20(1)	24(1)	-1(1)	-2(1)	7(1)
C(17)	22(1)	18(1)	28(1)	-2(1)	-2(1)	12(1)
C(18)	23(1)	18(1)	22(1)	-3(1)	0(1)	8(1)
C(19)	19(1)	23(1)	19(1)	-5(1)	1(1)	12(1)
C(20)	16(1)	22(1)	25(1)	3(1)	1(1)	10(1)
O(1)	14(1)	21(1)	14(1)	4(1)	1(1)	6(1)
O(2)	20(1)	22(1)	33(1)	7(1)	-1(1)	3(1)
O(3)	36(1)	33(1)	35(1)	-6(1)	3(1)	22(1)
O(4)	22(1)	21(1)	50(1)	1(1)	3(1)	3(1)
O(5)	47(1)	30(1)	24(1)	-2(1)	-12(1)	16(1)
O(6)	21(1)	24(1)	31(1)	-4(1)	6(1)	4(1)
O(7)	31(1)	34(1)	28(1)	7(1)	-3(1)	15(1)
Si(1)	10(1)	21(1)	18(1)	1(1)	1(1)	5(1)
Si(2)	17(1)	15(1)	20(1)	3(1)	-2(1)	7(1)
P	10(1)	12(1)	13(1)	1(1)	0(1)	4(1)
W	12(1)	13(1)	17(1)	0(1)	0(1)	6(1)

Table vi.5. Hydrogen coordinates ($\times 10^4$) and isotropic displacement parameters ($\text{Å}^2 \times 10^3$) for [34].

	x	y	z	U(eq)
H(1A)	7621	8994	8682	19
H(4A)	12475	11208	8130	32
H(5A)	13295	10013	9268	35
H(6A)	11771	8112	10164	31
H(7A)	9360	7302	9878	25
H(8C)	10131	11935	6560	71
H(8B)	11318	11408	6596	71
H(8A)	11239	12403	7539	71
H(9A)	5038	6294	6691	16
H(10A)	4605	8432	9377	36

H(10B)	5317	7562	9921	36
H(10C)	3700	7144	10091	36
H(11A)	4703	4692	8979	36
H(11B)	3560	4049	8032	36
H(11C)	3097	4246	9225	36
H(12A)	2146	5700	7081	46
H(12B)	2400	7127	7651	46
H(12C)	1596	5732	8276	46
H(13A)	3464	8388	6102	45
H(13B)	3768	7287	5413	45
H(13C)	4398	8842	5048	45
H(14A)	6946	10355	7858	47
H(14B)	5315	9936	7912	47
H(14C)	6226	10934	6995	47
H(15C)	7496	9951	5286	39
H(15B)	6999	8358	5023	39
H(15A)	8048	9081	6015	39

Table vi.6. Torsion angles [deg] for [34].

O(1)-C(1)-C(2)-C(7)	-9.1(3)
P-C(1)-C(2)-C(7)	-79.5(2)
O(1)-C(1)-C(2)-C(3)	170.67(17)
P-C(1)-C(2)-C(3)	100.2(2)
C(7)-C(2)-C(3)-O(2)	179.28(18)
C(1)-C(2)-C(3)-O(2)	-0.5(3)
C(7)-C(2)-C(3)-C(4)	0.3(3)
C(1)-C(2)-C(3)-C(4)	-179.40(19)
O(2)-C(3)-C(4)-C(5)	-178.0(2)
C(2)-C(3)-C(4)-C(5)	0.8(3)
C(3)-C(4)-C(5)-C(6)	-1.6(3)
C(4)-C(5)-C(6)-C(7)	1.3(3)
C(3)-C(2)-C(7)-C(6)	-0.7(3)
C(1)-C(2)-C(7)-C(6)	179.06(19)
C(5)-C(6)-C(7)-C(2)	-0.2(3)
C(2)-C(1)-O(1)-P	-115.48(16)
C(4)-C(3)-O(2)-C(8)	1.6(3)
C(2)-C(3)-O(2)-C(8)	-177.3(2)
P-C(9)-Si(1)-C(11)	-52.54(12)
Si(2)-C(9)-Si(1)-C(11)	169.40(11)
P-C(9)-Si(1)-C(10)	69.72(12)
Si(2)-C(9)-Si(1)-C(10)	-68.35(13)
P-C(9)-Si(1)-C(12)	-169.03(12)
Si(2)-C(9)-Si(1)-C(12)	52.90(15)
P-C(9)-Si(2)-C(14)	-83.09(13)
Si(1)-C(9)-Si(2)-C(14)	54.26(14)
P-C(9)-Si(2)-C(15)	38.54(14)
Si(1)-C(9)-Si(2)-C(15)	175.89(11)
P-C(9)-Si(2)-C(13)	155.62(12)
Si(1)-C(9)-Si(2)-C(13)	-67.03(14)
C(1)-O(1)-P-C(9)	-100.34(11)
C(1)-O(1)-P-W	115.39(8)
C(2)-C(1)-P-O(1)	102.86(18)
O(1)-C(1)-P-C(9)	97.71(10)
C(2)-C(1)-P-C(9)	-159.44(16)
O(1)-C(1)-P-W	-97.50(9)
C(2)-C(1)-P-W	5.4(2)
Si(2)-C(9)-P-O(1)	115.14(10)
Si(1)-C(9)-P-O(1)	-25.55(12)
Si(2)-C(9)-P-C(1)	62.18(12)
Si(1)-C(9)-P-C(1)	-78.51(12)

Si(2)-C(9)-P-W	-103.13(9)
Si(1)-C(9)-P-W	116.17(8)
O(3)-C(16)-W-C(18)	147(6)
O(3)-C(16)-W-C(17)	-125(6)
O(3)-C(16)-W-C(20)	-36(6)
O(3)-C(16)-W-C(19)	58(6)
O(3)-C(16)-W-P	-8(7)
O(5)-C(18)-W-C(16)	49(5)
O(5)-C(18)-W-C(17)	-41(5)
O(5)-C(18)-W-C(20)	-12(6)
O(5)-C(18)-W-C(19)	139(5)
O(5)-C(18)-W-P	-132(5)
O(4)-C(17)-W-C(16)	-40(5)
O(4)-C(17)-W-C(18)	51(5)
O(4)-C(17)-W-C(20)	-128(5)
O(4)-C(17)-W-C(19)	66(5)
O(4)-C(17)-W-P	144(5)
O(7)-C(20)-W-C(16)	-55(3)
O(7)-C(20)-W-C(18)	6(4)
O(7)-C(20)-W-C(17)	36(3)
O(7)-C(20)-W-C(19)	-145(3)
O(7)-C(20)-W-P	127(3)
O(6)-C(19)-W-C(16)	97(4)
O(6)-C(19)-W-C(18)	7(4)
O(6)-C(19)-W-C(17)	-9(5)
O(6)-C(19)-W-C(20)	-175(4)
O(6)-C(19)-W-P	-86(4)
O(1)-P-W-C(16)	-32.6(9)
C(1)-P-W-C(16)	26.1(9)
C(9)-P-W-C(16)	-171.1(9)
O(1)-P-W-C(18)	172.37(9)
C(1)-P-W-C(18)	-128.93(10)
C(9)-P-W-C(18)	33.88(10)
O(1)-P-W-C(17)	84.28(8)
C(1)-P-W-C(17)	142.98(10)
C(9)-P-W-C(17)	-54.21(10)
O(1)-P-W-C(20)	-4.62(8)
C(1)-P-W-C(20)	54.08(10)
C(9)-P-W-C(20)	-143.11(10)
O(1)-P-W-C(19)	-98.56(8)
C(1)-P-W-C(19)	-39.86(10)
C(9)-P-W-C(19)	122.95(9)

vii. [2-Bis(trimethylsilyl)methyl-3-*tert*-butyl-oxaphosphirane-*kP*]pentacarbonyltungsten (0) [36]

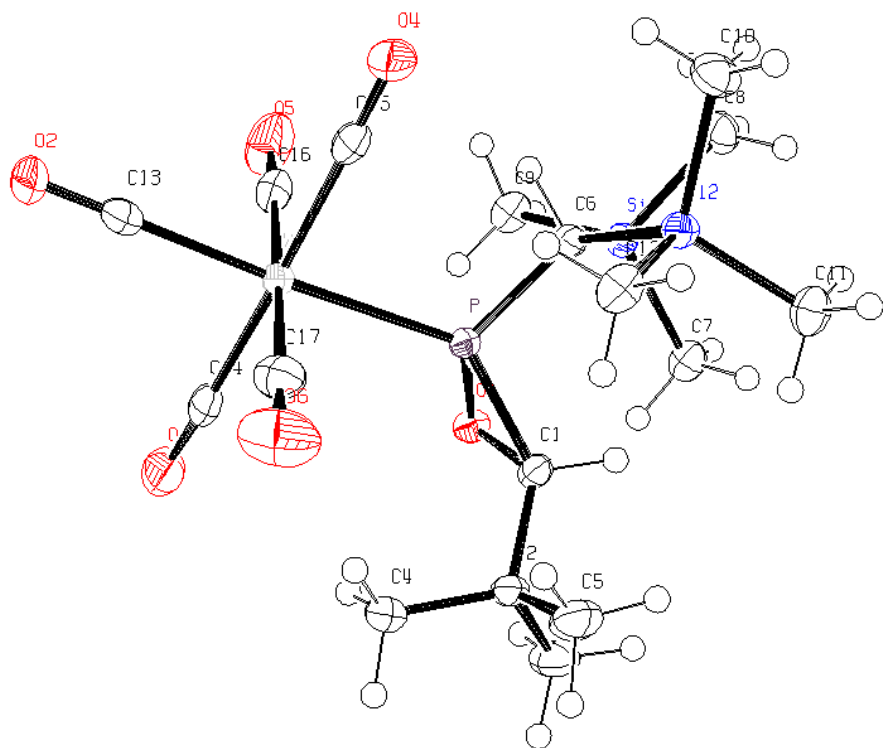


Table 1. Crystal data and structure refinement for [36].

Identification code	GSTR071, Greg661
Device Type	Nonius KappaCCD
Empirical formula	C17 H29 O6 P Si2 W
Formula weight	600.40
Temperature	123(2) K
Wavelength	0.71073 Å
Crystal system, space group	Monoclinic, P 21/n
Unit cell dimensions	a = 9.5099(3) Å alpha = 90 deg. b = 18.8095(6) Å beta = 91.237(2) deg. c = 13.6649(4) Å gamma = 90 deg.
Volume	2443.76(13) Å ³
Z, Calculated density	4, 1.632 Mg/m ³
Absorption coefficient	4.917 mm ⁻¹
F(000)	1184
Crystal size	0.36 x 0.32 x 0.20 mm
Theta range for data collection	2.64 to 28.00 deg.

Limiting indices $-12 \leq h \leq 12, -23 \leq k \leq 24, -18 \leq l \leq 14$
 Reflections collected / unique 18592 / 5796 [R(int) = 0.0518]
 Completeness to theta = 28.00 98.3 %
 Absorption correction Semi-empirical from equivalents
 Max. and min. transmission 0.38493 and 0.32928
 Refinement method Full-matrix least-squares on F²
 Data / restraints / parameters 5796 / 0 / 253
 Goodness-of-fit on F² 0.932
 Final R indices [I > 2sigma(I)] R1 = 0.0287, wR2 = 0.0522
 R indices (all data) R1 = 0.0454, wR2 = 0.0556
 Largest diff. peak and hole 0.984 and -1.770 e·Å⁻³

Table vii.2. Atomic coordinates ($x \times 10^4$) and equivalent isotropic displacement parameters ($A^2 \times 10^3$) for [36]. U(eq) is defined as one third of the trace of the orthogonalized Uij tensor.

	x	y	z	U(eq)
C(1)	-1477(3)	1830(2)	3482(2)	19(1)
C(2)	-2157(4)	1236(2)	4050(3)	23(1)
C(3)	-2326(4)	1507(2)	5098(3)	35(1)
C(4)	-1323(4)	546(2)	4053(3)	35(1)
C(5)	-3613(4)	1114(2)	3574(3)	35(1)
C(6)	-457(3)	2729(2)	1979(2)	16(1)
C(7)	-865(4)	3585(2)	3964(3)	25(1)
C(8)	-112(4)	4344(2)	2121(3)	29(1)
C(9)	2046(3)	3362(2)	3090(3)	26(1)
C(10)	-1889(4)	3347(2)	153(3)	33(1)
C(11)	-3561(3)	3290(2)	2029(3)	30(1)
C(12)	-2922(4)	1943(2)	916(3)	27(1)
C(13)	2457(4)	318(2)	892(3)	32(1)
C(14)	1801(4)	493(2)	2904(3)	28(1)
C(15)	667(4)	1464(2)	343(3)	26(1)
C(16)	2862(4)	1652(2)	1805(3)	30(1)
C(17)	-451(4)	288(2)	1460(3)	32(1)
O(1)	30(2)	1973(1)	3723(2)	20(1)
O(2)	3202(3)	-58(1)	484(2)	45(1)
O(3)	2166(3)	210(2)	3605(2)	44(1)
O(4)	410(3)	1743(2)	-385(2)	39(1)
O(5)	3815(3)	2020(2)	1886(2)	49(1)
O(6)	-1357(3)	-107(2)	1375(2)	55(1)
P	-236(1)	1857(1)	2522(1)	16(1)
Si(1)	135(1)	3493(1)	2812(1)	19(1)
Si(2)	-2216(1)	2831(1)	1284(1)	21(1)
W	1198(1)	978(1)	1629(1)	19(1)

Table vii.3. Bond lengths [Å] and angles [deg] for [36].

C(1)-O(1)	1.487(4)
C(1)-C(2)	1.514(4)
C(1)-P	1.784(3)
C(1)-H(1)	1.0000
C(2)-C(4)	1.520(5)
C(2)-C(3)	1.532(5)
C(2)-C(5)	1.534(5)
C(3)-H(3A)	0.9800
C(3)-H(3B)	0.9800
C(3)-H(3C)	0.9800
C(4)-H(4A)	0.9800
C(4)-H(4B)	0.9800
C(4)-H(4C)	0.9800
C(5)-H(5A)	0.9800
C(5)-H(5B)	0.9800
C(5)-H(5C)	0.9800
C(6)-P	1.811(3)
C(6)-Si(1)	1.910(3)
C(6)-Si(2)	1.915(3)
C(6)-H(6)	1.0000
C(7)-Si(1)	1.865(3)
C(7)-H(7A)	0.9800
C(7)-H(7B)	0.9800
C(7)-H(7C)	0.9800
C(8)-Si(1)	1.870(4)
C(8)-H(8A)	0.9800
C(8)-H(8B)	0.9800
C(8)-H(8C)	0.9800
C(9)-Si(1)	1.865(3)
C(9)-H(9A)	0.9800
C(9)-H(9B)	0.9800
C(9)-H(9C)	0.9800
C(10)-Si(2)	1.858(4)
C(10)-H(10A)	0.9800
C(10)-H(10B)	0.9800
C(10)-H(10C)	0.9800
C(11)-Si(2)	1.864(3)
C(11)-H(11A)	0.9800
C(11)-H(11B)	0.9800
C(11)-H(11C)	0.9800
C(12)-Si(2)	1.866(3)
C(12)-H(12A)	0.9800
C(12)-H(12B)	0.9800
C(12)-H(12C)	0.9800
C(13)-O(2)	1.154(4)
C(13)-W	2.010(4)
C(14)-O(3)	1.144(4)
C(14)-W	2.038(4)
C(15)-O(4)	1.147(4)
C(15)-W	2.035(4)
C(16)-O(5)	1.144(4)
C(16)-W	2.037(4)
C(17)-O(6)	1.142(4)
C(17)-W	2.045(4)
O(1)-P	1.669(2)
P-W	2.4804(8)
O(1)-C(1)-C(2)	116.1(3)
O(1)-C(1)-P	60.54(14)
C(2)-C(1)-P	134.0(3)

O(1)-C(1)-H(1)	111.4
C(2)-C(1)-H(1)	111.4
P-C(1)-H(1)	111.4
C(1)-C(2)-C(4)	113.8(3)
C(1)-C(2)-C(3)	106.8(3)
C(4)-C(2)-C(3)	110.3(3)
C(1)-C(2)-C(5)	106.6(3)
C(4)-C(2)-C(5)	109.8(3)
C(3)-C(2)-C(5)	109.5(3)
C(2)-C(3)-H(3A)	109.5
C(2)-C(3)-H(3B)	109.5
H(3A)-C(3)-H(3B)	109.5
C(2)-C(3)-H(3C)	109.5
H(3A)-C(3)-H(3C)	109.5
H(3B)-C(3)-H(3C)	109.5
C(2)-C(4)-H(4A)	109.5
C(2)-C(4)-H(4B)	109.5
H(4A)-C(4)-H(4B)	109.5
C(2)-C(4)-H(4C)	109.5
H(4A)-C(4)-H(4C)	109.5
H(4B)-C(4)-H(4C)	109.5
C(2)-C(5)-H(5A)	109.5
C(2)-C(5)-H(5B)	109.5
H(5A)-C(5)-H(5B)	109.5
C(2)-C(5)-H(5C)	109.5
H(5A)-C(5)-H(5C)	109.5
H(5B)-C(5)-H(5C)	109.5
P-C(6)-Si(1)	114.05(17)
P-C(6)-Si(2)	112.71(16)
Si(1)-C(6)-Si(2)	117.60(16)
P-C(6)-H(6)	103.4
Si(1)-C(6)-H(6)	103.4
Si(2)-C(6)-H(6)	103.4
Si(1)-C(7)-H(7A)	109.5
Si(1)-C(7)-H(7B)	109.5
H(7A)-C(7)-H(7B)	109.5
Si(1)-C(7)-H(7C)	109.5
H(7A)-C(7)-H(7C)	109.5
H(7B)-C(7)-H(7C)	109.5
Si(1)-C(8)-H(8A)	109.5
Si(1)-C(8)-H(8B)	109.5
H(8A)-C(8)-H(8B)	109.5
Si(1)-C(8)-H(8C)	109.5
H(8A)-C(8)-H(8C)	109.5
H(8B)-C(8)-H(8C)	109.5
Si(1)-C(9)-H(9A)	109.5
Si(1)-C(9)-H(9B)	109.5
H(9A)-C(9)-H(9B)	109.5
Si(1)-C(9)-H(9C)	109.5
H(9A)-C(9)-H(9C)	109.5
H(9B)-C(9)-H(9C)	109.5
Si(2)-C(10)-H(10A)	109.5
Si(2)-C(10)-H(10B)	109.5
H(10A)-C(10)-H(10B)	109.5
Si(2)-C(10)-H(10C)	109.5
H(10A)-C(10)-H(10C)	109.5
H(10B)-C(10)-H(10C)	109.5
Si(2)-C(11)-H(11A)	109.5
Si(2)-C(11)-H(11B)	109.5
H(11A)-C(11)-H(11B)	109.5
Si(2)-C(11)-H(11C)	109.5
H(11A)-C(11)-H(11C)	109.5
H(11B)-C(11)-H(11C)	109.5

Si(2)-C(12)-H(12A)	109.5
Si(2)-C(12)-H(12B)	109.5
H(12A)-C(12)-H(12B)	109.5
Si(2)-C(12)-H(12C)	109.5
H(12A)-C(12)-H(12C)	109.5
H(12B)-C(12)-H(12C)	109.5
O(2)-C(13)-W	178.5(4)
O(3)-C(14)-W	178.1(3)
O(4)-C(15)-W	177.9(3)
O(5)-C(16)-W	178.2(3)
O(6)-C(17)-W	178.7(4)
C(1)-O(1)-P	68.58(16)
O(1)-P-C(1)	50.88(13)
O(1)-P-C(6)	107.29(14)
C(1)-P-C(6)	104.68(15)
O(1)-P-W	119.87(9)
C(1)-P-W	136.25(12)
C(6)-P-W	117.58(11)
C(7)-Si(1)-C(9)	110.66(17)
C(7)-Si(1)-C(8)	106.67(16)
C(9)-Si(1)-C(8)	109.08(16)
C(7)-Si(1)-C(6)	115.06(15)
C(9)-Si(1)-C(6)	107.16(15)
C(8)-Si(1)-C(6)	108.09(16)
C(10)-Si(2)-C(11)	109.99(18)
C(10)-Si(2)-C(12)	108.00(18)
C(11)-Si(2)-C(12)	108.36(16)
C(10)-Si(2)-C(6)	107.75(15)
C(11)-Si(2)-C(6)	112.19(16)
C(12)-Si(2)-C(6)	110.47(15)
C(13)-W-C(15)	89.10(14)
C(13)-W-C(16)	88.54(15)
C(15)-W-C(16)	90.02(15)
C(13)-W-C(14)	89.54(14)
C(15)-W-C(14)	178.03(14)
C(16)-W-C(14)	88.53(15)
C(13)-W-C(17)	90.82(15)
C(15)-W-C(17)	90.70(15)
C(16)-W-C(17)	179.03(15)
C(14)-W-C(17)	90.73(15)
C(13)-W-P	176.14(11)
C(15)-W-P	89.81(9)
C(16)-W-P	87.76(10)
C(14)-W-P	91.46(10)
C(17)-W-P	92.90(10)

Table vii.4. Anisotropic displacement parameters ($\text{\AA}^2 \times 10^3$) for [36]
The anisotropic displacement factor exponent takes the form:
 $-2 \pi^2 [h^2 a^*^2 U_{11} + \dots + 2 h k a^* b^* U_{12}]$

	U11	U22	U33	U23	U13	U12
C(1)	17(2)	20(2)	21(2)	-1(2)	4(2)	-1(1)
C(2)	27(2)	17(2)	25(2)	2(2)	10(2)	-2(2)
C(3)	48(2)	34(2)	25(2)	2(2)	13(2)	-3(2)
C(4)	43(2)	26(2)	37(2)	10(2)	18(2)	6(2)
C(5)	29(2)	36(2)	40(3)	4(2)	9(2)	-8(2)

C(6)	18(2)	16(2)	15(2)	1(1)	0(1)	0(1)
C(7)	25(2)	23(2)	28(2)	-7(2)	2(2)	-1(2)
C(8)	31(2)	17(2)	40(2)	0(2)	2(2)	-1(2)
C(9)	22(2)	27(2)	29(2)	-8(2)	0(2)	-5(2)
C(10)	30(2)	39(2)	29(2)	10(2)	-5(2)	-1(2)
C(11)	21(2)	34(2)	34(2)	-3(2)	-3(2)	2(2)
C(12)	22(2)	34(2)	26(2)	-6(2)	-1(2)	-2(2)
C(13)	44(2)	26(2)	25(2)	9(2)	9(2)	7(2)
C(14)	31(2)	28(2)	26(2)	-2(2)	8(2)	10(2)
C(15)	28(2)	28(2)	23(2)	-6(2)	7(2)	5(2)
C(16)	25(2)	30(2)	35(2)	0(2)	6(2)	6(2)
C(17)	44(2)	27(2)	24(2)	-3(2)	4(2)	-4(2)
O(1)	19(1)	23(1)	19(1)	1(1)	1(1)	-2(1)
O(2)	68(2)	34(2)	36(2)	5(1)	22(2)	26(2)
O(3)	48(2)	54(2)	30(2)	11(2)	8(1)	24(2)
O(4)	43(2)	49(2)	24(2)	10(1)	8(1)	13(1)
O(5)	25(2)	45(2)	78(2)	-13(2)	8(2)	-6(1)
O(6)	71(2)	46(2)	49(2)	-4(2)	-4(2)	-33(2)
P	16(1)	15(1)	17(1)	1(1)	3(1)	0(1)
Si(1)	18(1)	16(1)	23(1)	-1(1)	2(1)	-1(1)
Si(2)	18(1)	24(1)	20(1)	2(1)	-1(1)	-1(1)
W	22(1)	15(1)	19(1)	1(1)	5(1)	3(1)

Table vii.5. Hydrogen coordinates ($\times 10^4$) and isotropic displacement parameters ($\text{\AA}^2 \times 10^3$) for [36].

	x	y	z	U(eq)
H(1)	-2050	2276	3502	23
H(3A)	-1402	1636	5376	53
H(3B)	-2744	1133	5497	53
H(3C)	-2940	1926	5092	53
H(4A)	-1248	371	3381	52
H(4B)	-1805	191	4449	52
H(4C)	-380	632	4330	52
H(5A)	-4120	1567	3533	52
H(5B)	-4144	778	3971	52
H(5C)	-3504	919	2915	52
H(6)	249	2734	1448	19
H(7A)	-717	3161	4370	38
H(7B)	-1869	3636	3805	38
H(7C)	-534	4006	4323	38
H(8A)	-1119	4430	2007	43
H(8B)	357	4310	1491	43
H(8C)	296	4737	2502	43
H(9A)	2387	3744	3520	39
H(9B)	2567	3370	2479	39
H(9C)	2188	2903	3416	39
H(10A)	-2767	3391	-231	49
H(10B)	-1186	3101	-237	49
H(10C)	-1541	3822	328	49
H(11A)	-3233	3770	2194	44
H(11B)	-3710	3021	2633	44
H(11C)	-4448	3320	1653	44
H(12A)	-3785	2005	521	41
H(12B)	-3130	1666	1503	41
H(12C)	-2222	1691	531	41

Table vii.6. Torsion angles [deg] for [36].

O(1)-C(1)-C(2)-C(4)	-50.4(4)
P-C(1)-C(2)-C(4)	22.8(5)
O(1)-C(1)-C(2)-C(3)	71.4(4)
P-C(1)-C(2)-C(3)	144.7(3)
O(1)-C(1)-C(2)-C(5)	-171.6(3)
P-C(1)-C(2)-C(5)	-98.3(4)
C(2)-C(1)-O(1)-P	127.7(3)
C(1)-O(1)-P-C(6)	95.11(18)
C(1)-O(1)-P-W	-127.34(15)
C(2)-C(1)-P-O(1)	-99.1(4)
O(1)-C(1)-P-C(6)	-100.54(17)
C(2)-C(1)-P-C(6)	160.4(3)
O(1)-C(1)-P-W	94.52(18)
C(2)-C(1)-P-W	-4.6(4)
Si(1)-C(6)-P-O(1)	15.1(2)
Si(2)-C(6)-P-O(1)	-122.37(16)
Si(1)-C(6)-P-C(1)	68.1(2)
Si(2)-C(6)-P-C(1)	-69.4(2)
Si(1)-C(6)-P-W	-123.58(13)
Si(2)-C(6)-P-W	98.95(15)
P-C(6)-Si(1)-C(7)	-62.8(2)
Si(2)-C(6)-Si(1)-C(7)	72.4(2)
P-C(6)-Si(1)-C(9)	60.7(2)
Si(2)-C(6)-Si(1)-C(9)	-164.07(18)
P-C(6)-Si(1)-C(8)	178.09(17)
Si(2)-C(6)-Si(1)-C(8)	-46.6(2)
P-C(6)-Si(2)-C(10)	-140.33(19)
Si(1)-C(6)-Si(2)-C(10)	83.8(2)
P-C(6)-Si(2)-C(11)	98.5(2)
Si(1)-C(6)-Si(2)-C(11)	-37.4(2)
P-C(6)-Si(2)-C(12)	-22.6(2)
Si(1)-C(6)-Si(2)-C(12)	-158.41(18)
O(2)-C(13)-W-C(15)	130(13)
O(2)-C(13)-W-C(16)	40(12)
O(2)-C(13)-W-C(14)	-48(12)
O(2)-C(13)-W-C(17)	-139(12)
O(2)-C(13)-W-P	57(13)
O(4)-C(15)-W-C(13)	-60(9)
O(4)-C(15)-W-C(16)	28(9)
O(4)-C(15)-W-C(14)	-14(12)
O(4)-C(15)-W-C(17)	-151(9)
O(4)-C(15)-W-P	116(9)
O(5)-C(16)-W-C(13)	12(12)
O(5)-C(16)-W-C(15)	-77(12)
O(5)-C(16)-W-C(14)	102(12)
O(5)-C(16)-W-C(17)	61(17)
O(5)-C(16)-W-P	-167(12)
O(3)-C(14)-W-C(13)	8(11)
O(3)-C(14)-W-C(15)	-39(14)
O(3)-C(14)-W-C(16)	-81(11)
O(3)-C(14)-W-C(17)	98(11)
O(3)-C(14)-W-P	-169(11)
O(6)-C(17)-W-C(13)	61(17)
O(6)-C(17)-W-C(15)	150(17)
O(6)-C(17)-W-C(16)	12(22)
O(6)-C(17)-W-C(14)	-29(17)
O(6)-C(17)-W-P	-120(17)
O(1)-P-W-C(13)	-87.7(17)
C(1)-P-W-C(13)	-150.8(17)
C(6)-P-W-C(13)	45.7(17)

O(1)-P-W-C(15)	-161.26(14)
C(1)-P-W-C(15)	135.63(19)
C(6)-P-W-C(15)	-27.89(16)
O(1)-P-W-C(16)	-71.23(15)
C(1)-P-W-C(16)	-134.3(2)
C(6)-P-W-C(16)	62.13(16)
O(1)-P-W-C(14)	17.24(14)
C(1)-P-W-C(14)	-45.9(2)
C(6)-P-W-C(14)	150.60(16)
O(1)-P-W-C(17)	108.05(14)
C(1)-P-W-C(17)	44.9(2)
C(6)-P-W-C(17)	-118.59(16)

viii. [2-Bis(trimethylsilyl)methyl-3-dimethyl-oxaphosphirane-
kP]pentacarbonyltungsten (0) **[42]**

(A1)

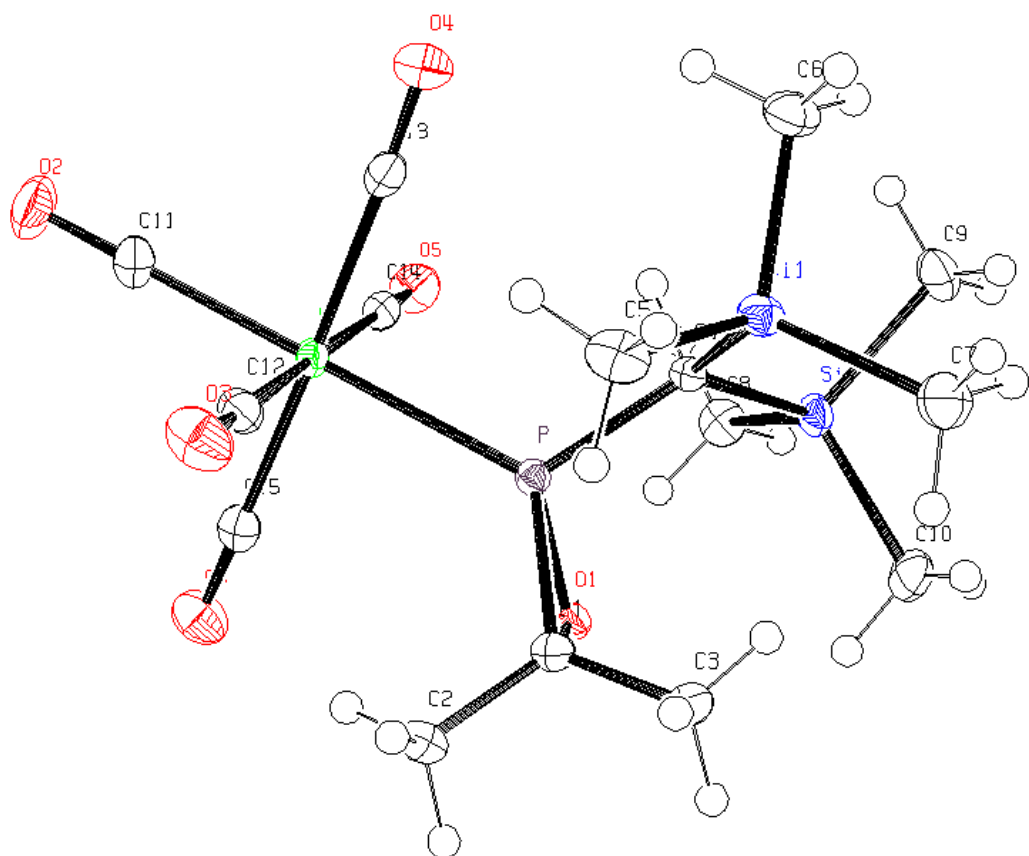


Table viii.1. Crystal data and structure refinement for **[42]**.

Identification code	GSTR100, Greg954
Device Type	X8-KappaApexII
Empirical formula	C15 H25 O6 P Si2 W
Formula weight	572.35

Temperature	100(2) K
Wavelength	0.71073 Å
Crystal system, space group	Monoclinic, P 21/n
Unit cell dimensions	a = 10.8795(3) Å alpha = 90 deg. b = 18.9957(5) Å beta = 108.1870(10) deg.
	c = 11.2893(4) Å gamma = 90 deg.
Volume	2216.53(12) Å ³
Z, Calculated density	4, 1.715 Mg/m ³
Absorption coefficient	5.416 mm ⁻¹
F(000)	1120
Crystal size	0.56 x 0.44 x 0.44 mm
Theta range for data collection	2.86 to 28.00 deg.
Limiting indices	-14<=h<=14, -24<=k<=25, -14<=l<=14
Reflections collected / unique	100210 / 5336 [R(int) = 0.0845]
Completeness to theta = 28.00	99.8 %
Absorption correction	Semi-empirical from equivalents
Max. and min. transmission	0.25339 and 0.12202
Refinement method	Full-matrix least-squares on F ²
Data / restraints / parameters	5336 / 0 / 234
Goodness-of-fit on F ²	1.100
Final R indices [I>2sigma(I)]	R1 = 0.0179, wR2 = 0.0412
R indices (all data)	R1 = 0.0197, wR2 = 0.0416
Largest diff. peak and hole	0.710 and -1.497 e.Å ⁻³

Table viii.2. Atomic coordinates (x 10⁴) and equivalent isotropic displacement parameters (Å² x 10³) for [42]. U(eq) is defined as one third of the trace of the orthogonalized Uij tensor.

	x	y	z	U(eq)
C(1)	2374(2)	2573(1)	3390(2)	17(1)
C(2)	1725(2)	2965(1)	4196(2)	22(1)
C(3)	2161(2)	2897(1)	2131(2)	24(1)
C(4)	3216(2)	1226(1)	2475(2)	14(1)
C(5)	236(2)	1280(1)	1314(2)	25(1)
C(6)	1841(2)	117(1)	616(2)	25(1)
C(7)	1850(2)	1582(1)	-397(2)	29(1)
C(8)	6104(2)	1350(1)	3854(2)	23(1)

C(9)	5200(2)	750(1)	1231(2)	27(1)
C(10)	4983(2)	2318(1)	1635(2)	26(1)
C(11)	2000(2)	362(1)	6701(2)	23(1)
C(12)	555(2)	1294(1)	4767(2)	20(1)
C(13)	1888(2)	112(1)	4212(2)	19(1)
C(14)	4313(2)	614(1)	5972(2)	19(1)
C(15)	3029(2)	1758(1)	6643(2)	19(1)
O(1)	3756(1)	2404(1)	4076(1)	17(1)
O(2)	1722(2)	30(1)	7421(2)	35(1)
O(3)	-493(1)	1466(1)	4391(2)	32(1)
O(4)	1557(1)	-364(1)	3573(1)	28(1)
O(5)	5365(1)	432(1)	6319(1)	26(1)
O(6)	3391(1)	2195(1)	7356(1)	30(1)
Si(1)	1783(1)	1072(1)	998(1)	17(1)
Si(2)	4861(1)	1430(1)	2291(1)	17(1)
P	2864(1)	1674(1)	3739(1)	13(1)
W	2440(1)	949(1)	5398(1)	14(1)

Table viii.3. Bond lengths [Å] and angles [deg] for **[42]**.

C(1)-O(1)	1.495(2)
C(1)-C(3)	1.499(3)
C(1)-C(2)	1.511(3)
C(1)-P	1.7949(18)
C(2)-H(2A)	0.9800
C(2)-H(2B)	0.9800
C(2)-H(2C)	0.9800
C(3)-H(3C)	0.9800
C(3)-H(3B)	0.9800
C(3)-H(3A)	0.9800
C(4)-P	1.8023(18)
C(4)-Si(2)	1.9046(18)
C(4)-Si(1)	1.9164(18)
C(4)-H(4A)	1.0000
C(5)-Si(1)	1.868(2)
C(5)-H(5A)	0.9800
C(5)-H(5B)	0.9800
C(5)-H(5C)	0.9800
C(6)-Si(1)	1.869(2)
C(6)-H(6A)	0.9800
C(6)-H(6B)	0.9800
C(6)-H(6C)	0.9800
C(7)-Si(1)	1.870(2)
C(7)-H(7A)	0.9800
C(7)-H(7B)	0.9800
C(7)-H(7C)	0.9800
C(8)-Si(2)	1.864(2)
C(8)-H(8A)	0.9800
C(8)-H(8B)	0.9800
C(8)-H(8C)	0.9800
C(9)-Si(2)	1.874(2)
C(9)-H(9A)	0.9800
C(9)-H(9B)	0.9800
C(9)-H(9C)	0.9800
C(10)-Si(2)	1.864(2)
C(10)-H(10C)	0.9800
C(10)-H(10B)	0.9800
C(10)-H(10A)	0.9800
C(11)-O(2)	1.143(2)
C(11)-W	2.019(2)
C(12)-O(3)	1.133(2)

C(12)-W	2.0576(19)
C(13)-O(4)	1.142(2)
C(13)-W	2.045(2)
C(14)-O(5)	1.142(2)
C(14)-W	2.0380(18)
C(15)-O(6)	1.137(2)
C(15)-W	2.045(2)
O(1)-P	1.6672(13)
P-W	2.4805(5)
O(1)-C(1)-C(3)	114.35(15)
O(1)-C(1)-C(2)	112.15(15)
C(3)-C(1)-C(2)	113.93(15)
O(1)-C(1)-P	60.08(8)
C(3)-C(1)-P	123.10(14)
C(2)-C(1)-P	119.94(14)
C(1)-C(2)-H(2A)	109.5
C(1)-C(2)-H(2B)	109.5
H(2A)-C(2)-H(2B)	109.5
C(1)-C(2)-H(2C)	109.5
H(2A)-C(2)-H(2C)	109.5
H(2B)-C(2)-H(2C)	109.5
C(1)-C(3)-H(3C)	109.5
C(1)-C(3)-H(3B)	109.5
H(3C)-C(3)-H(3B)	109.5
C(1)-C(3)-H(3A)	109.5
H(3C)-C(3)-H(3A)	109.5
H(3B)-C(3)-H(3A)	109.5
P-C(4)-Si(2)	115.46(9)
P-C(4)-Si(1)	116.41(9)
Si(2)-C(4)-Si(1)	118.27(9)
P-C(4)-H(4A)	100.6
Si(2)-C(4)-H(4A)	100.6
Si(1)-C(4)-H(4A)	100.6
Si(1)-C(5)-H(5A)	109.5
Si(1)-C(5)-H(5B)	109.5
H(5A)-C(5)-H(5B)	109.5
Si(1)-C(5)-H(5C)	109.5
H(5A)-C(5)-H(5C)	109.5
H(5B)-C(5)-H(5C)	109.5
Si(1)-C(6)-H(6A)	109.5
Si(1)-C(6)-H(6B)	109.5
H(6A)-C(6)-H(6B)	109.5
Si(1)-C(6)-H(6C)	109.5
H(6A)-C(6)-H(6C)	109.5
H(6B)-C(6)-H(6C)	109.5
Si(1)-C(7)-H(7A)	109.5
Si(1)-C(7)-H(7B)	109.5
H(7A)-C(7)-H(7B)	109.5
Si(1)-C(7)-H(7C)	109.5
H(7A)-C(7)-H(7C)	109.5
H(7B)-C(7)-H(7C)	109.5
Si(2)-C(8)-H(8A)	109.5
Si(2)-C(8)-H(8B)	109.5
H(8A)-C(8)-H(8B)	109.5
Si(2)-C(8)-H(8C)	109.5
H(8A)-C(8)-H(8C)	109.5
H(8B)-C(8)-H(8C)	109.5
Si(2)-C(9)-H(9A)	109.5
Si(2)-C(9)-H(9B)	109.5
H(9A)-C(9)-H(9B)	109.5
Si(2)-C(9)-H(9C)	109.5
H(9A)-C(9)-H(9C)	109.5

H(9B)-C(9)-H(9C)	109.5
Si(2)-C(10)-H(10C)	109.5
Si(2)-C(10)-H(10B)	109.5
H(10C)-C(10)-H(10B)	109.5
Si(2)-C(10)-H(10A)	109.5
H(10C)-C(10)-H(10A)	109.5
H(10B)-C(10)-H(10A)	109.5
O(2)-C(11)-W	178.42(18)
O(3)-C(12)-W	177.69(17)
O(4)-C(13)-W	177.76(16)
O(5)-C(14)-W	178.49(17)
O(6)-C(15)-W	177.78(16)
C(1)-O(1)-P	68.92(9)
C(5)-Si(1)-C(6)	110.30(10)
C(5)-Si(1)-C(7)	109.02(10)
C(6)-Si(1)-C(7)	107.11(10)
C(5)-Si(1)-C(4)	109.78(9)
C(6)-Si(1)-C(4)	105.81(8)
C(7)-Si(1)-C(4)	114.72(9)
C(8)-Si(2)-C(10)	109.25(10)
C(8)-Si(2)-C(9)	108.61(10)
C(10)-Si(2)-C(9)	108.49(10)
C(8)-Si(2)-C(4)	108.01(8)
C(10)-Si(2)-C(4)	114.36(9)
C(9)-Si(2)-C(4)	107.98(9)
O(1)-P-C(1)	51.00(7)
O(1)-P-C(4)	108.69(7)
C(1)-P-C(4)	113.35(8)
O(1)-P-W	121.41(5)
C(1)-P-W	125.55(6)
C(4)-P-W	118.15(6)
C(11)-W-C(14)	92.11(8)
C(11)-W-C(15)	90.52(8)
C(14)-W-C(15)	87.06(7)
C(11)-W-C(13)	87.68(8)
C(14)-W-C(13)	91.43(7)
C(15)-W-C(13)	177.61(7)
C(11)-W-C(12)	89.45(8)
C(14)-W-C(12)	178.27(7)
C(15)-W-C(12)	93.66(7)
C(13)-W-C(12)	87.90(7)
C(11)-W-P	177.11(6)
C(14)-W-P	90.62(5)
C(15)-W-P	90.56(5)
C(13)-W-P	91.31(5)
C(12)-W-P	87.80(6)

Table viii.4. Anisotropic displacement parameters ($\text{\AA}^2 \times 10^3$) for [42]

The anisotropic displacement factor exponent takes the form:
 $-2 \pi^2 [h^2 a^{*2} U_{11} + \dots + 2 h k a^* b^* U_{12}]$

	U11	U22	U33	U23	U13	U12
C(1)	17(1)	14(1)	19(1)	-1(1)	5(1)	-1(1)
C(2)	24(1)	18(1)	24(1)	-2(1)	9(1)	3(1)
C(3)	33(1)	17(1)	24(1)	4(1)	11(1)	2(1)
C(4)	16(1)	12(1)	14(1)	-1(1)	5(1)	0(1)

C(5)	18(1)	25(1)	28(1)	-5(1)	1(1)	0(1)
C(6)	29(1)	21(1)	24(1)	-6(1)	5(1)	-3(1)
C(7)	40(1)	27(1)	17(1)	1(1)	4(1)	1(1)
C(8)	16(1)	27(1)	26(1)	-2(1)	6(1)	-2(1)
C(9)	30(1)	30(1)	27(1)	-5(1)	16(1)	2(1)
C(10)	27(1)	28(1)	27(1)	0(1)	14(1)	-8(1)
C(11)	23(1)	27(1)	21(1)	2(1)	10(1)	1(1)
C(12)	20(1)	20(1)	21(1)	-4(1)	8(1)	-1(1)
C(13)	17(1)	19(1)	22(1)	6(1)	9(1)	2(1)
C(14)	22(1)	17(1)	19(1)	2(1)	9(1)	1(1)
C(15)	15(1)	23(1)	20(1)	3(1)	5(1)	4(1)
O(1)	16(1)	16(1)	21(1)	-3(1)	6(1)	-2(1)
O(2)	42(1)	38(1)	33(1)	12(1)	21(1)	-1(1)
O(3)	18(1)	36(1)	40(1)	-9(1)	7(1)	3(1)
O(4)	31(1)	21(1)	30(1)	-5(1)	9(1)	-2(1)
O(5)	19(1)	27(1)	33(1)	6(1)	7(1)	5(1)
O(6)	27(1)	33(1)	26(1)	-9(1)	3(1)	-1(1)
Si(1)	19(1)	16(1)	14(1)	-1(1)	2(1)	0(1)
Si(2)	17(1)	20(1)	18(1)	-2(1)	9(1)	-2(1)
P	12(1)	13(1)	13(1)	0(1)	4(1)	0(1)
W	13(1)	15(1)	14(1)	1(1)	6(1)	1(1)

Table viii.5. Hydrogen coordinates ($\times 10^4$) and isotropic displacement parameters ($\text{\AA}^2 \times 10^3$) for [42].

	x	y	z	U(eq)
H(2A)	784	2930	3827	33
H(2B)	1983	3461	4251	33
H(2C)	1987	2758	5033	33
H(3C)	2563	2601	1643	36
H(3B)	2550	3367	2229	36
H(3A)	1231	2934	1697	36
H(4A)	3366	737	2816	17
H(5A)	267	1763	1625	38
H(5B)	117	953	1942	38
H(5C)	-489	1232	543	38
H(6A)	1699	-168	1284	38
H(6B)	2690	6	534	38
H(6C)	1166	14	-171	38
H(7A)	2674	1489	-549	44
H(7B)	1776	2086	-247	44
H(7C)	1134	1437	-1127	44
H(8A)	6084	872	4176	35
H(8B)	5918	1690	4428	35
H(8C)	6962	1444	3780	35
H(9A)	4598	811	387	41
H(9B)	5089	279	1537	41
H(9C)	6090	804	1214	41
H(10C)	5842	2376	1540	39
H(10B)	4849	2680	2200	39
H(10A)	4321	2365	819	39

Table viii.6. Torsion angles [deg] for [42].

C(3)-C(1)-O(1)-P	-115.54(15)
C(2)-C(1)-O(1)-P	112.80(15)

P-C(4)-Si(1)-C(5)	-10.66(13)
Si(2)-C(4)-Si(1)-C(5)	-154.96(10)
P-C(4)-Si(1)-C(6)	-129.67(11)
Si(2)-C(4)-Si(1)-C(6)	86.03(12)
P-C(4)-Si(1)-C(7)	112.48(12)
Si(2)-C(4)-Si(1)-C(7)	-31.81(14)
P-C(4)-Si(2)-C(8)	48.09(12)
Si(1)-C(4)-Si(2)-C(8)	-167.28(10)
P-C(4)-Si(2)-C(10)	-73.76(12)
Si(1)-C(4)-Si(2)-C(10)	70.86(12)
P-C(4)-Si(2)-C(9)	165.38(10)
Si(1)-C(4)-Si(2)-C(9)	-50.00(13)
C(1)-O(1)-P-C(4)	105.33(10)
C(1)-O(1)-P-W	-112.46(9)
C(3)-C(1)-P-O(1)	101.11(18)
C(2)-C(1)-P-O(1)	-99.81(16)
O(1)-C(1)-P-C(4)	-95.72(10)
C(3)-C(1)-P-C(4)	5.39(18)
C(2)-C(1)-P-C(4)	164.47(14)
O(1)-C(1)-P-W	104.22(8)
C(3)-C(1)-P-W	-154.67(13)
C(2)-C(1)-P-W	4.41(17)
Si(2)-C(4)-P-O(1)	23.97(12)
Si(1)-C(4)-P-O(1)	-121.33(9)
Si(2)-C(4)-P-C(1)	78.69(11)
Si(1)-C(4)-P-C(1)	-66.61(12)
Si(2)-C(4)-P-W	-119.66(8)
Si(1)-C(4)-P-W	95.04(9)
O(2)-C(11)-W-C(14)	-154(7)
O(2)-C(11)-W-C(15)	119(7)
O(2)-C(11)-W-C(13)	-62(7)
O(2)-C(11)-W-C(12)	26(7)
O(2)-C(11)-W-P	8(8)
O(5)-C(14)-W-C(11)	-62(7)
O(5)-C(14)-W-C(15)	29(7)
O(5)-C(14)-W-C(13)	-149(7)
O(5)-C(14)-W-C(12)	143(6)
O(5)-C(14)-W-P	119(7)
O(6)-C(15)-W-C(11)	70(5)
O(6)-C(15)-W-C(14)	-22(5)
O(6)-C(15)-W-C(13)	29(6)
O(6)-C(15)-W-C(12)	159(5)
O(6)-C(15)-W-P	-113(5)
O(4)-C(13)-W-C(11)	21(4)
O(4)-C(13)-W-C(14)	113(4)
O(4)-C(13)-W-C(15)	62(5)
O(4)-C(13)-W-C(12)	-69(4)
O(4)-C(13)-W-P	-156(4)
O(3)-C(12)-W-C(11)	-91(5)
O(3)-C(12)-W-C(14)	64(6)
O(3)-C(12)-W-C(15)	178(100)
O(3)-C(12)-W-C(13)	-4(5)
O(3)-C(12)-W-P	88(5)
O(1)-P-W-C(11)	127.5(12)
C(1)-P-W-C(11)	65.5(12)
C(4)-P-W-C(11)	-93.7(12)
O(1)-P-W-C(14)	-71.48(8)
C(1)-P-W-C(14)	-133.45(9)
C(4)-P-W-C(14)	67.36(8)
O(1)-P-W-C(15)	15.59(7)
C(1)-P-W-C(15)	-46.38(9)
C(4)-P-W-C(15)	154.42(8)
O(1)-P-W-C(13)	-162.93(7)

C(1)-P-W-C(13)	135.10(9)
C(4)-P-W-C(13)	-24.09(8)
O(1)-P-W-C(12)	109.23(8)
C(1)-P-W-C(12)	47.26(9)
C(4)-P-W-C(12)	-111.94(8)

ix.[2-Bis(trimethylsilyl)methyl-3-diphenyl-oxaphosphirane-

kP]pentacarbonyltungsten (0) [41]

(A1)

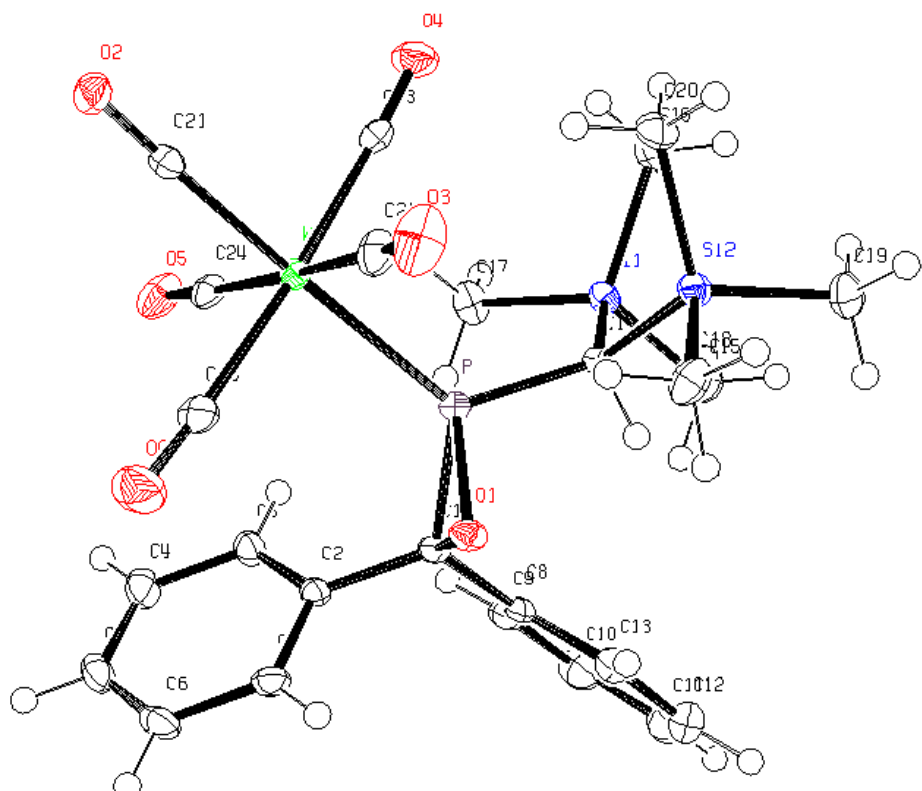


Table ix.1. Crystal data and structure refinement for [41].

Identification code	Greg1216g, GSTR145
Device Type	Bruker X8-KappaApex II
Empirical formula	C ₂₅ H ₂₉ O ₆ P Si ₂ W
Formula weight	696.48

Temperature	100(2) K
Wavelength	0.71073 Å
Crystal system, space group	Orthorhombic, F d d 2
Unit cell dimensions	a = 53.5138(16) Å alpha = 90 deg. b = 21.2300(6) Å beta = 90 deg. c = 10.0069(3) Å gamma = 90 deg.
Volume	11368.8(6) Å ³
Z, Calculated density	16, 1.628 Mg/m ³
Absorption coefficient	4.240 mm ⁻¹
F(000)	5504
Crystal size	0.48 x 0.22 x 0.12 mm
Theta range for data collection	3.49 to 28.00 deg.
Limiting indices	-70<=h<=60, -27<=k<=28, -13<=l<=8
Reflections collected / unique	23349 / 5472 [R(int) = 0.0363]
Completeness to theta = 28.00	99.7 %
Absorption correction	Semi-empirical from equivalents
Refinement method	Full-matrix least-squares on F ²
Data / restraints / parameters	5472 / 32 / 323
Goodness-of-fit on F ²	0.982
Final R indices [I>2sigma(I)]	R1 = 0.0174, wR2 = 0.0361
R indices (all data)	R1 = 0.0189, wR2 = 0.0366
Absolute structure parameter	0.997(5)
Largest diff. peak and hole	0.574 and -0.398 e.Å ⁻³

Table ix.2. Atomic coordinates (x 10⁴) and equivalent isotropic displacement parameters (Å² x 10³) for [41].

U(eq) is defined as one third of the trace of the orthogonalized Uij tensor.

	x	y	z	U(eq)
C(1)	-1808(1)	-5807(1)	8111(3)	14(1)
C(2)	-1931(1)	-6276(1)	7209(3)	14(1)
C(3)	-2187(1)	-6295(1)	7074(3)	18(1)
C(4)	-2300(1)	-6729(1)	6219(3)	24(1)
C(5)	-2155(1)	-7140(2)	5498(3)	25(1)
C(6)	-1897(1)	-7126(1)	5606(3)	25(1)
C(7)	-1784(1)	-6696(1)	6464(3)	19(1)
C(8)	-1746(1)	-5190(1)	7475(3)	17(1)

C(9)	-1934(1)	-4832(1)	6859(3)	22(1)
C(10)	-1877(1)	-4267(1)	6232(3)	28(1)
C(11)	-1634(1)	-4059(2)	6195(4)	32(1)
C(12)	-1447(1)	-4402(2)	6780(4)	32(1)
C(13)	-1503(1)	-4966(2)	7428(3)	23(1)
C(14)	-1762(1)	-5189(1)	10711(3)	13(1)
C(15)	-1951(1)	-3881(1)	10058(3)	25(1)
C(16)	-2120(1)	-4442(1)	12688(3)	21(1)
C(17)	-2330(1)	-4958(1)	10124(3)	22(1)
C(18)	-1260(1)	-5718(1)	11669(4)	23(1)
C(19)	-1423(1)	-4400(1)	12450(4)	23(1)
C(20)	-1662(1)	-5542(1)	13761(3)	21(1)
C(21)	-2181(1)	-7588(1)	11925(3)	16(1)
C(22)	-1714(1)	-7008(2)	11977(3)	22(1)
C(23)	-2184(1)	-6286(1)	12445(3)	18(1)
C(24)	-2370(1)	-6738(1)	9989(3)	18(1)
C(25)	-1914(1)	-7429(1)	9498(3)	21(1)
O(1)	-1596(1)	-6079(1)	8878(2)	16(1)
O(2)	-2259(1)	-8014(1)	12495(2)	23(1)
O(3)	-1535(1)	-7135(1)	12520(3)	38(1)
O(4)	-2278(1)	-5994(1)	13259(2)	28(1)
O(5)	-2561(1)	-6705(1)	9479(2)	29(1)
O(6)	-1849(1)	-7786(1)	8731(3)	37(1)
P	-1835(1)	-5920(1)	9898(1)	12(1)
Si(1)	-2042(1)	-4631(1)	10913(1)	15(1)
Si(2)	-1533(1)	-5225(1)	12166(1)	16(1)
W	-2039(1)	-6838(1)	10980(1)	13(1)

Table ix.3. Bond lengths [Å] and angles [deg] for **[41]**.

C(1)-O(1)	1.485(3)
C(1)-C(8)	1.494(4)
C(1)-C(2)	1.495(4)
C(1)-P	1.811(3)
C(2)-C(3)	1.378(4)
C(2)-C(7)	1.403(4)
C(3)-C(4)	1.395(4)
C(3)-H(3)	0.9500
C(4)-C(5)	1.373(5)
C(4)-H(4)	0.9500
C(5)-C(6)	1.385(5)
C(5)-H(5)	0.9500
C(6)-C(7)	1.391(4)
C(6)-H(6)	0.9500
C(7)-H(7)	0.9500
C(8)-C(13)	1.389(4)
C(8)-C(9)	1.403(5)
C(9)-C(10)	1.387(4)
C(9)-H(9)	0.9500
C(10)-C(11)	1.374(5)
C(10)-H(10)	0.9500
C(11)-C(12)	1.367(5)
C(11)-H(11)	0.9500
C(12)-C(13)	1.393(5)
C(12)-H(12)	0.9500
C(13)-H(13)	0.9500
C(14)-P	1.794(3)
C(14)-Si(2)	1.905(3)
C(14)-Si(1)	1.923(3)
C(14)-H(14)	1.0000
C(15)-Si(1)	1.871(3)

C(15)-H(15A)	0.9800
C(15)-H(15B)	0.9800
C(15)-H(15C)	0.9800
C(16)-Si(1)	1.868(3)
C(16)-H(16A)	0.9800
C(16)-H(16B)	0.9800
C(16)-H(16C)	0.9800
C(17)-Si(1)	1.864(3)
C(17)-H(17A)	0.9800
C(17)-H(17B)	0.9800
C(17)-H(17C)	0.9800
C(18)-Si(2)	1.862(3)
C(18)-H(18A)	0.9800
C(18)-H(18B)	0.9800
C(18)-H(18C)	0.9800
C(19)-Si(2)	1.868(3)
C(19)-H(19A)	0.9800
C(19)-H(19B)	0.9800
C(19)-H(19C)	0.9800
C(20)-Si(2)	1.865(3)
C(20)-H(20A)	0.9800
C(20)-H(20B)	0.9800
C(20)-H(20C)	0.9800
C(21)-O(2)	1.148(3)
C(21)-W	2.002(3)
C(22)-O(3)	1.136(4)
C(22)-W	2.034(3)
C(23)-O(4)	1.141(4)
C(23)-W	2.033(3)
C(24)-O(5)	1.146(4)
C(24)-W	2.042(3)
C(25)-O(6)	1.135(4)
C(25)-W	2.053(3)
O(1)-P	1.671(2)
P-W	2.4802(8)
O(1)-C(1)-C(8)	113.0(2)
O(1)-C(1)-C(2)	112.9(2)
C(8)-C(1)-C(2)	115.1(2)
O(1)-C(1)-P	59.96(13)
C(8)-C(1)-P	123.7(2)
C(2)-C(1)-P	118.3(2)
C(3)-C(2)-C(7)	119.2(3)
C(3)-C(2)-C(1)	121.0(3)
C(7)-C(2)-C(1)	119.8(3)
C(2)-C(3)-C(4)	120.6(3)
C(2)-C(3)-H(3)	119.7
C(4)-C(3)-H(3)	119.7
C(5)-C(4)-C(3)	119.9(3)
C(5)-C(4)-H(4)	120.1
C(3)-C(4)-H(4)	120.1
C(4)-C(5)-C(6)	120.6(3)
C(4)-C(5)-H(5)	119.7
C(6)-C(5)-H(5)	119.7
C(5)-C(6)-C(7)	119.6(3)
C(5)-C(6)-H(6)	120.2
C(7)-C(6)-H(6)	120.2
C(6)-C(7)-C(2)	120.1(3)
C(6)-C(7)-H(7)	119.9
C(2)-C(7)-H(7)	119.9
C(13)-C(8)-C(9)	118.1(3)
C(13)-C(8)-C(1)	121.6(3)
C(9)-C(8)-C(1)	120.2(3)

C(10)-C(9)-C(8)	120.6(3)
C(10)-C(9)-H(9)	119.7
C(8)-C(9)-H(9)	119.7
C(11)-C(10)-C(9)	119.9(3)
C(11)-C(10)-H(10)	120.0
C(9)-C(10)-H(10)	120.0
C(12)-C(11)-C(10)	120.6(3)
C(12)-C(11)-H(11)	119.7
C(10)-C(11)-H(11)	119.7
C(11)-C(12)-C(13)	120.0(3)
C(11)-C(12)-H(12)	120.0
C(13)-C(12)-H(12)	120.0
C(8)-C(13)-C(12)	120.7(3)
C(8)-C(13)-H(13)	119.6
C(12)-C(13)-H(13)	119.6
P-C(14)-Si(2)	116.96(15)
P-C(14)-Si(1)	114.22(15)
Si(2)-C(14)-Si(1)	116.49(14)
P-C(14)-H(14)	101.9
Si(2)-C(14)-H(14)	101.9
Si(1)-C(14)-H(14)	101.9
Si(1)-C(15)-H(15A)	109.5
Si(1)-C(15)-H(15B)	109.5
H(15A)-C(15)-H(15B)	109.5
Si(1)-C(15)-H(15C)	109.5
H(15A)-C(15)-H(15C)	109.5
H(15B)-C(15)-H(15C)	109.5
Si(1)-C(16)-H(16A)	109.5
Si(1)-C(16)-H(16B)	109.5
H(16A)-C(16)-H(16B)	109.5
Si(1)-C(16)-H(16C)	109.5
H(16A)-C(16)-H(16C)	109.5
H(16B)-C(16)-H(16C)	109.5
Si(1)-C(17)-H(17A)	109.5
Si(1)-C(17)-H(17B)	109.5
H(17A)-C(17)-H(17B)	109.5
Si(1)-C(17)-H(17C)	109.5
H(17A)-C(17)-H(17C)	109.5
H(17B)-C(17)-H(17C)	109.5
Si(2)-C(18)-H(18A)	109.5
Si(2)-C(18)-H(18B)	109.5
H(18A)-C(18)-H(18B)	109.5
Si(2)-C(18)-H(18C)	109.5
H(18A)-C(18)-H(18C)	109.5
H(18B)-C(18)-H(18C)	109.5
Si(2)-C(19)-H(19A)	109.5
Si(2)-C(19)-H(19B)	109.5
H(19A)-C(19)-H(19B)	109.5
Si(2)-C(19)-H(19C)	109.5
H(19A)-C(19)-H(19C)	109.5
H(19B)-C(19)-H(19C)	109.5
Si(2)-C(20)-H(20A)	109.5
Si(2)-C(20)-H(20B)	109.5
H(20A)-C(20)-H(20B)	109.5
Si(2)-C(20)-H(20C)	109.5
H(20A)-C(20)-H(20C)	109.5
H(20B)-C(20)-H(20C)	109.5
O(2)-C(21)-W	178.3(3)
O(3)-C(22)-W	176.5(3)
O(4)-C(23)-W	176.2(3)
O(5)-C(24)-W	176.4(3)
O(6)-C(25)-W	175.7(3)
C(1)-O(1)-P	69.74(14)

O(1)-P-C(14)	106.51(12)
O(1)-P-C(1)	50.29(12)
C(14)-P-C(1)	108.45(13)
O(1)-P-W	116.33(7)
C(14)-P-W	125.25(9)
C(1)-P-W	124.73(10)
C(17)-Si(1)-C(16)	107.32(16)
C(17)-Si(1)-C(15)	109.77(16)
C(16)-Si(1)-C(15)	108.11(15)
C(17)-Si(1)-C(14)	111.66(13)
C(16)-Si(1)-C(14)	114.03(14)
C(15)-Si(1)-C(14)	105.86(15)
C(18)-Si(2)-C(20)	108.41(15)
C(18)-Si(2)-C(19)	108.71(15)
C(20)-Si(2)-C(19)	108.95(15)
C(18)-Si(2)-C(14)	108.76(14)
C(20)-Si(2)-C(14)	115.43(14)
C(19)-Si(2)-C(14)	106.41(14)
C(21)-W-C(23)	88.37(12)
C(21)-W-C(22)	87.17(13)
C(23)-W-C(22)	94.34(13)
C(21)-W-C(24)	88.98(12)
C(23)-W-C(24)	87.57(13)
C(22)-W-C(24)	175.65(13)
C(21)-W-C(25)	88.76(12)
C(23)-W-C(25)	176.02(14)
C(22)-W-C(25)	88.28(14)
C(24)-W-C(25)	89.62(13)
C(21)-W-P	176.00(9)
C(23)-W-P	91.73(8)
C(22)-W-P	88.83(9)
C(24)-W-P	95.03(8)
C(25)-W-P	91.33(9)

Table ix.4. Anisotropic displacement parameters ($\text{Å}^2 \times 10^3$) for [41]
The anisotropic displacement factor exponent takes the form:
 $-2 \pi^2 [h^2 a^{*2} U_{11} + \dots + 2 h k a^* b^* U_{12}]$

	U11	U22	U33	U23	U13	U12
C(1)	13(2)	17(1)	11(1)	-1(1)	2(1)	1(1)
C(2)	20(2)	12(1)	10(1)	1(1)	1(1)	-1(1)
C(3)	18(2)	16(2)	19(2)	-3(1)	0(1)	0(1)
C(4)	28(2)	25(2)	18(2)	0(1)	-6(2)	-6(1)
C(5)	46(2)	17(2)	13(2)	0(1)	-2(2)	-8(2)
C(6)	44(2)	14(2)	17(2)	-2(1)	9(2)	2(2)
C(7)	20(2)	17(2)	19(2)	0(1)	8(1)	2(1)
C(8)	26(2)	17(2)	8(1)	-1(1)	3(1)	-6(1)
C(9)	32(2)	20(2)	14(2)	-2(1)	5(1)	-2(1)
C(10)	38(2)	24(1)	23(2)	-1(1)	0(1)	3(1)
C(11)	46(2)	25(1)	23(2)	2(1)	2(1)	-9(1)
C(12)	34(2)	34(2)	29(2)	-5(1)	4(1)	-15(1)
C(13)	28(2)	25(2)	17(2)	-2(1)	1(2)	-6(1)
C(14)	14(2)	14(1)	11(2)	-1(1)	1(1)	-1(1)
C(15)	31(2)	16(2)	27(2)	4(1)	2(2)	0(1)
C(16)	21(2)	19(2)	23(2)	-4(1)	0(1)	4(1)
C(17)	18(2)	21(2)	27(2)	-4(1)	-6(1)	5(1)

C(18)	15(2)	22(2)	31(2)	5(1)	-1(2)	0(1)
C(19)	18(2)	24(2)	27(2)	-4(1)	-5(1)	-2(1)
C(20)	25(2)	25(2)	14(2)	3(1)	-3(1)	0(1)
C(21)	19(2)	16(1)	13(1)	-1(1)	-2(1)	2(1)
C(22)	24(2)	18(2)	25(2)	5(1)	-4(1)	-3(1)
C(23)	20(2)	15(2)	18(2)	3(1)	2(1)	-3(1)
C(24)	19(1)	16(1)	18(2)	6(1)	0(1)	-2(1)
C(25)	29(2)	14(2)	21(2)	4(1)	4(1)	2(1)
O(1)	12(1)	21(1)	15(1)	-2(1)	1(1)	3(1)
O(2)	31(1)	19(1)	21(1)	4(1)	-2(1)	-6(1)
O(3)	31(2)	31(1)	52(2)	15(1)	-18(1)	1(1)
O(4)	40(2)	22(1)	22(1)	-2(1)	10(1)	2(1)
O(5)	23(1)	33(1)	30(1)	14(1)	-6(1)	-6(1)
O(6)	51(1)	27(1)	34(1)	-4(1)	11(1)	5(1)
P	12(1)	13(1)	12(1)	1(1)	0(1)	1(1)
Si(1)	16(1)	13(1)	16(1)	-1(1)	-1(1)	3(1)
Si(2)	14(1)	18(1)	14(1)	0(1)	-2(1)	0(1)
W	16(1)	12(1)	12(1)	1(1)	0(1)	0(1)

Table ix.5. Hydrogen coordinates ($\times 10^4$) and isotropic displacement parameters ($\text{\AA}^2 \times 10^3$) for [41].

	x	y	z	U(eq)
H(3)	-2288	-6009	7568	21
H(4)	-2476	-6741	6137	28
H(5)	-2232	-7436	4919	30
H(6)	-1797	-7408	5097	30
H(7)	-1607	-6686	6546	23
H(9)	-2102	-4978	6872	26
H(10)	-2006	-4025	5829	34
H(11)	-1595	-3674	5758	38
H(12)	-1280	-4255	6746	39
H(13)	-1373	-5199	7842	28
H(14)	-1661	-4969	10012	16
H(15A)	-2091	-3586	10083	37
H(15B)	-1907	-3971	9127	37
H(15C)	-1807	-3695	10517	37
H(16A)	-2250	-4115	12712	32
H(16B)	-1970	-4289	13148	32
H(16C)	-2182	-4822	13135	32
H(17A)	-2376	-5352	10569	33
H(17B)	-2298	-5039	9175	33
H(17C)	-2467	-4654	10212	33
H(18A)	-1129	-5682	12346	34
H(18B)	-1196	-5573	10805	34
H(18C)	-1313	-6159	11593	34
H(19A)	-1563	-4140	12753	35
H(19B)	-1356	-4229	11613	35
H(19C)	-1291	-4400	13131	35
H(20A)	-1532	-5535	14450	32
H(20B)	-1719	-5976	13623	32
H(20C)	-1803	-5281	14049	32

Table ix.6. Torsion angles [deg] for [41].

O(1)-C(1)-C(2)-C(3)

139.2(3)

C(8)-C(1)-C(2)-C(3)	-89.0(3)
P-C(1)-C(2)-C(3)	72.2(3)
O(1)-C(1)-C(2)-C(7)	-42.1(4)
C(8)-C(1)-C(2)-C(7)	89.7(3)
P-C(1)-C(2)-C(7)	-109.2(3)
C(7)-C(2)-C(3)-C(4)	0.6(4)
C(1)-C(2)-C(3)-C(4)	179.3(3)
C(2)-C(3)-C(4)-C(5)	-0.4(5)
C(3)-C(4)-C(5)-C(6)	-0.2(5)
C(4)-C(5)-C(6)-C(7)	0.6(5)
C(5)-C(6)-C(7)-C(2)	-0.4(5)
C(3)-C(2)-C(7)-C(6)	-0.2(4)
C(1)-C(2)-C(7)-C(6)	-178.9(3)
O(1)-C(1)-C(8)-C(13)	10.6(4)
C(2)-C(1)-C(8)-C(13)	-121.1(3)
P-C(1)-C(8)-C(13)	78.9(4)
O(1)-C(1)-C(8)-C(9)	-171.8(2)
C(2)-C(1)-C(8)-C(9)	56.4(4)
P-C(1)-C(8)-C(9)	-103.6(3)
C(13)-C(8)-C(9)-C(10)	-0.5(5)
C(1)-C(8)-C(9)-C(10)	-178.1(3)
C(8)-C(9)-C(10)-C(11)	0.9(5)
C(9)-C(10)-C(11)-C(12)	-0.5(5)
C(10)-C(11)-C(12)-C(13)	-0.3(5)
C(9)-C(8)-C(13)-C(12)	-0.3(5)
C(1)-C(8)-C(13)-C(12)	177.3(3)
C(11)-C(12)-C(13)-C(8)	0.7(5)
C(8)-C(1)-O(1)-P	116.8(2)
C(2)-C(1)-O(1)-P	-110.4(2)
C(1)-O(1)-P-C(14)	-100.54(16)
C(1)-O(1)-P-W	114.54(13)
Si(2)-C(14)-P-O(1)	-79.07(17)
Si(1)-C(14)-P-O(1)	139.91(14)
Si(2)-C(14)-P-C(1)	-131.94(16)
Si(1)-C(14)-P-C(1)	87.03(17)
Si(2)-C(14)-P-W	61.83(19)
Si(1)-C(14)-P-W	-79.19(16)
C(8)-C(1)-P-O(1)	-99.1(3)
C(2)-C(1)-P-O(1)	101.5(3)
O(1)-C(1)-P-C(14)	96.45(16)
C(8)-C(1)-P-C(14)	-2.6(3)
C(2)-C(1)-P-C(14)	-162.0(2)
O(1)-C(1)-P-W	-97.24(14)
C(8)-C(1)-P-W	163.7(2)
C(2)-C(1)-P-W	4.3(3)
P-C(14)-Si(1)-C(17)	-3.2(2)
Si(2)-C(14)-Si(1)-C(17)	-144.37(17)
P-C(14)-Si(1)-C(16)	118.71(16)
Si(2)-C(14)-Si(1)-C(16)	-22.5(2)
P-C(14)-Si(1)-C(15)	-122.57(17)
Si(2)-C(14)-Si(1)-C(15)	96.21(18)
P-C(14)-Si(2)-C(18)	46.4(2)
Si(1)-C(14)-Si(2)-C(18)	-173.45(15)
P-C(14)-Si(2)-C(20)	-75.6(2)
Si(1)-C(14)-Si(2)-C(20)	64.49(19)
P-C(14)-Si(2)-C(19)	163.36(17)
Si(1)-C(14)-Si(2)-C(19)	-56.5(2)
O(2)-C(21)-W-C(23)	-60(11)
O(2)-C(21)-W-C(22)	35(11)
O(2)-C(21)-W-C(24)	-147(11)
O(2)-C(21)-W-C(25)	123(11)
O(2)-C(21)-W-P	32(12)
O(4)-C(23)-W-C(21)	-48(4)

O(4)-C(23)-W-C(22)	-135(4)
O(4)-C(23)-W-C(24)	41(4)
O(4)-C(23)-W-C(25)	-4(6)
O(4)-C(23)-W-P	136(4)
O(3)-C(22)-W-C(21)	43(5)
O(3)-C(22)-W-C(23)	131(5)
O(3)-C(22)-W-C(24)	15(6)
O(3)-C(22)-W-C(25)	-46(5)
O(3)-C(22)-W-P	-137(5)
O(5)-C(24)-W-C(21)	12(5)
O(5)-C(24)-W-C(23)	-76(5)
O(5)-C(24)-W-C(22)	40(6)
O(5)-C(24)-W-C(25)	101(5)
O(5)-C(24)-W-P	-168(5)
O(6)-C(25)-W-C(21)	-14(4)
O(6)-C(25)-W-C(23)	-58(5)
O(6)-C(25)-W-C(22)	73(4)
O(6)-C(25)-W-C(24)	-103(4)
O(6)-C(25)-W-P	162(4)
O(1)-P-W-C(21)	67.9(13)
C(14)-P-W-C(21)	-69.6(13)
C(1)-P-W-C(21)	126.3(13)
O(1)-P-W-C(23)	159.27(12)
C(14)-P-W-C(23)	21.70(15)
C(1)-P-W-C(23)	-142.35(15)
O(1)-P-W-C(22)	64.96(13)
C(14)-P-W-C(22)	-72.61(15)
C(1)-P-W-C(22)	123.34(16)
O(1)-P-W-C(24)	-113.03(13)
C(14)-P-W-C(24)	109.40(15)
C(1)-P-W-C(24)	-54.64(15)
O(1)-P-W-C(25)	-23.29(13)
C(14)-P-W-C(25)	-160.86(15)
C(1)-P-W-C(25)	35.09(16)

x. [1-Oxa-2-(bis(trimethylsilyl)methyl)phosphaspiro[2.5]octane-
*k*P]pentacarbonyltungsten (0) **[46a]**

(B1)

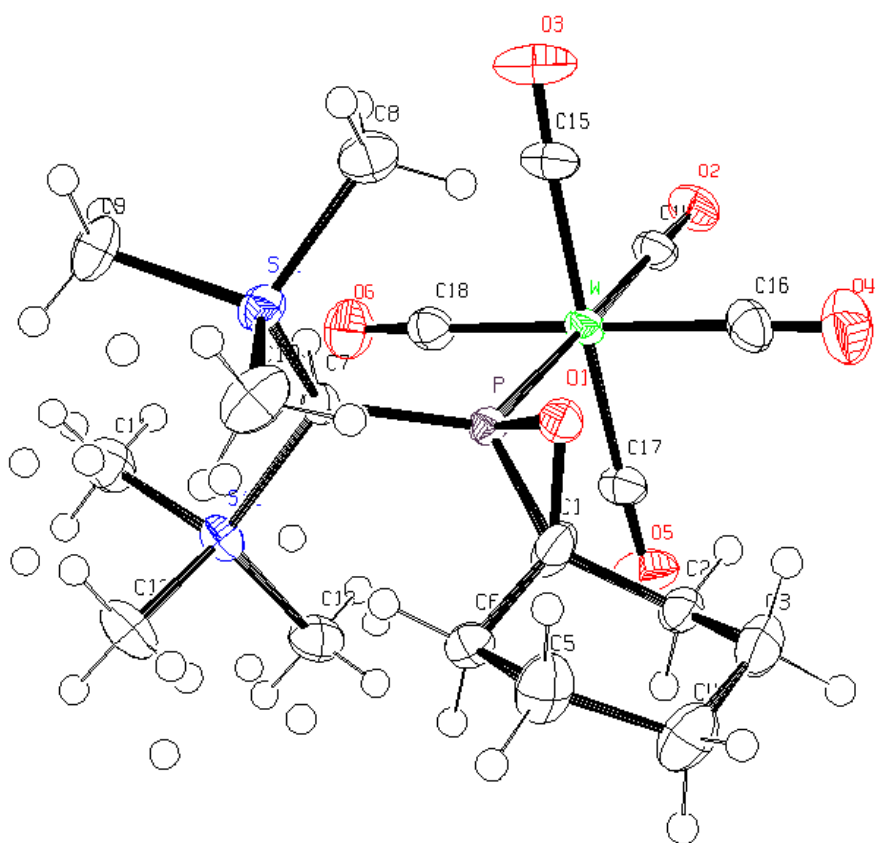


Table x.1. Crystal data and structure refinement for **[46a]**.

Identification code	GSTR138, Greg1236f
Device Type	Bruker X8-KappaApex II
Empirical formula	C ₁₈ H ₂₉ O ₆ P Si ₂ W
Formula weight	612.41
Temperature	100(2) K
Wavelength	0.71073 Å
Crystal system, space group	Triclinic, P -1
Unit cell dimensions deg.	a = 9.0075(3) Å alpha = 72.526(2) b = 10.6148(4) Å beta = 79.663(2) deg.

	c = 14.7863(6) Å	gamma =
66.018(2) deg.		
Volume	1229.43(8) Å ³	
Z, Calculated density	2, 1.654 Mg/m ³	
Absorption coefficient	4.888 mm ⁻¹	
F(000)	604	
Crystal size	0.600 x 0.357 x 0.162 mm	
Theta range for data collection	2.48 to 28.00 deg.	
Limiting indices	-11<=h<=11, -10<=k<=14, -19<=l<=19	
Reflections collected / unique	18872 / 5858 [R(int) = 0.0286]	
Completeness to theta = 28.00	98.8 %	
Absorption correction	Semi-empirical from equivalents	
Max. and min. transmission	0.45765 and 0.14175	
Refinement method	Full-matrix least-squares on F ²	
Data / restraints / parameters	5858 / 30 / 341	
Goodness-of-fit on F ²	1.116	
Final R indices [I>2sigma(I)]	R1 = 0.0227, wR2 = 0.0496	
R indices (all data)	R1 = 0.0267, wR2 = 0.0511	
Largest diff. peak and hole	1.699 and -1.139 e.Å ⁻³	

Table x.2. Atomic coordinates (x 10⁴) and equivalent isotropic displacement parameters (Å² x 10³) for **[46a]**.
U(eq) is defined as one third of the trace of the orthogonalized Uij tensor.

	x	y	z	U(eq)
C(1)	7818(4)	3847(3)	8600(2)	34(1)
C(2)	8239(4)	4925(4)	8892(3)	26(1)
C(2S)	7020(20)	5003(17)	9284(13)	34(4)
C(3)	8207(4)	4561(4)	9949(3)	42(1)
C(4)	9289(5)	3049(4)	10389(3)	40(1)
C(5)	9093(5)	1962(3)	10006(2)	40(1)
C(6)	9076(4)	2338(3)	8934(3)	24(1)
C(6S)	8000(20)	2339(16)	9382(11)	30(4)
C(7)	6851(3)	2894(3)	7159(2)	20(1)
C(8)	3535(5)	2919(5)	8186(4)	44(1)
C(9)	5477(6)	784(5)	7042(3)	38(1)
C(10)	6555(6)	441(5)	8968(3)	39(1)
C(10S)	6990(20)	-177(19)	8558(14)	37(2)
C(8S)	4160(20)	2600(20)	8714(17)	43(3)
C(9S)	4630(30)	1480(20)	7015(15)	41(3)
C(11)	8559(5)	1888(5)	5399(3)	36(1)

C(12)	10085(5)	148(4)	7247(3)	36(1)
C(13)	10166(5)	3127(5)	6332(4)	33(1)
C(12S)	10571(16)	720(17)	7527(12)	31(4)
C(11S)	8880(20)	1000(20)	5822(15)	41(4)
C(13S)	9830(20)	3380(19)	5866(14)	30(4)
C(14)	4075(3)	8817(3)	5883(2)	27(1)
C(15)	3131(3)	6474(3)	6884(3)	35(1)
C(16)	4625(4)	7568(3)	7849(3)	33(1)
C(17)	7350(3)	7200(3)	6479(2)	28(1)
C(18)	5878(3)	6131(3)	5449(2)	29(1)
O(1)	6171(3)	3978(2)	8784(2)	24(1)
O(1S)	8583(6)	4126(14)	7680(5)	52(4)
O(2)	3381(2)	9954(2)	5453(2)	35(1)
O(3)	1929(3)	6311(3)	7036(2)	58(1)
O(4)	4296(4)	8009(3)	8505(2)	52(1)
O(5)	8501(3)	7430(3)	6389(2)	42(1)
O(6)	6223(3)	5766(2)	4760(2)	41(1)
Si(1)	5666(1)	1739(1)	7863(1)	25(1)
Si(2)	8951(1)	1999(1)	6576(1)	24(1)
P	6642(1)	4374(1)	7611(1)	19(1)
W	5244(1)	6828(1)	6658(1)	22(1)

Table x.3. Bond lengths [Å] and angles [deg] for **[46a]**.

C(1)-O(1S)	1.414(4)
C(1)-O(1)	1.416(4)
C(1)-C(2)	1.531(4)
C(1)-C(6)	1.531(4)
C(1)-C(6S)	1.634(14)
C(1)-C(2S)	1.676(16)
C(1)-P	1.778(3)
C(2)-C(3)	1.491(5)
C(2)-H(2A)	0.9900
C(2)-H(2B)	0.9900
C(2S)-C(3)	1.424(15)
C(2S)-H(2S1)	0.9900
C(2S)-H(2S2)	0.9900
C(3)-C(4)	1.509(5)
C(3)-H(3A)	0.9900
C(3)-H(3B)	0.9900
C(4)-C(5)	1.509(5)
C(4)-H(4A)	0.9900
C(4)-H(4B)	0.9900
C(5)-C(6S)	1.328(16)
C(5)-C(6)	1.515(5)
C(5)-H(5A)	0.9900
C(5)-H(5B)	0.9900
C(6)-H(6A)	0.9900
C(6)-H(6B)	0.9900
C(6S)-H(6S1)	0.9900
C(6S)-H(6S2)	0.9900
C(7)-P	1.816(3)
C(7)-Si(1)	1.903(3)
C(7)-Si(2)	1.916(3)
C(7)-H(7)	1.0000
C(8)-Si(1)	1.886(4)
C(8)-H(8A)	0.9800
C(8)-H(8B)	0.9800
C(8)-H(8C)	0.9800
C(9)-Si(1)	1.867(4)
C(9)-H(9A)	0.9800

C(9)-H(9B)	0.9800
C(9)-H(9C)	0.9800
C(10)-Si(1)	1.852(4)
C(10)-H(10A)	0.9800
C(10)-H(10B)	0.9800
C(10)-H(10C)	0.9800
C(10S)-Si(1)	1.957(18)
C(10S)-H(10D)	0.9800
C(10S)-H(10E)	0.9800
C(10S)-H(10F)	0.9800
C(8S)-Si(1)	1.83(2)
C(8S)-H(8SA)	0.9800
C(8S)-H(8SB)	0.9800
C(8S)-H(8SC)	0.9800
C(9S)-Si(1)	1.831(19)
C(9S)-H(9SA)	0.9800
C(9S)-H(9SB)	0.9800
C(9S)-H(9SC)	0.9800
C(11)-Si(2)	1.883(4)
C(11)-H(11A)	0.9800
C(11)-H(11B)	0.9800
C(11)-H(11C)	0.9800
C(12)-Si(2)	1.857(4)
C(12)-H(12A)	0.9800
C(12)-H(12B)	0.9800
C(12)-H(12C)	0.9800
C(13)-Si(2)	1.851(5)
C(13)-H(13A)	0.9800
C(13)-H(13B)	0.9800
C(13)-H(13C)	0.9800
C(12S)-Si(2)	1.982(16)
C(12S)-H(12D)	0.9800
C(12S)-H(12E)	0.9800
C(12S)-H(12F)	0.9800
C(11S)-Si(2)	1.779(19)
C(11S)-H(11D)	0.9800
C(11S)-H(11E)	0.9800
C(11S)-H(11F)	0.9800
C(13S)-Si(2)	1.899(19)
C(13S)-H(13D)	0.9800
C(13S)-H(13E)	0.9800
C(13S)-H(13F)	0.9800
C(14)-O(2)	1.149(3)
C(14)-W	2.013(3)
C(15)-O(3)	1.138(4)
C(15)-W	2.039(3)
C(16)-O(4)	1.141(4)
C(16)-W	2.039(3)
C(17)-O(5)	1.136(3)
C(17)-W	2.047(3)
C(18)-O(6)	1.144(4)
C(18)-W	2.038(3)
O(1)-P	1.676(3)
O(1S)-P	1.677(3)
P-W	2.4740(7)
O(1S)-C(1)-O(1)	124.3(3)
O(1S)-C(1)-C(2)	92.4(5)
O(1)-C(1)-C(2)	115.7(3)
O(1S)-C(1)-C(6)	95.1(5)
O(1)-C(1)-C(6)	115.2(3)
C(2)-C(1)-C(6)	110.7(3)
O(1S)-C(1)-C(6S)	130.5(9)

O(1)-C(1)-C(6S)	79.0(6)
C(2)-C(1)-C(6S)	117.6(6)
C(6)-C(1)-C(6S)	39.4(6)
O(1S)-C(1)-C(2S)	125.1(9)
O(1)-C(1)-C(2S)	76.0(6)
C(2)-C(1)-C(2S)	41.0(6)
C(6)-C(1)-C(2S)	123.4(6)
C(6S)-C(1)-C(2S)	101.4(9)
O(1S)-C(1)-P	62.16(16)
O(1)-C(1)-P	62.10(15)
C(2)-C(1)-P	121.2(2)
C(6)-C(1)-P	122.8(2)
C(6S)-C(1)-P	118.8(6)
C(2S)-C(1)-P	111.5(6)
C(3)-C(2)-C(1)	108.9(3)
C(3)-C(2)-H(2A)	109.9
C(1)-C(2)-H(2A)	109.9
C(3)-C(2)-H(2B)	109.9
C(1)-C(2)-H(2B)	109.9
H(2A)-C(2)-H(2B)	108.3
C(3)-C(2S)-C(1)	104.7(9)
C(3)-C(2S)-H(2S1)	110.8
C(1)-C(2S)-H(2S1)	110.8
C(3)-C(2S)-H(2S2)	110.8
C(1)-C(2S)-H(2S2)	110.8
H(2S1)-C(2S)-H(2S2)	108.9
C(2S)-C(3)-C(2)	45.6(8)
C(2S)-C(3)-C(4)	126.7(7)
C(2)-C(3)-C(4)	114.0(3)
C(2S)-C(3)-H(3A)	63.2
C(2)-C(3)-H(3A)	108.8
C(4)-C(3)-H(3A)	108.8
C(2S)-C(3)-H(3B)	124.2
C(2)-C(3)-H(3B)	108.8
C(4)-C(3)-H(3B)	108.8
H(3A)-C(3)-H(3B)	107.7
C(3)-C(4)-C(5)	113.3(3)
C(3)-C(4)-H(4A)	108.9
C(5)-C(4)-H(4A)	108.9
C(3)-C(4)-H(4B)	108.9
C(5)-C(4)-H(4B)	108.9
H(4A)-C(4)-H(4B)	107.7
C(6S)-C(5)-C(4)	121.5(7)
C(6S)-C(5)-C(6)	43.6(7)
C(4)-C(5)-C(6)	114.6(3)
C(6S)-C(5)-H(5A)	65.8
C(4)-C(5)-H(5A)	108.6
C(6)-C(5)-H(5A)	108.6
C(6S)-C(5)-H(5B)	129.1
C(4)-C(5)-H(5B)	108.6
C(6)-C(5)-H(5B)	108.6
H(5A)-C(5)-H(5B)	107.6
C(5)-C(6)-C(1)	108.8(3)
C(5)-C(6)-H(6A)	109.9
C(1)-C(6)-H(6A)	109.9
C(5)-C(6)-H(6B)	109.9
C(1)-C(6)-H(6B)	109.9
H(6A)-C(6)-H(6B)	108.3
C(5)-C(6S)-C(1)	113.1(10)
C(5)-C(6S)-H(6S1)	109.0
C(1)-C(6S)-H(6S1)	109.0
C(5)-C(6S)-H(6S2)	109.0
C(1)-C(6S)-H(6S2)	109.0

H(6S1)-C(6S)-H(6S2)	107.8
P-C(7)-Si(1)	116.38(15)
P-C(7)-Si(2)	115.27(13)
Si(1)-C(7)-Si(2)	118.57(13)
P-C(7)-H(7)	100.5
Si(1)-C(7)-H(7)	100.5
Si(2)-C(7)-H(7)	100.5
Si(1)-C(8)-H(8A)	109.5
Si(1)-C(8)-H(8B)	109.5
Si(1)-C(8)-H(8C)	109.5
Si(1)-C(9)-H(9A)	109.5
Si(1)-C(9)-H(9B)	109.5
Si(1)-C(9)-H(9C)	109.5
Si(1)-C(10)-H(10A)	109.5
Si(1)-C(10)-H(10B)	109.5
Si(1)-C(10)-H(10C)	109.5
Si(1)-C(10S)-H(10D)	109.5
Si(1)-C(10S)-H(10E)	109.5
H(10D)-C(10S)-H(10E)	109.5
Si(1)-C(10S)-H(10F)	109.5
H(10D)-C(10S)-H(10F)	109.5
H(10E)-C(10S)-H(10F)	109.5
Si(1)-C(8S)-H(8SA)	109.5
Si(1)-C(8S)-H(8SB)	109.5
H(8SA)-C(8S)-H(8SB)	109.5
Si(1)-C(8S)-H(8SC)	109.5
H(8SA)-C(8S)-H(8SC)	109.5
H(8SB)-C(8S)-H(8SC)	109.5
Si(1)-C(9S)-H(9SA)	109.5
Si(1)-C(9S)-H(9SB)	109.5
H(9SA)-C(9S)-H(9SB)	109.5
Si(1)-C(9S)-H(9SC)	109.5
H(9SA)-C(9S)-H(9SC)	109.5
H(9SB)-C(9S)-H(9SC)	109.5
Si(2)-C(11)-H(11A)	109.5
Si(2)-C(11)-H(11B)	109.5
Si(2)-C(11)-H(11C)	109.5
Si(2)-C(12)-H(12A)	109.5
Si(2)-C(12)-H(12B)	109.5
Si(2)-C(12)-H(12C)	109.5
Si(2)-C(13)-H(13A)	109.5
Si(2)-C(13)-H(13B)	109.5
Si(2)-C(13)-H(13C)	109.5
Si(2)-C(12S)-H(12D)	109.5
Si(2)-C(12S)-H(12E)	109.5
H(12D)-C(12S)-H(12E)	109.5
Si(2)-C(12S)-H(12F)	109.5
H(12D)-C(12S)-H(12F)	109.5
H(12E)-C(12S)-H(12F)	109.5
Si(2)-C(11S)-H(11D)	109.5
Si(2)-C(11S)-H(11E)	109.5
H(11D)-C(11S)-H(11E)	109.5
Si(2)-C(11S)-H(11F)	109.5
H(11D)-C(11S)-H(11F)	109.5
H(11E)-C(11S)-H(11F)	109.5
Si(2)-C(13S)-H(13D)	109.5
Si(2)-C(13S)-H(13E)	109.5
H(13D)-C(13S)-H(13E)	109.5
Si(2)-C(13S)-H(13F)	109.5
H(13D)-C(13S)-H(13F)	109.5
H(13E)-C(13S)-H(13F)	109.5
O(2)-C(14)-W	178.7(3)
O(3)-C(15)-W	177.1(3)

O(4)-C(16)-W	178.2(3)
O(5)-C(17)-W	178.5(3)
O(6)-C(18)-W	178.7(3)
C(1)-O(1)-P	69.59(17)
C(1)-O(1S)-P	69.60(17)
C(8S)-Si(1)-C(9S)	109.4(10)
C(8S)-Si(1)-C(10)	81.9(8)
C(9S)-Si(1)-C(10)	127.2(6)
C(8S)-Si(1)-C(9)	129.9(6)
C(9S)-Si(1)-C(9)	25.4(6)
C(10)-Si(1)-C(9)	109.9(2)
C(8S)-Si(1)-C(8)	29.3(7)
C(9S)-Si(1)-C(8)	82.9(7)
C(10)-Si(1)-C(8)	108.0(2)
C(9)-Si(1)-C(8)	106.8(2)
C(8S)-Si(1)-C(7)	111.0(6)
C(9S)-Si(1)-C(7)	107.6(6)
C(10)-Si(1)-C(7)	115.87(15)
C(9)-Si(1)-C(7)	106.61(16)
C(8)-Si(1)-C(7)	109.36(16)
C(8S)-Si(1)-C(10S)	107.8(9)
C(9S)-Si(1)-C(10S)	105.6(8)
C(10)-Si(1)-C(10S)	28.6(6)
C(9)-Si(1)-C(10S)	83.8(6)
C(8)-Si(1)-C(10S)	128.8(6)
C(7)-Si(1)-C(10S)	115.2(5)
C(11S)-Si(2)-C(13)	126.1(7)
C(11S)-Si(2)-C(12)	78.6(7)
C(13)-Si(2)-C(12)	111.7(2)
C(11S)-Si(2)-C(11)	29.1(7)
C(13)-Si(2)-C(11)	107.6(2)
C(12)-Si(2)-C(11)	106.8(2)
C(11S)-Si(2)-C(13S)	109.3(10)
C(13)-Si(2)-C(13S)	22.5(6)
C(12)-Si(2)-C(13S)	127.2(6)
C(11)-Si(2)-C(13S)	86.5(7)
C(11S)-Si(2)-C(7)	112.2(6)
C(13)-Si(2)-C(7)	110.54(17)
C(12)-Si(2)-C(7)	113.94(15)
C(11)-Si(2)-C(7)	105.76(16)
C(13S)-Si(2)-C(7)	110.5(6)
C(11S)-Si(2)-C(12S)	108.4(8)
C(13)-Si(2)-C(12S)	83.7(5)
C(12)-Si(2)-C(12S)	32.4(5)
C(11)-Si(2)-C(12S)	133.4(5)
C(13S)-Si(2)-C(12S)	103.9(8)
C(7)-Si(2)-C(12S)	112.2(5)
O(1)-P-O(1S)	96.5(3)
O(1)-P-C(1)	48.31(13)
O(1S)-P-C(1)	48.23(14)
O(1)-P-C(7)	108.46(12)
O(1S)-P-C(7)	102.6(5)
C(1)-P-C(7)	113.27(13)
O(1)-P-W	118.69(8)
O(1S)-P-W	108.6(4)
C(1)-P-W	127.26(10)
C(7)-P-W	118.43(9)
C(14)-W-C(16)	89.42(12)
C(14)-W-C(18)	89.52(12)
C(16)-W-C(18)	178.54(11)
C(14)-W-C(15)	89.64(12)
C(16)-W-C(15)	88.94(13)
C(18)-W-C(15)	92.05(13)

C(14)-W-C(17)	90.65(11)
C(16)-W-C(17)	88.95(13)
C(18)-W-C(17)	90.07(12)
C(15)-W-C(17)	177.86(13)
C(14)-W-P	179.06(8)
C(16)-W-P	90.71(9)
C(18)-W-P	90.37(8)
C(15)-W-P	89.43(9)
C(17)-W-P	90.29(8)

Table x.4. Anisotropic displacement parameters ($\text{\AA}^2 \times 10^3$) for [46a]
The anisotropic displacement factor exponent takes the form:
 $-2 \pi^2 [h^2 a^{*2} U_{11} + \dots + 2 h k a^* b^* U_{12}]$

	U11	U22	U33	U23	U13	U12
C(1)	44(2)	24(1)	38(2)	-7(1)	-22(2)	-11(1)
C(2)	27(2)	23(2)	32(2)	-8(1)	-6(2)	-11(1)
C(2S)	30(8)	38(8)	38(11)	-19(7)	-12(7)	-8(7)
C(3)	47(2)	42(2)	43(2)	-22(2)	-12(2)	-13(2)
C(4)	56(2)	44(2)	27(2)	-5(1)	-11(2)	-25(2)
C(5)	57(2)	35(2)	26(2)	-3(1)	-13(2)	-15(2)
C(6)	25(2)	23(2)	22(2)	-2(1)	-5(2)	-10(1)
C(6S)	46(9)	32(8)	11(8)	7(6)	-2(7)	-23(7)
C(7)	20(1)	18(1)	22(2)	-6(1)	-1(1)	-7(1)
C(8)	30(2)	49(2)	64(4)	-24(2)	10(2)	-25(2)
C(9)	52(3)	32(2)	43(3)	-10(2)	-3(2)	-28(2)
C(10)	52(3)	45(2)	28(3)	1(2)	-4(2)	-34(2)
C(10S)	48(4)	44(4)	29(5)	-1(4)	-7(4)	-31(4)
C(8S)	31(4)	47(4)	63(5)	-22(4)	10(4)	-26(4)
C(9S)	50(5)	35(4)	43(4)	-6(4)	-3(4)	-25(4)
C(11)	36(2)	40(2)	29(2)	-13(2)	1(2)	-9(2)
C(12)	32(2)	26(2)	35(2)	-6(2)	1(2)	1(2)
C(13)	24(2)	41(2)	34(3)	-10(2)	6(2)	-14(2)
C(12S)	10(6)	29(7)	39(10)	-3(7)	8(6)	-1(5)
C(11S)	28(8)	44(11)	49(13)	-15(9)	-5(8)	-8(8)
C(13S)	26(9)	33(9)	20(10)	-5(8)	7(7)	-4(7)
C(14)	21(1)	22(1)	33(2)	-6(1)	-4(1)	-4(1)
C(15)	19(1)	38(2)	43(2)	-7(1)	-6(1)	-8(1)
C(16)	33(2)	26(1)	41(2)	-12(1)	6(1)	-12(1)
C(17)	22(1)	26(1)	33(2)	-4(1)	-5(1)	-7(1)
C(18)	26(1)	24(1)	32(2)	-4(1)	-6(1)	-7(1)
O(1)	22(1)	29(1)	25(1)	-11(1)	3(1)	-12(1)
O(1S)	52(4)	52(4)	53(4)	-13(1)	-4(1)	-20(2)
O(2)	29(1)	25(1)	39(1)	-3(1)	-5(1)	-3(1)
O(3)	25(1)	74(2)	71(2)	-8(2)	-9(1)	-21(1)
O(4)	65(2)	53(2)	48(2)	-27(1)	20(1)	-30(1)
O(5)	30(1)	45(1)	50(2)	-1(1)	-8(1)	-19(1)
O(6)	52(1)	41(1)	31(2)	-11(1)	-2(1)	-19(1)
Si(1)	26(1)	25(1)	28(1)	-6(1)	-1(1)	-14(1)
Si(2)	23(1)	21(1)	22(1)	-5(1)	2(1)	-5(1)
P	18(1)	18(1)	23(1)	-5(1)	-3(1)	-7(1)
W	18(1)	17(1)	29(1)	-5(1)	-4(1)	-4(1)

Table x.5. Hydrogen coordinates ($\times 10^4$) and isotropic displacement parameters ($\text{\AA}^2 \times 10^3$) for [46a].

	X	Y	Z	U(eq)
H(2A)	9334	4895	8614	31
H(2B)	7440	5900	8654	31
H(2S1)	6823	5989	8898	40
H(2S2)	5974	4959	9613	40
H(3A)	7073	4714	10211	50
H(3B)	8547	5220	10135	50
H(4A)	9038	2834	11085	48
H(4B)	10438	2965	10271	48
H(5A)	8063	1839	10291	48
H(5B)	9996	1035	10213	48
H(6A)	8790	1651	8743	28
H(6B)	10168	2290	8638	28
H(6S1)	6930	2421	9727	36
H(6S2)	8319	1581	9045	36
H(7)	6201	3416	6586	24
H(8A)	2969	3498	7605	65
H(8B)	3585	3545	8540	65
H(8C)	2943	2326	8580	65
H(9A)	6539	54	6931	57
H(9B)	5102	1466	6436	57
H(9C)	4690	330	7328	57
H(10A)	5945	-186	9228	58
H(10B)	6495	953	9434	58
H(10C)	7696	-131	8826	58
H(10D)	7820	-662	8117	55
H(10E)	6295	-719	8851	55
H(10F)	7528	-109	9053	55
H(8SA)	4712	2724	9175	65
H(8SB)	3533	2006	9047	65
H(8SC)	3419	3534	8376	65
H(9SA)	5439	1024	6555	61
H(9SB)	3873	2404	6681	61
H(9SC)	4028	869	7357	61
H(11A)	7903	2840	5037	55
H(11B)	7971	1250	5507	55
H(11C)	9598	1516	5041	55
H(12A)	11088	-278	6876	54
H(12B)	9407	-416	7365	54
H(12C)	10360	163	7855	54
H(13A)	10438	3164	6934	50
H(13B)	9533	4092	5977	50
H(13C)	11171	2721	5956	50
H(12D)	10658	1264	7932	46
H(12E)	11633	312	7200	46
H(12F)	10222	-49	7920	46
H(11D)	8501	241	6196	61
H(11E)	9977	573	5531	61
H(11F)	8138	1628	5323	61
H(13D)	9842	3951	6275	45
H(13E)	9164	4003	5330	45
H(13F)	10948	2898	5625	45

Table x.6. Torsion angles [deg] for [46a].

O(1S)-C(1)-C(2)-C(3)	-157.9(4)
O(1)-C(1)-C(2)-C(3)	71.9(4)
C(6)-C(1)-C(2)-C(3)	-61.5(4)
C(6S)-C(1)-C(2)-C(3)	-18.8(8)
C(2S)-C(1)-C(2)-C(3)	56.1(9)
P-C(1)-C(2)-C(3)	143.5(3)
O(1S)-C(1)-C(2S)-C(3)	-101.2(10)
O(1)-C(1)-C(2S)-C(3)	136.5(11)
C(2)-C(1)-C(2S)-C(3)	-58.2(8)
C(6)-C(1)-C(2S)-C(3)	25.3(14)
C(6S)-C(1)-C(2S)-C(3)	61.0(12)
P-C(1)-C(2S)-C(3)	-171.5(7)
C(1)-C(2S)-C(3)-C(2)	53.2(7)
C(1)-C(2S)-C(3)-C(4)	-35.6(15)
C(1)-C(2)-C(3)-C(2S)	-63.7(9)
C(1)-C(2)-C(3)-C(4)	54.9(4)
C(2S)-C(3)-C(4)-C(5)	3.9(11)
C(2)-C(3)-C(4)-C(5)	-47.5(4)
C(3)-C(4)-C(5)-C(6S)	-3.3(10)
C(3)-C(4)-C(5)-C(6)	45.9(5)
C(6S)-C(5)-C(6)-C(1)	59.0(10)
C(4)-C(5)-C(6)-C(1)	-51.6(4)
O(1S)-C(1)-C(6)-C(5)	154.0(4)
O(1)-C(1)-C(6)-C(5)	-74.2(3)
C(2)-C(1)-C(6)-C(5)	59.5(4)
C(6S)-C(1)-C(6)-C(5)	-49.3(9)
C(2S)-C(1)-C(6)-C(5)	15.3(8)
P-C(1)-C(6)-C(5)	-146.0(3)
C(4)-C(5)-C(6S)-C(1)	37.9(15)
C(6)-C(5)-C(6S)-C(1)	-55.8(8)
O(1S)-C(1)-C(6S)-C(5)	94.0(12)
O(1)-C(1)-C(6S)-C(5)	-140.0(12)
C(2)-C(1)-C(6S)-C(5)	-26.6(15)
C(6)-C(1)-C(6S)-C(5)	62.9(10)
C(2S)-C(1)-C(6S)-C(5)	-66.8(13)
P-C(1)-C(6S)-C(5)	170.6(8)
O(1S)-C(1)-O(1)-P	0.8(7)
C(2)-C(1)-O(1)-P	113.3(3)
C(6)-C(1)-O(1)-P	-115.4(3)
C(6S)-C(1)-O(1)-P	-131.1(6)
C(2S)-C(1)-O(1)-P	124.0(6)
O(1)-C(1)-O(1S)-P	-0.8(7)
C(2)-C(1)-O(1S)-P	-124.4(3)
C(6)-C(1)-O(1S)-P	124.6(3)
C(6S)-C(1)-O(1S)-P	105.4(8)
C(2S)-C(1)-O(1S)-P	-97.8(7)
P-C(7)-Si(1)-C(8S)	13.4(8)
Si(2)-C(7)-Si(1)-C(8S)	157.7(8)
P-C(7)-Si(1)-C(9S)	133.1(7)
Si(2)-C(7)-Si(1)-C(9S)	-82.5(7)
P-C(7)-Si(1)-C(10)	-77.7(2)
Si(2)-C(7)-Si(1)-C(10)	66.7(2)
P-C(7)-Si(1)-C(9)	159.71(19)
Si(2)-C(7)-Si(1)-C(9)	-55.9(2)
P-C(7)-Si(1)-C(8)	44.6(2)
Si(2)-C(7)-Si(1)-C(8)	-171.0(2)
P-C(7)-Si(1)-C(10S)	-109.4(7)
Si(2)-C(7)-Si(1)-C(10S)	34.9(7)

P-C(7)-Si(2)-C(11S)	-160.5(8)
Si(1)-C(7)-Si(2)-C(11S)	54.8(8)
P-C(7)-Si(2)-C(13)	-14.2(2)
Si(1)-C(7)-Si(2)-C(13)	-159.0(2)
P-C(7)-Si(2)-C(12)	112.5(2)
Si(1)-C(7)-Si(2)-C(12)	-32.2(2)
P-C(7)-Si(2)-C(11)	-130.45(19)
Si(1)-C(7)-Si(2)-C(11)	84.8(2)
P-C(7)-Si(2)-C(13S)	-38.2(7)
Si(1)-C(7)-Si(2)-C(13S)	177.0(7)
P-C(7)-Si(2)-C(12S)	77.2(6)
Si(1)-C(7)-Si(2)-C(12S)	-67.5(6)
C(1)-O(1)-P-O(1S)	-0.6(5)
C(1)-O(1)-P-C(7)	105.08(16)
C(1)-O(1)-P-W	-115.90(14)
C(1)-O(1S)-P-O(1)	0.6(5)
C(1)-O(1S)-P-C(7)	-110.1(4)
C(1)-O(1S)-P-W	123.8(4)
O(1S)-C(1)-P-O(1)	-179.2(7)
C(2)-C(1)-P-O(1)	-104.6(3)
C(6)-C(1)-P-O(1)	103.5(3)
C(6S)-C(1)-P-O(1)	57.5(8)
C(2S)-C(1)-P-O(1)	-59.9(7)
O(1)-C(1)-P-O(1S)	179.2(7)
C(2)-C(1)-P-O(1S)	74.6(7)
C(6)-C(1)-P-O(1S)	-77.3(7)
C(6S)-C(1)-P-O(1S)	-123.2(10)
C(2S)-C(1)-P-O(1S)	119.4(10)
O(1S)-C(1)-P-C(7)	86.2(6)
O(1)-C(1)-P-C(7)	-94.52(17)
C(2)-C(1)-P-C(7)	160.9(3)
C(6)-C(1)-P-C(7)	8.9(3)
C(6S)-C(1)-P-C(7)	-37.0(8)
C(2S)-C(1)-P-C(7)	-154.4(7)
O(1S)-C(1)-P-W	-81.8(6)
O(1)-C(1)-P-W	97.48(15)
C(2)-C(1)-P-W	-7.1(4)
C(6)-C(1)-P-W	-159.1(2)
C(6S)-C(1)-P-W	155.0(7)
C(2S)-C(1)-P-W	37.6(7)
Si(1)-C(7)-P-O(1)	26.06(18)
Si(2)-C(7)-P-O(1)	-119.46(15)
Si(1)-C(7)-P-O(1S)	127.5(3)
Si(2)-C(7)-P-O(1S)	-18.1(3)
Si(1)-C(7)-P-C(1)	77.77(19)
Si(2)-C(7)-P-C(1)	-67.8(2)
Si(1)-C(7)-P-W	-113.08(13)
Si(2)-C(7)-P-W	101.40(13)
O(2)-C(14)-W-C(16)	-51(12)
O(2)-C(14)-W-C(18)	130(12)
O(2)-C(14)-W-C(15)	38(12)
O(2)-C(14)-W-C(17)	-140(12)
O(2)-C(14)-W-P	47(16)
O(4)-C(16)-W-C(14)	-54(10)
O(4)-C(16)-W-C(18)	-10(13)
O(4)-C(16)-W-C(15)	-143(10)
O(4)-C(16)-W-C(17)	37(10)
O(4)-C(16)-W-P	127(10)
O(6)-C(18)-W-C(14)	9(12)
O(6)-C(18)-W-C(16)	-34(14)
O(6)-C(18)-W-C(15)	99(12)
O(6)-C(18)-W-C(17)	-81(12)
O(6)-C(18)-W-P	-172(12)

O(3)-C(15)-W-C(14)	-74(6)
O(3)-C(15)-W-C(16)	15(6)
O(3)-C(15)-W-C(18)	-163(6)
O(3)-C(15)-W-C(17)	24(8)
O(3)-C(15)-W-P	106(6)
O(5)-C(17)-W-C(14)	58(11)
O(5)-C(17)-W-C(16)	-31(11)
O(5)-C(17)-W-C(18)	148(11)
O(5)-C(17)-W-C(15)	-40(13)
O(5)-C(17)-W-P	-122(11)
O(1)-P-W-C(14)	-78(6)
O(1S)-P-W-C(14)	173(13)
C(1)-P-W-C(14)	-136(6)
C(7)-P-W-C(14)	57(6)
O(1)-P-W-C(16)	19.72(13)
O(1S)-P-W-C(16)	-89.0(4)
C(1)-P-W-C(16)	-37.85(17)
C(7)-P-W-C(16)	154.69(13)
O(1)-P-W-C(18)	-161.27(13)
O(1S)-P-W-C(18)	90.0(4)
C(1)-P-W-C(18)	141.17(17)
C(7)-P-W-C(18)	-26.29(13)
O(1)-P-W-C(15)	-69.22(14)
O(1S)-P-W-C(15)	-177.9(4)
C(1)-P-W-C(15)	-126.78(18)
C(7)-P-W-C(15)	65.76(14)
O(1)-P-W-C(17)	108.67(13)
O(1S)-P-W-C(17)	0.0(4)
C(1)-P-W-C(17)	51.10(17)
C(7)-P-W-C(17)	-116.36(13)

xi.[2-(Bis(trimethylsilyl)methyl)-2,5-diphenyl-1,3,4-dioxaphospholane]pentacarbonylchromium(0) } [62a]
 (A1)

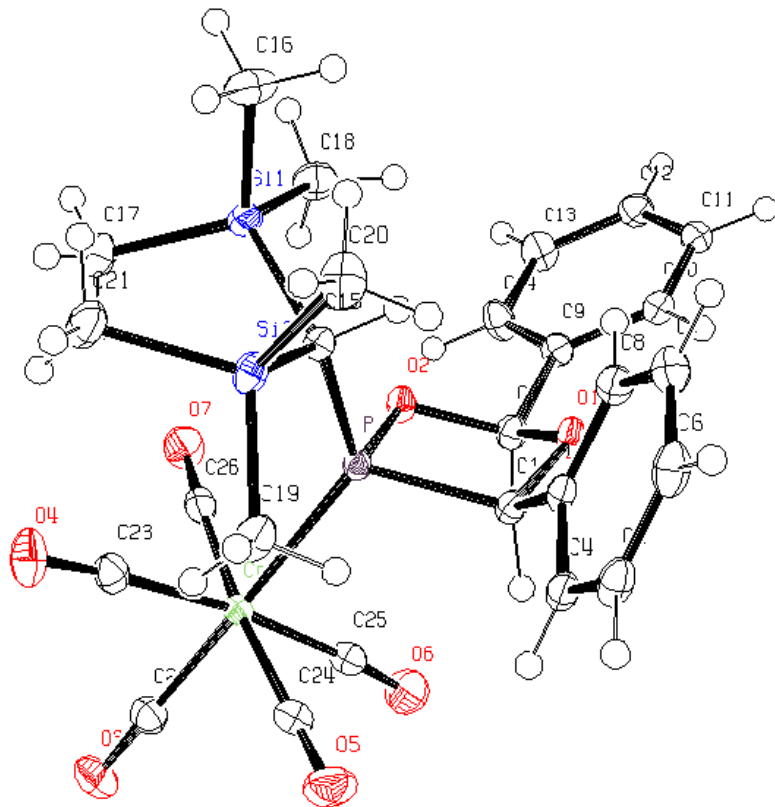


Table xi.1. Crystal data and structure refinement for [62a].

Identification code	GSTR099, Greg942f
Device Type	X8-KappaApexII
Empirical formula	C ₂₆ H ₃₁ Cr O ₇ P Si ₂
Formula weight	594.66
Temperature	100(2) K
Wavelength	0.71073 Å
Crystal system, space group	Monoclinic, P 21/n
Unit cell dimensions	a = 12.6086(5) Å alpha = 90 deg. b = 13.4086(5) Å beta = 92.515(2) deg. c = 16.9676(7) Å gamma = 90 deg.
Volume	2865.8(2) Å ³
Z, Calculated density	4, 1.378 Mg/m ³
Absorption coefficient	0.580 mm ⁻¹

F(000)	1240
Crystal size	0.60 x 0.20 x 0.20 mm
Theta range for data collection	1.97 to 28.00 deg.
Limiting indices	-16<=h<=16, -16<=k<=17, -22<=l<=22
Reflections collected / unique	70810 / 6918 [R(int) = 0.0314]
Completeness to theta = 28.00	99.8 %
Absorption correction	Semi-empirical from equivalents
Max. and min. transmission	0.8928 and 0.7223
Refinement method	Full-matrix least-squares on F^2
Data / restraints / parameters	6918 / 0 / 340
Goodness-of-fit on F^2	1.078
Final R indices [I>2sigma(I)]	R1 = 0.0246, wR2 = 0.0659
R indices (all data)	R1 = 0.0273, wR2 = 0.0679
Largest diff. peak and hole	0.411 and -0.327 e.A^-3

Table xi.2. Atomic coordinates (x 10^4) and equivalent isotropic displacement parameters (A^2 x 10^3) for **[62a]**.
U(eq) is defined as one third of the trace of the orthogonalized Uij tensor.

	x	y	z	U(eq)
C(1)	-754(1)	3456(1)	1022(1)	15(1)
C(2)	-2460(1)	2883(1)	1095(1)	17(1)
C(3)	-102(1)	4391(1)	1048(1)	16(1)
C(4)	907(1)	4388(1)	736(1)	19(1)
C(5)	1516(1)	5252(1)	745(1)	22(1)
C(6)	1122(1)	6130(1)	1046(1)	24(1)
C(7)	112(1)	6147(1)	1341(1)	23(1)
C(8)	-498(1)	5281(1)	1346(1)	19(1)
C(9)	-3610(1)	3158(1)	1160(1)	17(1)
C(10)	-3992(1)	4068(1)	882(1)	17(1)
C(11)	-5064(1)	4295(1)	928(1)	19(1)
C(12)	-5749(1)	3621(1)	1256(1)	21(1)
C(13)	-5370(1)	2708(1)	1532(1)	24(1)
C(14)	-4301(1)	2476(1)	1482(1)	23(1)
C(15)	-526(1)	3358(1)	2789(1)	15(1)
C(16)	-1277(1)	4203(1)	4333(1)	30(1)
C(17)	-1037(1)	1918(1)	4187(1)	28(1)
C(18)	-2854(1)	2982(1)	3383(1)	27(1)
C(19)	1942(1)	3249(1)	2445(1)	24(1)
C(20)	1019(1)	5037(1)	3242(1)	30(1)
C(21)	1352(1)	3108(1)	4123(1)	26(1)
C(22)	359(1)	-378(1)	1579(1)	23(1)
C(23)	853(1)	951(1)	2652(1)	21(1)
C(24)	1058(1)	1443(1)	1113(1)	22(1)
C(25)	-883(1)	814(1)	776(1)	22(1)

C(26)	-1257(1)	544(1)	2288(1)	20(1)
O(1)	-1850(1)	3724(1)	932(1)	18(1)
O(2)	-2046(1)	2486(1)	1834(1)	16(1)
O(3)	602(1)	-1191(1)	1487(1)	31(1)
O(4)	1430(1)	896(1)	3188(1)	31(1)
O(5)	1713(1)	1726(1)	725(1)	34(1)
O(6)	-1356(1)	663(1)	197(1)	34(1)
O(7)	-2010(1)	310(1)	2591(1)	28(1)
Si(1)	-1411(1)	3096(1)	3661(1)	18(1)
Si(2)	919(1)	3652(1)	3142(1)	18(1)
P	-738(1)	2576(1)	1918(1)	13(1)
Cr	-54(1)	954(1)	1729(1)	15(1)

Table xi.3. Bond lengths [Å] and angles [deg] for **[62a]**.

C(1)-O(1)	1.4295(13)
C(1)-C(3)	1.4990(16)
C(1)-P	1.9239(12)
C(1)-H(1A)	1.0000
C(2)-O(1)	1.3988(14)
C(2)-O(2)	1.4377(14)
C(2)-C(9)	1.5055(16)
C(2)-H(2A)	1.0000
C(3)-C(8)	1.3969(17)
C(3)-C(4)	1.3981(16)
C(4)-C(5)	1.3896(18)
C(4)-H(4A)	0.9500
C(5)-C(6)	1.385(2)
C(5)-H(5A)	0.9500
C(6)-C(7)	1.3888(19)
C(6)-H(6A)	0.9500
C(7)-C(8)	1.3921(18)
C(7)-H(7A)	0.9500
C(8)-H(8A)	0.9500
C(9)-C(10)	1.3867(17)
C(9)-C(14)	1.3917(17)
C(10)-C(11)	1.3906(16)
C(10)-H(10A)	0.9500
C(11)-C(12)	1.3840(18)
C(11)-H(11A)	0.9500
C(12)-C(13)	1.3881(18)
C(12)-H(12A)	0.9500
C(13)-C(14)	1.3908(18)
C(13)-H(13A)	0.9500
C(14)-H(14A)	0.9500
C(15)-P	1.8208(12)
C(15)-Si(1)	1.9249(12)
C(15)-Si(2)	1.9334(12)
C(15)-H(15A)	1.0000
C(16)-Si(1)	1.8744(14)
C(16)-H(16A)	0.9800
C(16)-H(16B)	0.9800
C(16)-H(16C)	0.9800
C(17)-Si(1)	1.8644(14)
C(17)-H(17A)	0.9800
C(17)-H(17B)	0.9800
C(17)-H(17C)	0.9800
C(18)-Si(1)	1.8657(14)
C(18)-H(18A)	0.9800
C(18)-H(18B)	0.9800
C(18)-H(18C)	0.9800

C(19)-Si(2)	1.8688(13)
C(19)-H(19A)	0.9800
C(19)-H(19B)	0.9800
C(19)-H(19C)	0.9800
C(20)-Si(2)	1.8676(15)
C(20)-H(20A)	0.9800
C(20)-H(20B)	0.9800
C(20)-H(20C)	0.9800
C(21)-Si(2)	1.8767(13)
C(21)-H(21A)	0.9800
C(21)-H(21B)	0.9800
C(21)-H(21C)	0.9800
C(22)-O(3)	1.1447(17)
C(22)-Cr	1.8805(13)
C(23)-O(4)	1.1412(16)
C(23)-Cr	1.8989(13)
C(24)-O(5)	1.1434(16)
C(24)-Cr	1.9016(13)
C(25)-O(6)	1.1442(17)
C(25)-Cr	1.8952(13)
C(26)-O(7)	1.1430(16)
C(26)-Cr	1.9054(13)
O(2)-P	1.6536(8)
P-Cr	2.3673(4)
O(1)-C(1)-C(3)	108.66(9)
O(1)-C(1)-P	102.39(7)
C(3)-C(1)-P	120.23(8)
O(1)-C(1)-H(1A)	108.3
C(3)-C(1)-H(1A)	108.3
P-C(1)-H(1A)	108.3
O(1)-C(2)-O(2)	106.84(9)
O(1)-C(2)-C(9)	110.88(10)
O(2)-C(2)-C(9)	109.96(9)
O(1)-C(2)-H(2A)	109.7
O(2)-C(2)-H(2A)	109.7
C(9)-C(2)-H(2A)	109.7
C(8)-C(3)-C(4)	119.02(11)
C(8)-C(3)-C(1)	121.37(10)
C(4)-C(3)-C(1)	119.55(11)
C(5)-C(4)-C(3)	120.31(12)
C(5)-C(4)-H(4A)	119.8
C(3)-C(4)-H(4A)	119.8
C(6)-C(5)-C(4)	120.36(12)
C(6)-C(5)-H(5A)	119.8
C(4)-C(5)-H(5A)	119.8
C(5)-C(6)-C(7)	119.79(12)
C(5)-C(6)-H(6A)	120.1
C(7)-C(6)-H(6A)	120.1
C(6)-C(7)-C(8)	120.22(13)
C(6)-C(7)-H(7A)	119.9
C(8)-C(7)-H(7A)	119.9
C(7)-C(8)-C(3)	120.27(11)
C(7)-C(8)-H(8A)	119.9
C(3)-C(8)-H(8A)	119.9
C(10)-C(9)-C(14)	119.89(11)
C(10)-C(9)-C(2)	120.83(11)
C(14)-C(9)-C(2)	119.26(11)
C(9)-C(10)-C(11)	119.87(11)
C(9)-C(10)-H(10A)	120.1
C(11)-C(10)-H(10A)	120.1
C(12)-C(11)-C(10)	120.29(12)
C(12)-C(11)-H(11A)	119.9

C(10)-C(11)-H(11A)	119.9
C(11)-C(12)-C(13)	120.01(11)
C(11)-C(12)-H(12A)	120.0
C(13)-C(12)-H(12A)	120.0
C(12)-C(13)-C(14)	119.86(12)
C(12)-C(13)-H(13A)	120.1
C(14)-C(13)-H(13A)	120.1
C(13)-C(14)-C(9)	120.08(12)
C(13)-C(14)-H(14A)	120.0
C(9)-C(14)-H(14A)	120.0
P-C(15)-Si(1)	116.73(6)
P-C(15)-Si(2)	118.18(6)
Si(1)-C(15)-Si(2)	111.61(6)
P-C(15)-H(15A)	102.4
Si(1)-C(15)-H(15A)	102.4
Si(2)-C(15)-H(15A)	102.4
Si(1)-C(16)-H(16A)	109.5
Si(1)-C(16)-H(16B)	109.5
H(16A)-C(16)-H(16B)	109.5
Si(1)-C(16)-H(16C)	109.5
H(16A)-C(16)-H(16C)	109.5
H(16B)-C(16)-H(16C)	109.5
Si(1)-C(17)-H(17A)	109.5
Si(1)-C(17)-H(17B)	109.5
H(17A)-C(17)-H(17B)	109.5
Si(1)-C(17)-H(17C)	109.5
H(17A)-C(17)-H(17C)	109.5
H(17B)-C(17)-H(17C)	109.5
Si(1)-C(18)-H(18A)	109.5
Si(1)-C(18)-H(18B)	109.5
H(18A)-C(18)-H(18B)	109.5
Si(1)-C(18)-H(18C)	109.5
H(18A)-C(18)-H(18C)	109.5
H(18B)-C(18)-H(18C)	109.5
Si(2)-C(19)-H(19A)	109.5
Si(2)-C(19)-H(19B)	109.5
H(19A)-C(19)-H(19B)	109.5
Si(2)-C(19)-H(19C)	109.5
H(19A)-C(19)-H(19C)	109.5
H(19B)-C(19)-H(19C)	109.5
Si(2)-C(20)-H(20A)	109.5
Si(2)-C(20)-H(20B)	109.5
H(20A)-C(20)-H(20B)	109.5
Si(2)-C(20)-H(20C)	109.5
H(20A)-C(20)-H(20C)	109.5
H(20B)-C(20)-H(20C)	109.5
Si(2)-C(21)-H(21A)	109.5
Si(2)-C(21)-H(21B)	109.5
H(21A)-C(21)-H(21B)	109.5
Si(2)-C(21)-H(21C)	109.5
H(21A)-C(21)-H(21C)	109.5
H(21B)-C(21)-H(21C)	109.5
O(3)-C(22)-Cr	179.43(13)
O(4)-C(23)-Cr	175.51(12)
O(5)-C(24)-Cr	178.18(12)
O(6)-C(25)-Cr	175.24(12)
O(7)-C(26)-Cr	176.60(11)
C(2)-O(1)-C(1)	108.29(9)
C(2)-O(2)-P	111.74(7)
C(17)-Si(1)-C(18)	105.94(7)
C(17)-Si(1)-C(16)	111.47(7)
C(18)-Si(1)-C(16)	106.20(7)
C(17)-Si(1)-C(15)	112.33(6)

C(18)-Si(1)-C(15)	114.33(6)
C(16)-Si(1)-C(15)	106.49(6)
C(20)-Si(2)-C(19)	107.41(7)
C(20)-Si(2)-C(21)	106.88(7)
C(19)-Si(2)-C(21)	105.46(6)
C(20)-Si(2)-C(15)	106.87(6)
C(19)-Si(2)-C(15)	114.30(5)
C(21)-Si(2)-C(15)	115.46(6)
O(2)-P-C(15)	102.89(5)
O(2)-P-C(1)	90.05(4)
C(15)-P-C(1)	106.52(5)
O(2)-P-Cr	106.76(3)
C(15)-P-Cr	126.69(4)
C(1)-P-Cr	116.58(4)
C(22)-Cr-C(25)	86.36(6)
C(22)-Cr-C(23)	87.07(6)
C(25)-Cr-C(23)	173.28(6)
C(22)-Cr-C(24)	92.17(6)
C(25)-Cr-C(24)	87.60(6)
C(23)-Cr-C(24)	91.25(5)
C(22)-Cr-C(26)	91.39(6)
C(25)-Cr-C(26)	88.55(5)
C(23)-Cr-C(26)	93.01(5)
C(24)-Cr-C(26)	174.58(5)
C(22)-Cr-P	174.70(4)
C(25)-Cr-P	90.96(4)
C(23)-Cr-P	95.70(4)
C(24)-Cr-P	92.28(4)
C(26)-Cr-P	83.97(4)

Table xi.4. Anisotropic displacement parameters ($\text{A}^2 \times 10^3$) for [62a]
The anisotropic displacement factor exponent takes the form:
 $-2 \pi^2 [h^2 a^{*2} U_{11} + \dots + 2 h k a^* b^* U_{12}]$

	U11	U22	U33	U23	U13	U12
C(1)	12(1)	20(1)	14(1)	3(1)	0(1)	0(1)
C(2)	16(1)	19(1)	17(1)	2(1)	-1(1)	-1(1)
C(3)	14(1)	20(1)	13(1)	5(1)	-1(1)	-1(1)
C(4)	16(1)	24(1)	16(1)	6(1)	1(1)	1(1)
C(5)	15(1)	31(1)	21(1)	9(1)	0(1)	-3(1)
C(6)	22(1)	24(1)	25(1)	8(1)	-5(1)	-7(1)
C(7)	25(1)	20(1)	24(1)	3(1)	-2(1)	-1(1)
C(8)	16(1)	22(1)	20(1)	3(1)	1(1)	0(1)
C(9)	13(1)	19(1)	18(1)	0(1)	-1(1)	0(1)
C(10)	17(1)	18(1)	16(1)	1(1)	0(1)	-1(1)
C(11)	19(1)	20(1)	18(1)	1(1)	1(1)	4(1)
C(12)	15(1)	28(1)	21(1)	0(1)	2(1)	2(1)
C(13)	18(1)	24(1)	31(1)	5(1)	4(1)	-4(1)
C(14)	18(1)	18(1)	33(1)	6(1)	2(1)	0(1)
C(15)	16(1)	16(1)	14(1)	1(1)	1(1)	0(1)
C(16)	35(1)	31(1)	25(1)	-8(1)	9(1)	-2(1)
C(17)	35(1)	27(1)	22(1)	8(1)	5(1)	1(1)
C(18)	21(1)	33(1)	27(1)	2(1)	9(1)	0(1)
C(19)	16(1)	34(1)	21(1)	4(1)	0(1)	-5(1)
C(20)	33(1)	25(1)	30(1)	0(1)	-9(1)	-8(1)
C(21)	26(1)	35(1)	18(1)	2(1)	-4(1)	1(1)
C(22)	20(1)	24(1)	24(1)	1(1)	1(1)	2(1)
C(23)	19(1)	19(1)	25(1)	4(1)	2(1)	0(1)

C(24)	22(1)	22(1)	23(1)	-1(1)	3(1)	5(1)
C(25)	24(1)	20(1)	23(1)	-1(1)	3(1)	4(1)
C(26)	22(1)	17(1)	21(1)	2(1)	-2(1)	2(1)
O(1)	11(1)	23(1)	21(1)	8(1)	-1(1)	-1(1)
O(2)	12(1)	19(1)	18(1)	6(1)	0(1)	-1(1)
O(3)	33(1)	21(1)	41(1)	-1(1)	3(1)	7(1)
O(4)	27(1)	33(1)	32(1)	11(1)	-10(1)	-3(1)
O(5)	32(1)	35(1)	35(1)	1(1)	17(1)	0(1)
O(6)	37(1)	40(1)	25(1)	-6(1)	-7(1)	4(1)
O(7)	24(1)	28(1)	33(1)	6(1)	7(1)	-2(1)
Si(1)	21(1)	19(1)	15(1)	1(1)	5(1)	1(1)
Si(2)	18(1)	22(1)	15(1)	2(1)	-3(1)	-3(1)
P	11(1)	15(1)	13(1)	2(1)	0(1)	0(1)
Cr	15(1)	16(1)	16(1)	1(1)	1(1)	2(1)

Table xi.5. Hydrogen coordinates ($\times 10^4$) and isotropic displacement parameters ($\text{Å}^2 \times 10^3$) for [62a].

	x	y	z	U(eq)
H(1A)	-562	3061	549	18
H(2A)	-2388	2376	669	21
H(4A)	1177	3792	518	22
H(5A)	2207	5240	543	27
H(6A)	1541	6719	1051	28
H(7A)	-164	6751	1541	28
H(8A)	-1186	5296	1552	23
H(10A)	-3523	4534	660	20
H(11A)	-5327	4917	733	23
H(12A)	-6479	3783	1291	25
H(13A)	-5841	2244	1755	29
H(14A)	-4041	1850	1669	27
H(15A)	-790	4022	2598	18
H(16A)	-1489	4808	4042	45
H(16B)	-538	4266	4529	45
H(16C)	-1736	4115	4779	45
H(17A)	-355	2008	4477	42
H(17B)	-977	1378	3803	42
H(17C)	-1584	1749	4558	42
H(18A)	-2992	2330	3139	40
H(18B)	-3060	3511	3009	40
H(18C)	-3267	3045	3857	40
H(19A)	1712	3435	1906	35
H(19B)	2032	2524	2477	35
H(19C)	2619	3577	2586	35
H(20A)	455	5279	3573	44
H(20B)	940	5345	2719	44
H(20C)	1712	5213	3486	44
H(21A)	1317	2379	4095	40
H(21B)	884	3347	4528	40
H(21C)	2084	3314	4259	40

Table xi.6. Torsion angles [deg] for [62a].

O(1)-C(1)-C(3)-C(8)	29.86(14)
P-C(1)-C(3)-C(8)	-87.45(12)
O(1)-C(1)-C(3)-C(4)	-147.34(10)

P-C(1)-C(3)-C(4)	95.34(12)
C(8)-C(3)-C(4)-C(5)	1.83(17)
C(1)-C(3)-C(4)-C(5)	179.10(10)
C(3)-C(4)-C(5)-C(6)	-1.40(18)
C(4)-C(5)-C(6)-C(7)	-0.01(19)
C(5)-C(6)-C(7)-C(8)	0.96(19)
C(6)-C(7)-C(8)-C(3)	-0.51(19)
C(4)-C(3)-C(8)-C(7)	-0.88(17)
C(1)-C(3)-C(8)-C(7)	-178.09(11)
O(1)-C(2)-C(9)-C(10)	15.50(15)
O(2)-C(2)-C(9)-C(10)	133.43(11)
O(1)-C(2)-C(9)-C(14)	-166.37(11)
O(2)-C(2)-C(9)-C(14)	-48.45(15)
C(14)-C(9)-C(10)-C(11)	0.15(18)
C(2)-C(9)-C(10)-C(11)	178.26(11)
C(9)-C(10)-C(11)-C(12)	0.50(18)
C(10)-C(11)-C(12)-C(13)	-0.74(19)
C(11)-C(12)-C(13)-C(14)	0.3(2)
C(12)-C(13)-C(14)-C(9)	0.3(2)
C(10)-C(9)-C(14)-C(13)	-0.6(2)
C(2)-C(9)-C(14)-C(13)	-178.71(12)
O(2)-C(2)-O(1)-C(1)	49.63(11)
C(9)-C(2)-O(1)-C(1)	169.44(9)
C(3)-C(1)-O(1)-C(2)	-166.15(9)
P-C(1)-O(1)-C(2)	-37.96(10)
O(1)-C(2)-O(2)-P	-37.65(11)
C(9)-C(2)-O(2)-P	-158.05(8)
P-C(15)-Si(1)-C(17)	72.77(8)
Si(2)-C(15)-Si(1)-C(17)	-67.43(8)
P-C(15)-Si(1)-C(18)	-48.00(9)
Si(2)-C(15)-Si(1)-C(18)	171.80(6)
P-C(15)-Si(1)-C(16)	-164.95(7)
Si(2)-C(15)-Si(1)-C(16)	54.85(8)
P-C(15)-Si(2)-C(20)	127.63(7)
Si(1)-C(15)-Si(2)-C(20)	-92.81(7)
P-C(15)-Si(2)-C(19)	8.94(9)
Si(1)-C(15)-Si(2)-C(19)	148.51(6)
P-C(15)-Si(2)-C(21)	-113.67(8)
Si(1)-C(15)-Si(2)-C(21)	25.90(9)
C(2)-O(2)-P-C(15)	119.49(8)
C(2)-O(2)-P-C(1)	12.52(8)
C(2)-O(2)-P-Cr	-105.36(7)
Si(1)-C(15)-P-O(2)	41.05(7)
Si(2)-C(15)-P-O(2)	178.59(6)
Si(1)-C(15)-P-C(1)	135.00(6)
Si(2)-C(15)-P-C(1)	-87.47(7)
Si(1)-C(15)-P-Cr	-81.59(7)
Si(2)-C(15)-P-Cr	55.94(8)
O(1)-C(1)-P-O(2)	14.19(8)
C(3)-C(1)-P-O(2)	134.67(9)
O(1)-C(1)-P-C(15)	-89.28(8)
C(3)-C(1)-P-C(15)	31.20(10)
O(1)-C(1)-P-Cr	123.03(6)
C(3)-C(1)-P-Cr	-116.49(8)
O(3)-C(22)-Cr-C(25)	-48(12)
O(3)-C(22)-Cr-C(23)	134(12)
O(3)-C(22)-Cr-C(24)	-135(12)
O(3)-C(22)-Cr-C(26)	41(12)
O(3)-C(22)-Cr-P	12(12)
O(6)-C(25)-Cr-C(22)	-2.2(15)
O(6)-C(25)-Cr-C(23)	9.9(18)
O(6)-C(25)-Cr-C(24)	90.2(15)
O(6)-C(25)-Cr-C(26)	-93.6(15)

O(6)-C(25)-Cr-P	-177.6(15)
O(4)-C(23)-Cr-C(22)	17.4(15)
O(4)-C(23)-Cr-C(25)	5.4(18)
O(4)-C(23)-Cr-C(24)	-74.7(15)
O(4)-C(23)-Cr-C(26)	108.7(15)
O(4)-C(23)-Cr-P	-167.1(15)
O(5)-C(24)-Cr-C(22)	70(4)
O(5)-C(24)-Cr-C(25)	-16(4)
O(5)-C(24)-Cr-C(23)	157(4)
O(5)-C(24)-Cr-C(26)	-61(4)
O(5)-C(24)-Cr-P	-107(4)
O(7)-C(26)-Cr-C(22)	-107(2)
O(7)-C(26)-Cr-C(25)	-20(2)
O(7)-C(26)-Cr-C(23)	166(2)
O(7)-C(26)-Cr-C(24)	25(2)
O(7)-C(26)-Cr-P	71(2)
O(2)-P-Cr-C(22)	-8.1(5)
C(15)-P-Cr-C(22)	112.9(4)
C(1)-P-Cr-C(22)	-106.8(4)
O(2)-P-Cr-C(25)	51.45(5)
C(15)-P-Cr-C(25)	172.44(6)
C(1)-P-Cr-C(25)	-47.28(6)
O(2)-P-Cr-C(23)	-129.43(5)
C(15)-P-Cr-C(23)	-8.44(6)
C(1)-P-Cr-C(23)	131.84(5)
O(2)-P-Cr-C(24)	139.08(5)
C(15)-P-Cr-C(24)	-99.92(6)
C(1)-P-Cr-C(24)	40.36(6)
O(2)-P-Cr-C(26)	-36.99(5)
C(15)-P-Cr-C(26)	84.00(6)
C(1)-P-Cr-C(26)	-135.71(5)

xii.[2-(Bis(trimethylsilyl)methyl)-2,5-diphenyl-1,3,4-dioxaphospholane]pentacarbonyltungsten(0) [64a]
 (A1)

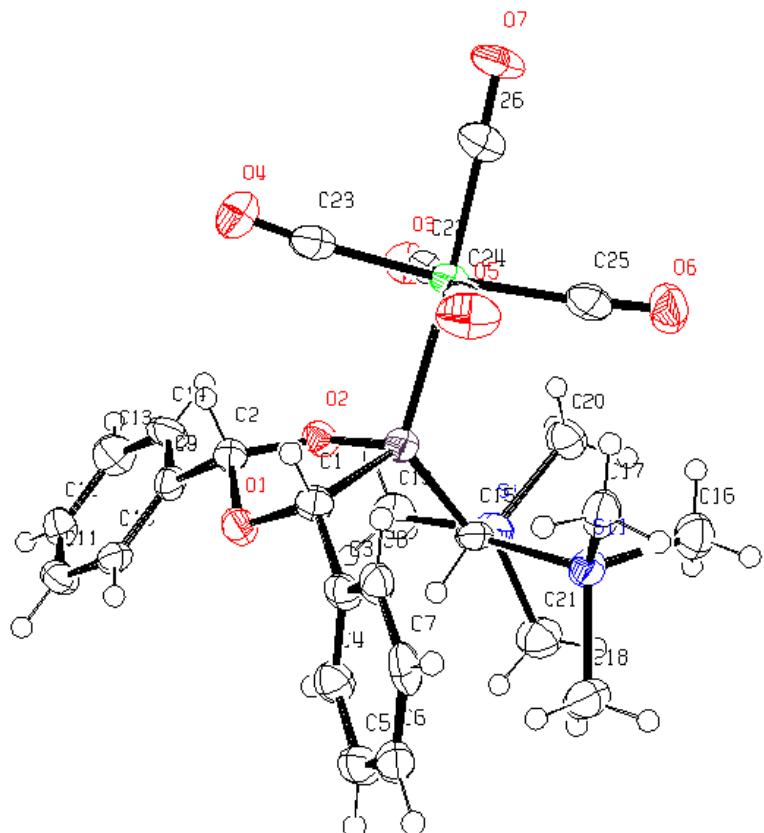


Table xii.1. Crystal data and structure refinement for [60a].

Identification code	GSTR137, Greg1181
Device Type	Nonius KappaCCD
Empirical formula	C ₂₆ H ₃₁ O ₇ P Si ₂ W
Formula weight	726.51
Temperature	123(2) K
Wavelength	0.71073 Å
Crystal system, space group	Monoclinic, P 21/c
Unit cell dimensions	a = 12.707(2) Å alpha = 90 deg. b = 13.545(2) Å beta = 124.298(9) deg.
	c = 20.703(3) Å gamma = 90 deg.
Volume	2943.7(8) Å ³
Z, Calculated density	4, 1.639 Mg/m ³
Absorption coefficient	4.100 mm ⁻¹

F(000)	1440
Crystal size	0.44 x 0.28 x 0.28 mm
Theta range for data collection	2.82 to 26.00 deg.
Limiting indices	-15<=h<=14, -15<=k<=16, -25<=l<=23
Reflections collected / unique	17559 / 5735 [R(int) = 0.1067]
Completeness to theta = 26.00	99.0 %
Absorption correction	Semi-empirical from equivalents
Max. and min. transmission	0.3931 and 0.2656
Refinement method	Full-matrix least-squares on F^2
Data / restraints / parameters	5735 / 0 / 340
Goodness-of-fit on F^2	0.895
Final R indices [I>2sigma(I)]	R1 = 0.0444, wR2 = 0.0812
R indices (all data)	R1 = 0.0897, wR2 = 0.0930
Largest diff. peak and hole	1.435 and -2.323 e.A^-3

Table xii.2. Atomic coordinates ($\times 10^4$) and equivalent isotropic displacement parameters ($\text{\AA}^2 \times 10^3$) for **[64a]**. U(eq) is defined as one third of the trace of the orthogonalized U_{ij} tensor.

	x	y	z	U(eq)
C(1)	-1833(6)	-8458(5)	-1026(4)	28(2)
C(2)	-3600(7)	-7886(5)	-1096(4)	31(2)
C(3)	-1191(7)	-9385(5)	-1045(4)	29(2)
C(4)	-1875(7)	-10261(5)	-1351(4)	34(2)
C(6)	32(7)	-11090(5)	-1032(4)	37(2)
C(7)	727(7)	-10218(6)	-723(4)	35(2)
C(8)	102(7)	-9374(5)	-725(4)	31(2)
C(9)	-4798(6)	-8149(5)	-1156(4)	26(2)
C(10)	-4920(7)	-9053(5)	-888(4)	30(2)
C(11)	-6034(7)	-9261(5)	-926(4)	34(2)
C(12)	-7018(7)	-8604(5)	-1232(4)	37(2)
C(13)	-6891(7)	-7692(6)	-1499(4)	42(2)
C(14)	-5784(7)	-7474(5)	-1458(4)	39(2)
C(15)	-3339(7)	-8361(5)	-2792(4)	29(2)
C(16)	-2714(7)	-8062(6)	-4077(4)	43(2)
C(17)	-521(7)	-8252(6)	-2417(4)	40(2)
C(18)	-2224(8)	-10009(5)	-3244(5)	49(2)
C(19)	-6205(7)	-7958(6)	-3388(4)	44(2)
C(20)	-5140(7)	-6901(5)	-4151(4)	42(2)
C(21)	-5562(7)	-9142(6)	-4328(4)	47(2)
C(22)	-3587(8)	-5479(5)	-2288(4)	32(2)
C(23)	-1673(7)	-5755(5)	-695(5)	37(2)
C(24)	23(8)	-6397(6)	-1066(4)	36(2)
C(25)	-1724(7)	-5879(5)	-2676(5)	37(2)
C(26)	-1157(7)	-4483(6)	-1542(5)	39(2)

C(5)	-1264(7)	-11109(5)	-1347(4)	37(2)
O(1)	-2834(4)	-8714(3)	-933(3)	31(1)
O(2)	-3913(4)	-7507(3)	-1837(2)	29(1)
O(3)	-4674(5)	-5274(4)	-2595(3)	46(1)
O(4)	-1609(6)	-5612(4)	-130(3)	54(2)
O(5)	1081(6)	-6714(4)	-670(3)	55(2)
O(6)	-1668(5)	-5820(4)	-3211(3)	51(2)
O(7)	-852(5)	-3667(4)	-1449(3)	51(2)
P	-2690(2)	-7594(1)	-1916(1)	28(1)
Si(1)	-2214(2)	-8640(2)	-3126(1)	34(1)
Si(2)	-5036(2)	-8070(2)	-3647(1)	34(1)
W	-1765(1)	-5893(1)	-1708(1)	30(1)

Table xii.3. Bond lengths [Å] and angles [deg] for **[64a]**.

C(1)-O(1)	1.433(7)
C(1)-C(3)	1.510(9)
C(1)-P	1.920(7)
C(1)-H(1A)	1.0000
C(2)-O(1)	1.396(7)
C(2)-O(2)	1.445(7)
C(2)-C(9)	1.498(9)
C(2)-H(2A)	1.0000
C(3)-C(8)	1.382(9)
C(3)-C(4)	1.394(9)
C(4)-C(5)	1.384(9)
C(4)-H(4A)	0.9500
C(6)-C(5)	1.389(10)
C(6)-C(7)	1.394(10)
C(6)-H(6A)	0.9500
C(7)-C(8)	1.391(9)
C(7)-H(7A)	0.9500
C(8)-H(8A)	0.9500
C(9)-C(14)	1.384(9)
C(9)-C(10)	1.390(9)
C(10)-C(11)	1.400(9)
C(10)-H(10A)	0.9500
C(11)-C(12)	1.365(10)
C(11)-H(11A)	0.9500
C(12)-C(13)	1.400(10)
C(12)-H(12A)	0.9500
C(13)-C(14)	1.392(10)
C(13)-H(13A)	0.9500
C(14)-H(14A)	0.9500
C(15)-P	1.835(7)
C(15)-Si(2)	1.906(7)
C(15)-Si(1)	1.943(7)
C(15)-H(15A)	1.0000
C(16)-Si(1)	1.867(7)
C(16)-H(16A)	0.9800
C(16)-H(16B)	0.9800
C(16)-H(16C)	0.9800
C(17)-Si(1)	1.871(7)
C(17)-H(17A)	0.9800
C(17)-H(17B)	0.9800
C(17)-H(17C)	0.9800
C(18)-Si(1)	1.869(7)
C(18)-H(18A)	0.9800
C(18)-H(18B)	0.9800
C(18)-H(18C)	0.9800
C(19)-Si(2)	1.849(7)

C(19)-H(19A)	0.9800
C(19)-H(19B)	0.9800
C(19)-H(19C)	0.9800
C(20)-Si(2)	1.860(7)
C(20)-H(20A)	0.9800
C(20)-H(20B)	0.9800
C(20)-H(20C)	0.9800
C(21)-Si(2)	1.865(7)
C(21)-H(21A)	0.9800
C(21)-H(21B)	0.9800
C(21)-H(21C)	0.9800
C(22)-O(3)	1.184(8)
C(22)-W	1.995(8)
C(23)-O(4)	1.144(8)
C(23)-W	2.041(8)
C(24)-O(5)	1.192(8)
C(24)-W	1.998(9)
C(25)-O(6)	1.153(8)
C(25)-W	2.034(8)
C(26)-O(7)	1.150(8)
C(26)-W	2.017(8)
C(5)-H(5A)	0.9500
O(2)-P	1.656(4)
P-W	2.5107(19)
O(1)-C(1)-C(3)	109.6(5)
O(1)-C(1)-P	102.1(4)
C(3)-C(1)-P	120.3(5)
O(1)-C(1)-H(1A)	108.1
C(3)-C(1)-H(1A)	108.1
P-C(1)-H(1A)	108.1
O(1)-C(2)-O(2)	106.2(5)
O(1)-C(2)-C(9)	111.4(5)
O(2)-C(2)-C(9)	109.7(5)
O(1)-C(2)-H(2A)	109.8
O(2)-C(2)-H(2A)	109.8
C(9)-C(2)-H(2A)	109.8
C(8)-C(3)-C(4)	119.7(6)
C(8)-C(3)-C(1)	119.5(6)
C(4)-C(3)-C(1)	120.7(6)
C(5)-C(4)-C(3)	119.9(7)
C(5)-C(4)-H(4A)	120.0
C(3)-C(4)-H(4A)	120.0
C(5)-C(6)-C(7)	120.5(7)
C(5)-C(6)-H(6A)	119.7
C(7)-C(6)-H(6A)	119.7
C(8)-C(7)-C(6)	118.8(7)
C(8)-C(7)-H(7A)	120.6
C(6)-C(7)-H(7A)	120.6
C(3)-C(8)-C(7)	121.0(7)
C(3)-C(8)-H(8A)	119.5
C(7)-C(8)-H(8A)	119.5
C(14)-C(9)-C(10)	119.1(6)
C(14)-C(9)-C(2)	120.0(6)
C(10)-C(9)-C(2)	120.9(6)
C(9)-C(10)-C(11)	119.4(6)
C(9)-C(10)-H(10A)	120.3
C(11)-C(10)-H(10A)	120.3
C(12)-C(11)-C(10)	121.9(7)
C(12)-C(11)-H(11A)	119.1
C(10)-C(11)-H(11A)	119.1
C(11)-C(12)-C(13)	118.6(7)
C(11)-C(12)-H(12A)	120.7

C(13)-C(12)-H(12A)	120.7
C(14)-C(13)-C(12)	120.0(7)
C(14)-C(13)-H(13A)	120.0
C(12)-C(13)-H(13A)	120.0
C(9)-C(14)-C(13)	121.0(7)
C(9)-C(14)-H(14A)	119.5
C(13)-C(14)-H(14A)	119.5
P-C(15)-Si(2)	116.3(3)
P-C(15)-Si(1)	116.8(4)
Si(2)-C(15)-Si(1)	112.6(3)
P-C(15)-H(15A)	102.8
Si(2)-C(15)-H(15A)	102.8
Si(1)-C(15)-H(15A)	102.8
Si(1)-C(16)-H(16A)	109.5
Si(1)-C(16)-H(16B)	109.5
H(16A)-C(16)-H(16B)	109.5
Si(1)-C(16)-H(16C)	109.5
H(16A)-C(16)-H(16C)	109.5
H(16B)-C(16)-H(16C)	109.5
Si(1)-C(17)-H(17A)	109.5
Si(1)-C(17)-H(17B)	109.5
H(17A)-C(17)-H(17B)	109.5
Si(1)-C(17)-H(17C)	109.5
H(17A)-C(17)-H(17C)	109.5
H(17B)-C(17)-H(17C)	109.5
Si(1)-C(18)-H(18A)	109.5
Si(1)-C(18)-H(18B)	109.5
H(18A)-C(18)-H(18B)	109.5
Si(1)-C(18)-H(18C)	109.5
H(18A)-C(18)-H(18C)	109.5
H(18B)-C(18)-H(18C)	109.5
Si(2)-C(19)-H(19A)	109.5
Si(2)-C(19)-H(19B)	109.5
H(19A)-C(19)-H(19B)	109.5
Si(2)-C(19)-H(19C)	109.5
H(19A)-C(19)-H(19C)	109.5
H(19B)-C(19)-H(19C)	109.5
Si(2)-C(20)-H(20A)	109.5
Si(2)-C(20)-H(20B)	109.5
H(20A)-C(20)-H(20B)	109.5
Si(2)-C(20)-H(20C)	109.5
H(20A)-C(20)-H(20C)	109.5
H(20B)-C(20)-H(20C)	109.5
Si(2)-C(21)-H(21A)	109.5
Si(2)-C(21)-H(21B)	109.5
H(21A)-C(21)-H(21B)	109.5
Si(2)-C(21)-H(21C)	109.5
H(21A)-C(21)-H(21C)	109.5
H(21B)-C(21)-H(21C)	109.5
O(3)-C(22)-W	175.3(6)
O(4)-C(23)-W	175.4(6)
O(5)-C(24)-W	178.0(7)
O(6)-C(25)-W	176.1(7)
O(7)-C(26)-W	177.3(7)
C(4)-C(5)-C(6)	120.1(7)
C(4)-C(5)-H(5A)	120.0
C(6)-C(5)-H(5A)	120.0
C(2)-O(1)-C(1)	108.9(5)
C(2)-O(2)-P	111.5(4)
O(2)-P-C(15)	102.3(3)
O(2)-P-C(1)	90.3(3)
C(15)-P-C(1)	107.4(3)
O(2)-P-W	107.02(18)

C(15)-P-W	126.5(2)
C(1)-P-W	115.9(2)
C(16)-Si(1)-C(18)	107.7(3)
C(16)-Si(1)-C(17)	105.4(3)
C(18)-Si(1)-C(17)	107.5(4)
C(16)-Si(1)-C(15)	114.4(3)
C(18)-Si(1)-C(15)	106.7(3)
C(17)-Si(1)-C(15)	114.7(3)
C(19)-Si(2)-C(20)	106.2(3)
C(19)-Si(2)-C(21)	106.2(4)
C(20)-Si(2)-C(21)	110.9(3)
C(19)-Si(2)-C(15)	114.9(3)
C(20)-Si(2)-C(15)	112.5(3)
C(21)-Si(2)-C(15)	106.0(3)
C(22)-W-C(24)	174.3(3)
C(22)-W-C(26)	92.3(3)
C(24)-W-C(26)	91.6(3)
C(22)-W-C(25)	94.0(3)
C(24)-W-C(25)	90.4(3)
C(26)-W-C(25)	86.5(3)
C(22)-W-C(23)	88.2(3)
C(24)-W-C(23)	87.9(3)
C(26)-W-C(23)	86.8(3)
C(25)-W-C(23)	173.0(3)
C(22)-W-P	83.3(2)
C(24)-W-P	92.7(2)
C(26)-W-P	174.9(2)
C(25)-W-P	96.3(2)
C(23)-W-P	90.6(2)

Table xii.4. Anisotropic displacement parameters ($\text{Å}^2 \times 10^3$) for [64a]

The anisotropic displacement factor exponent takes the form:
 $-2 \pi^2 [h^2 a^{*2} U11 + \dots + 2 h k a^* b^* U12]$

	U11	U22	U33	U23	U13	U12
C(1)	27(4)	26(4)	29(4)	1(3)	15(3)	1(3)
C(2)	43(5)	22(4)	33(4)	3(3)	26(4)	5(3)
C(3)	31(5)	26(4)	29(4)	8(3)	17(3)	6(3)
C(4)	34(5)	34(4)	35(4)	4(3)	19(4)	3(4)
C(6)	50(6)	32(5)	39(4)	7(3)	31(4)	9(4)
C(7)	31(5)	48(5)	35(4)	14(4)	25(4)	7(4)
C(8)	37(5)	31(4)	29(4)	7(3)	22(4)	8(3)
C(9)	27(4)	30(4)	28(4)	-3(3)	19(3)	-2(3)
C(10)	39(5)	22(4)	30(4)	-1(3)	20(3)	4(4)
C(11)	40(5)	26(4)	46(5)	3(3)	30(4)	-2(4)
C(12)	43(5)	38(5)	37(4)	2(4)	27(4)	-4(4)
C(13)	37(5)	41(5)	47(5)	4(4)	24(4)	7(4)
C(14)	50(5)	19(4)	56(5)	8(4)	35(4)	5(4)
C(15)	38(5)	19(4)	31(4)	-2(3)	19(4)	0(3)
C(16)	47(5)	47(5)	36(4)	2(4)	25(4)	2(4)
C(17)	45(5)	47(5)	39(5)	3(4)	29(4)	7(4)
C(18)	69(6)	35(5)	48(5)	-4(4)	36(5)	6(5)
C(19)	31(5)	50(5)	43(5)	9(4)	16(4)	13(4)
C(20)	49(5)	36(5)	37(4)	5(4)	23(4)	2(4)
C(21)	48(5)	44(5)	43(5)	-7(4)	22(4)	-7(4)
C(22)	44(5)	24(4)	36(4)	1(3)	26(4)	-4(4)

C(23)	42(5)	23(4)	47(5)	0(4)	25(4)	-1(4)
C(24)	43(6)	32(4)	39(5)	-5(4)	26(4)	-11(4)
C(25)	38(5)	23(4)	48(5)	10(4)	23(4)	8(4)
C(26)	36(5)	31(5)	49(5)	3(4)	23(4)	-4(4)
C(5)	41(5)	28(4)	45(5)	6(3)	26(4)	5(4)
O(1)	36(3)	28(3)	40(3)	8(2)	28(3)	7(2)
O(2)	29(3)	27(3)	34(3)	5(2)	19(2)	3(2)
O(3)	46(4)	41(3)	49(3)	-1(3)	25(3)	-1(3)
O(4)	79(5)	50(4)	41(3)	-9(3)	38(3)	-5(3)
O(5)	48(4)	41(4)	65(4)	-5(3)	24(3)	-5(3)
O(6)	72(4)	45(3)	53(4)	16(3)	46(3)	15(3)
O(7)	63(4)	25(3)	65(4)	-3(3)	37(3)	-15(3)
P	31(1)	24(1)	28(1)	1(1)	17(1)	1(1)
Si(1)	45(1)	30(1)	30(1)	1(1)	23(1)	4(1)
Si(2)	36(1)	27(1)	31(1)	0(1)	14(1)	-1(1)
W	36(1)	22(1)	34(1)	1(1)	20(1)	-1(1)

Table xii.5. Hydrogen coordinates ($\times 10^4$) and isotropic displacement parameters ($\text{\AA}^2 \times 10^3$) for [54a].

	x	y	z	U(eq)
H(1A)	-1187	-8061	-561	33
H(2A)	-3115	-7377	-679	37
H(4A)	-2760	-10276	-1562	41
H(6A)	449	-11675	-1027	44
H(7A)	1610	-10202	-515	42
H(8A)	570	-8781	-504	37
H(10A)	-4254	-9527	-680	36
H(11A)	-6107	-9876	-734	41
H(12A)	-7774	-8762	-1263	44
H(13A)	-7560	-7221	-1709	50
H(14A)	-5705	-6853	-1641	47
H(15A)	-3432	-9022	-2613	35
H(16A)	-2711	-7342	-4030	64
H(16B)	-3573	-8286	-4486	64
H(16C)	-2118	-8254	-4213	64
H(17A)	-208	-8516	-1898	61
H(17B)	-471	-7529	-2392	61
H(17C)	4	-8506	-2590	61
H(18A)	-3105	-10240	-3589	73
H(18B)	-1823	-10327	-2732	73
H(18C)	-1750	-10177	-3472	73
H(19A)	-6082	-7327	-3122	66
H(19B)	-6084	-8501	-3039	66
H(19C)	-7070	-7987	-3864	66
H(20A)	-4918	-7029	-4526	62
H(20B)	-4547	-6416	-3764	62
H(20C)	-6011	-6642	-4428	62
H(21A)	-5520	-9746	-4054	71
H(21B)	-5002	-9207	-4510	71
H(21C)	-6439	-9035	-4776	71
H(5A)	-1731	-11704	-1560	44

Table xii.6. Torsion angles [deg] for [54a].

O(1)-C(1)-C(3)-C(8) -145.9(6)

P-C(1)-C(3)-C(8)	96.3(7)
O(1)-C(1)-C(3)-C(4)	31.4(8)
P-C(1)-C(3)-C(4)	-86.4(7)
C(8)-C(3)-C(4)-C(5)	-1.3(10)
C(1)-C(3)-C(4)-C(5)	-178.6(6)
C(5)-C(6)-C(7)-C(8)	1.0(10)
C(4)-C(3)-C(8)-C(7)	1.8(10)
C(1)-C(3)-C(8)-C(7)	179.2(6)
C(6)-C(7)-C(8)-C(3)	-1.7(9)
O(1)-C(2)-C(9)-C(14)	-167.7(6)
O(2)-C(2)-C(9)-C(14)	-50.4(8)
O(1)-C(2)-C(9)-C(10)	14.5(9)
O(2)-C(2)-C(9)-C(10)	131.8(6)
C(14)-C(9)-C(10)-C(11)	-0.2(10)
C(2)-C(9)-C(10)-C(11)	177.6(6)
C(9)-C(10)-C(11)-C(12)	1.0(10)
C(10)-C(11)-C(12)-C(13)	-1.2(11)
C(11)-C(12)-C(13)-C(14)	0.7(11)
C(10)-C(9)-C(14)-C(13)	-0.3(11)
C(2)-C(9)-C(14)-C(13)	-178.1(6)
C(12)-C(13)-C(14)-C(9)	0.1(11)
C(3)-C(4)-C(5)-C(6)	0.6(10)
C(7)-C(6)-C(5)-C(4)	-0.5(10)
O(2)-C(2)-O(1)-C(1)	49.9(6)
C(9)-C(2)-O(1)-C(1)	169.3(5)
C(3)-C(1)-O(1)-C(2)	-166.5(5)
P-C(1)-O(1)-C(2)	-37.8(5)
O(1)-C(2)-O(2)-P	-38.3(6)
C(9)-C(2)-O(2)-P	-158.9(4)
C(2)-O(2)-P-C(15)	121.3(4)
C(2)-O(2)-P-C(1)	13.4(4)
C(2)-O(2)-P-W	-103.9(4)
Si(2)-C(15)-P-O(2)	41.9(4)
Si(1)-C(15)-P-O(2)	178.8(3)
Si(2)-C(15)-P-C(1)	136.2(4)
Si(1)-C(15)-P-C(1)	-86.9(4)
Si(2)-C(15)-P-W	-80.4(4)
Si(1)-C(15)-P-W	56.5(4)
O(1)-C(1)-P-O(2)	13.4(4)
C(3)-C(1)-P-O(2)	134.9(5)
O(1)-C(1)-P-C(15)	-89.7(4)
C(3)-C(1)-P-C(15)	31.9(6)
O(1)-C(1)-P-W	122.5(3)
C(3)-C(1)-P-W	-115.9(5)
P-C(15)-Si(1)-C(16)	-112.9(4)
Si(2)-C(15)-Si(1)-C(16)	25.6(5)
P-C(15)-Si(1)-C(18)	128.1(4)
Si(2)-C(15)-Si(1)-C(18)	-93.4(4)
P-C(15)-Si(1)-C(17)	9.2(5)
Si(2)-C(15)-Si(1)-C(17)	147.6(3)
P-C(15)-Si(2)-C(19)	-49.0(5)
Si(1)-C(15)-Si(2)-C(19)	172.4(3)
P-C(15)-Si(2)-C(20)	72.6(5)
Si(1)-C(15)-Si(2)-C(20)	-66.0(4)
P-C(15)-Si(2)-C(21)	-166.0(4)
Si(1)-C(15)-Si(2)-C(21)	55.4(4)
O(3)-C(22)-W-C(24)	6(10)
O(3)-C(22)-W-C(26)	-127(8)
O(3)-C(22)-W-C(25)	147(8)
O(3)-C(22)-W-C(23)	-40(8)
O(3)-C(22)-W-P	51(8)
O(5)-C(24)-W-C(22)	-4(22)
O(5)-C(24)-W-C(26)	128(20)

O(5)-C(24)-W-C(25)	-145(20)
O(5)-C(24)-W-C(23)	42(20)
O(5)-C(24)-W-P	-49(20)
O(7)-C(26)-W-C(22)	26(15)
O(7)-C(26)-W-C(24)	-149(15)
O(7)-C(26)-W-C(25)	120(15)
O(7)-C(26)-W-C(23)	-62(15)
O(7)-C(26)-W-P	-3(18)
O(6)-C(25)-W-C(22)	100(9)
O(6)-C(25)-W-C(24)	-84(9)
O(6)-C(25)-W-C(26)	8(9)
O(6)-C(25)-W-C(23)	-8(11)
O(6)-C(25)-W-P	-176(9)
O(4)-C(23)-W-C(22)	-82(9)
O(4)-C(23)-W-C(24)	102(9)
O(4)-C(23)-W-C(26)	10(9)
O(4)-C(23)-W-C(25)	26(10)
O(4)-C(23)-W-P	-165(9)
O(2)-P-W-C(22)	-36.7(3)
C(15)-P-W-C(22)	83.6(3)
C(1)-P-W-C(22)	-135.6(3)
O(2)-P-W-C(24)	139.3(3)
C(15)-P-W-C(24)	-100.4(3)
C(1)-P-W-C(24)	40.4(3)
O(2)-P-W-C(26)	-8(3)
C(15)-P-W-C(26)	113(3)
C(1)-P-W-C(26)	-107(3)
O(2)-P-W-C(25)	-130.0(3)
C(15)-P-W-C(25)	-9.7(3)
C(1)-P-W-C(25)	131.1(3)
O(2)-P-W-C(23)	51.4(3)
C(15)-P-W-C(23)	171.7(4)
C(1)-P-W-C(23)	-47.5(3)

xiii.[2-(Bis(trimethylsilyl)methyl)-2-*iso*-propyl-5-phenyl-1,3,4-dioxaphospholane]pentacarbonyltungsten(0) [62a]
(B1)

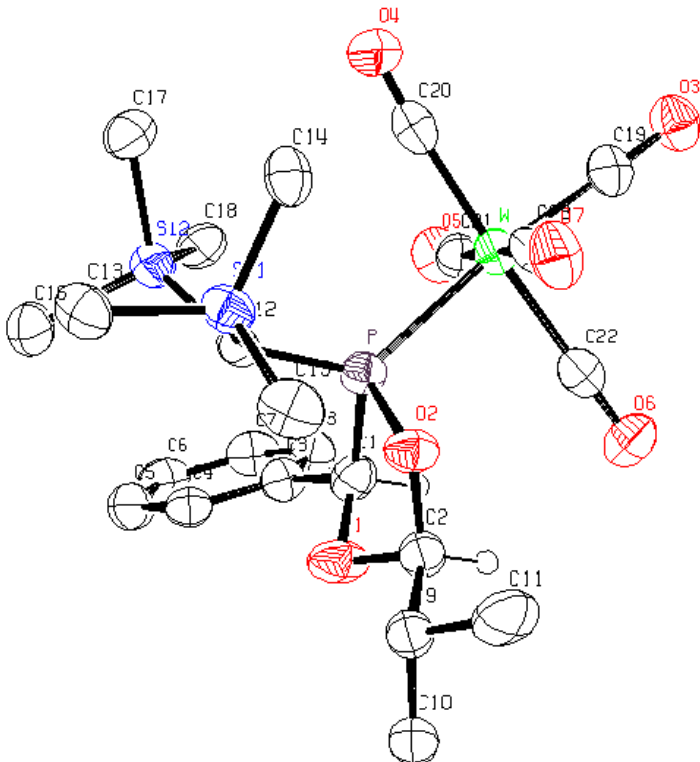


Table xiii.1. Crystal data and structure refinement for [62a].

Identification code	GSTR139, Greg1199
Device Type	Nonius KappaCCD
Empirical formula	C ₂₃ H ₃₃ O ₇ P Si ₂ W
Formula weight	692.49
Temperature	123(2) K
Wavelength	0.71073 Å
Crystal system, space group	Monoclinic, P 21/c
Unit cell dimensions	a = 11.0063(16) Å alpha = 90 deg. b = 14.099(3) Å beta = c = 20.512(3) Å gamma = 90 deg.
Volume	2853.5(8) Å ³
Z, Calculated density	4, 1.612 Mg/m ³
Absorption coefficient	4.225 mm ⁻¹
F(000)	1376
Crystal size	0.42 x 0.24 x 0.12 mm

Theta range for data collection 2.52 to 25.25 deg.
 Limiting indices -13<=h<=13, -15<=k<=16, -24<=l<=24
 Reflections collected / unique 18082 / 4984 [R(int) = 0.1264]
 Completeness to theta = 25.25 96.4 %
 Absorption correction Semi-empirical from equivalents
 Max. and min. transmission 0.6311 and 0.2699
 Refinement method Full-matrix least-squares on F^2
 Data / restraints / parameters 4984 / 36 / 332
 Goodness-of-fit on F^2 0.994
 Final R indices [I>2sigma(I)] R1 = 0.0496, wR2 = 0.0925
 R indices (all data) R1 = 0.1199, wR2 = 0.1145
 Largest diff. peak and hole 2.286 and -1.771 e.A^-3

Table xiii.2. Atomic coordinates ($\times 10^4$) and equivalent isotropic displacement parameters ($\text{\AA}^2 \times 10^3$) for **[62a]**. U(eq) is defined as one third of the trace of the orthogonalized U_{ij} tensor.

	x	y	z	U(eq)
C(1)	7302(9)	-7967(7)	1018(5)	43(2)
C(2)	9337(16)	-7591(11)	1112(11)	42(3)
C(2S)	9760(40)	-7860(30)	1500(30)	42(3)
C(3)	6268(9)	-8715(6)	928(5)	38(2)
C(4)	6600(8)	-9552(6)	1324(5)	38(2)
C(5)	5621(10)	-10220(7)	1227(6)	49(3)
C(6)	4291(10)	-10061(7)	743(6)	48(3)
C(7)	3962(10)	-9236(7)	348(6)	52(3)
C(8)	4933(9)	-8559(7)	438(5)	47(3)
C(9)	10768(16)	-7914(11)	1324(11)	42(3)
C(10)	10786(10)	-8595(7)	749(6)	55(3)
C(11)	11575(10)	-6997(8)	1357(7)	69(3)
C(9S)	10310(40)	-7620(30)	1000(30)	42(3)
C(10S)	10786(10)	-8595(7)	749(6)	55(3)
C(11S)	11575(10)	-6997(8)	1357(7)	69(3)
C(12)	8374(8)	-7695(6)	2612(5)	37(2)
C(13)	10496(9)	-8106(7)	4163(5)	51(3)
C(14)	9721(9)	-6028(6)	3721(5)	46(3)
C(15)	11495(9)	-7131(7)	3224(6)	57(3)
C(16)	7264(10)	-9309(6)	3209(6)	53(3)
C(17)	7063(10)	-7305(7)	3704(5)	52(3)
C(18)	5236(8)	-7872(7)	2205(5)	48(3)
C(23)	8676(10)	-4956(7)	1975(6)	43(2)
C(20)	6445(10)	-5299(7)	2308(6)	45(3)
C(21)	4889(10)	-6050(7)	868(5)	41(2)
C(22)	7158(9)	-5596(7)	539(6)	43(2)
C(19)	6014(9)	-4204(7)	1070(6)	42(3)
O(1)	8536(6)	-8405(5)	1109(4)	56(2)
O(2)	9315(6)	-6988(4)	1693(3)	43(2)

O(7)	9774(7)	-4687(5)	2273(4)	57(2)
O(4)	6251(7)	-5131(5)	2799(4)	61(2)
O(5)	3805(6)	-6350(5)	564(4)	54(2)
O(6)	7404(7)	-5649(5)	53(4)	56(2)
O(3)	5558(6)	-3457(5)	873(4)	53(2)
P	7889(2)	-7072(2)	1763(1)	36(1)
Si(1)	9982(3)	-7223(2)	3412(2)	43(1)
Si(2)	7011(3)	-8031(2)	2922(2)	40(1)
W	6780(1)	-5480(1)	1423(1)	38(1)

Table xiii.3. Bond lengths [Å] and angles [deg] for **[62a]**.

C(1)-O(1)	1.427(10)
C(1)-C(3)	1.501(12)
C(1)-P	1.862(10)
C(1)-H(1A)	1.0000
C(2)-O(1)	1.446(15)
C(2)-O(2)	1.472(16)
C(2)-C(9)	1.51(3)
C(2)-H(2A)	1.0000
C(2S)-O(2)	1.44(4)
C(2S)-O(1)	1.45(4)
C(2S)-C(9S)	1.45(7)
C(2S)-H(2AS)	1.0000
C(3)-C(8)	1.381(12)
C(3)-C(4)	1.387(12)
C(4)-C(5)	1.377(11)
C(4)-H(4A)	0.9500
C(5)-C(6)	1.375(13)
C(5)-H(5A)	0.9500
C(6)-C(7)	1.371(13)
C(6)-H(6A)	0.9500
C(7)-C(8)	1.383(12)
C(7)-H(7A)	0.9500
C(8)-H(8A)	0.9500
C(9)-C(10)	1.528(17)
C(9)-C(11)	1.553(17)
C(9)-H(9A)	1.0000
C(10)-H(10A)	0.9800
C(10)-H(10B)	0.9800
C(10)-H(10C)	0.9800
C(11)-H(11A)	0.9800
C(11)-H(11B)	0.9800
C(11)-H(11C)	0.9800
C(9S)-H(9AS)	1.0000
C(12)-P	1.808(9)
C(12)-Si(1)	1.922(9)
C(12)-Si(2)	1.929(9)
C(12)-H(12A)	1.0000
C(13)-Si(1)	1.862(10)
C(13)-H(13A)	0.9800
C(13)-H(13B)	0.9800
C(13)-H(13C)	0.9800
C(14)-Si(1)	1.867(9)
C(14)-H(14A)	0.9800
C(14)-H(14B)	0.9800
C(14)-H(14C)	0.9800
C(15)-Si(1)	1.873(9)
C(15)-H(15A)	0.9800
C(15)-H(15B)	0.9800
C(15)-H(15C)	0.9800

C(16)-Si(2)	1.878(9)
C(16)-H(16A)	0.9800
C(16)-H(16B)	0.9800
C(16)-H(16C)	0.9800
C(17)-Si(2)	1.882(9)
C(17)-H(17A)	0.9800
C(17)-H(17B)	0.9800
C(17)-H(17C)	0.9800
C(18)-Si(2)	1.866(9)
C(18)-H(18A)	0.9800
C(18)-H(18B)	0.9800
C(18)-H(18C)	0.9800
C(23)-O(7)	1.151(10)
C(23)-W	2.022(10)
C(20)-O(4)	1.145(11)
C(20)-W	2.023(12)
C(21)-O(5)	1.154(10)
C(21)-W	2.043(10)
C(22)-O(6)	1.143(11)
C(22)-W	2.039(11)
C(19)-O(3)	1.160(10)
C(19)-W	1.983(10)
O(2)-P	1.642(6)
P-W	2.502(2)
O(1)-C(1)-C(3)	109.8(7)
O(1)-C(1)-P	102.8(6)
C(3)-C(1)-P	123.1(7)
O(1)-C(1)-H(1A)	106.7
C(3)-C(1)-H(1A)	106.7
P-C(1)-H(1A)	106.7
O(1)-C(2)-O(2)	103.5(10)
O(1)-C(2)-C(9)	108.6(14)
O(2)-C(2)-C(9)	109.3(15)
O(1)-C(2)-H(2A)	111.7
O(2)-C(2)-H(2A)	111.7
C(9)-C(2)-H(2A)	111.7
O(2)-C(2S)-O(1)	105(3)
O(2)-C(2S)-C(9S)	107(4)
O(1)-C(2S)-C(9S)	108(4)
O(2)-C(2S)-H(2AS)	112.2
O(1)-C(2S)-H(2AS)	112.2
C(9S)-C(2S)-H(2AS)	112.2
C(8)-C(3)-C(4)	118.7(8)
C(8)-C(3)-C(1)	118.8(9)
C(4)-C(3)-C(1)	122.5(8)
C(5)-C(4)-C(3)	120.7(8)
C(5)-C(4)-H(4A)	119.6
C(3)-C(4)-H(4A)	119.6
C(6)-C(5)-C(4)	120.4(9)
C(6)-C(5)-H(5A)	119.8
C(4)-C(5)-H(5A)	119.8
C(7)-C(6)-C(5)	118.9(9)
C(7)-C(6)-H(6A)	120.6
C(5)-C(6)-H(6A)	120.6
C(6)-C(7)-C(8)	121.4(10)
C(6)-C(7)-H(7A)	119.3
C(8)-C(7)-H(7A)	119.3
C(3)-C(8)-C(7)	119.8(9)
C(3)-C(8)-H(8A)	120.1
C(7)-C(8)-H(8A)	120.1
C(2)-C(9)-C(10)	109.7(15)
C(2)-C(9)-C(11)	105.4(14)

C(10)-C(9)-C(11)	110.7(11)
C(2)-C(9)-H(9A)	110.3
C(10)-C(9)-H(9A)	110.3
C(11)-C(9)-H(9A)	110.3
C(9)-C(10)-H(10A)	109.5
C(9)-C(10)-H(10B)	109.5
H(10A)-C(10)-H(10B)	109.5
C(9)-C(10)-H(10C)	109.5
H(10A)-C(10)-H(10C)	109.5
H(10B)-C(10)-H(10C)	109.5
C(9)-C(11)-H(11A)	109.5
C(9)-C(11)-H(11B)	109.5
H(11A)-C(11)-H(11B)	109.5
C(9)-C(11)-H(11C)	109.5
H(11A)-C(11)-H(11C)	109.5
H(11B)-C(11)-H(11C)	109.5
C(2S)-C(9S)-H(9AS)	110.1
P-C(12)-Si(1)	114.9(5)
P-C(12)-Si(2)	119.7(5)
Si(1)-C(12)-Si(2)	111.1(4)
P-C(12)-H(12A)	102.8
Si(1)-C(12)-H(12A)	102.8
Si(2)-C(12)-H(12A)	102.8
Si(1)-C(13)-H(13A)	109.5
Si(1)-C(13)-H(13B)	109.5
H(13A)-C(13)-H(13B)	109.5
Si(1)-C(13)-H(13C)	109.5
H(13A)-C(13)-H(13C)	109.5
H(13B)-C(13)-H(13C)	109.5
Si(1)-C(14)-H(14A)	109.5
Si(1)-C(14)-H(14B)	109.5
H(14A)-C(14)-H(14B)	109.5
Si(1)-C(14)-H(14C)	109.5
H(14A)-C(14)-H(14C)	109.5
H(14B)-C(14)-H(14C)	109.5
Si(1)-C(15)-H(15A)	109.5
Si(1)-C(15)-H(15B)	109.5
H(15A)-C(15)-H(15B)	109.5
Si(1)-C(15)-H(15C)	109.5
H(15A)-C(15)-H(15C)	109.5
H(15B)-C(15)-H(15C)	109.5
Si(2)-C(16)-H(16A)	109.5
Si(2)-C(16)-H(16B)	109.5
H(16A)-C(16)-H(16B)	109.5
Si(2)-C(16)-H(16C)	109.5
H(16A)-C(16)-H(16C)	109.5
H(16B)-C(16)-H(16C)	109.5
Si(2)-C(17)-H(17A)	109.5
Si(2)-C(17)-H(17B)	109.5
H(17A)-C(17)-H(17B)	109.5
Si(2)-C(17)-H(17C)	109.5
H(17A)-C(17)-H(17C)	109.5
H(17B)-C(17)-H(17C)	109.5
Si(2)-C(18)-H(18A)	109.5
Si(2)-C(18)-H(18B)	109.5
H(18A)-C(18)-H(18B)	109.5
Si(2)-C(18)-H(18C)	109.5
H(18A)-C(18)-H(18C)	109.5
H(18B)-C(18)-H(18C)	109.5
O(7)-C(23)-W	176.9(9)
O(4)-C(20)-W	175.2(8)
O(5)-C(21)-W	177.8(8)
O(6)-C(22)-W	178.1(8)

O(3)-C(19)-W	178.9(9)
C(1)-O(1)-C(2)	101.6(8)
C(1)-O(1)-C(2S)	116.2(16)
C(2)-O(1)-C(2S)	32.9(16)
C(2S)-O(2)-C(2)	32.7(17)
C(2S)-O(2)-P	114.6(15)
C(2)-O(2)-P	112.8(7)
O(2)-P-C(12)	103.5(4)
O(2)-P-C(1)	88.6(4)
C(12)-P-C(1)	107.9(4)
O(2)-P-W	106.1(2)
C(12)-P-W	127.1(3)
C(1)-P-W	115.5(3)
C(13)-Si(1)-C(14)	111.0(4)
C(13)-Si(1)-C(15)	104.2(5)
C(14)-Si(1)-C(15)	107.0(4)
C(13)-Si(1)-C(12)	107.6(4)
C(14)-Si(1)-C(12)	112.4(4)
C(15)-Si(1)-C(12)	114.5(4)
C(18)-Si(2)-C(16)	108.7(5)
C(18)-Si(2)-C(17)	103.4(4)
C(16)-Si(2)-C(17)	108.1(5)
C(18)-Si(2)-C(12)	114.0(4)
C(16)-Si(2)-C(12)	108.0(4)
C(17)-Si(2)-C(12)	114.4(4)
C(19)-W-C(23)	92.2(4)
C(19)-W-C(20)	89.8(4)
C(23)-W-C(20)	90.2(4)
C(19)-W-C(22)	88.3(4)
C(23)-W-C(22)	87.7(4)
C(20)-W-C(22)	177.1(4)
C(19)-W-C(21)	89.5(4)
C(23)-W-C(21)	178.2(4)
C(20)-W-C(21)	90.2(4)
C(22)-W-C(21)	91.8(4)
C(19)-W-P	172.7(3)
C(23)-W-P	85.2(3)
C(20)-W-P	97.1(3)
C(22)-W-P	84.8(3)
C(21)-W-P	93.0(3)

Table xiii.4. Anisotropic displacement parameters ($\text{\AA}^2 \times 10^3$) for [62a]

The anisotropic displacement factor exponent takes the form:
 $-2 \pi^2 [h^2 a^{*2} U_{11} + \dots + 2 h k a^* b^* U_{12}]$

	U11	U22	U33	U23	U13	U12
C(1)	39(6)	50(6)	43(7)	2(5)	21(5)	0(5)
C(2)	37(7)	41(7)	53(9)	6(6)	25(7)	4(5)
C(2S)	37(7)	41(7)	53(9)	6(6)	24(7)	4(5)
C(3)	35(5)	39(6)	40(6)	-5(5)	16(5)	-7(4)
C(4)	33(5)	42(5)	40(6)	-5(6)	17(5)	0(5)
C(5)	52(6)	44(6)	56(7)	-2(5)	28(6)	-4(5)
C(6)	43(6)	48(6)	62(8)	-16(6)	32(6)	-16(5)
C(7)	42(6)	60(7)	51(7)	-10(6)	19(6)	-3(5)
C(8)	49(6)	45(6)	46(7)	0(5)	22(6)	0(5)

C(9)	38(7)	42(7)	53(9)	6(6)	24(7)	4(5)
C(10)	61(7)	49(6)	73(8)	13(6)	45(7)	15(5)
C(11)	58(7)	76(8)	93(10)	-7(8)	53(8)	-4(6)
C(9S)	37(7)	41(7)	53(9)	6(6)	24(7)	4(5)
C(10S)	61(7)	49(6)	73(8)	13(6)	45(7)	15(5)
C(11S)	58(7)	76(8)	93(10)	-7(8)	53(8)	-4(6)
C(12)	41(5)	30(5)	38(6)	1(4)	17(5)	6(4)
C(13)	44(6)	49(6)	46(7)	0(5)	7(6)	8(5)
C(14)	44(6)	40(6)	45(7)	3(5)	13(5)	-10(5)
C(15)	40(6)	61(7)	60(8)	-4(6)	13(6)	3(5)
C(16)	64(7)	45(7)	57(7)	2(5)	31(6)	-6(5)
C(17)	60(7)	58(7)	41(7)	-2(5)	24(6)	2(5)
C(18)	42(6)	57(7)	58(7)	0(6)	34(6)	0(5)
C(23)	47(6)	30(5)	52(7)	-2(5)	21(6)	3(5)
C(20)	43(6)	34(6)	49(7)	3(5)	11(6)	-1(4)
C(21)	38(6)	43(6)	43(7)	5(5)	20(5)	4(5)
C(22)	33(5)	36(6)	55(7)	0(5)	15(5)	-1(4)
C(19)	36(5)	38(6)	44(7)	-7(5)	12(5)	-14(5)
O(1)	49(4)	50(4)	87(6)	-20(4)	47(4)	-11(3)
O(2)	37(4)	46(4)	51(5)	-8(3)	22(4)	-1(3)
O(7)	43(4)	50(5)	66(5)	10(4)	15(4)	-4(4)
O(4)	79(5)	55(5)	59(6)	1(4)	41(5)	13(4)
O(5)	31(4)	58(5)	62(5)	0(4)	11(4)	-4(3)
O(6)	53(4)	72(5)	47(5)	6(4)	26(4)	3(4)
O(3)	42(4)	48(5)	64(5)	9(4)	19(4)	6(4)
P	30(1)	38(1)	40(2)	-3(1)	16(1)	-2(1)
Si(1)	38(2)	40(2)	43(2)	-3(1)	12(2)	5(1)
Si(2)	43(2)	36(2)	44(2)	0(1)	22(2)	0(1)
W	32(1)	37(1)	42(1)	2(1)	15(1)	0(1)

Table xiii.5. Hydrogen coordinates ($\times 10^4$) and isotropic displacement parameters ($\text{Å}^2 \times 10^3$) for [62a].

	x	y	z	U(eq)
H(1A)	6949	-7606	551	52
H(2A)	8941	-7258	632	50
H(2AS)	10434	-8205	1940	51
H(4A)	7512	-9667	1666	46
H(5A)	5866	-10794	1497	59
H(6A)	3611	-10514	683	57
H(7A)	3048	-9127	5	62
H(8A)	4683	-7988	164	56
H(9A)	11151	-8230	1811	51
H(10A)	11719	-8800	886	83
H(10B)	10427	-8273	277	83
H(10C)	10224	-9150	715	83
H(11A)	12521	-7161	1487	103
H(11B)	11541	-6567	1724	103
H(11C)	11173	-6685	881	103
H(9AS)	9605	-7288	562	51
H(10D)	10005	-9018	514	83
H(10E)	11483	-8909	1178	83
H(10F)	11156	-8444	406	83
H(11D)	11924	-6853	1003	103
H(11E)	12270	-7335	1772	103
H(11F)	11343	-6405	1525	103
H(12A)	8672	-8327	2513	44
H(13A)	10618	-8727	3986	61

H(13B)	9790	-8149	4330	61
H(13C)	11350	-7905	4567	61
H(14A)	9114	-6083	3953	55
H(14B)	9318	-5602	3301	55
H(14C)	10596	-5771	4071	55
H(15A)	11339	-6634	2861	68
H(15B)	11640	-7739	3037	68
H(15C)	12297	-6972	3674	68
H(16A)	8220	-9418	3542	64
H(16B)	7002	-9714	2779	64
H(16C)	6702	-9462	3455	64
H(17A)	6877	-6640	3555	63
H(17B)	7962	-7358	4117	63
H(17C)	6377	-7540	3846	63
H(18A)	5082	-8279	1788	58
H(18B)	5092	-7208	2049	58
H(18C)	4602	-8046	2402	58

Table xiii.6. Torsion angles [deg] for [62a].

O(1)-C(1)-C(3)-C(8)	-141.4(9)
P-C(1)-C(3)-C(8)	97.5(10)
O(1)-C(1)-C(3)-C(4)	39.4(12)
P-C(1)-C(3)-C(4)	-81.7(11)
C(8)-C(3)-C(4)-C(5)	0.5(14)
C(1)-C(3)-C(4)-C(5)	179.7(9)
C(3)-C(4)-C(5)-C(6)	-1.0(14)
C(4)-C(5)-C(6)-C(7)	1.3(15)
C(5)-C(6)-C(7)-C(8)	-1.2(15)
C(4)-C(3)-C(8)-C(7)	-0.5(14)
C(1)-C(3)-C(8)-C(7)	-179.7(9)
C(6)-C(7)-C(8)-C(3)	0.8(15)
O(1)-C(2)-C(9)-C(10)	64(2)
O(2)-C(2)-C(9)-C(10)	176.1(9)
O(1)-C(2)-C(9)-C(11)	-176.9(10)
O(2)-C(2)-C(9)-C(11)	-65(2)
C(3)-C(1)-O(1)-C(2)	174.4(10)
P-C(1)-O(1)-C(2)	-52.9(10)
C(3)-C(1)-O(1)-C(2S)	-154(2)
P-C(1)-O(1)-C(2S)	-22(2)
O(2)-C(2)-O(1)-C(1)	55.0(13)
C(9)-C(2)-O(1)-C(1)	171.0(14)
O(2)-C(2)-O(1)-C(2S)	-66(3)
C(9)-C(2)-O(1)-C(2S)	50(3)
O(2)-C(2S)-O(1)-C(1)	0(4)
C(9S)-C(2S)-O(1)-C(1)	-114(3)
O(2)-C(2S)-O(1)-C(2)	70(3)
C(9S)-C(2S)-O(1)-C(2)	-44(4)
O(1)-C(2S)-O(2)-C(2)	-68(3)
C(9S)-C(2S)-O(2)-C(2)	46(4)
O(1)-C(2S)-O(2)-P	26(4)
C(9S)-C(2S)-O(2)-P	141(3)
O(1)-C(2)-O(2)-C(2S)	67(3)
C(9)-C(2)-O(2)-C(2S)	-48(3)
O(1)-C(2)-O(2)-P	-32.9(14)
C(9)-C(2)-O(2)-P	-148.5(12)
C(2S)-O(2)-P-C(12)	74(2)
C(2)-O(2)-P-C(12)	109.9(10)
C(2S)-O(2)-P-C(1)	-34(2)
C(2)-O(2)-P-C(1)	1.8(10)
C(2S)-O(2)-P-W	-150(2)

C(2)-O(2)-P-W	-114.4(9)
Si(1)-C(12)-P-O(2)	46.8(5)
Si(2)-C(12)-P-O(2)	-176.9(5)
Si(1)-C(12)-P-C(1)	139.8(5)
Si(2)-C(12)-P-C(1)	-84.0(6)
Si(1)-C(12)-P-W	-75.9(5)
Si(2)-C(12)-P-W	60.4(6)
O(1)-C(1)-P-O(2)	30.1(6)
C(3)-C(1)-P-O(2)	154.4(8)
O(1)-C(1)-P-C(12)	-73.6(6)
C(3)-C(1)-P-C(12)	50.6(9)
O(1)-C(1)-P-W	137.3(5)
C(3)-C(1)-P-W	-98.4(8)
P-C(12)-Si(1)-C(13)	-168.2(5)
Si(2)-C(12)-Si(1)-C(13)	51.9(6)
P-C(12)-Si(1)-C(14)	69.3(6)
Si(2)-C(12)-Si(1)-C(14)	-70.6(6)
P-C(12)-Si(1)-C(15)	-53.0(6)
Si(2)-C(12)-Si(1)-C(15)	167.1(4)
P-C(12)-Si(2)-C(18)	11.3(7)
Si(1)-C(12)-Si(2)-C(18)	149.0(4)
P-C(12)-Si(2)-C(16)	132.2(6)
Si(1)-C(12)-Si(2)-C(16)	-90.1(5)
P-C(12)-Si(2)-C(17)	-107.4(6)
Si(1)-C(12)-Si(2)-C(17)	30.4(6)
O(3)-C(19)-W-C(23)	-103(48)
O(3)-C(19)-W-C(20)	-13(48)
O(3)-C(19)-W-C(22)	170(48)
O(3)-C(19)-W-C(21)	78(48)
O(3)-C(19)-W-P	-172(100)
O(7)-C(23)-W-C(19)	-127(17)
O(7)-C(23)-W-C(20)	144(17)
O(7)-C(23)-W-C(22)	-39(17)
O(7)-C(23)-W-C(21)	38(27)
O(7)-C(23)-W-P	46(17)
O(4)-C(20)-W-C(19)	-19(11)
O(4)-C(20)-W-C(23)	73(11)
O(4)-C(20)-W-C(22)	28(16)
O(4)-C(20)-W-C(21)	-108(11)
O(4)-C(20)-W-P	159(11)
O(6)-C(22)-W-C(19)	86(27)
O(6)-C(22)-W-C(23)	-7(27)
O(6)-C(22)-W-C(20)	39(31)
O(6)-C(22)-W-C(21)	175(100)
O(6)-C(22)-W-P	-92(27)
O(5)-C(21)-W-C(19)	-47(23)
O(5)-C(21)-W-C(23)	148(20)
O(5)-C(21)-W-C(20)	43(23)
O(5)-C(21)-W-C(22)	-135(23)
O(5)-C(21)-W-P	140(23)
O(2)-P-W-C(19)	31(2)
C(12)-P-W-C(19)	152(2)
C(1)-P-W-C(19)	-66(2)
O(2)-P-W-C(23)	-39.1(4)
C(12)-P-W-C(23)	82.6(5)
C(1)-P-W-C(23)	-135.4(4)
O(2)-P-W-C(20)	-128.7(4)
C(12)-P-W-C(20)	-7.1(4)
C(1)-P-W-C(20)	135.0(4)
O(2)-P-W-C(22)	49.1(4)
C(12)-P-W-C(22)	170.7(4)
C(1)-P-W-C(22)	-47.2(4)
O(2)-P-W-C(21)	140.7(4)

C(12)-P-W-C(21)
C(1)-P-W-C(21)

-97.7(4)
44.4(4)

xiv. { η^2 -[phenylmethylene

(bis(trimethylsilyl)methyl)hydroxypyrophosphonium]pentacarbonyltungsten(0)}_{2,3},
4,5,6,7,8,9,10,11,12-undecachloro-1-carbadodecaborate [73]

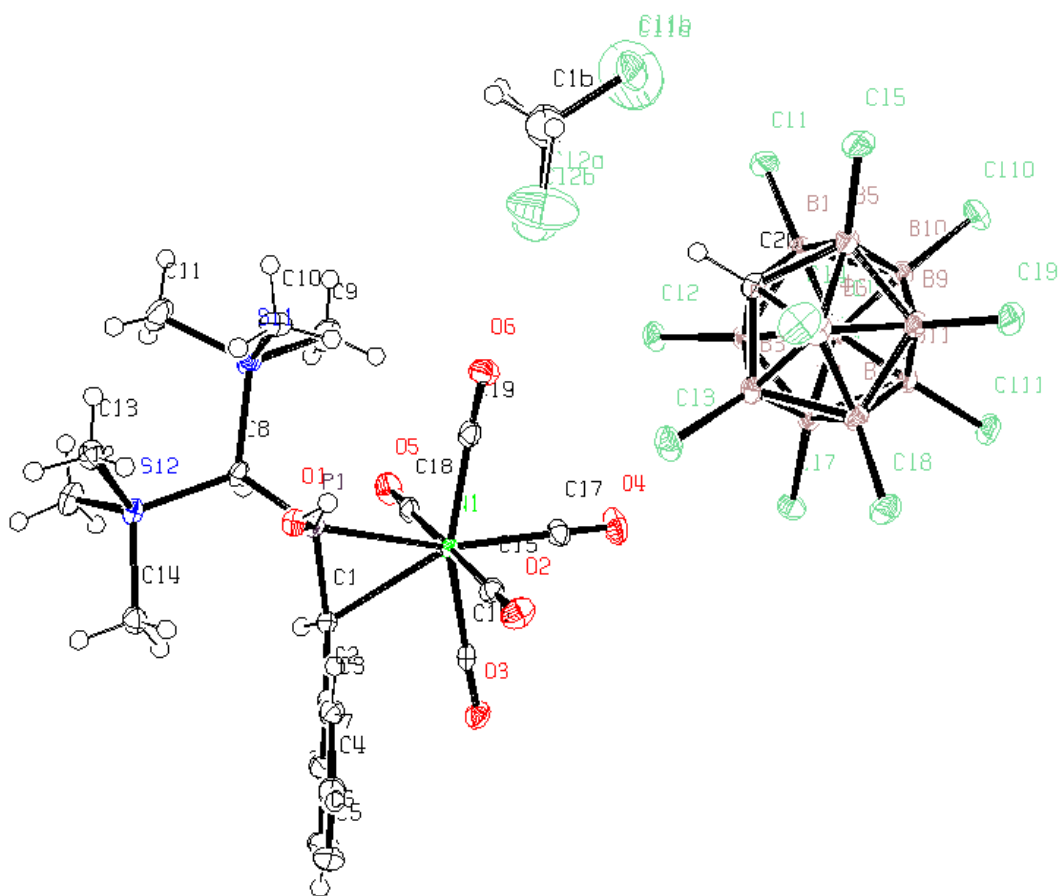


Table xiv.1. Crystal data and structure refinement for [73]

Empirical formula	C ₂₁ H ₂₉ B ₁₁ C ₁₁₃ O ₆ PSi ₂ W
Formula weight	1228.20
Temperature	0(2) K
Wavelength	0.71073 Å
Crystal system	Triclinic
Space group	P-1
Unit cell dimensions	a = 9.5558(12) Å alpha = 86.1740(10)° b = 14.2372(17) Å beta = 86.5200(10)°

	c = 17.852(2) Å	gamma = 70.7550(10)°
Volume	2285.9(5) Å ³	
Z	2	
Density (calculated)	1.784 Mg/m ³	
Absorption coefficient	3.410 mm ⁻¹	
F(000)	1192	
Crystal size	0.51 x 0.13 x 0.12 mm ³	
Theta range for data collection	1.85 to 29.19°	
Index ranges	-12<=h<=12, -18<=k<=17, -22<=l<=23	
Reflections collected	19052	
Independent reflections	10829 [R(int) = 0.0118]	
Completeness to theta = 29.19°	87.5 %	
Absorption correction	Sadabs	
Max. and min. transmission	0.6851 and 0.2752	
Refinement method	Full-matrix least-squares on F ²	
Data / restraints / parameters	10829 / 0 / 538	
Goodness-of-fit on F ²	1.043	
Final R indices [I>2sigma(I)]	R1 = 0.0174, wR2 = 0.0426	
R indices (all data)	R1 = 0.0184, wR2 = 0.0430	
Extinction coefficient	0.00010(7)	
Largest diff. peak and hole	0.914 and -0.839 e.Å ⁻³	

Table xiv.2. Atomic coordinates (x 10⁴) and equivalent isotropic displacement parameters (Å²x 10³) for [73]

1. U(eq) is defined as one third of the trace of the orthogonalized U^{ij} tensor.

	x	y	z	U(eq)
W(1)	8996(1)	2079(1)	1893(1)	12(1)
P(1)	11391(1)	1736(1)	2468(1)	12(1)
Si(1)	11144(1)	1547(1)	4216(1)	22(1)
Si(2)	14203(1)	469(1)	3267(1)	16(1)
O(1)	12227(2)	2541(1)	2408(1)	16(1)
O(2)	9410(2)	3902(1)	845(1)	26(1)
O(3)	9156(2)	894(1)	408(1)	23(1)
O(4)	5554(2)	2644(1)	1583(1)	31(1)
O(5)	8562(2)	279(1)	2926(1)	26(1)
O(6)	7715(2)	3641(1)	3175(1)	27(1)

C(1)	11595(2)	1073(1)	1662(1)	14(1)
C(2)	12327(2)	1190(1)	925(1)	15(1)
C(3)	12787(2)	2005(2)	702(1)	19(1)
C(4)	13466(2)	2056(2)	0(1)	25(1)
C(5)	13681(2)	1297(2)	-493(1)	30(1)
C(6)	13252(2)	482(2)	-276(1)	29(1)
C(7)	12589(2)	419(2)	429(1)	21(1)
C(8)	12054(2)	972(1)	3292(1)	16(1)
C(9)	9241(2)	1452(2)	4348(1)	34(1)
C(10)	11095(3)	2865(2)	4215(1)	30(1)
C(11)	12194(3)	806(2)	5026(1)	34(1)
C(12)	14738(2)	-776(2)	3775(1)	25(1)
C(13)	14966(2)	1348(2)	3701(1)	21(1)
C(14)	14985(2)	308(2)	2282(1)	20(1)
C(15)	9293(2)	3250(1)	1208(1)	18(1)
C(16)	9125(2)	1301(1)	933(1)	16(1)
C(17)	6765(2)	2483(1)	1689(1)	20(1)
C(18)	8735(2)	917(1)	2556(1)	18(1)
C(19)	8200(2)	3084(2)	2731(1)	19(1)
C(20)	3221(2)	6337(1)	2849(1)	17(1)

	x	y	z	U(eq)
B(1)	1572(2)	6168(2)	3152(1)	17(1)
B(2)	2949(2)	5264(2)	2613(1)	16(1)
B(3)	3888(2)	5899(2)	1973(1)	17(1)
B(4)	3076(3)	7206(2)	2118(1)	21(1)
B(5)	1655(2)	7369(2)	2844(1)	19(1)
B(6)	1060(2)	5644(2)	2381(1)	16(1)
B(7)	2478(2)	5476(2)	1650(1)	17(1)
B(8)	2564(2)	6682(2)	1343(1)	19(1)
B(9)	1183(3)	7593(2)	1884(1)	19(1)
B(10)	240(2)	6954(2)	2525(1)	18(1)
B(11)	809(2)	6525(2)	1594(1)	18(1)
C1(1)	1213(1)	5891(1)	4110(1)	25(1)
C1(2)	3939(1)	4101(1)	3054(1)	21(1)
C1(3)	5810(1)	5383(1)	1763(1)	27(1)
C1(4)	4202(1)	7976(1)	2063(1)	34(1)
C1(5)	1374(1)	8305(1)	3498(1)	27(1)

C1(6)	-10(1)	4821(1)	2528(1)	23(1)
C1(7)	2876(1)	4499(1)	1022(1)	24(1)
C1(8)	3114(1)	6947(1)	403(1)	28(1)
C1(9)	270(1)	8812(1)	1496(1)	28(1)
C1(10)	-1648(1)	7502(1)	2816(1)	29(1)
C1(11)	-515(1)	6616(1)	918(1)	29(1)
C(1A)	5774(7)	5856(5)	4850(4)	39(1)
C1(1A)	4305(9)	6803(6)	4926(5)	146(3)
C1(2A)	6803(4)	6024(3)	4035(2)	84(1)
C(1B)	6298(6)	6404(5)	4688(4)	62(2)
C1(1B)	4306(2)	6878(1)	4948(1)	40(1)
C1(2B)	6705(2)	5536(2)	4029(1)	58(1)

Table xiv.3. Bond lengths [Å] and angles [°] for [73]

W(1)-C(18)	2.043(2)	W(1)-C(17)	2.0667(19)
W(1)-C(19)	2.0713(19)	W(1)-C(16)	2.0784(19)
W(1)-C(15)	2.086(2)	W(1)-C(1)	2.4489(17)
W(1)-P(1)	2.4513(5)	P(1)-O(1)	1.5935(14)
P(1)-C(1)	1.7394(18)	P(1)-C(8)	1.7865(18)
Si(1)-C(10)	1.861(3)	Si(1)-C(9)	1.867(2)
Si(1)-C(11)	1.867(2)	Si(1)-C(8)	1.9193(19)
Si(2)-C(12)	1.863(2)	Si(2)-C(14)	1.867(2)
Si(2)-C(13)	1.8705(19)	Si(2)-C(8)	1.9380(19)
O(1)-H(1A)	0.75(3)	O(2)-C(15)	1.129(2)
O(3)-C(16)	1.129(2)	O(4)-C(17)	1.128(2)
O(5)-C(18)	1.138(2)	O(6)-C(19)	1.126(2)
C(1)-C(2)	1.479(2)	C(2)-C(3)	1.397(3)
C(2)-C(7)	1.404(3)	C(3)-C(4)	1.386(3)
C(4)-C(5)	1.394(3)	C(5)-C(6)	1.379(4)
C(6)-C(7)	1.385(3)	C(20)-B(2)	1.715(3)
C(20)-B(4)	1.716(3)	C(20)-B(5)	1.718(3)
C(20)-B(1)	1.723(3)	C(20)-B(3)	1.729(3)
C(20)-H(20)	1.14(3)	B(1)-Cl(1)	1.767(2)
B(1)-B(6)	1.775(3)	B(1)-B(10)	1.787(3)
B(1)-B(5)	1.788(3)	B(1)-B(2)	1.792(3)
B(2)-Cl(2)	1.772(2)	B(2)-B(6)	1.772(3)
B(2)-B(7)	1.785(3)	B(2)-B(3)	1.790(3)

B(3)-Cl(3)	1.765(2)	B(3)-B(8)	1.785(3)
B(3)-B(7)	1.785(3)	B(3)-B(4)	1.794(3)
B(4)-Cl(4)	1.766(2)	B(4)-B(9)	1.777(3)
B(4)-B(8)	1.780(3)	B(4)-B(5)	1.788(3)
B(5)-Cl(5)	1.774(2)	B(5)-B(10)	1.779(3)
B(5)-B(9)	1.780(3)	B(6)-B(7)	1.791(3)
B(6)-Cl(6)	1.791(2)	B(6)-B(11)	1.791(3)
B(6)-B(10)	1.799(3)	B(7)-Cl(7)	1.773(2)
B(7)-B(11)	1.793(3)	B(7)-B(8)	1.794(3)
B(8)-Cl(8)	1.781(2)	B(8)-B(11)	1.791(3)
B(8)-B(9)	1.800(3)	B(9)-Cl(9)	1.779(2)
B(9)-B(11)	1.788(3)	B(9)-B(10)	1.796(3)
B(10)-Cl(10)	1.775(2)	B(10)-B(11)	1.800(3)
B(11)-Cl(11)	1.769(2)	C(1A)-Cl(1A)	1.600(10)
C(1A)-Cl(2A)	1.754(7)	C(1B)-Cl(2B)	1.699(5)
C(1B)-Cl(1B)	1.839(6)		
C(18)-W(1)-C(17)	87.22(8)	C(18)-W(1)-C(19)	93.27(8)
C(17)-W(1)-C(19)	82.01(7)	C(18)-W(1)-C(16)	90.83(7)
C(17)-W(1)-C(16)	80.48(7)	C(19)-W(1)-C(16)	161.79(7)
C(18)-W(1)-C(15)	179.07(7)	C(17)-W(1)-C(15)	93.36(8)
C(19)-W(1)-C(15)	87.53(8)	C(16)-W(1)-C(15)	88.55(7)
C(18)-W(1)-C(1)	88.35(7)	C(17)-W(1)-C(1)	152.10(7)
C(19)-W(1)-C(1)	125.76(6)	C(16)-W(1)-C(1)	72.06(6)
C(15)-W(1)-C(1)	90.79(7)	C(18)-W(1)-P(1)	87.29(5)
C(17)-W(1)-P(1)	164.93(6)	C(19)-W(1)-P(1)	84.30(5)
C(16)-W(1)-P(1)	113.63(5)	C(15)-W(1)-P(1)	92.32(5)
C(1)-W(1)-P(1)	41.58(4)	O(1)-P(1)-C(1)	113.91(8)
O(1)-P(1)-C(8)	105.42(8)	C(1)-P(1)-C(8)	113.84(9)
O(1)-P(1)-W(1)	121.02(6)	C(1)-P(1)-W(1)	69.14(6)
C(8)-P(1)-W(1)	127.86(6)	C(10)-Si(1)-C(9)	111.32(12)
C(10)-Si(1)-C(11)	110.44(11)	C(9)-Si(1)-C(11)	105.42(11)
C(10)-Si(1)-C(8)	110.09(9)	C(9)-Si(1)-C(8)	109.72(10)
C(11)-Si(1)-C(8)	109.75(10)	C(12)-Si(2)-C(14)	108.43(10)
C(12)-Si(2)-C(13)	112.09(9)	C(14)-Si(2)-C(13)	107.55(9)
C(12)-Si(2)-C(8)	106.63(9)	C(14)-Si(2)-C(8)	111.21(8)
C(13)-Si(2)-C(8)	110.95(9)	P(1)-O(1)-H(1A)	114(2)
C(2)-C(1)-P(1)	130.08(14)	C(2)-C(1)-W(1)	118.94(12)
P(1)-C(1)-W(1)	69.28(6)	C(3)-C(2)-C(7)	118.77(17)

C(3)-C(2)-C(1)	124.06(16)	C(7)-C(2)-C(1)	117.16(17)
C(4)-C(3)-C(2)	120.39(18)	C(3)-C(4)-C(5)	120.1(2)
C(6)-C(5)-C(4)	120.1(2)	C(5)-C(6)-C(7)	120.2(2)
C(6)-C(7)-C(2)	120.5(2)	P(1)-C(8)-Si(1)	114.32(10)
P(1)-C(8)-Si(2)	111.05(9)	Si(1)-C(8)-Si(2)	114.77(9)
O(2)-C(15)-W(1)	177.81(17)	O(3)-C(16)-W(1)	178.12(16)
O(4)-C(17)-W(1)	175.82(18)	O(5)-C(18)-W(1)	178.78(16)
O(6)-C(19)-W(1)	177.36(16)	B(2)-C(20)-B(4)	114.46(14)
B(2)-C(20)-B(5)	114.61(14)	B(4)-C(20)-B(5)	62.75(13)
B(2)-C(20)-B(1)	62.83(12)	B(4)-C(20)-B(1)	114.64(15)
B(5)-C(20)-B(1)	62.62(12)	B(2)-C(20)-B(3)	62.63(12)
B(4)-C(20)-B(3)	62.77(12)	B(5)-C(20)-B(3)	114.92(14)
B(1)-C(20)-B(3)	114.93(14)	B(2)-C(20)-H(20)	117.7(14)
B(4)-C(20)-H(20)	117.8(14)	B(5)-C(20)-H(20)	118.0(14)
B(1)-C(20)-H(20)	117.8(14)	B(3)-C(20)-H(20)	117.2(14)
C(20)-B(1)-Cl(1)	121.20(13)	C(20)-B(1)-B(6)	104.01(14)
Cl(1)-B(1)-B(6)	125.40(15)	C(20)-B(1)-B(10)	104.51(15)
Cl(1)-B(1)-B(10)	125.49(14)	B(6)-B(1)-B(10)	60.66(12)
C(20)-B(1)-B(5)	58.55(12)	Cl(1)-B(1)-B(5)	120.82(13)
B(6)-B(1)-B(5)	107.78(15)	B(10)-B(1)-B(5)	59.68(12)
C(20)-B(1)-B(2)	58.37(11)	Cl(1)-B(1)-B(2)	119.91(13)
B(6)-B(1)-B(2)	59.59(11)	B(10)-B(1)-B(2)	108.28(14)
B(5)-B(1)-B(2)	107.60(15)	C(20)-B(2)-Cl(2)	120.63(13)
C(20)-B(2)-B(6)	104.45(14)	Cl(2)-B(2)-B(6)	125.28(14)
C(20)-B(2)-B(7)	104.85(14)	Cl(2)-B(2)-B(7)	125.89(13)
B(6)-B(2)-B(7)	60.45(12)	C(20)-B(2)-B(3)	59.06(12)
Cl(2)-B(2)-B(3)	120.40(13)	B(6)-B(2)-B(3)	108.31(14)
B(7)-B(2)-B(3)	59.92(12)	C(20)-B(2)-B(1)	58.80(11)
Cl(2)-B(2)-B(1)	119.13(14)	B(6)-B(2)-B(1)	59.74(11)
B(7)-B(2)-B(1)	108.45(14)	B(3)-B(2)-B(1)	108.67(14)
C(20)-B(3)-Cl(3)	121.30(13)	C(20)-B(3)-B(8)	104.21(14)
Cl(3)-B(3)-B(8)	125.10(15)	C(20)-B(3)-B(7)	104.28(14)
Cl(3)-B(3)-B(7)	125.84(14)	B(8)-B(3)-B(7)	60.33(12)
C(20)-B(3)-B(2)	58.31(11)	Cl(3)-B(3)-B(2)	120.99(14)
B(8)-B(3)-B(2)	107.95(15)	B(7)-B(3)-B(2)	59.92(12)
C(20)-B(3)-B(4)	58.28(12)	Cl(3)-B(3)-B(4)	120.09(14)
B(8)-B(3)-B(4)	59.65(12)	B(7)-B(3)-B(4)	107.66(15)
B(2)-B(3)-B(4)	107.22(15)	C(20)-B(4)-Cl(4)	120.41(14)
C(20)-B(4)-B(9)	104.83(15)	Cl(4)-B(4)-B(9)	125.22(15)

C(20)-B(4)-B(8)	104.93(15)	C1(4)-B(4)-B(8)	125.69(15)
B(9)-B(4)-B(8)	60.81(12)	C(20)-B(4)-B(5)	58.66(12)
C1(4)-B(4)-B(5)	119.49(14)	B(9)-B(4)-B(5)	59.92(13)
B(8)-B(4)-B(5)	108.60(16)	C(20)-B(4)-B(3)	58.95(12)
C1(4)-B(4)-B(3)	120.06(15)	B(9)-B(4)-B(3)	108.69(15)
B(8)-B(4)-B(3)	59.92(12)	B(5)-B(4)-B(3)	108.41(15)
C(20)-B(5)-C1(5)	121.00(14)	C(20)-B(5)-B(10)	105.07(14)
C1(5)-B(5)-B(10)	125.06(15)	C(20)-B(5)-B(9)	104.63(15)
C1(5)-B(5)-B(9)	125.08(14)	B(10)-B(5)-B(9)	60.61(13)
C(20)-B(5)-B(4)	58.59(12)	C1(5)-B(5)-B(4)	120.06(15)
B(10)-B(5)-B(4)	108.38(15)	B(9)-B(5)-B(4)	59.73(13)
C(20)-B(5)-B(1)	58.82(12)	C1(5)-B(5)-B(1)	120.22(14)
B(10)-B(5)-B(1)	60.14(12)	B(9)-B(5)-B(1)	108.47(14)
B(4)-B(5)-B(1)	108.10(15)	B(2)-B(6)-B(1)	60.67(12)
B(2)-B(6)-B(7)	60.14(12)	B(1)-B(6)-B(7)	108.94(15)
B(2)-B(6)-C1(6)	121.42(14)	B(1)-B(6)-C1(6)	120.68(14)
B(7)-B(6)-C1(6)	121.81(13)	B(2)-B(6)-B(11)	108.03(15)
B(1)-B(6)-B(11)	108.19(14)	B(7)-B(6)-B(11)	60.05(12)
C1(6)-B(6)-B(11)	122.19(13)	B(2)-B(6)-B(10)	108.60(14)
B(1)-B(6)-B(10)	60.00(12)	B(7)-B(6)-B(10)	108.71(15)
C1(6)-B(6)-B(10)	121.02(14)	B(11)-B(6)-B(10)	60.18(12)
C1(7)-B(7)-B(3)	122.28(14)	C1(7)-B(7)-B(2)	122.68(14)
B(3)-B(7)-B(2)	60.16(12)	C1(7)-B(7)-B(6)	121.88(14)
B(3)-B(7)-B(6)	107.68(14)	B(2)-B(7)-B(6)	59.42(12)
C1(7)-B(7)-B(11)	121.25(13)	B(3)-B(7)-B(11)	107.69(14)
B(2)-B(7)-B(11)	107.40(14)	B(6)-B(7)-B(11)	59.98(12)
C1(7)-B(7)-B(8)	121.48(14)	B(3)-B(7)-B(8)	59.82(12)
B(2)-B(7)-B(8)	107.74(14)	B(6)-B(7)-B(8)	107.80(14)
B(11)-B(7)-B(8)	59.92(12)	B(4)-B(8)-C1(8)	121.27(15)
B(4)-B(8)-B(3)	60.43(12)	C1(8)-B(8)-B(3)	120.58(14)
B(4)-B(8)-B(11)	107.21(15)	C1(8)-B(8)-B(11)	123.15(14)
B(3)-B(8)-B(11)	107.79(15)	B(4)-B(8)-B(7)	107.90(15)
C1(8)-B(8)-B(7)	121.86(14)	B(3)-B(8)-B(7)	59.85(12)
B(11)-B(8)-B(7)	60.00(12)	B(4)-B(8)-B(9)	59.51(12)
C1(8)-B(8)-B(9)	122.42(14)	B(3)-B(8)-B(9)	108.07(15)
B(11)-B(8)-B(9)	59.72(12)	B(7)-B(8)-B(9)	107.86(15)
B(4)-B(9)-C1(9)	121.59(15)	B(4)-B(9)-B(5)	60.35(13)
C1(9)-B(9)-B(5)	122.05(13)	B(4)-B(9)-B(11)	107.49(14)
C1(9)-B(9)-B(11)	121.97(14)	B(5)-B(9)-B(11)	107.66(15)

B(4)-B(9)-B(10)	108.11(15)	C1(9)-B(9)-B(10)	121.88(15)
B(5)-B(9)-B(10)	59.66(12)	B(11)-B(9)-B(10)	60.30(12)
B(4)-B(9)-B(8)	59.69(12)	C1(9)-B(9)-B(8)	121.25(14)
B(5)-B(9)-B(8)	108.06(14)	B(11)-B(9)-B(8)	59.89(12)
B(10)-B(9)-B(8)	108.40(14)	C1(10)-B(10)-B(5)	121.69(14)
C1(10)-B(10)-B(1)	121.48(15)	B(5)-B(10)-B(1)	60.18(12)
C1(10)-B(10)-B(9)	122.17(14)	B(5)-B(10)-B(9)	59.73(12)
B(1)-B(10)-B(9)	107.80(15)	C1(10)-B(10)-B(6)	122.50(15)
B(5)-B(10)-B(6)	107.14(14)	B(1)-B(10)-B(6)	59.34(11)
B(9)-B(10)-B(6)	107.22(15)	C1(10)-B(10)-B(11)	122.72(14)
B(5)-B(10)-B(11)	107.19(15)	B(1)-B(10)-B(11)	107.28(14)
B(9)-B(10)-B(11)	59.63(12)	B(6)-B(10)-B(11)	59.70(12)
C1(11)-B(11)-B(9)	122.10(14)	C1(11)-B(11)-B(8)	122.08(14)
B(9)-B(11)-B(8)	60.39(12)	C1(11)-B(11)-B(6)	121.22(14)
B(9)-B(11)-B(6)	107.90(14)	B(8)-B(11)-B(6)	107.92(14)
C1(11)-B(11)-B(7)	121.26(13)	B(9)-B(11)-B(7)	108.46(14)
B(8)-B(11)-B(7)	60.08(12)	B(6)-B(11)-B(7)	59.97(12)
C1(11)-B(11)-B(10)	121.03(14)	B(9)-B(11)-B(10)	60.07(12)
B(8)-B(11)-B(10)	108.62(14)	B(6)-B(11)-B(10)	60.12(12)
B(7)-B(11)-B(10)	108.59(14)	C1(1A)-C(1A)-C1(2A)	109.2(5)
C1(2B)-C(1B)-C1(1B)	112.7(3)		

Table xiv.4. Anisotropic displacement parameters ($\text{\AA}^2 \times 10^3$). The anisotropic displacement factor exponent takes the form: $-2\alpha^2 [h^2 a^{*2} U^{11} + \dots + 2 h k a^{*} b^{*} U^{12}]$

	U ¹¹	U ²²	U ³³	U ²³	U ¹³	U ¹²
W(1)	11(1)	13(1)	13(1)	0(1)	-2(1)	-4(1)
P(1)	12(1)	15(1)	11(1)	1(1)	-2(1)	-6(1)
Si(1)	18(1)	38(1)	12(1)	3(1)	-1(1)	-11(1)
Si(2)	14(1)	16(1)	17(1)	2(1)	-5(1)	-6(1)
O(1)	17(1)	15(1)	20(1)	-1(1)	-3(1)	-8(1)
O(2)	37(1)	22(1)	22(1)	3(1)	-2(1)	-13(1)
O(3)	25(1)	20(1)	22(1)	-4(1)	-8(1)	-5(1)
O(4)	16(1)	28(1)	48(1)	-6(1)	-8(1)	-4(1)
O(5)	23(1)	24(1)	31(1)	7(1)	1(1)	-8(1)

	U ¹¹	U ²²	U ³³	U ²³	U ¹³	U ¹²

O(6)	23(1)	33(1)	25(1)	-9(1)	1(1)	-6(1)
C(1)	13(1)	14(1)	15(1)	0(1)	-2(1)	-4(1)
C(2)	10(1)	19(1)	14(1)	0(1)	-2(1)	-3(1)
C(3)	17(1)	22(1)	17(1)	1(1)	-1(1)	-7(1)
C(4)	18(1)	32(1)	23(1)	7(1)	-1(1)	-8(1)
C(5)	22(1)	47(1)	18(1)	-2(1)	5(1)	-6(1)
C(6)	24(1)	39(1)	22(1)	-13(1)	3(1)	-6(1)
C(7)	17(1)	24(1)	22(1)	-6(1)	-1(1)	-5(1)
C(8)	17(1)	19(1)	13(1)	5(1)	-5(1)	-8(1)
C(9)	21(1)	64(2)	19(1)	9(1)	0(1)	-17(1)
C(10)	29(1)	38(1)	21(1)	-10(1)	3(1)	-7(1)
C(11)	27(1)	59(2)	17(1)	10(1)	-4(1)	-18(1)
C(12)	28(1)	21(1)	27(1)	5(1)	-12(1)	-9(1)
C(13)	19(1)	22(1)	25(1)	-3(1)	-3(1)	-10(1)
C(14)	17(1)	21(1)	22(1)	-2(1)	-2(1)	-6(1)
C(15)	18(1)	18(1)	17(1)	-2(1)	-3(1)	-5(1)
C(16)	12(1)	15(1)	21(1)	4(1)	-5(1)	-4(1)
C(17)	18(1)	17(1)	24(1)	-3(1)	-2(1)	-4(1)
C(18)	12(1)	21(1)	20(1)	0(1)	-2(1)	-5(1)
C(19)	14(1)	24(1)	19(1)	1(1)	-3(1)	-7(1)
C(20)	20(1)	15(1)	17(1)	1(1)	-4(1)	-7(1)
B(1)	19(1)	15(1)	16(1)	0(1)	-2(1)	-4(1)
B(2)	16(1)	13(1)	18(1)	2(1)	-3(1)	-4(1)
B(3)	18(1)	15(1)	20(1)	3(1)	-3(1)	-6(1)
B(4)	26(1)	17(1)	21(1)	2(1)	-5(1)	-10(1)
B(5)	24(1)	13(1)	20(1)	-1(1)	-6(1)	-4(1)
B(6)	16(1)	14(1)	20(1)	-1(1)	-1(1)	-4(1)
B(7)	17(1)	13(1)	19(1)	-1(1)	-3(1)	-3(1)
B(8)	24(1)	16(1)	16(1)	2(1)	-4(1)	-6(1)
B(9)	26(1)	11(1)	19(1)	1(1)	-7(1)	-2(1)
B(10)	19(1)	13(1)	20(1)	-2(1)	-4(1)	-2(1)
B(11)	17(1)	15(1)	19(1)	-2(1)	-6(1)	-2(1)

	U ¹¹	U ²²	U ³³	U ²³	U ¹³	U ¹²
C1(1)	30(1)	26(1)	17(1)	1(1)	2(1)	-5(1)
C1(2)	20(1)	14(1)	26(1)	6(1)	-2(1)	-2(1)

C1(3)	16(1)	30(1)	33(1)	4(1)	1(1)	-7(1)
C1(4)	46(1)	29(1)	37(1)	4(1)	-5(1)	-28(1)
C1(5)	41(1)	18(1)	23(1)	-6(1)	-8(1)	-8(1)
C1(6)	18(1)	20(1)	34(1)	-4(1)	1(1)	-9(1)
C1(7)	29(1)	16(1)	25(1)	-7(1)	-2(1)	-3(1)
C1(8)	35(1)	27(1)	18(1)	6(1)	-1(1)	-8(1)
C1(9)	41(1)	12(1)	27(1)	3(1)	-9(1)	-1(1)
C1(10)	19(1)	26(1)	35(1)	-6(1)	0(1)	3(1)
C1(11)	26(1)	30(1)	27(1)	-6(1)	-14(1)	-2(1)
C(1A)	37(3)	39(4)	36(3)	5(3)	11(3)	-10(3)
C1(1A)	122(5)	154(6)	135(6)	-8(4)	1(4)	-8(4)
C1(2A)	106(2)	86(2)	72(2)	-24(2)	43(2)	-52(2)
C(1B)	57(3)	54(3)	67(4)	-25(3)	-23(3)	2(3)
C1(1B)	39(1)	24(1)	49(1)	-4(1)	-9(1)	5(1)
C1(2B)	49(1)	78(1)	45(1)	-24(1)	3(1)	-15(1)

Table xiv.5. Hydrogen coordinates ($\times 10^4$) and isotropic displacement parameters ($\text{\AA}^2 \times 10^{-3}$)

	x	y	z	U(eq)
H(1)	11748	354	1797	17
H(3)	12632	2527	1034	22
H(4)	13786	2609	-146	30
H(5)	14124	1342	-979	37
H(6)	13411	-39	-610	35
H(7)	12309	-149	578	25
H(8)	11741	372	3257	19
H(9A)	9300	753	4333	52
	x	y	z	U(eq)
H(9B)	8622	1844	3944	52
H(9C)	8804	1709	4834	52
H(10A)	10840	3106	4723	45
H(10B)	10349	3277	3870	45
H(10C)	12072	2907	4051	45
H(11A)	13210	828	4990	51

H(11B)	12217	114	5016	51
H(11C)	11705	1088	5497	51
H(12A)	14262	-1198	3552	37
H(12B)	14416	-698	4305	37
H(12C)	15818	-1088	3734	37
H(13A)	14519	1486	4207	31
H(13B)	14736	1971	3392	31
H(13C)	16045	1047	3730	31
H(14A)	16063	-15	2288	30
H(14B)	14759	961	2014	30
H(14C)	14544	-108	2026	30
H(1A1)	5503	5245	4823	47
H(1A2)	6378	5777	5296	47
H(1B1)	6627	6968	4493	75
H(1B2)	6855	6107	5143	75
H(1A)	11720 (30)	3070(20)	2417(16)	34(8)
H(20)	4080 (30)	6270(20)	3288(15)	37(7)

xv.[(Bis(trimethylsilyl)methyl)chloro-(1,1-hydroxyphenyl)
methyl)phosphane]pentacarbonyltungsten(0) [85c]

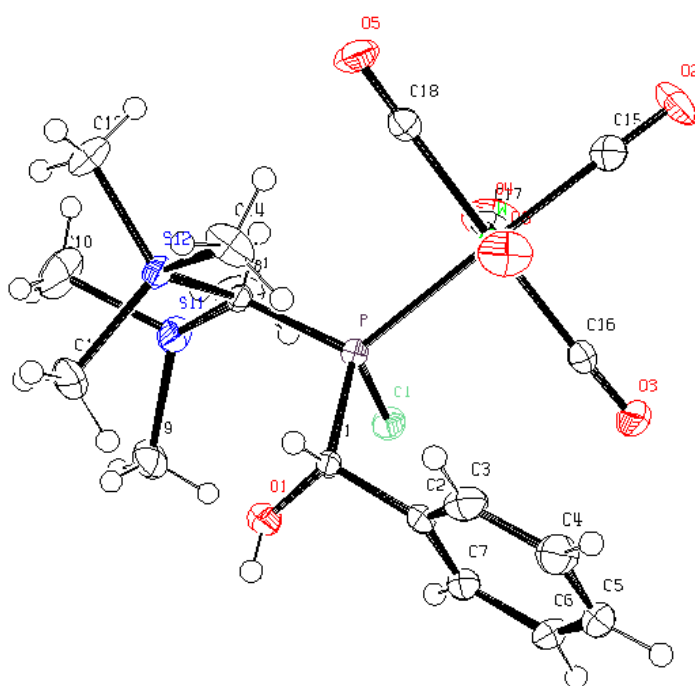


Table xv.1. Crystal data and structure refinement for [85c].

Identification code	GSTR074, Greg672
Device Type	Nonius KappaCCD
Empirical formula	C19 H26 Cl O6 P Si2 W
Formula weight	656.85
Temperature	123(2) K
Wavelength	0.71073 Å
Crystal system, space group	Triclinic, P -1
Unit cell dimensions	a = 9.021 Å alpha = 88.96 deg. b = 10.386 Å beta = 89.59 deg. c = 14.292 Å gamma = 68.52 deg.
Volume	1245.7 Å ³
Z, Calculated density	2, 1.751 Mg/m ³
Absorption coefficient	4.935 mm ⁻¹
F(000)	644
Crystal size	0.43 x 0.34 x 0.15 mm
Theta range for data collection	2.85 to 28.00 deg.
Limiting indices	-11<=h<=11, -13<=k<=11, -18<=l<=18
Reflections collected / unique	14138 / 5784 [R(int) = 0.0392]
Completeness to theta = 28.00	95.9 %
Absorption correction	Semi-empirical from equivalents
Max. and min. transmission	0.48000 and 0.39425
Refinement method	Full-matrix least-squares on F ²
Data / restraints / parameters	5784 / 6 / 289
Goodness-of-fit on F ²	1.064
Final R indices [I>2sigma(I)]	R1 = 0.0267, wR2 = 0.0629
R indices (all data)	R1 = 0.0293, wR2 = 0.0637
Largest diff. peak and hole	2.058 and -1.507 e.Å ⁻³

Table xv.2. Atomic coordinates ($\times 10^4$) and equivalent isotropic displacement parameters ($\text{Å}^2 \times 10^3$) for [85c].
 U(eq) is defined as one third of the trace of the orthogonalized U_{ij} tensor.

	x	y	z	U(eq)
C(1)	6683(4)	4919(4)	8490(2)	20(1)
C(1S)	6683(4)	4919(4)	8490(2)	20(1)
C(2)	5463(5)	6154(4)	8955(3)	22(1)
C(3)	3954(5)	6781(4)	8565(3)	28(1)
C(4)	2822(5)	7938(5)	8971(3)	33(1)
C(5)	3210(5)	8457(4)	9783(3)	33(1)
C(6)	4690(5)	7820(4)	10189(3)	28(1)
C(7)	5822(5)	6677(4)	9778(3)	26(1)
C(8)	9340(4)	3784(3)	7154(2)	16(1)
C(9)	11086(5)	2128(4)	8972(3)	33(1)
C(10)	12287(6)	1032(5)	7060(4)	51(1)
C(11)	12714(5)	3608(5)	7653(3)	36(1)
C(12)	9307(5)	1919(5)	5516(3)	31(1)
C(13)	7979(6)	1449(4)	7434(3)	34(1)
C(14)	6172(5)	3906(5)	6128(3)	30(1)
C(15)	6616(5)	9264(4)	5895(3)	24(1)
C(16)	6422(5)	8662(4)	7845(3)	22(1)
C(17)	9377(5)	7547(4)	6849(3)	25(1)
C(18)	7853(4)	6400(4)	5476(3)	21(1)
C(19)	4897(4)	7535(4)	6418(2)	20(1)
Cl	9448(1)	5781(1)	8743(1)	25(1)
O(1)	7598(4)	3914(4)	9108(2)	29(1)
O(1S)	6183(17)	4080(15)	8144(10)	37(4)
O(2)	6344(4)	10277(3)	5477(2)	36(1)
O(3)	6033(4)	9332(3)	8488(2)	35(1)
O(4)	10595(4)	7604(4)	6971(2)	47(1)
O(5)	8220(4)	5804(3)	4792(2)	34(1)
O(6)	3666(3)	7575(3)	6235(2)	35(1)
P	8083(1)	5396(1)	7692(1)	17(1)
Si(1)	11303(1)	2665(1)	7739(1)	26(1)
Si(2)	8186(1)	2767(1)	6580(1)	20(1)
W	7149(1)	7511(1)	6662(1)	14(1)

Table xv.3. Bond lengths [Å] and angles [deg] for [85c].

C(1)-O(1)	1.378(5)
C(1)-C(2)	1.511(5)
C(1)-P	1.886(3)
C(1)-H(1)	1.0000
C(2)-C(3)	1.392(6)
C(2)-C(7)	1.393(6)
C(3)-C(4)	1.393(6)
C(3)-H(3A)	0.9500
C(4)-C(5)	1.388(6)
C(4)-H(4A)	0.9500
C(5)-C(6)	1.381(6)
C(5)-H(5A)	0.9500
C(6)-C(7)	1.388(5)
C(6)-H(6A)	0.9500
C(7)-H(7A)	0.9500
C(8)-P	1.823(3)

C(8)-Si(1)	1.915(4)
C(8)-Si(2)	1.929(4)
C(8)-H(8A)	1.0000
C(9)-Si(1)	1.869(4)
C(9)-H(9A)	0.9800
C(9)-H(9B)	0.9800
C(9)-H(9C)	0.9800
C(10)-Si(1)	1.885(5)
C(10)-H(10A)	0.9800
C(10)-H(10B)	0.9800
C(10)-H(10C)	0.9800
C(11)-Si(1)	1.871(5)
C(11)-H(11A)	0.9800
C(11)-H(11B)	0.9800
C(11)-H(11C)	0.9800
C(12)-Si(2)	1.867(4)
C(12)-H(12A)	0.9800
C(12)-H(12B)	0.9800
C(12)-H(12C)	0.9800
C(13)-Si(2)	1.877(4)
C(13)-H(13A)	0.9800
C(13)-H(13B)	0.9800
C(13)-H(13C)	0.9800
C(14)-Si(2)	1.879(4)
C(14)-H(14C)	0.9800
C(14)-H(14B)	0.9800
C(14)-H(14A)	0.9800
C(15)-O(2)	1.146(5)
C(15)-W	2.010(4)
C(16)-O(3)	1.137(5)
C(16)-W	2.050(4)
C(17)-O(4)	1.136(5)
C(17)-W	2.044(4)
C(18)-O(5)	1.147(5)
C(18)-W	2.031(4)
C(19)-O(6)	1.128(5)
C(19)-W	2.055(4)
Cl-P	2.0830(13)
O(1)-H(1A)	0.8400
O(1S)-H(1S1)	0.8400
P-W	2.5000(9)
O(1)-C(1)-C(2)	114.0(3)
O(1)-C(1)-P	107.6(3)
C(2)-C(1)-P	113.2(2)
O(1)-C(1)-H(1)	107.2
C(2)-C(1)-H(1)	107.2
P-C(1)-H(1)	107.2
C(3)-C(2)-C(7)	119.0(3)
C(3)-C(2)-C(1)	120.1(3)
C(7)-C(2)-C(1)	120.9(4)
C(2)-C(3)-C(4)	121.0(4)
C(2)-C(3)-H(3A)	119.5
C(4)-C(3)-H(3A)	119.5
C(5)-C(4)-C(3)	119.1(4)
C(5)-C(4)-H(4A)	120.5
C(3)-C(4)-H(4A)	120.5
C(6)-C(5)-C(4)	120.3(4)
C(6)-C(5)-H(5A)	119.9
C(4)-C(5)-H(5A)	119.9
C(5)-C(6)-C(7)	120.5(4)
C(5)-C(6)-H(6A)	119.7
C(7)-C(6)-H(6A)	119.7

C(6)-C(7)-C(2)	120.0(4)
C(6)-C(7)-H(7A)	120.0
C(2)-C(7)-H(7A)	120.0
P-C(8)-Si(1)	119.70(19)
P-C(8)-Si(2)	114.47(18)
Si(1)-C(8)-Si(2)	114.97(17)
P-C(8)-H(8A)	101.1
Si(1)-C(8)-H(8A)	101.1
Si(2)-C(8)-H(8A)	101.1
Si(1)-C(9)-H(9A)	109.5
Si(1)-C(9)-H(9B)	109.5
H(9A)-C(9)-H(9B)	109.5
Si(1)-C(9)-H(9C)	109.5
H(9A)-C(9)-H(9C)	109.5
H(9B)-C(9)-H(9C)	109.5
Si(1)-C(10)-H(10A)	109.5
Si(1)-C(10)-H(10B)	109.5
H(10A)-C(10)-H(10B)	109.5
Si(1)-C(10)-H(10C)	109.5
H(10A)-C(10)-H(10C)	109.5
H(10B)-C(10)-H(10C)	109.5
Si(1)-C(11)-H(11A)	109.5
Si(1)-C(11)-H(11B)	109.5
H(11A)-C(11)-H(11B)	109.5
Si(1)-C(11)-H(11C)	109.5
H(11A)-C(11)-H(11C)	109.5
H(11B)-C(11)-H(11C)	109.5
Si(2)-C(12)-H(12A)	109.5
Si(2)-C(12)-H(12B)	109.5
H(12A)-C(12)-H(12B)	109.5
Si(2)-C(12)-H(12C)	109.5
H(12A)-C(12)-H(12C)	109.5
H(12B)-C(12)-H(12C)	109.5
Si(2)-C(13)-H(13A)	109.5
Si(2)-C(13)-H(13B)	109.5
H(13A)-C(13)-H(13B)	109.5
Si(2)-C(13)-H(13C)	109.5
H(13A)-C(13)-H(13C)	109.5
H(13B)-C(13)-H(13C)	109.5
Si(2)-C(14)-H(14C)	109.5
Si(2)-C(14)-H(14B)	109.5
H(14C)-C(14)-H(14B)	109.5
Si(2)-C(14)-H(14A)	109.5
H(14C)-C(14)-H(14A)	109.5
H(14B)-C(14)-H(14A)	109.5
O(2)-C(15)-W	177.7(3)
O(3)-C(16)-W	177.8(3)
O(4)-C(17)-W	177.7(4)
O(5)-C(18)-W	178.1(4)
O(6)-C(19)-W	176.1(3)
C(8)-P-C(1)	105.60(15)
C(8)-P-Cl	106.26(12)
C(1)-P-Cl	96.68(13)
C(8)-P-W	116.92(11)
C(1)-P-W	122.03(12)
Cl-P-W	106.45(5)
C(9)-Si(1)-C(11)	111.7(2)
C(9)-Si(1)-C(10)	107.0(2)
C(11)-Si(1)-C(10)	104.9(2)
C(9)-Si(1)-C(8)	114.31(18)
C(11)-Si(1)-C(8)	108.35(18)
C(10)-Si(1)-C(8)	110.11(19)
C(12)-Si(2)-C(13)	111.0(2)

C(12)-Si(2)-C(14)	104.5(2)
C(13)-Si(2)-C(14)	110.1(2)
C(12)-Si(2)-C(8)	108.06(17)
C(13)-Si(2)-C(8)	109.73(18)
C(14)-Si(2)-C(8)	113.29(18)
C(15)-W-C(18)	89.34(15)
C(15)-W-C(17)	88.15(15)
C(18)-W-C(17)	91.25(15)
C(15)-W-C(16)	89.70(15)
C(18)-W-C(16)	179.02(14)
C(17)-W-C(16)	88.92(16)
C(15)-W-C(19)	89.30(15)
C(18)-W-C(19)	87.73(14)
C(17)-W-C(19)	177.26(14)
C(16)-W-C(19)	92.05(15)
C(15)-W-P	173.17(11)
C(18)-W-P	92.93(11)
C(17)-W-P	85.36(11)
C(16)-W-P	88.04(11)
C(19)-W-P	97.22(10)

Table xv.4. Anisotropic displacement parameters ($\text{\AA}^2 \times 10^3$) for [85c]
The anisotropic displacement factor exponent takes the form:
 $-2 \pi^2 [h^2 a^* a^2 U_{11} + \dots + 2 h k a^* b^* U_{12}]$

	U11	U22	U33	U23	U13	U12
C(1)	26(2)	13(2)	21(2)	-1(1)	12(2)	-8(1)
C(1S)	26(2)	13(2)	21(2)	-1(1)	12(2)	-8(1)
C(2)	29(2)	15(2)	21(2)	2(1)	8(2)	-9(2)
C(3)	29(2)	34(2)	23(2)	-2(2)	5(2)	-14(2)
C(4)	26(2)	33(2)	33(2)	5(2)	3(2)	-1(2)
C(5)	37(2)	22(2)	30(2)	1(2)	13(2)	-1(2)
C(6)	37(2)	24(2)	22(2)	-5(2)	10(2)	-9(2)
C(7)	27(2)	22(2)	25(2)	2(2)	7(2)	-5(2)
C(8)	17(2)	14(2)	15(2)	-2(1)	1(1)	-3(1)
C(9)	40(2)	25(2)	28(2)	8(2)	-11(2)	-7(2)
C(10)	35(3)	41(3)	49(3)	-13(2)	-7(2)	20(2)
C(11)	18(2)	58(3)	31(2)	3(2)	-2(2)	-13(2)
C(12)	31(2)	35(2)	26(2)	-15(2)	5(2)	-11(2)
C(13)	48(3)	25(2)	34(2)	3(2)	2(2)	-21(2)
C(14)	22(2)	39(2)	35(2)	14(2)	-9(2)	-17(2)
C(15)	25(2)	27(2)	24(2)	-2(2)	-2(2)	-14(2)
C(16)	27(2)	17(2)	23(2)	2(2)	0(2)	-9(2)
C(17)	23(2)	33(2)	21(2)	8(2)	-1(2)	-12(2)
C(18)	18(2)	22(2)	24(2)	2(2)	1(2)	-7(2)
C(19)	21(2)	21(2)	19(2)	3(1)	-1(1)	-7(2)
Cl	32(1)	24(1)	20(1)	-2(1)	-6(1)	-10(1)
O(1)	33(2)	22(2)	25(2)	4(1)	6(2)	-4(2)
O(1S)	38(4)	37(5)	38(5)	-1(2)	2(2)	-15(2)
O(2)	50(2)	28(2)	33(2)	16(1)	-16(1)	-21(1)
O(3)	56(2)	23(2)	27(2)	-8(1)	10(1)	-16(1)
O(4)	30(2)	83(3)	40(2)	10(2)	-5(1)	-36(2)
O(5)	40(2)	41(2)	22(1)	-8(1)	9(1)	-15(1)
O(6)	19(2)	50(2)	35(2)	2(1)	-3(1)	-14(1)
P	18(1)	14(1)	16(1)	-1(1)	1(1)	-5(1)
Si(1)	20(1)	24(1)	25(1)	-1(1)	-4(1)	1(1)
Si(2)	22(1)	18(1)	20(1)	-4(1)	2(1)	-7(1)

W	14(1)	13(1)	15(1)	1(1)	0(1)	-5(1)
---	-------	-------	-------	------	------	-------

Table xv.5. Hydrogen coordinates ($\times 10^4$) and isotropic displacement parameters ($\text{Å}^2 \times 10^3$) for [85c].

	x	y	z	U(eq)
H(1)	6087	4487	8095	24
H(1S)	7377	4393	9017	24
H(3A)	3691	6414	8013	34
H(4A)	1799	8366	8696	40
H(5A)	2453	9253	10062	39
H(6A)	4936	8168	10753	34
H(7A)	6841	6250	10059	31
H(8A)	9738	4142	6589	19
H(9A)	10381	1600	8987	49
H(9B)	10628	2953	9357	49
H(9C)	12134	1551	9219	49
H(10A)	12508	1271	6421	77
H(10B)	11577	510	7039	77
H(10C)	13289	465	7366	77
H(11A)	12468	4302	8144	54
H(11B)	12604	4067	7038	54
H(11C)	13809	2949	7731	54
H(12A)	10266	1138	5705	47
H(12B)	9613	2591	5151	47
H(12C)	8631	1583	5133	47
H(13A)	7554	1898	8027	50
H(13B)	9024	722	7543	50
H(13C)	7250	1040	7179	50
H(14C)	5570	3331	5950	45
H(14B)	6303	4436	5580	45
H(14A)	5593	4544	6618	45
H(1A)	7001	3688	9476	43
H(1S1)	6452	3361	8482	56

Table xv.6. Torsion angles [deg] for [85c].

O(1)-C(1)-C(2)-C(3)	-141.0(4)
P-C(1)-C(2)-C(3)	95.5(4)
O(1)-C(1)-C(2)-C(7)	38.6(5)
P-C(1)-C(2)-C(7)	-84.9(4)
C(7)-C(2)-C(3)-C(4)	1.7(6)
C(1)-C(2)-C(3)-C(4)	-178.7(3)
C(2)-C(3)-C(4)-C(5)	-0.8(6)
C(3)-C(4)-C(5)-C(6)	-0.9(6)
C(4)-C(5)-C(6)-C(7)	1.6(6)
C(5)-C(6)-C(7)-C(2)	-0.6(6)
C(3)-C(2)-C(7)-C(6)	-1.1(5)
C(1)-C(2)-C(7)-C(6)	179.3(3)
Si(1)-C(8)-P-C(1)	-90.6(2)
Si(2)-C(8)-P-C(1)	51.9(2)
Si(1)-C(8)-P-Cl	11.3(2)
Si(2)-C(8)-P-Cl	153.84(14)
Si(1)-C(8)-P-W	129.96(16)
Si(2)-C(8)-P-W	-87.54(18)
O(1)-C(1)-P-C(8)	56.9(3)

C(2)-C(1)-P-C(8)	-176.2(3)
O(1)-C(1)-P-Cl	-52.1(3)
C(2)-C(1)-P-Cl	74.9(3)
O(1)-C(1)-P-W	-166.3(2)
C(2)-C(1)-P-W	-39.3(3)
P-C(8)-Si(1)-C(9)	56.7(3)
Si(2)-C(8)-Si(1)-C(9)	-85.7(2)
P-C(8)-Si(1)-C(11)	-68.6(2)
Si(2)-C(8)-Si(1)-C(11)	149.04(19)
P-C(8)-Si(1)-C(10)	177.2(3)
Si(2)-C(8)-Si(1)-C(10)	34.8(3)
P-C(8)-Si(2)-C(12)	144.9(2)
Si(1)-C(8)-Si(2)-C(12)	-70.8(2)
P-C(8)-Si(2)-C(13)	-93.9(2)
Si(1)-C(8)-Si(2)-C(13)	50.4(2)
P-C(8)-Si(2)-C(14)	29.6(2)
Si(1)-C(8)-Si(2)-C(14)	173.88(18)
O(2)-C(15)-W-C(18)	-127(9)
O(2)-C(15)-W-C(17)	-36(9)
O(2)-C(15)-W-C(16)	53(9)
O(2)-C(15)-W-C(19)	145(9)
O(2)-C(15)-W-P	-17(9)
O(5)-C(18)-W-C(15)	-29(10)
O(5)-C(18)-W-C(17)	-118(10)
O(5)-C(18)-W-C(16)	-18(16)
O(5)-C(18)-W-C(19)	60(10)
O(5)-C(18)-W-P	157(10)
O(4)-C(17)-W-C(15)	70(9)
O(4)-C(17)-W-C(18)	159(9)
O(4)-C(17)-W-C(16)	-20(9)
O(4)-C(17)-W-C(19)	91(9)
O(4)-C(17)-W-P	-108(9)
O(3)-C(16)-W-C(15)	-30(10)
O(3)-C(16)-W-C(18)	-42(15)
O(3)-C(16)-W-C(17)	58(10)
O(3)-C(16)-W-C(19)	-120(10)
O(3)-C(16)-W-P	143(10)
O(6)-C(19)-W-C(15)	38(5)
O(6)-C(19)-W-C(18)	-52(5)
O(6)-C(19)-W-C(17)	16(7)
O(6)-C(19)-W-C(16)	127(5)
O(6)-C(19)-W-P	-144(5)
C(8)-P-W-C(15)	-97.2(9)
C(1)-P-W-C(15)	130.5(9)
Cl-P-W-C(15)	21.3(9)
C(8)-P-W-C(18)	12.18(17)
C(1)-P-W-C(18)	-120.16(18)
Cl-P-W-C(18)	130.70(11)
C(8)-P-W-C(17)	-78.84(17)
C(1)-P-W-C(17)	148.83(18)
Cl-P-W-C(17)	39.68(12)
C(8)-P-W-C(16)	-167.91(17)
C(1)-P-W-C(16)	59.75(18)
Cl-P-W-C(16)	-49.39(12)
C(8)-P-W-C(19)	100.26(16)
C(1)-P-W-C(19)	-32.08(18)
Cl-P-W-C(19)	-141.22(11)

xvi. [2-Bis(trimethylsilyl)methyl-3-phenyl-oxaphosphirane-
kP]pentacarbonyltungsten(0) **[16b]**

(A1)

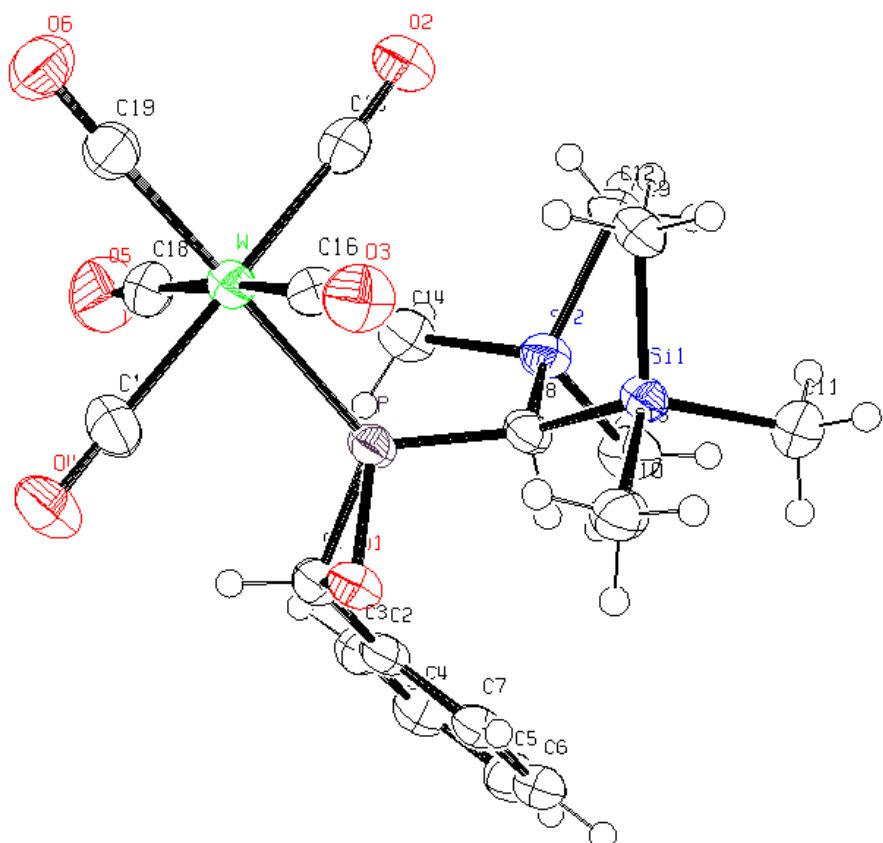


Table xvi.1. Crystal data and structure refinement for **[16b]**.

Identification code	GSTR146, Greg1188
Device Type	Nonius KappaCCD
Empirical formula	C ₁₉ H ₂₅ O ₆ P Si ₂ W
Formula weight	620.39
Temperature	123(2) K
Wavelength	0.71073 Å
Crystal system, space group	Monoclinic, P 21/c
Unit cell dimensions	a = 14.1951(8) Å alpha = 90 deg. b = 11.0928(9) Å beta = 108.497(4) deg.
	c = 16.3457(12) Å gamma = 90 deg.
Volume	2440.9(3) Å ³

Z, Calculated density	4, 1.688 Mg/m^3
Absorption coefficient	4.926 mm^-1
F(000)	1216
Crystal size	0.40 x 0.20 x 0.12 mm
Theta range for data collection	2.58 to 28.00 deg.
Limiting indices	-16<=h<=18, -14<=k<=13, -15<=l<=21
Reflections collected / unique	18831 / 5708 [R(int) = 0.0802]
Completeness to theta = 28.00	96.8 %
Absorption correction	Semi-empirical from equivalents
Max. and min. transmission	0.5894 and 0.2433
Refinement method	Full-matrix least-squares on F^2
Data / restraints / parameters	5708 / 2 / 268
Goodness-of-fit on F^2	0.905
Final R indices [I>2sigma(I)]	R1 = 0.0395, wR2 = 0.0753
R indices (all data)	R1 = 0.0730, wR2 = 0.0828
Largest diff. peak and hole	1.695 and -1.986 e.A^-3

Table xvi.2. Atomic coordinates (x 10^4) and equivalent isotropic displacement parameters (A^2 x 10^3) for **[16b]**. U(eq) is defined as one third of the trace of the orthogonalized Uij tensor.

	x	y	z	U(eq)
C(1)	2378(3)	8245(5)	4546(3)	33(1)
C(2)	2146(4)	9428(5)	4841(3)	32(1)
C(3)	2892(4)	10135(5)	5385(3)	39(1)
C(4)	2688(4)	11262(6)	5638(3)	44(2)
C(5)	1728(4)	11720(6)	5354(4)	45(2)
C(6)	968(4)	11011(5)	4822(3)	40(1)
C(7)	1176(4)	9884(5)	4572(3)	32(1)
C(8)	1971(4)	9254(5)	2824(3)	30(1)
C(9)	1366(4)	8234(5)	926(3)	35(1)
C(10)	-44(4)	8067(5)	1994(3)	39(1)
C(11)	404(4)	10495(6)	1358(3)	45(2)
C(12)	3275(4)	10509(5)	1813(3)	40(1)
C(13)	2593(4)	11842(5)	3153(4)	47(2)
C(14)	4209(4)	9952(6)	3688(3)	43(2)
C(15)	3649(4)	6996(5)	2194(3)	32(1)
C(16)	1969(4)	5549(5)	2290(3)	34(1)
C(17)	2852(4)	5230(5)	4069(3)	41(1)
C(18)	4540(4)	6670(6)	4085(4)	45(2)
C(19)	3960(4)	4699(5)	2896(3)	37(1)
O(1)	1537(2)	7588(3)	3940(2)	32(1)

O(2)	3872(3)	7399(4)	1634(2)	43(1)
O(3)	1240(3)	5186(4)	1832(2)	46(1)
O(4)	2595(3)	4712(4)	4557(3)	60(1)
O(5)	5242(3)	6956(5)	4625(3)	67(1)
O(6)	4355(3)	3865(4)	2724(3)	52(1)
P	2389(1)	7916(1)	3469(1)	29(1)
Si(1)	942(1)	8991(1)	1766(1)	31(1)
Si(2)	3007(1)	10366(2)	2852(1)	33(1)
W	3269(1)	6147(1)	3148(1)	32(1)

Table xvi.3. Bond lengths [Å] and angles [deg] for [16b].

C(1)-C(2)	1.470(8)
C(1)-O(1)	1.480(6)
C(1)-P	1.804(5)
C(1)-H(1A)	1.0000
C(2)-C(3)	1.390(7)
C(2)-C(7)	1.401(7)
C(3)-C(4)	1.376(8)
C(3)-H(3A)	0.9500
C(4)-C(5)	1.388(8)
C(4)-H(4A)	0.9500
C(5)-C(6)	1.394(8)
C(5)-H(5A)	0.9500
C(6)-C(7)	1.375(7)
C(6)-H(6A)	0.9500
C(7)-H(7A)	0.9500
C(8)-P	1.808(5)
C(8)-Si(1)	1.899(5)
C(8)-Si(2)	1.909(5)
C(8)-H(8A)	1.0000
C(9)-Si(1)	1.864(5)
C(9)-H(9C)	0.9800
C(9)-H(9B)	0.9800
C(9)-H(9A)	0.9800
C(10)-Si(1)	1.866(5)
C(10)-H(10C)	0.9800
C(10)-H(10B)	0.9800
C(10)-H(10A)	0.9800
C(11)-Si(1)	1.869(6)
C(11)-H(11A)	0.9800
C(11)-H(11B)	0.9800
C(11)-H(11C)	0.9800
C(12)-Si(2)	1.861(5)
C(12)-H(12C)	0.9800
C(12)-H(12B)	0.9800
C(12)-H(12A)	0.9800
C(13)-Si(2)	1.857(6)
C(13)-H(13C)	0.9800
C(13)-H(13B)	0.9800
C(13)-H(13A)	0.9800
C(14)-Si(2)	1.874(5)
C(14)-H(14C)	0.9800
C(14)-H(14B)	0.9800
C(14)-H(14A)	0.9800
C(15)-O(2)	1.149(6)
C(15)-W	2.036(6)
C(16)-O(3)	1.141(6)
C(16)-W	2.042(6)
C(17)-O(4)	1.133(6)
C(17)-W	2.054(6)

C(18)-O(5)	1.147(7)
C(18)-W	2.045(6)
C(19)-O(6)	1.161(6)
C(19)-W	1.992(6)
O(1)-P	1.668(3)
P-W	2.4692(14)
C(2)-C(1)-O(1)	116.2(4)
C(2)-C(1)-P	124.9(4)
O(1)-C(1)-P	60.1(2)
C(2)-C(1)-H(1A)	114.7
O(1)-C(1)-H(1A)	114.7
P-C(1)-H(1A)	114.7
C(3)-C(2)-C(7)	118.0(5)
C(3)-C(2)-C(1)	120.6(5)
C(7)-C(2)-C(1)	121.4(5)
C(4)-C(3)-C(2)	121.0(5)
C(4)-C(3)-H(3A)	119.5
C(2)-C(3)-H(3A)	119.5
C(3)-C(4)-C(5)	120.7(6)
C(3)-C(4)-H(4A)	119.7
C(5)-C(4)-H(4A)	119.7
C(4)-C(5)-C(6)	119.0(6)
C(4)-C(5)-H(5A)	120.5
C(6)-C(5)-H(5A)	120.5
C(7)-C(6)-C(5)	120.1(5)
C(7)-C(6)-H(6A)	119.9
C(5)-C(6)-H(6A)	119.9
C(6)-C(7)-C(2)	121.2(5)
C(6)-C(7)-H(7A)	119.4
C(2)-C(7)-H(7A)	119.4
P-C(8)-Si(1)	114.8(3)
P-C(8)-Si(2)	114.1(3)
Si(1)-C(8)-Si(2)	119.1(3)
P-C(8)-H(8A)	101.7
Si(1)-C(8)-H(8A)	101.7
Si(2)-C(8)-H(8A)	101.7
Si(1)-C(9)-H(9C)	109.5
Si(1)-C(9)-H(9B)	109.5
H(9C)-C(9)-H(9B)	109.5
Si(1)-C(9)-H(9A)	109.5
H(9C)-C(9)-H(9A)	109.5
H(9B)-C(9)-H(9A)	109.5
Si(1)-C(10)-H(10C)	109.5
Si(1)-C(10)-H(10B)	109.5
H(10C)-C(10)-H(10B)	109.5
Si(1)-C(10)-H(10A)	109.5
H(10C)-C(10)-H(10A)	109.5
H(10B)-C(10)-H(10A)	109.5
Si(1)-C(11)-H(11A)	109.5
Si(1)-C(11)-H(11B)	109.5
H(11A)-C(11)-H(11B)	109.5
Si(1)-C(11)-H(11C)	109.5
H(11A)-C(11)-H(11C)	109.5
H(11B)-C(11)-H(11C)	109.5
Si(2)-C(12)-H(12C)	109.5
Si(2)-C(12)-H(12B)	109.5
H(12C)-C(12)-H(12B)	109.5
Si(2)-C(12)-H(12A)	109.5
H(12C)-C(12)-H(12A)	109.5
H(12B)-C(12)-H(12A)	109.5
Si(2)-C(13)-H(13C)	109.5
Si(2)-C(13)-H(13B)	109.5

H(13C)-C(13)-H(13B)	109.5
Si(2)-C(13)-H(13A)	109.5
H(13C)-C(13)-H(13A)	109.5
H(13B)-C(13)-H(13A)	109.5
Si(2)-C(14)-H(14C)	109.5
Si(2)-C(14)-H(14B)	109.5
H(14C)-C(14)-H(14B)	109.5
Si(2)-C(14)-H(14A)	109.5
H(14C)-C(14)-H(14A)	109.5
H(14B)-C(14)-H(14A)	109.5
O(2)-C(15)-W	175.4(5)
O(3)-C(16)-W	177.6(5)
O(4)-C(17)-W	177.7(5)
O(5)-C(18)-W	178.3(5)
O(6)-C(19)-W	178.0(5)
C(1)-O(1)-P	69.7(2)
O(1)-P-C(1)	50.26(19)
O(1)-P-C(8)	107.2(2)
C(1)-P-C(8)	107.4(2)
O(1)-P-W	114.50(14)
C(1)-P-W	121.99(19)
C(8)-P-W	128.55(17)
C(9)-Si(1)-C(10)	109.8(2)
C(9)-Si(1)-C(11)	109.3(2)
C(10)-Si(1)-C(11)	108.3(3)
C(9)-Si(1)-C(8)	113.9(2)
C(10)-Si(1)-C(8)	108.2(2)
C(11)-Si(1)-C(8)	107.3(3)
C(13)-Si(2)-C(12)	109.9(3)
C(13)-Si(2)-C(14)	108.4(3)
C(12)-Si(2)-C(14)	106.5(2)
C(13)-Si(2)-C(8)	105.6(2)
C(12)-Si(2)-C(8)	114.3(2)
C(14)-Si(2)-C(8)	112.0(2)
C(19)-W-C(15)	87.0(2)
C(19)-W-C(16)	89.6(2)
C(15)-W-C(16)	91.5(2)
C(19)-W-C(18)	90.4(2)
C(15)-W-C(18)	93.3(2)
C(16)-W-C(18)	175.3(2)
C(19)-W-C(17)	91.5(2)
C(15)-W-C(17)	177.3(2)
C(16)-W-C(17)	86.3(2)
C(18)-W-C(17)	89.0(2)
C(19)-W-P	178.87(16)
C(15)-W-P	94.02(15)
C(16)-W-P	89.78(15)
C(18)-W-P	90.06(17)
C(17)-W-P	87.45(17)

Table xvi.4. Anisotropic displacement parameters ($\text{Å}^2 \times 10^3$) for [16b]
The anisotropic displacement factor exponent takes the form:
 $-2 \pi^2 [h^2 a^{*2} U_{11} + \dots + 2 h k a^* b^* U_{12}]$

	U11	U22	U33	U23	U13	U12
C(1)	23(3)	45(4)	29(3)	2(2)	6(2)	-4(2)

C(2)	33(3)	42(4)	22(3)	2(2)	12(2)	-4(3)
C(3)	36(3)	49(4)	33(3)	4(3)	12(2)	1(3)
C(4)	50(4)	50(4)	35(3)	-3(3)	15(3)	-4(3)
C(5)	60(4)	39(4)	42(3)	1(3)	24(3)	8(3)
C(6)	41(3)	51(4)	32(3)	5(3)	18(2)	5(3)
C(7)	36(3)	38(4)	24(3)	-1(2)	13(2)	-3(2)
C(8)	33(3)	36(3)	20(2)	-1(2)	8(2)	-1(2)
C(9)	40(3)	42(4)	23(3)	2(2)	11(2)	1(3)
C(10)	33(3)	53(4)	31(3)	-2(3)	10(2)	2(3)
C(11)	41(3)	51(4)	41(3)	5(3)	11(3)	12(3)
C(12)	42(3)	46(4)	41(3)	7(3)	24(3)	-1(3)
C(13)	55(4)	39(4)	54(4)	-5(3)	25(3)	-11(3)
C(14)	33(3)	55(4)	39(3)	-1(3)	10(2)	-12(3)
C(15)	32(3)	24(3)	38(3)	-7(2)	6(2)	-2(2)
C(16)	33(3)	38(4)	35(3)	5(3)	16(2)	8(3)
C(17)	57(4)	33(4)	32(3)	2(2)	13(2)	-1(3)
C(18)	38(3)	55(4)	42(3)	9(3)	12(3)	13(3)
C(19)	37(3)	36(3)	40(3)	2(3)	14(2)	-1(2)
O(1)	34(2)	37(2)	26(2)	0(2)	13(2)	-6(2)
O(2)	46(2)	50(3)	36(2)	1(2)	16(2)	-6(2)
O(3)	37(2)	54(3)	44(2)	-6(2)	10(2)	-6(2)
O(4)	82(3)	64(3)	43(3)	15(2)	33(2)	8(3)
O(5)	50(3)	86(4)	50(3)	-7(2)	-7(2)	0(3)
O(6)	48(3)	47(3)	64(3)	2(2)	24(2)	9(2)
P	29(1)	37(1)	22(1)	2(1)	9(1)	-1(1)
Si(1)	29(1)	42(1)	22(1)	2(1)	9(1)	3(1)
Si(2)	33(1)	38(1)	32(1)	0(1)	14(1)	-3(1)
W	31(1)	37(1)	27(1)	2(1)	10(1)	3(1)

Table xvi.5. Hydrogen coordinates ($\times 10^4$) and isotropic displacement parameters ($\text{\AA}^2 \times 10^3$) for [16b].

	x	y	z	U(eq)
H(1A)	2834	7734	5008	39
H(3A)	3553	9836	5586	47
H(4A)	3208	11731	6010	53
H(5A)	1592	12506	5519	54
H(6A)	306	11306	4632	48
H(7A)	652	9408	4212	38
H(8A)	1609	9691	3168	36
H(9C)	807	8163	391	53
H(9B)	1620	7429	1127	53
H(9A)	1895	8713	818	53
H(10C)	-632	8041	1479	58
H(10B)	-221	8429	2472	58
H(10A)	203	7246	2150	58
H(11A)	914	10997	1239	67
H(11B)	169	10889	1794	67
H(11C)	-154	10389	826	67
H(12C)	3804	11104	1876	61
H(12B)	2673	10772	1361	61
H(12A)	3488	9726	1656	61
H(13C)	3141	12422	3273	71
H(13B)	2389	11742	3668	71
H(13A)	2030	12139	2676	71
H(14C)	4679	10623	3767	64
H(14B)	4487	9235	3500	64
H(14A)	4091	9782	4236	64

 Table xvi.6. Torsion angles [deg] for **[16b]**.

O(1)-C(1)-C(2)-C(3)	-177.5(4)
P-C(1)-C(2)-C(3)	-107.1(5)
O(1)-C(1)-C(2)-C(7)	1.4(7)
P-C(1)-C(2)-C(7)	71.8(6)
C(7)-C(2)-C(3)-C(4)	-1.4(8)
C(1)-C(2)-C(3)-C(4)	177.5(5)
C(2)-C(3)-C(4)-C(5)	0.0(8)
C(3)-C(4)-C(5)-C(6)	1.4(8)
C(4)-C(5)-C(6)-C(7)	-1.3(8)
C(5)-C(6)-C(7)-C(2)	-0.2(8)
C(3)-C(2)-C(7)-C(6)	1.5(7)
C(1)-C(2)-C(7)-C(6)	-177.4(5)
C(2)-C(1)-O(1)-P	116.9(4)
C(1)-O(1)-P-C(8)	-98.7(3)
C(1)-O(1)-P-W	112.2(3)
C(2)-C(1)-P-O(1)	-102.7(5)
C(2)-C(1)-P-C(8)	-4.5(5)
O(1)-C(1)-P-C(8)	98.2(3)
C(2)-C(1)-P-W	160.6(3)
O(1)-C(1)-P-W	-96.7(2)
Si(1)-C(8)-P-O(1)	-76.8(3)
Si(2)-C(8)-P-O(1)	140.7(2)
Si(1)-C(8)-P-C(1)	-129.6(3)
Si(2)-C(8)-P-C(1)	87.9(3)
Si(1)-C(8)-P-W	66.6(3)
Si(2)-C(8)-P-W	-75.9(3)
P-C(8)-Si(1)-C(9)	-73.7(3)
Si(2)-C(8)-Si(1)-C(9)	66.8(4)
P-C(8)-Si(1)-C(10)	48.6(3)
Si(2)-C(8)-Si(1)-C(10)	-170.8(3)
P-C(8)-Si(1)-C(11)	165.3(3)
Si(2)-C(8)-Si(1)-C(11)	-54.2(4)
P-C(8)-Si(2)-C(13)	-127.3(3)
Si(1)-C(8)-Si(2)-C(13)	92.0(3)
P-C(8)-Si(2)-C(12)	111.8(3)
Si(1)-C(8)-Si(2)-C(12)	-28.9(4)
P-C(8)-Si(2)-C(14)	-9.5(4)
Si(1)-C(8)-Si(2)-C(14)	-150.3(3)
O(6)-C(19)-W-C(15)	-32(14)
O(6)-C(19)-W-C(16)	60(14)
O(6)-C(19)-W-C(18)	-125(14)
O(6)-C(19)-W-C(17)	146(14)
O(6)-C(19)-W-P	118(13)
O(2)-C(15)-W-C(19)	21(5)
O(2)-C(15)-W-C(16)	-69(5)
O(2)-C(15)-W-C(18)	111(5)
O(2)-C(15)-W-C(17)	-35(9)
O(2)-C(15)-W-P	-158(5)
O(3)-C(16)-W-C(19)	76(11)
O(3)-C(16)-W-C(15)	163(11)
O(3)-C(16)-W-C(18)	-15(13)
O(3)-C(16)-W-C(17)	-15(11)
O(3)-C(16)-W-P	-103(11)
O(5)-C(18)-W-C(19)	-109(19)
O(5)-C(18)-W-C(15)	164(19)
O(5)-C(18)-W-C(16)	-18(21)
O(5)-C(18)-W-C(17)	-17(19)
O(5)-C(18)-W-P	70(19)

O(4)-C(17)-W-C(19)	-88(14)
O(4)-C(17)-W-C(15)	-32(17)
O(4)-C(17)-W-C(16)	1(14)
O(4)-C(17)-W-C(18)	-179(100)
O(4)-C(17)-W-P	91(14)
O(1)-P-W-C(19)	7(8)
C(1)-P-W-C(19)	64(8)
C(8)-P-W-C(19)	-134(8)
O(1)-P-W-C(15)	156.63(19)
C(1)-P-W-C(15)	-146.3(2)
C(8)-P-W-C(15)	15.5(3)
O(1)-P-W-C(16)	65.2(2)
C(1)-P-W-C(16)	122.2(2)
C(8)-P-W-C(16)	-76.0(3)
O(1)-P-W-C(18)	-110.1(2)
C(1)-P-W-C(18)	-53.0(3)
C(8)-P-W-C(18)	108.7(3)
O(1)-P-W-C(17)	-21.1(2)
C(1)-P-W-C(17)	35.9(2)
C(8)-P-W-C(17)	-162.3(3)

xvii. [(bis(trimethylsilyl)methyl)fluoro-1,1-

(hydroxyphenyl)methylphosphane]pentacarbonyl tungsten(0) [91]

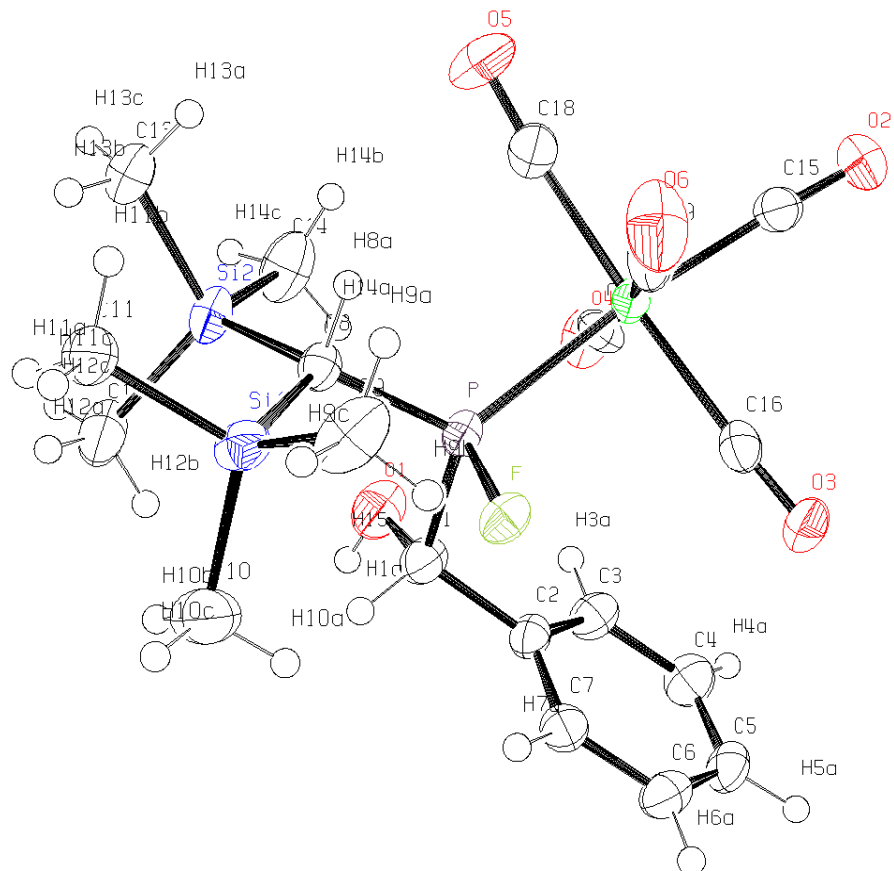


Table xvii.1. Crystal data and structure refinement for [91].

Identification code	GSTR167, Greg1367
Device Type	Nonius KappaCCD
Empirical formula	C19 H26 F O6 P Si2 W
Formula weight	640.40
Temperature	123(2) K
Wavelength	0.71073 Å
Crystal system, space group	Monoclinic, P 21/n
Unit cell dimensions deg.	a = 10.9714(3) Å alpha = 90 deg. b = 12.2708(4) Å beta = 96.280(2) c = 18.5295(5) Å gamma = 90 deg.
Volume	2479.62(12) Å^3
Z, Calculated density	4, 1.715 Mg/m^3
Absorption coefficient	4.857 mm^-1
F(000)	1256
Crystal size	0.60 x 0.48 x 0.40 mm
Theta range for data collection	1.99 to 28.00 deg.
Limiting indices	-14<=h<=14, -15<=k<=16, -24<=l<=24
Reflections collected / unique	38680 / 5964 [R(int) = 0.0954]
Completeness to theta = 28.00	99.4 %
Absorption correction	Semi-empirical from equivalents
Max. and min. transmission	0.13667 and 0.06361
Refinement method	Full-matrix least-squares on F^2
Data / restraints / parameters	5964 / 0 / 278
Goodness-of-fit on F^2	1.047
Final R indices [I>2sigma(I)]	R1 = 0.0395, wR2 = 0.0782
R indices (all data)	R1 = 0.0523, wR2 = 0.0827
Largest diff. peak and hole	2.232 and -1.956 e.Å^-3

Table xvii.2. Atomic coordinates ($\times 10^4$) and equivalent isotropic displacement parameters ($\text{\AA}^2 \times 10^3$) for [91].
 U(eq) is defined as one third of the trace of the orthogonalized U_{ij} tensor.

	x	y	z	U(eq)
C(1)	10585(4)	3453(4)	9276(3)	32(1)
C(2)	9370(4)	3717(4)	9558(2)	27(1)
C(3)	8585(5)	4485(4)	9211(3)	33(1)
C(4)	7460(5)	4693(4)	9454(3)	36(1)
C(5)	7098(4)	4132(4)	10042(3)	34(1)
C(6)	7891(5)	3390(4)	10403(3)	34(1)
C(7)	9029(4)	3181(4)	10162(3)	31(1)
C(8)	11959(4)	1754(4)	8559(2)	26(1)
C(9)	11746(6)	-438(4)	9374(3)	51(2)
C(10)	12845(6)	1499(6)	10219(3)	57(2)
C(11)	14209(5)	341(5)	9090(3)	40(1)
C(12)	14038(5)	3457(5)	8909(4)	50(2)
C(13)	14044(5)	1960(5)	7591(3)	41(1)
C(14)	12286(5)	3776(5)	7522(3)	50(2)
C(15)	7350(5)	2012(4)	6880(3)	32(1)
C(16)	7574(4)	2172(4)	8391(3)	31(1)
C(17)	8838(4)	3773(4)	7484(3)	34(1)
C(18)	9967(5)	1949(4)	6877(3)	41(1)
C(19)	8932(4)	476(4)	7758(3)	39(1)
F	10033(2)	1426(2)	9290(1)	31(1)
O(1)	11024(4)	4287(3)	8862(2)	45(1)
O(2)	6500(3)	1956(3)	6467(2)	41(1)
O(3)	6861(3)	2127(3)	8797(2)	43(1)
O(4)	8849(3)	4677(3)	7333(2)	43(1)
O(5)	10583(4)	1793(4)	6421(3)	72(1)
O(6)	9047(4)	-443(3)	7803(3)	61(1)
P	10428(1)	2224(1)	8672(1)	24(1)
Si(1)	12683(1)	817(1)	9319(1)	34(1)
Si(2)	13064(1)	2755(1)	8170(1)	32(1)
W	8811(1)	2125(1)	7638(1)	25(1)

Table xvii.3. Bond lengths [Å] and angles [deg] for [91].

C(1)-O(1)	1.396(6)
C(1)-C(2)	1.518(6)
C(1)-P	1.874(5)
C(1)-H(1A)	1.0000
C(2)-C(7)	1.385(7)
C(2)-C(3)	1.387(7)
C(3)-C(4)	1.383(7)
C(3)-H(3A)	0.9500
C(4)-C(5)	1.383(7)
C(4)-H(4A)	0.9500
C(5)-C(6)	1.380(7)
C(5)-H(5A)	0.9500
C(6)-C(7)	1.395(7)
C(6)-H(6A)	0.9500
C(7)-H(7A)	0.9500
C(8)-P	1.810(4)
C(8)-Si(2)	1.920(5)
C(8)-Si(1)	1.920(5)
C(8)-H(8A)	1.0000
C(9)-Si(1)	1.861(6)
C(9)-H(9A)	0.9800
C(9)-H(9B)	0.9800
C(9)-H(9C)	0.9800
C(10)-Si(1)	1.858(6)
C(10)-H(10A)	0.9800
C(10)-H(10B)	0.9800
C(10)-H(10C)	0.9800
C(11)-Si(1)	1.865(5)
C(11)-H(11A)	0.9800
C(11)-H(11B)	0.9800
C(11)-H(11C)	0.9800
C(12)-Si(2)	1.854(6)
C(12)-H(12A)	0.9800
C(12)-H(12B)	0.9800
C(12)-H(12C)	0.9800
C(13)-Si(2)	1.875(5)
C(13)-H(13A)	0.9800
C(13)-H(13B)	0.9800
C(13)-H(13C)	0.9800
C(14)-Si(2)	1.876(6)
C(14)-H(14A)	0.9800
C(14)-H(14B)	0.9800
C(14)-H(14C)	0.9800
C(15)-O(2)	1.142(6)
C(15)-W	2.016(5)
C(16)-O(3)	1.144(6)
C(16)-W	2.051(5)
C(17)-O(4)	1.145(6)
C(17)-W	2.043(5)
C(18)-O(5)	1.154(7)
C(18)-W	2.009(6)
C(19)-O(6)	1.137(6)
C(19)-W	2.038(5)
F-P	1.603(3)
O(1)-H(15)	0.8400
P-W	2.4684(12)
O(1)-C(1)-C(2)	113.7(4)
O(1)-C(1)-P	106.0(3)

C(2)-C(1)-P	110.5(3)
O(1)-C(1)-H(1A)	108.8
C(2)-C(1)-H(1A)	108.8
P-C(1)-H(1A)	108.8
C(7)-C(2)-C(3)	119.2(4)
C(7)-C(2)-C(1)	120.2(4)
C(3)-C(2)-C(1)	120.6(4)
C(4)-C(3)-C(2)	120.4(5)
C(4)-C(3)-H(3A)	119.8
C(2)-C(3)-H(3A)	119.8
C(5)-C(4)-C(3)	120.5(5)
C(5)-C(4)-H(4A)	119.7
C(3)-C(4)-H(4A)	119.7
C(6)-C(5)-C(4)	119.3(4)
C(6)-C(5)-H(5A)	120.3
C(4)-C(5)-H(5A)	120.3
C(5)-C(6)-C(7)	120.4(5)
C(5)-C(6)-H(6A)	119.8
C(7)-C(6)-H(6A)	119.8
C(2)-C(7)-C(6)	120.1(5)
C(2)-C(7)-H(7A)	119.9
C(6)-C(7)-H(7A)	119.9
P-C(8)-Si(2)	118.1(2)
P-C(8)-Si(1)	114.9(2)
Si(2)-C(8)-Si(1)	115.5(2)
P-C(8)-H(8A)	101.4
Si(2)-C(8)-H(8A)	101.4
Si(1)-C(8)-H(8A)	101.4
Si(1)-C(9)-H(9A)	109.5
Si(1)-C(9)-H(9B)	109.5
H(9A)-C(9)-H(9B)	109.5
Si(1)-C(9)-H(9C)	109.5
H(9A)-C(9)-H(9C)	109.5
H(9B)-C(9)-H(9C)	109.5
Si(1)-C(10)-H(10A)	109.5
Si(1)-C(10)-H(10B)	109.5
H(10A)-C(10)-H(10B)	109.5
Si(1)-C(10)-H(10C)	109.5
H(10A)-C(10)-H(10C)	109.5
H(10B)-C(10)-H(10C)	109.5
Si(1)-C(11)-H(11A)	109.5
Si(1)-C(11)-H(11B)	109.5
H(11A)-C(11)-H(11B)	109.5
Si(1)-C(11)-H(11C)	109.5
H(11A)-C(11)-H(11C)	109.5
H(11B)-C(11)-H(11C)	109.5
Si(2)-C(12)-H(12A)	109.5
Si(2)-C(12)-H(12B)	109.5
H(12A)-C(12)-H(12B)	109.5
Si(2)-C(12)-H(12C)	109.5
H(12A)-C(12)-H(12C)	109.5
H(12B)-C(12)-H(12C)	109.5
Si(2)-C(13)-H(13A)	109.5
Si(2)-C(13)-H(13B)	109.5
H(13A)-C(13)-H(13B)	109.5
Si(2)-C(13)-H(13C)	109.5
H(13A)-C(13)-H(13C)	109.5
H(13B)-C(13)-H(13C)	109.5
Si(2)-C(14)-H(14A)	109.5
Si(2)-C(14)-H(14B)	109.5
H(14A)-C(14)-H(14B)	109.5
Si(2)-C(14)-H(14C)	109.5
H(14A)-C(14)-H(14C)	109.5

H(14B)-C(14)-H(14C)	109.5
O(2)-C(15)-W	177.9(4)
O(3)-C(16)-W	175.4(4)
O(4)-C(17)-W	173.8(4)
O(5)-C(18)-W	175.5(5)
O(6)-C(19)-W	176.5(5)
C(1)-O(1)-H(15)	109.5
F-P-C(8)	102.43(18)
F-P-C(1)	94.55(18)
C(8)-P-C(1)	107.5(2)
F-P-W	107.27(11)
C(8)-P-W	119.46(16)
C(1)-P-W	120.95(17)
C(10)-Si(1)-C(9)	108.8(3)
C(10)-Si(1)-C(11)	110.2(3)
C(9)-Si(1)-C(11)	105.6(3)
C(10)-Si(1)-C(8)	112.3(3)
C(9)-Si(1)-C(8)	110.4(2)
C(11)-Si(1)-C(8)	109.3(2)
C(12)-Si(2)-C(13)	110.1(3)
C(12)-Si(2)-C(14)	110.3(3)
C(13)-Si(2)-C(14)	103.3(3)
C(12)-Si(2)-C(8)	110.9(3)
C(13)-Si(2)-C(8)	107.9(2)
C(14)-Si(2)-C(8)	114.0(2)
C(18)-W-C(15)	91.1(2)
C(18)-W-C(19)	86.1(2)
C(15)-W-C(19)	92.6(2)
C(18)-W-C(17)	89.4(2)
C(15)-W-C(17)	89.65(19)
C(19)-W-C(17)	175.0(2)
C(18)-W-C(16)	175.0(2)
C(15)-W-C(16)	86.59(19)
C(19)-W-C(16)	89.6(2)
C(17)-W-C(16)	95.04(19)
C(18)-W-P	95.44(16)
C(15)-W-P	173.23(14)
C(19)-W-P	86.08(15)
C(17)-W-P	92.24(13)
C(16)-W-P	86.77(13)

Symmetry transformations used to generate equivalent atoms:

Table xvii.4. Anisotropic displacement parameters ($\text{Å}^2 \times 10^3$) for [91].
The anisotropic displacement factor exponent takes the form:
 $-2 \pi^2 [h^2 a^{*2} U_{11} + \dots + 2 h k a^* b^* U_{12}]$

	U11	U22	U33	U23	U13	U12
C(1)	31(3)	31(2)	36(3)	-7(2)	10(2)	-4(2)
C(2)	24(2)	25(2)	32(2)	-7(2)	7(2)	-2(2)
C(3)	35(3)	28(2)	37(3)	-1(2)	12(2)	1(2)
C(4)	34(3)	32(3)	43(3)	-2(2)	5(2)	10(2)
C(5)	25(2)	34(3)	45(3)	-12(2)	10(2)	2(2)
C(6)	39(3)	30(2)	35(3)	-5(2)	14(2)	-4(2)
C(7)	30(3)	31(2)	32(2)	-5(2)	3(2)	3(2)
C(8)	23(2)	24(2)	32(2)	-2(2)	5(2)	1(2)
C(9)	55(4)	37(3)	65(4)	18(3)	25(3)	15(3)
C(10)	57(4)	77(4)	36(3)	-3(3)	3(3)	27(4)
C(11)	35(3)	46(3)	39(3)	0(2)	1(2)	14(2)
C(12)	30(3)	44(3)	77(4)	-21(3)	12(3)	-4(2)
C(13)	30(3)	47(3)	49(3)	2(2)	12(2)	0(2)
C(14)	41(3)	41(3)	70(4)	19(3)	18(3)	2(3)
C(15)	34(3)	34(3)	30(2)	-4(2)	8(2)	-3(2)
C(16)	26(2)	29(2)	38(3)	-4(2)	-1(2)	-3(2)
C(17)	34(3)	38(3)	29(2)	-11(2)	-4(2)	-3(2)
C(18)	32(3)	46(3)	46(3)	-8(2)	6(2)	-1(2)
C(19)	25(3)	28(3)	63(4)	-5(2)	1(2)	-2(2)
F	31(2)	28(1)	34(1)	3(1)	12(1)	-1(1)
O(1)	42(2)	35(2)	61(2)	-12(2)	17(2)	-7(2)
O(2)	35(2)	48(2)	39(2)	-4(2)	-4(2)	-4(2)
O(3)	30(2)	56(2)	46(2)	-10(2)	15(2)	-12(2)
O(4)	37(2)	34(2)	58(2)	11(2)	9(2)	2(2)
O(5)	54(3)	101(4)	65(3)	-27(3)	34(2)	-3(3)
O(6)	43(2)	31(2)	106(4)	-10(2)	0(2)	0(2)
P	21(1)	22(1)	30(1)	-1(1)	6(1)	0(1)
Si(1)	34(1)	36(1)	31(1)	3(1)	6(1)	13(1)
Si(2)	23(1)	28(1)	47(1)	2(1)	10(1)	0(1)
W	20(1)	26(1)	31(1)	-3(1)	5(1)	-1(1)

Table xvii.5. Hydrogen coordinates ($\times 10^4$) and isotropic displacement parameters ($\text{\AA}^2 \times 10^3$) for [91].

	x	y	z	U(eq)
H(1A)	11209	3297	9698	39
H(3A)	8820	4870	8804	39
H(4A)	6932	5226	9216	44
H(5A)	6312	4257	10196	41
H(6A)	7659	3019	10817	41
H(7A)	9571	2671	10414	37
H(8A)	11792	1228	8148	31
H(9A)	11547	-743	8887	77
H(9B)	10986	-257	9581	77
H(9C)	12211	-975	9685	77
H(10A)	12030	1654	10364	85
H(10B)	13298	2183	10189	85
H(10C)	13293	1020	10579	85
H(11A)	14794	947	9144	60
H(11B)	14133	79	8588	60
H(11C)	14502	-252	9418	60
H(12A)	14565	2923	9185	75
H(12B)	13516	3817	9233	75
H(12C)	14549	4002	8699	75
H(13A)	13523	1493	7257	62
H(13B)	14621	1507	7901	62
H(13C)	14502	2464	7311	62
H(14A)	11653	4161	7756	74
H(14B)	11908	3400	7087	74
H(14C)	12892	4301	7383	74
H(15)	11272	4806	9135	68

Table xvii.6. Torsion angles [deg] for [91].

O(1)-C(1)-C(2)-C(7)	-157.3(4)
P-C(1)-C(2)-C(7)	83.6(5)
O(1)-C(1)-C(2)-C(3)	23.4(6)
P-C(1)-C(2)-C(3)	-95.7(5)
C(7)-C(2)-C(3)-C(4)	-1.7(7)
C(1)-C(2)-C(3)-C(4)	177.6(4)
C(2)-C(3)-C(4)-C(5)	-0.6(8)
C(3)-C(4)-C(5)-C(6)	2.5(7)
C(4)-C(5)-C(6)-C(7)	-2.1(7)
C(3)-C(2)-C(7)-C(6)	2.0(7)
C(1)-C(2)-C(7)-C(6)	-177.3(4)
C(5)-C(6)-C(7)-C(2)	-0.2(7)
Si(2)-C(8)-P-F	-156.4(2)
Si(1)-C(8)-P-F	-14.6(3)
Si(2)-C(8)-P-C(1)	-57.5(3)
Si(1)-C(8)-P-C(1)	84.3(3)
Si(2)-C(8)-P-W	85.4(3)
Si(1)-C(8)-P-W	-132.84(19)
O(1)-C(1)-P-F	175.9(3)
C(2)-C(1)-P-F	-60.5(4)
O(1)-C(1)-P-C(8)	71.3(4)
C(2)-C(1)-P-C(8)	-165.0(3)
O(1)-C(1)-P-W	-70.8(3)
C(2)-C(1)-P-W	52.8(4)
P-C(8)-Si(1)-C(10)	-60.8(4)
Si(2)-C(8)-Si(1)-C(10)	82.0(3)
P-C(8)-Si(1)-C(9)	60.8(3)
Si(2)-C(8)-Si(1)-C(9)	-156.4(3)
P-C(8)-Si(1)-C(11)	176.5(3)
Si(2)-C(8)-Si(1)-C(11)	-40.7(3)
P-C(8)-Si(2)-C(12)	94.6(3)
Si(1)-C(8)-Si(2)-C(12)	-47.0(3)
P-C(8)-Si(2)-C(13)	-144.8(3)
Si(1)-C(8)-Si(2)-C(13)	73.7(3)
P-C(8)-Si(2)-C(14)	-30.7(4)
Si(1)-C(8)-Si(2)-C(14)	-172.2(3)
O(5)-C(18)-W-C(15)	-45(7)
O(5)-C(18)-W-C(19)	48(7)
O(5)-C(18)-W-C(17)	-134(7)
O(5)-C(18)-W-C(16)	17(9)
O(5)-C(18)-W-P	134(7)
O(2)-C(15)-W-C(18)	-171(12)
O(2)-C(15)-W-C(19)	103(12)
O(2)-C(15)-W-C(17)	-82(12)
O(2)-C(15)-W-C(16)	13(12)
O(2)-C(15)-W-P	25(13)
O(6)-C(19)-W-C(18)	10(9)
O(6)-C(19)-W-C(15)	101(9)
O(6)-C(19)-W-C(17)	-15(10)
O(6)-C(19)-W-C(16)	-173(9)
O(6)-C(19)-W-P	-86(9)
O(4)-C(17)-W-C(18)	41(4)
O(4)-C(17)-W-C(15)	-50(4)
O(4)-C(17)-W-C(19)	66(5)
O(4)-C(17)-W-C(16)	-137(4)
O(4)-C(17)-W-P	136(4)
O(3)-C(16)-W-C(18)	2(7)
O(3)-C(16)-W-C(15)	65(5)
O(3)-C(16)-W-C(19)	-28(5)

O(3)-C(16)-W-C(17)	154(5)
O(3)-C(16)-W-P	-114(5)
F-P-W-C(18)	-133.07(19)
C(8)-P-W-C(18)	-17.3(2)
C(1)-P-W-C(18)	120.5(2)
F-P-W-C(15)	31.2(12)
C(8)-P-W-C(15)	147.0(12)
C(1)-P-W-C(15)	-75.3(12)
F-P-W-C(19)	-47.41(19)
C(8)-P-W-C(19)	68.3(2)
C(1)-P-W-C(19)	-153.9(2)
F-P-W-C(17)	137.36(18)
C(8)-P-W-C(17)	-106.9(2)
C(1)-P-W-C(17)	30.9(2)
F-P-W-C(16)	42.44(17)
C(8)-P-W-C(16)	158.2(2)
C(1)-P-W-C(16)	-64.0(2)

xviii. [Benzyl(bis(trimethylsilyl)methyl)chlorophosphane]pentacarbonyl tungsten(0) [113]

(A1)

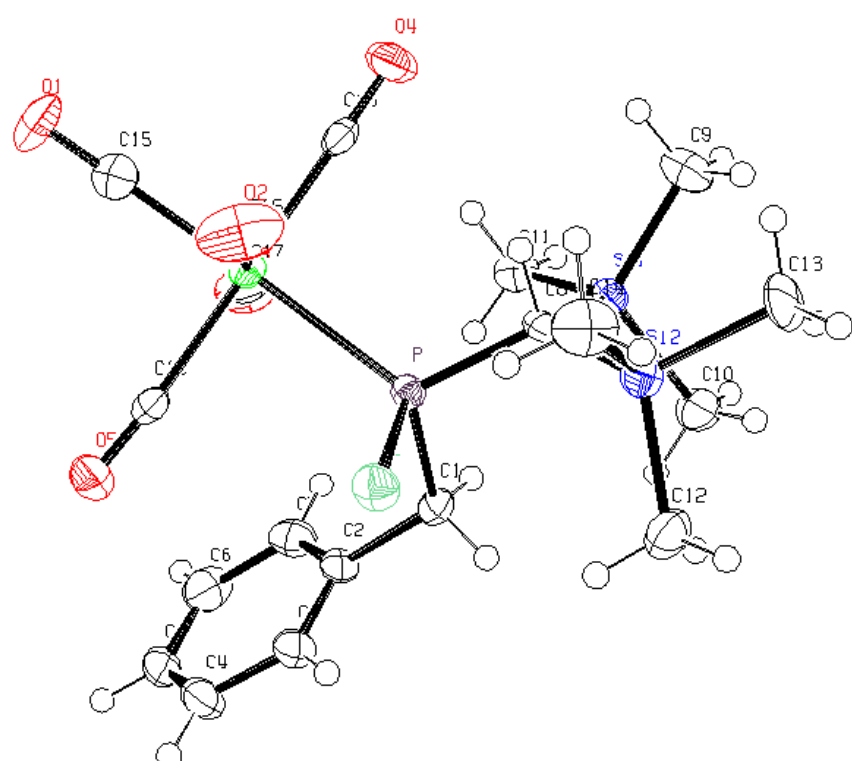


Table xviii.1. Crystal data and structure refinement for [113].

Identification code	GSTR070, Greg660
Device Type	Nonius KappaCCD
Empirical formula	C19 H26 Cl O5 P Si2 W
Formula weight	640.85
Temperature	123(2) K
Wavelength	0.71073 Å
Crystal system, space group	Triclinic, P -1
Unit cell dimensions deg.	a = 9.0076(5) Å alpha = 88.090(3) 88.596(3) deg. b = 10.3098(5) Å beta = 68.414(2) deg. c = 14.2857(5) Å gamma =
Volume	1232.83(10) Å^3

Z, Calculated density	2, 1.726 Mg/m^3
Absorption coefficient	4.981 mm^-1
F(000)	628
Crystal size	0.40 x 0.20 x 0.16 mm
Theta range for data collection	2.59 to 27.99 deg.
Limiting indices	-11<=h<=10, -13<=k<=13, -18<=l<=18
Reflections collected / unique	15005 / 5752 [R(int) = 0.0807]
Completeness to theta = 27.99	96.8 %
Absorption correction	Multi-Scan
Max. and min. transmission	0.49051 and 0.32225
Refinement method	Full-matrix least-squares on F^2
Data / restraints / parameters	5752 / 15 / 317
Goodness-of-fit on F^2	0.998
Final R indices [I>2sigma(I)]	R1 = 0.0422, wR2 = 0.0902
R indices (all data)	R1 = 0.0549, wR2 = 0.0940
Largest diff. peak and hole	2.118 and -2.542 e.A^-3

Table xviii.2. Atomic coordinates ($\times 10^4$) and equivalent isotropic displacement parameters ($\text{Å}^2 \times 10^3$) for [113].
 U(eq) is defined as one third of the trace of the orthogonalized U_{ij} tensor.

	x	y	z	U(eq)
C(1)	6651(7)	4862(6)	8474(4)	24(1)
C(2)	5406(7)	6060(6)	8954(4)	24(1)
C(3)	5727(8)	6591(6)	9768(4)	29(1)
C(4)	4572(8)	7739(7)	10177(4)	36(2)
C(5)	3079(8)	8336(7)	9797(4)	38(2)
C(6)	2717(8)	7805(7)	9000(4)	40(2)
C(7)	3866(8)	6687(7)	8567(4)	32(1)
C(8)	9320(6)	3773(5)	7150(3)	20(1)
C(15)	6557(7)	9318(6)	5910(4)	29(1)
C(16)	9301(8)	7577(7)	6839(4)	35(2)
C(17)	4860(7)	7529(6)	6421(4)	27(1)
C(18)	7818(7)	6459(6)	5460(4)	25(1)
C(19)	6357(7)	8650(6)	7863(4)	26(1)
O(1)	6272(6)	10355(5)	5484(3)	44(1)
O(2)	10536(6)	7629(6)	6961(3)	58(2)
O(3)	3619(5)	7566(5)	6239(3)	44(1)
O(4)	8198(6)	5860(5)	4781(3)	39(1)
O(5)	5950(6)	9326(5)	8500(3)	44(1)
C(9)	9287(8)	1893(7)	5532(4)	37(2)
C(10)	7926(9)	1435(7)	7464(4)	37(2)
C(11)	6146(9)	3895(8)	6123(6)	28(2)
C(12)	10835(8)	2172(7)	9013(4)	37(2)
C(14)	12688(8)	3527(8)	7691(5)	42(2)
C(13)	12223(10)	957(8)	7141(6)	47(2)
P	8017(2)	5380(2)	7685(1)	19(1)
Cl	9375(2)	5773(2)	8733(1)	31(1)
Si(1)	8161(2)	2757(2)	6583(1)	22(1)
Si(2)	11216(2)	2632(2)	7770(1)	28(1)
C(9S)	9287(8)	1893(7)	5532(4)	37(2)
C(10S)	7926(9)	1435(7)	7464(4)	37(2)
C(11S)	10280(30)	5430(30)	8810(30)	18(11)
C(12S)	10835(8)	2172(7)	9013(4)	37(2)
C(14S)	12688(8)	3527(8)	7691(5)	42(2)
PS	7394(18)	5098(16)	7291(11)	24(4)
ClS	5910(20)	4420(20)	6525(13)	39(5)
Si(1S)	9610(20)	1955(17)	6773(12)	32(4)
Si(2S)	10800(20)	3749(18)	8174(10)	29(4)
C(13S)	11830(90)	760(80)	6740(50)	51(7)
W	7091(1)	7537(1)	6658(1)	20(1)

Table xviii.3. Bond lengths [Å] and angles [deg] for [113].

C(1)-C(2)	1.501(8)
C(1)-PS	1.843(15)
C(1)-P	1.856(5)
C(1)-H(1A)	0.9900
C(1)-H(1B)	0.9900
C(2)-C(3)	1.383(8)
C(2)-C(7)	1.414(8)
C(3)-C(4)	1.391(9)

C(3)-H(3)	0.9500
C(4)-C(5)	1.374(10)
C(4)-H(4)	0.9500
C(5)-C(6)	1.375(9)
C(5)-H(5)	0.9500
C(6)-C(7)	1.386(9)
C(6)-H(6)	0.9500
C(7)-H(7)	0.9500
C(8)-PS	1.781(15)
C(8)-P	1.821(5)
C(8)-Si(1S)	1.890(16)
C(8)-Si(2)	1.901(6)
C(8)-Si(1)	1.934(5)
C(8)-Si(2S)	1.998(16)
C(8)-H(8)	1.0000
C(15)-O(1)	1.159(7)
C(15)-W	1.998(6)
C(16)-O(2)	1.151(7)
C(16)-W	2.030(6)
C(17)-O(3)	1.141(7)
C(17)-W	2.049(6)
C(18)-O(4)	1.143(7)
C(18)-W	2.032(6)
C(19)-O(5)	1.134(7)
C(19)-W	2.058(6)
C(9)-Si(1)	1.852(6)
C(9)-H(9A)	0.9800
C(9)-H(9B)	0.9800
C(9)-H(9C)	0.9800
C(10)-Si(1)	1.889(6)
C(10)-H(10A)	0.9800
C(10)-H(10B)	0.9800
C(10)-H(10C)	0.9800
C(11)-Si(1)	1.883(8)
C(11)-H(11A)	0.9800
C(11)-H(11B)	0.9800
C(11)-H(11C)	0.9800
C(12)-Si(2)	1.880(6)
C(12)-H(12A)	0.9800
C(12)-H(12B)	0.9800
C(12)-H(12C)	0.9800
C(14)-Si(2)	1.873(7)
C(14)-H(14A)	0.9800
C(14)-H(14B)	0.9800
C(14)-H(14C)	0.9800
C(13)-Si(2)	1.877(8)
C(13)-H(13A)	0.9800
C(13)-H(13B)	0.9800
C(13)-H(13C)	0.9800
P-Cl	2.098(2)
P-W	2.5032(16)
C(11S)-Si(2S)	1.8800(10)
C(11S)-H(11D)	0.9800
C(11S)-H(11E)	0.9800
C(11S)-H(11F)	0.9800
PS-ClS	2.07(3)
PS-W	2.563(15)
Si(1S)-C(13S)	1.93(7)
C(13S)-H(13D)	0.9800
C(13S)-H(13E)	0.9800
C(13S)-H(13C)	0.9800

C(2)-C(1)-PS 120.7(6)

C(2)-C(1)-P	114.1(4)
PS-C(1)-P	29.1(5)
C(2)-C(1)-H(1A)	108.7
PS-C(1)-H(1A)	80.2
P-C(1)-H(1A)	108.7
C(2)-C(1)-H(1B)	108.7
PS-C(1)-H(1B)	124.4
P-C(1)-H(1B)	108.7
H(1A)-C(1)-H(1B)	107.6
C(3)-C(2)-C(7)	118.4(5)
C(3)-C(2)-C(1)	121.6(5)
C(7)-C(2)-C(1)	120.0(5)
C(2)-C(3)-C(4)	120.4(6)
C(2)-C(3)-H(3)	119.8
C(4)-C(3)-H(3)	119.8
C(5)-C(4)-C(3)	120.6(6)
C(5)-C(4)-H(4)	119.7
C(3)-C(4)-H(4)	119.7
C(4)-C(5)-C(6)	120.0(6)
C(4)-C(5)-H(5)	120.0
C(6)-C(5)-H(5)	120.0
C(5)-C(6)-C(7)	120.2(6)
C(5)-C(6)-H(6)	119.9
C(7)-C(6)-H(6)	119.9
C(6)-C(7)-C(2)	120.3(6)
C(6)-C(7)-H(7)	119.9
C(2)-C(7)-H(7)	119.9
PS-C(8)-P	29.8(6)
PS-C(8)-Si(1S)	122.4(8)
P-C(8)-Si(1S)	147.8(6)
PS-C(8)-Si(2)	145.1(6)
P-C(8)-Si(2)	119.4(3)
Si(1S)-C(8)-Si(2)	76.7(6)
PS-C(8)-Si(1)	84.3(6)
P-C(8)-Si(1)	113.1(3)
Si(1S)-C(8)-Si(1)	39.4(6)
Si(2)-C(8)-Si(1)	114.6(3)
PS-C(8)-Si(2S)	112.4(8)
P-C(8)-Si(2S)	83.7(5)
Si(1S)-C(8)-Si(2S)	112.0(8)
Si(2)-C(8)-Si(2S)	36.7(5)
Si(1)-C(8)-Si(2S)	145.1(6)
PS-C(8)-H(8)	102.0
P-C(8)-H(8)	102.1
Si(1S)-C(8)-H(8)	101.0
Si(2)-C(8)-H(8)	102.1
Si(1)-C(8)-H(8)	102.1
Si(2S)-C(8)-H(8)	103.8
O(1)-C(15)-W	178.7(5)
O(2)-C(16)-W	178.0(6)
O(3)-C(17)-W	175.9(5)
O(4)-C(18)-W	178.7(5)
O(5)-C(19)-W	176.3(5)
Si(1)-C(9)-H(9A)	109.5
Si(1)-C(9)-H(9B)	109.5
H(9A)-C(9)-H(9B)	109.5
Si(1)-C(9)-H(9C)	109.5
H(9A)-C(9)-H(9C)	109.5
H(9B)-C(9)-H(9C)	109.5
Si(1)-C(10)-H(10A)	109.5
Si(1)-C(10)-H(10B)	109.5
H(10A)-C(10)-H(10B)	109.5
Si(1)-C(10)-H(10C)	109.5

H(10A)-C(10)-H(10C)	109.5
H(10B)-C(10)-H(10C)	109.5
Si(1)-C(11)-H(11A)	109.5
Si(1)-C(11)-H(11B)	109.5
H(11A)-C(11)-H(11B)	109.5
Si(1)-C(11)-H(11C)	109.5
H(11A)-C(11)-H(11C)	109.5
H(11B)-C(11)-H(11C)	109.5
Si(2)-C(12)-H(12A)	109.5
Si(2)-C(12)-H(12B)	109.5
H(12A)-C(12)-H(12B)	109.5
Si(2)-C(12)-H(12C)	109.5
H(12A)-C(12)-H(12C)	109.5
H(12B)-C(12)-H(12C)	109.5
Si(2)-C(14)-H(14A)	109.5
Si(2)-C(14)-H(14B)	109.5
H(14A)-C(14)-H(14B)	109.5
Si(2)-C(14)-H(14C)	109.5
H(14A)-C(14)-H(14C)	109.5
H(14B)-C(14)-H(14C)	109.5
Si(2)-C(13)-H(13A)	109.5
Si(2)-C(13)-H(13B)	109.5
H(13A)-C(13)-H(13B)	109.5
Si(2)-C(13)-H(13C)	109.5
H(13A)-C(13)-H(13C)	109.5
H(13B)-C(13)-H(13C)	109.5
C(8)-P-C(1)	105.3(2)
C(8)-P-Cl1	105.56(19)
C(1)-P-Cl1	97.06(19)
C(8)-P-W	117.11(18)
C(1)-P-W	122.89(19)
Cl-P-W	105.74(8)
C(9)-Si(1)-C(11)	104.2(3)
C(9)-Si(1)-C(10)	111.1(3)
C(11)-Si(1)-C(10)	109.7(3)
C(9)-Si(1)-C(8)	108.5(3)
C(11)-Si(1)-C(8)	114.2(3)
C(10)-Si(1)-C(8)	109.2(3)
C(14)-Si(2)-C(13)	104.5(4)
C(14)-Si(2)-C(12)	112.1(3)
C(13)-Si(2)-C(12)	107.6(4)
C(14)-Si(2)-C(8)	108.7(3)
C(13)-Si(2)-C(8)	110.9(3)
C(12)-Si(2)-C(8)	112.7(3)
Si(2S)-C(11S)-H(11D)	109.5
Si(2S)-C(11S)-H(11E)	109.5
H(11D)-C(11S)-H(11E)	109.5
Si(2S)-C(11S)-H(11F)	109.5
H(11D)-C(11S)-H(11F)	109.5
H(11E)-C(11S)-H(11F)	109.5
C(8)-PS-C(1)	107.6(8)
C(8)-PS-ClS	104.1(10)
C(1)-PS-ClS	98.5(9)
C(8)-PS-W	115.9(7)
C(1)-PS-W	120.5(7)
ClS-PS-W	107.6(9)
C(8)-Si(1S)-C(13S)	112(2)
C(11S)-Si(2S)-C(8)	115.4(13)
Si(1S)-C(13S)-H(13D)	109.5
Si(1S)-C(13S)-H(13E)	109.5
H(13D)-C(13S)-H(13E)	109.5
Si(1S)-C(13S)-H(13F)	109.5
H(13D)-C(13S)-H(13F)	109.5

H(13E)-C(13S)-H(13F)	109.5
C(15)-W-C(16)	88.0(2)
C(15)-W-C(18)	89.3(2)
C(16)-W-C(18)	91.1(2)
C(15)-W-C(17)	90.1(2)
C(16)-W-C(17)	177.6(2)
C(18)-W-C(17)	87.5(2)
C(15)-W-C(19)	90.0(2)
C(16)-W-C(19)	88.7(3)
C(18)-W-C(19)	179.2(2)
C(17)-W-C(19)	92.8(2)
C(15)-W-P	173.07(16)
C(16)-W-P	85.59(17)
C(18)-W-P	93.48(15)
C(17)-W-P	96.39(16)
C(19)-W-P	87.19(16)
C(15)-W-PS	165.6(4)
C(16)-W-PS	102.7(4)
C(18)-W-PS	80.9(4)
C(17)-W-PS	79.0(4)
C(19)-W-PS	99.8(4)
P-W-PS	21.1(4)

Table xviii.4. Anisotropic displacement parameters ($\text{\AA}^2 \times 10^3$) for [113]

The anisotropic displacement factor exponent takes the form:
 $-2 \pi^2 [h^2 a^* a^2 U_{11} + \dots + 2 h k a^* b^* U_{12}]$

	U11	U22	U33	U23	U13	U12
C(1)	28(3)	20(3)	25(3)	2(2)	3(2)	-10(3)
C(2)	23(3)	25(3)	25(3)	-2(2)	12(2)	-9(3)
C(3)	31(3)	31(3)	26(3)	-3(2)	6(2)	-11(3)
C(4)	47(4)	34(4)	29(3)	-11(3)	13(3)	-17(3)
C(5)	43(4)	25(3)	36(4)	-3(3)	23(3)	-2(3)
C(6)	26(4)	43(4)	41(4)	8(3)	5(3)	-3(3)
C(7)	32(4)	41(4)	27(3)	-2(3)	5(3)	-18(3)
C(8)	19(3)	22(3)	17(3)	-2(2)	5(2)	-5(2)
C(15)	27(3)	35(4)	34(3)	-3(3)	-2(3)	-20(3)
C(16)	30(4)	49(4)	28(3)	20(3)	-1(3)	-20(3)
C(17)	22(3)	33(3)	26(3)	7(2)	6(2)	-11(3)
C(18)	21(3)	21(3)	30(3)	9(2)	5(2)	-5(2)
C(19)	32(3)	21(3)	24(3)	6(2)	2(2)	-9(3)
O(1)	58(3)	33(3)	47(3)	19(2)	-17(2)	-25(2)
O(2)	35(3)	102(5)	50(3)	15(3)	-6(2)	-43(3)
O(3)	23(3)	69(4)	45(3)	5(2)	-2(2)	-24(2)
O(4)	45(3)	44(3)	29(2)	-10(2)	13(2)	-17(2)
O(5)	69(4)	32(3)	34(3)	-9(2)	15(2)	-23(3)
C(9)	36(4)	46(4)	32(3)	-14(3)	8(3)	-20(3)
C(10)	51(4)	32(4)	35(3)	-2(3)	8(3)	-23(3)
C(11)	25(4)	36(4)	29(4)	0(3)	-1(3)	-18(4)
C(12)	38(4)	32(4)	36(4)	9(3)	-6(3)	-8(3)
C(14)	24(4)	62(5)	41(4)	2(3)	-7(3)	-16(3)
C(13)	35(5)	35(4)	45(5)	-4(4)	-3(4)	19(4)
P	18(1)	19(1)	19(1)	-2(1)	2(1)	-6(1)
C1	32(1)	32(1)	29(1)	-4(1)	-6(1)	-13(1)
Si(1)	21(1)	21(1)	23(1)	-4(1)	3(1)	-8(1)

Si(2)	21(1)	29(1)	29(1)	0(1)	-3(1)	-2(1)
C(9S)	36(4)	46(4)	32(3)	-14(3)	8(3)	-20(3)
C(10S)	51(4)	32(4)	35(3)	-2(3)	8(3)	-23(3)
C(11S)	18(14)	16(14)	15(14)	7(9)	0(9)	-2(10)
C(12S)	38(4)	32(4)	36(4)	9(3)	-6(3)	-8(3)
C(14S)	24(4)	62(5)	41(4)	2(3)	-7(3)	-16(3)
PS	14(8)	26(8)	27(8)	-3(6)	7(6)	-2(6)
CLS	34(10)	60(13)	34(10)	-7(8)	1(8)	-29(9)
Si(1S)	32(10)	18(8)	46(10)	-3(7)	3(8)	-8(8)
Si(2S)	28(9)	38(10)	22(8)	-3(7)	0(6)	-12(8)
C(13S)	39(11)	37(11)	49(12)	-1(11)	-2(11)	20(10)
W	17(1)	21(1)	22(1)	2(1)	1(1)	-8(1)

Table xvii.5. Hydrogen coordinates ($\times 10^4$) and isotropic displacement parameters ($\text{\AA}^2 \times 10^3$) for [113].

	x	y	z	U(eq)
H(1A)	6109	4375	8104	29
H(1B)	7292	4193	8956	29
H(3)	6743	6169	10050	35
H(4)	4818	8115	10725	43
H(5)	2296	9115	10084	45
H(6)	1677	8205	8746	48
H(7)	3618	6340	8008	38
H(8)	9751	4131	6589	24
H(9A)	10365	1277	5711	55
H(9B)	9353	2602	5076	55
H(9C)	8737	1342	5252	55
H(10A)	7326	1918	8012	55
H(10B)	8983	789	7658	55
H(10C)	7347	912	7179	55
H(11A)	5468	4399	6641	43
H(11B)	5647	3312	5832	43
H(11C)	6274	4565	5656	43
H(12A)	10062	1707	9023	55
H(12B)	10408	3025	9376	55
H(12C)	11838	1545	9290	55
H(14A)	12247	4420	8008	64
H(14B)	12902	3695	7031	64
H(14C)	13684	2935	7991	64
H(13A)	11519	423	7150	70
H(13B)	13224	408	7453	70
H(13C)	12450	1165	6491	70
H(9S1)	8224	2563	5371	55
H(9S2)	9364	951	5378	55
H(9S3)	10099	2130	5175	55
H(10D)	8070	1457	8140	55
H(10E)	8023	494	7295	55
H(10F)	6866	2101	7294	55
H(11D)	9228	5667	9108	27
H(11E)	10264	6178	8361	27
H(11F)	11083	5324	9287	27
H(12D)	9759	2350	9266	55
H(12E)	11568	2076	9530	55
H(12F)	11196	1310	8660	55
H(14D)	13102	2650	7355	64
H(14E)	13420	3502	8193	64
H(14F)	12593	4307	7255	64

H(13D)	12260	639	7378	77
H(13E)	12423	1188	6333	77
H(13F)	11940	-149	6503	77

Table xviii.6. Torsion angles [deg] for [113].

PS-C(1)-C(2)-C(3)	-115.7(8)
P-C(1)-C(2)-C(3)	-83.7(6)
PS-C(1)-C(2)-C(7)	63.4(9)
P-C(1)-C(2)-C(7)	95.4(6)
C(7)-C(2)-C(3)-C(4)	-1.8(8)
C(1)-C(2)-C(3)-C(4)	177.3(5)
C(2)-C(3)-C(4)-C(5)	2.1(9)
C(3)-C(4)-C(5)-C(6)	-0.5(10)
C(4)-C(5)-C(6)-C(7)	-1.4(10)
C(5)-C(6)-C(7)-C(2)	1.7(9)
C(3)-C(2)-C(7)-C(6)	-0.1(9)
C(1)-C(2)-C(7)-C(6)	-179.2(5)
PS-C(8)-P-C(1)	68.1(10)
Si(1S)-C(8)-P-C(1)	26.2(12)
Si(2)-C(8)-P-C(1)	-87.3(3)
Si(1)-C(8)-P-C(1)	52.2(3)
Si(2S)-C(8)-P-C(1)	-96.0(5)
PS-C(8)-P-Cl	170.2(10)
Si(1S)-C(8)-P-Cl	128.2(11)
Si(2)-C(8)-P-Cl	14.7(3)
Si(1)-C(8)-P-Cl	154.2(2)
Si(2S)-C(8)-P-Cl	6.0(5)
PS-C(8)-P-W	-72.5(10)
Si(1S)-C(8)-P-W	-114.5(11)
Si(2)-C(8)-P-W	132.1(2)
Si(1)-C(8)-P-W	-88.5(3)
Si(2S)-C(8)-P-W	123.3(5)
C(2)-C(1)-P-C(8)	-177.0(4)
PS-C(1)-P-C(8)	-66.8(10)
C(2)-C(1)-P-Cl	74.7(4)
PS-C(1)-P-Cl	-175.1(10)
C(2)-C(1)-P-W	-39.2(5)
PS-C(1)-P-W	71.0(10)
PS-C(8)-Si(1)-C(9)	138.0(6)
P-C(8)-Si(1)-C(9)	145.9(3)
Si(1S)-C(8)-Si(1)-C(9)	-55.7(9)
Si(2)-C(8)-Si(1)-C(9)	-72.6(4)
Si(2S)-C(8)-Si(1)-C(9)	-100.4(10)
PS-C(8)-Si(1)-C(11)	22.3(6)
P-C(8)-Si(1)-C(11)	30.2(4)
Si(1S)-C(8)-Si(1)-C(11)	-171.4(9)
Si(2)-C(8)-Si(1)-C(11)	171.7(3)
Si(2S)-C(8)-Si(1)-C(11)	144.0(10)
PS-C(8)-Si(1)-C(10)	-100.8(6)
P-C(8)-Si(1)-C(10)	-92.9(3)
Si(1S)-C(8)-Si(1)-C(10)	65.5(9)
Si(2)-C(8)-Si(1)-C(10)	48.6(4)
Si(2S)-C(8)-Si(1)-C(10)	20.9(10)
PS-C(8)-Si(2)-C(14)	-93.0(11)
P-C(8)-Si(2)-C(14)	-71.8(4)
Si(1S)-C(8)-Si(2)-C(14)	138.4(6)
Si(1)-C(8)-Si(2)-C(14)	149.3(3)
Si(2S)-C(8)-Si(2)-C(14)	-57.1(8)
PS-C(8)-Si(2)-C(13)	152.7(11)
P-C(8)-Si(2)-C(13)	174.0(4)

Si(1S)-C(8)-Si(2)-C(13)	24.1(7)
Si(1)-C(8)-Si(2)-C(13)	35.1(4)
Si(2S)-C(8)-Si(2)-C(13)	-171.4(9)
PS-C(8)-Si(2)-C(12)	32.0(11)
P-C(8)-Si(2)-C(12)	53.2(4)
Si(1S)-C(8)-Si(2)-C(12)	-96.6(6)
Si(1)-C(8)-Si(2)-C(12)	-85.7(3)
Si(2S)-C(8)-Si(2)-C(12)	67.8(8)
P-C(8)-PS-C(1)	-71.0(10)
Si(1S)-C(8)-PS-C(1)	84.0(11)
Si(2)-C(8)-PS-C(1)	-31.7(16)
Si(1)-C(8)-PS-C(1)	94.3(8)
Si(2S)-C(8)-PS-C(1)	-53.9(11)
P-C(8)-PS-ClS	-174.8(15)
Si(1S)-C(8)-PS-ClS	-19.8(12)
Si(2)-C(8)-PS-ClS	-135.5(9)
Si(1)-C(8)-PS-ClS	-9.5(7)
Si(2S)-C(8)-PS-ClS	-157.8(8)
P-C(8)-PS-W	67.2(9)
Si(1S)-C(8)-PS-W	-137.8(9)
Si(2)-C(8)-PS-W	106.5(9)
Si(1)-C(8)-PS-W	-127.5(7)
Si(2S)-C(8)-PS-W	84.3(9)
C(2)-C(1)-PS-C(8)	156.7(6)
P-C(1)-PS-C(8)	71.8(10)
C(2)-C(1)-PS-ClS	-95.6(10)
P-C(1)-PS-ClS	179.6(15)
C(2)-C(1)-PS-W	20.7(12)
P-C(1)-PS-W	-64.1(9)
PS-C(8)-Si(1S)-C(13S)	-177(3)
P-C(8)-Si(1S)-C(13S)	-154(3)
Si(2)-C(8)-Si(1S)-C(13S)	-29(3)
Si(1)-C(8)-Si(1S)-C(13S)	166(3)
Si(2S)-C(8)-Si(1S)-C(13S)	-39(3)
PS-C(8)-Si(2S)-C(11S)	-22.6(19)
P-C(8)-Si(2S)-C(11S)	-14.2(17)
Si(1S)-C(8)-Si(2S)-C(11S)	-165.1(18)
Si(2)-C(8)-Si(2S)-C(11S)	179(2)
Si(1)-C(8)-Si(2S)-C(11S)	-136.3(17)
O(1)-C(15)-W-C(16)	-17(25)
O(1)-C(15)-W-C(18)	-108(25)
O(1)-C(15)-W-C(17)	164(25)
O(1)-C(15)-W-C(19)	72(25)
O(1)-C(15)-W-P	5(26)
O(1)-C(15)-W-PS	-155(25)
O(2)-C(16)-W-C(15)	78(15)
O(2)-C(16)-W-C(18)	167(15)
O(2)-C(16)-W-C(17)	114(15)
O(2)-C(16)-W-C(19)	-12(15)
O(2)-C(16)-W-P	-100(15)
O(2)-C(16)-W-PS	-112(15)
O(4)-C(18)-W-C(15)	-74(20)
O(4)-C(18)-W-C(16)	-162(20)
O(4)-C(18)-W-C(17)	16(20)
O(4)-C(18)-W-C(19)	-94(26)
O(4)-C(18)-W-P	112(20)
O(4)-C(18)-W-PS	95(20)
O(3)-C(17)-W-C(15)	30(8)
O(3)-C(17)-W-C(16)	-7(12)
O(3)-C(17)-W-C(18)	-59(8)
O(3)-C(17)-W-C(19)	120(8)
O(3)-C(17)-W-P	-152(8)
O(3)-C(17)-W-PS	-140(8)

O(5)-C(19)-W-C(15)	-11(9)
O(5)-C(19)-W-C(16)	77(9)
O(5)-C(19)-W-C(18)	9(23)
O(5)-C(19)-W-C(17)	-101(9)
O(5)-C(19)-W-P	163(9)
O(5)-C(19)-W-PS	180(100)
C(8)-P-W-C(15)	-100.2(15)
C(1)-P-W-C(15)	126.6(15)
Cl-P-W-C(15)	17.0(15)
C(8)-P-W-C(16)	-77.7(3)
C(1)-P-W-C(16)	149.1(3)
Cl-P-W-C(16)	39.5(2)
C(8)-P-W-C(18)	13.1(3)
C(1)-P-W-C(18)	-120.1(3)
Cl-P-W-C(18)	130.34(18)
C(8)-P-W-C(17)	101.0(3)
C(1)-P-W-C(17)	-32.3(3)
Cl-P-W-C(17)	-141.81(18)
C(8)-P-W-C(19)	-166.5(3)
C(1)-P-W-C(19)	60.2(3)
Cl-P-W-C(19)	-49.33(18)
C(8)-P-W-PS	66.5(9)
C(1)-P-W-PS	-66.7(9)
Cl-P-W-PS	-176.3(9)
C(8)-PS-W-C(15)	105.5(15)
C(1)-PS-W-C(15)	-122.1(13)
ClS-PS-W-C(15)	-10.6(19)
C(8)-PS-W-C(16)	-31.4(9)
C(1)-PS-W-C(16)	101.0(9)
ClS-PS-W-C(16)	-147.5(8)
C(8)-PS-W-C(18)	57.6(8)
C(1)-PS-W-C(18)	-169.9(9)
ClS-PS-W-C(18)	-58.4(8)
C(8)-PS-W-C(17)	146.8(9)
C(1)-PS-W-C(17)	-80.7(9)
ClS-PS-W-C(17)	30.8(8)
C(8)-PS-W-C(19)	-122.3(8)
C(1)-PS-W-C(19)	10.2(9)
ClS-PS-W-C(19)	121.7(8)
C(8)-PS-W-P	-68.1(10)
C(1)-PS-W-P	64.3(10)
ClS-PS-W-P	175.8(15)
